National Research Council Canada

Conseil national de recherches Canada

NRC · CNRC

Canadian Journal of Fisheries and Aquatic Sciences

Journal canadien des sciences halieutiques et aquatiques

http://www.nrc.ca/cisti/journals

ISSN 0706-652X / CJFSDX 56(7) 1143–1327 (1999)

The *Canadian Journal of Fisheries and Aquatic Sciences*, previously published as *Contributions to Canadian Biology* 1901–1925, *Contributions to Canadian Biology and Fisheries* 1926–1934, *Journal of the Biological Board of Canada* 1934–1937, and *Journal of the Fisheries Research Board of Canada* 1938–1979, is issued monthly to form annual volumes of 12 numbers plus supplements.

Editorial policy: The Journal publishes original research articles, perspectives (syntheses, critiques, re-evaluations), discussions (comment and reply), and rapid communications. Manuscripts may concern cells, organisms, populations, communities, ecosystems, or processes that affect aquatic systems. They may cover a range of disciplines including biology and ecology of marine and freshwater organisms, limnology, oceanography, physiology, toxicology, genetics, economics, disease, and management. Preference will be given to manuscripts that emphasize understanding of observed phenomena and interpretation of experimental results. The Journal encourages papers that lead from clearly stated purpose or rationale and from testable hypotheses, concepts, or questions to identifiable conclusions or syntheses. Such papers may amplify, modify, question, or redirect accumulated knowledge embodied in contemporary perceptions of a particular state of aquatic sciences. The Journal discourages papers that are essentially descriptive, except in emerging disciplines; have only site-specific or local applications (a certain year, place, taxon, chemical compound, etc.); only confirm previously established principles; or apply standard techniques without breaking new methodological ground.

Manuscripts for publication should be submitted to the Editors, Canadian Journal of Fisheries and Aquatic Sciences, Department of Zoology, University of Guelph, Guelph, ON N1G 2W1, Canada (519-824-4120 ext. 2646; fax: 519-767-9798; e-mail: cjfas@uoguelph.ca).

Submissions in either English or French are acceptable. The information must be original, that is, not copyrighted, published, or submitted elsewhere except in abstract form or unless by written consent of the Editor. NRC accepts no responsibility for statements or opinions expressed by a contributor. Acceptance of an advertisement, announcement, or other material does not imply endorsement by either the *Journal*'s Editors or NRC. The use of proprietary names does not imply endorsement of the product or company.

Correspondence concerning accepted manuscripts and corrected proofs should be sent to NRC Research Press, National Research Council of Canada, Ottawa, ON K1A 0R6, Canada.

Instructions to Authors are published once a year in the first issue of each volume. Copies are available from NRC Research Press or from our Web site. The **Publication Policy** of NRC Research Press is also available at our Web site:
http://www.nrc.ca/cisti/journals/rj.html

Microfilm: Issues from 1934 through the current volume can be purchased on 16- or 35-mm microfilm. Photocopies of individual articles or issues can be purchased from University Microfilms International, 330 North Zeeb Road, Ann Arbor, MI 48106, U.S.A.

U.S. periodical postage paid at Champlain, N.Y., and at additional mailing offices. Attention U.S. POSTMASTER: Send address changes to **Canadian Journal of Fisheries and Aquatic Sciences**, c/o USACAN Media Distribution Center, P.O. Box 2888, Plattsburg, NY 12901, U.S.A.

Publié sans interruption depuis 1901, le *Journal canadien des sciences halieutiques et aquatiques* a paru sous plusieurs titres : *Contributions to Canadian Biology* 1901–1925, *Contributions to Canadian Biology and Fisheries* 1926–1934, *Journal of the Biological Board of Canada* 1934–1937, et *Journal of the Fisheries Research Board of Canada* 1938–1979. Le *Journal* paraît tous les mois, formant ainsi un volume de 12 numéros, et offre en plus jusqu'à deux suppléments par année.

Politique éditoriale : On publie, dans le Journal, des articles rendant compte de recherche originale, des perspectives (synthèses, critiques et réévaluations), des discussions (commentaires et réponses) et des communications rapides. Les documents peuvent porter sur les cellules, organismes, populations, communautés, écosystèmes ou processus qui affectent les systèmes aquatiques. Ils peuvent relever de divers domaines y compris la biologie et l'écologie des organismes marins et d'eau douce, la limnologie, l'océanographie, la physiologie, la toxicologie, la génétique, l'économie, la pathologie et la gestion. On accorde la préséance aux articles qui contribuent à la compréhension de phénomènes observés et à l'interprétation de résultats expérimentaux. On invite les auteurs à soumettre des articles ayant des objectifs précis ou relevant d'hypothèses, de concepts ou de questions vérifiables et se terminant par de solides conclusions ou d'utiles synthèses. Ces articles enrichissent, changent, mettent en question ou réorientent les connaissances acquises sur divers aspects des sciences aquatiques. On décourage toutefois la soumission d'articles simplement descriptifs (à moins qu'il ne s'agisse de nouvelles disciplines), d'application très limitée (applicables à une seule année, une seule région ou un seul taxon, portant sur un unique composé chimique, etc.); d'articles qui ne font que reprendre les principes énoncés dans des articles précédents; et d'articles rendant compte de l'application de normes sans gain de méthodologie.

Les auteurs voudront adresser leurs **manuscrits** aux directeurs scientifiques, Journal canadien des sciences halieutiques et aquatiques, Département de Zoologie, University of Guelph, Guelph, ON N1G 2W1, Canada (519-824-4120 poste. 2646; télécopieur : 519-767-9798; adresse électronique : cjfas@uoguelph.ca).

Les contributions peuvent être en anglais ou en français. Elles doivent être originales, c.-à.-d. qu'elles ne doivent pas avoir fait l'objet d'un copyright, avoir été publiées ou soumises ailleurs, sauf sous forme abrégée ou avec le consentement du rédacteur. Le CNRC ne se tient en aucune façon responsable des opinions exprimées par un collaborateur ou des déclarations qui pourrait faire ce dernier. La publication d'annonces publicitaires, d'avis et autres n'implique pas l'endossement de leur contenu par les directeurs du *Journal* ou du CNRC. L'utilisation des noms de marques de commerce ne signifie aucunement une sanction du produit en question ou de la compagnie qui le fabrique.

La correspondance ayant trait aux manuscrits acceptés et les **épreuves corrigés** doivent être envoyées aux Presses scientifiques du CNRC, Conseil national de recherches du Canada, Ottawa, ON K1A 0R6, Canada.

Recommandations aux auteurs sont publiés une fois par année dans le premier numéro de chaque volume. Des copies, ainsi que la **Politique de publication**, sont disponibles auprès des Presses scientifiques du CNRC ou au site Web :
http://www.nrc.ca/cisti/journals/rj.html

Microfilms : On peut acheter sur microfilms de 16 ou 35 mm tous les numéros depuis 1934. Des photocopies d'articles ou de numéros individuels sont aussi en vente auprès de University Microfilms International, 330 North Zeeb Road, Ann Arbor, MI 48106, É.-U.

This journal is indexed or abstracted in / Ce journal est signalé ou résumé dans
Aquatic Sciences and Fisheries Abstracts, Biological & Agricultural Index, CAB Abstracts (Centre for Agriculture and Biosciences), Chemical Abstracts, Current Awareness in Biological Sciences, Current Contents, FAO Freshwater and Aquaculture Contents Tables, FAO Marine Science Contents Tables, GEOBASE – Geo Abstracts, Meteorological and Geoastrophysical Abstracts, Oceanic Abstracts, Science Citation Index, Biological Abstracts, Environment Abstracts, Environmental Periodicals Bibliography, GEOREF, Life Sciences Collection, ABSEARCH, and PASCAL Database

Volume 56, Number 7, July 1999

Canadian Journal of Fisheries and Aquatic Sciences

Published by the National Research Council of Canada

Volume 56, numéro 7, juillet 1999

Journal canadien des sciences halieutiques et aquatiques

Publié par le Conseil national de recherches du Canada

Editors / directeurs scientifiques John C. Roff and Moira M. Ferguson

Assistant to the Editors / adjointe aux directeurs scientifiques **Holly Foster**

Associate Editors / directeurs scientifique associés

D. Boisclair, *Université de Montréal*
U. Borgmann, *Environment Canada, Burlington*
S.E. Campana, *DFO/MPO, Dartmouth*
D.G. Dixon, *University of Waterloo*
A.E. Dizon, *National Marine Fisheries Service, La Jolla, Calif.*
J.J. Dodson, *Université Laval*
J.A. Downing, *Iowa State University*
K.T. Frank, *DFO/MPO, Dartmouth*
D.F. Houlihan, *University of Aberdeen, Aberdeen, Scotland*
F.A. Huntingford, *University of Glasgow*
J.A. Hutchings, *Dalhousie University*
G.S. Jamieson, *DFO/MPO, Nanaimo*
B. Jonsson, *Norwegian Institute for Nature Research, Oslo, Norway*
L. Legendre, *Université Laval*
D.M. Mason, *Purdue University, West Lafayette, Ind.*
A. Mazumder, *University of Victoria*
D.L. Parrish, *Vermont Cooperative Fish and Wildlife Research Unit (USGS/BRD), University of Vermont*
P. Pepin, *DFO/MPO, St. John's*
R.M. Peterman, *Simon Fraser University*
E.E. Prepas, *University of Alberta*
T.M. Powell, *University of California, Berkeley, Calif.*
T.J. Quinn II, *University of Alaska–Fairbanks, Juneau, Alaska*
T.P. Quinn, *University of Washington*
R.D. Robarts, *Environment Canada, Saskatoon*
B. Sainte-Marie, *DFO/MPO, Mont-Joli*
P.F. Sale, *University of Windsor*
D.W. Schindler, *University of Alberta*
S.J. Smith, *DFO/MPO, Dartmouth*
W.G. Sprules, *University of Toronto*
R.J. Thompson, *Memorial University of Newfoundland*
C.J. Walters, *University of British Columbia*
R.D. Ward, *CSIRO Division of Fisheries, Australia*
C.M. Wood, *McMaster University*
B. de Young, *Memorial University of Newfoundland*

NRC Research Press / Presses scientifiques du CNRC

Editor-in-chief / directeur général **Bruce P. Dancik**

Assistant Editor-in-chief / directeur général adjoint **Iain E.P. Taylor**

Journals Program / Programme des revues

(Fax / télécopieur : 613-952-7656; e-mail / adresse électronique : research.journals@nrc.ca;
URL: http://www.nrc.ca/cisti/journals/)

Director / directrice **Aldyth Holmes**

Business Manager / gestionnaire des affaires **Paul McClymont**

Managing Editor / rédactrice administrative **Cecily M. Pearson (613-993-9099)**

Publication Officer / agente de publication **Jennifer McColl**

Advertising / annonces publicitaires **Judy Heyman (613-993-0151)**

Reprints / tirés à part **Roxanne Landriault (613-990-2254)**

Subscriptions / abonnements **Helen Goulet (613-993-9084)**

© National Research Council of Canada 1999. World rights reserved.
No part of this publication may be reproduced, stored, or transmitted in any form or by any means, without the written permission of the publisher, except as stated below.

The National Research Council of Canada grants **permission*** to individuals to make single copies of articles for personal use. Any person may reproduce short excerpts from articles in the journal for any purpose that respects the moral rights of authors, provided that the source is fully acknowledged. As a courtesy, the consent of authors of such material should be obtained directly from the author.

Authorization to reproduce items for other than personal use, as stated above, is granted by the National Research Council of Canada provided that the copyright fee of $7.00 per copy is paid directly to CANCOPY, One Yonge Street, Suite 1900, Toronto, ON M5E 1E5, Canada.

*The above permission does not extend to other kinds of copying, such as copying for general distribution, for advertising, or promotional purposes, for creating new collective works, or for resale. For such copying, arrangements must be made with the publisher, National Research Council of Canada, Ottawa, ON K1A 0R6, Canada.

© Conseil national de recherches du Canada 1999. Tous droits réservés.
Il est interdit de reproduire, de sauvegarder ou de transmettre quelque partie de la présente publication dans quelque format ou de quelque façon sans le consentement écrit de l'éditeur, à l'exception des conditions suivantes.

Le Conseil national de recherches du Canada accorde aux particuliers le droit de faire des copies individuelles pour leur usage personnel. Toute personne peut reproduire de courts extraits des articles de la Revue pour autant que les droits moraux de l'auteur soient respectés et que la mention de provenance soit clairement indiquée. Il est de convenance de demander le consentement de l'auteur avant de faire mention de son travail.

On obtiendra l'autorisation de reproduire des articles à d'autres fins que l'usage personnel (tel qu'on l'a décrit ci-dessus) auprès du Conseil national de recherches du Canada pour autant que des redevances de droits d'auteurs de 7,00 $/copie soient versées au CANCOPY, One Yonge Street, Suite 1900, Toronto, ON M5E 1E5, Canada.

*La permission ci-dessus ne s'applique pas à la reproduction à grande échelle, telle que la reproduction aux fins de distribution générale, publicitaire ou promotionnelle, de compilation de nouveaux ouvrages collectifs ou de revente. Dans de tels cas, il faudra ratifier une entente particulière avec l'éditeur, le Conseil national de recherches du Canada, Ottawa, ON K1A 0R6, Canada.

Subscription information

The *Canadian Journal of Fisheries and Aquatic Sciences* (ISSN 0706-652X) is published monthly by the National Research Council of Canada. 1999 annual subscription rates (second class postage) for Canada are $578CAN institutional and $182CAN personal, for US & foreign $578US institutional and $182US personal. For air mail add $150US to foreign rate. Canadian customers please include 7% GST (business no. 12149 1807 RT 0275). Subscriptions are entered for the calendar year. Remittances should be made payable to the Receiver General for Canada credit NRC. Price for regular single issues: institutional, $75.00; personal, $25.00. Supplements will be priced separately. Special rates apply to members of Canadian scientific and engineering societies if they subscribe through their respective societies.

There are no refunds on cancelled subscriptions once delivery has begun. Claims for missing issues should be made within four months (N. America) or six months (outside N. America) following the date of publication. The publisher expects to supply missing issues only when losses have occurred in transit and when the reserve stock will permit. For change of address and subscription enquiries: Subscription Office, NRC Research Press, National Research Council of Canada, Ottawa, ON K1A 0R6, Canada; tel: 613-993-9084; fax: 613-952-7656; e-mail: research.journals@nrc.ca.

Microform backfiles are available from UMI, P.O. Box 1346, Ann Arbor, MI 48106-1346, U.S.A., and Micromedia Ltd., 20 Victoria St., Toronto, ON M5C 2N8, Canada.

The 1999 issues of the *Canadian Journal of Fisheries and Aquatic Sciences* are available on the Web. Pricing information can be found at

http://www.nrc.ca/cisti/journals/

Renseignements sur l'abonnement

Journal canadien des sciences halieutiques et aquatiques (ISSN 0706-652X) est une publication mensuelle du Conseil national de recherches du Canada. Le prix de l'abonnement annuel au Canada (courrier de deuxième classe) est de 578 $CAN pour les organismes et de 182 $CAN pour les particuliers. À l'étranger (y compris les É.-U.), le prix de l'abonnement est de 578 $US pour les organismes et de 182 $US pour les particuliers. L'expédition par avion exige des frais de 150 $US en sus du prix d'abonnement à l'étranger. Les clients du Canada doivent ajouter la TPS de 7% (numéro d'entreprise 12149 1807 RT 0275). Les abonnements sont pour l'année civile. Tout paiement doit être adressé au Receveur général du Canada, crédit du CNRC. Le prix par numéro est de 75 $ pour les organismes et de 25 $ pour les particuliers. Le prix des hors-série varie. Les membres des sociétés canadiennes de sciences et de génie bénéficient de taux préférentiels en s'abonnant via leurs sociétés respectives.

Aucun remboursement ne sera accordé ni aucune annulation acceptée une fois que les livraisons auront commencé. Les réclamations de numéros manquants devront être soumises dans les quatre mois (Amérique du Nord) ou dans les six mois (à l'extérieur de l'Amérique du Nord) suivant la date de publication. L'éditeur ne fournira de numéros manquants que si le document a été perdu pendant l'expédition et que si le stock le permet. Adressez tout changement d'adresse ou toute question quant à l'abonnement au : Bureau des abonnements, Presses scientifiques du CNRC, Conseil national de recherches Canada, Ottawa, ON K1A 0R6, Canada; téléphone : 613-993-9084; télécopieur : 613-952-7656; adresse électronique : research.journals@nrc.ca.

On peut obtenir les fichiers rétrospectifs sur **microforme** auprès de UMI, P.O. Box 1346, Ann Arbor, MI 48106-1346, É.-U., et auprès de Micromedia Ltée, 20 rue Victoria, Toronto, ON M5C 2N8, Canada.

Les numéros de 1999 de *Journal canadien des sciences halieutiques et aquatiques* sont accessibles sur le Web. On trouvera des renseignements sur les tarifs à

http://www.nrc.ca/cisti/journals/rjfr.html

Relative importance of water and food as cadmium sources to the predatory insect *Sialis velata* (Megaloptera)

Isabelle Roy and Landis Hare

Abstract: A key aspect of modeling contaminant uptake by animals is knowledge of the route taken by the contaminant to enter the animal. To determine the relative importance of food and water as Cd sources for benthic insects, we measured Cd accumulation by the predatory alderfly *Sialis velata* (Megaloptera) from either water alone or from chironomid prey (*Cryptochironomus* sp.). We determined that Cd uptake from prey was far more important than that from water. Chironomid prey fed to *S. velata* also appeared to take up the bulk of their Cd from food (meiobenthic organisms). The efficiency with which Cd was assimilated by the predator from its prey is high (50%) and comparable with values reported for several other insects. In the predator, Cd taken up from food was largely stored in gut tissues (as is the case for insect larvae in nature), whereas a greater proportion of the metal taken up from water was stored in other animal parts.

Résumé : La connaissance de la voie par laquelle les contaminants entrent dans les animaux est essentielle pour la modélisation de l'absorption des contaminants par les animaux. Pour déterminer la contribution relative des aliments et de l'eau comme sources du Cd présent chez les insectes benthiques, nous avons mesuré l'accumulation dans le sialidé *Sialis velata* (Megaloptera), un insecte prédateur, du Cd provenant de l'eau seule ou de ses proies du groupe des chironomides (*Cryptochironomus* sp.). Nous avons établi que le Cd absorbé par cet insecte provenait beaucoup plus de ses proies que de l'eau. De plus, la plus grande partie du Cd absorbé par les chironomides donnés en pâture à *S. velata* semblait provenir de leurs aliments (organismes méiobenthiques). L'efficacité avec laquelle le Cd des proies était assimilé par le prédateur est élevée (50%) et comparable aux valeurs signalées pour plusieurs autres insectes. Chez le prédateur, le Cd provenant de ses aliments était en grande partie stocké dans les tissus intestinaux (comme c'est le cas pour les larves d'insectes dans la nature), tandis qu'une plus grande proportion du métal provenant de l'eau était stockée dans d'autres organes.

[Traduit par la Rédaction]

Introduction

Human activities are responsible for recent increases in the global fluxes of many trace metals to the biosphere (Pacyna et al. 1995). Because metals can be transported great distances in the atmosphere, they have contaminated large numbers of remote aquatic systems (Franzin et al. 1979; Verta et al. 1986). Given the potential toxicity of metals to aquatic animals (Hare 1992), we require some means of measuring the risk that they pose to aquatic life. Although measurements of metals in sediment and water can be of some use in this regard, they often necessitate assumptions about bioavailability that can be circumvented by making measurements in the animals themselves (Phillips and Rainbow 1993). The effective use of animals as biomonitoring tools depends on the development of models that reliably relate metal concentrations in a biomonitor to those in its surroundings (Hare and Tessier 1996). A key element in modeling metal accumulation in animals is a knowledge of the relative importance of food and water as metal sources (Hare 1992; Luoma et al. 1992).

There is little reliable information on metal uptake routes in freshwater animals (e.g., Timmermans et al. 1992; Stephenson and Turner 1993; Munger and Hare 1997), in part due to the technical difficulties inherent in separating food and water as metal vectors (Kay 1985). Many investigators appear to ignore metal uptake from food because they measure bioaccumulation and effects subsequent to water-only exposures (Luoma 1995). However, a recent study has shown that Cd uptake by the insect *Chaoborus punctipennis* is mainly from its planktonic prey (Munger and Hare 1997). We conducted experiments on a benthic insect, the alderfly *Sialis*, to determine if food is also an important Cd source for this opportunistic predator on benthic invertebrates (Evans and Neunzig 1996). We chose *Sialis* larvae for our experiments because of their potential as a benthic Cd biomonitor (Roy and Hare 1998) in complement to the planktonic Cd biomonitor *Chaoborus* (Hare and Tessier 1996, 1998; Croteau et al. 1998).

Received September 10, 1998. Accepted February 5, 1999. J14782

I. Roy and L. Hare.[1] Institut national de la recherche scientifique – Eau (INRS-Eau), Université du Québec, Sainte-Foy, QC G1V 4C7, Canada.

[1]Author to whom all correspondence should be addressed. e-mail: landis@inrs-eau.uquebec.ca

Methods

Experimental design

We used an experimental trophic chain to determine the relative

© 1999 NRC Canada

Fig. 1. Simple food chain used in our laboratory experiments, indicating potential Cd sources at each trophic level.

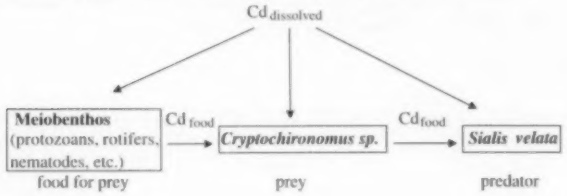

importance of water and food as Cd sources to *Sialis velata* (Megaloptera) larvae (Fig. 1). Laboratory comparisons of prey and water as metal sources for a predator are most realistic when (*i*) prey have been exposed to the metal in both food and water, as would occur in nature, and (*ii*) stress on predators exposed to metal in water only has been minimized by offering uncontaminated prey as food (Kay 1985; Fisher and Reinfelder 1995). With this in mind, we exposed prey (the chironomid *Cryptochironomus* sp.) (Fig. 1) to Cd in both water and meiobenthic food, and we fed all predatory larvae (*S. velata*), i.e., in the case of the food-only exposure the predator was offered ^{109}Cd-contaminated prey, whereas in the water-only exposure, predators were fed ^{109}Cd-free prey (Table 1). Furthermore, we conducted predator Cd exposures in artificial lake water of known composition so as to better control aqueous Cd speciation. Predator Cd accumulation was measured in both whole animals and various animal parts (Table 1).

Collection of insects and preparation of Cd exposure solutions

Larvae of *S. velata* and *Cryptochironomus* sp. were collected with an Ekman grab at a 5 m water depth in Lake St. Joseph, Québec (46°55′N, 71°40′W). The water of this Canadian Shield lake has a pH of 6.6 and a dissolved organic C concentration of 3 mg $C \cdot L^{-1}$ (Hare and Tessier 1996). Grab samples were sieved in the field and the animals retained transported to the laboratory where they were held in aerated aquariums at 10°C in unsieved Lake St. Joseph sediment until required.

Artificial lake water was used in the holding aquariums as well as for all experimental exposures. Major ions in the artificial lake water were present in the same concentrations as in Lake St. Joseph water (micromolar): Ca, 97; Mg, 19; Na, 39, K, 2.5; SO_4, 42; Cl, 16. All labware was soaked in 15% nitric acid for 1 day and rinsed repeatedly in deionized water before use. To contaminate our trophic chain, we prepared stock solutions by adding sufficient $^{109+112}$Cd to artificial lake water to attain a total dissolved Cd concentration of 3, 10, or 30 nM. Concentrations of dissolved Cd as high as 20 nM have been reported in Cd-contaminated lakes (Croteau et al. 1998). Chemical speciation calculations indicate that Cd added to our artificial lake water was present largely as the free metal ion (≈98%; HYDRAQL speciation program, Papelis et al. 1988). A control group of *S. velata* larvae held in 30-mL high-density polyethylene (HDPE) containers with clean artificial lake water and fed uncontaminated *Cryptochironomus* sp. prey daily for 4 days showed no mortality, as was the case for larvae at all of the Cd treatment levels, suggesting that neither the experimental conditions nor the Cd concentrations used in our whole-insect Cd accumulation experiment were deleterious to larvae. Total dissolved Cd concentrations to which both prey and the predator were exposed (measured in 0.5-mL water samples taken with a polyethylene syringe fitted with a 0.45-μm Millipore HA filter) were within 10% of the nominal Cd values (Cd measurement methods described below).

Cadmium exposure of prey and their food

Because the preferred food of *Cryptochironomus* sp. larvae is not known, we reared a mixture of meiobenthic organisms as food for these potential prey. An innoculum, obtained from organic debris in a fish-holding tank, was distributed in several 1-L HDPE containers filled with artificial lake water. Air was bubbled continuously and the cultures were kept in the dark for 2 weeks at 20°C. Small pieces of hydroponic lettuce were added as a nutrient source for the meiobenthos at regular intervals. The biomass of these cultures was dominated, in decreasing order, by protozoans, rotifers, naidid oligochaetes, and nematodes (based on microscopic examination).

Meiobenthos and *Cryptochironomus* sp. were exposed together to each of the three nominal Cd concentrations so as to produce a supply of *Cryptochironomus* sp. prey for *S. velata* at the rate of one prey per predator per day. To achieve this end, third-instar *Cryptochironomus* sp. larvae were contaminated in groups of four individuals in the dark at 17°C in 100-mL polypropylene containers for 16 days. To determine if the prey took up their Cd mainly from food, we also exposed *Cryptochironomus* sp. larvae (1 per 30-mL HDPE vial) to water at the intermediate Cd concentration (10 nM) without food for 7 days; a longer exposure time resulted in prey mortality, presumably due to starvation. Because of the small size of the meiobenthic organisms, it was not possible to measure their ^{109}Cd concentration. Prey (*Cryptochironomus* sp.) ^{109}Cd concentrations were measured over time (described below). Prey fresh weights were converted to dry weights using a factor of 0.17, based on the dry and fresh weights of a series of third-instar *Cryptochironomus* sp. samples (n = 6 samples of five pooled individuals). This series of prey samples was subsequently digested in a microwave oven and Cd contents were measured by graphite furnace atomic absorption spectrophotometry (Croteau et al. 1998) to estimate total Cd in *Cryptochironomus* sp. larvae.

Cadmium exposure regimes of the predator *S. velata*

We selected *S. velata* larvae of uniform length and weight for our experiments to avoid variations due to differences in Cd accumulation with animal size. Larvae at the beginning of our whole-insect water versus food experiment (Table 1) were 12.7 ± 1.7 mm in length and had a dry weight of 6.3 ± 1.8 mg (means ± SD), and larval length and weight were not significantly different among treatments at either the beginning or the end of our experiments ($p > 0.05$, Kruskal–Wallis Dunn's test). Prior to Cd exposure, each *S. velata* larva was held at 10°C in a 30-mL HDPE vial filled with artificial lake water for a 3-day acclimation period during which time it was fed one uncontaminated *Cryptochironomus* sp. larva daily.

In the experiment designed to measure Cd accumulation in the whole insect, we exposed the predator *S. velata* for 4 days to Cd in either food or water (Table 1). In the food-only exposure, each predator was fed daily a live Cd-contaminated *Cryptochironomus* sp. larva that had been exposed to the metal for 16 days at one of the three nominal Cd concentrations (prey exposure described above). Prey were not depurated prior to consumption by the predator for two reasons: (*i*) prey depuration would not necessarily occur in nature and (*ii*) trial periods of prey depuration led to only small Cd losses (<10% after 2 days). Prey size (third instar) was chosen to ensure that one individual would fill the predator's gut (prey were visible in the predator's gut), and larvae were fed daily because previous observations revealed that *S. velata* larvae will not feed within 15 h of consuming a large prey.

The predator consumed its prey within 15 min, during which time the Cd lost from prey was not measurable (in either prey or water). To ensure that Cd concentrations in water remained negligible, water in the vials was changed daily; ^{109}Cd concentrations in water were always below the detection limit of 0.06 ± 0.01 Bq (mean ± SD). Following the 4-day predator exposure period, *S. velata* larvae were fed uncontaminated prey of another chironomid genus (*Procladius* sp.) to allow us to confirm the complete

© 1999 NRC Canada

Table 1. Cadmium exposure routes used in our experiments designed to compare Cd accumulation by the alderfly *S. velata* from water and from its prey (the chironomid *Cryptochironomus* sp.) as well as to measure Cd efflux from the predator.

Cd source for predator (exposure duration)	Number of *S. velata*	[Cd] (nM)	Cd source for prey (exposure duration)	Efflux duration (days)
Whole animal				
Food (4 days)	9	3, 10, 30	Food + water (16 days)	—
Water (4 days)	9	3, 10, 30	—	6
Internal distribution				
Food (7 days)	12	10	Water (7 days)	—
Water (7 days)	12	10	—	—

evacuation of contaminated gut contents (by the presence of *Procladius* sp. head capsules in the predator's fecal pellets). Cadmium concentrations in *S. velata* larvae were measured 1 day after their last Cd-contaminated meal (see analytical methods below).

In the water-only treatment of the whole-insect experiment, *S. velata* larvae were exposed for 4 days to each of the three nominal Cd concentrations (Table 1). To avoid stress due to starvation, larvae were fed one uncontaminated *Cryptochironomus* sp. larva daily. We verified that the predator consumed its prey rapidly (in <15 min) and that prey took up no measurable Cd from water during this short feeding period (prey were subjected to an EDTA rinse prior to Cd measurement, as described below). Cd concentrations in water remained constant during the experiment (coefficients of variation ≈ 5%). Because the gut contents of *S. velata* were not contaminated, as they were in the food-only exposure, we were able to make repeated measurements over time of ^{109}Cd concentrations in individual *S. velata* larva (Cd analyses described below).

We measured ^{109}Cd losses from the predator for up to 6 days subsequent to the ^{109}Cd exposure period. *Sialis velata* larvae were placed in 30 mL of Cd-free water containing 0.1 mM EDTA to ensure that any ^{109}Cd released by insects would be complexed. Results of a preliminary experiment showed that the presence of EDTA in water did not influence Cd efflux from the predator. During this period, each *S. velata* larva was fed daily one uncontaminated *Cryptochironomus* sp. larva, and water in the vials was changed daily to avoid Cd buildup in water.

Internal distribution of Cd in *S. velata*

To measure differences in internal Cd localization with exposure route, *S. velata* larvae were exposed for 7 days to either Cd in prey or Cd in water (Table 1). In the food-only exposure, the predator was exposed to Cd through a daily feeding of a *Cryptochironomus* sp. larva that had been previously exposed to 10 nM Cd in artificial lake water for 7 d; although prey were not fed, this should not compromise the comparison of relative Cd distribution patterns in *Sialis* larvae. In the water-only exposure, the predator was exposed to 10 nM Cd and fed one ^{109}Cd-free *Cryptochironomus* sp. larva daily. In both cases, the predator was separated by dissection into gills, gut tissues, and remaining body parts (as described in Hare et al. 1989). Cadmium losses during dissection were <10% of the larval total-Cd.

Cadmium analyses

Cadmium-109 concentrations were measured in water and animal samples in a gamma-counter (Wallac NaI-well type); both counting efficiency (70%) and sample geometry were taken into account. The specific activity of aqueous Cd was used to convert ^{109}Cd counts to total Cd accumulated by predators exposed to Cd in water. For predators exposed to Cd in prey, ^{109}Cd measurements in prey consumed by the predator were first converted to $^{109+112}$Cd concentrations from the specific activity of Cd in the water to which the prey had been exposed. The quantity of ^{112}Cd initially present in the prey was then added to the $^{109+112}$Cd that they accumulated in the laboratory and a new specific activity was calculated for the total Cd present in prey. This new specific activity was used to convert the ^{109}Cd counts measured in the predator to the total Cd accumulated by *S. velata* larvae from prey during our 4-day experiment.

Prior to ^{109}Cd measurements in live prey or the predator, insects were weighed and rinsed for 10 min in 0.1 mM EDTA solution to remove adsorbed Cd (Munger and Hare 1997). At the end of an experiment, each predator or its parts were placed on pieces of Teflon in a petri dish (Hare et al. 1989), frozen at –40°C, dried to constant weight in a lyophilizer, and weighed on a Mettler ME30 electronic microbalance.

Results

An increase in Cd concentrations in the surroundings of *Cryptochironomus* sp. larvae was accompanied by an increase in larval Cd concentrations (Fig. 2). Concentrations of Cd in *Cryptochironomus* sp. tended to plateau after between 2 and 3 weeks of Cd exposure, and a longer exposure period (38 days at 10 nM Cd) did not lead to further increases in prey Cd (Fig. 2). Thus, we fixed the Cd exposure time for prey to be offered to the predator at 16 days.

Cadmium accumulated by prey during their 16-day exposure in the laboratory represented from 13% (3 nM nominal Cd exposure) to 70% (30 nM nominal Cd exposure) of their initial Cd values (13 ± 1 nmol·g dry weight (dw)$^{-1}$) (mean ± SD). Initial prey Cd concentrations are low compared with those measured in *Cryptochironomus* sp. larvae from lakes exposed to emissions from metal smelters (up to 145 nmol·g dw^{-1}, L. Hare, unpublished). The modest extent of Cd increases in prey, even at the highest Cd exposure regime, suggests that the meiobenthic food used in our experiments either was not an optimal food source for *Cryptochironomus* sp. larvae or was not contaminated adequately with Cd. In either case, the importance of food as a Cd source to the predator *S. velata* may have been underestimated in our experiments.

Cryptochironomus sp. larvae exposed to Cd in water alone accumulated less Cd than those exposed to the metal in both water and food. That is, a water-only exposure to 10 nM Cd led to an net increase in prey Cd concentrations of only 1.0 ± 0.4 nmol Cd·g dw^{-1}, whereas a comparable food and water exposure resulted in an increase of 6.1 ± 1.5 nmol Cd·g dw^{-1} (means ± SD for a 7-day Cd exposure). On the basis of these measurements, we decided to expose *Cryptochironomus* sp. larvae to be offered as prey in the Cd

© 1999 NRC Canada

Fig. 2. Increases in Cd concentrations (mean ± SD) above initial values in *Cryptochironomus* sp. (prey for *S. velata*) exposed to Cd in both water and food (meiobenthos) for up to 18 days at one of three nominal Cd concentrations (3, 10, and 30 nM; open symbols). Shaded squares represent Cd concentrations in prey exposed to the metal for up to 38 days at a nominal aqueous Cd concentration of 10 nM.

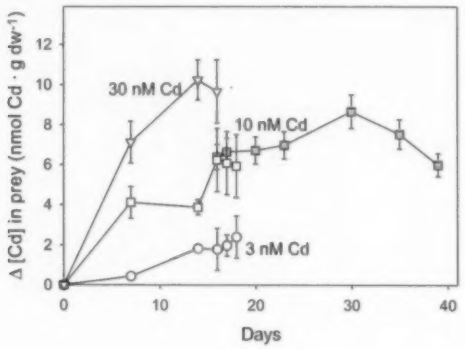

Fig. 3. Accumulation rate of Cd (mean ± SD) in *S. velata* larvae exposed to the metal for 4 days in either water (solid circles) or prey (open circles) as a function of dissolved Cd concentrations in the exposure media of either the predator or its prey, respectively. The equation for the regression line (values ± 95% CI) for Cd uptake directly from water is $y = (0.013 \pm 0.002)x + (0.03 \pm 0.03)$. Cadmium accumulation rates from food are best described by a saturation-type curve (see eq. 1).

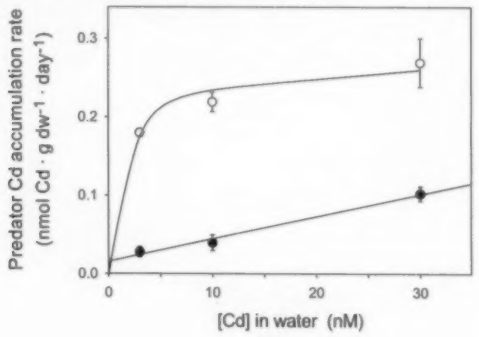

source determination experiment to Cd in both water and food, as would occur in nature.

For the same dissolved Cd concentration, *S. velata* larvae exposed to Cd via prey accumulated Cd more quickly than did those exposed to Cd via water (Fig. 3). From Fig. 3, we estimate that the Cd accumulated by *S. velata* larvae from food represented ≈80% of the estimated total Cd that this predator would have accumulated if it had been exposed to Cd in prey and water simultaneously (assuming that Cd accumulation from food and water is additive). The relationship between the Cd accumulation rate in *S. velata* and dissolved Cd concentrations was direct and linear when Cd uptake was via water (Fig. 3, solid circles; $r^2 = 0.95$, $p < 0.05$). However, the rate of Cd accumulation by the predator from food was not linearly related to Cd exposure concentrations in the water to which prey were exposed (Fig. 3, open

Fig. 4. Accumulation rate of Cd by individual *S. velata* larvae as a function of the mean total Cd concentrations in the *Cryptochironomus* sp. prey that they consumed during our 4-day experiment. The equation for the regression line (values ± 95% CI) is $y = (0.037 \pm 0.003)x + (0.1 \pm 0.1)$.

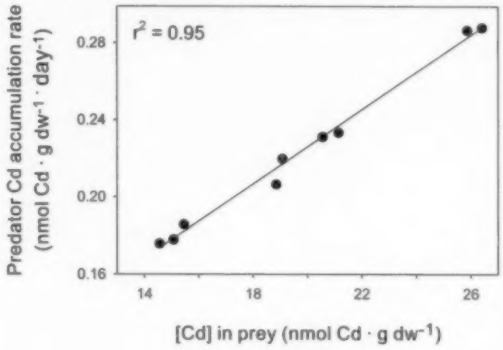

Fig. 5. Distribution of total larval weight and of the Cd accumulated during our experiment (means ± SD) between the gut tissues and remaining animal parts of *S. velata* exposed to the metal for 10 days in either water only or food only. Values in gills are not given because gills represented <5% of the total mass and their Cd concentrations were below the detection limit. Different letters indicate a significant difference ($p < 0.05$, Kruskal–Wallis Dunn's test) in the proportion of either animal weight (A and B) or Cd content (C and D) between animal parts.

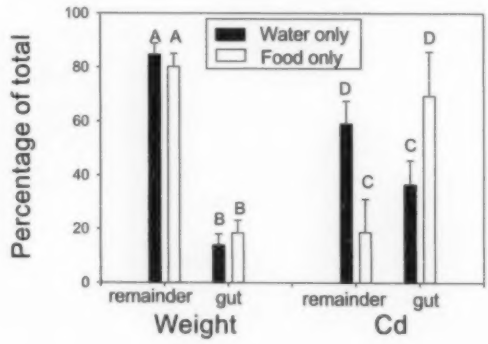

circles) and can be described by a Michaelis–Menten type equation of the form

$$(1) \quad \frac{\Delta[Cd]_{Sialis}}{\Delta t} = \frac{V_{max}[Cd]}{HSC + [Cd]}$$

where [Cd] is the dissolved Cd concentration, V_{max} (maximum uptake rate) = 0.27 nmol·g^{-1}·day^{-1}, and HSC (half saturation constant) = 1.74 nmol·L^{-1} (values of best fit determined by iteration). A model curve based on eq. 1 fits the observed data well (Fig. 3).

The mean Cd concentration of prey consumed by an individual predator (irrespective of the dissolved Cd concentration to which the prey had been exposed) was directly related to the rate at which the predator accumulated Cd dur-

© 1999 NRC Canada

Fig. 6. Increases in Cd concentrations above initial values (mean ± SD) in *S. velata* larvae exposed for 4 days to Cd in water at one of three nominal Cd concentrations (3, 10, and 30 nM). Following Cd exposure, larvae were held in Cd-free water and fed uncontaminated prey to measure Cd efflux.

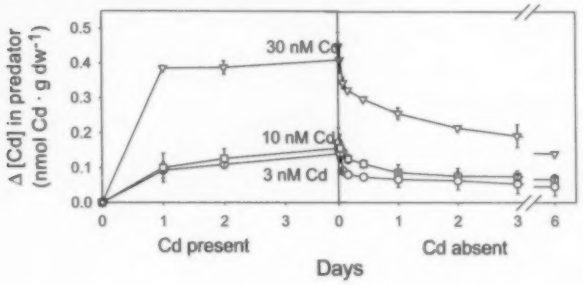

ing our experiment (Fig. 4; $r^2 = 0.95$, $p < 0.05$), which can be expressed by the following equation for a straight line:

$$(2) \qquad \frac{\Delta[\mathrm{Cd}]_{Sialis}}{\Delta t} = F[\mathrm{Cd}]_{Cryptochironomus}$$

having F as a proportionality constant equal to the value of the slope of the regression line (0.037 ± 0.003 (±95% CI), Fig. 4) and a y-intercept equal to 0 (0.1 ± 0.1 (±95% CI), Fig. 4).

Combining eqs. 1 and 2, we obtain

$$(3) \qquad [\mathrm{Cd}]_{Cryptochironomus} = \frac{S_T[\mathrm{Cd}]}{\mathrm{HSC} + [\mathrm{Cd}]}$$

where the total number of adsorption sites, S_T, equals V_{max}/F, which suggests a saturation-type relationship between prey Cd and dissolved Cd concentrations. Saturation is also suggested by the data in Fig. 2 in which a threefold increase in dissolved Cd concentrations between 10 and 30 nM is accompanied by an approximately twofold increase in prey Cd concentrations. Saturation in Cd could have occurred at the level of prey themselves or at a lower level in our experimental trophic chain, if we assume that food is the main Cd source for each consumer and that there is a direct relationship between the Cd in each consumer and the Cd in its food. The most likely level at which saturation occurred is that of the organic matter (lettuce) offered as a food source for the meiobenthos on which the *Cryptochironomus* sp. larvae fed. Because the organic matter offered to meiobenthos was not grown in a Cd-rich medium, the majority of its Cd could have been bound at surface sites that became saturated at high Cd concentrations. A saturation-type curve would probably not be observed in nature where organisms at all trophic levels would be exposed to ambient Cd during their growth.

We estimate the efficiency with which *S. velata* assimilated Cd from its food to have been 50 ± 8% (±SD, $n = 9$). Assimilation efficiencies were calculated by dividing the quantity of Cd accumulated by the predator during our experiment (after gut evacuation) by the quantity of Cd consumed as prey. This estimate is likely to represent a minimum because it ignores Cd losses from the predator during our experiment. Cadmium accumulated by *S. velata* from food was found mainly in gut tissues, whereas the remainder of the animal (animal minus gut and gills) was the site of the majority of the Cd when exposure was directly via water (Fig. 5). Cadmium concentrations in gills were below the detection limit in all samples.

Cadmium was taken up rapidly from water by *S. velata* larvae and was lost equally rapidly when larvae were placed in Cd-free water (Fig. 6). The mean ±SD biological half-life of Cd taken up from water by *S. velata* larvae at the three nominal aqueous Cd exposures was 1.4 ± 1.0 days, as estimated from an exponential equation describing Cd loss from the predator. The form of the efflux curve suggests rapid loss from a less strongly bound Cd pool and slower Cd loss from a more strongly bound Cd pool. The lack of a significant decline in the Cd concentrations of *S. velata* larvae exposed to Cd in food ($p > 0.05$, Kruskal–Wallis test) (data not shown; measurements done subsequent to gut depuration) suggests that Cd in gut tissues is tightly bound.

Discussion

Our experimental results suggest that food is a much more important source of Cd than is water for both the predator *S. velata* and its chironomid prey *Cryptochironomus* sp. The distribution pattern of Cd within *S. velata* larvae also supports the importance of food as its main Cd source in nature; larvae exposed to the metal either in nature (Hare et al. 1991) or via food only (our experiment) had the majority of their Cd in gut tissues, whereas other animal parts were the major site of Cd accumulation in larvae exposed to the metal in water only. Admittedly, assumptions about Cd uptake routes from internal distribution patterns must be made with some caution (Craig et al. 1998). The internal distribution of Cd supports a two-compartment model for Cd accumulation in *S. velata* by which the metal enters the insect via both its gut and other body regions (perhaps the gills); however, entry via the gut seems to be by far the most important route.

Food is reported to be an important source of Cd for other predatory arthropods including the caddisfly *Mystacides* (Timmermans et al. 1992), the water mite *Limnesia maculata* (Timmermans et al. 1992), and the phantom midge *C. punctipennis* (Munger and Hare 1997). The importance of food as a Cd source for this diverse group of arthropods suggests that water-only exposures to the metal would be likely to underestimate Cd bioaccumulation and toxic effects in such invertebrates (Kay 1985; Luoma 1995). For experimental studies, the importance for prey of Cd in their food underlines the necessity of ensuring that animals at lower trophic levels are exposed to Cd in both food and water before they are offered to predators (Kay 1985). Our laboratory results suggest that models designed to describe Cd movements in natural aquatic food webs should not be based solely on water as a Cd source for animals.

The efficiency with which larvae of *S. velata* assimilated Cd from prey was high (≈50%) and could be explained by the fact that these larvae swallow live prey whole, with no loss due to sloppy feeding. Furthermore, *Sialis* larvae retain prey in their gut for a long period of time (≈1 day from our observations; see also Evans and Neunzig 1996). High Cd assimilation efficiencies have also been reported for a water mite feeding on chironomid larvae (61% for *L. maculata*

© 1999 NRC Canada

feeding on *Chironomus riparius* larvae, Timmermans et al. 1992) as well as for a mysid crustacean feeding on cladocerans (72% for *Mysis relicta* feeding on *Daphnia magna*, Smokorowski et al. 1998). Although neither water mites nor mysids consume the exoskeleton of their prey (Smith and Cook 1991 and Lasenby and Fürst 1981, respectively), they would probably ingest the bulk of their prey's Cd because it is likely to be located in prey digestive tissues (Hare et al. 1991). In contrast, the caddisfly *Mystacides* is reported to assimilate Cd from chironomids with only a 5% efficiency because it eats prey piecemeal, i.e., because of its sloppy feeding habits (Timmermans et al. 1992). These estimates of assimilation efficiencies should probably be considered as values within a range for a given taxon. For example, the assimilation efficiency of Cd by *Chaoborus* larvae is reported to vary from a low of 4% for *C. punctipennis* feeding on cladocerans (Munger and Hare 1997) to a high of 50% for *Chaoborus americanus* feeding on copepods. Furthermore, assimilation efficiencies of Cd by *Chaoborus* larvae consuming a given prey type are influenced by the rate at which prey are ingested as well as ambient temperature (M.-N. Croteau and C. Munger, unpublished data).

Sialis larvae are reported to be promising candidates for use as biomonitors of Cd concentrations in lakes (Roy and Hare 1998) and would provide a benthic alternative to the mainly planktonic biomonitor *Chaoborus*. As has been shown for *Chaoborus* larvae (Hare and Tessier 1996, 1998; Croteau et al. 1998), the use of an effective biomonitor must be based on an appropriate model that relates the biomonitor's metal concentrations to those in water or sediment. Our study suggests that consideration may have to be given to Cd concentrations in the prey of *Sialis* if a simple relationship cannot be found between Cd concentrations in *Sialis* larvae and those in water or sediment.

Acknowledgments

Funding was provided by Human Resources Development Canada, the Fonds pour la Formation de Chercheurs et l'Aide à la Recherche, the Natural Sciences and Engineering Research Council of Canada, the CNTC MITE Research Network, and the U.S. Environmental Protection Agency. Comments on the manuscript were kindly provided by U. Borgmann, M.-N. Croteau, C. Munger, A. Tessier, and K.R. Timmermans. Technical assistance was furnished by M.-R. Doyon, B. Patry, and J.-P. Baillargeon.

References

Craig, A., Hare, L., Charest, P.-M., and Tessier, A. 1998. Effect of exposure regime on the internal distribution of cadmium in *Chironomus staegeri* larvae (Insecta, Diptera). Aquat. Toxicol. **41**: 265–275.

Croteau, M.-N., Hare, L., and Tessier, A. 1998. Refining and testing a trace metal biomonitor (*Chaoborus*) in highly acidic lakes. Environ. Sci. Technol. **32**: 1348–1353.

Evans, E.D., and Neunzig, H.H. 1996. Megaloptera and aquatic Neuroptera. *In* An introduction to the aquatic insects of North America. 3rd ed. *Edited by* R.W. Merritt and K.W. Cummins. Kendall/Hunt Publishing Company, Dubuque, Iowa. pp. 298–308.

Fisher, N.S., and Reinfelder, J.R. 1995. The trophic transfer of metals in marine systems. *In* Metal speciation and bioavailability in aquatic systems. *Edited by* A. Tessier and D.R. Turner. Wiley, New York. pp. 363–406.

Franzin, W.G., McFarlane, G.A., and Lutz, A. 1979. Atmospheric fallout in the vicinity of a base metal smelter at Flin Flon, Manitoba. Environ. Sci. Technol. **13**: 1513–1522.

Hare, L. 1992. Aquatic insects and trace metals: bioavailability, bioaccumulation, and toxicity. Crit. Rev. Toxicol. **22**: 327–369.

Hare, L., and Tessier, A. 1996. Predicting animal cadmium concentrations in lakes. Nature (Lond.), **380**: 430–432.

Hare, L., and Tessier, A. 1998. The aquatic insect *Chaoborus* as a biomonitor of trace metals in lakes. Limnol. Oceanogr. **43**: 1850–1859.

Hare, L., Campbell, P.G.C., Tessier, A., and Belzile, N. 1989. Gut sediment in a burrowing mayfly (Ephemeroptera, *Hexagenia limbata*): their contribution to animal trace element burdens, their removal, and the efficacy of a correction for their presence. Can. J. Fish. Aquat. Sci. **46**: 451–456.

Hare, L., Tessier, A., and Campbell, P.G.C. 1991. Trace element distributions in aquatic insects: variations among genera, elements, and lakes. Can. J. Fish. Aquat. Sci. **48**: 1481–1491.

Kay, S.H. 1985. Cadmium in aquatic food webs. Residue Rev. **96**: 13–43.

Lasenby, D.C., and Fürst, M. 1981. Feeding of *Mysis relicta* Lovén on macrozooplankton. Inst. Freshwater Res. Drottningholm Rep. **59**: 75–80.

Luoma, S.N. 1995. Prediction of metal toxicity in nature from bioassays: limitations and research needs. *In* Metal speciation and bioavailability in aquatic systems. *Edited by* A. Tessier and D.R. Turner. Wiley, New York. pp. 609–660.

Luoma, S.N., Johns, C., Fisher, N.S., Steinberg, N.A., Oremland, R.S., and Reinfelder, J.R. 1992. Determination of selenium bioavailability to a benthic bivalve from particulate and solute pathways. Environ. Sci. Technol. **26**: 485–491.

Munger, C., and Hare, L. 1997. Relative importance of water and food as cadmium sources to an aquatic insect (*Chaoborus punctipennis*): implications for predicting Cd bioaccumulation in nature. Environ. Sci. Technol. **31**: 891–895.

Pacyna, J.M., Scholtz, M.T., and Li, Y.-F.A. 1995. Global budget of trace metal sources. Environ. Rev. **3**: 145–159.

Papelis, C., Hayes, K.F., and Leckie, J.O. 1988. HYDRAQL: a program for the computation of chemical equilibrium composition of aqueous batch systems including surface complexation modeling of ion adsorption at the oxide/solution interface. Tech. Rep. 306. Department of Civil Engineering, Stanford University, Stanford, Calif.

Phillips, D.J.H., and Rainbow, P.S. 1993. Biomonitoring of trace aquatic contaminants. Elsevier, London.

Roy, I., and Hare, L. 1998. Eastward range extension in Canada of the alderfly *Sialis velata* Ross (Megaloptera; Sialidae) and the potential of the genus as a contaminant monitor. Entomol. News, **109**: 285–287.

Smith, I.M., and Cook, D.R. 1991. Water mites. *In* Ecology and classification of North American freshwater invertebrates. *Edited by* J.H. Thorp and A.P. Covich. Academic Press, New York. pp. 523–593.

Smokorowski, K.E., Lasenby, D.C., and Evans, R.D. 1998. Quantifying the uptake and release of Cd and Cu by the opossum shrimp *Mysis relicta* preying upon the cladoceran *Daphnia magna* using stable isotope tracers. Can. J. Fish. Aquat. Sci. **55**: 909–916.

Stephenson, M., and Turner, M.A. 1993. A field study of cadmium dynamics in periphyton and in *Hyalella azteca* (Crustacea: Amphipoda). Water Air Soil Pollut. **68**: 341–361.

© 1999 NRC Canada

Timmermans, K.R., Spijkerman, E., Tonkes, M., and Govers, H.A.J. 1992. Cadmium and zinc uptake by two species of aquatic freshwater invertebrate predators from dietary and aqueous sources. Can. J. Fish. Aquat. Sci. **49**: 655–662.

Verta, M., Rekolainen, S., Mannio, J., and Surma-Aho, K. 1986. The origin and level of mercury in Finnish forest lakes. Public Water Res. Inst. Natl. Board Waters Finland, **65**: 21–31.

© 1999 NRC Canada

Water quality prediction and probability network models

Kenneth H. Reckhow

Abstract: It is a common strategy in surface water quality modeling to attempt to remedy predictive inadequacies by incorporating additional mechanistic detail into the model. This approach reflects the reasonable belief that enhanced scientific understanding of basic processes can be used to improve predictive modeling. However, nature is complex, and even the most detailed simulation model is extremely simple in comparison. At some point, additional detail exceeds our ability to simulate and predict with reasonable error levels. In those situations, an attractive alternative may be to express the complex behavior probabilistically, as in statistical mechanics, for example. This viewpoint is the basis for consideration of Bayesian probability networks for surface water quality assessment and prediction. To begin this examination of Bayes nets, some simple water quality examples are used for the illustration of basic ideas. This is followed by discussion of a set of proposed probability network models for the eutrophication of the Neuse River estuary in North Carolina. The presentation concludes with consideration of applications and opportunities for Bayes nets in predictive water quality modeling.

Résumé : Dans la modélisation de la qualité des eaux de surface, on tente couramment de corriger les défauts relatifs à la prévision en incorporant de nouveaux éléments mécanistes dans le modèle. Cette approche est fondée sur la croyance suivant laquelle les progrès scientifiques concernant les processus fondamentaux peuvent être utilisés pour améliorer les modèles prédictifs. Cependant, la nature est complexe, et le modèle de simulation le plus détaillé est en comparaison infiniment plus simple. En ajoutant des détails, il arrive un point où l'on ne peut plus simuler et prévoir avec des niveaux d'erreur raisonnables. Dans de telles situations, il peut être attrayant d'exprimer le comportement complexe d'un système en termes probabilistes, comme en mécanique statistique, par exemple. On s'est inspiré de cette approche pour appliquer des réseaux bayesiens de probabilité à l'évaluation et à la prévision de la qualité des eaux de surface. Pour commencer cet examen des réseaux bayesiens, on utilise des exemples simples relatifs à la qualité des eaux pour illustrer les idées de base. On examine ensuite un ensemble de modèles de réseau de probabilité pour l'eutrophisation de l'estuaire du Neuse, en Caroline du Nord. On termine en considérant les applications et les possibilités des réseaux bayesiens dans la modélisation prédictive de la qualité des eaux.

[Traduit par la Rédaction]

Nature of useful predictive science in support of water quality management

In an ideal world, decision makers would have access to perfect predictions of the impacts of their actions at any spatial/temporal scale and any level of substantive detail. In the real world, scientific predictions are uncertain, and resources are limited. In an ideal world, decision makers would have the time and inclination to acquire perfect knowledge of outcomes. In the real world, decisions are made with limited time for understanding.

In water quality modeling, one approach to the dilemma of limited resources and limited knowledge is to build predictive models that characterize as much of this knowledge, or mechanism, as possible and then depend heavily on these models for decision. Unfortunately, experience indicates that this strategy results in models with high forecast uncertainty. An alternative strategy is to build simple models that do not tax either resources or scientific understanding. Unfortunately, these models may not directly address the problem of concern. This dilemma provides the rationale for the study presented in this paper, which is an examination of the usefulness of probability (or Bayesian) networks for water quality modeling.

Received April 30, 1998. Accepted February 16, 1999.
J14565

K.H. Reckhow. UNC Water Resources Research Institute, North Carolina State University, Raleigh, NC 27695, U.S.A., and Nicholas School of the Environment, Duke University, Durham, NC 27708, U.S.A. e-mail: ken_reckhow@ncsu.edu

Mechanistic models and prediction

The premise in support of the use and development of mechanistic water quality simulation models is that the most accurate and flexible forecasts result from a model that correctly describes detailed processes. These models are accurate (it is believed) because the models are assumed to correctly characterize processes, and they are flexible because detail-rich forecasts can always be aggregated over space/time (but not vice versa) if necessary. The need to forecast implies that extrapolation beyond the bounds of observation may be necessary, and this is believed to be reliable only if mechanisms are correctly characterized.

Mechanistic advection–diffusion–reaction (transport–fate–effects) models are typically large in order to simulate processes. Despite this, they are still quite simple in the description of complex chemical and biological processes, relative to the real world. For example, in these models, virtually all

© 1999 NRC Canada

chemical reactions are assumed to be first order, and one or at most a few species of organisms are modeled at each level of the food chain. Small-scale temporal and spatial resolution gives the illusion of substantial knowledge.

In fact, it is not complexity in model description that leads to prediction accuracy; rather, it is the underlying scientific knowledge and observational evidence that provide the basis for accurate prediction. Unfortunately, current practice suggests that knowledge and observation may support accurate prediction at only a very gross level of detail. For example, the prediction from a simple model for annual average total nitrogen concentration in a water body may have less information but also may have less predictive uncertainty than that for a large model of daily concentrations of organic and inorganic forms of nitrogen. Simply stated, when less detail is required in a predictive model, the resultant forecast is likely to be less uncertain. In other words, given fixed scientific knowledge, prediction of mean annual chlorophyll *a* concentration in a lake should be more precise than prediction of the maximum chlorophyll *a* on July 4 in the public beach swimming area.

Why is this conclusion generally true? In basic terms, accurate prediction of aquatic ecosystem behavior in small regions of time (e.g., 15-min or 1-day intervals) and space (e.g., a small embayment of a water body) requires scientific understanding, observational evidence, and mathematical descriptions that far exceed current practice.

In natural aquatic systems, we know which chemical reactions can take place, but the rate of reaction is difficult to predict. For example, reaction rates are highly temperature dependent, and temperature varies considerably in space and time. The conventional temperature adjustment expression for mathematical models is approximate; this fact, coupled with space/time temperature variability, can lead to an exploding forecast error over time.

In addition, models of aquatic ecosystems typically have one phytoplankton compartment, two zooplankton compartments, and no fish. Even for those larger models that include a few additional compartments, the number of distinct species at each level of the food chain model is far below that in real aquatic systems. Here, the limited species variability in the model means that no one would confuse the extreme simplicity in the descriptive mathematics with the species complexity of the real world.

Beyond that, most model parameters (e.g., reaction rates, feeding preferences, settling velocities) are not measured in situ. Instead, they are typically selected from the model users manual (e.g., Bicknell et al. 1993) or a tabulation of model coefficients (e.g., Bowie et al. 1985); these tabulated values sometimes reflect very little actual observational or experimental evidence (see Reckhow 1994). The selected parameters are sometimes adjusted from the initial value to improve model fit. This ad hoc task of "parameter tuning" is often the only "contribution" from the aquatic system being modeled to the determination of model parameters.

The conclusion concerning poor prediction accuracy in large water quality models reflects the results of error propagation studies (e.g., Di Toro and van Straten 1979; Scavia et al. 1981; Beck and Halfon 1991) and prediction/observation comparisons in a reasonable verification exercise (see graphs in Chapra and Reckhow 1983, chap. 16). Note that this conclusion is not consistent with some model calibration studies reported in the literature. However, it must be pointed out that calibration, involving the selection of many parameters in a large model, provides an opportunity for the modeler to "tune" the parameters so that model predictions closely match observations. Of primary interest should be how the model performs on a substantially different data set (verification data), and unfortunately, these assessments are extremely rare.

Indeed, since a primary objective in the application of these models is prediction, one should reasonably expect that users manuals (e.g., Ambrose et al. 1988; Bicknell et al. 1993) and textbooks (e.g., Chapra and Reckhow 1983; Thomann and Mueller 1987) would be filled with examples (graphs and statistics) illustrating prediction success. In fact, there is little evidence presented in these references demonstrating that the models discussed have been rigorously verified, and there is no complete error propagation assessment presented in these references for any of the mechanistic models.

Simulation models for the management of natural systems will never replicate the complexity in nature. That statement is obvious. Less clear is the conclusion that the prudent environmental modeling strategy is often to avoid detailed mathematical characterization of natural processes for models used in policy analysis. This recommendation, from those who have studied environmental simulation and policy (e.g., Mar 1974; Freedman et al. 1983; Morgan and Walters 1986; Hodges 1987; Henrion 1990), is based on the observation that the most useful predictive models are often extremely simple. As Levin (1985) concluded in his assessment of ecological models, "Overly detailed models are useless as predictive devices, and techniques for aggregation and simplification are essential".

Most decision makers are interested in models not because they replicate detailed environmental processes, but because they want techniques that are credible, reliable, and provide useful answers to questions. The questions of interest to decision makers broadly concern the relationship between a management option and an attribute of concern to the public. For example, will the frequency (probability) of fishkills in the Neuse River estuary in North Carolina be reduced to a tolerable level by forested buffers and nitrogen removal at wastewater treatment plants?

Complex environmental simulation models are not essential to answer questions of that nature, as there is too much unpredictability in nature to mathematically describe all of the mechanisms affecting fish survival in natural waters. An alternative approach has been employed by the physicist who uses probabilistic expressions to capture the aggregate response of molecular motion in statistical mechanics. In a similar manner, the water quality modeler could summarize small-scale processes with probabilistic expressions that characterize the aggregate response of interest to the decision maker.

For example, application of a useful environmental policy model might yield the following statement: "if nitrogen loading to the Neuse River is reduced by 40% or more, the probability of a major fishkill in a given year is less than 0.25" or "if nitrogen loading to the Neuse River is reduced by 40% or more and June–August streamflow does not drop

© 1999 NRC Canada

Fig. 1. Schematic of a multispecies phosphorus model (modified from Chapra and Reckhow 1983).

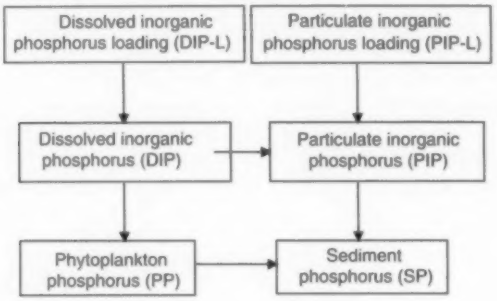
Dissolved inorganic phosphorus loading (DIP-L)
Particulate inorganic phosphorus loading (PIP-L)
Dissolved inorganic phosphorus (DIP)
Particulate inorganic phosphorus (PIP)
Phytoplankton phosphorus (PP)
Sediment phosphorus (SP)

below 500 ft^3/s (152.4 m^3/s) for a 1-week period, then the probability of a major fishkill in a given year is less than 0.15". Generally speaking, most decision makers want reliable, low-cost solutions. In other words, decision makers are likely to be concerned about cost and about being wrong (prediction error).

These observations about models and prediction reflect a decision analytic perspective (Clemen 1996) and lead to consideration of influence diagrams (Marshall and Oliver 1995) and probability network models for the evaluation and presentation of scientific relationships for policy analysis. Probability network models, or Bayes nets (Lauritzen and Spiegelhalter 1988; Pearl 1990; Jensen 1996), may be used to express uncertain, complex associations among variables using probability analysis. Models can be as simple or as complex as scientific judgment and data allow, provided that uncertainties are adequately represented probabilistically.

Probability (inference) networks

It is common modeling practice to develop a flow diagram consisting of "boxes and arrows" to describe relationships among key variables in an aquatic ecosystem and use this diagram as a device to guide model development and explanation. A simple example is given in Fig. 1 (modified from Chapra and Reckhow 1983, p. 311) for phosphorus species in eutrophication.

The probability modeling approach of interest here typically begins with a diagram like that in Fig. 1, with the requirement that presence (absence) of an arrow connecting two boxes specifies conditional dependence (independence). To fix ideas on this concept, consider the relationships implied by the presence or absence of arrows in Fig. 1. The connecting arrow pointing from dissolved inorganic phosphorus loading (DIP-L) to dissolved inorganic phosphorus (DIP) expresses the fact that DIP-L is the sole determinant or "parent" of DIP. In a similar manner, DIP is represented as the sole parent of phytoplankton phosphorus (PP). Likewise, particulate inorganic phosphorus (PIP) has two parents (DIP and PIP-L), and sediment phosphorus (SP) also has two parents (PIP and PP).

It is important to recognize that conditional independence is not the same as complete independence, a feature that is likely to be quite rare in systems of interest (Matzkevich and Abramson 1995). For example, limnological knowledge suggests that the variables in Fig. 1 are likely to be interrelated or interdependent. However, the arrows in Fig. 1 indicate that conditional on DIP, PP is independent of all other variables. This means that once DIP is known, knowledge of other variables does not change the probability for PP (p(PP)).

The usefulness of these dependence/independence relationships is apparent when we consider the joint probability for the variables displayed in Fig. 1 while initially ignoring the independencies conveyed in the diagram. The chain rule may be used to calculate a joint probability for a system of variables. According to the chain rule, this joint probability is

$$\begin{aligned}(1)\quad & p(\text{DIP-L,PIP-L,DIP,PIP,PP,SP}) \\ &= p(\text{DIP-L})p(\text{PIP-L}|\text{DIP-L}) \\ &\quad \times p(\text{DIP}|\text{DIP-L,PIP-L}) \\ &\quad \times p(\text{PIP}|\text{DIP-L,PIP-L,DIP}) \\ &\quad \times p(\text{PP}|\text{DIP-L,PIP-L,DIP,PIP}) \\ &\quad \times p(\text{SP}|\text{DIP-L,PIP-L,DIP,PIP,PP})\end{aligned}$$

where $p(x|y)$ is read as the "probability of x conditional on, or given, y". The joint probability, p(DIP-L,PIP-L,DIP,PIP, PP,SP), contains all the information available on these six variables.

In principal, the joint probability in eq. 1 is sufficient for any analysis, but is this of practical value? Probably not, since as Pearl (1990) noted, most people do not think in terms of large, multiple-variable joint distributions. Instead, human reasoning typically occurs on a marginal or conditional basis, focused on only one or two variables at a time. In addition, most scientific analyses concern the probability of a single variable as the principal quantity of interest (often conditioned on one or more controlled or assumed levels of other factors). This is true for the example above, where the most interesting probability is likely to be the probability associated with the phytoplankton (PP) variable.

To determine the probability p(PP), it seems from eq. 1 that we need to define the joint distribution and then solve for the quantity of interest, which in this case appears to be p(PP|DIP-L,PIP-L DIP,PIP). This is not a simple task, and it becomes more difficult as the number of variables in a system increases. Fortunately, thanks to conditional independence, the relationships conveyed in Fig. 1 indicate that PP is dependent only on DIP. This conclusion comes directly from the interpretation of the graphical model and the presence/absence of arrows defining the dependence/independence relationships. Thus the probability model for PP may be written by modifying eq. 1 to express these conditional independence relationships:

$$\begin{aligned}(2)\quad & p(\text{DIP-L,PIP-L,DIP,PIP,PP,SP}) \\ &= p(\text{DIP-L})p(\text{PIP-L})p(\text{DIP}|\text{DIP-L}) \\ &\quad \times p(\text{PIP}|\text{PIP-L,DIP})p(\text{PP}|\text{DIP})p(\text{SP}|\text{PP,PIP}).\end{aligned}$$

To apply this model, the probabilities must be estimated, typically using expert judgment and (or) scientific data.

Diagrams similar to Fig. 1 have been used for years in applied statistics, associated with path analysis, structural equations, and causal models. Recently, interest in these

© 1999 NRC Canada

Fig. 2. Probability network model for the Neuse River estuary. Probabilities adjacent to the ovals and diamond are hypothetical examples. NR, nitrogen load reduction; MMS, March–May daily streamflow at Kinston; JAS, June–August daily streamflow at Kinston; TN, total nitrogen concentration.

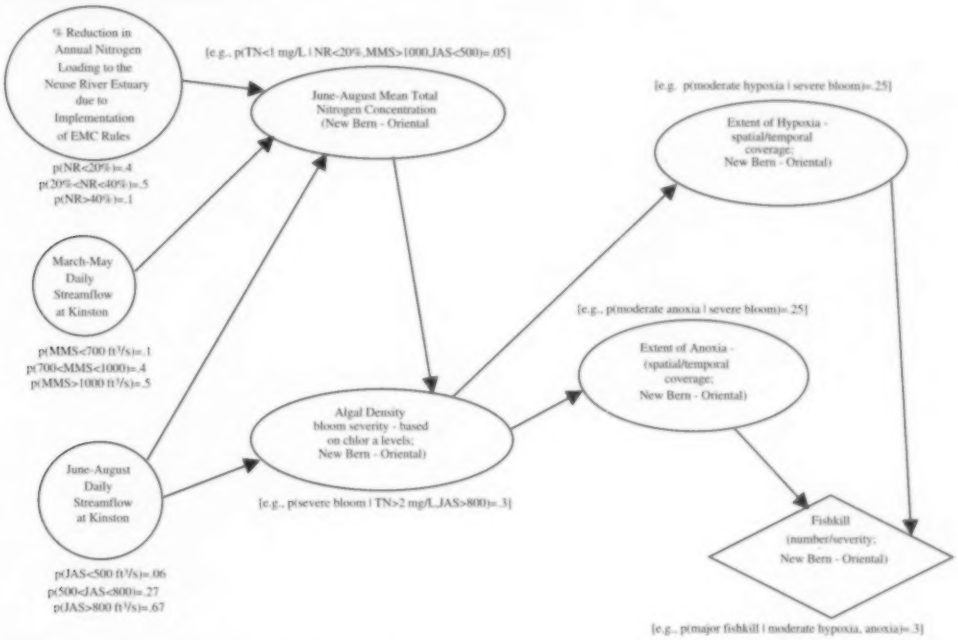
% Reduction in Annual Nitrogen Loading to the Neuse River Estuary due to Implementation of EMC Rules
p(NR<20%)=.4
p(20%<NR<40%)=.5
p(NR>40%)=.1
[e.g., p(TN<1 mg/L | NR<20%,MMS>1000,JAS<500)=.05]
June-August Mean Total Nitrogen Concentration (New Bern - Oriental
March-May Daily Streamflow at Kinston
p(MMS<700 ft³/s)=.1
p(700<MMS<1000)=.4
p(MMS>1000 ft³/s)=.5
June-August Daily Streamflow at Kinston
p(JAS<500 ft³/s)=.06
p(500<JAS<800)=.27
p(JAS>800 ft³/s)=.67
Algal Density bloom severity - based on chlor a levels; New Bern - Oriental)
[e.g., p(severe bloom | TN>2 mg/L,JAS>800)=.3]
[e.g. p(moderate hypoxia | severe bloom)=.25]
Extent of Hypoxia - spatial/temporal coverage; New Bern - Oriental)
[e.g., p(moderate anoxia | severe bloom)=.25]
Extent of Anoxia - (spatial/temporal coverage; New Bern - Oriental)
Fishkill (number/severity; New Bern - Oriental)
[e.g., p(major fishkill | moderate hypoxia, anoxia)=.3]

"graphical models" (Whittaker 1990) has increased as it has become recognized that the conditional independence implied by the omission of connecting arrows may be exploited to reduce information needs and simplify probability modeling. This, in part, has sparked developments in the emerging area of "Bayesian probability networks" or "Bayes nets", which uses the graphical model as an expression by the scientific expert of the functional dependencies (and independencies) for the system of interest, and then data and expert judgment are used to probabilistically quantify all linkages. A closely related area concerns chains of reasoning (Schum 1994; Kadane and Schum 1996), which employ often very detailed models of linkages and dependencies to assess evidence in legal studies. With that background in mind, consider next how Bayes nets might be applied to probabilistic prediction of eutrophication in the Neuse River in North Carolina.

Probabilistic model for policy analysis

The most effective way to explore the nature of a probability-based model to guide decisions on Neuse River eutrophication is to work with examples. Figure 2 displays an initial example to help fix ideas, using notation associated with influence diagrams. In the graphical model in Fig. 2, oval nodes represent uncertain events and diamond nodes represent uncertain attributes. Note that this model provides a probabilistic and predictive link between a management action ("percent reduction in annual nitrogen loading due to implementation of EMC rules") proposed by the North Carolina Environmental Management Commission (EMC) and an important estuarine response ("fishkills").

The input to the model in Fig. 2 reflects a decision or management action (here, the EMC decision) expressed in terms of a predicted reduction in nitrogen loading. This nitrogen loading assessment may result from a direct probabilistic assessment by an expert or from an application of a detailed model like HSP-F (Bicknell et al. 1993). Both of these are unlikely; the direct probability assessment is far too complex for a single scientific judgment, while complete uncertainty analyses are not currently feasible for large mechanistic models such as HSP-F. A more likely source of this assessment is a pollutant loading function (Haith and Shoemaker 1987; Dodd and Tippett 1994) analysis linked to a simple river model characterizing transport and loss. Figure 3 displays a probability network model that might be used to summarize that analysis. In essence, Fig. 3 is an expansion of the single element in the upper left of Fig. 2. In principle, any expansion or level of detail may be captured in a probability network model; in practice, the level of detail is likely to be quite constrained by the requirement that uncertainties must be estimated for all relationships.

Where do the numbers come from in Fig. 3? Any proposed management plan (e.g., the proposed EMC plan) will contain requirements/assumptions on point source controls, land use restrictions, best management practices, and background or uncontrolled sources. For example, the proposed EMC rules for large wastewater treatment plants require optimization for nitrogen removal. In addition, new point sources must reduce nitrogen in the discharge to 3.5 mg/L, so that collectively, these point source rules achieve 30% overall point source reduction. Predictive modeling and (or) expert judgment can be used in conjunction with plant-specific information to yield a prediction of the overall flow-

© 1999 NRC Canada

Fig. 3. Nitrogen loading model. Probabilities adjacent to the ovals and diamond are hypothetical examples. N_{WWT}, wastewater nitrogen concentration; New Dev N, nitrogen loading from new urban development; Agr N Red, percent reduction in nitrogen loading from agricultural runoff; Atm N, percent total nitrogen loading from atmospheric deposition.

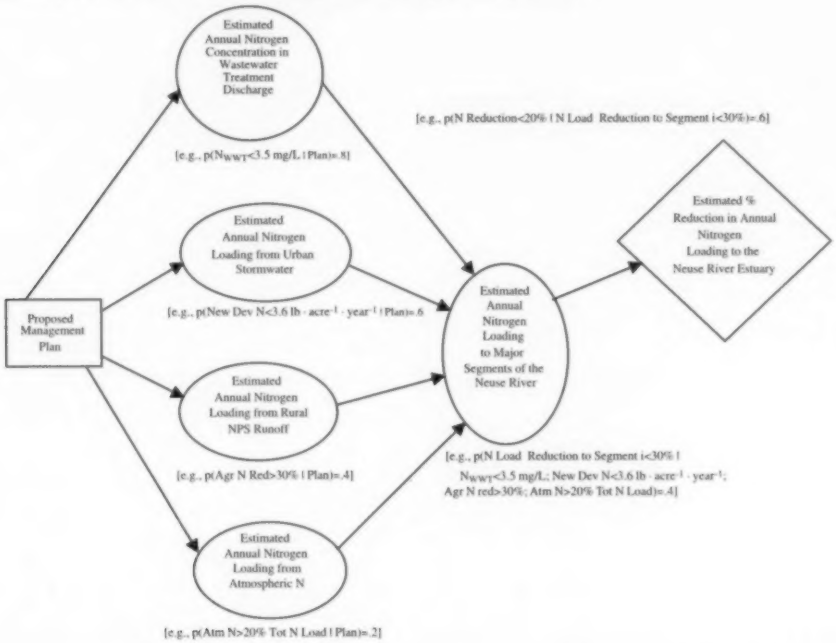
Estimated Annual Nitrogen Concentration in Wastewater Treatment Discharge
[e.g., p(N_WWT<3.5 mg/L | Plan)=.8]
[e.g., p(N Reduction<20% | N Load Reduction to Segment i<30%)=.6]
Estimated % Reduction in Annual Nitrogen Loading to the Neuse River Estuary
Estimated Annual Nitrogen Loading from Urban Stormwater
[e.g., p(New Dev N<3.6 lb · acre⁻¹ · year⁻¹ | Plan)=.6
Proposed Management Plan
Estimated Annual Nitrogen Loading to Major Segments of the Neuse River
Estimated Annual Nitrogen Loading from Rural NPS Runoff
[e.g., p(Agr N Red>30% | Plan)=.4]
[e.g., p(N Load Reduction to Segment i<30% | N_WWT<3.5 mg/L; New Dev N<3.6 lb · acre⁻¹ · year⁻¹; Agr N red>30%; Atm N>20% Tot N Load)=.4]
Estimated Annual Nitrogen Loading from Atmospheric N
[e.g., p(Atm N>20% Tot N Load | Plan)=.2]

weighted nitrogen concentration. Uncertainty analysis applied to this predictive assessment can then be used to estimate the probability that any particular concentration goal can be achieved; in this case, the probability that the weighted average discharge concentration will be less than 3.5 mg/L is represented in Fig. 3.

A predictive model, such as the nutrient loading function model, can be used to estimate the total nitrogen loading to each segment of the Neuse River. Using uncertainty analysis, this is to be expressed probabilistically as shown in Fig. 3. Finally, a river transport/transformation model is needed to yield the final response in Fig. 3: the probability that the reduction in nitrogen loading to the Neuse River estuary will achieve a specified goal.

Note that all except the initial probabilities (characterizing the initial forcing functions) are conditional. This "conditional dependence" feature is an important aspect of a probability network model, as it reflects the associations, or dependencies, that are assumed among the variables. For example, in Fig. 2 the probability of a major fishkill is conditional on hypoxia and anoxia, hypoxia and anoxia are expressed as dependent on algal density, and so on. Thus, fishkills are dependent on algal density, but only through the effect of algal density on hypoxia and anoxia.

In summary, the schematics in Figs. 2 and 3 display the key dependencies or linkages. These models can have more or less detail, provided that uncertainty analysis is possible. To illustrate this, the nitrogen input box (or node) from Fig. 2 was expanded into a loading model in Fig. 3; expansions of a similar nature are likely as this model is implemented for the algae–oxygen–fishkills relationships in the estuary. Finally, note that for these probability network models, uncertainties are expressed probabilistically and outcomes are expressed as discrete levels (e.g., less than or greater than 3.5 mg/L) to facilitate computation and explanation for decision makers and the public.

Example

To fix ideas on possible expansion of a probability network model for nitrogen enrichment and algal blooms in the Neuse River, Fig. 4 presents a general graphical model for this analysis. The relationships in Fig. 4 reflect current scientific thinking on associations and, in many cases, on cause and effect. To operationalize this model and make it useful, metrics are needed for each variable. For example, (*i*) what is the space/time scale for "dissolved oxygen concentration"? and (*ii*) what is the categorization scheme for "dominant algal species"? Beyond that, scientific knowledge, available data, and management information needs may allow or require additional features to enhance the usefulness of the model; for example, the nitrogen compartment might be expanded to nitrate, ammonium, and organic nitrogen or a zooplankton compartment might be added.

To examine possible applications, the graphical model in Fig. 4 is simplified and modified slightly to that in Fig. 5. This model is also in need of greater specificity (e.g., what is the metric for each variable?), but it nonetheless does provide a convenient device to present some of the key relationships.

To apply the model in Fig. 5, probabilities must be estimated for all relationships. The initial forcing functions

© 1999 NRC Canada

Fig. 4. Graphical model for eutrophication in the Neuse River.

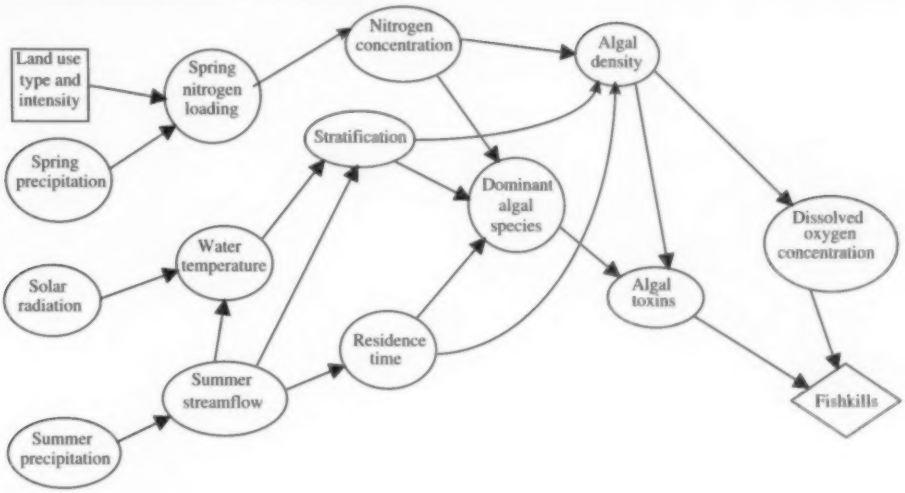

Fig. 5. Simplified alternative graphical model for eutrophication in the Neuse River.

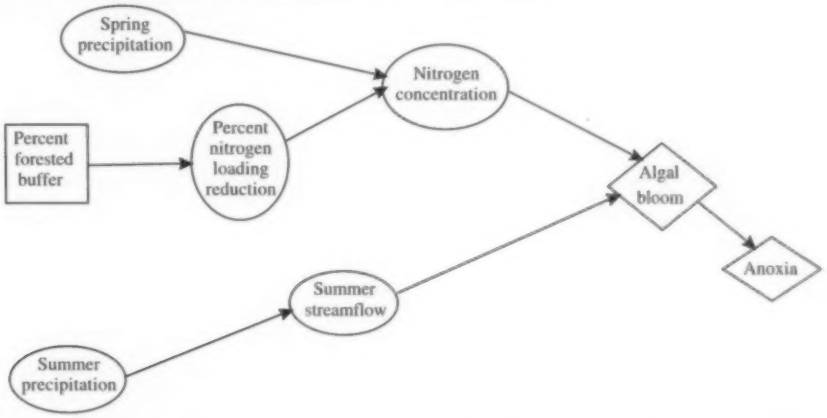

Table 1. Marginal probabilities for spring and summer precipitation and % forested buffer.

Spring and summer precipitation	
Below average	0.33
Average	0.34
Above average	0.33
% forested buffer	
70–80	0.2
80–95	0.6
95–100	0.2

"spring precipitation" and "summer precipitation" are expressed as marginal probabilities that can be easily assessed from statistics on historic precipitation data in the watershed. For this model, the distributions for spring and summer data were simply segmented into three equally likely precipitation ranges (below average, average, above average). In addition, the probabilities for "percent forested buffer" reflect a judgmental assessment of the total perennial stream miles in the Neuse River watershed that would be required to have a maintained minimum width buffer, based on the projected outcome of proposed management plans. The resultant marginal probability estimates are given in Table 1.

Next, conditional probabilities were assessed for the three intermediate variables and reported in Table 2. In the model, the "percent nitrogen load reduction" is conditional on only the percent forested buffer, so a scientific expert can be consulted for a probabilistic statement reflecting the expected reduction in total nitrogen loading due to buffers alone. The "total nitrogen concentration" is expressed in Fig. 5 as a function of spring precipitation and nitrogen load reduction; in the absence of data to fit a statistical model for these variables, the conditional probabilities for total nitrogen concentration were based on scientific judgment. Finally, the relationship between summer precipitation and "summer streamflow" could be based on a statistical model developed from precipitation and streamflow data; here, too, judgment was the basis for the probabilities reported in Table 2.

The conditional probabilities for the response variable "al-

© 1999 NRC Canada

Table 2. Conditional probabilities for intermediate variables % N load reduction, TN concentration, and summer streamflow.

	% forested buffer								
% N load reduction	70–80			80–95			95–100		
<5	0.95			0.2			0		
5–15	0.05			0.6			0.05		
>15	0			0.2			0.95		
	Spring precipitation								
	<5% N load reduction			5–15% N load reduction			>15% N load reduction		
TN concentration (mg/L)	Below average	Average	Above average	Below average	Average	Above average	Below average	Average	Above average
<1.4	0.6	0.3	0.2	0.45	0.28	0.27	0.8	0.75	0.7
1.4–1.7	0.3	0.4	0.3	0.28	0.45	0.28	0.1	0.15	0.2
>1.7	0.1	0.3	0.5	0.27	0.27	0.45	0.1	0.1	0.1
	Summer precipitation								
Summer streamflow (ft^3/s)	Below average			Average			Above average		
<500	0.5			0.15			0.15		
500–800	0.35			0.7			0.35		
>800	0.15			0.15			0.5		

Table 3. Conditional probabilities for response variables algal bloom and anoxia.

	Summer flow (ft^3/s)								
	TN < 1.4 mg/L			1.4 mg/L < TN < 1.7 mg/L			TN > 1.7 mg/L		
Algal bloom	<500	500–800	>800	<500	500–800	>800	<500	500–800	>800
None	0.1	0.35	0.9	0	0.2	0.8	0	0.1	0.7
Slight	0.35	0.3	0.1	0.3	0.35	0.2	0.1	0.2	0.3
Moderate	0.35	0.25	0	0.4	0.25	0	0.3	0.3	0
Severe	0.2	0.1	0	0.3	0.2	0	0.6	0.4	0
	Algal bloom								
Anoxia	None			Slight			Moderate		Severe
Anoxia	0.1			0.2			0.4		0.7
No anoxia	0.9			0.8			0.6		0.3

gal bloom" were based in part on scientific judgment (for the effect of nitrogen concentration) and in part on the interpretation of chlorophyll *a* versus flow data presented in fig. 3 in Christian et al. (1986). Using the data in Christian et al. (1986), the chlorophyll levels were grouped into algal bloom categories, and the flow data were grouped into flow categories. The relative frequency of data points in each algal bloom/flow group determined the initial probabilities; these probabilities were further decomposed, using judgment, to account for the effect of total nitrogen concentration. The conditional probabilities for "anoxia" were based on judgment. These response variable conditional probabilities are presented in Table 3.

For this example, the probabilities in Tables 1–3 can be combined into a joint probability on all variables (as in eq. 2), which then allows us to solve for a number of interesting quantities. While all marginal and conditional probabilities can be easily calculated using the estimates in Tables 1–3, computation in larger problems is facilitated with Bayes nets software (e.g., Hugin; see Jensen 1996).

From the probabilities expressed in Tables 1–3, the simple (or marginal) probability of anoxia is 0.30; in Bayesian terms, this calculation reflects only prior probabilities. If the implemented management option could assure that at least 95% of the streams had the required buffer (p(95–100% forested buffer) = 1.0), then the anoxia probability drops slightly to 0.27. This calculation, although hypothetical, is indicative of the types of policy-related questions that can be addressed with a complete probability network model.

As another example, the baseline case in Tables 1–3 yields

$$p(\text{severe algal bloom}) = 0.18.$$

In this example, we can make the Bayes net more useful by combining the prior probabilities in the network with new (sample) information to produce a posterior probability, using Bayes Theorem. For example, if spring precipitation is observed to be above average, then the (conditional) probability becomes

$$p(\text{severe algal bloom}|\text{above-average spring precipitation}) = 0.21.$$

If, instead, summer streamflow is extremely low (<500 ft^3/s), then:

$$p(\text{severe algal bloom}|\text{summer flow} < 500\ ft^3/s) = 0.33.$$

Both events together yield

© 1999 NRC Canada

$$p(\text{severe algal bloom} \mid \text{above-average spring precipitation, summer flow} < 500\ \text{ft}^3/\text{s}) = 0.37.$$

These types of "what if" probabilistic calculations are relatively quick and easy, even with a much larger and more realistic probability network model. In addition, since Bayes Theorem allows the new observational information to be combined with the prior probabilities, as more observational information is incorporated into the analysis, the often-subjective prior is dominated by the newer data-based sample evidence.

Outcomes expressed as probabilities are an acknowledgment of the lack of precision in predictive models. The probabilities, and relative change in probabilities between scenarios, give decision makers and stakeholders an explicit characterization of risk. For example, is the probability of a severe algal bloom of 0.37 unacceptably high? If a management action could reduce this probability from 0.37 to 0.20, is that worthwhile, given the costs and changes in other attributes? Questions like these are of interest to stakeholders and can be examined using probability network models.

Estimation and elicitation of probabilities

The example discussed above suggests that the primary sources of the information used to characterize probabilities are (*i*) observational/experimental evidence or data and (*ii*) expert scientific judgment. In conventional modeling studies, observational information that is based on precise measurements of the variable or relationship of interest is likely to be the least controversial and most useful information. Experimental evidence may also be useful, but legitimate questions may arise for some experimental setups concerning the applicability of this evidence to the natural, uncontrolled ecosystem. Finally, expert judgment is an essential source of information for most models, but it is also the information source "of last resort" due to its perceived lack of reliability.

It is an unfortunate but common fact that observational data for parameterization of water quality models are almost always woefully inadequate for the task. As a consequence, experimental evidence is sometimes used, but primarily the gap is filled with judgmental parameter selection. This fact has been "institutionalized" through the publication of tabulations of model reaction rates (e.g., Bowie et al. 1985); these tables are routinely used by modelers for judgmental selection of many or most parameters in mechanistic water quality simulation models.

Scientific knowledge or judgment, of course, is the basis for the functional relationships that form the equations in the model. That fact, coupled with the routine use of scientific judgment for model parameter selection, should result in easy acceptance of judgmental (subjective) probabilities. This remains to be shown, as it may not be the "judgment" aspect but rather the "probability" aspect that hinders acceptance among water quality modelers.

Fortunately, there are some well-established techniques (see von Winterfeldt and Edwards 1986; Cooke 1991; Meyer and Booker 1991) for eliciting probabilities. Unfortunately, there is a great deal of evidence that people are not, in general, particularly good in making judgments under uncertainty. Evidence suggests that scientists are better in judgmentally characterizing scientific knowledge in their fields of expertise, but good probability elicitation technique is helpful to insure success.

Discussion and conclusions

What should be the basis for selection of a predictive model? Few will argue against the viewpoint that a model should be as simple as possible. However, it is also true that few will argue against the viewpoint that a model should be as accurate as possible, and it is likely that few will argue against the viewpoint that a model should correctly characterize processes. Unfortunately, these desirable features for models are often in conflict with one another.

In this study, a probability network model is recommended as a predictive model to guide Neuse River decision making because uncertainty, or accuracy, is believed to be an essential attribute for a predictive model. Does this mean that we can ignore correct process description and focus on probabilities? No! At the same time, we should not be trapped in the view that there is only one true process model, and it is CE-QUAL-W2 (Cole and Buchak 1995), or WASP (Ambrose et al. 1988), or....

All of the graphical models presented in this paper characterize processes at some level of detail. Mechanistic models, such as CE-QUAL-W2, provide process description, but this description is far from complete. Consider the variety of species of fish, zooplankton, and phytoplankton in a normal aquatic ecosystem, consider the importance of their role, and then consider the fact that aquatic ecosystem models have few (often one) species of phytoplankton and zooplankton and usually no fish species.

It is important to recognize that any process model can be easily incorporated into a probability network model if the accuracy of the mathematical process description can be quantified and is acceptable. For example, any (or all) of the mechanistic process descriptions in CE-QUAL-W2 can be represented in a probability network model *if* all relationships are expressed probabilistically. For this to happen, of course, a complete uncertainty analysis must be undertaken for the CE-QUAL-W2 process descriptions.

At this point, it seems likely that the complexities of error analysis for mechanistic models such as CE-QUAL-W2 will prevent inclusion of models of that nature into a probability network. This should not weaken a study like the Neuse River eutrophication analysis, as there is a distinct, useful role for mechanistic models. CE-QUAL-W2 is a large, relatively detailed research model that approximates process descriptions. As a consequence, CE-QUAL-W2 can be used to present and assess scientific hypotheses and relationships and therefore augment scientific judgment. Beyond that, it can be used for predictive assessment to augment or support policy evaluation undertaken using a probability network model.

However, given the large prediction errors inherent in mechanistic eutrophication models, and given the absence of a thorough prediction uncertainty analysis, the risks associated with policy guidance supported alone by a model like CE-QUAL-W2 may be large. Further, the expertise and time required to run the model make it less suitable for policy

© 1999 NRC Canada

evaluation and communication than is a probability network model that has less detail and structure due to the requirement of a complete uncertainty analysis.

A carefully devised and calibrated probability network model is ideally designed to communicate at the interface between scientists, stakeholders, and decision makers. The graphical model provides a description of relationships so that stakeholders and decision makers can easily grasp the nature of the model. Scenarios can be run quickly so that the implications of a range of options are rapidly understood. The probabilities of various outcomes can be described in a relative sense; this gives the stakeholders and decision makers a realistic appraisal of the chances of achieving desirable goals. We know that scientific assessment and prediction are far from certain. By acknowledging the sometimes-substantial uncertainty in model predictions, we enhance, rather than diminish, the value of predictive modeling by focusing on the ability of the model to estimate risk.

References

Ambrose, R.B., Jr., Wool, T.A., Connolly, J.P., and Schanz, R.W. 1988. WASP4, a hydrodynamic and water quality model — model theory, user's manual, and programmer's guide. U.S. Environmental Protection Agency, Environmental Research Laboratory, Office of Research and Development, Athens, Ga. EPA/600/3-87/039.

Beck, M.B., and Halfon, E. 1991. Uncertainty, identifiability, and the propagation of prediction errors: a case study of Lake Ontario. J. Forecasting, **10**: 135–161.

Bicknell, B.R., Imhoff, J.C., Kittle, J.L., Jr., Donigian, A.S., Jr., and Johanson, R.C. 1993. Hydrologic simulation program — FORTRAN. User's manual for release 10. U.S. Environmental Protection Agency, Environmental Research Laboratory, Office of Research and Development, Athens, Ga. EPA/600/R-93/174.

Bowie, G.L., Mills, W.B., Porcella, D.B., Campbell, C.L., Pagenkopf, J.R., Rupp, G.L., Johnson, K.M., Chan, P.W.H., Gherini, S.A., and Chamberlin, C.E. 1985. Rates, constants, and kinetics formulations in surface water quality modeling. U.S. Environmental Protection Agency, Environmental Research Laboratory, Office of Research and Development, Athens, Ga. EPA/600/3-85/040.

Chapra, S.C., and Reckhow, K.H. 1983. Engineering approaches for lake management. Vol. II: mechanistic modeling. Butterworths Publ., Boston, Mass.

Christian, R.R., Bryant, W.L., Jr., and Stanley, D.W. 1986. The relationship between river flow and *Microcystis aeruginosa* blooms in the Neuse River, North Carolina. Rep. No. 223. UNC Water Resources Research Institute, North Carolina State University, Raleigh, N.C.

Clemen, R.T. 1996. Making hard decisions. Duxbury Press, Belmont, Calif.

Cole, T.M., and Buchak, E.M. 1995. CE-QUAL-W2: a two-dimensional, laterally averaged hydrodynamic and water quality model, version 2.0. Draft user's manual. Instruction Rep. EL-95-02. Waterways Experiment Station, Vicksburg, Miss.

Cooke, R.M. 1991. Experts in uncertainty, opinion and subjective probability in science. Oxford University Press, New York.

Di Toro, D.M., and van Straten, G. 1979. Uncertainty in the parameters and predictions of phytoplankton models. Working Pap. WP-79-27. International Institute for Applied Systems Analysis, Laxenburg, Austria.

Dodd, R.C., and Tippett, J.P. 1994. Nutrient modeling and management in the Tar-Pamlico River Basin. Draft report. Research Triangle Institute, Research Triangle Park, N.C.

Freedman, D., Rothenberg, T., and Sutch, R. 1983. On energy policy models (with discussion). J. Bus. Econ. Stat. **1**: 24–36.

Haith, D.A., and Shoemaker, L.L. 1987. Generalized watershed loading functions for stream flow nutrients. Water Resour. Bull. **23**: 471–478.

Hodges, J.S. 1987. Uncertainty, policy analysis, and statistics (with discussion). J. Am. Stat. Assoc. **2**: 259–291.

Jensen, F.V. 1996. An introduction to Bayesian networks. Springer, New York.

Kadane, J.B., and Schum, D.A. 1996. A probabilistic analysis of the Sacco and Vanzetti evidence. Wiley, New York.

Lauritzen, S.L., and Spiegelhalter, D.J. 1988. Local computations with probabilities on graphical structures and their application to expert systems (with discussion). J. R. Stat. Soc. Ser. B (Methodol.), **50**: 157–224.

Levin, S.A. 1985. Scale and predictability in ecological modeling. *In* Modeling and management of resources under uncertainty. *Edited by* T.L. Vincent, Y. Cohen, W.J. Grantham, G.P. Kirkwood, and J.M. Skowronski. Lecture Notes in Biomathematics No. 72. Springer-Verlag, Berlin. pp. 1–8.

Mar, B.W. 1974. Problems encountered in multi-disciplinary resources and environmental simulation models development. J. Environ. Manage. **2**: 83–100.

Marshall, K.T., and Oliver, R.M. 1995. Decision making and forecasting. McGraw-Hill, New York.

Matzkevich, I., and Abramson, B. 1995. Decision analytic networks in artificial intelligence. Manage. Sci. **41**: 1–22.

Meyer, M., and Booker, J. 1991. Eliciting and analyzing expert judgment, a practical guide. Academic Press, London, U.K.

Morgan, M.G., and Henrion, M. 1990. Uncertainty. Cambridge University Press, New York.

Pearl, J. 1990. Probabilistic reasoning in intelligent systems: networks of plausible inference. Morgan Kaufmann, San Mateo, Calif.

Reckhow, K.H. 1994. Water quality simulation modeling and uncertainty analysis for risk assessment and decision making. Ecol. Model. **72**: 1–20.

Scavia, D., Canale, R.P., Powers, W.F., and Moody, J.L. 1981. Variance estimates for a dynamic eutrophication model of Saginaw Bay, Lake Huron. Water Resour. Res. **17**: 1115–1124.

Schum, D.A. 1994. Evidential foundations of probabilistic reasoning. Wiley, New York.

Thomann, R.V., and Mueller, J.A. 1987. Principles of surface water quality modeling. Harper & Row, New York.

von Winterfeldt, D., and Edwards, W. 1986. Decision analysis and behavioral research. Cambridge University Press, Cambridge, U.K.

Walters, C. 1986. Adaptive management of renewable resources. Macmillan Publishing Company, New York.

Whittaker, J. 1990. Graphical models in applied multivariate statistics. Wiley, Chichester, U.K.

© 1999 NRC Canada

Effects of migration distance on whole-body and tissue-specific energy use in American shad (*Alosa sapidissima*)

Jill B.K. Leonard and Stephen D. McCormick

Abstract: We examined total and tissue-specific energy content of upstream-migrating American shad (*Alosa sapidissima*) in the Connecticut River. Total energy depletion over the course of the 228-km migration ranged from 35 to 60%. The approximate contributions of different tissues to energy use during migration were white muscle 57%, subdermal fat 27%, red muscle 8%, viscera 6%, and liver 2%. American shad preferentially use energy stores in the skin and its subdermal fat layer (depleted by 63%) while sparing red muscle protein. Both lipid and protein were used as energy sources throughout migration, although lipids were depleted to a greater extent (e.g., white muscle lipid decreased 48% and protein 30%). Large fish expended 2–21% more energy during migration than small fish. Migrating to upriver sites (198–228 km) is 50–100% more energetically expensive than to lower river sections for females. This suggests that upriver range expansion may be limited by females in that they may have reached a threshold level of energy expenditure in this upriver area. American shad may possess physiological mechanisms for tissue-specific energy use allowing maintenance of critical tissues necessary for postspawning survival.

Résumé : Nous avons étudié les réserves énergétiques totales et de divers tissus chez l'alose savoureuse (*Alosa sapidissima*) en montaison dans le fleuve Connecticut. La baisse totale des réserves énergétiques au cours de cette migration de 228 km variait de 35 à 60%. Les contributions approximatives des différents tissus à la dépense d'énergie durant la migration étaient les suivantes : muscles blancs 57%, graisse sous-dermique 27%, muscles rouges 8%, viscères 6% et foie 2%. L'alose savoureuse utilise préférentiellement les réserves énergétiques de la peau et de la couche de graisse sous-dermique (appauvrie de 63%) et économise les protéines de ses muscles rouges. Des lipides et des protéines ont été utilisés comme sources d'énergie durant la migration, mais ce sont les teneurs en lipides qui ont le plus diminué (p. ex., les teneurs des muscles blancs en lipides ont baissé de 48%, tandis que pour les protéines, la diminution est de 30%). Les gros poissons ont dépensé 2 à 21% plus d'énergie que les petits poissons durant la migration. La migration vers les sites d'amont (198–228 km) est 50 à 100% plus coûteuse énergétiquement que celle vers les secteurs du cours inférieur pour les femelles. Cela laisse penser que l'expansion de l'aire de l'espèce plus en amont pourrait être limitée par les femelles, qui pourraient avoir atteint leur plafond de dépense énergétique. L'alose savoureuse pourrait disposer de mécanismes physiologiques lui permettant d'utiliser sélectivement les réserves énergétiques de certains tissus et assurant ainsi la protection de tissus critiques pour la survie post-fraye.

[Traduit par la Rédaction]

Introduction

It is commonly believed that fish migration is energetically costly given the locomotor demands of long-distance travel (Gross et al. 1988; Roff 1988; Dingle 1996). Therefore, energy availability has the potential to be a limiting factor in migration, particularly in those species that do not feed during migration. There have been numerous studies describing the energetic costs of migration in fish (e.g., Idler and Bitners 1958, 1959; Glebe and Leggett 1981*a*, 1981*b*; Crawford et al. 1986; Lambert and Dodson 1990*a*; Reid et al. 1993; Hatano et al. 1995; Jorgensen et al. 1997). Most of these studies have concentrated on whole-body energy use over the course of migration or have described an in-depth examination of energy usage in a single tissue. These approaches provide limited insight into any potentially adaptive physiological mechanisms of energy utilization that may result from differential liberation of energy from different tissues or storage forms throughout the animal. Further, most of this work, with the exception of Glebe and Leggett (1981*a*, 1981*b*), Crawford et al. (1986), and Lambert and Dodson (1990*a*), has focused on salmonids, particularly semelparous Pacific species. These fish do not need to conserve stored energy in order to power the return downstream migration as iteroparous fishes presumably must. Lambert and Dodson (1990*a*, 1990*b*) have demonstrated correlations between costs of migration, overwintering condition, postspawning survival, and lifetime fecundity in iteroparous coregonines (cisco (*Coregonus artedi*) and lake whitefish (*Coregonus clupeaformis*)). More recently, Jonsson et al. (1997) have evaluated energy use in Atlantic salmon (*Salmo salar*) and have shown that iteroparous populations can sus-

Received June 25, 1998. Accepted March 4, 1999.
J14669

J.B.K. Leonard[1] and S.D. McCormick. S.O. Conte Anadromous Fish Research Center, Biological Resources Division, U.S. Geological Survey, Turners Falls, MA 01376, U.S.A., and Department of Biology, University of Massachusetts, Amherst, MA 01003, U.S.A.

[1]Author to whom all correspondence should be addressed.
e-mail: jbkleonard@hotmail.com

© 1999 NRC Canada

tain energetic losses of 60–70% during upstream migration. Berg et al. (1998) have also demonstrated differences in energy accumulation and survivorship between virgin and repeat-spawning brown trout (*Salmo trutta*), suggesting an impact of energetic constraints on repeat-spawning ability. However, physiological mechanisms for tissue-specific energy conservation by iteroparous fishes remain unexplored.

The American shad (*Alosa sapidissima*) is an abundant, anadromous clupeid ranging from Florida to Atlantic Canada. American shad display a clinal variation in postspawning survival from completely semelparous populations in the south to largely iteroparous populations in the north (Glebe and Leggett 1981*b*). In the Connecticut River, American shad are iteroparous, with about 30–40% of returning fish having spawned in a previous year (Glebe and Leggett 1981*b*). In the Connecticut River, spawning occurs in May and June at water temperatures between 10 and 22°C. While this is an apparently large thermal window, May–June is a period of rapid temperature increase in the river, with migration and spawning lasting only 6–8 weeks each year. Fish migrate as much as 300 km upriver during this period and may spawn several times during this journey. Further, American shad have been impacted by human modification of rivers throughout their range, leading to reduced populations in many river systems, although restoration efforts are currently underway in some of these rivers (Rulifson 1994; St. Pierre 1994). Mitigation efforts frequently include fish ladders that permit passage past dams. In the Connecticut River, American shad pass through as many as four mainstem hydroelectric power dams, each of which is equipped with a fish passage facility (one fish elevator, three fish ladders of varied design).

There has been considerable work addressing energy use in migrating American shad in previous studies. Notably, Leggett and Trump (1978) and Glebe and Leggett (1981*a*, 1981*b*) have provided a groundwork for our research. We have chosen to expand upon these studies for several reasons. Firstly, it is unknown whether there are mechanisms available to American shad by which they can spare certain tissue energy sources while still utilizing others during upstream migration. Tissues where energy sparing occurs could presumably be used to power downstream migration and (or) enhance recovery from migration while in the ocean. Knowledge of these mechanisms is critical to understanding energy management in migratory fishes, particularly iteroparous species. Secondly, the work of Leggett and collaborators was done in the 1970's at a period when shad were not successfully passing over the first hydroelectric power dam (Holyoke Dam, km 139). Fish now migrate past a facility 280 km (Bellows Falls Dam) from the mouth of the river, with 42–63% of the population migrating above the Holyoke Dam in recent years (data from 1990–1997, Connecticut River Coordinators Office, personal communication). We wish to understand whether energy use has been altered since the installation of fish passage facilities, whether fish traveling far up the river may be unable to successfully return to the ocean because of excessive energy depletion, or if other factors are involved in the upstream range expansion of this population.

In this study, we document differential use of energy derived from different substrates and energy storage areas. We also examine the impact of migration distance, fish size, and sex on total and tissue-specific energy use. This allows us to assess the overall cost of migration in American shad and to gain an understanding of how the increased metabolic costs of migration are apportioned between different tissues and energy supplies.

Fig. 1. Map showing the Connecticut River drainage area including the four river sampling sites (stars) for American shad located at km 1 (Old Lyme, Conn.), km 139 (Holyoke, Mass.), km 198 (Turners Falls, Mass.), and km 228 (Vernon, Vt.).

Materials and methods

Fish

Adult migratory American shad were sampled at four sites on the Connecticut River (Old Lyme, Conn. (km 1), Holyoke Dam, Holyoke, Mass. (km 139), Cabot Station, Turners Falls, Mass. (km 198), and Vernon Dam, Vernon, Vt. (km 228)), during spring in 1993 and 1994 (Fig. 1). Efforts were made to sample fish within 1 week of the arrival of the first migratory cohort at each location to minimize the confounding effects of variable amounts of time spent in the river prior to sampling. It is difficult to know precisely when fish first enter the estuary, and fish ladders are not necessarily operated with the arrival of the fish, but rather in compliance with federal regulations based on river discharge. Therefore, there may be some variation that we could not control in our sampling time relative to the arrival of cohorts at each location. American

© 1999 NRC Canada

shad were also sampled at an ocean site off Barnagut Light, N.J., in the spring of 1995. At the ocean site and at Old Lyme (km 1), fish were captured using 14- and 15-cm stretch mesh gill nets. At other sites, fish were captured at fish-trapping facilities built into fish passageways at hydroelectric dams. At each location, about 10 males and 10 females were sampled.

Fish were removed from the net or trap and immediately anesthetized with tricaine methanesulfonate (MS 222) at 50 $mg \cdot L^{-1}$ (buffered with 0.24 mM $NaHCO_3$ and adjusted to pH 7.0 with NaOH). Fish were bled from the caudal vessels using heparinized syringes and then placed on ice until tissue samples could be removed (<2 h). Gonad, liver, and remaining viscera were removed, weighed, and frozen at –80°C. The remaining body was then frozen and later sliced to produce a series of cross sections posterior to the head. Each cross section was then dissected on the left side to separate white muscle, red muscle, and the skin including the subdermal fat layer (SDF). This resulted in all the somatic tissue from one half of the carcass being separated by tissue type. For each fish, all left-side red muscle, white muscle, and skin/SDF were weighed and frozen separately. Samples of red and white muscle tissue were also taken from the right side of the body anterior to the dorsal fin for determination of muscle moisture content by drying to a constant weight at 60°C for 24 h.

Proximate analysis

Frozen gonad, liver, red and white muscle, and skin/SDF were homogenized with one volume of deionized water. The resulting homogenates were divided into aliquots for total lipid, total protein, and glycogen determination. Total lipid aliquots were extracted immediately, while protein and glycogen aliquots were frozen for later assay. Total lipid was determined using the protocol of Sheridan et al. (1983). Lipids were extracted from the homogenate (1 mL) using 20 volumes of 1:1 chloroform–methanol (Folch et al. 1957). Extracted lipid was spectrophotometrically determined using extracted and gravimetrically quantified cod liver oil as a standard (Frings et al. 1972). The aliquot for protein analysis was thawed, resuspended, and sonicated (two 5-s bursts) in 0.1 N NaOH (1:20 w/v). Protein was then quantified using the methods of Lowry et al. (1951) with bovine serum albumin as a standard. Glycogen was estimated in thawed aliquots after resuspension in 100 mM sodium citrate buffer (pH 5.0, 1:10 w/v) using the methods of Carr and Neff (1984) and Busacker et al. (1990). Samples were digested with amyloglucosidase (125 $\mu g \cdot mL$ $homogenate^{-1}$) for 2 h at 55°C and compared with undigested controls. Glucose in digested and undigested samples (glucose control) was assayed in a spectrophotometer using the glucose oxidase – *o*-dianisidine – peroxidase reaction (Raabo and Terkildsen 1960).

All values of mass of lipid, protein, and glycogen were transformed into their energetic content using the energetic equivalents of 35.52 $kJ \cdot g^{-1}$ for extracted lipid and 23.63 $kJ \cdot g^{-1}$ for total protein (Craig et al. 1978) and 17.2 $kJ \cdot g^{-1}$ for glycogen (Brafield 1985). Note that the conversion factor used for lipid is lower than is typical of many earlier studies because Craig et al. (1978) suggested that this is a more realistic conversion factor for samples extracted using the chloroform–methanol method employed in this study.

In order to obtain estimates of total tissue and total body energy content, caloric equivalents (kilojoules per gram) of protein, lipids, and glycogen from each tissue aliquot were extrapolated to the total mass of the tissue (in the cases of white and red muscle and skin/SDF, this value was doubled to account for the unsampled tissue on the right side of the fish). Total body content was then calculated as the total of all the tissue contents (white muscle, red muscle, skin/SDF, gonad, liver, remaining viscera). Note that this method of calculating total body energy content does not include the head, spinal column and ribs, or fins. The reported values are therefore underestimates of true content, although it is unlikely that energy can be easily mobilized from these excluded areas of the body.

Gonadosomatic index (GSI) was calculated as gonad mass/(total mass – gonad mass) × 100.

Statistics

Data were analyzed using the general linear models analysis of covariance (ANCOVA) with a three-way classification with fish fork length as the covariate using the SAS statistical package (SAS Institute Inc., Cary, N.C.) at $\alpha = 0.05$ followed by least squares means comparisons (as needed). Use of the length covariate was chosen because American shad display a sexual size dimorphism where spawning males are consistently smaller than same-age females. This analytic technique generates adjusted means for the tested groups based on the length regressions for all fish (either all within-river individuals or the estuary/km 1 groups) sampled including all sites, sexes, and years. These adjusted means were then tested for homogeneity in a manner similar to that employed by analysis of variance (ANOVA). The primary assumption of this analysis is that the slopes of the regressions of a measured variable on length for all site–sex–year combinations are homogeneous. Other test assumptions include significance of the relevant regressions and linearity of the response as well as ANOVA assumptions of randomness, homoscedasticity, and normality (Snedecor and Cochran 1989; Sokal and Rohlf 1995). All these assumptions were satisfactorily met in this study.

Actual values of energy content for fish captured at the different locations are presented as well as the least squares means corrected for length (adjusted means). All statistics presented take variation in fish size into account (Tables 1 and 2). Our intent is to clarify our data with respect to the sexual length dimorphism while still detailing the absolute costs of migration in the species.

Results

Length differed between males and females at all sites except the ocean sampling location (Table 1). There was a significant decrease in the size of females from both years and males from 1994 at the most upriver site.

Total energy was depleted by 35–61% from estuarine levels over the course of the 228-km upriver migration and differed significantly between the sexes and between years (Table 1; Fig. 2). Total energy was also significantly higher in the ocean (1995) than in the estuary (Old Lyme, km 1) in 1993 and 1994 (Table 1).

In white muscle, both lipid and protein were utilized over the course of migration in both sexes (Figs. 3 and 4; Table 1). Overall, lipid-based energy was used more extensively (48% depletion over 228 km for length-corrected means) than protein-based energy (30% depletion). Both lipid-derived energy and protein-derived energy were utilized from the earliest portions of the migration. As expected, relatively more energy (26% calculated over all river sites) is available in female white muscle than in male white muscle given the generally larger size of females. When size is taken into account, however, there was no difference in white muscle energy at a given site between the sexes. Levels of energy available from lipid in the ocean were higher than levels seen in the estuary in 1993 and 1994. Oceanic protein-derived energy content of white muscle was higher than the estuary samples in 1993 but not in 1994. Greater energy depletion occurred in 1994 than in 1993.

© 1999 NRC Canada

Table 1. Mean absolute energy values (kJ) for muscle and cumulative energy content in American shad captured at four river locations, estuary (km 1), Holyoke Dam (km 139), Cabot Station (km 198), and Vernon Dam (km 228), and at an oceanic site, Barnagut Light, N.J.

	A	B	1995 males	1995 females	1993 males			
Site (km)			Ocean	Ocean	1	139	198	228
N			7	11	10	10	13	13
Length	s, l (a, a, b, c) sy, ly	s′, gs′	45.6	46.9	43.2	42.7	42.0	43.0
			(0.7)	(0.5)	(0.4)	(0.4)	(0.4)	(0.3)
Total mass	l (a, b, c, d), s, sy	g (ab, a, b), s′, sg	1 550	1 678	1219	1103	987	1028
			(40)	(54)	(38)	(44)	(23)	(39)
Total	f, l (a, b, b, c), y, sy, ly	f′, g (a, b, b)	11 807	12 327	8316	7502	5264	4959
			(471)	(899)	(651)	(703)	(474)	(346)
White total	f, l (a, a, b, c), y, sy, ly	f′, g (a, b, b)	7 516	7 907	4916	5252	3471	3064
			(377)	(681)	(411)	(469)	(350)	(214)
White protein	f, l (a, b, c, d), y, sl, ly	f′, g (a, b, a)	3 027	3 085	2087	2211	1645	1835
			(152)	(107)	(1060)	(129)	(151)	(92)
White lipid	f, l (a, a, b, c), y, sy, ly	f′, g (a, b, b)	4 489	4 822	2830	3042	1826	1229
			(304)	(587)	(320)	(357)	(360)	(202)
White glycogen			0.7	0.8	0.0	0.0	0.4	0.0
			(0.1)	(0.0)	(0.0)	(0.0)	(0.3)	(0.0)
White % H_2O	l (a, b, b, b)	g (a, b, b)	52.7	52.5	65	67	71	71
			(4.5)	(3.6)	(1)	(2)	(1)	(2)
Red total	f, l (a, bc, ab, c), y, sy, ly	f′, g (a, b, a)	718	733	847	794	643	585
			(31)	(51)	(95)	(59)	(60)	(46)
Red protein	f, s, y, sy	f′	315	332	290	307	248	247
			(15)	(21)	(24)	(18)	(21)	(13)
Red lipid	f, l (a, bc, a, c), y, sy, ly	f′, g (a, b, a)	402	402	557	487	395	338
			(20)	(34)	(62)	(44)	(26)	(36)
Red glycogen		f′, s′	0.1	0.1	0.2	0.0	0.0	
			(0.0)	(0.0)	(0.1)	(0.0)	(0.0)	
Red % H_2O	l (a, b, c, b), y, ly	g (a, b, c)	28.4	28.3	89	69	67	68
			(1.4)	(1.3)	(1)	(3)	(1)	(1)

Note: Also included are data for fork length (cm), total wet mass (g), and muscle moisture content (% mass). Parenthetical numbers are 1 SE of the mean. Column A indicates the results of ANCOVA (for length only, ANOVA) and multiple comparisons analysis of riverine data; column B indicates the results of similar analyses comparing the ocean and estuarine sites. "y" indicates a significant effect of year, "s" a significant effect of sex for riverine sites, "l" a significant effect of location for riverine sites, "f" a significant effect of length for riverine sites, "sl" a significant interaction between sex and location for riverine sites, "sy" a significant interaction between sex and year for riverine sites, "ly" a significant interaction between location and year for riverine sites, "g" a significant difference between sites for the ocean–estuary comparison, "s′" a significant effect of sex on the ocean–estuary comparison, "gs" a significant interaction between location and sex for the ocean–estuary comparison, and "f′" a significant effect of length for the ocean–estuary comparison on a given parameter as indicated by ANCOVA ($\alpha = 0.05$). Parenthetical letters after "l" and "g" indicate the results of multiple comparisons testing for riverine location (km 0, km 139, km 198, and km 228, respectively) and ocean–estuary groups (ocean, estuary 1993, and estuary 1994, respectively).

White muscle moisture increased significantly after American shad entered freshwater.

Utilization of lipid-based energy (32%), but not protein, is seen in red muscle (Figs. 3 and 4; Table 1). There was no difference between the ocean site and the estuary in protein-based energy of red muscle, and the difference between ocean and estuary lipid-based energy was only significant in 1993. There was a significant effect of sampling sex and year on energy utilized from protein but not energy from lipid. Red muscle energy content was length dependent. Sex was only a significant factor in riverine lipid content depletion. Red muscle energy content was initially lower and more rapidly used in 1994 than in 1993. Red muscle moisture increased sharply after American shad entered freshwa-

© 1999 NRC Canada

1994 males				1993 females				1994 females			
1	139	198	228	1	139	198	228	1	139	198	228
8	9	11	11	18	10	10	7	11	11	10	10
44.5	43.4	40.2	37.6	48.3	48.0	46.9	45.6	49.8	48.5	47.6	45.5
(0.9)	(1.0)	(1.1)	(0.7)	(0.6)	(0.7)	(0.7)	(0.7)	(0.8)	(0.5)	(0.5)	(0.7)
1445	1151	908	679	1 781	1 660	1533	1269	2 088	1775	1602	1285
(104)	(73)	(69)	(51)	(60)	(70)	(103)	(82)	(89)	(61)	(50)	(73)
9818	5503	4485	2931	11 167	10 531	8836	6405	12 461	8441	7328	4280
(1213)	(471)	(489)	(388)	(585)	(1042)	(1197)	(817)	(572)	(441)	(343)	(552)
6097	3928	3073	2058	6 477	7 037	5274	4015	7 389	5267	4603	2493
(682)	(334)	(375)	(275)	(445)	(732)	(869)	(549)	(461)	(275)	(254)	(491)
3010	2217	1712	1321	3 087	2 928	2319	1886	3 627	2927	2666	1597
(226)	(187)	(155)	(134)	(155)	(229)	(233)	(205)	(203)	(129)	(94)	(266)
3087	1711	1360	737	3 390	4 109	2955	2129	3 762	2340	1937	895
(471)	(183)	(248)	(147)	(318)	(534)	(668)	(355)	(276)	(159)	(185)	(258)
0.2	0.1	0.1	0.0	0.6	0.1	0.1	0.0	0.2	0.0	0.4	0.1
(0.1)	(0.0)	(0.0)	(0.0)	(0.6)	(0.0)	(0.1)	(0.0)	(0.1)	(0.0)	(0.2)	(0.1)
64	71	67	65	65	70	67	69	64	69	68	72
(2)	(1)	(1)	(7)	(1)	(2)	(1)	(1)	(1)	(2)	(1)	(1)
567	405	401	234	1 100	1 020	1051	716	799	526	602	423
(56)	(42)	(49)	(29)	(80)	(111)	(113)	(64)	(44)	(36)	(34)	(45)
279	226	205	128	386	383	375	318	360	292	313	235
(27)	(18)	(30)	(14)	(25)	(41)	(42)	(23)	(26)	(18)	(17)	(20)
287	178	196	106	714	637	676	398	437	234	289	188
(36)	(29)	(26)	(16)	(59)	(74)	(72)	(45)	(26)	(22)	(20)	(27)
0.7	0.1	0.0	0.0	0.3	0.1	0.2	0.1	2.6	0.1	0.1	0.0
(0.2)	(0.1)	(0.0)	(0.0)	(0.1)	(0.0)	(0.1)	(0.0)	(2.3)	(0.1)	(0.1)	(0.0)
61	67	63	66	90	66	64	69	59	67	64	68
(1)	(1)	(1)	(1)	(1)	(1)	(1)	(1)	(2)	(1)	(1)	(1)

ter. After river entry, a generalized increase was seen at more upriver sites, although moisture content was extremely high in both sexes in 1993 in the estuary.

In the liver, both lipid-based energy and protein-based energy are utilized (76 and 38%, respectively) with lipid providing a greater proportion of the fuel for migration (Fig. 3; Table 2). The liver in general contributes a proportion of its available energy similar to that of red and white muscle; however, because of its small mass, it only accounts for about 2% of the energy consumed during migration (Fig. 3). Stored, lipid-based energy was significantly higher in the ocean fish than in the estuary samples. Fork length and sex were both significant factors in total liver energy use, primarily because of the effect of length and sex on female liver protein.

Visceral stores of both lipid-based energy and protein-based energy were depleted (57 and 34%, respectively) during migration (Fig. 3; Table 2), with more energy being pro-

© 1999 NRC Canada

Fig. 2. Total adjusted mean energy content for male and female adult American shad captured at four sites (km 1, km 139, km 198, and km 228) in the Connecticut River in (*a*) 1993 and (*b*) 1994. Bars indicate the contribution from white muscle (open), gonad (diagonal hatch), red muscle (cross-hatch), liver (horizontal hatch), viscera (solid), and skin (squares) at each site. Values above bars indicate the percent depletion of total energy at that site relative to total content of fish captured at km 1 based on adjusted means.

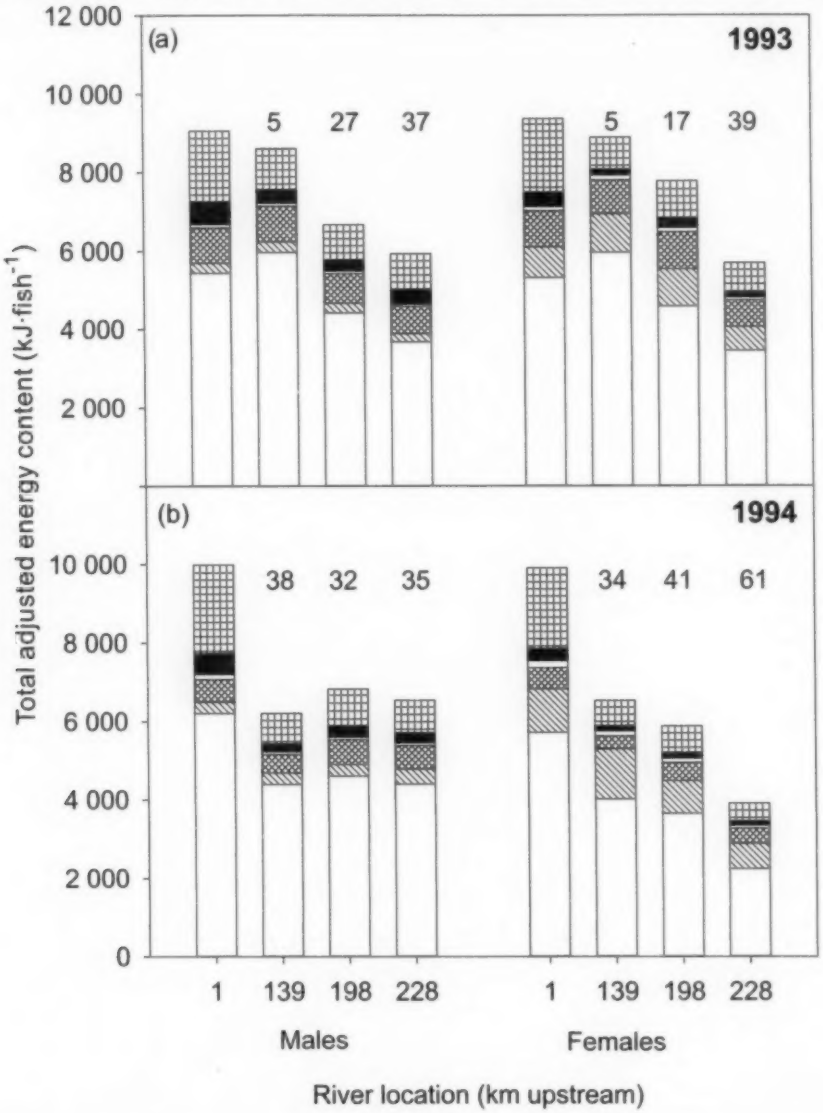

vided by lipid than by protein in both sexes. Much of this depletion occurred during the first phases of migration between the estuary and the first dam (km 139). Visceral energy was also significantly affected by both fork length and sex, primarily because males have higher visceral stores than females.

GSI was higher in females than in males except in the ocean (Table 2). There was a small increase in GSI from the estuary to Holyoke Dam (km 139). Thereafter, there was little change in GSI as the fish moved upriver until they reached the most upriver site where there was a significant decrease. Gonads had decreased lipid- and protein-based energy in both sexes over the course of migration (Table 2). Gonad energy content differed with sex (female > male), fork length (large > small), and year (1994 > 1993).

Protein could not be measured in raw skin/SDF homogenates because of the high lipid content in the tissue. The portion of tissue unhomogenized was largely the skin itself (dermis and epidermis), which is unlikely to be mobilized as an energy source during migration, given its relative insolubility (Whitear 1984). Lipid-based energy was extremely high on a per gram basis, with skin/SDF lipid providing about 33% of the total energy available from total body lipid (Table 2). Only white muscle has a larger lipid store.

© 1999 NRC Canada

Fig. 3. Adjusted mean tissue energy content for migrating (*a*) male and (*b*) female adult American shad in 1993 sampled in (1) the estuary (km 1), (2) Holyoke Dam (km 139), (3) Cabot Station (km 198), and (4) Vernon Dam (km 228). Bars indicate energy from protein (solid) and lipid (open). Values above the bar sets indicate the percent total energy depletion for the indicated tissue between km 1 and km 228 based on adjusted means. Values in parentheses indicate the percent contribution of the indicated tissue to the whole-body energy depletion between km 1 and km 228 for the groups shown.

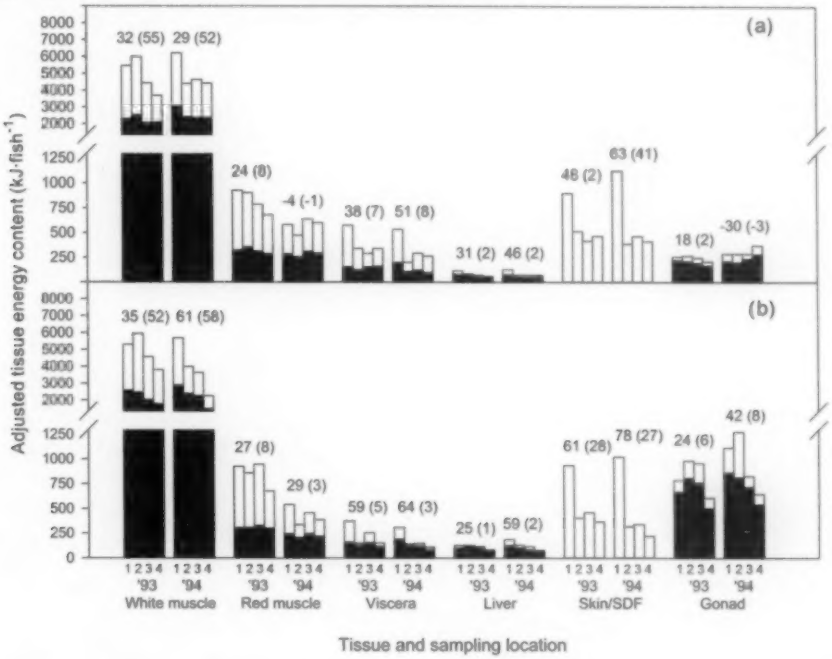

Fig. 4. White (open circles) and red (solid circles) muscle adjusted mean protein-based tissue energy content in female American shad sampled at four different sites in the Connecticut River in 1993 (solid line) and 1994 (broken line). For white muscle, different letters indicate significantly different energy contents. There were no differences in red muscle protein between the sites.

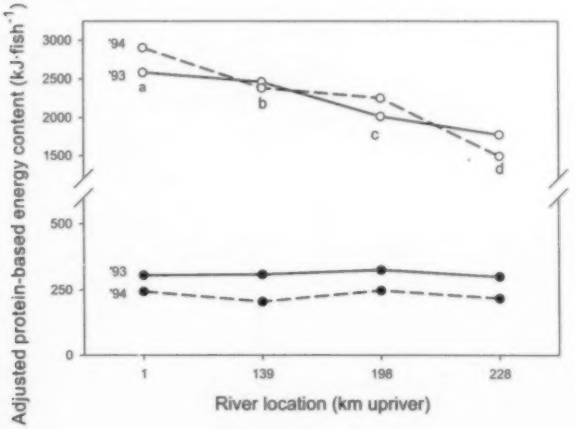

Skin/SDF energy was depleted throughout migration by 48–80% (Fig. 3; Table 2). Skin/SDF energy content was significantly affected by fish length such that larger fish depleted this source more rapidly than smaller fish.

In all tissues examined, glycogen was marginally detectable and contributed very little energy (<1%) relative to lipid and protein (Tables 1 and 2).

Discussion

Our results parallel and expand upon those of Glebe and Leggett (1981*a*), who also worked with the Connecticut River American shad population. They found that somatic tissue contributed over 90% of the energy required for migration, including the downstream migration. In our study, somatic tissues (red and white muscle and skin/SDF) provided about 90% of the energy for upstream migration. The studies differ, however, in that Glebe and Leggett (1981*a*) reported an approximately 26–30% depletion of the somatic stores in the first 139 km of the migration. Our work found an approximately 29–61% depletion (Fig. 3) in the white muscle stores alone over the entire 228-km upstream migration. When Glebe and Leggett (1981*a*) gathered their data, km 139 (Holyoke Dam) was the functional upriver extent of the migration. Currently, American shad are able to move upstream more than 228 km, an increase of 64%. Estimates suggest that a substantial portion of the population utilized this upstream portion of the range (42–63% for 1990–1997, Connecticut River Coordinators Office, personal

© 1999 NRC Canada

Table 2. Mean absolute energy values (kJ) for tissue energy content in American shad captured at four river locations, estuary (km 1), Holyoke Dam (km 139), Cabot Station (km 198), and Vernon Dam (km 228), and at an oceanic site, Barnagut Light, N.J.

	A	B	1995 males	1995 females	1993 males			
Site (km)			Ocean	Ocean	1	139	198	228
Viscera total	f, s, l (a, b, b, b), y	f′, s′	556	235	553	309	248	312
			(61)	(30)	(84)	(62)	(39)	(159)
Viscera protein	f, l (a, b, b, b), ly	f′, g (a, a, b)	189	146	149	116	140	153
			(15)	(11)	(12)	(11)	(9)	(64)
Viscera lipid	s, l (a, b, b, b), y	f′, s′	366	89	405	193	108	159
			(49)	(27)	(72)	(56)	(34)	(86)
Viscera glycogen	l (a, b, abc, c)	f′	0.0	0.0	0.0	0.0	0.0	0.0
			(0.0)	(0.0)	(0.0)	(0.0)	(0.0)	(0.0)
Liver total	f, s, l (a, b, b, c), y, ly	f′, g (a, b, a)	181	152	109	71	57	49
			(19)	(13)	(14)	(12)	(5)	(4)
Liver protein	f, s, l (a, a, b, c), sl, sy	f′	89	93	73	58	42	39
			(9)	(6)	(6)	(11)	(3)	(12)
Liver lipid	l (a, b, b, c), y, ly	g (a, b, c)	92	59	35	12	15	10
			(14)	(8)	(5)	(2)	(2)	(1)
Liver glycogen	f, l (a, b, b, b), y, sl, ly	g (a, b, a)	0.0	0.1	1.1	0.0	0.2	0.0
			(0.0)	(0.1)	(0.4)	(0.0)	(0.1)	(0.0)
Skin total	f, l (a, b, b, b), ly	f′, g (a, b, a)	2634	2430	1693	890	707	815
			(130)	(208)	(114)	(132)	(77)	(89)
Skin lipid	f, l (a, b, b, b), ly	f′, g (a, b, a)	2634	2430	1693	890	707	815
			(130)	(208)	(114)	(132)	(77)	(89)
Gonad total	f, s, l (a, b, a, c), y, sl, ly	f′, s′, g (a, a, b), gs	203	891	198	185	138	134
			(15)	(71)	(13)	(11)	(8)	(10)
Gonad protein	f, s, l (a, a, a, b), y, sl	f′, s′, g (a, a, b)	155	753	176	149	110	109
			(12)	(59)	(10)	(7)	(7)	(7)
Gonad lipid	f, s, l (a, b, ac, c), y, sl, sy, ly	f′, s′, g (a, a, b), gs	48	138	23	36	28	25
			(6)	(14)	(4)	(5)	(4)	(4)
GSI	s, sl, l (ac, b, ab, c)	s′, gs	11.4	9.9	7.5	8.3	6.6	6.3
			(1.5)	(0.5)	(0.3)	(0.4)	(0.2)	(0.4)

Note: Also included are data for GSI (%). Parenthetical numbers are 1 SE of the mean. Column A indicates the results of ANCOVA (for length only, ANOVA) and multiple comparisons analysis of riverine data; column B indicates the results of similar analyses comparing the ocean and estuarine sites. "y" indicates a significant effect of year, "s" a significant effect of sex for riverine sites, "l" a significant effect of location for riverine sites, "f" a significant effect of length for riverine sites, "sl" a significant interaction between sex and location for riverine sites, "sy" a significant interaction between sex and year for riverine sites, "ly" a significant interaction between location and year for riverine sites, "g" a significant difference between sites for the ocean–estuary comparison, "s′" a significant effect of sex on the ocean–estuary comparison, "gs" a significant interaction between location and sex for the ocean–estuary comparison, and "f′" a significant effect of length for the ocean–estuary comparison on a given parameter as indicated by ANCOVA ($\alpha = 0.05$). Parenthetical letters after "l" and "g" indicate the results of multiple comparisons testing for riverine location (km 0, km 139, km 198, and km 228, respectively) and ocean–estuary groups (ocean, estuary 1993, and estuary 1994, respectively).

communication). The data show that, at the maximum upriver site in both studies, fish had similar levels of energy depletion. It is not clear why this occurs, although it could be the result of behavioral changes in the migration of American shad over time leading to changes in migration speed.

If we compare, instead, the energy depleted to reach km 139 in both our study and Glebe and Leggett (1981*a*), we find differences that highlight annual effects on migration. In our study, white muscle energy content in 1993 did not change substantially between km 1 and km 139, while in 1994, there was a decrease in white muscle energy content (29.1% males, 32.8% females) between km 1 and km 139, similar to the expenditure (26–30% somatic) seen by Glebe and Leggett (1981*a*). This suggests that there are large year-to-year differences affecting energy expenditure, including the expenditure of energy prior to the first mainstem passage obstacle (Holyoke Dam, km 139). This expenditure between km 1 and km 139 (1994), combined with the large female expenditures between km 198 and km 228, is respon-

© 1999 NRC Canada

1994 males				1993 females				1994 females			
1	139	198	228	1	139	198	228	1	139	198	228
530	182	225	162	423	198	285	162	378	195	191	119
(140)	(15)	(23)	(27)	(38)	(12)	(57)	(19)	(55)	(15)	(19)	(11)
198	101	103	65	173	144	164	122	210	139	135	88
(14)	(4)	(8)	(8)	(9)	(6)	(17)	(11)	(20)	(8)	(10)	(3)
332	82	122	97	250	54	122	40	168	56	56	32
(129)	(11)	(18)	(20)	(32)	(8)	(44)	(10)	(43)	(9)	(10)	(10)
0.0	0.1	0.0	0.0	0.0	0.0	0.0	0.0	0.0	0.1	0.1	0.0
(0.0)	(0.0)	(0.0)	(0.0)	(0.0)	(0.0)	(0.0)	(0.0)	(0.0)	(0.1)	(0.1)	(0.0)
127	62	46	31	148	145	129	85	212	149	129	79
(28)	(5)	(6)	(4)	(14)	(15)	(13)	(6)	(13)	(11)	(8)	(6)
76	47	32	26	115	128	108	72	147	118	96	72
(9)	(3)	(4)	(3)	(12)	(13)	(10)	(5)	(9)	(7)	(6)	(6)
50	15	13	5	30	17	21	14	64	31	34	7
(19)	(2)	(2)	(1)	(4)	(3)	(5)	(1)	(6)	(4)	(2)	(1)
0.4	0.0	0.0	0.0	3.2	0.0	0.2	0.3	1.2	0.2	0.0	0.1
(0.2)	(0.0)	(0.0)	(0.0)	(0.7)	(0.0)	(0.1)	(0.1)	(0.3)	(0.1)	(0.0)	(0.0)
2222	690	629	355	2097	1024	1059	781	2373	882	867	490
(324)	(128)	(64)	(62)	(104)	(188)	(138)	(122)	(58)	(104)	(78)	(74)
2222	690	629	355	2097	1024	1059	781	2373	822	867	490
(324)	(18)	(64)	(62)	(104)	(188)	(138)	(122)	(58)	(104)	(78)	(74)
276	236	111	91	922	1107	1038	646	1310	1421	937	677
(26)	(19)	(7)	(13)	(47)	(57)	(94)	(108)	(85)	(151)	(88)	(52)
203	161	101	68	775	904	823	526	1012	924	802	562
(19)	(12)	(8)	(6)	(40)	(49)	(75)	(83)	(68)	(100)	(76)	(43)
73	75	11	24	147	203	216	120	298	497	135	114
(9)	(9)	(2)	(7)	(11)	(11)	(20)	(45)	(21)	(54)	(13)	(13)
8.1	8.1	6.9	5.9	13.4	16.3	18.0	13.7	15.2	18.6	16.9	14.4
(0.3)	(0.3)	(0.4)	(0.3)	(0.6)	(0.9)	(1.5)	(1.6)	(0.5)	(1.2)	(1.2)	(1.0)

sible for the very large (61%) total energy depletion seen in females in 1994. The source of year-to-year variation is somewhat unclear, although the two sampling years in our study were quite different, particularly in water flow; 1994 was characterized by high river discharge during the migration (25% greater than in 1993 as measured by the U.S. Geological Survey gauging station at Montague, Mass.), indicating that high water flow may be involved in the greater energy expenditure of fish migrating in 1994 compared with 1993. This is particularly relevant given that, in both males and females, fish sampled in 1994 from the estuary (km 1) had a greater energy reserve than those migrating in 1993. This type of large variation in energy availability was also seen by Glebe and Leggett (1981*a*), who saw much larger energy reserves in fish migrating through the estuary in 1972 (compared with 1973). These data suggest that not only is annual variation large and likely critical to migratory success, but annual effects may be acting prior to river entry (energy storing) as well as during the upstream migration (energy expending).

© 1999 NRC Canada

Fig. 5. Energy expenditure per kilometre of river traversed per reach of river sampled: (1) Old Lyme to Holyoke Dam (km 1 to km 139), (2) Holyoke Dam to Cabot Station (km 139 to km 198), and (3) Cabot Station to Vernon Dam (km 198 to km 228). Bars indicate data from 1993 (solid) and 1994 (open) Values are based on differences between standardized means for each sex at two adjacent sites. When values are pooled across years (based on a priori individual standardization), there is a significant difference between female energy expenditure in reach 3 and all other male and female reach expenditures (ANOVA, $p < 0.05$).

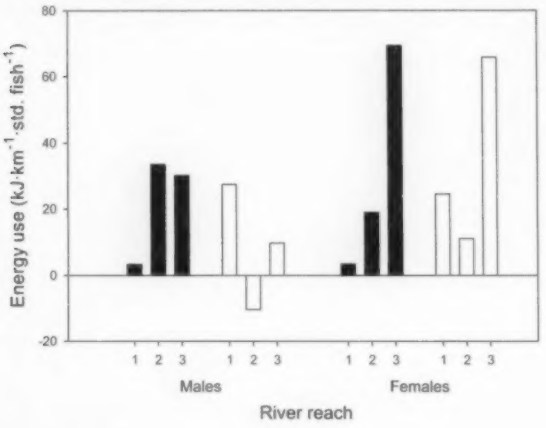

Glebe and Leggett (1981*a*) found that smaller American shad (males) consumed greater proportions of their somatic muscle than did larger shad. In our study, large fish (females) expended a slightly larger amount of energy (using length-corrected values for comparison) than did small fish (males), but this effect varied strongly between years. In 1993, females expended 39% of total energy, while males expended 37%. In 1994, however, females expended 60% of total energy, while males expended only 35%. Our data are in agreement with the observations of Jonsson et al. (1997), who found that migrating large Atlantic salmon of either sex expended more energy than small fish, but it is difficult to definitively separate the effects of sex and length in American shad. The differences between our study and Glebe and Leggett (1981*a*) may be the result of annual variability in energy use, perhaps resulting from differences in river discharge or temperature. Based on comparison of American shad from semelparous and iteroparous populations, Glebe and Leggett (1981*b*) suggested that populations of fish expending more than 60% of their total energy during migration would tend to be semelparous. The Connecticut River American shad population is partially semelparous, and they may represent a threshold population that encounters a high level of energy expenditure in intermittent years or only in one sex. The use of the 60% energy expenditure threshold is, however, subjective, as pointed out by Jonsson et al. (1997). They demonstrated that Atlantic salmon can endure 60–70% energy expenditure in iteroparous populations, although greater than 62% energy depletion resulted in less than 15% postspawning survival. Perhaps threshold levels of energy expenditure leading to semelparity are species dependent. Threshold values are only useful, however, when the premigratory condition of the fish is known and invariable. We have very little information on oceanic condition of American shad, or other anadromous fishes, and no knowledge of how premigratory condition might relate to postspawning survival or migratory success. The relationship between energy expenditure and iteroparity must continue to be examined in a variety of species before generalizations can be accepted.

Differences in mean energy content were adjusted for distance between the sampling sites and the adjusted means plotted versus the region of the river between the sampling sites (Fig. 5). The cost of migration on a per distance traveled basis for American shad (about 25 $kJ \cdot km^{-1} \cdot fish^{-1}$) in our study is similar to that proposed for alewife (*Alosa pseudoharengus*) and blueback herring (*Alosa aestivalis*) in Nova Scotia (Crawford et al. 1986) as well as to that demonstrated for American shad in the lower reaches of the Connecticut River (Glebe and Leggett 1981*a*). In the present study, the areas between the estuary and Holyoke Dam (km 139) and between Holyoke Dam and Cabot Station (km 198) were not different in energy utilization (when the years were pooled and the individual-based means tested for differences using ANOVA). However, female American shad use a consistently higher amount of energy between Cabot Station (km 198) and Vernon Dam (km 228) than earlier in the migration and higher than that used by males (ANOVA, $p < 0.05$) in the same river reach. The cause of this difference is unclear because there are no known costs that would apply only to females in the upper river reaches. Spawning might be more energetically expensive for females than for males, but spawning also occurs below km 198, as evidenced by decreasing GSI and gonadal condition (this study; Glebe and Leggett 1981*a*), and we see no evidence of sex-differential energy usage below km 198. It is possible that there are behaviors inherent in traversing either fish ladders or the power canal in this river reach that make these structures more challenging to females. Regardless of the cause of this increased energy expenditure, it may explain the greater number of males than females that passed over the Vernon Dam (km 228).

Despite the energetic expense of migration in the last reach of the river sampled (between Cabot Station and Vernon Dam), fish captured at Vernon Dam (km 228) still have a considerable store of energy. While skin/SDF energy was depleted by about 63%, total white muscle energy was depleted by about 41%. Overall standardized energy use by adult American shad was about 44% over the 228-km migration distance. It seems likely that some of the remaining energy could be used to return to the sea, although the downstream migration is aided by the river current. It is unclear how the balance between returning successfully to the sea and making advances farther upriver is determined in these fish or how much further these animals could successfully expand their range in the river. The 35–40% energy expenditure seen in American shad (with the exception of 1994 females) may represent a threshold for iteroparity in this population. Perhaps greater energy expenditure depletes the stored energy resource to the point where postspawning survival is minimal. The balance between the advantage of further upriver migration after this depletion relative to postspawning mortality would then be crucial in determining the proportion of semelparity in the population.

© 1999 NRC Canada

We assume that our sampling was from a single cohort of animals moving upriver together, and our sampling protocol of capturing the earliest fish arriving at a passage facility was intended to facilitate this assumption. Several aspects of our data suggest that we may not have been entirely successful. The higher white muscle energy reserves in fish captured in 1993 at km 139 (relative to km 1) suggest that these fish may be a specific subset of the population that chooses to migrate upriver past the spawning sites nearest the ocean (km 50–137, Glebe and Leggett 1981*a*). The males in 1994 also suggest that there may be different cohorts of fish moving through the upstream areas, since there is no increase in total depletion of energy above km 139, suggesting that an approximately 35% depletion is typical and individuals (at least males) are unlikely to expend more than this amount of energy. Passage data through Holyoke Dam (km 139), Cabot Station (km 198), and Vernon Dam (km 228) suggest that about 10% of fish passing Holyoke Dam will ascend the Cabot Station ladder and only about 1% of Holyoke Dam fish will pass Vernon Dam (D. Pugh, Massachusetts Fish and Wildlife Cooperative Unit, personal communication). We were sampling a dwindling subset of the population as we moved upstream, but whether these fish are substantially different from the rest of the population remains unknown.

Tissue-specific energy expenditure patterns may reveal some of the metabolic control mechanisms used by American shad during their migration. Our data demonstrate large differences in the patterns of energy utilization between tissues and between lipid and protein energy sources. Although all tissues examined contributed significantly to the energy used during migration, white muscle and the skin/SDF contributed the most energy (Figs. 3 and 4). Skin/SDF lipid contributed about 21% to the entire energy pool in American shad, despite the fact that skin/SDF comprises less than 5% of the whole-animal weight. White muscle lipid contributed about 35% and white muscle protein about 24% of the energy in the whole body. White muscle lipid was consistently lower (Table 1) between the ocean and the estuarine sampling site, suggesting that river entry itself is powered by white muscle lipid stores. White muscle protein was not used prior to freshwater entry, nor were red muscle energy stores. The large contribution of subdermal lipid stores to migration is unusual for those anadromous fishes that have been studied, and skin/SDF can be thought of as a specialized tissue for energy storage in American shad. The SDF is part of the hypodermal area of the integumentary region and is enlarged in some other fishes, including Atlantic mackerel (*Scomber scombrus*) (Whitear 1984), bogue (*Boops boops*) (Kapoulas and Miniadis-Meimaroglou 1985), and cyclostomes. Sea lampreys (*Petromyzon marinus*) use lipid from this area (the fat column or myeloid region) to provide energy for upstream migration (Beamish et al. 1979). The SDF storage site differs from that of salmonid species that typically mobilize lipid from muscle and viscera during migration (Sheridan 1988), although recent evidence from Arctic char (*Salvelinus alpinus*) suggests that some salmonids may also use lipid stored in the skin (Jorgensen et al. 1997).

There were no significant differences in protein content of red muscle (length adjusted) between any of our samplings (Fig. 4), yet significant utilization of protein occurred in all other tissues examined. This suggests that energy sparing of red muscle occurs in American shad during migration. It is unknown whether sparing occurs in other species, since red muscle is generally not separated from white muscle in other energetic studies. Integrity of the protein structure of red muscle may be crucial to the aerobic swimming capacity that is necessary for continued upstream migration and return to the ocean. Either white muscle can sustain a reduction in protein while retaining function (burst swimming) or the animal sacrifices white muscle function in exchange for energy. Extensive white muscle depletion has been shown to compromise swimming ability in salmonids (Williams and Brett 1987). If white muscle function is compromised in American shad, the importance of burst swimming to total reproductive success may be lower than sustained swimming. Salmonids, however, may use white muscle more extensively during the process of nest building and spawning (Hendry 1998) than American shad, since American shad are nonnesting, broadcast spawners.

There are few absolute energetic differences between the sexes that cannot be attributed to a length effect based on the sexual length dimorphism (females larger than males) seen in this species. An effect of length on proximate composition is to be expected, given the known effects of scaling on metabolic parameters. Aerobic pathways scale such that relative aerobic costs decrease with increasing size (Goolish 1991). This suggests that upstream migration would be more costly for smaller individuals (Weihs 1977). However, both Jonsson et al. (1997) and our study found that larger fish expended more energy during migration. There was some suggestion from Somero and Childress (1980) that, in fish, anaerobic metabolism scales such that larger fish have greater costs for anaerobic activity, and this may be partially responsible for the length-dependent patterns seen in our study. However, we have also measured metabolic enzyme changes in American shad and found few sex-independent, length-dependent effects on either aerobic or anaerobic enzymes during migration (Leonard and McCormick 1999). The mechanisms behind the larger energy expenditure of only slightly larger migratory individuals of the same species remain unclear, although individual behavioral choices could play a significant role.

Sex differences that are independent of length are only seen in liver protein content, visceral lipid content, and red muscle protein (Tables 1 and 2). Elevated liver protein levels in females may be the result of vitellogenin production in the liver during reproductive maturation. This function was also suggested as the basis for elevated lipid levels in female landlocked *Alosa fallax lacustris* (Luzzana et al. 1996), and yet we did not see this difference in liver lipid in this study. Increased visceral lipid in males (also found by Glebe and Leggett 1981*a*) may be a result of relatively smaller gonads, which are probably energetically less costly to maintain, allowing males to use the visceral space taken up in females by large gonads for fat storage. It is unclear why males should have relatively more protein in their red muscle than females, although this relationship could play a role in the greater migration distances achieved by males in the Connecticut River.

American shad use lipid- and protein-based energy throughout the course of their migration, although the relative use of lipid is greater. The contemporaneous use of these energy

© 1999 NRC Canada

sources is somewhat unusual, since several other fishes have been shown to use lipid first and then use protein later in migration. Protein is typically mobilized after lipid in sea lamprey (Beamish et al. 1979). Sockeye salmon (*Oncorhynchus nerka*) use both lipid and protein during their migration, but lipid plays a much larger role early in migration, while protein is more important later in migration and during spawning (Idler and Bitners 1958, 1959). Crawford et al. (1986) demonstrated that migrating alewife and blueback herring use lipid, but not protein, as their energy source for upstream migration in the LeHave and Margaree rivers in Nova Scotia. This suggests that within the alosines, there is a difference in the pattern of energy source mobilization, since American shad use protein in the early stages of migration. The migrations characterized in Crawford et al. (1986), however, were relatively short (<35 km) and do not rule out the use of protein as an energy source for longer migration in these species.

Clearly, upstream anadromous migration is energetically expensive for American shad. White and red muscle, SDF, liver, and viscera all contribute to energy use during migration. However, we have shown that white muscle and SDF store most of the energy that powers migration. Red muscle protein is spared during migration. Additionally, American shad are probably not energetically exhausted at the end of their current maximum migratory distance in the Connecticut River, since 40% energy depletion is common, but 60% depletion is possible. Differential use of energy between the sexes in the last region of the river encountered may indicate a sex-specific limitation on migration that may represent an energetic constraint on the extent of migration.

Acknowledgements

The authors would like to thank Dr. Mark Sheridan, the Massachusetts Fish and Wildlife Cooperative Research Unit (especially Don Pugh), the New Jersey Department of Environmental Protection (especially Russ Allen), the Vermont Department of Fish and Wildlife (especially Ken Cox), the Connecticut River Coordinators Office, Northeast Utilities, New England Electric Co., Harry Root, the crew of the FV *Compromise*, and particularly Todd Dubreuil and the students and staff of the S.O. Conte Anadromous Fish Research Center for their help in conducting this study. We would also like to acknowledge the assistance of Drs. Kevin Whalen, Joseph Zydlewski, and Andrew Hendry and two anonymous reviewers for their careful evaluation of previous versions of the manuscript.

References

Beamish, F.W.H., Potter, I.C., and Thomas, E. 1979. Proximate composition of the adult anadromous sea lamprey, *Petromyzon marinus*, in relation to feeding, migration and reproduction. J. Anim. Ecol. **48**: 1–19.

Berg, O.K., Thronaes, E., and Brenset, G. 1998. Energetics and survival of virgin and repeat spawning brown trout (*Salmo trutta*). Can. J. Fish. Aquat. Sci. **55**: 47–53.

Brafield, A.E. 1985. Laboratory studies of energy budgets. *In* Fish energetics: new perspectives. *Edited by* P. Tytler and P. Calow. Croom Helm, London, U.K. pp. 257–282.

Busacker, G.P., Adelman, I.R., and Goolish, E.M. 1990. Growth. *In* Methods for fish biology. *Edited by* C.B. Schreck and P.B. Moyle. American Fisheries Society, Bethesda, Md. pp. 363–388.

Carr, R.S., and Neff, J.M. 1984. Quantitative semiautomated enzymatic assay for tissue glycogen. Comp. Biochem. Physiol. B. Comp. Biochem. **77**: 447–449.

Craig, J.F., Kenley, M.J., and Talling, J.F. 1978. Comparative estimations of the energy content of fish tissue from bomb calorimetry, wet oxidation and proximate analysis. Freshwater Biol. **8**: 585–590.

Crawford, R.H., Cusak, R.R., and Parlee, T.R. 1986. Lipid content and energy expenditure on the spawning migration of alewife (*Alosa pseudoharengus*) and blueback herring (*Alosa aestivalis*). Can. J. Zool. **64**: 1902–1907.

Dingle, H. 1996. Migration: the biology of life on the move. Oxford University Press, New York.

Folch, J., Lees, M., and Stanley, G.H.S. 1957. A simple method for the isolation and purification of total lipids from animal tissues. J. Biol. Chem. **226**: 497–509.

Frings, C.S., Fendley, T.W., Dunn, R.T., and Queen, C.A. 1972. Improved determination of total serum lipids by the sulphophospho-vanillin reaction. Clin. Chem. **18**: 673–674.

Glebe, B.D., and Leggett, W.C. 1981*a*. Temporal, intra-population differences in energy allocation and use by American shad (*Alosa sapidissima*) during the spawning migration. Can. J. Fish. Aquat. Sci. **38**: 795–805.

Glebe, B.D., and Leggett, W.C. 1981*b*. Latitudinal differences in energy allocation and use during the freshwater migrations of American shad (*Alosa sapidissima*) and their life history consequences. Can. J. Fish. Aquat. Sci. **38**: 806–820.

Goolish, E.M. 1991. Aerobic and anaerobic scaling in fish. Biol. Rev. Camb. Philos. Soc. **66**: 3–56.

Gross, M.R., Coleman, R.M., and McDowall, R.M. 1988. Aquatic productivity and the evolution of diadromous fish migration. Science (Washington, D.C.), **239**: 1291–1293.

Hatano, M., Takahashi, K., Mathisen, O.A., and Amma, G. 1995. Biochemical differences in sockeye salmon that are ocean feeding and on the spawning grounds. J. Food Biochem. **19**: 269–284.

Hendry, A.P. 1998. Reproductive energetics of Pacific salmon: strategies, tactics, and trade-offs. Ph.D. thesis, University of Washington, Seattle, Wash.

Idler, D.R., and Bitners, I. 1958. Biochemical studies on sockeye salmon during spawning migration. II. Cholesterol, fat, protein, and water in the flesh of standard fish. Can. J. Biochem. Physiol. **36**: 793–798.

Idler, D.R., and Bitners, I. 1959. Biochemical studies on sockeye salmon during spawning migration. V. Cholesterol, fat, protein and water in the body of the standard fish. J. Fish. Res. Board Can. **16**: 235–241.

Jonsson, N., Jonsson, B., and Hansen, L.P. 1997. Changes in proximate composition and estimates of energetic costs during upstream migration and spawning in Atlantic salmon *Salmo salar*. J. Anim. Ecol. **66**: 425–436.

Jorgensen, E.H., Johansen, S.J.S., and Jobling, M. 1997. Seasonal patterns of growth, lipid deposition and lipid depletion in anadromous Arctic charr. J. Fish Biol. **51**: 312–326.

Kapoulas, V.M., and Miniadis-Meimaroglou, S. 1985. Composition and distribution of lipids in tissues of bogue (*Boops boops*). Z. Naturforsch. Sect. C. Biosci. **40**: 562–565.

Lambert, Y., and Dodson, J.J. 1990*a*. Freshwater migration as a determinant factor in the somatic cost of reproduction of two anadromous coregonines of James Bay. Can. J. Fish. Aquat. Sci. **47**: 318–334.

© 1999 NRC Canada

Lambert, Y., and Dodson, J.J. 1990*b*. Influence of freshwater migration on the reproductive patterns of anadromous populations of cisco (*Coregonus artedii*) and lake whitefish (*C. clupeaformis*). Can. J. Fish. Aquat. Sci. **47**: 335–345.

Leggett, W.C., and Trump, C.L. 1978. Energetics of migration in American shad. *In* Animal migration, navigation and homing. *Edited by* K. Schmidt-Koenig and W.T. Keeton. Springer-Verlag, New York. pp. 370–377.

Leonard, J.B.K., and McCormick, S.D. 1999. The effect of migration distance and timing on metabolic enzyme activity in an anadromous clupeid, the American shad (*Alosa sapidissima*). Fish Physiol. Biochem. **20**: 163–179.

Lowry, O.H., Rosenbrough, N.J., Farr, A.L., and Randall, R.J. 1951. Protein measurement with the folin phenol reagent. J. Biol. Chem. **193**: 265–275.

Luzzana, U., Serrini, G., Moretti, V.M., Grimaldi, P., Paleari, M.A., and Valfre, F. 1996. Seasonal variations in fat content and fatty acid composition of male and female coregonid 'bondella' from Lake Maggiore and landlocked shad from Lake Como (northern Italy). J. Fish Biol. **48**: 352–366.

Raabo, E., and Terkildsen, T.C. 1960. On the enzymatic determination of blood glucose. Scand. J. Clin. Lab. Invest. **12**: 402.

Reid, R.A., Durance, T.D., Walker, D.C., and Reid, P.E. 1993. Structural and chemical changes in the muscle of chum salmon (*Oncorhynchus keta*) during spawning migration. Food Res. Int. **26**: 1–9.

Roff, D.A. 1988. The evolution of migration and some life history parameters in marine fishes. Environ. Biol. Fishes, **22**: 133–146.

Rulifson, R.A. 1994. Status of anadromous *Alosa* along the east coast of North America. *In* Anadromous Alosa Symposium. *Edited by* J.E. Cooper, R.T. Eades, R.J. Klauda, and J.G. Loesch. American Fisheries Society, Bethesda, Md. pp. 134–158.

Sheridan, M. 1988. Lipid dynamics in fish: aspects of absorption, transportation, deposition and mobilization. Comp. Biochem. Physiol. B. Comp. Biochem. **90**: 679–690.

Sheridan, M., Allen, W.V., and Kerstetter, T.H. 1983. Seasonal variations in the lipid composition of the steelhead trout, *Salmo gairdneri* Richardson, associated with the parr–smolt transformation. J. Fish Biol. **23**: 125–134.

Snedecor, G.W., and Cochran, W.G. 1989. Statistical methods. 8th ed. Iowa State University Press, Ames, Iowa.

Sokal, R.R., and Rohlf, F.J. 1995. Biometry. 3rd ed. W.H. Freeman and Co., New York.

Somero, G.N., and Childress, J.J. 1980. A violation of the metabolism-size scaling paradigm: activities of glycolytic enzymes increase in larger-size fish. Physiol. Zool. **53**: 322–337.

St. Pierre, R. 1994. American shad restoration in the Susquehanna River. *In* Anadromous Alosa Symposium. *Edited by* J.E. Cooper, R.T. Eades, R.J. Klauda, and J.G. Loesch. American Fisheries Society, Bethesda, Md. pp. 81–85.

Weihs, D. 1977. Effects of size on sustained swimming speeds of aquatic organisms. *In* Scale effects in animal locomotion. *Edited by* T.J. Pedley. Academic Press, New York. pp. 333–338.

Whitear, M. 1984. Dermis. *In* The skin of fishes including cyclostomes. *Edited by* J. Bereiter-Hahn, A.G. Matoltsy, and K. Sylvia-Richards. Springer-Verlag, New York. pp. 39–64.

Williams, I.V., and Brett, J.R. 1987. Critical swimming speed of Fraser and Thompson River pink salmon (*Oncorhynchus gorbuscha*). Can. J. Fish. Aquat. Sci. **44**: 348–358.

© 1999 NRC Canada

Exceptions to semelparity: postmaturation survival, morphology, and energetics of male chinook salmon (*Oncorhynchus tshawytscha*)

M.J. Unwin, M.T. Kinnison, and T.P. Quinn

Abstract: Between 2.1 and 6.8% of fall-run male chinook salmon (*Oncorhynchus tshawytscha*) reared in two New Zealand hatcheries matured as yearling parr, of similar size to immature siblings. The incidence of mature parr in 58 half-sib families ranged from 0 to 69% of the available males. Although chinook salmon are normally semelparous, about 80% of mature parr survived to mature again at age 2, and all fish held for another year matured again at age 3. All three ages produced milt that successfully fertilized eggs. Morphological development in mature parr and repeat-maturing males was consistent with that of older, first time maturing males. The gonadosomatic index for mature age-2 males was 11.7, 7.2, and 5.4% for repeat-maturing males, freshwater-reared males, and sea-run males, respectively. Muscle energy density for repeat-maturing males (4.45 kJ/g) was lower than for normal males (5.20–5.45 kJ/g) and negatively correlated with the gonadosomatic index. Although we think it unlikely that repeat maturation occurs regularly in the wild, our results indicate that under favorable conditions, chinook salmon can exhibit some iteroparous traits. We hypothesize an evolutionary continuum between semelparity and iteroparity in salmonids, primarily characterized by modifications in a few key energetic and physiological thresholds.

Résumé : De 2,1 à 6,8% de la remonte d'automne de quinnats (*Oncorhynchus tshawytscha*) mâles élevés dans deux écloseries de la Nouvelle-Zélande ont atteint la maturité sexuelle alors qu'ils étaient des tacons d'un an de taille similaire à leurs congénères immatures issus des mêmes géniteurs. La proportion de tacons matures dans 58 familles à demi-apparentées était de 0 à 69% des mâles existants. Bien que le quinnat soit normalement sémelpare, environ 80% des tacons matures ont survécu pour atteindre une seconde maturité sexuelle à l'âge de 2 ans, et tous les poissons gardés pour une autre année ont atteint une nouvelle maturité à l'âge de 3 ans. Les poissons de ces trois âges ont produit une laitance qui a pu féconder des oeufs avec succès. Le développement morphologique des tacons matures et des mâles qui ont atteint plusieurs maturités sexuelles était semblable à celui des mâles plus vieux qui ont atteint leur première maturité à un âge plus avancé. Les indices gonadosomatiques des mâles matures de 2 ans étaient de 11,7, 7,2 et 5,4% chez les mâles à maturation multiple, les mâles élevés en eau douce et les mâles anadromes, respectivement. La densité énergétique des muscles chez les mâles à maturation multiple (4,45 kJ/g) était inférieure à celle observée chez les mâles normaux (5,20–5,45 kJ/g) et corrélée négativement avec l'indice gonadosomatique. Bien que nous jugions improbable que la maturation multiple se produise régulièrement dans la nature, nos résultats indiquent que, dans des conditions favorables, le quinnat peut montrer certains caractères d'itéroparité. Nous formulons une hypothèse suivant laquelle il y aurait un continuum évolutionnaire entre la sémelparité et l'itéroparité chez les salmonidés, principalement caractérisé par des modifications de quelques seuils énergétiques et physiologiques importants.

[Traduit par la Rédaction]

Introduction

Salmonid fishes display a variety of interrelated life history traits (Scott and Crossman 1973; Groot and Margolis 1991). Key traits include variation in age at first maturation, the proportion of each population that survives to spawn more than once (iteroparity), frequency of spawning events for given individuals, and migration between freshwater spawning and incubation sites to marine feeding areas (anadromy). Anadromy is generally associated with high growth rate, early age at maturation, and lower probability of repeat spawning. These life history traits vary within the family, ranging from fully freshwater, iteroparous, long-lived species such as lake trout (*Salvelinus namaycush*) to invariably semelparous, short-lived, anadromous species such as pink salmon (*Oncorhynchus gorbuscha*). There is also great variation among populations within species and between males and females in life history patterns and the degree of anadromy (e.g., Groot and Margolis 1991; Jonsson and Jonsson 1993). Such variation presumably reflects evolutionary adaptations to the fact that marine waters occupied by salmonids provide greater opportunities for growth than

Received July 28, 1998. Accepted February 5, 1999.
J14716

M.J. Unwin. National Institute of Water and Atmospheric Research, Box 8602, Christchurch, New Zealand.
M.T. Kinnison[1] and T.P. Quinn. School of Fisheries, Box 357 980, University of Washington, Seattle, WA 98195, U.S.A.

[1]Author to whom all correspondence should be addressed: Department of Biological Sciences, Dartmouth College, Gilman Hall, Hanover, NH 03755, U.S.A. e-mail: mike.kinnison@Dartmouth.EDU

© 1999 NRC Canada

freshwater habitats, but exploitation of these rich feeding areas exposes them to a higher mortality rate and a sometimes arduous return migration to the spawning site.

Chinook salmon (*Oncorhynchus tshawytscha*) are generally considered to be entirely semelparous and anadromous within their natural range but vary widely in timing of migrations and age at maturity, both between and within populations. Age at maturation is most commonly between 3 and 5 but ranges from 2 to 8 (Healey 1991; Roni and Quinn 1995). The species is often divided into ocean-type populations, in which juveniles spend a few months in freshwater prior to seaward migration, and stream-type populations, in which juveniles migrate after a full year or more in the river (e.g., Healey 1983). Modal age at maturity tends to be younger for ocean-type populations, and in many populations, some males (termed "jacks") mature at a younger age than the youngest females in the population (Healey 1991; Roni and Quinn 1995). Age at maturation in chinook salmon is partially subject to genetic control (Hankin et al. 1993; Heath et al. 1994*a*), but as in most salmonids (see Thorpe 1986) is also strongly influenced by growth rate. For example, age at maturity tends to be younger for hatchery-produced chinook salmon than for related wild fish (e.g., Unwin and Glova 1997).

In a number of chinook salmon populations, a small proportion of male parr mature at the end of their first year of life, while still resident in freshwater, in a phenomenon often termed "precocious" maturation. Unlike jacks, which have gone to sea and returned at a younger age than females of their population, mature parr have remained in freshwater throughout their first year of life. However, because the term "precocious" could apply to jacks as well as to mature parr, and also because it implies some abnormality (cf. Thorpe 1986), we avoid it in this paper. To remove any possible ambiguity, we use the term "mature male parr" to refer specifically to stream- or hatchery-resident male chinook salmon maturing towards the end of their first year of life, with both a total age (measured from the date of fertilization) and a freshwater age of about 12 months. (An exception to this definition would be stream-type populations in which some individuals rear in streams for 2 years prior to seaward migration (e.g., Beacham et al. 1989); such mature parr might be 2 years old.)

Parr maturation has been reported in populations of both natural and hatchery origin in many river systems (e.g., Robertson 1957; Flain 1970; Taylor 1989; Bernier et al. 1993). These fish produce viable sperm (e.g., Robertson 1957) and can survive into their second year and reinitiate gonad development under hatchery conditions (Flain 1971) or after transfer to seawater (Bernier et al. 1993). Understanding the processes that underlie parr maturation and repeat maturation may provide important insights into the evolution of salmonid life histories, particularly with regard to semelparity and iteroparity. However, some important questions remain unanswered. Is parr maturation necessarily associated with stream-type populations (e.g., Taylor 1989; Healey 1991) or can it occur more generally? To what extent do the physical changes associated with parr and repeat maturation mirror the normal maturation process in older fish? Is repeat maturation limited to fish transferred to seawater after first maturing as parr (cf. Bernier et al. 1993) or can it occur entirely in freshwater? If so, how many times can individual males mature? How do energetic and physiological influences affect early and repeat maturation? Taking these issues into account, is repeat maturation of chinook salmon likely under natural conditions, and what does the process reflect about the evolutionary association between semelparity and iteroparity?

The objectives of this study were to document the incidence of mature male parr among hatchery-reared chinook salmon in New Zealand and test the hypotheses that (*i*) ocean-type parents as well as stream-type parents can produce mature male parr, (*ii*) mature parr are larger than immature fish at the time of maturation, (*iii*) mature parr are unevenly distributed among families, (*iv*) the offspring of mature parr show a higher incidence of mature parr than offspring sired by older males, and (*v*) mature parr necessarily die at the end of the spawning season. The last hypothesis was falsified and many such mature parr survived the first spawning season, allowing us to test the additional hypotheses that growth, gonad size, energy density, and morphology of repeat-maturing individuals are similar to those traits in mature male parr and males maturing for the first time at age 2 or greater.

Methods

Study populations

New Zealand's chinook salmon populations are derived from fall-run (ocean-type) Sacramento River stock (McDowall 1994; Quinn et al. 1996) and are primarily confined to the large, glacier-fed rivers on the east coast of the South Island where spawning typically occurs from mid-April to early June (Quinn and Unwin 1993). Fish in this study were mostly derived from Glenariffe Stream (43°18′S, 171°22′E), a spring-fed headwater tributary of the upper Rakaia River, in which chinook salmon have been studied since 1965 (Unwin 1986, 1997). Prior to 1979, this population was maintained by natural spawning, with some hatchery supplementation during the 1980's after hatchery facilities were developed in the late 1970's (Unwin and Glova 1997). During the latter period, maturing male parr were frequently encountered during routine husbandry operations or coded-wire tag (CWT) application. Mature parr were distinguishable from immature fish by their darker, less silvery body color compared with immature parr, a greenish pigmentation in the fins, and a less-streamlined body (cf. Taylor 1989). The mature parr tended to expel milt freely when handled, and their musculature was noticeably less firm to the touch than that of immature parr.

There were two large-scale experimental programs on chinook salmon, conducted from 1982 to 1984 and from 1994 to 1998. They allowed us to collect data on mature male parr to test our hypotheses but were not designed expressly for that purpose. Consequently, some characteristics of our data were constrained by the design and (or) logistic requirements of the main programs. When presenting our data, these constraints are noted only when they are relevant to interpretation of our results.

Between April 1982 and November 1984, 923 000 fry from the 1982 and 1983 brood years were raised at Glenariffe Stream as part of a study of the effects of date and size at release on survival of chinook salmon smolts. All fry were reared in concrete hatchery raceways at ambient stream temperature (7–14°C) and were fed a standard OMP diet. The date and size protocol was to divide the fish into 102 groups (over 2 years), representing predetermined size ranges (range of mean weights 10–150 g), and release them at selected monthly intervals to include a range of sizes on each

© 1999 NRC Canada

release date. Each group was marked with CWT's and released from March to November, corresponding to ages of 10–18 months postfertilization (Unwin 1997). About 100 fry from each CWT group were sacrificed 1 day before release for measurement of fork length (FL) and weight and recovery of CWT's. All fish were sexed by dissection and examination of the gonads, and any maturing parr were identified.

In addition, an intensive experimental program was initiated at Glenariffe Stream in 1994 to determine whether New Zealand chinook salmon have developed into genetically distinct populations over the 90 years since their introduction (Kinnison et al. 1998*a*). We collected gametes from 108 mature adults in two study streams, Glenariffe Stream and the Hakataramea River (44°43′S, 170°30′E), a tributary of the Waitaki River 150 km southwest of the Rakaia River. The gametes were taken to the Silverstream Research Station (44°43′S, 170°30′E) on the lower Waimakariri River and used to establish a total of 72 full-sib families nested within 36 half-sib families by crossing each male with two females. These were subsequently culled to 58 full-sib families within 29 half-sib families, evenly divided between the two populations. Unless otherwise specified, the term "family" refers to one full-sib family. We determined the age and life history type (i.e., ocean, stream, or hatchery) for all adults by scale pattern analysis (Unwin and Lucas 1993). When culling families, we tried to retain those for which both parents were of natural (ocean or stream) rather than hatchery origin. Families were individually incubated, hatched, and reared in ambient (12.4°C) well water (Kinnison et al. 1998*a*). At about 6 months postfertilization, each family was randomly assigned to one of 29 3000-L circular tanks, with two families (one marked by excision of the adipose fin) sharing each tank.

Incidence, size, and growth of mature male parr

For each family, we estimated mean fry weight on 12 occasions between 10 August 1994 and 18 April 1995 (Kinnison et al. 1998*b*). We examined about 300 fish from each family for the presence of mature male parr between 24 April and 4 May 1995 (about 12 months postfertilization) as a prelude to tagging and further experimental protocols. We calculated the incidence of mature male parr on the assumption that 50% of the fish examined were males. We used a nested ANOVA on arcsine square root transformed proportions, with sires nested within populations, to determine if there were significant population and sire effects that would suggest heritable influences on incidence.

Fertilization trials and postmaturation survival

We used the combined pool of mature parr from all experimental families to initiate several further experiments. First, we tested the viability of milt from six mature parr by fertilizing six samples of 100–200 ova (collected from two mature females) and incubating these at Silverstream under standard hatchery conditions. We estimated fertilization rates for each male by counting the number of live and dead ova after shocking (by brief physical agitation) 29 days after fertilization. All surviving ova were hatched and reared for a further 12 months, initially at Silverstream (to a weight of about 5 g) and then at Glenariffe. In April 1996, these fish were individually examined to determine the incidence of mature male parr.

We retained about 150 of the mature parr collected in April and May 1995 in a 6-m-diameter circular holding pond at Glenariffe, where they were reared (under standard hatchery procedures) to determine whether they could survive for a second year. At age 2 (26 April 1996), 118 surviving fish were collected. All of these had matured a second time, and milt from six mature individuals was used in another fertilization trial at Silverstream, using the same protocol as in 1995. Most of the remaining fish were sacrificed for collection of ancillary data (see next paragraph), but 10 fish were reared for another year. All survived and matured for a third time (at age 3) in April 1997, at which time, we used milt from six individuals to conduct a third fertilization trial.

Reproductive output and energy density

Representative individuals from all experimental groups (i.e., the mature parr collected in April 1995, their survivors in 1996 and 1997, and the age-1 progeny of the 1995 fertilization trial) were sacrificed for measurement of FL, weight, and gonad weight. We measured gonad weight by removing the testes from the body cavity and weighing the total mass, taking care to include any expressed milt. We calculated the gonadosomatic index (GSI) for each fish, where GSI is the wet gonad weight as a percentage of the total body weight (including gonads), to compare gonad development and relative gonad size between groups, excluding any individuals visually assessed as underripe (i.e., with testes not fully developed) or overripe (i.e., with testes partially or wholly spent).

To provide additional comparisons with "normal" fish (i.e., those maturing no earlier than the end of their second year), we drew on two parallel experimental groups established in April 1995 from siblings of the Glenariffe and Hakataramea families. One group consisted of 2900 fish (50 from each of 58 families), individually marked with passive integrated transponder (PIT) tags and subsequently reared in captivity at Glenariffe. A second group (totaling 141 000 fish marked with CWT's) was released from Glenariffe Stream in July 1995, thereby gaining access to the South Pacific Ocean via the Rakaia River and returning as sea-run fish from 1996. Mature 2-year-old fish from both groups were examined at Glenariffe in April and May 1996, allowing for measurement of size and GSI using the same protocols as above. We used a somatic condition factor ($CF_{som} = 10^5 \times W_{som}/FL^3$, where W_{som} = total body weight – testes weight) to provide a measure of body robustness independent of gonad development. For most groups of fish, we also dissected about 10 g of tissue from the dorsolateral muscle, anterior to the dorsal fin. After oven drying this tissue at 95°C for 24 h, we calculated the ratio of dry weight to total weight (each measured to ± 0.0001 g) and used the general nonlinear model for energy density (ED, joules per gram) given by Hartman and Brandt (1995) ($ED = 45.29 \times (\%\ \text{dry weight})^{1.507}$) to estimate specific ED for each individual. To obtain ED estimates for yearling parr (which was not measured in autumn 1995), we collected additional tissue samples from two yearling groups held at Glenariffe in April 1996 and May 1998.

Body morphology and salinity tolerance

We analyzed morphology based on a series of landmark points (Table 1) to characterize morphological differences between immature parr, mature parr, mature 2-year-old males, and 2-year-old repeat-maturing males. Parr were placed on a sheet of paper and a pin was used to mark each landmark point for subsequent data capture via a digitizing pad. To characterize morphological development in normal males, we collected similar data for 109 PIT-tagged fish sampled in November 1995 (at an age of 18 months) from the captive freshwater group at Glenariffe and later (as mature 2-year-old males) in April 1996. The morphology of these fish at maturation was also compared with that of 78 repeat-maturing males collected at the same time and age. For these (and all subsequent fish), morphometric data were obtained by placing each fish on its left side (alongside a 40-cm ruler), taking a photograph from a camera mounted directly overhead, and digitizing all points of interest from the resulting print.

In most cases, we compared landmark arrangements via relative warps analysis (Rohlf 1993). To allow for the substantial size difference between repeat- and first time maturing age-2 males, and possible allometric effects in this comparison, we calculated four univariate measures likely to differ between groups (snout length: point 1 to point 17; hump size: point 14 to point 19; belly depth: point 4 to point 20; anal region depth: point 12 to point 5) from the

© 1999 NRC Canada

Table 1. Landmark points used for morphometric and relative warps analysis.

Point	Description
1	Tip of snout
2	Outline point directly ventral to posterior end of maxilla
3	Outline point directly ventral to pectoral fin insertion
4	Outline point directly ventral to pelvic fin insertion
5	Anterior insertion of anal fin
6	Posterior insertion of anal fin
7	Ventral insertion of caudal fin
8	Central point of hypural flexure
9	Caudal fork
10	Dorsal insertion of caudal fin
11	Posterior insertion of adipose fin
12	Anterior insertion of adipose fin
13	Posterior insertion of dorsal fin
14	Anterior insertion of dorsal fin
15	Outline point directly dorsal to point 16
16	Dorsal insertion of gill plate
17	Center of eye socket
18	Insertion of pectoral fin
19	Vertical projection of point 14 onto lateral line
20	Vertical projection of point 4 onto lateral line

landmark points. The groups were then compared relative to body length using ANCOVA of logged trait values versus logged mideye to hypural length.

We assessed the salinity tolerance of maturing male parr by including 10 individuals in a hypersalinity trial conducted on the main group of 58 families in May 1995. The challenge was implemented by placing the fish to be tested into water at a salinity of 45 ppt and recording time to death, FL, and weight for each fish. Full details of the experimental protocol and results of family- and population-level comparisons are given in Kinnison et al. (1998*b*).

Results

Incidence of mature male parr

Of 4624 male parr examined between 5 March and 1 November in 1983 and 1984, 96 (2.1%) were sexually mature. Mature parr were recorded in all months except November (when only 18 males were examined) but were most common in March (nine out of 288 fish; 3.1%) and April (38 out of 883 fish; 4.3%). They were less prevalent from June to October but still comprised 1.2% (30 fish) of 2590 parr examined over this period. Mature male parr were relatively more common in the 1995 families, comprising 572 of 16 853 parr examined (3.39% of the total, or 6.79% of the males).

The incidence of mature male parr within families varied greatly. Of the 58 families examined (all but four of which had between 293 and 304 individuals), 12 had no mature parr and another 16 families had fewer than five. By contrast, 15 families produced more than 15 mature males, including one family (of Glenariffe origin) that yielded 97 mature parr from the original 300 fish (69% of the estimated males). The family sharing the same tank yielded only two such fish out of 297 examined, indicating that the unusually high proportion of mature parr in the other family was not an artifact of the rearing regime in that particular tank. Despite family variation in the incidence of mature parr, nested ANOVA on transformed proportions did not indicate significant sire ($p = 0.23$) or population ($p = 0.12$) effects. Moderate deviations from a 50:50 sex ratio within each family would have relatively little effect on the estimated incidence of mature male parr and could not account for the observed level of variation. Even if the imbalance were as much as 2:1, so that a sample of 300 individuals could include between 100 and 200 males (much greater than the estimated 95% confidence interval of ± 17 males for 300 fish per family), a count of five or fewer mature parr out of 300 fish would represent a lower incidence of maturation (0–5%) than a count of 15 or more (at least 7.5%).

Scale pattern analysis of the parents indicated that mature male parr were descended from parents with an ocean-type life history. In 40 families for which both parents were positively identified as ocean-type individuals (including the family with 97 mature males), the incidence of mature parr was 445 out of 11 475, or 7.8% of the assumed males. The only family derived from a stream-type parent (crossed with an ocean-type individual) produced seven mature parr out of 300 (2.3%; similar to the average for all families combined).

Size and growth

Size differences between mature and immature parr were apparent in both 1983–1984 and 1995 but were inconsistent between seasons and were generally small compared with the size range within each cohort. Mature parr recorded in 1983–1984 were slightly longer than normal parr (nested ANOVA of log FL by month and maturity: all fish, $p = 0.001$; males only, $p = 0.006$). However, the size difference was small in absolute terms (mature males: FL = 132.5 mm; immature males: FL = 131.2 mm) and the significance of this result is primarily attributable to the large sample size ($N = 4510$) for immature male parr. By contrast, mature male parr recorded in 1995 were smaller than immature parr of unknown sex (mature: 161.5 mm, $N = 97$; immature: 167.7 mm, $N = 278$; t test, $p < 0.001$). Mature parr recorded in 1983–1984 lay within a much more restricted length range than immature male parr (Fig. 1). Only six (6%) of the 96 mature parr were smaller than 110 mm or larger than 160 mm FL whereas 41% of immature males fell outside this size range. However, no difference in variance was apparent in 1995.

Mature parr were heavier for their length than immature parr. ANCOVA of log W on maturity, with log FL as the covariate, showed no interaction between maturity and slope ($p = 0.23$) but a difference in elevation of the regression line for mature and immature parr ($p < 0.001$). This was equivalent to an average weight difference of 15.2% between mature and immature parr of the same length. Mean condition indices (unadjusted for gonad weight) were 1.33 for mature parr compared with 1.13 for immature parr.

The incidence of mature parr in each family was uncorrelated with mean weight within the family, as measured on 18 April 1995 ($p = 0.92$) or at any of the 11 earlier weigh-ups ($p > 0.05$ in all cases), with mean alevin weight ($p > 0.16$ for all four weigh-ups), and with mean ova weight ($p = 0.83$). We looked for evidence of a family-level correlation between the incidence of mature parr and growth rate by considering all possible pairs of dates for the 12 successive fry weigh-ups, estimating mean specific growth rate

© 1999 NRC Canada

Fig. 1. Box and whisker plots showing variation in FL between mature and immature parr by month for combined 1983 and 1984 data. Sample sizes (mature parr in italics) are shown above each box. Each plot shows the median, the upper and lower quartiles, the upper and lower inner fences, and any outlying points (asterisk). Variations in mean FL between months are an artifact of the 1982–1983 time and size at release protocol.

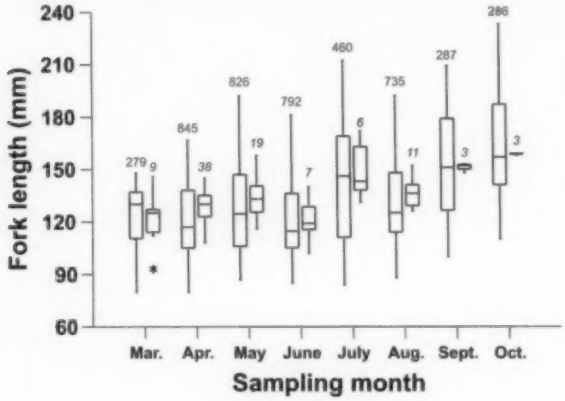

(percent weight gain per day) for each family over the 132 (12 × 11) date intervals, and calculating the Pearson correlation coefficient. Only three of these coefficients (ranging from –0.27 to –0.30, all corresponding to intervals from September 1994 to March 1995) were significant at $p < 0.05$, and none were significant at $p < 0.01$. Because this result is more or less what would be expected by chance in a set of 132 randomly generated correlation coefficients, we conclude that our data show no evidence of a correlation between growth rate and maturation.

Body morphology

Differences in body morphology between 278 immature and 97 mature male parr were clearly apparent via analysis of relative warps. The first relative warp (analogous to a principal component of geometric shape) described 32% of the morphometric variation in the two groups combined. This relative warp also best described the morphometric difference between mature parr and their immature relatives ($p < 0.001$) (Fig. 2*a*). Physically, this warp describes increased development of the hump and snout in mature parr, together with a "deepening" of the anal region (Fig. 2*b*). By contrast, their immature relatives had a more streamlined body with a longer and shallower caudal peduncle more typical of fish undergoing smolt transformation. Relative warp 7 also differed slightly between the immature and mature parr, but it explained only 4.0% of variation in shape, did not have a clear biological interpretation, and contributed much less to group separation than warp 1 (Fig. 2*a*).

The pattern of development in mature male parr strongly resembled the morphological development that we observed, from 18 to 24 months of age, in repeated measures of 109 of their individually tagged male siblings that matured at age 2. The first relative warp captured 34% of the morphometric variation and best described the difference between fish before and after maturation ($p < 0.001$) (Fig. 3). Development of the snout and hump and deepening of the anal region

Fig. 2. Relative warps analysis results for mature male parr (solid symbols) and immature fish of the same age (open symbols) in terms of (*a*) relative warp 1 versus relative warp 7 scores and (*b*) extremes of relative warp 1 (exaggerated for clarity) along the axis best describing shape differences between the groups. Landmark points are numbered as in Table 1 and are aligned relative to points 1 and 9.

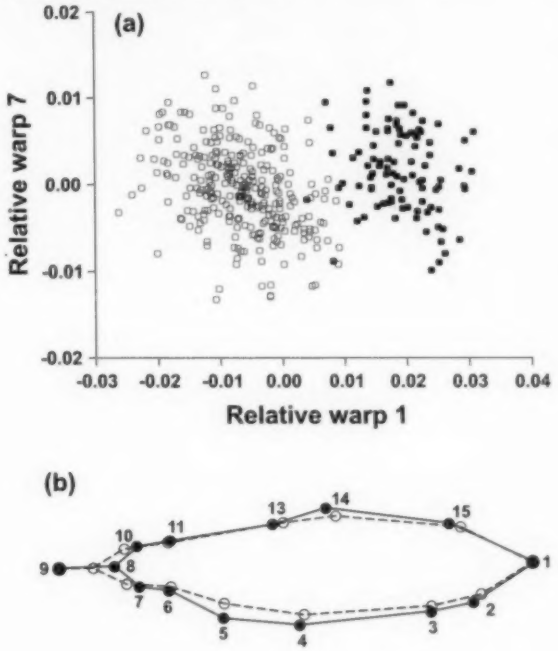

were again characteristic and were slightly more pronounced than in mature male parr. Warp 12 showed a relatively small amount of group separation compared with warp 1 (Fig. 3) but explained only 1.6% of the variation in shape and lacked a clear biological interpretation. Comparison of univariate size-adjusted traits indicated that repeat-maturing fish were 13.9% greater in belly depth and 6.6% greater in anal region depth ($p < 0.001$ in both cases) than males reared in freshwater and maturing for the first time at age 2.

Fertilization trials

All six mature yearling parr tested in April 1995 produced viable milt. Of 1030 ova shocked, 986 were fully viable and survived at least until hatching, 35 had weak or malformed embryos, and only nine showed no evidence of successful fertilization. Mean fertilization rate (for the fully viable ova) was 95.5%, ranging from 87 to 98% for the six individual males. Similar results were obtained for six freshwater-reared fish spawning a second time in April 1996 (mean 87.2%, range 71–94%) and for a final group of six of these fish maturing for the third successive year (at age 3) in April 1997 (mean 93.3%, range 92–95%). The fertilization rate exceeded 90% for 14 of the 18 individuals tested over the three seasons. This compares with rates of 75–85% for routine hatchery operations at Silverstream, based on delayed (4–6 h) fertilization (National Institute of Water and Atmospheric Research, unpublished data).

© 1999 NRC Canada

Fig. 3. Relative warps analysis results for 109 individually marked males that matured at age 2, at 18 months (6 months prior to maturation) (open symbols), and at 24 months (fully mature) (solid symbols) in terms of (*a*) relative warp 1 versus relative warp 12 scores and (*b*) extremes of relative warp 1 (exaggerated for clarity) along the axis best describing shape differences between the groups. Landmark points are numbered as in Table 1 and are aligned relative to points 1 and 9.

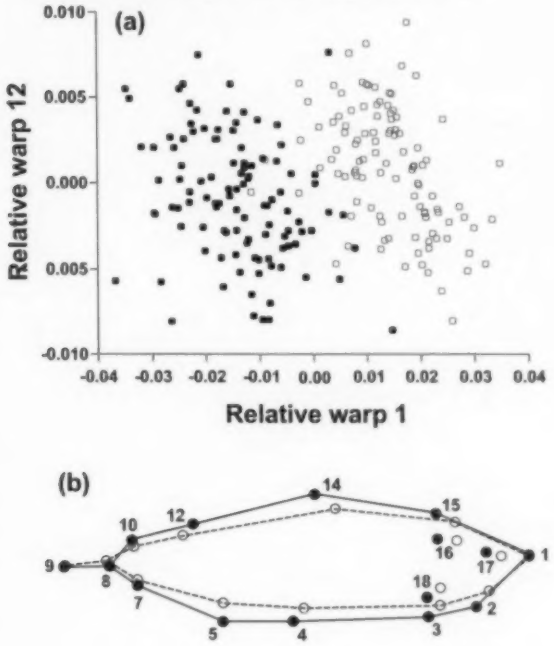

Of 728 progeny from the April 1995 fertilization trial (using mature parr as sires) examined in April 1996, 27 (3.7%) were mature male parr, representing 7.4% of the assumed male half of the population. This proportion did not differ from the 6.79% incidence of mature parr among their parent stock, as determined in April 1995 ($\chi^2 = 0.22$, $p = 0.64$).

Postmaturation survival, growth, and reproductive output

Survival of mature parr to the end of their second year was high (118 out of about 150 individuals, or about 80%), but growth during this period was extremely poor. By April 1996, their mean weight had increased from 57 g (in April 1995) to 333 g, but they were well under half the weight of their freshwater-reared male siblings maturing for the first time at age 2 and less than 30% as heavy as mature sea-run age-2 males (ANOVA with post hoc Bonferroni tests, $p < 0.001$ for all paired comparisons) (Table 2). Examination of stomach contents from repeat-maturing males in April 1996 suggested that they were feeding actively at that time, with nearly all fish examined having undigested food in their gut. However, in most individuals the gut wall showed signs of partial degradation, appearing thinner and less muscular than in immature parr.

Reproductive output for mature male parr was high relative to body weight (Table 2). Mean GSI for parr maturing in April 1995 (9.14%) was substantially greater than for either of their sibling groups maturing for the first time at age 2 (freshwater reared: 7.23%; sea-run: 5.39%; ANOVA with post hoc Bonferroni tests, $p < 0.001$ for all paired comparisons). Mean GSI for age-2 repeat-maturing fish was higher still, averaging 11.67% and ranging from 4.7 to 16%. The 10 males maturing for a third successive year had a mean GSI of 7.9% (range 4.8–10.3%). We retained 10 mature parr (collected in April 1996 from a 1995 spawning) at Glenariffe until 26 November 1996, at which time, nine surviving fish were sacrificed to determine the state of their gonads midway through the second year of life. Their testes were greatly reduced in size compared with the previous autumn, with a mean GSI of 1.2% (range 0.8–1.7%). However, all individuals retained the general appearance of mature male parr (including enlarged fins and dark coloring) and still exuded a small quantity of milt (of unknown viability) when squeezed gently around the vent.

Specific ED for 2-year-old males varied among the three sibling groups maturing in 1996, being highest for freshwater-reared males, slightly lower for sea-run males, and lowest for the repeat-maturing males (ANOVA with post hoc Bonferroni tests, $p < 0.001$ for all paired comparisons) (Table 2). Specific ED was negatively correlated with GSI for all three groups combined ($r = -0.62$, $p < 0.001$) (Fig. 4), although when each life history type was considered separately, only the repeat-maturing males exhibited the same trend ($r = -0.59$, $p < 0.001$). The loss in energy with increasing GSI for this latter group was substantial, predicted ED (based on linear regression of ED on GSI) declining from 4.33 kJ/g for a fish with a GSI of 10% to 3.47 kJ/g for a GSI of 15%. This trend was partially confounded by a negative correlation between CF_{som} and GSI ($r = -0.55$, $p < 0.001$) and a positive correlation between CF_{som} and ED ($r = 0.70$, $p < 0.001$), both of which are consistent with an energetic trade-off between gonad development and production of somatic tissue. However, regression analysis and examination of residuals confirmed a tendency for ED to decline with increasing GSI independent of CF_{som} ($r = -0.29$, $p = 0.014$). CD_{som} did not differ between 2- and 3-year-old repeat-maturing fish (t test, $p = 0.07$) despite their differences in mean ED (Table 2). Mean ED's for yearling parr were 5.81 kJ/g (April 1996 immature: mean FL = 224 mm, $N = 30$), 5.23 kJ/g (April 1996 mature: FL = 212 mm, $N = 10$), and 4.60 kJ/g (May 1998 mature: FL = 133 mm, $N = 47$), respectively. ED for both groups of mature parr was less than for immature parr but also differed between seasons for the two groups of mature parr (ANOVA with post hoc Bonferroni tests, $p < 0.001$ for all paired comparisons).

Mature male parr were less able to withstand hypersaline conditions than their immature counterparts. Mean survival time for the 10 mature parr subjected to the hypersalinity challenge was 11 h 8 min compared with 29 h 53 min for immature parr ($p < 0.001$).

Discussion

Based on our observations at Glenariffe and Silverstream, maturation of male chinook salmon parr was a common (although not routine) occurrence in the populations that we examined. Such males were able to survive and mature

© 1999 NRC Canada

Table 2. Mean (± 1 SE) size (FL and weight), reproductive output (testes weight and GSI), and muscle ED for five groups of sibling chinook salmon maturing over three consecutive seasons (1995–1997).

Maturation number	First	First	First	Second	Third
Age at first maturation	1	2	2	1	1
Age at this maturation	1	2	2	2	3
Rearing environment	Hatchery	Sea-run	Hatchery	Hatchery	Hatchery
N	81	87	126	78	10
FL (mm)	161±9	454±6	373±5	278±7	342±7
Weight (g)	57.0±1.0	1177±45	796±37	333±47	645±62
Testes weight (g)	5.21±0.14	63.6±3.6	57.8±3.0	37.7±3.8	50.5±6.2
GSI (%)	9.14±0.18	5.39±0.32	7.23±0.27	11.67±0.34	7.87±0.56
ED (kJ/g)[a]	—	5.20±0.12	5.45±0.10	4.45±0.12	5.15±0.24

[a]*N* = 73–108 for 2-year-old groups.

Fig. 4. Muscle ED versus GSI for three sibling groups of 2-year-old male chinook salmon maturing in autumn 1996. Individual groups are sea-run fish maturing for the first time (○), hatchery-reared fish maturing for the first time (+), and hatchery-reared fish maturing for the second time (●).

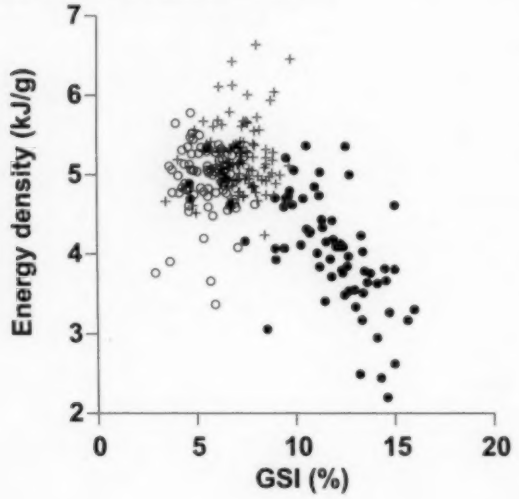

again for at least two more seasons while remaining in a freshwater hatchery environment. Our studies also suggest that parr maturation is not limited to stream-type populations but can occur under some conditions in ocean-type populations (e.g., when juveniles were held in freshwater for a year). Taken together, these results suggest that the phenomena of parr and repeat maturation in male chinook salmon occur under a wider range of conditions than has been recognized to date.

Maturation of chinook salmon parr is generally regarded as a characteristic of stream-type populations (Healey 1991; Mullan et al. 1992), which are, in turn, traditionally associated with spring-run adults (Healey 1983, 1991). In a laboratory study of four British Columbia chinook salmon populations, Taylor (1989) found that mature parr comprised 12–29% of the males in two stream-type populations (Slim Creek and Bowron River) but did not occur in two ocean-type populations (Harrison River and Nanaimo River). New Zealand chinook salmon are descended from fall-run Sacramento River stocks (McDowall 1994; Quinn et al. 1996), and both the seasonal timing of the adult spawning migration (Quinn and Unwin 1993) and the migration patterns of newly emerged fry (Unwin 1986) are consistent with fall run/ocean-type behavior. The mature parr in this study therefore appear to be derived from an ocean-type population.

Because maturation in salmon commences some months before external signs become apparent (Silverstein et al. 1997), the time of year when individual male parr begin to mature and the processes that trigger this development are unclear. Under natural conditions, parr maturation and smolting are usually incompatible (cf. Thorpe 1986); parr from ocean-type chinook salmon populations generally smolt and migrate to sea within 3–6 months of emergence, excluding any prospect of maturing in freshwater. Morphological differences between immature and mature parr, particularly the lengthening of the caudal region in immature (apparently smolted) fish compared with their mature siblings, also suggest that the developmental trajectory leading to maturation began before the onset of smolt transformation in the remainder of the cohort. Our observations of mature parr in March, together with Flain's (1970) records of mature parr from Lake Heron (in the upper Rakaia catchment) in February, are consistent with Robertson's (1957) finding that mature parr first appeared at about 10 months.

Age at maturity in most salmonid species is inversely related to growth rate (Thorpe 1994). The onset of maturation in Atlantic salmon (*Salmo salar*) has been linked to increased mesenteric fat reserves during the previous spring (Rowe et al. 1991), and similar mechanisms may apply to chinook salmon. Silverstein et al. (1997) found that amago salmon (*Oncorhynchus masu ishikawai*) that matured at 12 months of age had higher triacylglycerol levels than immature controls as early as 1 week after the beginning of exogenous feeding. We found no correlation between the incidence of mature parr in the 1994 experimental families and their mean size or growth rate at any time during their first year, although analysis of individual growth trajectories would provide a more sensitive method for detecting such correlations. Our finding that mature parr were either of similar length (in 1983–1984) or smaller (in 1995) than immature parr from the same cohort, and (in 1983–1984) less variable in size, also contrasts with previous studies. For example, Gebhards (1960) and Taylor (1989) found that mature chinook salmon parr were larger than immature parr,

© 1999 NRC Canada

and Silverstein et al. (1997) noted that mature amago salmon yearlings were more variable in size than immature parr. Nevertheless, the virtual absence of mature parr among the lower quartile of the populations sampled in 1983 and 1984 (Fig. 1) suggests that the slowest growing fish in these cohorts were unable to mature and is consistent with a minimum size or growth threshold for maturation (Rowe et al. 1991). Whether mature parr are larger or smaller than their immature counterparts may depend on a number of factors, including how much initial growth advantage maturing parr had at the onset of maturation and when sampling occurs relative to when maturing parr reduce their food consumption.

Maturation of male parr was subject to strong family-level variability. However, the lack of significant sire or population effects and the absence of any increase in maturation rate among the progeny of the mature parr spawned in 1995 (cf. Robertson 1957) suggest that any additive genetic effects (and consequently, heritability) are weak. These findings differ from those of Heath et al. (1994*a*), who reported significant sire effects and heritability for the incidence of jacks in chinook salmon. However, jack maturation does not necessarily reflect the same trait as parr maturation, which occurs at a younger life history stage and without any marine phase. Indeed, Heath et al. (1994*b*) found no evidence for genetic family contributions to parr maturation in chinook salmon but did find evidence for genetic contributions to jack maturation. Our results are also consistent with the low additive genetic variation and heritability for parr maturation in coho salmon (*Oncorhynchus kisutch*) (Silverstein and Hershberger 1992).

By making use of relative warps, our results provide a more comprehensive depiction of body development in mature parr than previously presented (Taylor 1989). In addition to being consistent with previous observations of deeper bodies and increased snout development in mature male parr (Taylor 1989), we were also able to graphically depict development of the hump and anal region in mature fish as well the lengthening of the caudal region in immature fish. While the morphological changes associated with parr maturation are subtle to the naked eye, we were able to determine that they are similar to those occurring in older and larger males, suggesting that their subtle development represents a lower endpoint along an allometric gradient. The tendency for deepening of the body and enlargement of the anal region to be more pronounced in repeat-maturing males than in first time maturing males is consistent with their high GSI's.

A striking feature of our results was the negative correlation between ED and GSI for 2-year-old repeat-maturing fish. We interpret this as reflecting the energetic costs associated with gonad production in a situation where energy reserves prior to the onset of maturation were severely limited, probably due to incomplete recovery after initial maturation. Fish spawning for a third successive season had condition indices similar to those of their 2-year-old counterparts, with lower GSI's and higher energy reserves, indicating a reduced investment in gonad development during their third year. The substantially lower ED for 2-year-old repeat-maturing males, compared with sea-run males maturing for the first time, is equally striking given that the latter group would have had to allocate some of their energy reserves to upstream migration (Glenariffe Stream is 100 km upriver at an elevation of 430 m). The discrepancy in ED between 2-year-old sea-run fish and their freshwater-reared siblings that first matured at age 2, although somewhat smaller, is also consistent with an energetic trade-off between gonad production and return migration.

Whether naturally occurring mature male parr could survive for a second year outside the hatchery environment is uncertain. Twenty-five mature male chinook salmon returning to the University of Washington hatchery at 1 year of age in autumn 1995 were held (with food provided) in freshwater, but all died within a week of capture (M. Kinnison, unpublished data). At 12 months the mature parr in our study performed poorly in a hypersalinity challenge compared with normal parr, although Bernier at al. (1993) found that mature parr reared in freshwater for 21 months (i.e., until late summer) were generally seawater tolerant. In naturally spawning populations, however, stream-type or yearling juveniles migrate to sea somewhat earlier than this, about 16–17 months postfertilization (i.e., early spring), both in the Pacific Northwest (Healey 1983) and in New Zealand (Unwin 1986; Unwin and Lucas 1993), and the seawater tolerance of mature parr at this age is unknown.

Even if smolt transformation and migration do not occur, energetic considerations weigh against postmaturation survival under all but highly favorable circumstances. Although specific ED's for mature parr varied widely, they were generally lower than for 2-year-old first time maturing males. Thus, mature parr would have had to overcome a significant energy deficit if they were to survive in the wild during their second year. This energy deficit (and perhaps some further nutritional effects related to gut atrophy) is evidenced by the large discrepancy in mean weight (at age 2) between previously mature parr and fish maturing for the first time at age 2 in our study. Despite much higher growth than encountered in the wild during their first year (hatchery FL: 132–212 mm; wild FL: 92–131 mm; Flain 1970) and an abundant food supply during their second year, repeat-maturing fish were incapable of allocating as much energy to growth. Their ability to survive for a third year, despite their low ED's, indicates that in the absence of other factors, low energy reserves do not inevitably result in death. Nonetheless, natural environments are likely to be much less conducive to postmaturation survival than hatchery environments, and this energy deficit might be a particularly important barrier to repeat maturation in stream-type chinook salmon populations within their natural range. Such populations are usually in regions with comparatively poor growing conditions, especially in the postspawning (winter) period (Taylor 1990).

Taking these factors into account, we think that mature male parr of natural origin might occasionally survive for a second (or even third) year if they remained in freshwater and obtained enough energy but would be extremely unlikely to survive downriver migration, seawater entry, and a return spawning migration up the Rakaia River within a 6- to 12-month time span. A nil return from a 1986 brood year release of 501 CWT-marked mature male parr from Glenariffe in July 1987 (National Institute of Water and Atmospheric Research, unpublished data) further supports this

© 1999 NRC Canada

conclusion. Although marine survival for the 1986 brood was poor (Unwin 1997), this group remains the only one of 247 CWT groups released from Glenariffe between 1978 and 1993 that failed to generate any adult returns.

The ability of some individuals to mature in up to three consecutive seasons confirms and extends previous findings that semelparity in male chinook salmon is not inevitable (Robertson 1957; Flain 1971; Bernier et al. 1993). However, four considerations suggest that the physiological changes associated with parr maturation were never fully reversed: (*i*) the persistence of mature male parr in samples collected over at least 8 months of the year, at ages ranging from 10 to 18 months, (*ii*) the ability of at least some such fish to express milt as late as the end of November (19–20 months, viability unknown) despite a significant decrease in GSI, (*iii*) the fact that, without exception, all mature male parr that survived for a second year matured again at age 2, and (*iv*) the extremely high GSI's for the age-2 repeat-maturing males. Thus, although mature parr in this study clearly exhibited one iteroparous characteristic (i.e., the ability to survive after spawning), it is unclear whether maturation reversal and subsequent redevelopment of the testes occurred to the same degree as in nominally iteroparous salmonids such as rainbow trout (*Oncorhynchus mykiss*).

The appearance of some iteroparous tendencies in male chinook salmon suggests an intermediate state in a continuum from fully semelparous Pacific salmonids (*O. gorbuscha*, chum salmon (*O. keta*), sockeye salmon (*O. nerka*), and *O. kisutch*) to more strongly iteroparous species such as brown trout (*Salmo trutta*) and char (*Salvelinus* spp). This intermediate state approaches a life history variant that occurs in some populations of masu salmon (*Oncorhynchus masou*), in which males sometimes mature in freshwater at the end of their first year before migrating to sea to return and spawn again (Tsiger et al. 1994). Females of this species less commonly mature in freshwater and are apparently always semelparous (Kato 1991). The most strongly iteroparous species within the genus *Oncorhynchus* are steelhead (*O. mykiss*) and cutthroat trout (*O. clarki*), both of which are capable of repeat spawning after successive return migrations between their freshwater and marine habitats (e.g., Scott and Crossman 1973). By contrast, repeat maturation in chinook salmon (and *O. masou*) appears to occur only after initial maturation in freshwater (i.e., parr maturation), suggesting a link between anadromy and semelparity.

Although mature male chinook salmon parr are unlikely to represent more than a minority of any population, we believe that they should be more widely acknowledged. Within naturally spawning New Zealand populations, mature male parr are probably about as common (in a demographic sense) as 2-year-old females and 5-year-old fish of either sex (Quinn and Unwin 1993). More generally, their small size would make them difficult to sample in the larger rivers often used by chinook salmon, so they are probably underrepresented in spawner surveys. The incidence of mature parr in our study was not correlated with size or growth rate at any time during the first year of life, and the mechanisms that trigger maturation of individual parr remain unclear. Nevertheless, given the apparent ease with which iteroparous male chinook salmon developed within a hatchery environment, in an intrinsically "ocean-type" population, the distinction between semelparous and iteroparous species of *Oncorhynchus* may not represent a large evolutionary gulf. Our results suggest that such a difference could evolve through small changes in a few key energetic and physiological thresholds.

Acknowledgements

We thank all staff associated with fish husbandry at Glenariffe and Silverstream throughout this study, particularly Tim Dodgshun, Selwyn Hawke, Martin Tawa, and Lindsay Hawke. Additional technical support was provided by Nelson Boustead, Fred Lucas, Tom Gough, Susan James, Carl Burton, and Larry Lehman. Bob McDowall, Gavin James, Clive Howard-Williams, and two anonymous referees reviewed earlier drafts of the manuscript. Special thanks is given to Andrew Hendry who participated in data collection and initial discussions on early and repeat maturation in New Zealand chinook salmon. The study was funded by the Foundation for Research, Science and Technology through contract CO1501 (in New Zealand) and by a consortium of North West American power utilities (in the United States). M.T. Kinnison was supported by an H. Mason Keeler Endowment.

References

Beacham, T.D., Murray, C.B., and Withler, R.E. 1989. Age, morphology, and biochemical genetic variation of Yukon River chinook salmon. Trans. Am. Fish. Soc. **118**: 46–63.

Bernier, N.J., Heath, D.D., Randall, D.J., and Iwama, G.K. 1993. Repeat sexual maturation of precocious male chinook salmon (*Oncorhynchus tshawytscha*). Can. J. Zool. **71**: 683–688.

Flain, M. 1970. Precocious male quinnat salmon *Oncorhynchus tshawytscha* (Walbaum) in New Zealand. N.Z. J. Mar. Freshwater Res. **4**: 217–222.

Flain, M. 1971. Repeated spawning and survival of male quinnat salmon in New Zealand. N.Z. J. Mar. Freshwater Res. **5**: 519–521.

Gebhards, S.V. 1960. Biological notes on precocious male chinook salmon parr in the Salmon River drainage, Idaho. Prog. Fish-Cult. **22**: 121–123.

Groot, C., and Margolis, L. 1991. Pacific salmon life histories. University of British Columbia Press, Vancouver, B.C.

Hankin, D.G., Nicholas, J.W., and Downey, T.W. 1993. Evidence for inheritance of age of maturity in chinook salmon (*Oncorhynchus tshawytscha*). Can. J. Fish. Aquat. Sci. **50**: 347–358.

Hartman, K.J., and Brandt, S.B. 1995. Estimating energy density of fish. Trans. Am. Fish. Soc. **124**: 347–355.

Healey, M.C. 1983. Coastwide distribution and ocean migration patterns of stream- and ocean-type chinook salmon, *Oncorhynchus tshawytscha*. Can. Field-Nat. **97**: 427–433.

Healey, M.C. 1991. Life history of chinook salmon (*Oncorhynchus tshawytscha*). *In* Pacific salmon life histories. *Edited by* G. Groot and L. Margolis. University of British Columbia Press, Vancouver, B.C. pp. 311–393.

Heath, D.D., Devlin, R.H., Heath, J.W., and Iwama, G.K. 1994*a*. Genetic, environmental and interaction effects on the incidence of jacking in *Oncorhynchus tshawytscha* (chinook salmon). Heredity, **72**: 146–154.

Heath, D.H., Iwama, G.K., and Devlin, R.H. 1994*b*. DNA fingerprinting used to test for family effects on precocious sexual mat-

© 1999 NRC Canada

uration in two populations of *Oncorhynchus tshawytscha* (chinook salmon). Heredity, **73**: 616–624.

Jonsson, B., and Jonsson, N. 1993. Partial migration: niche shift versus sexual maturation in fishes. Rev. Fish Biol. Fish. **3**: 348–365.

Kato, F. 1991. Life histories of masu and amago salmon. *In* Pacific salmon life histories. *Edited by* C. Groot and L. Margolis. University of British Columbia Press, Vancouver, B.C. pp. 447–520.

Kinnison, M.T., Unwin, M.J., Hershberger, W.K., and Quinn, T.P. 1998*a*. Egg size, fecundity, and development rate of two introduced New Zealand chinook salmon (*Oncorhynchus tshawytscha*) populations. Can. J. Fish. Aquat. Sci. **55**: 1946–1953.

Kinnison, M.T., Unwin, M.J., and Quinn, T.P. 1998*b*. Growth and salinity tolerance of juvenile chinook salmon (*Oncorhynchus tshawytscha*) from two introduced New Zealand populations. Can. J. Zool. **76**: 2219–2226.

McDowall, R.M. 1994. The origins of New Zealand's chinook salmon, *Oncorhynchus tshawytscha*. Mar. Fish. Rev. **56**: 1–7.

Mullan, J.W., Rockhold, A., and Chrisman, C.R. 1992. Life histories and precocity of chinook salmon in the mid-Columbia River. Prog. Fish-Cult. **54**: 25–28.

Quinn, T.P., and Unwin, M.J. 1993. Variation in life history patterns among New Zealand chinook salmon (*Oncorhynchus tshawytscha*) populations. Can. J. Fish. Aquat. Sci. **50**: 1414–1421.

Quinn, T.P., Neilsen, J.L., Gan, C., Unwin, M.J., Wilmot, R., Gutherie, C., and Utter, F.M. 1996. Origin and genetic structure of chinook salmon, *Oncorhynchus tshawytscha*, transplanted from California to New Zealand: allozyme and mtDNA evidence. Fish. Bull. U.S. **94**: 506–521.

Robertson, O.H. 1957. Survival of precociously mature king salmon male parr (*Oncorhynchus tshawytscha* Juv.) after spawning. Calif. Fish Game, **43**: 119–130.

Rohlf, F.J. 1993. Relative warp analysis and an example of its application to mosquito wings. *In* Contributions to morphometrics. *Edited by* L.F. Marcus, E. Bello, and A. Garcia-Valedcasas. Museo Nacional de Ciencias Naturales, Madrid, Spain. pp. 131–159.

Roni, P., and Quinn, T.P. 1995. Geographic variation in size and age of North American chinook salmon (*Oncorhynchus tshawytscha*). N. Am. J. Fish. Manage. **15**: 325–345.

Rowe, D.K., Thorpe, J.E., and Shanks, A.M. 1991. Role of fat stores in the maturation of male Atlantic salmon (*Salmo salar*) parr. Can. J. Fish. Aquat. Sci. **48**: 405–413.

Scott, W.B., and Crossman, E.J. 1973. Freshwater fishes of Canada. Bull. Fish. Res. Board Can. No. 184.

Silverstein, J.T., and Hershberger, W.K. 1992. Precocious maturation in coho salmon (*Oncorhynchus kisutch*): estimation of the additive genetic variance. J. Hered. **83**: 282–286.

Silverstein, J.T., Shimma, H., and Ogata, H. 1997. Early maturity in amago salmon (*Oncorhynchus masu ishikawai*): an association with energy storage. Can. J. Fish. Aquat. Sci. **54**: 444–451.

Taylor, E.B. 1989. Precocial male maturation in laboratory-reared populations of chinook salmon, *Oncorhynchus tshawytscha*. Can. J. Zool. **67**: 1665–1669.

Taylor, E.B. 1990. Environmental correlates of life-history variation in juvenile chinook salmon, *Oncorhynchus tshawytscha* (Walbaum). J. Fish Biol. **37**: 1–17.

Thorpe, J.E. 1986. Age at first maturity in Atlantic salmon, *Salmo salar*: freshwater period influences and conflicts with smolting. *In* Salmonid age at maturity. *Edited by* D.J. Meerburg. Can. Spec. Publ. Fish. Aquat. Sci. No. 89. pp. 7–14.

Thorpe, J.E. 1994. An alternative view of smolting in salmonids. Aquaculture, **121**: 105–113.

Tsiger, V.V., Skirin, V.I., Krupyanko, N.I., Kashlin, K.A., and Semenchenko, A.Y. 1994. Life history form of male masu salmon (*Oncorhynchus masou*) in South Primor'e, Russia. Can. J. Fish. Aquat. Sci. **51**: 197–208.

Unwin, M.J. 1986. Stream residence time, size characteristics, and migration patterns of juvenile chinook salmon (*Oncorhynchus tshawytscha*) from a tributary of the Rakaia River, New Zealand. N.Z. J. Mar. Freshwater Res. **20**: 231–252.

Unwin, M.J. 1997. Fry-to-adult survival of wild and hatchery chinook salmon (*Oncorhynchus tshawytscha*) from a common origin. Can. J. Fish. Aquat. Sci. **54**: 1246–1254.

Unwin, M.J., and Glova, G.J. 1997. Changes in life history parameters in a wild population of chinook salmon (*Oncorhynchus tshawytscha*) associated with releases of hatchery-reared fish. Can. J. Fish. Aquat. Sci. **54**: 1235–1245.

Unwin, M.J., and Lucas, D.H. 1993. Scale characteristics of wild and hatchery chinook salmon (*Oncorhynchus tshawytscha*) in the Rakaia River, New Zealand, and their use in stock identification. Can. J. Fish. Aquat. Sci. **50**: 2475–2484.

© 1999 NRC Canada

The rich krill aggregation of the Saguenay – St. Lawrence Marine Park: hydroacoustic and geostatistical biomass estimates, structure, variability, and significance for whales

Yvan Simard and Diane Lavoie

Abstract: The euphausiid aggregation at the head of the main channel of the estuary and Gulf of St. Lawrence was surveyed using 120- and 38-kHz hydroacoustics in the summers of 1994 and 1995. A systematic sampling grid covering an area of 1319 km^2 was visited eight times. Fish echoes were separated from krill echoes using the difference in backscattering strength at the two frequencies. Global estimates were obtained from geostatistical methods for both total biomass and the fraction exceeding 5 g wet·m^{-3}. The euphausiids were always exclusively composed of individuals of the oldest cohorts (2+) of the two species *Thysanoessa raschi* and *Meganyctiphanes norvegica*. Total biomass varied from 8 ± 2 to 96 ± 8 kt and cutoff biomass from 0 to 56 ± 6 kt. The two types of estimates were linearly related. Biomass was autocorrelated up to distances of 10–15 km. An anisotropic structure with radii of ~2 × 5 km, stretched along the channel axis, was discernible at a small scale. The particular size distribution of euphausiids and the large variations in the global estimates appear to be controlled by horizontal transport. The study area appears to be the richest krill aggregation site yet documented in the northwest Atlantic, with densities similar to the rich krill aggregation areas of the Antarctic. The krill aggregation is at the heart of this traditional whale feeding ground.

Résumé : L'agrégation d'euphausides à la tête du chenal principal de l'estuaire et du golfe du St-Laurent a été échantillonnée par hydroacoustique à 120 et 38 kHz aux étés 1994 et 1995. Un réseau d'échantillonnage systématique couvrant une zone de 1 319 km^2 a été visité à huit occasions. Les échos des poissons on été séparés de ceux du krill d'après la différence d'intensité de réflection acoustique aux deux fréquences. Des estimés globaux tant pour la biomasse totale que pour la fraction excédant 5 g de poids frais·m^{-3} ont été calculés par méthodes géostatistiques. Les euphausides étaient toujours composés exclusivement d'individus de la cohorte la plus agée (2+) des deux espèces *Thysanoessa raschi* et *Meganyctiphanes norvegica*. La biomasse totale était de 8 ± 2 à 96 ± 8 kt et celle de la fraction dense de 0 à 56 ± 6 kt. Les deux types d'estimés étaient linéairement reliés. La biomasse était autocorrelée jusqu'à des distances de 10–15 km. Des structures anisotropiques de ~2 × 5 km de rayon, allongées dans l'axe du chenal, étaient notables à petite échelle. La structure de taille particulière des euphausides et les variations importantes des estimés globaux seraient contrôlées par le transport horizontal. La région d'étude serait la plus riche zone d'agrégation de krill documentée à ce jour dans le nord-ouest de l'Atlantique. Ses densités sont comparables aux riches agrégations de krill de l'Antarctique. Cette agrégation de krill est au coeur de ce site d'alimentation traditionnel des baleines.

Introduction

Euphausiids form dense aggregations in various environments, notably in the Antarctic (Sameoto 1982, 1983; Simard et al. 1986*b*; Greene et al. 1988; Simard and Mackas 1989; Cochrane and Sameoto 1991; Hewitt and Demer 1993 and references therein). These zooplankton aggregations are in turn a source of predator concentrations, especially for pelagic fish and whales during their feeding season. A web of intensive trophic exchanges is then maintained at those feeding grounds by the zooplankton aggregation dynamics instead of local production. Understanding these locally rich areas, where larger scale production is concentrated and transferred to higher trophic levels, is essential for a comprehensive view of the ecosystem. The global biomass contained in the zooplankton aggregation and its temporal fluctuations are a basic requirement to estimate how many predators the area can support and for how long. This is the objective of this paper.

The estimation of global biomass in a given area requires adequate survey design, sampling strategies, sample quality, and statistical model. For lower levels of pelagic marine food webs on continental shelves or in the open ocean, we most often rely on sparse sets of point-measurements made in this three-dimensional environment. Such measurements are of limited interest because they cannot resolve the complex spatial–temporal structures of zooplankton patchiness

Received February 9, 1998. Accepted March 19, 1999. J14421

Y. Simard[1] and D. Lavoie. Department of Fisheries and Oceans, Fish and Marine Mammal Division, Maurice Lamontagne Institute, P.O. Box 1000, 850 route de la Mer, Mont-Joli, QC G5H 3Z4, Canada.

[1]Author to whom all correspondence should be addressed. e-mail: simardy@mpo-dfo.gc.ca

© 1999 NRC Canada

Fig. 1. Map of the study area showing the systematic sampling grid with primary (single letters) and secondary (double letters) acoustic transects. The polygon delimits the 1319-km^2 study area used for biomass estimation.

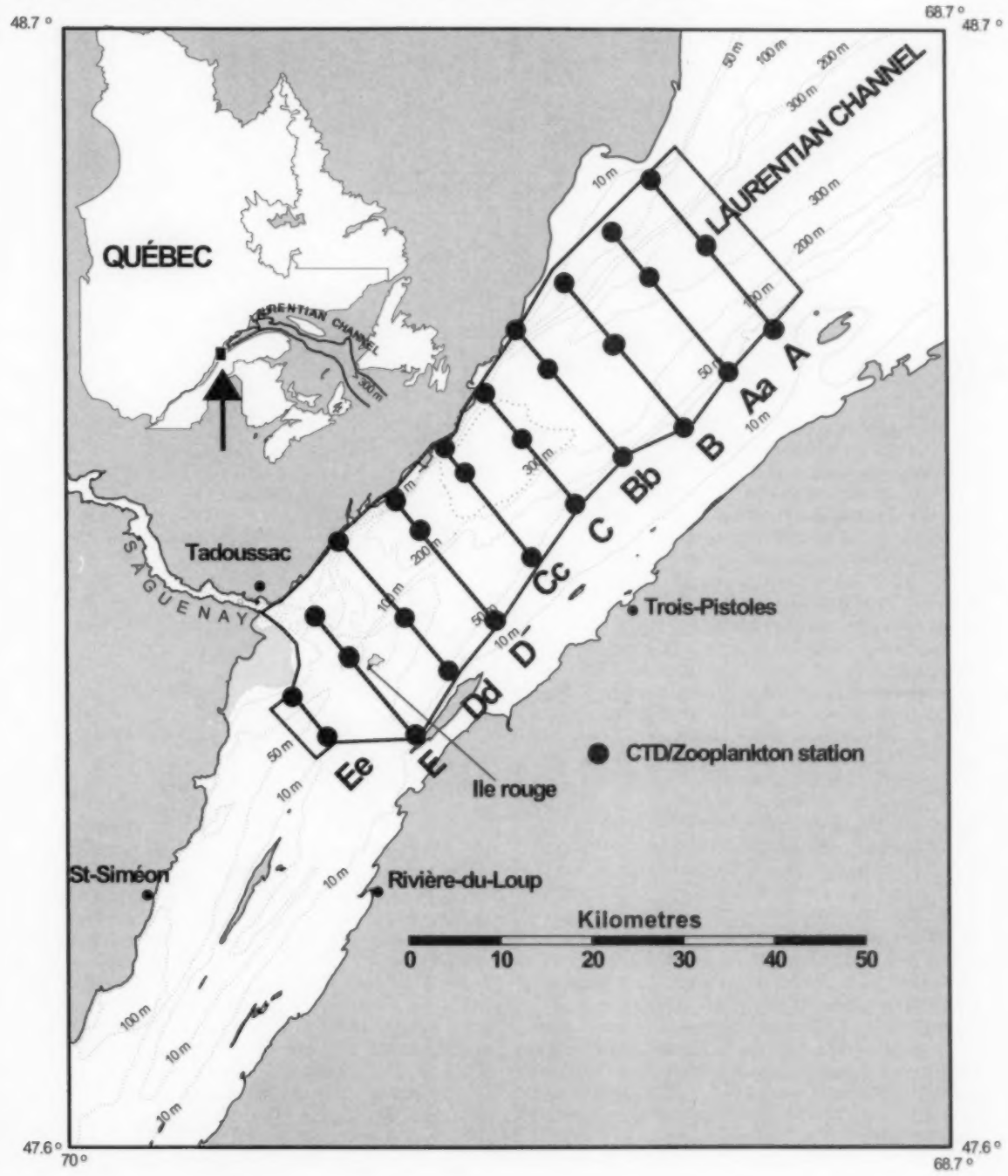

(Haury et al. 1978; Mackas et al. 1985). The latter make the acquisition of satisfactory samples difficult and generally far beyond the limits of sampling means (Herman and Platt 1980). Besides, intrusive samplers are often avoided by the target organisms, sometimes to a large extent by euphausiids (Sameoto et al. 1993). In contrast, the hydroacoustics technique (MacLennan 1990; MacLennan and Simmonds 1992; Holliday and Pieper 1995) does not have such limitations. It

© 1999 NRC Canada

Table 1. Survey attributes for each visit of the sampling grid and the echoclassification used over the transects.

	Mission 1 (*Calanus II*)		Mission 2 (*F.G. Creed*)		Mission 3 (*Parizeau*)		Mission 4 (*F.G. Creed*)	
	Visit 1	Visit 2	Visit 1	Visit 2	Visit 1	Visit 2	Visit 1	Visit 2
Dates	June 28–29, 1994	July 2–3, 1994	July 26–27, 1994	July 31 – Aug. 1, 1994	Aug. 24–25, 1994	Aug. 28–29, 1994	Aug. 7–8, 1995	Aug. 17–18, 1995
Days from last spring tide	4–5	8–9	2–3	7–8	2–3	6–7	10–11	5–6
Transect No.	7	7	8	10	7	7	9	10
Speed (kn)	~6	~6	~8	~8	~6	~6	~8	~8
Echointegration unit (m)	~30	~30	~80	~80	~60	~30	~80	-80
Bz No.	2905	2673	1520	1931	1536	3161	1758	2057
Classification krill/fish								
Depth <35 m	C1	C1	C1	C1	C1	Fish	C1	C1
Depth >35 m	C3	C2	C1	C1	C1	C3	C4	C2

Note: C1, 120/38 kHz MVBS ratio on transects A–Dd and fish on transects E and Ee; C2, krill on transects A–Dd and fish on transects E and Ee; C3, krill on transects A–D and 35–105 m on transect Dd and fish on transects E and Ee and >105 m on transect Dd; C4, krill on transects A–D and >105 m on transect Dd and fish on transects E and Ee and 35–105 m on transect Dd.

allows two-dimensional nonintrusive biomass measurements on large volumes along ship routes or sampler paths over a wide range of scales that comprise most of the significant spatial structure. Combined with proper sampling designs and biomass transfer functions, it is now commonly used for estimating pelagic fish stocks around the world (e.g., Simmonds and MacLennan 1996). With appropriate wavelengths and scattering model (Stanton 1989; Holliday and Pieper 1995), it is also employed to detect and estimate macrozooplankton/micronekton biomass in areas where the echo is dominated by a particular species. The present paper uses this technique combined with survey design and geostatistical methods (Simard et al. 1992, 1993; Petitgas 1993, 1996; Simmonds and Fryer 1996) to produce global biomass estimates of euphausiids in a rich area of the Canadian continental shelf, where many species of whales gather during summer. This region is now a protected area under the Saguenay – St. Lawrence Marine Park Act. To our knowledge, it is the first structured acoustic global estimation of krill biomass over a delimited area in the northwest Atlantic; all previous acoustic estimates were for specific locations (point or transect lines) and not from a sampling strategy designed to produce a global estimate over a delimited area of the ocean.

The study area is the head of the main channel of the Gulf of St. Lawrence, the Laurentian channel (Fig. 1). This submarine valley is 300–500 m deep and ~1400 km long. It ends abruptly near Tadoussac, which coincides with the entrance of the Saguenay fjord, in an area marked by several shoals, reefs, and islands. The head of the channel is a very dynamic and rich area (cf. El-Sabh and Silverberg 1990). Many physical oceanographic processes are simultaneously taking place: tidal upwelling of cold and nutrient-rich deep water (Ingram 1975; Therriault and Lacroix 1976; Gratton et al. 1988), generation of internal tides (Forrester 1974) and high-frequency internal waves (Ingram 1978), fronts (Ingram 1976, 1985), and complex tidal current dynamics (Service hydrographique du Canada 1997) which are combined with the two-layer estuarine circulation (El-Sabh 1979). The region is the site of a rich aggregation of krill (Simard et al. 1986*a*, 1986*b*) attributed to the interaction of the vertical migration and phototactic behavior of euphausiids with the circulation pattern (Simard et al. 1986*b*). Juvenile capelin also appear to aggregate over the shallows at the channel head (Bailey et al. 1977; Laurin 1982; Marchand 1997; Ménard 1998). Since the 1970's, a flourishing ecotourism industry (Michaud et al. 1997) has been established in the region to observe many species of whales (minkes, fins, blues, humpbacks, sperms) that gather in the area during summer along with other marine mammals, either residents, such as the local beluga population (Kingsley 1998), or visitors (Sergeant 1977; Edds and Macfarlane 1987; Lynas and Sylvestre 1988; Lavigueur et al. 1993).

One of the key factors for the attractiveness of the area for marine mammals is the aggregation of krill and its links with the other abundant prey species, especially capelin. The needs of cetaceans for highly concentrated food is well documented (Nemoto 1970; Brodie et al. 1978; Kawamura 1980). Aggregations of food, at a range of scales from bite size up to that of the entire feeding ground, favor a positive energy budget by minimizing energy lost in searching activity. Rich patches are of little interest if they are not imbedded in an area where the probability of encountering other rich patches is also high. Feeding grounds are such areas where rich food patches are strongly autocorrelated. In its search for food, a migratory predator such as the baleen whale must be aware of both the feeding ground units (Kawamura 1980) and their assemblages along its migratory route. We therefore need to locate these important feeding grounds and to document their intrinsic properties, such as the global prey biomass they embody, the biomass exceeding cutoff concentrations significant for predators, their food patchiness and concentration dynamics, their predictability, and their stability over time. The present paper aims to determine the latter krill biomass characteristics of the whale feeding ground at the head of the Laurentian channel in the St. Lawrence estuary. Global estimates of total biomass as well as cutoff biomass are presented for eight acoustic surveys performed in 1994 and 1995 using the geostatistical es-

© 1999 NRC Canada

Fig. 2. Acoustic separation of krill from fish by their relative backscattering strength (Sv = 10 log MVBS) at 120 and 38 kHz. Sv bins: dots, krill BIONESS samples; open symbols, krill samples from the small-mesh Marinovich pelagic trawl; solid symbols, fish samples from the same trawl. Line: $Y = X$.

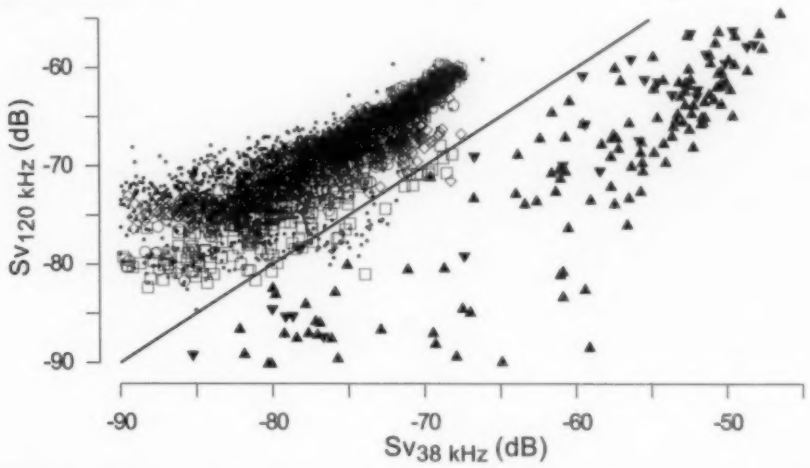

timation methodology. The weekly and monthly fluctuations in summer are presented and the results are compared with other aggregation sites. Description of the spatial patterns dymanics is beyond the scope of this paper and will be presented elsewhere.

Materials and methods

Sampling

Sampling was carried out during three missions in the summer of 1994 and one mission in the summer of 1995. A regular grid of 10 transects crossing the head of the Laurentian channel at intervals of 7.4 km delimited a study area of 1319 km^2 (Table 1; Fig. 1). The grid was surveyed twice during each mission to obtain two short-term estimates from 3 to 10 days apart depending on the mission. In 1994, the three missions were separated by 1 month to examine monthly fluctuations in biomass. To avoid possible acoustic bias during night, related to diel vertical migrations of euphausiids (Sameoto 1980; Demer and Hewitt 1995), visits of the grid were done during daytime only, when the krill scattering layers (SL's) were at their daytime depth (Simard et al. 1986*b*) and well separated from fish echoes in the upper water column. The survey speed was 6 or 8 kn. A complete visit of the grid took 2 days. To restrict the survey time to 2 days, a few secondary transects (Fig. 1) had to be omitted on some visits (Table 1). A grid of punctual stations (Fig. 1) was sampled at each mission to obtain CTD profiles (Lavoie et al. 1996) and some zooplankton samples over the entire water column from either 0.28-m^2 Bongo nets or a 1-m^2 BIONESS (0.33-mm mesh).

The acoustic system was composed of a Biosonics 102 echo sounder, equipped with two dual-beam transducers operating at 120 kHz (3.3 and 10°) and 38 kHz (10 and 25°). They were triggered alternatively every 0.5 s, except for the second visit of mission 3 where only 120 kHz was used. Pulse width was 0.5 ms. All raw data were digitally logged on magnetic tapes by means of a Biosonics 171 interface. The echo sounder was also linked to a computer via a Biosonics ESP A/D interface and the ESP_EI echointegration software, which simultaneously recorded positions from a GPS receiver (Magnavox 200). The system was regularly calibrated using the standard sphere method for each frequency (Foote et al. 1987). Given the negligible differences between the results of the different calibrations, the same calibration parameters were used for all missions. At mission 4, the 38-kHz transducer was replaced with a new one with its own calibration parameters.

Echointegration (Burczynski 1982; Johannesson and Mitson 1983) from the narrow beam of the transducers was done along transects on vertical strata of 5 m, from ranges of 2 to 202 or 207 m, and of 30 or 50 m for deeper strata down to a range of 250 m, which included all the krill SL's. In the 30-m layer off the bottom, echoes were integrated with a higher resolution from a secondary set of 1-m-thick bottom-locked strata. Horizontally, echointegration was done every 20 pings, except for mission 1 and the second visit of mission 3 where echointegration was done every 10 pings. Corresponding distances are given in Table 1. At the beginning of each mission, the ambient noise level at the survey speed were recorded for each frequency with the transducers in listening mode (i.e., not transmitting). An echo voltage threshold slightly higher than the noise level for each strata was then introduced for acquisition by ESP_EI.

Data analysis

Mean volume backscattering strength data (MVBS, Johanesson and Mitson 1983) were cleaned of acoustic interference and the first metre off the bottom was ignored. The MVBS were corrected for the absorption (François and Garrison 1982) and sound speed profile associated with the vertical structure of the water column for each mission (e.g., see Fig. 4B). A single representative profile was used for each mission, since the horizontal variability (Lavoie et al. 1996) was negligible for this purpose. The MVBS at 120 kHz were used for the present krill biomass estimates after fish echoes were sorted out using the MVBS ratio at the two frequencies (Simard 1998; Foote et al. 1990; Madureira et al. 1993) and high-resolution echograms. This classification proved to be correct from spot-checks with direct sampling of the krill SL's and fish aggregations with a BIONESS and a small-mesh Marinovich pelagic trawl (codend mesh of 5 mm, opening of ~3 × 5 m) (Fig. 2). Classifications were doubtful, however, in cases of strong MVBS in the upper water column in frontal regions, where adjacent MVBS bins were classified on either side. In these cases, we played back the raw data recorded on tapes to use the high-resolution spatial pattern to make the proper classification of fish and krill SL's. For the MVBS bins having a low 38-kHz signal to noise ratio, because of vessel noise, and for the second visit of mission 3 where only the

© 1999 NRC Canada

Table 2. Parameters of the biomass conversion factors at 120 kHz from eqs. 2–5 for the four missions separately and for all missions combined.

Parameter	Mission 1	Mission 2	Mission 3	Mission 4	All
$\langle\bar{\sigma}_{bs}\rangle_N$ ($\times 10^{-8}$ m^2)	1.78	3.54	2.82	1.77	2.47
$\overline{TS}_N$ (dB)	–77.5	–74.5	–75.6	–77.5	–76.1
$\bar{w}$ (g)	0.131	0.287	0.219	0.132	0.192
$\overline{TS}_W \cdot g^{-1}$ (dB)	–68.7	–69.1	–69.0	–68.7	–68.9

120-kHz signal was available, MVBS were classified with the high-resolution echograms (see Table 1).

The MVBS to biomass (B) conversion factors were computed for each mission (m) using the relationship of euphausiid target strength (TS) at 120 kHz to total length (L, from the tip of the rostrum to the end of the telson). We employed the same function as Hewitt and Demer (1993) for Antarctic krill, based on the bent cylinder model (Stanton 1989) and the Greene et al. (1991) prediction. The average euphausiid weight was computed using weighted size–frequency distributions of the two species (*i*) *Meganyctiphanes norvegica* and *Thysanoessa raschi* estimated from the zooplankton samples collected at the punctual stations (s), the local dry weight versus length relationships ($c_i(L_{ij})^{k_i}$) for these species in the St. Lawrence (Sameoto 1976*b*), and a factor (wd) of 5 for converting dry weight to wet weight (Kulka and Corey 1982; Falk-Petersen 1985). We did not use a wet weight versus length regression because none was available for this region and because the natural variability of those curves (e.g., Falk-Petersen 1985) did not warrant a better precision than our approach. The equations are

$$(1)\qquad B = \mathrm{MVBS} / 10^{(\overline{TS}_W /10)}$$

$$(2)\qquad \overline{TS}_W = \overline{TS}_N - 10 \log \bar{w}$$

$$(3)\qquad \bar{w} = \sum_i \sum_{L_j} f_{iL_j m}\ \mathrm{wd}\ c_i (L_{ij})^{k_i}$$

where wd = 5 and c_i and k_i are, respectively, 0.00000029 and 3.50 for *M. norvegica* and 0.000000717 and 3.17 for *T. raschi*, L_j is length-class j in millimetres and $\bar{w}$ is in grams, and

$$f_{iL_j m} = \frac{\left(\sum_s f_{iL_j} d_{is}\right)}{\left(\sum_s \sum_i d_{is}\right)}$$

is the proportion of length-class L_j of species i in the total length–frequency distribution for the two species combined ($\sum_i \sum_{L_j} f_{iL_j m} = 1.0$) for mission m where d_{is} is the density (number per square metre) of species i at station s and

$$(4)\qquad \overline{TS}_N = 10 \log (\bar{\sigma}_{bs})$$

where $\bar{\sigma}_{bs} = \dfrac{\bar{\sigma}}{4\pi}$

$$(5)\qquad \bar{\sigma}_{bs} = \sum_i \sum_{L_j} f_{iL_j m} 10^{(TS_{NL_{ij}} /10)}$$

$$= \sum_i \sum_{L_j} f_{iL_j m} 10^{\left[(a_N + b_N \log L_{ij})/10\right]}$$

where $a_N = -127.45$ and $b_N = 34.85$ for L in millimetres. Table 2 shows the computed parameters for eqs. 2–5. Since the values of $\overline{TS}_W$ were very similar from one mission to another, a $\overline{TS}_W$ of –69 dB·g^{-1} was used for all missions.

The biomass per cubic metre (B) was computed for each echointegration bin. It was then summed over the water column to obtain the total biomass per square metre (Bz) along the transects. A second sum integrated the bins where the biomass exceeded 5 g·m^{-3} to obtain the cutoff biomass per square metre ($Bz_{B>5}$). This cutoff level is an estimate of the krill concentration that baleen whales need for efficient feeding from Nemoto's (1970) data.

To take advantage of the autocorrelation structure to map the krill biomass over the study area and to estimate the global biomass and its uncertainty level, geostatistical methods were used, as they are well adapted for such a type of autocorrelated data and survey design used here (Simard et al. 1992, 1993; Petitgas 1993, 1996; Simmonds and Fryer 1996). Besides, the interpretation of the computed autocorrelation structure allows useful inferences on krill patchiness and its significance for predators. Global estimates over the study area were computed from punctual kriging (Journel and Huijbregts 1978). The 1-km mesh kriging grid delimited by the survey area had 1319 nodes for depths >10 m. A general variogram (γ_{all}) was computed from the pair (p_v) weighted average of the variograms of each visit (γ_v), standardized by the corresponding variance of observations ($\sigma^2_{Bz_v}$ or $\sigma^2_{Bz_{vB>5}}$) for both Bz and $Bz_{B>5}$:

$$(6)\qquad \gamma_{all} = \frac{\sum_v \dfrac{\gamma_v}{\sigma^2_{Bz_v} \text{ or } \sigma^2_{Bz_{vB>5}}} p_v}{\sum_v p_v}$$

for each distance class. To take into account the anisotropy of the spatial structure, the variograms were computed in the cross-channel direction (130° trigonometric) and along the main axis of the estuary (40° trigonometric). An elliptic neighborhood oriented along the axis of the estuary was used, with radii of 2 and 16 km. The search was done by iteration on four quadrants to obtain a maximum of eight observations belonging to at least two quadrants. The global biomass estimates over the study area for each visit ($\hat{BT}_v$ or $\hat{BT}_{vB>5}$) were obtained by expanding the mean of the kriged local estimates at the n nodes of the grid ($\hat{Bz}_v$ or $\hat{Bz}_{vB>5}$) to the surface area (A) of the study area (1319 km^2):

$$(7)\qquad \hat{\mathrm{BT}}_v = \frac{1}{n} \sum_1^n \hat{\mathrm{Bz}}_v\ A$$

$$\hat{\mathrm{BT}}_{vB>5} = \frac{1}{n} \sum_1^n \hat{\mathrm{Bz}}_{vB>5}\ A$$

where n is the number of local estimates.

The estimation variance is obtained from the geostatistical equation

© 1999 NRC Canada

Fig. 3. Average relative distribution of krill for the eight visits to the study area. Mean of centered and standardized local biomass estimates for each visit ($[\hat{B}z_v - \overline{\hat{B}z_v}]/\sigma_{\hat{B}z_v}$). Kriged grid mesh: 1 × 1 km.

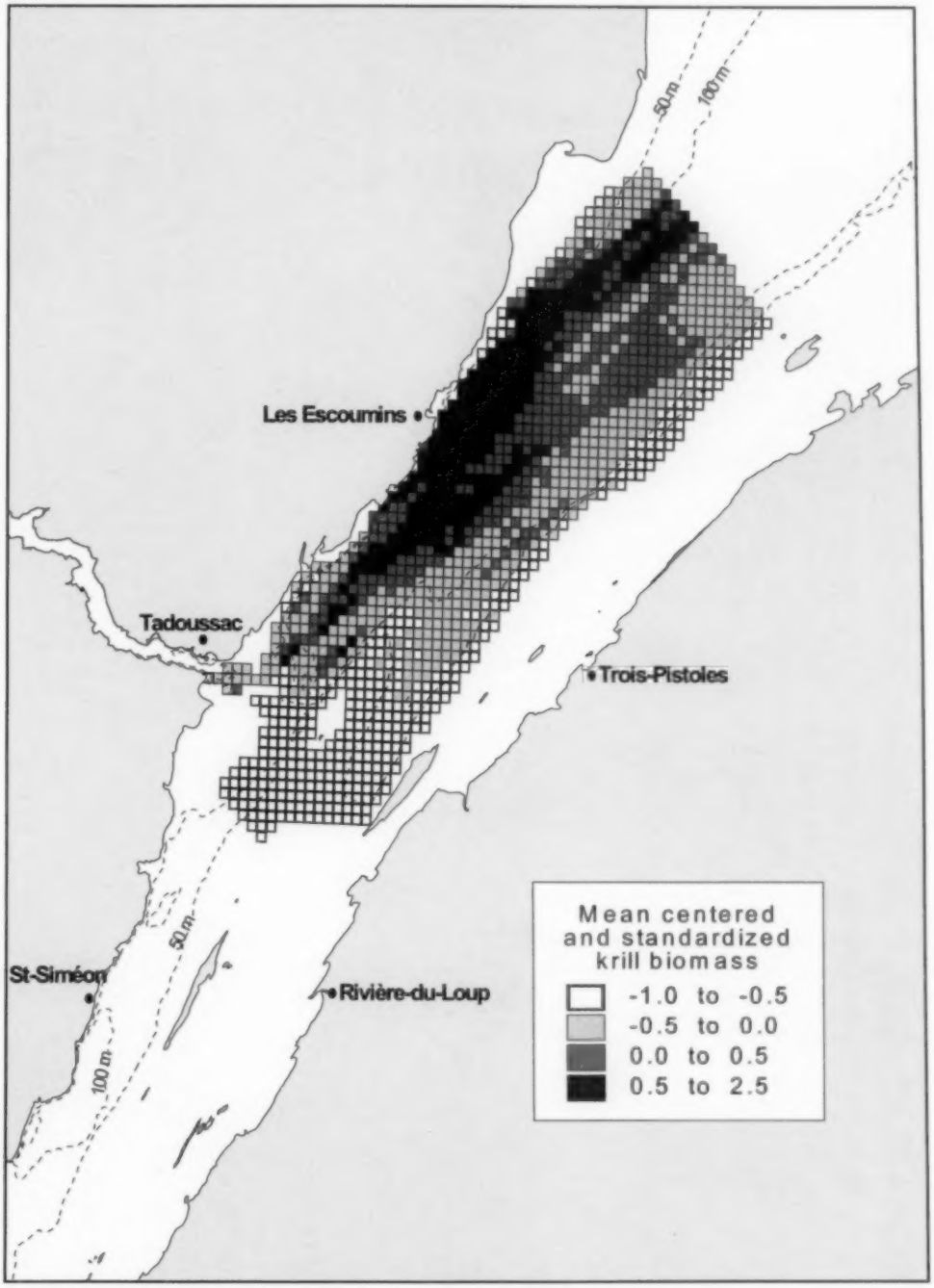

$$\sigma_{\hat{B}z_v \text{ or } \hat{B}z_{vB>5}} = 2\bar{\gamma}(x_{va}, S) - \bar{\gamma}(S, S) - \bar{\gamma}(x_{va}, x_{vb}) \quad (8)$$

where x_{va} and x_{vb} are the positions of the observations and S is the estimation polygon. The variograms used in this equation were the general standardized variogram rescaled by the variance of the observations of the corresponding visit (i.e., were multiplied by the $\sigma^2_{Bz_v}$ or $\sigma^2_{Bz_{vB>5}}$ of eq. 6). The estimation standard deviation and the 95% confidence limits of the mean are expanded to the estimation

© 1999 NRC Canada

Fig. 4. Typical echointegrated data for (A) a cross-channel section of the krill SL with (B) corresponding temperature and salinity (dashed line) profiles and for (C) a Bioness tow sampling the northern slope concentration with boxes delimiting MVBS bins associated with the net sample paths and (D) the catch for each net sample. Sv = 10 log MVBS. Note the change of 5 dB in the Sv palette between the two echograms. The echoes above the thermocline are not from krill.

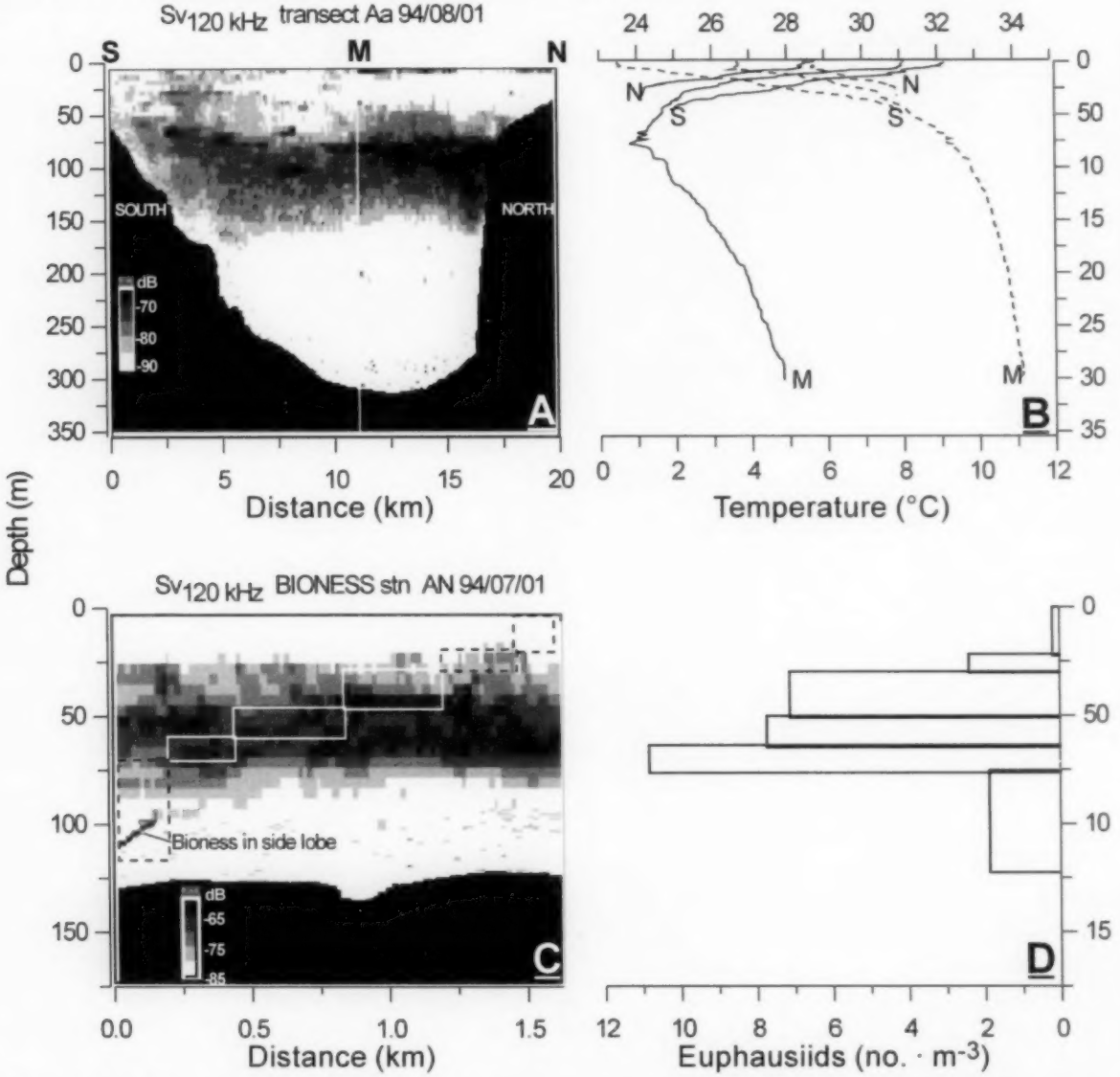

polygon by multiplying by its area to obtain the error statistics of the global estimates, $\sigma_{\hat{B}T_v \text{ or } \hat{B}T_{v,B>5}}$ and $CI95\%_{\hat{B}T_v \text{ or } \hat{B}T_{v,B>5}}$.

Results

The krill aggregation was concentrated in the part of the study area downstream of transect D, often with higher concentrations along the northern slope of the channel, enlarging off Les Escoumins, and occasional rich patches along the southern slope (Fig. 3). Most of the SL was found between 30 and 160 m (Fig. 4A), sometimes extending deeper, and showed a good continuity over the channel. Pelagic fish were generally located above the thermocline (Fig. 4B) and the krill SL and (or) around the SL boundaries, especially on the shallows upstream of the study area (Ménard 1998). The euphausiid density from the BIONESS samples in the SL (e.g., Figs. 4C and 4D) was strongly correlated with the MVBS ($r^2 = 0.80$, $p < 0.01$). It closely matched the expected euphausiid density from the MVBS. The slope was close to 1, but higher resolution MVBS and more accurate spatial alignment of the two sample types are needed to obtain its precise estimate.

Over all four missions, only the 2+ cohort (cf. Berkes 1976) of both *T. raschi* and *M. norvegica* was found in the

© 1999 NRC Canada

Fig. 5. Length–frequency distributions of *T. raschi* (open bars) and *M. norvegica* (solid bars) for each mission and for all missions combined.

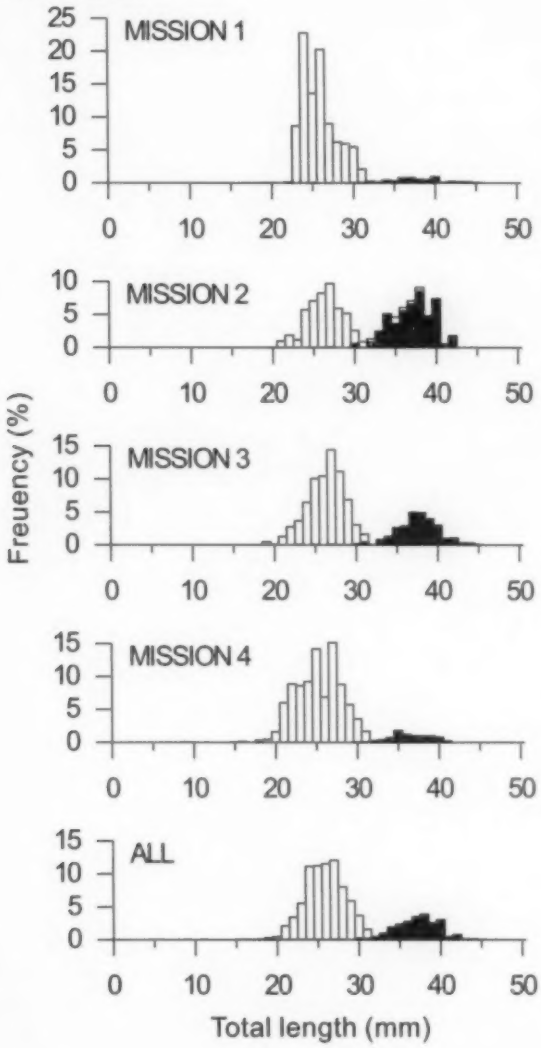

study area (Fig. 5). The relative proportion of the two species appeared to change from one visit to another, but this could result from variations in the number of samples and (or) their location relative to the center of mass. The average over all missions likely gives a better species ratio. The variations in length–frequency distribution had little effect on the biomass conversion factor ($\overline{TS}_W$, Table 2). As Hewitt and Demer (1993) showed, the increase in TS_N with krill length compensates for the decrease in number of krill per weight unit to produce a stable $\overline{TS}_W$.

Variograms of the total biomass (Fig. 6) indicated that all the variance observed at scales larger than our echo-integration unit of 30–80 m could be explained by the spatial structure (see Simard et al. (1992) or Petitgas (1996) for elementary variogram interpretation). Since the variogram reached zero at the origin, no small-scale unresolved variability (nugget variance is the intercept of the variogram at the origin) could be discerned. This nugget variance did not contribute to the total variance, which was therefore essentially due to the structural component. The along-transect autocorrelation (Fig. 6A) was strong up to distances of about 2 km, after which it decreased slowly but did not stabilized to a plateau (sill of the variogram). The continuous increase in the variance with distance indicates that a gradient was present and was generally not completely sampled at a distance of 10 km. The break in the monotone relationship at a distance of 2 km indicates that an approximately 2-km radius spatial structure was present and fused in the larger gradient. Along the channel axis (Fig. 6B), the large distance between the transects allowed the computation of coarse-scale variance only. The relative semivariance in that direction increased steadily up to 10–15 km. At larger distances, it reached a plateau where it fluctuated around a value of 1.0 (the variance of the observations) and no significant autocorrelation was present. We therefore modeled the general variogram with an isotropic exponential model having a practical range of 25 km to which a small structure was added in the cross-channel direction via another exponential model having a practical range of 1.2 km (Table 3). The variograms of the cutoff biomass (Fig. 6C) stepped more rapidly at the origin, indicating a more patchy spatial organization for the dense concentrations of krill. The model was adapted accordingly and took into account a small zonal anisotropy (Table 3).

Total krill biomass in the study area varied from 8 to 96 kt (Table 4), which corresponded to mean densities of 6–73 t·km^{-2}. The estimates tended to be more alike within missions than between them, even though the differences were significant (t test, $p < 0.001$). However, a large change of 55 kt was observed in 4 days during the first mission and a decrease of 88 kt was observed in 24 days between missions 2 and 3. The within-mission variation rate was ± 4–21%·day^{-1}. The relative error of the estimates varied from 8 to 23%, the highest values going along with the poor coverages of the grid (Table 1). The cutoff biomass for concentrations >5 g·m^{-3} varied from 0 to 56 kt and also showed large short-term fluctuations. The relative errors of these cutoff estimates were larger than those for the total biomass because of their lower global biomass and the shorter spatial continuity of the rich concentrations, as depicted by their variogram (Fig. 6). The proportion of total biomass exceeding the cutoff level varied widely, from 1 to 63%, but a simple linear relationship appeared to link the estimates of $\hat{B}T_v$ and $\hat{B}T_{vB>5}$ (Fig. 7). About 60% of the biomass in excess of a threshold of 10–15 kt (7.5–11.3 t·km^{-2}) appeared to be concentrated in the rich patches.

Discussion

Unusual euphausiid age-class composition

An important characteristic of the euphausiids of this part of the St. Lawrence system is that they are exclusively represented by the oldest individuals of the regional stocks. Simard et al. (1986*a*) also observed only old individuals of *T. raschi* in the adjacent area downstream. Unpublished data (Simard et al.) from a 1.5-year sampling series in the lower

© 1999 NRC Canada

Fig. 6. General experimental variogram of total and cutoff biomasses computed from eq. 6 in the cross- and along-channel directions, with the fitted model.

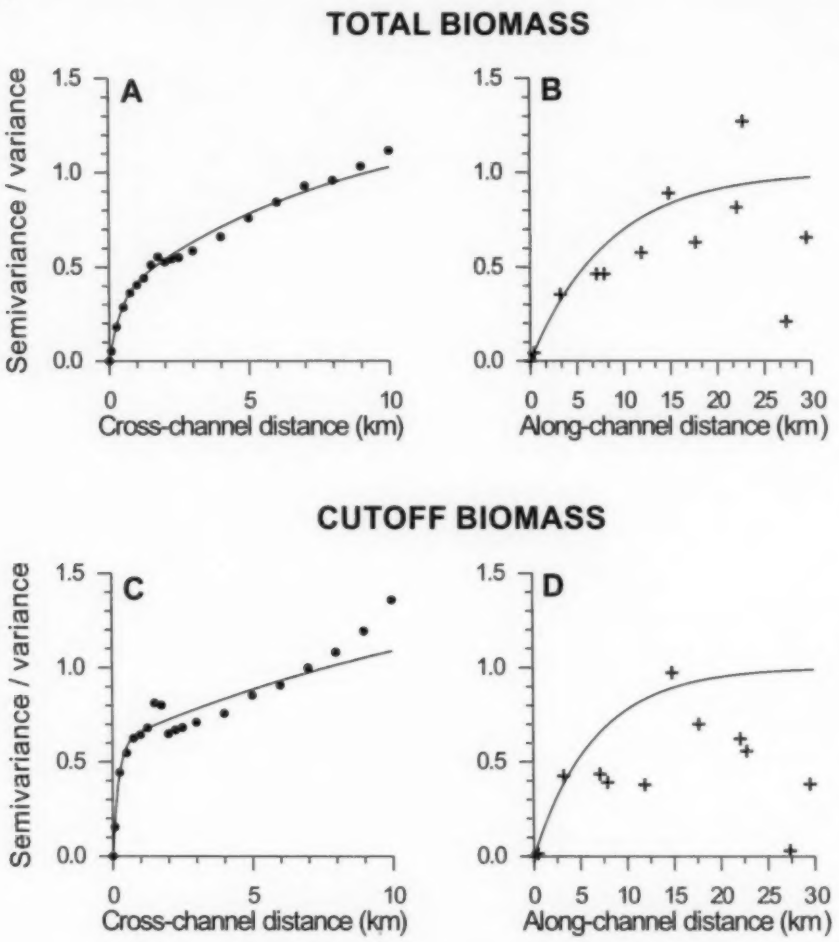

Table 3. General standardized variogram models for total and cutoff biomasses and standard deviations observed for each visit.

	Mission 1		Mission 2		Mission 3		Mission 4	
	Visit 1	Visit 2	Visit 1	Visit 2	Visit 1	Visit 2	Visit 1	Visit 2
Total biomass								
Model 1	Exponential: $a = 25/3$, $C = 1.0$, $C_0 = 0$							
Model 2	Exponential: $a_{130°} = 1.2/3$, $C = 0.33$, $C_0 = 0$							
σ_{Bz}	111.8	24.2	64.3	112.3	12.1	25.2	74.0	49.3
Cutoff biomass								
Model 1	Exponential: $a_{130°} = 45/3$, $a_{40°} = 20/3$, $C = 1.0$, $C_0 = 0$							
Model 2	Exponential: $a_{130°} = 0.63/3$, $C = 0.6$, $C_0 = 0$							
$\sigma_{Bz_{z\geq 5}}$	102.9	16.4	40.1	89.0	1.3	11.8	66.8	43.3

Note: The expotential model is $\gamma(h) = C\,[1 - \exp(-h/a)]$; practical range = $3a$.

St. Lawrence estuary (Therriault and Levasseur 1985) indicate that this is a persistent characteristic of the local euphausiids. Further downstream in the Gulf of St. Lawrence, an additional smaller cohort (1+) is present for both species (Berkes 1976). It appears therefore that a sorting mechanism is acting here to concentrate the oldest euphausiids at the head of the Laurentian channel and to exclude the young euphausiids from that area. According to the aggregation

© 1999 NRC Canada

Table 4. Global estimates of total biomass ($\hat{BT}_v$) and cutoff biomass (>5 g wet·m^{-3}, $\hat{BT}_{vB>5}$) in the study area for the eight visits to the sampling grid.

	Mission 1		Mission 2		Mission 3		Mission 4	
	Visit 1	Visit 2	Visit 1	Visit 2	Visit 1	Visit 2	Visit 1	Visit 2
Dates	June 28–29, 1994	July 2–3, 1994	July 26–27, 1994	July 31 – Aug. 1, 1994	Aug. 24–25, 1994	Aug. 28–29, 1994	Aug. 7–8, 1995	Aug. 17–18, 1995
Total biomass								
$\hat{BT}_v$ (kt)	78.8	23.8	76.6	95.9	7.9	19.3	52.5	30.4
$\sigma_{\hat{BT}}$ (kt)	16.2	3.4	7.4	7.6	1.8	3.8	7.1	3.4
CI95%$_{\hat{BT}_v}$ (kt)	47.1, 110.5	17.1, 30.5	62.1, 91.0	81.1, 110.8	4.4, 11.5	12.0, 26.7	38.7, 66.4	23.7, 37.0
Cutoff biomass								
$\hat{BT}_{vB>5}$ (kt)	49.5	6.6	23.6	55.9	0.1	2.2	32.5	13.4
$\sigma_{\hat{BT}_{vB>5}}$ (kt)	14.9	2.3	4.6	6.0	0.2	1.8	6.4	3.0
CI95%$_{\hat{BT}_{vB>5}}$ (kt)	20.3, 78.8	2.0, 11.1	14.5, 32.6	44.2, 67.7	0, 0.4	0, 5.7	20.1, 45.0	7.6, 19.2
Ratio								
$\%\hat{BT}_{vB>5}$	63	28	31	58	1	11	62	44

Fig. 7. Relationship between the global estimates of cutoff biomass (>5 g wet·m^{-3}) and total biomass. Bars are the 95% confidence intervals of the estimates.

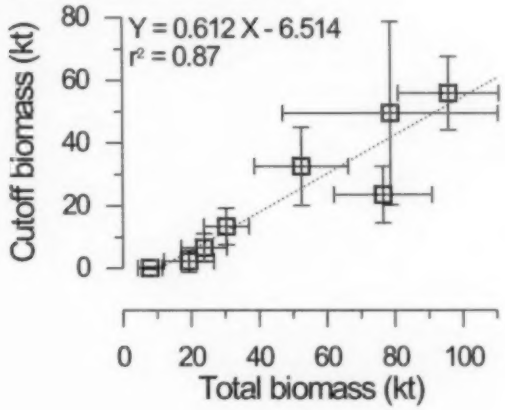

mechanism proposed by Simard et al. (1986*b*), the deep current of the two-layer estuarine circulation should slowly import the old individuals from the Gulf. The initial pulse in that direction was noted by Berkes (1976), who found that adult euphausiids were concentrating in the western Gulf after the larval and juvenile dispersion phase in summer. The same two-layer and cyclonic estuarine circulation pattern involved in Simard et al.'s (1986*b*) model is likely responsible for the rapid flushing of the young euphausiids. The early developmental stages, up to furcilia IV, grow in the upper water column and do not exhibit significant vertical migrations (Lacroix 1961). By inhabiting this superficial water mass, they are rapidly exported to the Gulf and the Magdalen shallows (Berkes 1976) by the downstream surface flow. Numerical simulations of vertical migrations in a two-layer circulation pattern representative of the currents off the northern and southern coasts of the lower estuary confirmed that the import of adults from the Gulf takes many months and that the young euphausiids are flushed out in a few months (Simard et al., unpublished data). The two-layer strong estuarine circulation cell of the St. Lawrence system (Koutitonsky and Bugden 1991), combined with the ontogenic development of the euphausiid diel vertical migration behavior, likely causes the krill aggregation at the head of the Laurentian channel to be essentially composed of "elderly" euphausiids. More information on the three-dimensional coupling of the circulation with the euphausiid distributions over the range of scales that they experienced during a complete life cycle is needed to refine this gross size/age sorting mechanism.

Variability of global estimates of euphausiid biomass

What is at the origin of the short-term variability of the global biomass in the study area? Possible causes include sampling errors, ecological factors, and physical oceanographic contributions. Sources of error in hydroacoustic estimation of biomass are numerous (Simmonds et al. 1992), but we do not have any reason to believe that some are especially involved here to explain the observed large variations. Sampling was done during daytime only to eliminate the possibility of day/night bias due to changes in euphausiid TS because of vertical migrations (Demer and Hewitt 1995). The local euphausiids were always exclusively composed of the large 2+ individuals of the two species present. Therefore, no seasonal changes in size and body composition affected their detectability by the echo sounder and (or) the biomass conversion factor. This factor as well as the calibration parameters were kept constant over all missions. The MVBS was strongly correlated with the catch from BIONESS samples, and both samplers produced similar euphausiid densities. The narrow beam (3.3°) and the high source level used (229.5 dB re 1 µPa at 1 m) allowed easy detection of concentrations as low as 0.1 euphausiid·m^{-3}

© 1999 NRC Canada

Table 5. Krill biomass estimates at various aggregation areas in the northwest Atlantic.

Location	Area (km^2)	Species	Method
Northwest Atlantic			
St. Lawrence estuary channel head	1 319 (n = 8)	Tr, Mn	120-kHz EI
Lower St. Lawrence estuary	~2 300	Tr, Mn, Ti	104 kHz vs. Tucker in SL
Lower St. Lawrence estuary and northwest Gulf	23 800	Tr, Mn, Ti	BIONESS tows
Gulf of St. Lawrence	214 000	Tr	0.5-m net
Gulf of St. Lawrence	p	Tr, Mn, Ti	Bongo in SL
Gulf of St. Lawrence, Gaspé coast	p	Tr, Mn, Ti	120 kHz vs. BIONESS in SL
Gulf of St. Lawrence, Gaspé coast	p	Tr, Mn, Ti	120 kHz vs. BIONESS in SL
Scotian shelf basins	p	Mn	200-kHz EI
Scotian shelf basins	p	Mn	BIONESS tows in SL, lights on, OPC
Scotian shelf/slope	p	Tl, Mn, Nm, Ek	BIONESS tows in SL
Bay of Fundy	14 800 (n = 5)	Mn, Ti, other	Bongo net tows
Bay of Fundy, Brier Island	p	Mn	Surface swarms, visual
Bay of Fundy, Brier and Long islands	p	Mn	Surface swarms, photographs, and samples
Gulf of Maine, Wilkinson basin	p	Mn	120 kHz, 420-kHz DB, bioluminescence
Gulf of Maine basins and canyons off Georges Bank	p	Mn	Visual from submersible, lights off
Continental slope and canyons off Georges Bank	p	Mn, T.	420-kHz EI and DB
Antarctic			
Elephant Island	36 271 (n = 2) 7 203 (n = 2)	Es	120-kHz EI
	Historic review: 17 338 – 43 474	120- to 150-kHz EI	81–3720

Note: n, number of surveys; p, punctual measurements. Species: Ek, *Euphausia krohni*; Es, *Euphausia superba*; Mn, *Meganyctiphanes norvegica*; Nm, *Nematoscelis megalops*; Tr, *Thysanoessa raschi*; Ti, *Thysanoessa inermis*; Tl, *Thysanoessa longicaudata*; T., *Thysanoessa* spp. Method: DB, dual-beam technique; EI, echointegration; OPC, optical plankton counter; SL, scattering layer.

[a]Computed from Simard et al. (1986*b*) dry biomass per cubic metre in their table 1, and corresponding areas and average heights of water column in their fig. 1.

[b]Wet weight = 5 × dry weight.

[c]0.00047 g dry·m^{-3} × 5 × 34 550 km^3.

[d]Assuming a thickness of 20, 10, and 5 m, respectively, for the light, medium, and heavy SL's.

[e]Surface swarm biomass in t·m^{-3} × thickness of 1 m.

[f]Mean acoustic density estimate per cubic metre × 0.2 g·individual^{-1} × 25-m-thick SL.

[g]Mean visual density per cubic metre in demersal SL × 0.2 g·individual^{-1} × SL thickness.

[h]Mean density per cubic metre estimated from fecal pellet concentration × 0.2 g·individual^{-1} × 20 m for the thickness of the mixed layer.

over the entire range (<250 m) of the SL's in the water column. Noise was properly thresholded out at acquisition and other punctual interference was eliminated during postprocessing. The fraction of the SL's present in the 1-m-thick blind zone at the bottom interface, unavailable to the echo sounder, was very small, limited to the contact areas with the SL's horizons and equally distributed among the eight visits to the grid. Special care was taken with echoclassification to minimize possible incorrect interpretations. We are confident that this is not a significant problem here. The low error of the estimates indicates that the observed changes in biomass are all significant and that the sampling design is not involved. It appears that the high variability observed is most likely real and due to other factors.

Among the ecological factors, possible effects of euphausiid growth cannot explain the high variability in global biomass. The length–frequencies observed do not support any growth effect, which, in any case, would be slow and monotone (Berkes 1976). Possible effects of predation could be involved, since the area is a whale feeding ground and a nursery area for a capelin stock, the two most important local krill predators in summer. Their precise biomass is unfortunately not available at present, but the higher boundary of this possible predation effect can be estimated to be <0.6 kt·day^{-1} ((30 whales of 30 t × daily ration of 0.01) + (25 kt capelin × daily ration of 0.05 × 0.5 krill diet)). The resulting euphausiid mortality rate would be 4–23 times smaller than the decreases in total krill biomass observed in 1994 and 1995. Besides, predation loss could be partially or entirely compensated for by krill production.

Another cause of fluctuation is massive mortality. Environmentally driven mortality is unlikely, the water mass characteristics (Lavoie et al. 1996) being well within the vital range of both species. However, large mortality cannot be

© 1999 NRC Canada

Wet biomass			
Total (kt)	Mean ($t \cdot km^{-2}$)	Maximum ($t \cdot km^{-2}$)	Reference
8–96	6–73	127–1660	Present study
0–56 >5 $g \cdot m^{-3}$	0–42 >5 $g \cdot m^{-3}$	23–1654 >5 $g \cdot m^{-3}$	
10–15[a,b]	4–7[a,b]	111[a,b]	Simard et al. 1986*b*[a,b]
500–1000	21–42	—	Runge and Joly 1995
81[c]	0.4[c]	—	Berkes 1977[b,c]
—	p: 0–12[d]	23[d]	Sameoto 1976*a*[d]
—	p: 9–12	—	Sameoto 1980
—	p: 2–315	315	Sameoto 1983
—	p: 79 and 102	—	Cochrane and Sameoto 1991
—	p: 14–145	—	Sameoto et al. 1993
—	p: 1–46	46	Sameoto 1982
60–80	4–5	27	Kulka et al. 1982
—	—	200[e]	Brown et al. 1979[e]
—	—	16 – 154 000[e]	Nicol 1986[e]
—	p: 1–3[f]	—	Greene et al. 1992[f]
—	p: 105–5142[g] p: 28–272[h]	—	Youngbluth et al. 1989[g,h]
—	—	30 700	Greene et al. 1988
1075–2220	30–61	—	Hewitt and Demer 1993
424–729	59–101	—	
3–91	—		

excluded entirely for the (old) females of *M. norvegica*, which are at their spawning peak at the end of the summer. Daytime surface swarms of euphausiids were often observed by the whale-watching boats in August 1994, which gives some support to this speculation. However, this would affect exclusively the female fraction of a single species and it could not account for the large loss observed between missions 2 and 3. It appears therefore that other factors are involved.

Transport is the most likely cause of the fluctuations in the biomass in the study area. The site is an open segment of the St. Lawrence estuary, where the input/output balance is controlled by complex hydrodynamic processes occurring over a large range of frequencies, especially the semidiurnal and fortnight tidal periods. The amplitude of the residual currents at the daytime depths of the SL's in summer is on the order of 10–15 $cm \cdot s^{-1}$ (Ingram 1979; Lafleur et al. 1996). Such deep currents could advect the SL's over a distance of ~10 km over 24 h, which is 13% of the length of the study area. Diel vertical migrations of the euphausiids in the stronger flow of surface waters at night would amplify the horizontal advection. Tidal modulations would also add significant variability. It is thus conceivable that the fluctuations of the krill biomass in the region could be under the control of the hydrodynamic circulation, which would rapidly exchange the euphausiids with the adjacent areas through import/export processes. The shallows at the head of the channel limit the possible exchanges at the SL's day depth in the upstream direction in the upper estuary and Saguenay fjord, even though the strong tidal upwelling in this area (Ingram 1975; Therriault and Lacroix 1976; Gratton et al. 1988) indicates that some should occur. However, our present observations and those of others (Runge and Simard 1990 and references therein) and hydroacoustic mis-

© 1999 NRC Canada

sions carried out in 1997 and 1998 (Simard et al., unpublished data) do not evidence any significant concentration of krill upstream but only some weak SL's. The exchanges are therefore mostly limited to the downstream end of the study area. The relative stability of the length–frequency distribution, with an almost pure 2+ cohort for both species, pleads for a close krill pool for these fast exchanges with a fair amount of recirculation. Lack of meso- to large-scale (>15 km) continuity in the supply, because of the patchy nature of the krill aggregation, combined with the fluctuations in the circulation, is likely the source of the variations in biomass. The coincidence of the large decrease in global biomass between missions 2 and 3 with the most important changes in the deepwater mass observed during the study (Lavoie et al. 1996) agrees with this transport hypothesis.

Euphausiid biomass structure and ecological significance

The variograms indicated that variance of krill biomass at scales larger than 30–80 m was due to a well-defined spatial structure, bounded by the channel width in the along-transect direction, and extending up to ranges larger than10–15 km, for both total and cutoff biomasses. The structure was stronger in the cross-channel direction than along the channel axis. The sampling design used, with transects oriented in the direction of maximum variance at intervals of 7.4 km, about half the autocorrelation range, therefore properly allocated the sampling effort by taking advantage of the spatial structure for optimizing global biomass estimation. The variograms also revealed a cross-channel structure with a radius of about 2 km, narrowing to about 0.5 km for the dense concentrations. This structure was likely two to three times longer along the channel, from the range needed to reach the same variance level on the along-channel variograms shown in Fig. 6 and from other variograms (not shown) on additional transects in same direction. It corresponds to the richer band of biomass stretched along the slopes of the channel reported by Simard et al. (1986*a*, 1986*b*) and evidenced in Fig. 3.

Predators use many cues to minimize their search effort for food. For those relying on large concentrations of prey, such as fish schools and baleen whales, the structure of their prey at different scales must be one of them. What does the observed krill structure mean for a predator seeking high concentrations of prey? First, it says that there is a good continuity in biomass over a range of scales from 30–80 m up to 10–15 km. At larger scales, there is no structure in the krill organization that is helping to find the richest areas. The radius of the feeding ground unit is therefore given by the autocorrelation range. Hence, there is a high risk in leaving a feeding ground, besides the displacement cost. This should impose limits to short- to mid-term displacements during feeding season and favor a certain degree of site fidelity. Second, in their search for food at meso- and large scales, the detection of the feeding ground unit, based on the krill concentration, likely results from a threshold response, since there is no helpful information in biomass structure. Once a threshold concentration is detected, the predator is informed that, in a maximum distance of 10–15 km, there is a high probability of finding rich patches, and the biomass gradient can be used to find it. Third, to stay in the rich core of the patches, its displacements should be less than ~4 km in the cross-channel direction but they can be up to ~10 km along the channel, assuming that both predators and prey are advected at the same speed and in the same direction. The large fluctuations observed in the global biomass estimates stress that the feeding success of this type of predator relies on an efficient tactic to find the rich patches. These latter represent only a fraction of the total biomass, highly localized, and do not exist when the global biomass falls below a certain level. It is therefore expected that this type of predator would concentrate in a decreasing food environment, up to a point where they would leave to find a new feeding ground unit. The mesoscale assemblage of feeding ground units then becomes important. Whales have the advantage of being able to be remotely informed of the locations of these feeding grounds through infrasound calls from distant individuals, which propagate over large distances in the ocean (Cummings and Thompson 1971; Watkins et al. 1987). Fish probably do not have this ability and might choose the alternative strategies of exploring the mesoscale surroundings, which represent a high energetic cost, or of reducing their activity and waiting until more favorable food conditions are built up and advected.

Comparisons with other aggregations sites

How does the head of the Laurentian channel compare with the other euphausiid aggregation sites in the northwest Atlantic or Antarctic? Such comparisons are difficult for the northwest Atlantic, not only because there appears to be no other similar estimate, but also because a wide range of sampling methods were used and, so far, only a small fraction of known or potential aggregation sites have been documented. Keeping in mind these limitations and probable avoidance problems with some intrusive samplers (Sameoto et al. 1993), some gross scaling could be tempted. Simard et al. (1986*b*) mapped the same local aggregation in July 1982 over an area about twice that of the present study. The estimate that we can compute from their data (10–15 kt, Table 5) is comparable with the lowest of the present estimates. When only the rich upstream area is considered, their krill density could be raised, possibly by a factor of 2, but it is still low compared with the present estimates. Possible interannual variations and (or) net avoidance by euphausiids could partly explain their low estimates. For the lower estuary and the northwest Gulf of St. Lawrence, an area 18 times larger than the present study area, Runge and Joly (1995) obtained an estimate from BIONESS samples in September 1994. They estimated a gross average density of 21–42 $t \cdot km^{-2}$, which falls in the present range but is relatively high if net avoidance is as important as Sameoto et al. (1993) reported. Mackas et al. (1997) estimated a 0.25-m^2 BIONESS efficiency of about 50–75% in catching euphausiids. Our data for a 1.0-m^2 BIONESS indicate a higher efficiency of about 75–100%. Berkes (1977) estimated the average density of *T. raschi* over the whole Gulf of St. Lawrence, a region 162 times larger than the present study area, to be 0.4 $t \cdot km^{-2}$. Doubling this value to account for *M. norvegica* would still give a very low biomass for the entire Gulf. Clearly, the samples were too scarce and the

© 1999 NRC Canada

sampler probably too ineffective at catching euphausiids to support a reasonable estimation over such a large area. Other punctual estimates can be obtained from Sameoto's (1976*a*, 1980, 1983) work in the Gulf of St. Lawrence. They fall within the low end of the present range, even for the maximum value of 315 $t \cdot km^{-2}$. The acoustic estimates of the density of *M. norvegica* in Scotian shelf basins (Cochrane and Sameoto 1991) are within the present mean density range but in the low end of our maximum densities. BIONESS estimates in the same basins, using artificial light when fishing, produced similar densities (Sameoto et al. 1993). Unfortunately, punctual estimates cannot be directly compared with a mean estimate over an area, since neither the area they actually represent nor their probability distribution is known. At the Scotian shelf slope, punctual euphausiid densities from the BIONESS appear to be lower than those observed in our area. In the Bay of Fundy, Kulka et al. (1982) obtained consistent and relatively high global biomass estimates, given their sampling gear. Taking into account that their survey area was 10 times larger than ours, and the low efficiency of the net, their estimates compare well with the low range of ours. The Bay is also a site where high-density surface swarms of euphausiids are observed (Brown et al. 1979; Nicol 1986). However, these swarms represent small areas, and still, their densities fall within our maximum values over larger areas, except for an extreme density of 154 $kg \cdot m^{-2}$. In the Gulf of Maine, punctual acoustic estimates from a deep basin (Greene et al. 1992) appeared to be lower than our minimum average density. High concentrations appear to occur, however, at some locations in the Gulf of Maine and in canyons along the continental slope and off Georges Bank (Greene et al. 1988; Youngbluth et al. 1989). Except for a few high values, they are not inconsistent with our average or maximum densities. Finally, our estimates are very similar to the krill estimates of a rich Antarctic region obtained by Hewitt and Demer (1993) using the same methods.

Conclusion

The head of the main channel carved in the continental shelf of eastern Canada appears to be the site of the richest krill aggregation yet documented in the northwest Atlantic. This aggregation is composed of old euphausiids only, essentially belonging to the 2+ cohorts of two species, *T. raschi* and *M. norvegica*. The very efficient sorting mechanism is likely driven by the combination of the hydrodynamic circulation and the ontogenic development of the diel vertical migration behavior of euphausiids. The generation of the aggregation is adequately explained by the model proposed by Simard et al. (1986*b*), but significant short-term fluctuations in global biomass are common because of dynamic exchanges of krill patches with the immediate downstream area. The average patch radius was 10–15 km, with cores elongated along the channel slopes. Concentrations denser than 5 $g \cdot m^{-3}$ represent about 60% of the total biomass when mean densities are larger than ~10 $t \cdot km^{-2}$. The intrinsic characteristics of this krill aggregation are fundamental properties structuring, in time and space, trophic exchanges with predators, such as pelagic fish and baleen whales, food web dynamics, and mass energy transfer in the regional pelagic ecosystem. This krill aggregation is an important factor, if not the keystone, of the biological richness of the recent Saguenay – St. Lawrence Marine Park.

Acknowledgments

We thank the numerous persons who participated in data collection and the crews of the research vessels and the trawler *Lamie*. We are indebtful to D. Marcotte for geostatistical programs and helpful suggestions and to Y. Gratton. Comments from one anonymous reviewer contributed to improving the manuscript. This research was funded by the Department of Fisheries and Oceans and the St. Lawrence Vision 2000 program, project IML 113-94-9.

References

Bailey, R.F.J., Able, K.W., and Leggett, W.C. 1977. Seasonal and vertical distribution and growth of juvenile and adult capelin (*Mallotus villosus*) in the St. Lawrence estuary and western Gulf of St. Lawrence. J. Fish. Res. Board Can. **34**: 2030–2040.

Berkes, F. 1976. Ecology of euphausiids in the Gulf of St. Lawrence. J. Fish. Res. Board Can. **33**: 1894–1905.

Berkes, F. 1977. Production of the euphausiid crustacean *Thysanoessa raschii* in the Gulf of St. Lawrence. J. Fish. Res. Board Can. **34**: 443–446.

Brodie, P.F., Sameoto, D.D., and Sheldon, R.W. 1978. Population densities of euphausiids off Nova Scotia as indicated by net samples, whale stomach contents and sonar. Limnol. Oceanogr. **23**: 1264–1267.

Brown, R.G.B., Barker, S.P., and Gaskin, D.E. 1979. Daytime surface swarming by *Meganyctiphanes norvegica* (M. Sars) (Crustacea, Euphausiacea) off Brier Island, Bay of Fundy. Can. J. Zool. **57**: 2285–2291.

Burczynski, J. 1982. Introduction to the use of sonar systems for estimating fish biomass. FAO Fish. Tech. Pap. No. 191 (Rev. 1).

Cochrane, N.A., and Sameoto, D.D. 1991. Corrected euphausiid abundance estimates from hydroacoustics: comments on Cochrane et al. 1991. Can. J. Fish. Aquat. Sci. **48**: 2034–2035.

Cummings, W.C., and Thompson, P.O. 1971. Underwater sounds of the blue whale, *Balaenoptera musculus*. J. Acoust. Soc. Am. **50**: 1193–1198.

Demer, D.A., and Hewitt, R.P. 1995. Bias in acoustic estimates of *Euphausia superba* due to diel vertical migration. Deep-Sea Res. **42**: 455–475.

Edds, P.L., and Macfarlane, J.A.F. 1987. Occurrence and general behavior of balaenopterid cetaceans summering in the St. Lawrence Estuary, Canada. Can. J. Zool. **65**: 1363–1376.

El-Sabh, M.I. 1979. The lower St. Lawrence estuary as a physical system. Nat. Can. **106**: 55–73.

El-Sabh, M.I., and Silverberg, N. (*Editors*). 1990. Oceanography of a large-scale estuarine system: the St. Lawrence. Coastal Estuarine Stud. No. 39.

Falk-Petersen, S. 1985. Growth of the euphausiids *Thysanoessa inermis*, *Thysanoessa raschii*, and *Meganyctiphanes norvegica* in a subarctic fjord north Norway. Can. J. Fish. Aquat. Sci. **42**: 14–22.

Foote, K.G., Knudsen, H.P., Vestnes, G., MacLennan, D.N., and Simmonds, E.J. 1987. Calibration of acoustic instruments for fish density estimation: a practical guide. ICES Coop. Res. Rep. No. 144.

© 1999 NRC Canada

Foote, K.G., Everson, I., Watkins, J.L., and Bone, D.G. 1990. Target strengths of Antarctic krill (*Euphausia superba*). J. Acoust. Soc. Am. **87**: 16–24.

Forrester, W.D. 1974. Internal tides in St. Lawrence Estuary. J. Mar. Res. **32**: 55–66.

François, R.E., and Garrison, G.R. 1982. Sound absorption based on ocean measurements. Part II: Boric acid contribution and equation for total absorption. J. Acoust. Soc. Am. **72**: 1879–1890.

Gratton, Y., Mertz, G., and Gagné, J.A. 1988. Satellite observations of tidal upwelling and mixing in the St. Lawrence estuary. J. Geophys. Res. **93**: 6947–6954.

Greene, C.H., Wiebe, P.H., Burczynski, J., and Youngbluth, M.J. 1988. Acoustical detection of high-density demersal krill layers in the submarine canyons off Georges Bank. Science (Washington, D.C.), **241**: 359–361.

Greene, C.H., Stanton, T.K., Wiebe, P.H., and McClatchie, S. 1991. Acoustic estimates of Antarctic krill. Nature (Lond.), **349**: 110.

Greene, C.H., Youngbluth, M.J., Tamse, A., and Johnson, G.E. 1992. The migration behavior, fine structure, and bioluminescent activity of krill sound scattering layers. Limnol. Oceanogr. **37**: 650–658.

Haury, L.R., McGowan, J.A., and Wiebe, P.H. 1978. Patterns and processes in the time–space scales of plankton distributions. *In* Spatial pattern in plankton communities. *Edited by* J.H. Steele. Plenum Press, New York. pp. 277–327.

Herman, A.W., and Platt, T. 1980. Meso-scale spatial distribution of plankton: co-evolution of concepts and instrumentation. *In* Oceanography: the past. *Edited by* M. Sears and D. Merriman. Springer-Verlag, New York. pp. 204–225.

Hewitt, R.P., and Demer, D.A. 1993. Dispersion and abundance of Antarctic krill in the vicinity of Elephant Island in the 1992 austral summer. Mar. Ecol. Prog. Ser. **99**: 29–39.

Holliday, D.V., and Pieper, R.E. 1995. Bioacoustical oceanography at high frequencies. ICES J. Mar. Sci. **52**: 279–296.

Ingram, R.G. 1975. Influence of tidal-induced vertical mixing on primary productivity in the St. Lawrence estuary. Mém. Soc. R. Liège, **7**: 59–74.

Ingram, R.G. 1976. Characteristics of a tide-induced estuarine front. J. Geophys. Res. **81**: 1951–1959.

Ingram, R.G. 1978. Internal wave observations off Isle Verte. J. Mar. Res. **36**: 715–724.

Ingram, R.G. 1979. Water mass modification in the St. Lawrence estuary. Nat. Can. **106**: 45–54.

Ingram, R.G. 1985. Frontal characteristics at the head of the Laurentian trough. Nat. Can. **112**: 31–38.

Johannesson, K.A., and Mitson, R.B. 1983. Fisheries acoustics. A pratical manual for aquatic biomass estimation. FAO Fish. Tech. Pap. No. 240.

Journel, A.G., and Huijbregts, C.J. 1978. Mining geostatistics. Academic Press, New York.

Kawamura, A. 1980. A review of food of balaenopterid whales. Sci. Rep. Whales Res. Inst. Tokyo, **32**: 155–197.

Kingsley, M.C.S. 1998. Population index estimate for the St. Lawrence belugas, 1973–1995. Mar. Mammal Sci. **14**: 508–530.

Koutitonsky, V.G., and Bugden, G.L. 1991. The physical oceanography of the Gulf of St. Lawrence: a review with emphasis on the synoptic variability of the motion. *In* The Gulf of St. Lawrence: small ocean or big estuary? *Edited by* J.-C. Therriault. Can. Spec. Publ. Fish. Aquat. Sci. No. 113. pp. 57–90.

Kulka, D.W, and Corey, S. 1982. Length and weight relationships of euphausiids and caloric values of *Meganyctiphanes norvegica* (M. Sars) in the Bay of Fundy. J. Crustacean Biol. **2**: 239–247.

Kulka, D.W, Corey, S., and Iles, T.D. 1982. Community structure and biomass of euphausiids in the Bay of Fundy. Can. J. Fish. Aquat. Sci. **39**: 326–334.

Lacroix, G. 1961. Les migrations verticales des euphausides à l'entrée de la Baie des Chaleurs. Nat. Can. **88**: 257–316.

Lafleur, C., Gratton, Y., Chanut, J.P., Savenkoff, C., Vézina, A.F., and Vinet, P. 1996. Distribution des paramètres océanographiques des eaux de l'estuaire du Saint-Laurent au large de Rimouski (juin–juillet 1990). Rapp. Stat. Can. Sci. Halieut. Aquat. No. 981.

Laurin, J. 1982. Étude écologique et éthologique de la population de bélugas (*Delphinapterus leucas*) du fjord du Saguenay, Québec. M.Sc. thesis, University of Montréal, Montréal, Qué.

Lavigueur, L., Hammil, M.O., and Asselin, S. 1993. Distribution et biologie des phoques et autres mammifères marins dans la région du parc marin du Saguenay. Rapp. Manuscrit Can. Sci. Halieut. Aquat. No. 2220.

Lavoie, D., Simard, Y., Benoit, J., Larouche, P., and Thibeault, B. 1996. Distribution des masses d'eau à la tête du chenal Laurentien dans l'estuaire du Saint-Laurent aux étés 1994 et 1995. Rapp. Tech. Can. Hydrogr. Sci. Océaniques No. 176.

Lynas, E.M., and Sylvestre, J.P. 1988. Feeding techniques and foraging strategies of minke whales (*Balaenoptera acutorostrata*) in the St. Lawrence River Estuary. Aquat. Mamm. **14**: 21–32.

Mackas, D.L., Denman, K.L., and Abbott, M.R. 1985. Plankton patchiness: biology in the physical vernacular. Bull. Mar. Sci. **37**: 652–674.

Mackas, D.L., Kieser, R., Saunders, M., Yelland, D.R., Brown, R.M., and Moore, D.F. 1997. Aggregation of euphausiids and Pacific hake (*Merluccius productus*) along the outer continental shelf off Vancouver Island. Can. J. Fish. Aquat. Sci. **54**: 2080–2096.

MacLennan, D.N. 1990. Acoustical measurement of fish abundance. J. Acoust. Soc. Am. **87**: 1–15.

MacLennan, D.N., and Simmonds, E.J. 1992. Fisheries acoustics. Chapman and Hall, London, U.K.

Madureira, L.S.P, Everson, I., and Murphy, E.J. 1993. Interpretation of acoustic data at two frequencies to discriminate between Antarctic krill (*Euphausia superba* Dana) and other scatterers. J. Plankton Res. **15**: 787–802.

Marchand, C. 1997. Étude des agrégations de proies potentielles pour les rorquals détectées par acoustique dans les fronts à la tête du chenal Laurentien (estuaire maritime du Saint-Laurent, Québec). M.Sc. thesis, Université du Québec à Rimouski, Rimouski, Qué.

Ménard, N. 1998. Répartition spatiale et structure des bancs de poissons pélagiques dans une aire d'alimentation des cétacés de l'estuaire du Saint-Laurent. M.Sc. thesis, Université Laval, Ste-Foy, Qué.

Michaud, R., Bédard, C., Mingelbier, M., and Gilbert, M.C. 1997. Les activités d'observation en mer des cétacés dans l'estuaire maritime du Saint-Laurent 1985–1996: une étude de la répartition spatiale des activités et des facteurs favorisant la concentration des bateaux sur les sites d'observation. GREMM, C.P. 223, Tadoussac, Qué. Final report to Parks Canada, Canadian Heritage Department, Ottawa, Ont.

Nemoto, T. 1970. Feeding pattern of baleen whales in the ocean. *In* Marine food chains. *Edited by* J.H. Steele. University of California Press, Berkeley, Calif. pp. 241–252.

Nicol, S. 1986. Shape, size and density of daytime surface swarms of the euphausiid *Meganyctiphanes norvegica* in the bay of Fundy. J. Plankton Res. **8**: 29–39.

Petitgas, P. 1993. Geostatistics for fish stock assessments: a review and an acoustic application. ICES J. Mar. Sci. **50**: 285–298.

© 1999 NRC Canada

Petitgas, P. 1996. Geostatistics and their applications to fisheries survey data. *In* Computers in fisheries research. *Edited by* B.A. Megrey and E. Moksness. Chapman and Hall, London, U.K. pp. 113–142.

Runge, J., and Joly, P. 1995. Zooplancton (euphausiacés et *Calanus*) de l'estuaire et du golfe du Saint-Laurent. *In* Rapport sur l'état des invertébrés en 1994: crustacés et mollusques des côtes du Québec, crevette nordique et zooplancton de l'estuaire et du golfe du Saint-Laurent. *Edited by* L. Savard. Rapp. Manusrit Can. Sci. Halieut. Aquat. No. 2323. pp. 124–132.

Runge, J., and Simard, Y. 1990. Zooplankton of the St. Lawrence Estuary: the imprint of physical processes on its composition and distribution. *In* Oceanography of a large-scale estuarine system: the St. Lawrence. *Edited by* M.I. El-Sabh and N. Silverberg. Coastal Estuarine Stud. No. 39. pp. 296–320.

Sameoto, D.D. 1976*a*. Distribution of sound scattering layers caused by euphausiids and their relationship to chlorophyll *a* concentrations in the Gulf of St. Lawrence estuary. J. Fish. Res. Board Can. **33**: 681–687.

Sameoto, D.D. 1976*b*. Respiration rates, energy budgets, and molting frequencies of three species of euphausiids found in the Gulf of St. Lawrence. J. Fish. Res. Board Can. **33**: 2568–2576.

Sameoto, D.D. 1980. Quantitative measurements of euphausiids using a 120 kHz sounder and their in situ orientation. Can. J. Fish. Aquat. Sci. **37**: 693–702.

Sameoto, D.D. 1982. Zooplankton and micronekton abundance in acoustic scattering layers on the Nova Scotian slope. Can. J. Fish. Aquat. Sci. **39**: 760–777.

Sameoto, D.D. 1983. Euphausiid distribution in acoustic scattering layers and its significance to surface swarms. J. Plankton Res. **5**: 129–143.

Sameoto, D., Cochrane, N., and Herman, A. 1993. Convergence of acoustic, optical and net-catch estimates of euphausiid abundance: use of artificial light to reduce net avoidance. Can. J. Fish. Aquat. Sci. **50**: 334–346.

Sergeant, D.E. 1977. Stocks of fin whales *Balaenoptera physalus* L. in the north Atlantic Ocean. Rep. Int. Whaling Comm. **27**: 460–473.

Service hydrographique du Canada. 1997. Atlas des courants de marée, estuaire du Saint-Laurent du cap de Bon-Désir à Trois-Rivières. Department of Fisheries and Oceans, Ottawa, Ont.

Simard, Y. 1998. Fish'n krill: a 38/120 kHz acoustic separation. Proceedings of the 16th International Congress on Acoustics and of the 135th Meeting of the Acoustical Society of America, Seattle, Wash. pp. 2783–2784.

Simard, Y., and Mackas, D. 1989. Mesoscale aggregations of euphausiid sound scattering layers on the continental shelf of Vancouver Island. Can. J. Fish. Aquat. Sci. **46**: 1238–1249.

Simard, Y., Lacroix, G., and Legendre, L. 1986*a*. Diel vertical migrations and nocturnal feeding of a dense coastal krill scattering layer (*Thysanoessa raschi* and *Meganyctiphanes norvegica*) in stratified surface waters. Mar. Biol. **91**: 93–105.

Simard, Y., de Ladurantaye, R., and Therriault, J.-C. 1986*b*. Aggregation of euphausiids along a coastal shelf in an upwelling environment. Mar. Ecol. Prog. Ser. **32**: 203–215.

Simard, Y., Legendre, P., Lavoie, G., and Marcotte, D. 1992. Mapping, estimating biomass, and optimizing sampling programs for spatially autocorrelated data: case study of the northern shrimp. Can. J. Fish. Aquat. Sci. **49**: 32–45.

Simard, Y., Marcotte, D., and Bourgault, G. 1993. Exploration of geostatistical methods for mapping and estimating acoustic biomass of pelagic fish in the Gulf of St. Lawrence: size of echo-integration unit and auxiliary environmental variables. Aquat. Living Resour. **6**: 185–199.

Simmonds, E.J., and Fryer, R.J. 1996. Which are better, random or systematic acoustic surveys? A simulation using North Sea herring as an example. ICES J. Mar. Sci. **53**: 39–50.

Simmonds, E.J., and MacLennan, D.N. (*Editors*). 1996. Fisheries and plankton acoustics. Proceedings of an ICES international symposium held in Aberdeen, Scotland, 12–16 June 1995. ICES J. Mar. Sci. **53**.

Simmonds, E.J., Williamson, N.J., Gerlotto, F., and Aglen, A. 1992. Acoustic survey design and analysis procedures: a comprehensive review of current practice. ICES Coop. Res. Rep. No. 187.

Stanton, T.K. 1989. Simple approximate formulas for backscattering of sound by spherical and elongated objects. J. Acoust. Soc. Am. **86**: 1499–1510.

Therriault, J.-C., and Lacroix, G. 1976. Nutrients, chlorophyll and internal tides in the St. Lawrence estuary. J. Fish. Res. Board Can. **33**: 2747–2757.

Therriault, J.-C., and Levasseur, M. 1985. Control of phytoplankton production in the lower St. Lawrence estuary: light and freshwater runoff. Nat. Can. **112**: 77–96.

Watkins, W.A., Tyack, P., Moore, K.E., and Bird, J.E. 1987. The 20-Hz signals of finback whales (*Balaenoptera physalus*). J. Acoust. Soc. Am. **82**: 1901–1912.

Youngbluth, M.J., Bailey, T., Davoll, P.J., Jacoby, C.A., Blades-Eckelbarger, P.I., and Griswold, C.A. 1989. Fecal pellet production and diel migratory behavior by the euphausiid *Meganyctiphanes norvegica* effect benthic–pelagic coupling. Deep-Sea Res. **36**: 1491–1501.

© 1999 NRC Canada

Microsatellite evolution in sunfish (Centrarchidae)

Bryan D. Neff, Peng Fu, and Mart R. Gross

Abstract: We describe 10 microsatellite loci from bluegill (*Lepomis macrochirus*) and discuss their evolution within the Centrarchidae. All of the loci exhibit Mendelian inheritance and are unlinked. While six loci are conserved within the Centrarchidae (found also in pumpkinseed (*Lepomis gibbosus*) and largemouth bass (*Micropterus salmoides*)), four have origins outside the family and two predate it by 65–150 million years. The persistence of these loci in fish may be due to a slow rate of sequence divergence within their flanking sequences, estimated at 0.14–0.83% per million years. We examine the number of alleles, heterozygosity, range, modes, and the frequency of the most common allele and find that a two-phased model (TPM) or an infinite alleles-model (IAM) best describes the results, while a stepwise mutation model (SMM) is rejected. Therefore, population differentiation analyses utilizing these microsatellite loci should consider parameters based on the IAM (e.g., F_{ST}) and not the SMM.

Résumé : Nous décrivons 10 loci microsatellites du crapet arlequin (*Lepomis macrochirus*) et traitons de leur évolution au sein des Centrarchidae. Tous les loci obéissent à l'hérédité mendélienne et ne sont pas liés. Six loci sont conservés au sein des Centrarchidae (présents aussi chez le crapet-soleil (*Lepomis gibbosus*) et l'achigan à grande bouche (*Micropterus salmoides*)), tandis que quatre ont leur origine à l'extérieur de la famille, dont deux existaient 65 à 150 millions d'années avant l'apparition de cette dernière. La persistance de ces loci chez les poissons pourrait être attribuable à un faible taux de divergence des séquences dans leurs régions flanquantes, estimé à 0,14–0,83% par million d'années. Nous examinons le nombre d'allèles, l'hétérozygosité, la diversité des allèles, les modes et la fréquence de l'allèle le plus commun pour conclure qu'un modèle diphasé ou un modèle en nombre infini d'allèles donnent la meilleure description des résultats et qu'on doit rejeter le modèle de mutation par pas. Ainsi, les analyses de différenciation des populations utilisant ces loci microsatellites devraient considérer les paramètres fondés sur le modèle en nombre infini d'allèles (p. ex. F_{ST}) et non sur le modèle de mutation par pas.

[Traduit par la Rédaction]

Introduction

Microsatellite loci are powerful genetic markers with the potential to provide researchers with new insights into the behaviour, ecology, and genetic structure of fish (Avise 1994; Jarne and Lagoda 1996; O'Connell and Wright 1997). Here, we report an analysis of 10 microsatellites in the North American sunfish family Centrarchidae (eight new and two reported in Colbourne et al. 1996). We evaluate the microsatellite loci within the source species, across two species within the same genus, across two genera within the same family, and across three fish families. Our analyses infer the origins of these loci and their mode and rates of evolution as well as their expression and variability. Thus, this study provides an evolutionary perspective on microsatellites and a useful set of genetic markers.

Three prevailing models exist to explain the mode of mutation at genetic marker loci: the infinite-alleles model (IAM), the stepwise mutation model (SMM), and the two-phase model (TPM). These models relate to parameters used to estimate population differentiation and distance and are therefore important for considerations in fisheries management and conservation. The IAM (Kimura and Crow 1964) assumes that, within a population, each mutation gives rise to a unique allele and therefore, equivalent alleles are identical by descent. The SMM (Kimura and Ohta 1978; Shriver et al. 1993; Valdes et al. 1993) assumes that a mutation changes the allele by one unit and therefore infers that alleles of the same size are more closely related but not necessarily identical by descent. The TPM (Di Rienzo et al. 1994) is analogous to the SMM with the addition of occasional multistep mutations. This latter model requires estimates of the size (i.e., number of steps) and proportion of mutations that are multistep.

It is generally considered that the mode of mutation at microsatellite loci follows a stepwise mutational process (e.g., Schlötterer and Tautz 1992). However, allelic variation at many loci appears to conform to predictions based on the IAM and not the SMM (e.g., O'Connell et al. 1997). Further, measures of population differentiation calculated from parameters based on the IAM are often consistent with alternative estimates (e.g., estimates based on mtDNA; Di Rienzo et al. 1994). Di Rienzo et al. (1994) have suggested that multistep mutations may often give rise to novel alleles and could explain the apparent fit of microsatellite data to the IAM. However, few studies have tested the TPM, and to our knowledge, no study has yet tested all three models.

The Centrarchidae diverged from other fishes during the

Received August 28, 1998. Accepted March 18, 1999.
J14761

B.D. Neff,[1] P. Fu, and M.R. Gross.[2] Department of Zoology, University of Toronto, 25 Harbord Street, Toronto, ON M5S 3G5, Canada.

[1,2]Authors to whom all correspondence should be addressed.
e-mail: neff@zoo.utoronto.ca; mgross@zoo.utoronto.ca

© 1999 NRC Canada

Eocene, 39–54 million years ago (Wilson and Williams 1992). The family is now composed of 32 species in nine genera (Nelson 1984; Wainwright and Lauder 1992). These species are widely distributed throughout their native North America and through human transport have colonized other regions of the world (e.g., Lelek 1987; Coad et al. 1995). They are important members of the fish fauna wherever they are found. In North America, they are highly valued in the sport fishery, being the target species in over 80% of registered sport tournaments (Schramm et al. 1991). They are also a concern to conservation biologists, both because of endangered populations in North America and because they can displace native species when introduced elsewhere (Lelek 1987). In addition, they are of great interest to evolutionary ecologists for studies of life history, mating system, and behavioural evolution (Gross 1982, 1996; Wainwright and Lauder 1992; Baylis et al. 1993; Belk 1998).

In this study of microsatellite evolution, the source species is the bluegill (*Lepomis macrochirus*). Bluegill are thought to be a recent lineage within the Centrarchidae that diverged probably 2–4 million years ago during the late Pliocene to early Pleistocene (Miller 1958; Mabee 1988; Wainwright and Lauder 1992). The pumpkinseed (*Lepomis gibbosus*), which cohabits with bluegill in the northern part of its range, is used as the test species for cross-species amplification within the genus. The largemouth bass (*Micropterus salmoides*), probably the first of the centrarchids to have diverged 39–54 million years ago during the Eocene (Wainwright and Lauder 1992; Wilson and Williams 1992), is used as the test species for cross-genera amplification and comparison between the oldest and youngest groups within the family. We examine the level of polymorphism within four largemouth bass populations and compare this with that of bluegill. To determine whether the microsatellite loci are exclusive to the Centrarchidae, we test for their presence in the families Percidae (yellow perch (*Perca flavescens*)) and Esocidae (northern pike (*Esox lucius*)), an ancient group that diverged during the late Cretaceous, 65–150 million years ago (Wilson and Williams 1992). Yellow perch and northern pike are also important recreational and commercial species. To estimate the rate of sequence divergence at the loci, we analyze sequences from homologues of two loci in bluegill, pumpkinseed, and largemouth bass. We compare the rates with those found for other species in the literature and infer the relationship between microsatellite mutation rates and conservation. Finally, we test the IAM, SMM, and TPM to determine which model best explains the variation at the microsatellite loci.

Methods

Fish samples

The microsatellite loci were initially isolated from a bluegill in Lake Opinicon (Ontario, Canada). For each locus, inheritance of the microsatellite alleles was tested using up to three family crosses and a minimum of 20 offspring per family (see Colbourne et al. 1996 for details of the crosses). Linkage disequilibrium was examined using genotypes from 44 bluegill of mixed ages seined from several areas of Lake Opinicon. Cross-species amplifications were tested using DNA of five pumpkinseed, five largemouth bass, two yellow perch, and two northern pike netted or angled from Lake Opinicon. Sequence analyses used a single bluegill, pumpkinseed, and largemouth bass from Lake Opinicon. Comparison of allelic polymorphism was tested using 20 bluegill and largemouth bass taken from multiple populations to minimize population-specific biases: bluegill from Lake Opinicon (n = 10) and Lake Fork (Texas, U.S.A., n = 10) and largemouth bass from Lake Opinicon (n = 5), Everglades (Florida, U.S.A., n = 5), Lake Fork (n = 5), and Lake Erie (Minnesota, U.S.A., n = 5). The mutational models were tested using genotypes from 169 bluegill of mixed ages seined from several areas of Lake Opinicon.

Microsatellite protocols

We followed the protocols of Colbourne et al. (1996). Briefly, microsatellites were developed from a partial genomic library of bluegill DNA. Positive clones were sequenced and "forward" and "reverse" primers were designed for bluegill using the program PRIMER (Lincoln et al. 1991). Single-locus and multiplex polymerase chain reactions were then performed for all species using the same protocols. Two microsatellite loci were sequenced using DNA from a homozygous bluegill, pumpkinseed, and largemouth bass and a T_7 cycle sequencing kit (Pharmacia).

Inheritance

Conformity to Hardy–Weinberg proportions was tested following Guo and Thompson (1992), and linkage of loci was tested using the program Genepop, version 1.2 (Raymond and Roussett 1995). Null alleles were screened by testing for an excess of homozygotes, inconsistent Mendelian inheritance patterns, and non-amplifying individuals.

Cross-amplification

Cross-species amplifications of the bluegill microsatellite loci in pumpkinseed, largemouth bass, yellow perch, and northern pike provided intragenus, intergenera, and interfamily comparisons. Potential origins of the microsatellites were inferred from the cross-species amplifications and the known evolutionary relationships of the five species. To compare levels of variability of the microsatellites that were conserved within the Centrarchidae, four loci were amplified in a large sample (n = 20) of both bluegill and largemouth bass. Both the heterozygosity, estimated according to Nei (1978), and the number of alleles present were compared. Finally, for both bluegill and largemouth bass, the probability of identity (i.e., the probability that two individuals would have identical genotypes) was calculated using the frequency of most common genotypes following Edwards et al. (1992).

Mutation

We followed Rico et al. (1996) to estimate the rate of sequence divergence within the centrarchid flanking sequences. Briefly, sequences were aligned using CLUSTAL W with default settings (Thompson et al. 1994). Priming and repeat sequences were omitted. The estimate was based on the percent sequence similarity and the time since the divergence of the older *Micropterus* species (largemouth bass) and the more recent *Lepomis* species (bluegill and pumpkinseed). Estimates were made for two independent loci (Lma116 and Lma120).

We followed Di Rienzo et al. (1994) to estimate the frequency of slipped-strand mispairing. Briefly, the mutation rate (μ) was calculated from $\mu = m_2/(2N_e\sigma^2)$, where m_2 is the variance in allele size, N_e is the effective population size, and σ^2 is the net increase in variance under mutation (e.g., under the SMM, $\sigma^2 = 1$). Since we did not know the effective population size, we calculated a relative measure of the mutation rate for each locus from the relationship $\mu \propto m_2$.

Finally, we followed Estoup et al. (1995), Shriver et al. (1993), and Di Rienzo et al. (1994) to compare the allelic distribution of the microsatellites with those predicted by the IAM, SMM, and TPM, respectively. For the IAM, the expected number of alleles

© 1999 NRC Canada

Table 1. Primer and microsatellite sequences for 10 microsatellite loci isolated from bluegill.

Locus	Primer sequence[a,b]	Microsatellite sequence[b]	Cross-species amplification[c]	Additional analyses[d]
Lma21[e]	F: CAGCTCAATAGTTCTGTCAGG R: ACTACTGCTGAAGATATTGTAG	$(TC)_{19}(AC)_{11}$	PS, LB, PE	M, P
Lma87[e]	F: ATGACACAGACTCACCATGC R: CTCCTGCCCATAAATCAGAC	$(AC)_{15}A_5$	PS	M
Lma102	F: CTGTGAAAATGGTGTGAGCG R: AAACACAAAAGTCCACGCAC	$(GT)_{19}ATGTAT(GT)_4$	PS	M
Lma104	F: TCTAGCTGTAGTGCCACAGGG R: ACAGGGACGAAGATCCCAC	$(GT)_{17}$	PS, LB, PE, PI	M
Lma116	F: GAATCTGGCTGCACACTGAC R: GTATTGACCCATAGCAGCTGC	$(GT)_{25}$	PS, LB, PE, PI	M, P, S
Lma117 (short)	F: TCACTCTGCAACCTACAAGCC R: AGATCTACATGCCACTCATTGC	$(GT)_{22}$	PS	M
Lma117[f] (long)	F: CCACCAACAGCATGCAGAC R: CATGCCACTCATTGCACTG	$(GT)_{22}$	PS	—
Lma120	F: TGTCCACCCAAACTTAAGCC R: TAAGCCCATTCCCAATTATCC	$(GT)_{28}$	PS, LB	M, P, S
Lma121	F: CACTGGTGGGAGAGGAAGAG R: AGTGATTTTCCCCTGGCAG	$(GT)_{25}$	PS, LB	M, P
Lma122[f]	F: AAATAAAGTTTGGGATACCCTG R: GTCGTGAGCTATTGCTTAAATAC	$(GT)_{30}$	PS	—
Lma124	F: CATTCAATTTGTCGCGACACC R: AAACACAAAGCCACACCATG	$(TG)_{27}$	PS, LB, PE	M

Note: Successful cross-species amplifications and loci with additional analyses are also indicated.
[a]F, forward; R, reverse.
[b]Sequences are from 5′ to 3′.
[c]PS, Pumpkinseed; LB, largemouth bass; PE, yellow perch; PI, northern pike.
[d]M, mode of mutation; P, polymorphism; S, sequence (see text).
[e]Primer and microsatellite sequence previously reported in Colbourne et al. (1996).
[f]Null alleles detected (see text).

and heterozygosity was estimated according to Ewens (1972). For the SMM and TPM, simulations were performed to generate 95% confidence intervals (CI) for the number of alleles, frequency of the most common allele, range in allele size, number of modes (based on allele frequency and size), and heterozygosity. The effective population size was set at 1000 and the mutation rate was estimated according to $\mu = m_2/2N_e\sigma^2$. Since the SMM tests are sensitive to demographic history (Di Rienzo et al. 1994), we also examined the effects of coalescence time and population bottlenecks on the results of the simulations. The average coalescence time in generations (T) was estimated using $T = m_2/(\mu\sigma^2)$ (Di Rienzo et al. 1994), where, based on our data, $m_2 = 11$ and assuming only single-step mutations, $\mu \geq 10^{-2}$, and $\sigma^2 = 1$ (Jarne and Lagoda 1996). A modified SMM simulation that applied a bottleneck consistent with the founding time of the bluegill population in Lake Opinicon was also tested (Hudson 1990). For the TPM, we assumed that multistep mutations followed a geometric distribution (see Di Rienzo et al. 1994). We assumed that the associated change in repeat number was $j + 1$ (thus, multistep mutations were of at least two repeats units). In accordance with Di Rienzo et al. (1994), the proportion of multistep mutations was ≤20% and the variance in these mutations was either 50 or 100.

All of the simulations ran for 4000 ($4N_e$) generations after which 100 samples of 338 gametes were drawn and analyzed (338 is the number of gametes that were used to calculate the observed variance in allele size). Only samples that had a variance in allele size within 15% of m_2, the observed variance in allele size, were considered. The simulation was repeated 50 times, generating a total of 5000 (50 × 100) samples. The 95% CI was determined by extracting the 125th smallest and largest value for each summary measure (the 2.5 and 97.5 percentiles, respectively).

Results

Bluegill microsatellites

About 1.0×10^4 colonies were screened and hybridization revealed over 200 positive clones. Sixty-five were sequenced and 85% (55/65) contained a $(GT)_n$ microsatellite. Repeats ranged from five to 75 GT's (25 ± 15 SD), and 53% (29/55) were perfect, while 47% (26/55) were imperfect repeats. Primer sequences and the repeat motif for the 10 microsatellites are presented in Table 1.

Null alleles were detected for two microsatellite loci, Lma117 (long) and Lma122. Both had an individual for which no amplified product was observed (Lma117: one in 44 individuals; Lma122: one in 44 individuals; note that these were different individuals) and an excess of homozygotes (Lma117: $\chi^2 = 8.3$, df = 1, $p < 0.01$ ($n = 43$); Lma122: $\chi^2 = 6.3$, df = 1, $p < 0.05$ ($n = 43$)). For Lma117, both primers were redesigned (Lma117 (short)) and subsequent analysis revealed that the null allele consisted of a single allele with a frequency of 0.19. For Lma122, the microsatellite resided near the end of the plasmid insert and we therefore had insufficient sequence data to redesign the primers. However, by reducing the priming stringency, the null allele was amplified with weak product intensity. It consisted of at least four different alleles, all of which overlapped in length with other amplifying alleles. However, the "null" allele was less intense than the other alleles, and in some heterozygous individuals, it was undetectable through the stutter bands of

© 1999 NRC Canada

Fig. 1. Minimum estimates of the origin for 10 microsatellites isolated from bluegill. The phylogeny is based on the literature and the dates are based on the fossil record (see text). The number of microsatellites present in each species and a summary of the analyses (polymorphism (P), sequences (S), mode of mutation (M)) are indicated in parentheses. For example, six of the 10 microsatellites isolated in bluegill were also found in largemouth bass, and both the degree of polymorphism and sequence similarity were analyzed in the largemouth bass.

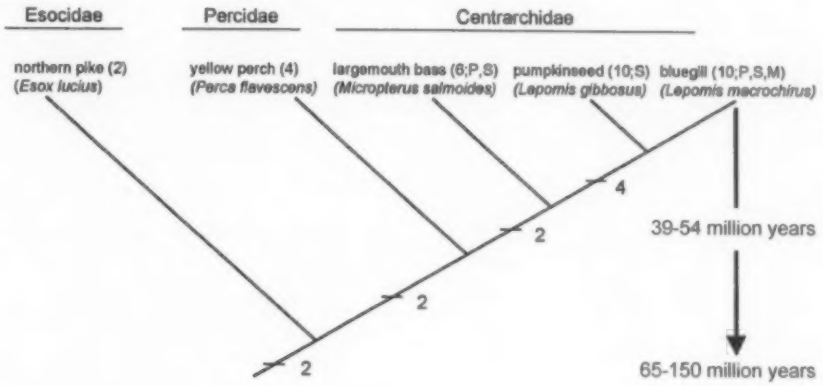

Table 2. Number of alleles, size range, and heterozygosity of the 10 microsatellites in bluegill (BG) and largemouth bass (LB).

	Number of alleles[a]		Allele size range[a,c]		Heterozygosity[a,c]	
Locus	BG	LB[d]	BG	LB[d]	BG	LB[d]
Lma21	5	15	158–182	124–222	0.61	0.82
Lma87	4	N	118–152	N	0.55	N
Lma102	5	N	88–102	N	0.64	N
Lma 104	2	NT	98, 100	NT	0.50	NT
Lma116	6	2	264–322	246–256	0.47	0.31
Lma117 (short)	5	N	152–176	N	0.60	N
Lma120	5	6	211–245	283–295	0.56	0.67
Lma121	4	5	176–196	174–178	0.53	0.15
Lma122	7	N	73–132	N	0.69	N
Lma 124	8	NT	152–176	NT	0.49	NT
Average	5±2	7±6	—	—	0.56±0.07	0.49±0.31

[a]Based on 20 individuals.
[b]Allele size range is expressed as the number of nucleotides.
[c]Nei (1978).
[d]N, no amplification; NT, not tested (see Table 1).

Table 3. Flanking sequence homology of microsatellites Lma116 and Lma120 for bluegill, pumpkinseed, and largemouth bass expressed as a proportion of the nucleotides that were identical (total nucleotides given in parentheses).

	Bluegill		Pumpkinseed	
	116	120	116	120
Pumpkinseed	0.97 (176)	0.99 (76)	—	—
Largemouth bass	0.68 (157)	0.92 (103)	0.67 (179)	0.92 (75)

the normal allele. To avoid possible inaccuracies introduced by the null allele, Lma122 was only considered in the cross-species amplifications.

The remaining eight microsatellite loci and the redesigned Lma117 (short) exhibited inheritance patterns that were consistent with their parents (χ^2 test, $p > 0.20$ for each of the nine loci), conformed to the expected Hardy–Weinberg proportions (exact test, $p > 0.40$), and were amplified in all individuals ($n = 44$). These nine microsatellite loci averaged 5 ± 2 alleles with a heterozygosity of 0.55 ± 0.06. There was no linkage between any of the loci (exact test, $p > 0.10$ for all pairs of loci). Within the Lake Opinicon bluegill population, given the number of loci and alleles identified, the probability that two random individuals would have identical genotypes was 0.0001 ($n = 9$ loci, mean for each locus = 0.38 ± 0.09).

Multiplexes

Three sets of four microsatellites were successfully coamplified in bluegill. One set contained Lma102, Lma87, Lma21, and Lma117 (long), another contained Lma102,

© 1999 NRC Canada

Table 4. Comparison of nine bluegill microsatellites with the predictions of three models: TPM, SMM, and IAM.

		Alleles[b]				Heterozygosity (%)				Range		
Locus	Var[a]	Obs	TPM	SMM	IAM	Obs	TPM	SMM	IAM	Obs	TPM	SMM
Lma21[c]	6.6	7	**5–10**	9–14	**2–10**	57	**48–83**	71–88	**16–68**	14	**7–28**	**8–14**
Lma87	13.9	4	**4–9**	12–18	**2–10**	58	**25–75**	83–91	**16–68**	17	**9–48**	**12–19**
Lma102	11.1	9	**7–13**	11–17	**4–14**	69	**50–86**	81–91	**37–78**	20	**9–42**	10–18
Lma104	0.25	2	**2–3**	**2–4**	**1–8**	50	**13–50**	**36–51**	**0–72**	1	**1–8**	**1–3**
Lma116	31.7	11	**6–14**	18–26	2–10	56	**47–85**	89–94	**16–68**	29	**15–61**	**18–32**
Lma117	16.6	6	**4–9**	13–20	**5–15**	70	**18–77**	84–92	**45–79**	12	**10–53**	14–22
Lma120	7.3	12	**6–12**	**9–13**	3–11	60	**60–86**	77–88	**28–71**	18	**7–31**	8–15
Lma121	6.9	7	**5–11**	9–13	**2–9**	52	**46–84**	77–88	**16–65**	9	**7–34**	**9–13**
Lma124	8.0	8	**5–12**	**9–14**	**2–8**	49	**48–85**	77–89	**16–61**	9	**8–24**	**9–15**
% fit			100	33	78		100	11	100		100	67

Note: Bold numbers indicate that the observed data fall within the 95% CI of the model's prediction. The proportion of the microsatellites that fit a model (% fit) is summarized.

[a]Variance in repeat number; variance and observed data are from 169 individuals except for Lma104, which is from 44.

[b]Observed data; 95% CI for TPM, SMM, and IAM.

[c]TPM parameters were $p = 0.05$ and $\sigma_g^2 = 50$ for Lma21, Lma102, Lma121, and Lma124, $p = 0.20$ and $\sigma_g^2 = 100$ for Lma87, Lma116, and Lma117, $p = 0.035$ and $\sigma_g^2 = 50$ for Lma120, and $p = 0.01$ and $\sigma_g^2 = 50$ for Lma104.

Fig. 2. Sequence alignments of microsatellites Lma116 and Lma120 in bluegill (BG), pumpkinseed (PS), and largemouth bass (LB). Dots indicate sequence homology, letters indicate point mutations, and dahes indicate deletions. The sequences are presented 5′ to 3′.

Lma116

```
BG   AATTCTATTCTACAGTCAGACAGAAACAGTGTGTGTGTGTGTGTGTGTGTGTGTGTGTGTGTG
PS   .......................G............C......A...A.----------------
LB   NNNNNNNNN..............G....C.......C...C....CC....A.------------

BG   TGTGTGTGTGTGTGGTAATGTGTTTGTGTGTCAGCGTGCGAGNCNNNNNNNAGGGAGNAAGAATG
PS   ----------.............................A..A.GGGAGTA......A.......
LB   ----------....T......C.................A.GGGAGGA..A...A.......

BG   NNAAGAGATAGATAATAAAAGAGAAAGGTGACGCAAGCGAAGCAGATGGAAGCNNNNCCAGAGAA
PS   AA.....................................T..............AAAA........
LB   AA..........A..G.G..AG.TG.AAA..GAT.T.AT..A-...GAA.G.TGACG.A..T..T

BG   ACAAACAGANATTCTACAAGAAAGAATGTATTTACAGCATTATATATTAAGTTGCA
PS   .........C....CT...T................................NNN
LB   G..G.TG..AGCGAA....A.C.AGCA.ACA..CT.CA..G.AGNNNNNNNNNNN
```

Lma120

```
BG   TGGTCTTCAATAGGCTTCCAAAAGTGTGTGTGTGTGTGTGTGTGTGTGTGTGTGTGTGTGT
PS   NNNNNNNNNNNNNNNNNN.....................................----------
LB   ..........G.....................................------------------

BG   GTGTGTGTGTGTGTTCACATGTAAATACACAAATACACTGTAATTGTAATTGTGTGCATGTGTTT
PS   --------------.................---------..A.....................
LB   --------------....G..C......G..GTAAT--.............................

BG   A-TATGTGTGTTTGCCTACATGTGTGTGTTCATGCGTGCATGTTTTTCAGGGCAGTTA
PS   .G.............................NNNNNNNNNNNNNNNNNNNNNNNNNNNN
LB   .-.........................A..NNNNNA.NNNNNNNNNNNNNNNNNNNNN
```

Lma116, Lma120, and either Lma21 or Lma121, and the final set contained Lma116, Lma120, Lma121, and Lma122. The band intensities within a set of loci were similar and apparently insensitive to small variations in primer concentrations.

Cross-amplification

All 10 of the bluegill microsatellites amplified in the congeneric pumpkinseed. Six amplified in the heterogeneric largemouth bass, four amplified in the yellow perch, and two amplified in the northern pike (Table 1).

Based on the evolutionary relationships of the five species and the amplification results, potential origins for the microsatellites were assessed (Fig. 1). For example, the four microsatellites that amplified only in the bluegill and pumpkinseed originated prior to the divergence of these species. The two microsatellites that amplified in all five species originated prior to their divergence, at least 65–150 million years ago.

© 1999 NRC Canada

Modes			Frequency (%)		
Obs	TPM	SMM	Obs	TPM	SMM
3	**0–4**	**1–5**	57	**25–70**	18–48
2	**0–3**	**2–6**	49	**36–86**	14–32
4	**1–4**	**2–6**	41	**21–68**	13–36
1	**1–2**	**0–1**	53	**52–93**	**50–78**
3	**1–5**	**3–8**	64	**23–70**	9–24
3	**0–4**	**2–6**	45	**31–91**	13–30
4	**1–4**	**1–5**	53	**20–59**	17–41
3	**1–4**	**1–5**	66	**22–68**	17–42
3	**1–5**	**1–5**	69	**22–70**	16–41
	100	100		100	11

The polymorphism of the microsatellite loci was determined for bluegill and largemouth bass (Table 2). It was not significantly different for the four microsatellites examined in both species. At these loci, the average number of alleles in bluegill and largemouth bass was 5.0 ± 0.8 and 7.0 ± 5.6 (paired t test, $t = 0.69$, df = 3, $p = 0.54$), respectively, and their expected heterozygosity was 0.54 ± 0.06 and 0.49 ± 0.31 (paired t test, $t = 0.41$, df = 3, $p = 0.71$), respectively. The probability that two random individuals had identical genotypes in the largemouth bass was 0.015 (n = 4 loci, mean for each locus = 0.45 ± 0.30).

Mutation

Large portions of the Lma116 and Lma120 sequences were similar in the bluegill, pumpkinseed, and largemouth bass (Fig. 2; Table 3). Alignments revealed significant homology, although substitution, deletion, and insertion mutations were observed. Lma120 had higher overall homology than Lma116 in both the repeat region and the flanking regions (average homology: Lma116, 0.77; Lma120, 0.94). Lma116 showed substantial degeneration of the repeat. For both loci, the repeat region was shorter in the nonsource species than that of the source species (Lma116: bluegill, 25 repeats; pumpkinseed, 11; largemouth bass, 12; Lma120: bluegill, 28; both others, 13). Based on the sequence similarity of all three centrarchid species, and assuming a divergence time of 39–54 million years, the estimated rate of sequence divergence at Lma116 was 0.83 ± 0.02 to 0.59 ± 0.01% per million years and at Lma120 was 0.20 ± 0.00 to 0.14 ± 0.00% per million years.

The variance in repeat number at the nine microsatellite loci ranged from 0.25 at Lma104 to 31.7 at Lma116 (Table 4). The large variance observed at Lma116 was attributed to two large gaps in allele sizes, of seven and 12 repeats, resulting in three "clusters" of alleles at this locus. The average variance was 11 ± 9 repeats. Since the rate of slipped-strand mispairing is directly proportional to the variance in repeat number, it showed over 100-fold variation (31.7/0.25) among the microsatellite loci.

The results from the IAM, SMM, and TPM analyses are summarized in Table 4. The nine microsatellite loci fit the TPM consistently, as it was possible to select values for the parameters p and σ^2 such that the microsatellite characters fit the model (i.e., fall within the 95% CI). For example, at $p = 0.05$ and $\sigma^2 = 50$, 56% (5/9) of the loci fell within the expected number of alleles, 67% (6/9) within the heterozygosity, 89% (8/9) within the range, 100% (9/9) within the number of modes, and 78% (7/9) within the frequency of the most common allele. All together, 44% (4/9) of the loci conformed to the TPM with these parameters at all five characters. Three of the remaining five loci conformed to the TPM at each of the five characters for $p = 0.20$ and $\sigma^2 = 100$. The last two loci fit the TPM at values of $p < 0.05$. In contrast, the observed microsatellite data deviated significantly from that expected under the SMM. Only one locus conformed to the SMM expectation at all of the characters. All nine microsatellite loci also conformed to the IAM for heterozygosity and 78% (7/9) conformed to the IAM for the number of alleles.

Discussion

Microsatellites

This study provides primers for 10 microsatellite loci that should be useful for centrarchid research including applications such as population differentiation and the study of life history, mating system, and behavioural evolution. The microsatellites are polymorphic, averaging over five alleles and a heterozygosity of 0.56 per locus. The low probability of identity associated with these loci should also make them useful for evolutionary and ecological studies requiring, for example, the tracking of individuals and parentage analyses.

Initially, two of the 10 microsatellite loci had a null allele. We were only able to inconsistently visualize the "null" alleles by reducing the primer annealing stringency. For one locus, we also redesigned primers and were successful at consistently amplifying its null allele. Therefore, redesigning primers may be a better approach to consistently detect a null allele (also see Paetkau and Strobeck 1995).

Some of the microsatellite loci are also found in the pumpkinseed, largemouth bass, yellow perch, and northern pike. Those that were conserved in largemouth bass were equally polymorphic as compared with bluegill, the microsatellite source species. It is likely that these loci will have similar levels of polymorphism in all of the species within the sunfish family, since largemouth bass are most distantly related to bluegill (e.g., see Primmer et al. 1996 for a discussion). The multiplexes that we have developed for bluegill should increase the efficiency of generating genotype data using the microsatellites and may also facilitate their use with other centrarchid species.

Evolution

Microsatellite loci generally have ancient origins and show considerable evolutionary conservation. For example, between freshwater and marine species of turtles, microsatellite homologues have shown at least 300 million years of conservation (FitzSimmons et al. 1995). In fish, homologues have been found between species from agnathans and gnathostomes, which diverged about 470 million years ago (Rico et al. 1996). Consistent with the long persistence of microsatellite loci, we found that two of the loci isolated

© 1999 NRC Canada

from bluegill were present in northern pike, indicating origins predating 65–150 million years. However, several of the loci have diverged sufficiently to be undetectable even in closely related species of the same genus (e.g., Lma87, Lma102, Lma117, and Lma122 were common only to bluegill and pumpkinseed). This suggests that not all microsatellite loci from poikilotherms show sufficient conservation of priming sites to be detectable over long periods of time.

The rate of sequence divergence of nuclear DNA is thought to be lower in poikilotherms than in homeotherms (Rico et al. 1996 and references within). For example, Rico et al. (1996) estimated the rates of sequence divergence for nuclear microsatellite flanking sequences in fish to be between 0.02 and 0.05% per million years, while in mammals, Pépin et al. (1995) estimated a rate of about 0.93% per million years. Our estimate of the rates of sequence divergence are 0.14–0.83% per million years, intermediate to the estimates in mammals and fish. Therefore, it is not clear whether there will be a consistent difference between poikilotherms and homeotherms. Further, our data suggest that this rate can be quite variable within a species. This may suggest that the rate of sequence divergence at microsatellite flanking sequences is dependent on the locus itself.

Our tests of the mode of mutation for microsatellites support the TPM and IAM while rejecting the SMM. The failure of the SMM to explain the observed variations in our data could not be attributed to a recent bottleneck. Bluegill entered Lake Opinicon only about 170 years ago (Curran et al. 1947). If this population was founded by only a few individuals (i.e., bottlenecked) followed by rapid population growth, it is expected that the time of coalescence would be close to the time of the bottleneck (Di Rienzo et al. 1994 and references within). However, our estimate of T (the average coalescence time), based on the SMM, is ≥1100 generations. This is considerably longer than the age of the Lake Opinicon population, suggesting that the population has not experienced a recent bottleneck. Furthermore, the observed data did not consistently fall within the predicted ranges based on the SMM simulations even when a population bottleneck was incorporated. For example, when assuming that the population was founded by 0.5% of the source population, only 22% (2/9) of the microsatellites conformed to all five microsatellite characteristics. Although we cannot exclude other historical effects on demography, it does not appear that a recent bottleneck can explain the observed rejection of the SMM for these microsatellites.

Although it is generally considered that microsatellite variation is generated via a stepwise mutational process (e.g., Schlötterer and Tautz 1992), our results indicate that this process may not involve only single repeats. Instead, the conformity to the TPM suggests that these microsatellite loci follow a stepwise mutational process with the occasional large mutation of multiple repeats. These large mutations are more likely to generate alleles of novel sizes than single-step mutations and may explain the conformity of such microsatellites to the IAM, since it assumes that mutations give rise to novel alleles (also see Di Rienzo et al. 1994). However, the TPM and IAM are not equivalent models. The IAM assumes that alleles of equivalent size are identical by descent, while no relationship can be inferred among alleles of different sizes. The TPM does not assume that alleles of equivalent size are identical by descent but that alleles of similar sizes are more closely related.

It is necessary to determine which mutation model best describes microsatellite allelic variation in order to select the appropriate test statistics for estimating population differentiation and distance. For example, Slatkin (1995) showed that unlike R_{ST}, F_{ST} tends to underestimate the true level of population differentiation when using microsatellites that conform to the SMM. As statistics based on the TPM are not yet available, those based on the IAM may be the most appropriate for the presented microsatellites that conform to both the IAM and TPM. However, since the IAM does not necessarily reflect the stepwise mutational process of microsatellites, the development of test statistics based on the TPM may provide more accurate estimations of population differentiation and structure. To our knowledge, this study represents that first test of all three mutation models showing the conformity of empirical data to both the TPM and IAM.

Acknowledgments

John Colbourne, Junjian Chen, and Paul Hebert are thanked for their advice and assistance in forming the DNA library. Lucy Dueck of the Texas Freshwater Fisheries Center and Douglas W. Nelson of the University of Michigan Museum of Zoology are thanked for supplying tissue samples. Ben Kim assisted with primer development. This work was supported by an NSERC research grant to M.R. Gross and an NSERC graduate fellowship to B.D. Neff.

References

Avise, J.C. 1994. Molecular markers, natural history and evolution. Chapman and Hall, New York.

Baylis, J.R., Wiegmann, D.D., and Hoff, M.H. 1993. Alternative life histories of smallmouth bass. Trans. Am. Fish. Soc. **122**: 500–510.

Belk, M.C. 1998. Predator-induced delayed maturity in bluegill sunfish (*Lepomis macrochirus*): variation among populations. Oecologia, **113**: 203–209.

Coad, B.W., Waszczuk, H., and Labignan, I. 1995. Encyclopedia of Canadian fishes. Canadian Museum of Nature and Canadian Sport Fishing Productions Inc., Ottawa, Ont.

Colbourne, J.K., Neff, B.D., Wright, J.M., and Gross, M.R. 1996. DNA fingerprinting of bluegill sunfish (*Lepomis macrochirus*) using $(GT)_n$ microsatellites and its potential for assessment of mating success. Can. J. Fish. Aquat. Sci. **53**: 342–349.

Curran, H.W., Bardach, J., Bowman, R.I., and Lawler, H.G. 1947. A biological survey of Lake Opinicon. Progress report. Hanson and Edgar, Kingston, Ont.

Di Rienzo, A., Peterson, A.C., Garza, J.C., Valdes, A.M., Slatkin, M., and Freimer, N.B. 1994. Mutational processes of simple-sequence repeat loci in human populations. Proc. Natl. Acad. Sci. U.S.A. **91**: 3166–3170.

Edwards, A., Hammond, H.A., Jin, L., Caskey, C.T., and Chakraborty, R. 1992. Genetic variation at five trimeric and tetrameric tandem repeat loci in four human population groups. Genomics, **12**: 241–253.

Estoup, A., Tailliez, C., Cornuet, J.-M., and Solignac, M. 1995. Size homoplasy and mutational processes of interrupted microsatellites in two bee species, *Apis mellifera* and *Bombus terrestris* (Apidae). Mol. Biol. Evol. **12**: 1074–1084.

© 1999 NRC Canada

Ewens, W.J. 1972. The sampling theory of selectively neutral alleles. Theor. Popul. Biol. **3**: 87–112.

FitzSimmons, N.N., Moritz, C., and Moore, S.S. 1995. Conservation and dynamics of microsatellite loci over 300 million years of marine turtle evolution. Mol. Biol. Evol. **12**: 432–440.

Gross, M.R. 1982. Sneakers, satellites and parentals: polymorphic mating strategies in North American sunfishes. Z. Tierpsychol. **60**: 1–26.

Gross, M.R. 1996. Alternative reproductive strategies and tactics: diversity within sexes. Trends Ecol. Evol. **11**: 92–98.

Guo, S.W., and Thompson, E.A. 1992. Performing the exact test of Hardy–Weinberg proportions for multiple alleles. Biometrics, **48**: 361–372.

Hudson, R.R. 1990. Gene genealogies and the coalescent process. Oxf. Surv. Evol. Biol. **7**: 1–44.

Jarne, P., and Lagoda, J.L. 1996. Microsatellites, from molecules to populations and back. Trends Ecol. Evol. **8**: 285–288.

Kimura, M., and Crow, J.F. 1964. The number of alleles that can be maintained in a finite population. Genetics, **49**: 725–738.

Kimura, M., and Ohta, T. 1978. Stepwise mutation model and distribution of allelic frequencies in a finite population. Proc. Natl. Acad. Sci. U.S.A. **75**: 2868–2872.

Lelek, A. 1987. The freshwater fishes of Europe. Vol. 9. Threatened fishes of Europe. AULA-Verlag GmbH, Wiesbaden, Germany.

Lincoln, S.E., Daly, M.J., and Lander, E.S. 1991. PRIMER: a computer program for automatically selecting PCR primers. Version 0.5. Whitehead Institute for Biochemical Research, Cambridge, MA 02142.

Mabee, P.M. 1988. Supraneural and predorsal bones in fishes: development and homologies. Copeia, **1988**: 827–838.

Miller, R.R. 1958. Origin and affinities of the freshwater fish fauna of western North America. *In* Zoogeography. *Edited by* C.L. Hubbs. Am. Assoc. Adv. Sci. Publ. No. 51. pp. 187–222.

Nei, M. 1978. Estimation of average heterozygosity and genetic distance from a small number of individuals. Genetics, **89**: 583–590.

Nelson, J.S. 1984. Fishes of the world. 2nd ed. John Wiley & Sons, New York.

O'Connell, M., and Wright, J.M. 1997. Microsatellite DNA in fishes. Rev. Fish Biol. Fish. **7**: 331–363.

O'Connell, M., Danzmann, R.G., Cornuet, J.-M., Wright, J.M., and Ferguson, M.M. 1997. Differentiation of rainbow trout (*Oncorhynchus mykiss*) populations in Lake Ontario and the evaluation of the stepwise mutation and infinite allele mutation models using microsatellite variability. Can. J. Fish. Aquat. Sci. **54**: 1391–1399.

Paetkau, D., and Strobeck, C. 1995. The molecular basis and evolutionary history of a microsatellite null allele in bears. Mol. Ecol. **4**: 519–520.

Pépin, L., Amigues, Y., Lépingle, A., Berthier, J., Bensaid, A., and Vaiman, D. 1995. Sequence conservation of microsatellites between *Bos taurus* (cattle), *Capra hircus* (goat) and related species. Examples of use in parentage testing and phylogeny analysis. Heredity, **74**: 53–61.

Primmer, C.R., Moller, A.P., and Ellegren, H. 1996. A wide-range survey of cross-species microsatellite amplification in birds. Mol. Ecol. **5**: 365–378.

Raymond, M., and Rousett, F. 1995. Genpop (version-1.2). Population genetics software for exact tests and ecumenicism. J. Hered. **86**: 248–249.

Rico, C., Rico, I., and Hewitt, G. 1996. 470 million years of conservation of microsatellite loci among fish species. Proc. R. Soc. Lond. Ser. B. Biol. Sci. **263**: 549–557.

Schlötterer, C., and Tautz, D. 1992. Slippage synthesis of simple sequence DNA. Nucleic Acids Res. **20**: 211–215.

Schramm, H.L., Jr., Armstrong, M.L., Funicelli, N.A., Green, D.M., Lee, D.P., Manns, R.E., Jr., Taubert, B.D., and Waters, S.J. 1991. The status of competitive sport fishing in North America. Fisheries (Bethesda), **16**: 4–12.

Shriver, M.D., Jin, L., Chakraborty, R., and Boerwinkle, E. 1993. VNTR allele frequency distribution under the stepwise mutation model. Genetics, **134**: 983–993.

Slatkin, M. 1995. A measure of population subdivision based on microsatellite allele frequencies. Genetics, **139**: 457–462.

Thompson, J.D., Higgins, D.G., and Gibson, T.J. 1994. CLUSTAL W: improving the sensitivity of progressive multiple sequence alignment through sequence weighting, position-specific gap penalties and weight matrix choice. Nucleic Acids Res. **22**: 4673–4680.

Valdes, A.M., Slatkin, M., and Freimer, N.B. 1993. Allele frequencies at microsatellite loci: the stepwise mutation model revisited. Genetics, **133**: 737–749.

Wainwright, P.C., and Lauder, G.V. 1992. The evolution of feeding biology in sunfishes (Centrarchidae). *In* Systematics, historical ecology, and North American freshwater fishes. *Edited by* R.L. Mayden. Standford University Press, Standford, Calif. pp. 472–491.

Wilson, M.V.H., and Williams, R.G. 1992. Phylogenetic, biogeographic, and ecological significance of early fossil records of North American freshwater teleostean fishes. *In* Systematics, historical ecology, and North American freshwater fishes. *Edited by* R.L. Mayden. Standford University Press, Standford, Calif. pp. 224–246.

© 1999 NRC Canada

Predation risk breaks size-dependent dominance in juvenile coho salmon (*Oncorhynchus kisutch*) and provides growth opportunities for risk-prone individuals

Ulrich G. Reinhardt

Abstract: Groups of coho salmon (*Oncorhynchus kisutch*) fry in stream tanks formed size-determined dominance hierarchies, which were upheld through aggressive interactions and led to smaller fish occupying inferior feeding positions. Under simulated predation risk, the frequency of agonistic interactions was reduced, but more intensive aggressive behaviours were performed. This allowed small fish to gain access to better feeding positions. The effect of the predation threat on coho behaviour seemed to extend across a riffle into a second pool that served as a refuge. Smaller fry that chose to be in the exposed pool had greater growth rates than those that mainly occupied the refuge, while large fry that exposed themselves to predation did not grow better than their risk-avoiding counterparts. Differences in risk taking and growth among small coho fry in this experiment may support reports for Atlantic salmon (*Salmo salar*) of a split into different life history trajectories. The observations suggest that the presence of predators creates opportunities for the expression of alternative behavioural strategies that are absent under size-dependent dominance hierarchies.

Résumé : Des groupes d'alevins de saumon coho (*Oncorhynchus kisutch*) dans des bassins en cours d'eau formaient des ordres hiérarchiques selon la taille, qui ont été établis par des interactions agressives, les poissons de petite taille finissant par avoir un accès plus difficile aux ressources alimentaires. Dans une simulation de risque de prédation, la fréquence des interactions agonistiques a été réduite, mais des comportements agressifs plus marqués se sont développés, ce qui a permis aux poissons de petite taille d'avoir un accès plus facile aux ressources alimentaires. L'effet de la menace de prédation sur le comportement du coho semblait s'étendre dans un radier jusque dans une deuxième fosse qui servait de refuge. Les alevins de petite taille qui choisissaient de demeurer dans la fosse exposée ont présenté un taux de croissance plus élevé que ceux qui n'ont fait qu'occuper le refuge, tandis que les alevins de grande taille qui s'exposaient à la prédation ne présentaient pas une meilleure croissance que leurs homologues qui ne prenaient pas de risque. Les différences au niveau de la prise de risque et de la croissance entre les alevins de petite taille dans cette expérience peuvent appuyer les observations, dans le cas du saumon atlantique (*Salmo salar*), d'une division en différents cycles vitaux. Selon les observations, la présence de prédateurs créerait des possibilités d'expression d'autres stratégies comportementales qui sont absentes dans des ordres hiérarchiques selon la taille.

[Traduit par la Rédaction]

Introduction

Nonlethal effects of predators can include the increase of intraspecific competition if prey concentrate in refuges or the decrease of competition if only parts of the prey population seek refuge (e.g., Mittelbach and Chesson 1987). Individual variation in predator avoidance behaviour within fish populations may be caused by differential susceptibility of prey to their predators (e.g., Werner et al. 1983) or by differences among the prey animals in their energy stores (Dill and Fraser 1984) or energy requirements (Abrahams and Dill 1989). Reinhardt and Healey (1997) showed that the reaction of age-0 coho salmon (*Oncorhynchus kisutch*) to predators was influenced by the body size of the individual in accordance with predictions from dynamic optimization models (Clark 1994). Larger individuals avoided exposure to a predation threat and had reduced growth rates, whereas smaller individuals were less cautious and maintained their growth rate in the presence of a threat. Growth depensation, which commonly results from size-dependent competitive exclusion from food sources in coho (Sandercock 1991; Ryer and Olla 1996) and other salmonids (e.g., Elliott 1990), did not occur under simulated predation threat.

In this study, I analyse observations of groups of coho competing for food in a laboratory environment. Following up on the results reported by Reinhardt and Healey (1997), I examine how the social dynamics that cause growth depensation are influenced by the presence of predators. Because recent studies on salmonids suggest that individual

Received October 16, 1998. Accepted March 5, 1999. J14837

U.G. Reinhardt.[1] Fisheries Centre, University of British Columbia, 2204 Main Mall, Vancouver, BC V6T 1Z4, Canada.

[1]Current address: Tomakomai Research Station, Hokkaido University Forests, Takaoka, Tomakomai City, Hokkaido, Japan, 053 0035. e-mail: reinhard@exfor.agr.hokudai.ac.jp

© 1999 NRC Canada

Fig. 1. Experimental setup. Coho salmon in the exposed pool were subjected to simulated predation risk by dipping an electrified bird model during the first 3 days out of a total of 5 days that behavioural observations were made. See text for more details.

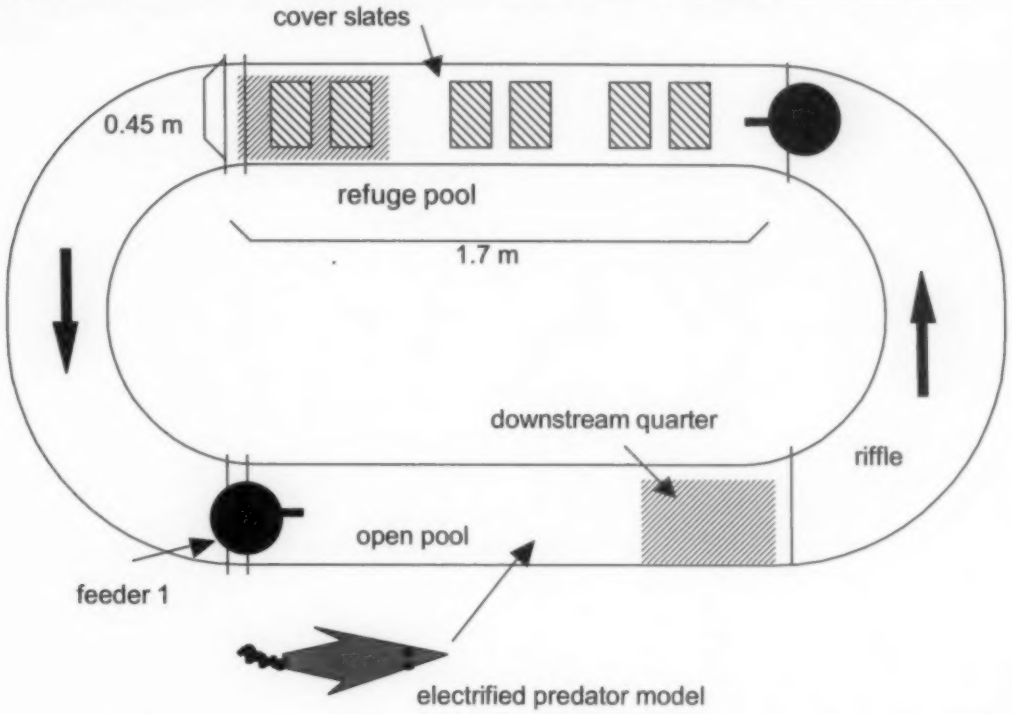

foraging behaviour and the rearing environment interact to influence fitness indicators (Metcalfe et al. 1989, 1995; Adams and Huntingford 1996), I also examine whether environments with different levels of predation risk favour the expression of different foraging phenotypes in coho.

Materials and methods

The experiment was designed to allow observation of territorial contests within groups of fish and individual differences in behaviour under the threat of predation. It was conducted at the University of British Columbia during July and August of 1995 using young-of-the-year coho captured at the fry stage from the Salmon River near Langley, B.C.

I simulated a predation threat to the fish by means of an electrified model of a kingfisher. By briefly (about 1 s) plunging the model into a tank containing fish and applying a shock (300 V/75 Hz), the fish were frightened. Before using the fish in the experiments, they were conditioned to the model in the holding tanks by two short presentations by the electrified model to ensure recognition of the model as a threat later in the experiments. Tests of the stress response of coho fry to the electrified model showed that the mild shock enhanced the fright response of the fish above that produced by the model alone but did not prolong the postpredation stress recovery period (Reinhardt and Healey 1999)

I divided each of three oval recirculating stream tanks into two pools (length 1.7 m, width 0.45 m, depth 0.28 m) separated by a riffle of about 2.5 m length and 2 cm depth (Fig. 1). One of the pools (refuge pool) contained six semitransparent Plexiglas plates suspended about 1 cm beneath the water surface as simulated overhead cover. The plates blocked access to food floating at the surface and occupied about a third of the surface of the pool (Fig. 1). Floating food (freeze-dried shrimp at 5% of the combined live weight of the 20 fish per day, equally divided between pools) was delivered continuously during daylight hours by automatic feeders at the head of the pool (Fig. 1). A stream of pressurized air blew the food particles a variable distance (up to 40 cm) downstream from the feeder so that no single fish could dominate the whole food delivery area. Uneaten food floated to skimmers at the tail of the pool and was removed from the tanks.

For each replicate of the experiment, 20 coho juveniles were netted from the holding tank, anaesthetized, weighed to the nearest 0.1 g, and marked individually by tattooing an ink mark on the side of the body. The 20 fish were released into a stream tank and allowed 60 h to choose between pools and establish a territorial hierarchy. I observed location and behaviour of the fish in the pools through glass windows from a darkened observation space in the centre of the tanks starting on day 3 of each experiment. After the first observation in the morning of day 3, a predation threat was simulated in the pool without cover (open pool) by dipping the electrified kingfisher model as described above. This procedure was repeated three times per day for 3 days, each time dipping the model one to four times at 30-s intervals. The fish in the refuge pool were spared the predation simulation. For the 3 days of simulated predation threat (during predation) and 2 days afterwards (after predation), I assessed the position and behaviour of all visible fish five times per day. For each fish, the pool it occupied was recorded and whether it was seen in the upstream three quarters of the pool or in the downstream quarter (farthest away from the feeder; Fig. 1). I determined the position by choosing an individual fish in order of its coded mark and recording its position relative to a painted line on the tank at the moment I first located it. I then observed the behaviour of the fish for three 5-s periods. During each 5-s period, three kinds of agonistic interactions were recorded in ascending order of intensity (after Swain and Holtby 1989): (*i*) lat-

© 1999 NRC Canada

Fig. 2. Distribution of agonistic activities for coho salmon fry above (large fish, solid bars) and below (small fish, open bars) median body weight in the control treatment. "Defensive" refers to a focal fish being the receiver of an agonistic action; "aggressive" refers to an attack by a focal fish.

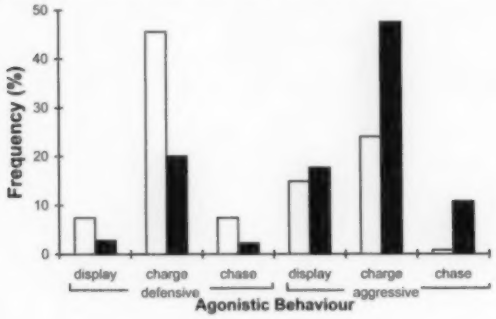

eral display (showing the side of the body with erected dorsal and pectoral fins), (*ii*) charge (rapid acceleration toward a conspecific to within one body length or less, sometimes followed by bumping into the other or nipping), and (*iii*) chase (chasing the other for more than two body lengths after a charge). I also recorded whether a fish attacked an opponent or received the attack. Agonistic interactions were recorded independent of their duration (e.g., 4 s of station holding and 1 s of attack counted as an attack), and if more than one interaction for any 5-s period occurred, only the first one was recorded. This resulted in a maximum of 15 observations for each fish and each day. The maximum total observation time in this experiment was about 6.5 min for each fish and 125 min for each replicate.

On day 7 of each experiment, all fish were removed, anaesthetized, and weighed to allow calculation of growth rates over the previous week. Four weeks of the experiment with predation treatment (12 replicates with fish of 1.9 g mean body weight) preceded 2 weeks of control observations (six replicates, 2.3 g mean weight) with the same setup, except that no simulated predation was performed and only three observation periods per day were conducted. I used different fish in each replicate. For further details on experimental protocol and the effect of conditioning fish of different sizes by electric shock, see Reinhardt and Healey (1997, 1999).

Data handling and statistics

A group of 20 fish, observed for 5 days, was considered one replicate for most statistical analyses, with the exception of χ^2 tests where pooled observations across replicates were used. For the analysis of social hierarchies, fish were divided into two groups: those heavier than the median weight of the 20 fish in the replicate and those lighter than the median weight. Since in the control observations (no predation), there were no differences in the number of fish and their behaviour between the two pools of the tanks, observations from the two sides were pooled for analysis. Data from the predation treatment were divided by location ("exposed" and "refuge" pools) and time relative to the predation simulation ("during" (days 2 and 3 of each trial) and "after" (days 4 and 5)). An aggression score was calculated for each fish for which I had observed a minimum of two agonistic interactions. A lateral display, charge, or chase performed by the focal fish was given a positive score of 1, 2, and 3 points, respectively, and equivalent negative scores when the focal fish was the receiver of such behaviours (e.g., a fish observed to have chased others twice while having been charged once would receive an aggression score of 3 + 3 − 2 = 4). The *P* values given for all statistical tests are two-tailed; $P = 0.05$ was used as the significance criterion throughout.

Fig. 3. Relationship between aggression score and growth rate of small (open circles) and large (solid diamonds) coho salmon fry in the control treatment. The correlation between the two factors was significant. See the text for calculation of the aggression score.

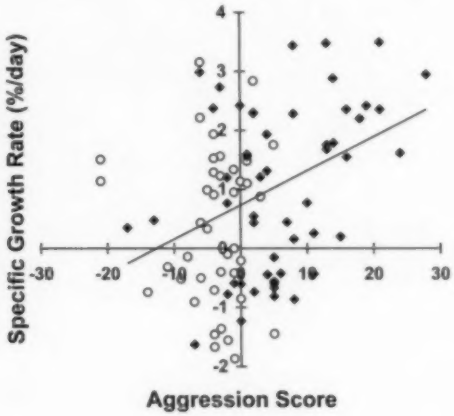

Results

Social interactions in absence of predation threat

Of all observed agonistic interactions, charges against an opponent were most frequent (about 70%), followed by lateral displays and chases (Fig. 2). Lateral displays against a focal fish were more difficult to detect, which probably accounts for their being less frequently recorded than lateral displays by the focal fish (Fig. 2). Large fish engaged in more agonistic behaviour than small fish (0.15 agonistic acts per 5-s observation period versus 0.11 for small fish; paired *t* test on arcsine-transformed frequencies: $t_5 = 2.94$, $P < 0.05$). Large fish were more often attackers than receivers (Fig. 2) (3:1 ratio of attacks/defenses when focal fish were large), whereas small fish were more often receivers of aggressive actions (4:6 ratio of attacks/defenses when focal fish were small). This difference in distribution of aggressive/defensive interactions between size-classes was significant (χ^2 test on observed against expected even distribution of pooled counts of aggressive and defensive interactions: $\chi^2_1 = 79.7$, $P < 0.001$).

The mean size of fish in the downstream quarter of the tank was significantly smaller than in the rest of the pool (paired *t* test on log-transformed mean weights of fish in the two areas of the tank: $t_5 = 7.25$, $P < 0.01$), which confirmed the visual impression that small fish mainly occupied the downstream part of a pool (farthest away from the feeder) where the frequency of agonistic interactions was lower (mean frequency of 0.07 per 5-s observation period in the downstream area versus 0.14 in the upstream part).

The specific growth rate was correlated with the aggression score of the individual fish (Fig. 3) (Pearson $r = 0.337$, $P < 0.05$) (see Data handling and statistics section for details on calculation). Division into negative and positive aggression scores (Fig. 3) reflects the division of fish into a small

© 1999 NRC Canada

Table 1. Relative frequency (%) and number (in parentheses) of three types of agonistic behaviour in coho salmon control and predation treatments divided into four combinations of location and time relative to the predation simulation.

Treatment	Display	Charge	Chase	Comparison	χ^2	P (∞)
Control	18 (112)	68 (420)	13 (80)			
I. Exposed/during	11 (23)	63 (132)	27 (56)	Control vs. I	28.2	<0.001
II. Refuge/during	10 (43)	68 (304)	23 (101)	Control vs. II	26.9	<0.001
III. Exposed/after	18 (48)	67 (176)	15 (38)	III vs. I	13.7	<0.01
IV. Refuge/after	13 (46)	73 (258)	13 (49)	IV vs. II	10.72	<0.05

Note: χ^2 values are given for significant pairwise comparisons among groups.

Fig. 4. Mean frequency (+2 SE) of coho salmon agonistic interactions in the control treatment (n = 6) and predation treatment (n = 12). Data for the predation treatment are divided by location (exposed/refuge pool) and time relative to the predation simulation (during/after). Asterisks denote significant differences among categories in single-degree-of-freedom tests.

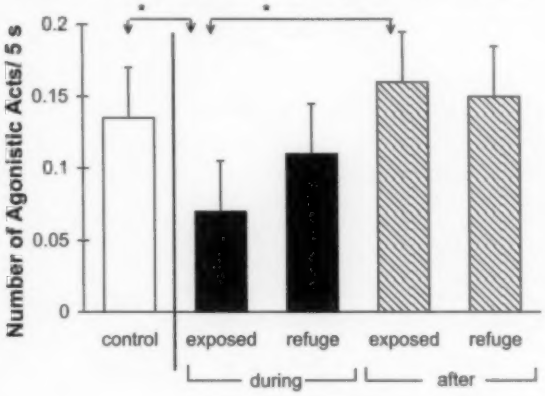

and a large group: only seven (15%) of the fish with a positive score were small and 10 (25%) of fish with a negative score were large.

Social interactions under simulated predation

During the days that the predator model was dipped into the exposed pool, the mean level of aggression in the exposed pool was reduced by about 50% compared with the control treatment (Fig. 4) (exposed pool: mean of 0.07 agonistic acts per observation period, range 0–0.16) and returned following predation simulation to values comparable with the control observations (control treatment: mean of 0.14, range 0.07–0.2). In the refuge, the mean frequency of agonistic interactions during simulation was intermediate between values for the exposed pool and the control treatment (Fig. 4). The frequencies of agonistic interactions differed significantly among the four location/time intervals (repeated-measures ANOVA on arcsine square root transformed frequencies: $F_{3,33} = 5.08$, $P < 0.01$). Single-degree-of-freedom tests showed significantly lower levels of agonistic behaviours during predation in the exposed pool but not in the refuge pool (Fig. 4) (t tests on arcsine square root transformed values: control versus exposed pool during, $t_{16} = -2.16$, $P < 0.05$; control versus refuge pool during, $t_{16} = -0.85$, not significant; Tukey test on transformed values: exposed pool during versus after, $q = 4.72$, $P < 0.05$; refuge pool during versus after, not significant).

During predation simulation in both the exposed and refuge pools, the relative frequency of lateral displays was reduced, while the relative frequency of chases was about twice that of the control observation (Table 1). I analysed the patterns in the distribution of the three types of agonistic interactions (display, charge, and chase) statistically with a series of pairwise χ^2 tests using pooled counts of agonistic interactions. In both the exposed and refuge pools, the distribution of agonistic interactions during predation differed significantly from the control and after-predation distributions (Table 1).

In the predation treatment, as in the control treatment, fish occupying the downstream end of the tank were on average smaller than those in the upstream part of the tank, closer to the feeder (Fig. 5). However, the size difference was smaller during the days of simulated predation (one-sample t test on log-transformed ratios of mean fish weight in the downstream quarter/weight in the upstream part: exposed pool during predation, $t_{11} = 1.84$, not significant, power = 0.12; refuge pool during predation, $t_{11} = -0.04$, not significant, power = 0.36). After predation simulation was halted, the fish in the back were again significantly smaller than those closer to the feeder (one-sample t test: exposed pool after predation, $t_{11} = -2.96$, $P < 0.05$; refuge pool after predation, $t_{11} = -2.78$, $P < 0.05$).

Choice of habitat and growth rate

To get an indication of habitat preference of the fish, I divided the number of times an individual was observed in either pool by the number of all observations for that fish. In the control and predation treatments, the majority of fish showed a strong preference for one of the two pools (Fig. 6), with a slight tendency for large fish to be more bound to a single pool (χ^2 test on the distribution of observations belonging to the three categories of pool fidelity: comparison between small and large fish (Fig. 6*a*), control, $\chi^2_4 = 5.29$; predation, $\chi^2_4 = 5.14$; both not significant; comparison between control and treatment, both size-classes pooled (Fig. 6*b*), $\chi^2_4 = 6.42$, not significant). This preference for one habitat was not due to a general lack of sampling of the available choices: the mean number of confirmed switches between pools (number of times an individual was observed in different pools in subsequent observations periods as a minimum estimate of switches) was 2.7 (median = 2) in the predation treatment and 1.6 (median = 1) in the control treatment. Small fish did not switch pools significantly more often than large fish (control, small mean number of switches = 1.4; large = 1.9; predation, small = 2.8; large = 2.6).

To compare growth rates between individuals willing to risk predation and those avoiding predation, I separated the

© 1999 NRC Canada

Fig. 5. Ratio of mean body weights (+2 SE) of coho salmon fry in the downstream quarter versus the upstream three quarters of a pool in the control treatment (n = 6) and predation treatment (n = 12) separated by location (exposed/refuge pool) and time relative to the predation simulation (during/after). Values below the horizontal line indicate that the fish in the back of the tank on average were smaller than those in the front. Asterisks denotes a significant deviation from the 1:1 ratio.

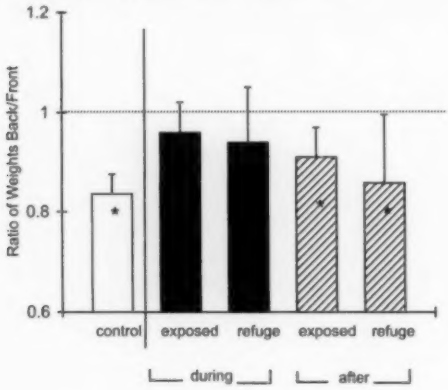

Fig. 6. Location fidelity of small (open bars) and large (solid bars) coho salmon fry in the control and predation treatments during 5 days of observations. The x-axis represents the frequency of observations in the pool that an individual was most often observed in (home pool).

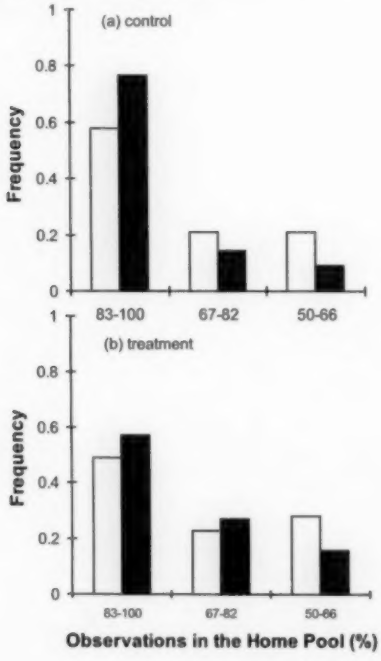

fish into two categories of habitat choice: those with ≥60% of all observations in the exposed pool ("risk takers") and those with ≥60% in the refuge pool ("risk avoiders"). In the

Fig. 7. Mean growth rate of large and small coho salmon in the control and predation treatments. Data for the predation treatment are divided into categories of risk taking, according to the preference of individual fish for the exposed pool (risk takers) or refuge pool (risk avoiders). Asterisks denote a statistically significant post hoc comparison. Data for the control treatment were previously published in Reinhardt and Healey (1997).

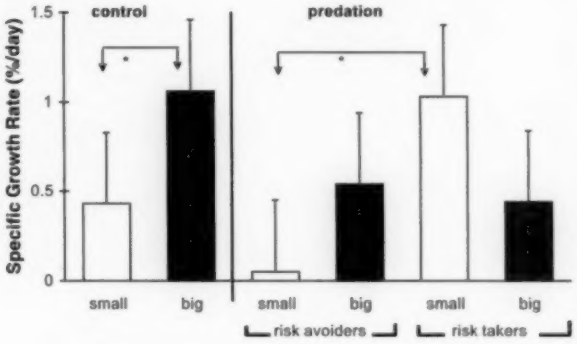

control treatment, large fish grew better than small fish (Fig. 7) (first reported in Reinhardt and Healey 1997). The risk-avoiding fish in the predation treatment showed a similar size-dependent growth pattern as the fish in the control treatment (Fig. 7), but among the risk takers, this pattern was reversed (Fig. 7) (two-way ANOVA on log-transformed specific growth rates: interaction between size and risk category, $F_{1,39}$ = 4.5, P = 0.04). Risk-taking fish on average grew 0.73 versus 0.29%/day for the risk avoiders, a difference that was not quite significant ($F_{1,39}$ = 3.3, P = 0.08). Small risk-taking fish grew significantly faster than small risk-avoiding fish (Fig. 7) (Tukey test: $P < 0.05$), whereas I found no difference in growth rate between risk-taking and risk-avoiding large fish (Tukey test: not significant).

Discussion

In the absence of predation risk, coho fry formed aggression hierarchies. The apparent dominance status, as determined by rate of aggression and proximity to the food source, increased with body size relative to the tank mates. This agrees with earlier studies that showed that coho juveniles form size-dependent hierarchies when food sources can be monopolized (e.g., Holtby et al. 1993; Ryer and Olla 1996; Grand 1997). The larger and more aggressive fish subsequently grew better, so that initial size differences in the group increased. In natural systems, this growth depensation has been shown to lead to mortality and emigration of the smaller members of a cohort (Elliott 1990; Sandercock 1991).

The presence of a predation threat changed the group dynamics and growth patterns considerably. As in previous experiments on coho behaviour in the presence of predation risk (Dill and Fraser 1984; Martel and Dill 1992; Healey and Reinhardt 1995), activity rates of fish were reduced following exposure to a predator. Small fish, which are more willing to feed under an apparent predation threat (Grant and Noakes 1987; Reinhardt and Healey 1997, 1999), were able

© 1999 NRC Canada

to profit from reduced levels of intraspecific aggression and gain access to food sources from which they previously had been excluded. Additionally, large fish tended to avoid the exposed pool (Reinhardt and Healey 1997), so that the presence of the disturbance indirectly provided growth opportunities for individuals willing to risk exposure to the (simulated) predator. A similar interaction among social status, antipredator behaviour, and release from intraspecific competition has previously been shown in field experiments with birds (Hegner 1985; Hogstad 1988; Koivula et al. 1994).

The greater relative frequency of chases versus aggressive displays during the days of simulated predation in this experiment is somewhat surprising, since previous studies have indicated that predators detect moving prey more easily (Martel and Dill 1995), and I had expected that the coho fry under threat would not only reduce the frequency of agonistic interactions, but also use less overt types of behaviour. However, since this increase in severity of agonistic acts was also observed in the refuge where no direct contact with the threat was present, it may have been caused by the need to reestablish aggression hierarchies in both pools accompanying the redistribution of the animals after the start of the predation simulation. The level of agonistic interactions and the spatial segregation by size within the pools after predation simulation were similar to the undisturbed pattern, which indicates that the social hierarchies within pools were quickly reestablished. Reinhardt and Healey (1997) showed that it takes longer for numerical and size distributions among pools to return to undisturbed levels, and in this study, I showed that individuals tend to spend most of their time in one pool. This relative stability in the distribution of fish is likely due to the costs that individuals have to pay for switching habitats, such as the cost of contesting a feeding spot against a prior territory holder (e.g., Cutts 1997).

Considering the distance between exposed and refuge pools and their visual isolation from one another, it is surprising to find indications of similar behavioural patterns in the refuge and exposed pools. Salmonids and other fish react to visual cues from conspecifics that were conditioned to a frightening stimulus (Suboski and Tempelton 1989), so that a mixed group of stimulus-naive and experienced fish reacts like an experienced group (Bams 1967; Olla and Davis 1989). Therefore, it is possible that in this experiment, fish that came in contact with the model predator moved into the refuge pool, where their frightened mood influenced the other fish.

Among small fish, the choice of individuals to occupy the exposed or refuge pool strongly affected their growth. The small fish in the predation treatment could be classified as those that avoided predation risk and grew slowly and those that were willing to accept predation risk and grew rapidly. This pattern is similar to the one observed in juvenile Atlantic salmon (*Salmo salar*), where smaller members of the cohort show reduced feeding motivation by July of their first feeding season and delay seaward migration for 1 year, whereas larger and (or) more dominant fry continue to compete for food vigorously through the fall and initiate seaward migration the following spring (Thorpe et al. 1992). Juvenile coho have been less well studied with regard to the behaviour of fish with different smolting strategies, but it is known that the proportion of fish that smoltify at age 1+ or age 2+ varies with growth conditions among geographical regions and years (Holtby and Hartman 1982; Randall et al. 1987). Furthermore, Reinhardt and Healey (1999) have shown that the predation risk avoidance of small coho fry increases in the fall. It is therefore possible that the two risk-taking and growth strategies of small coho in this study reflect the decision to smolt as 1- or 2-year olds, respectively. More experimentation is needed to decide whether coho and Atlantic salmon follow similar behavioural patterns with respect to their decision to smolt as 1- or 2-year-olds.

It is important to note that in this experiment, a high-risk, high-growth strategy for smaller, competetively inferior individuals was only possible in the presence of the predation threat. The disturbance caused by the predator model forced larger fish into risk-avoidance behaviour (Reinhardt and Healey 1997, 1999). This presented the opportunity for some small fish to grow at a relatively high rate while paying the cost of greater exposure to a predator. If these results have significance for natural systems, then predation should also be seen as creating a behavioural niche by breaking up size-dependent dominance hierarchies. Environments with frequent predator presence may thus result in similar fitness for a wider variety of foraging strategies than environments with low predation pressure, where growth, and thus fitness, are predominantly determined by an individual's ability to compete for a feeding territory.

Acknowledgments

I would like to thank Dr. Michael Healey for assistance at various stages of this study, including his comments on a draft manuscript of this paper. Funding was provided by an NSERC operating grant to Dr. Healey from the University of British Columbia and a Government of Canada awards scholarship to the author. Further advice was provided by Drs. Larry Dill, Robin Liley, Lee Gass, and Tony Pitcher, who served on my academic supervisory committee during the study period.

References

Abrahams, M.V., and Dill, L.M. 1989. A determination of the energetic equivalence of the risk of predation. Ecology, **70**: 999–1007.

Adams, C.E., and Huntingford, F.A. 1996. What is a successful fish? Determinants of competitive success in Arctic char (*Salvelinus alpinus*) in different social contexts. Can. J. Fish. Aquat. Sci. **53**: 2446–2450.

Bams, R.A. 1967. Differences in performance of naturally and artificially propagated sockeye salmon migrant fry as measured with swimming and predation tests. J. Fish. Res. Board Can. **24**: 1117–1153.

Clark, C.W. 1994. Antipredator behaviour and the asset-protection principle. Behav. Ecol. **5**: 159–170.

Cutts, C.J. 1997. Metabolic rate, territoriality, and life history strategies in juvenile Atlantic salmon (*Salmo salar* L). Ph.D. dissertation, University of Glasgow, Glasgow, Scotland.

Dill, L.M., and Fraser, A.G.H. 1984. Risk of predation and the feeding behaviour of juvenile coho (*Oncorhynchus kisutch*). Behav. Ecol. Sociobiol. **16**: 65–71.

© 1999 NRC Canada

Elliott, J.M. 1990. Mechanism responsible for population regulation in young migratory trout, *Salmo trutta*. III. The role of territorial behaviour. J. Anim. Ecol. **59**: 803–818.

Grand, T.C. 1997. Foraging site selection by juvenile coho salmon: ideal free distribution of unequal competitors. Anim. Behav. **45**: 185–195.

Grant, J.W.A., and Noakes, D.L.G. 1987. Escape behaviour and use of cover by young-of-the-year brook trout, *Salvelinus fontinalis*. Can. J. Fish. Aquat. Sci. **44**: 1390–1396.

Healey, M.C., and Reinhardt, U. 1995. Predator avoidance in naive and experienced juvenile coho and chinook salmon. Can. J. Fish. Aquat. Sci. **52**: 614–622.

Hegner, R.E. 1985. Dominance and anti-predator behaviour in blue tits (*Parus caerulus*). Anim. Behav. **33**: 762–768.

Hogstad, O. 1988. Social rank and antipredator behaviour of willow tits *Parus montanus* in winter flocks. Ibis, **130**: 45–46.

Holtby, L.B., and Hartman, G.F. 1982. The population dynamics of coho salmon (*Oncorhynchus kisutch*) in a West Coast rain forest stream subjected to logging. *In* Proceedings of the Carnation Creek Workshop, a 10 year review, February 24–26, 1982, Malaspina, Nanaimo. *Edited by* G.F. Hartman. Pacific Biological Station, Nanaimo, B.C. pp. 308–347.

Holtby, L.B., Swain, D.P., and Allan, G.M. 1993. Mirror-elicited agonistic behaviour and body morphology as predictors of dominance status in juvenile coho salmon (*Oncorhynchus kisutch*). Can. J. Fish. Aquat. Sci. **50**: 676–684.

Koivula, K., Kimma, L., Rytkonen, S., and Orell, M. 1994. Do subordinates expose themselves to predation? Field experiments on feeding site selection by willow tits. J. Avian Biol. **25**: 178–183.

Martel, G., and Dill, L.M. 1992. Feeding and aggressive behaviours in juvenile coho salmon (*Oncorhynchus kisutch*) under chemically-mediated risk of predation. Behav. Ecol. Sociobiol. **32**: 365–370.

Martel, G., and Dill, L.M. 1995. Influence of movement by coho salmon (*Oncorhynchus kisutch*) parr on their detection by common mergansers (*Mergus merganser*). Ethology, **99**:139–149.

Metcalfe, N.B., Huntingford, F.A., Graham, W.D., and Thorpe, J.E. 1989. Early social status and the development of life-history strategies in Atlantic salmon. Proc. R. Soc. Lond. Ser. B, Biol. Sci. **236**: 7–19.

Metcalfe, N.B., Taylor, A.C., and Thorpe, J.E. 1995. Metabolic rate, social status and life-history strategies in Atlantic salmon. Anim. Behav. **49**: 431–437.

Mittelbach, G.G., and Chesson, P.L. 1987. Predation risk: indirect effects on fish populations. *In* Predation: direct and indirect impacts on aquatic communities. *Edited by* W.C. Kerfoot and A. Sih. University of New England Press, Hanover, N.H. pp. 315–330.

Olla, B.L., and Davis, M.W. 1989. The role of learning and stress in predator avoidance of hatchery-reared coho salmon (*Oncorhynchus kisutch*) juveniles. Aquaculture, **76**: 209–214.

Randall, R.G., Healey, M.C., and Dempson, J.B. 1987. Variability in length of freshwater residence of salmon, trout and char. Am. Fish. Soc. Symp. **1**: 27–41.

Reinhardt, U.G., and Healey, M.C. 1997. Size-dependent foraging behaviour and use of cover in juvenile coho salmon under predation risk. Can. J. Zool. **75**: 1642–1651.

Reinhardt, U.G., and Healey, M.C. 1999. Season- and size-dependent risk taking in juvenile coho salmon: experimental evaluation of asset protection. Anim. Behav. **57**: 923–933.

Ryer, C.H., and Olla, B.L. 1996. Growth depensation and aggression in laboratory reared coho salmon: the effect of food distribution and ration size. J. Fish Biol. **48**: 686–694.

Sandercock, F.K. 1991. Life history of coho salmon. *In* Pacific salmon life histories. *Edited by* C. Groot and L. Margolis. University of British Columbia Press, Vancouver, B.C. pp. 395–445.

Suboski, M.D., and Tempelton, J.J. 1989. Life skills training for hatchery fish: social learning and survival. Fish. Res. **7**: 343–352.

Swain, D.P., and Holtby, L.B. 1989. Differences in morphology and behaviour between juvenile coho salmon (*Oncorynchus kisutch*) rearing in a lake and in its tributary stream. Can. J. Fish. Aquat. Sci. **46**: 1406–1414.

Thorpe, J.E., Metcalfe, N.B., and Huntingford, F.A. 1992. Behavioural influences on life-history variation in juvenile Atlantic salmon, *Salmo salar*. Environ. Biol. Fishes, **33**: 331–340.

Werner, E.E., Gilliam, J.F., Hall, D.J., and Mittelbach, G.G. 1983. An experimental test of the effects of predation risk on habitat use in fish. Ecology, **64**: 1540–1548.

© 1999 NRC Canada

Effects of oil sands related aquatic reclamation on yellow perch (*Perca flavescens*). I. Water quality characteristics and yellow perch physiological and population responses

M.R. van den Heuvel, M. Power, M.D. MacKinnon, T. Van Meer, E.P. Dobson, and D.G. Dixon

Abstract: In order to test the viability of oil sands aquatic reclamation techniques, yellow perch (*Perca flavescens*) were stocked into three experimental ponds. Pond substrates consisted of either oil sands fine tailings or clay and lean oil sands deposited by the mining operations. Yellow perch were stocked immediately postspawning and subsamples were sacrificed at 5 and 11 months to measure indicators of energy storage and utilization. These indicators included survival, age, spawning periodicity, condition factor, gonad size, fecundity, and liver size. Indicators generally showed patterns consistent with improved energy storage and utilization in the experimental pond yellow perch as compared with yellow perch in the lake from which the stocked fish originated. This was evidenced by increased gonad size, condition factor, and liver size and the disappearance of spawning periodicity. The patterns observed in experimental ponds suggest improved resource availability and (or) reduced intra- and interspecific competition. Yellow perch physiological indicators were also compared with those measured at several remote natural lakes in the area. Fisheries parameters measured in yellow perch from the experimental ponds generally fell within the range of those found in natural lakes.

Résumé : Pour vérifier la viabilité des techniques de récupération des sables bitumineux en milieu aquatique, on a introduit des perchaudes (*Perca flavescens*) dans trois étangs expérimentaux. Les substrats des étangs étaient constitués de résidus fins de sables bitumineux, ou d'argile et de sables bitumineux pauvres issus des opérations minières. Les perchaudes ont été introduites immédiatement après la fraye, et on a sacrifié des sous-échantillons à 5 et 11 mois pour mesurer les indicateurs suivants de stockage et d'utilisation de l'énergie : taux de survie, âge, périodicité de la fraye, coefficient de condition, taille des gonades, fécondité et taille du foie. Les indicateurs ont de façon générale montré une amélioration du stockage et de l'utilisation de l'énergie chez les perchaudes des étangs expérimentaux par rapport aux perchaudes du lac d'origine de ces perchaudes introduites. On a en effet observé un accroissement de la taille des gonades, du coefficient de condition et de la taille du foie et la disparition de la périodicité de la fraye. Les profils observés dans les étangs expérimentaux laissent croire qu'il y avait dans ces milieux davantage de ressources disponibles et (ou) une réduction de la compétition intraspécifique et interspécifique. On a aussi comparé les indicateurs physiologiques des perchaudes avec ceux mesurés dans plusieurs lacs naturels éloignés de la région. Les valeurs des paramètres halieutiques mesurés chez les perchaudes des étangs expérimentaux étaient généralement comparables à celles observées dans les lacs naturels.

[Traduit par la Rédaction]

Introduction

Oil sands deposits in northeastern Alberta, Canada, are a vast reservoir of fossil fuel estimated to contain one third of the world's known recoverable oil. Current levels of production from the Athabasca oil sands deposit represent 20% of Canada's petroleum needs. This level is certain to increase as conventional oil reserves dwindle and oil sands mining and extraction technologies improve.

The hot water flotation method for extraction of heavy hydrocarbons (bitumen) from oil sands produces large volumes of process water containing a suspension of solids as well as un-

Received August 25, 1998. Accepted February 17, 1999.
J14757

M.R. van den Heuvel,[1] **E.P. Dobson, and D.G. Dixon.** Department of Biology, University of Waterloo, Waterloo, ON N2L 3G1, Canada.
M. Power. Department of Agricultural Economics, University of Manitoba, Winnipeg, MB R3T 2N2, Canada.
M.D. MacKinnon. Syncrude Canada Ltd., Edmonton Research Center, 9421 17th Ave., Edmonton, AB T6N 1H4, Canada.
T. Van Meer. Syncrude Canada Ltd., Environment Department, P.O. Bag 4009, M.D. 0078, Fort McMurray, AB T9H 3L1, Canada.

[1]Author to whom all correspondence should be addressed. Present address: New Zealand Forest Research Institute, Private Bag 3020, Rotorua, New Zealand. e-mail: mike.vandenheuvel@forestresearch.co.nz

© 1999 NRC Canada

recovered hydrocarbons. These tailings segregate into deposits of sand and a slowly densifying suspension of water, fine clay particles (<22 μm), and unrecovered bitumen that is referred to as fine tailings. The oil sands fine tailings release pore water while densifying into mature fine tailings, a stable aqueous suspension containing 65% water (Fine Tailings Fundamentals Consortium 1995). The enormous volumes of fine tailings (hundreds of millions of cubic metres) cannot be easily incorporated into a dry landscape due to the fluid-like properties of the material. Currently, there is no single method of reclamation that could accommodate the volume of fine tailings produced and stored to date.

Two diverse methods are currently under consideration for reclaiming tailings into the landscape. The first method involves the incorporation of fine tailings into the bottoms of constructed lakes and is called the water-capping approach. The second method, called consolidated tailings, consists of adding gypsum to densified raw extraction tailings to which fine tailings have been added. Gypsum initiates the coagulation of the fine tailings fraction so that fine particles remain trapped within the coarse fraction from which fines-free water is released. Both methods would produce aquatic environments that would be influenced by oil sands related chemicals.

Elevated sulfate/chloride salinity, naphthenic acids, and polycyclic aromatic hydrocarbons are generally characteristic of oil sands tailing related water. Naphthenic acids are predominantly mono- and polycycloalkane carboxylic acids with aliphatic side chains of various lengths and have been identified as the family of compounds responsible for the acute lethality of fresh oil sands tailings water to fish (Verbeek 1994). Levels of priority, or parent polycyclic aromatic hydrocarbons, are generally relatively low as compared with the many alkane-substituted polycyclic aromatic hydrocarbons present. Experiments conducted using prototype ponds containing water-capped fine tailings at Syncrude's Mildred Lake site have demonstrated that primary production as well as macrophyte and invertebrate colonization proceed normally within 1–2 years of water capping (Boerger et al. 1992). Rainbow trout (*Oncorhynchus mykiss*) exposed to the overlying capping water within these ponds exhibited no acute toxicity over a period of several months (MacKinnon and Boerger 1986). However, chronic toxic effects, indirect effects such as limitations of primary and secondary productivity in the constructed systems, or nondirect effects such as the unsuitability of constructed habitats for particular life stages could compromise the viability of fish populations that will ultimately be exposed to oil sands tailings related waters. The potential of these factors to impact fish population status suggests the need for a diagnostic monitoring framework capable of determining which of the potential factors could be responsible for affecting fish populations.

Colby and Nepzy (1981) initiated such a framework based on the premise that fish population responses to particular stressors were distinct and could be used to predict fish population integrity. Munkittrick and Dixon (1989) and Gibbons and Munkittrick (1994) have refined the design to incorporate traditional fisheries data (growth, condition factor, age at maturity, reproductive potential, age and size structure) to compare potentially impacted with reference fish populations. Gibbons and Munkittrick (1994) have further classified fisheries data into three categories: age structure, energy expenditure, and energy storage.

The intent of this study was to examine the effects of the oil sands fine tailings water-capping option on survival and physiological indicators of energy storage and energy utilization in an indigenous species, yellow perch (*Perca flavescens*). A second goal of this study was to explore the utility of the monitoring framework based on physiological status measures by maintaining a single genetic stock and utilizing field stocking experiments. Finally, the results obtained were compared with data from natural yellow perch populations found within the same geophysical area as a means of examining the natural variability in measured parameters.

Materials and methods

Study site descriptions

In 1993, a 4-ha pond was constructed in the experimental pond facility located on the northwest corner of the Syncrude Canada Ltd. oil sands lease area located on the Athabasca oil sands deposit north of Fort McMurray, Alberta (Fig. 1). About 70 000 m^3 of mature oil sands fine tailings were pumped from the main tailings storage pond into the fine tailings water-capping demonstration pond, hereafter called Demonstration Pond (Table 1). After the addition of tailings, 70 000 m^3 of natural surface water (drainage water from muskeg area) was pumped into Demonstration Pond from a nearby canal to a depth of 2.8 m above the tailings–water interface. A second pond, located immediately adjacent to Demonstration Pond, was constructed simultaneously. This pond was designed as a demonstration deep wetland, hereafter called Deep Wetland, and consisted of a dug-out pit filled with surface drainage water from the same source as Demonstration Pond. During the filling of these experimental ponds, fathead minnow (*Pimephales promelas*), brook stickleback (*Culaea inconstans*), and a small number of lake chub (*Couesius plumbeus*) were inadvertently pumped into the experimental ponds. All three species have survived to date in Demonstration Pond, whereas only fathead minnow remain in Deep Wetland.

A third experimental pond was formed in 1987 as a drainage basin in an area designated to be reclaimed as bison pasture on the south portion of the oil sands lease. The basin, and the area surrounding the pond, received overburden and materials deemed not suitable for reclamation. These materials were saline/sodic in nature and quite likely contained lean oil sands material. Reclamation (capping with muskeg) of the area surrounding this pond, hereafter called South Bison Pond, was completed in 1995. There were no fish species present in South Bison Pond at the initiation of this study. To provide a yellow perch forage base, 800 fathead minnow were transplanted from Deep Wetland to South Bison Pond in June 1995. Fathead minnow have subsequently formed a large and apparently viable population in this pond.

The lake chosen as the source of the experimental yellow perch was Mildred Lake, located on the Syncrude Canada Ltd. mining lease and present prior to the initiation of mining. Beginning in 1975, Mildred Lake was modified from its natural state and currently serves as a reservoir for plant makeup water that is pumped into Mildred Lake from the Athabasca River. Mildred Lake has been known to contain an abundant population of yellow perch since fisheries work was initiated in 1978.

To provide an ecologically relevant context for data derived from stocking experiments, the fish populations of three reference lakes, located off the oil sands lease or off the Athabasca oil sands

© 1999 NRC Canada

Fig. 1. Location of the Athabasca oil sands deposit and experimental sites within Alberta, Canada. Oil sands deposits are shaded.

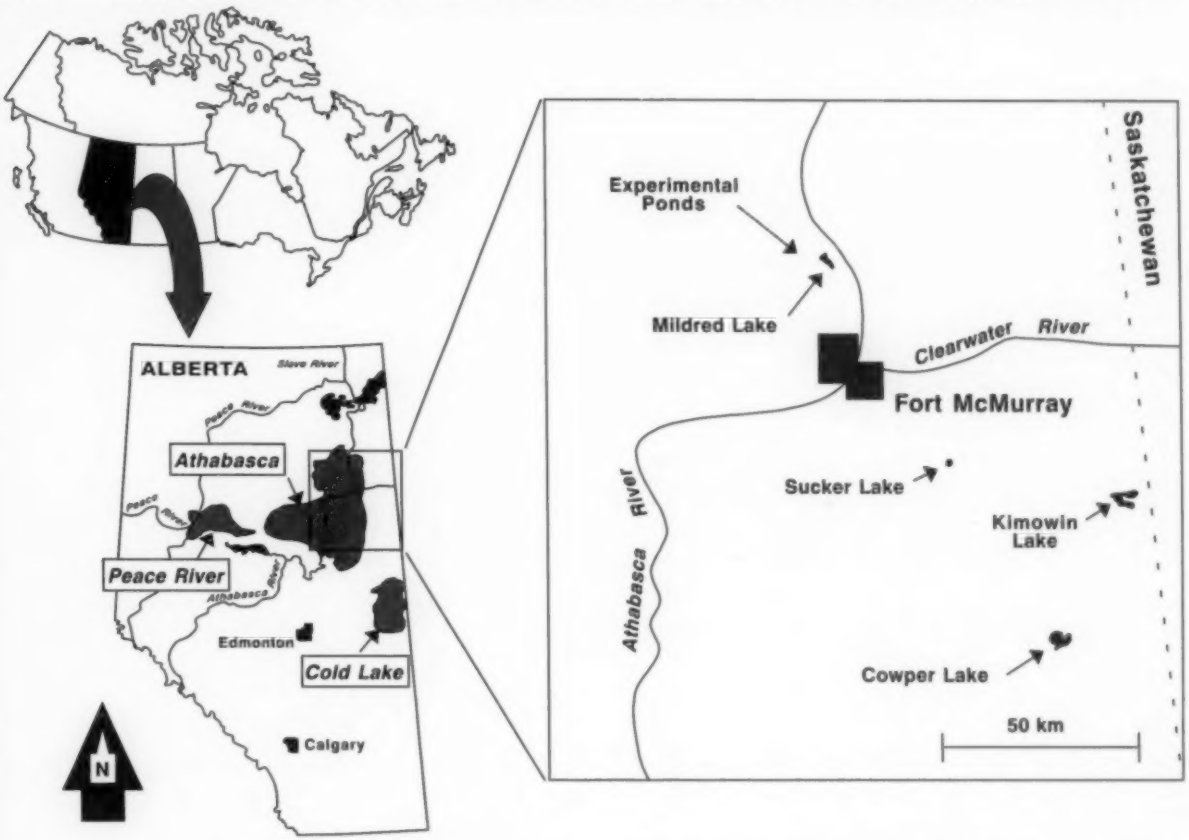

deposit altogether, were evaluated. These natural lakes (Fig. 1; Table 1), Sucker Lake, Kimowin Lake, and Cowper Lake, were added at varying intervals throughout the course of the stocking experiments.

Experimental fish stocking

From June 26 to 28, 1995, 300 yellow perch were stocked into each of Demonstration Pond, Deep Wetland, and South Bison Pond. Yellow perch were captured in Mildred Lake using a Smith-Root 7.5-GPP gasoline-powered electrofisher mounted on a Smith-Root-18 electrofishing boat. Electrofisher voltage was set at 500 V pulsed direct current and pulse frequency was adjusted to provide a measured current between 2.4 and 2.8 A. Yellow perch captured by dip net were placed in a 500-L live well with flow-through water circulation. Upon capture of 75–100 yellow perch, fish were transferred to wire mesh holding cages (0.75 m^3) at a density of about 50 per cage. Yellow perch length and weight were recorded and several scales from just posterior to the pectoral fin were removed for ageing. Yellow perch were transported to the experimental ponds in two aerated circular polyethylene tanks with a capacity of about 0.75 m^3. Transportation time to the experimental ponds was less than 30 min (50–75 fish per tank).

The sex ratio of individuals taken from Mildred Lake in the spring of 1995 was highly skewed toward females (female to male sex ratio of 5:1). Fish sampled in the experimental ponds in the fall of 1995 reflected the stocking ratio. Apparent poor summer survival made obtaining sufficient numbers of yellow perch for the scheduled fall sampling difficult and required that yellow perch be restocked in 1996 to continue experimentation.

To correct for both survival and sex ratio problems, several modifications were made to fish capture and transfer procedures. The sex bias problem was corrected by capturing male yellow perch using overnight hoop net sets (May 20–22, 1996). Hoop nets were 1.22 m wide × 0.91 m high at the opening with a 7.6-m leader and 8-mm mesh size and no diagonal wings at the opening. Yellow perch can still be sexed externally at this time, since male yellow perch are still expressing milt. This capture technique used nearshore during the spawning period generally captured exclusively male yellow perch. A total of 250 male yellow perch were transferred to each of Demonstration Pond and South Bison Pond. Deep Wetland, which had become anoxic the previous winter, was not included in the 1996 experiments.

A further 500 yellow perch (presumed to be mostly female) were captured by electrofishing (as previously described) on June 7, 1996; 250 were transferred to each of Demonstration Pond and South Bison Pond. All yellow perch transfers in 1996 were made as rapidly as possible, with less than 1.5 h elapsing between removal from Mildred Lake and placement in the destination ponds. No data were recorded from the stocked fish in 1996 in order to minimize handling.

Water chemistry analysis

Temperature, pH, conductivity, and dissolved oxygen profiles were measured using a Hydrolab model 4041 water chemistry me-

© 1999 NRC Canada

Table 1. Experimental lake descriptions.

Site	Coordinates	Area (ha)	Maximum depth (m)	Known fish species	Sampling dates
Demonstration Pond	57°4.94′N, 111°41.40′W	4	2.9 (overlying 12 m of mature fine tailings)	YP, BS, FM, LC	F95, F96, W97
Deep Wetland	57°4.94′N, 111°41.40′W	4	6.0	YP, FM	F95
South Bison Pond	56°59.78′N, 111°36.15′W	5	5.0	YP, FM	F95, F96, W97
Mildred Lake	57°3.07′N, 111°36.02′W	170	8.2	YP, WE, LW, SPO, WS, LN, B	F95, F96, W97
Sucker Lake	56°25.34′N, 110°51.73′W	55	6.0	YP, NP, WS, SPO, BS, LC	F96, W97
Kimowin Lake	56°11.75′N, 110°7.00′W	448	12.0	YP, NP, BS	F96, W97
Cowper Lake	55°54.36′N, 110°27.14′W	600	5.5	YP, NP	W97

Note: Fish species: YP, yellow perch (*Perca flavescens*); FM, fathead minnow (*Pimephales promelas*); BS, brook stickleback (*Culaea inconstans*); LC, lake chub (*Couesius plumbeus*); NP, northern pike (*Esox lucius*); WE, walleye (*Stizostedion vitreum*); WS, white sucker (*Catostomus commersoni*); LN, longnose sucker (*Catostomus catostomus*); B, burbot (*Lota lota*); LW, lake whitefish (*Coregonus clupeaformis*); SPO, spottail shiner (*Notropis hudsonius*). Sampling dates: F95, fall 1995 (September 20–29, 1995); F96, fall 1996 (September 19–28, 1996); W97, winter 1997 (March 9–25, 1997).

ter. Temperature and dissolved oxygen were measured continually in Demonstration Pond using a turbidity probe for temperature (D&A Instruments, model OBS-3) and a low-demand oxygen probe (Greenspan model D1015) for dissolved oxygen.

The following chemical methods were used as outlined in American Public Health Association (1985) and U.S. Environmental Protection Agency (1979) standard method descriptions. Total nitrogen was measured using the Kjeldahl method. Total phosphate was analysed by ammonium molybdate – ascorbic acid – potassium tartrate colour reagent after acid–persulfate hydrolysis. Ammonia was quantified by means of the Bertelot reaction in an autoanalyser. Dissolved organic carbon was determined by measuring the carbon dioxide infrared absorbance of an ultraviolet light-oxidized solution against dissolved organic carbon standards. Carbonate levels were calculated from dissolved inorganic carbon concentrations. Dissolved inorganic carbon was determined by infrared measurement of carbon dioxide stripped from an acidified water solution. Major cations (sodium, potassium, calcium, magnesium) and trace metals were quantified by atomic emission using radiofrequency inductively coupled plasma. Samples for metals analyses were acidified without filtering.

The following chemical methods were used for the remaining water chemistry parameters. Major anions (chloride, sulfate) were analysed using ion chromatography followed by conductivity detection. The trace metals arsenic and selenium were analysed as hydrides using cold-vapour atomic absorption spectroscopy. Total naphthenates in water were quantified by FTIR spectroscopy following methylene chloride extraction of water.

Yellow perch survival estimates and sampling protocol

Quantitative estimates of yellow perch survival in the experimental ponds were not performed in 1995. During fall 1995 and spring 1996, qualitative estimates of yellow perch survival were observed while capturing stocked yellow perch for sacrifice. After stocking in 1996, catch-per-unit-effort (CPUE) was periodically measured in Demonstration Pond and South Bison Pond to quantify the relative density of yellow perch over 1 year. Four identical hoop nets spaced at random intervals were set overnight around the perimeter of the experimental ponds. Netting was carried out over two or three consecutive nights, changing net location each night to provide replicate estimates of relative density. Nets were always set with the leader anchored to shore and the net set perpendicular to shore. The number of fish per net and the exact fishing time were recorded in order to calculate CPUE as number of fish per net per hour. CPUE measurement was initiated 7 days after the completion of stocking in 1996 (June 21) and repeated during August and September 1996 as well as May 1997.

Yellow perch were sacrificed for physiological measurements from September 20 to 29 in 1995 and from September 18 to 28 in 1996. Yellow perch were captured in daytime or overnight hoop net or trap net sets (1.83 m with 19-mm mesh and a 46-m leader). To compare fall parameters with those from a period of more advanced reproductive development, yellow perch were also captured during late winter 1997 (March 9–27, 1997). Winter sampling was chosen because of the difficulties encountered while attempting to capture prespawning yellow perch in May 1996. At the majority of sites sampled during winter, multimesh, monofilament gill nets (50-m lengths) were set under the ice in daytime or overnight sets. Nets consisted of 10-m panels of 38.1-, 50.8-, 63.5-, 76.2-, and 88.9-mm stretch mesh. Gill nets were checked at least every 4 h. At Kimowin Lake and Cowper Lake, yellow perch were captured by angling through the ice.

Yellow perch were maintained alive until sampling and were dispatched with a sharp blow to the head. Length, weight, liver weight, gonad weight, gender, and sexual maturity were recorded. Operculae were placed in envelopes, kept cool, and later frozen pending age determinations. To age yellow perch, operculae were thawed, boiled to remove attached flesh, and dried prior to age determination. Anular rings were read under bright incandescent illumination. Ovary samples (about 1 g) for fecundity analysis were frozen in liquid nitrogen and later transferred to a –20°C freezer. In the laboratory, ovarian tissue was thawed and 50–200 mg was weighed out to 0.1 mg using a Sartorius digital balance. All ovarian follicles in the subsamples were counted. The weights of ovarian tissue used were chosen to correspond to between 150 and 300 follicles per sample. Total fecundity was calculated by multiplying the total count by the ratio of gonad weight to subsample weight.

Statistics

CPUE data were not normally distributed and were tested using

© 1999 NRC Canada

Description
Contains 70 000 m^3 of mature fine tailings, capped with 70 000 m^3 of surface runoff water. Construction completed in October 1993
Dug-out area filled with surface runoff water. Completed in October 1993
Natural depression in reclaimed bison pasture
Natural lake on oil sands mining lease. Heavily modified in 1975 to act as a water reservoir. No angling pressure
Small boreal forest lake located in the Athabasca River basin. May receive drainage water from lakes overlying the oil sands deposit. No angling pressure
Medium-sized boreal forest lake located in the Beaver River basin 40 km west of the Athabasca oil sands deposit. Heavy angling exploitation in winter only
Medium-sized boreal forest lake located in the Athabasca River basin 30 km south (upstream) of the Athabasca oil sands deposit. Heavy angling exploitation in winter only

the nonparametric Mann–Whitney *U* test. Condition factor, liver size, gonad size, and fecundity data were analysed using analysis of covariance (ANCOVA) on base-10 logarithmically transformed variables. Corrected total weight (body weight – liver weight – gonad weight) was used for all statistical comparisons and calculations. It should be noted that although statistical comparisons using ANCOVA were completed on body, liver, and gonad weight and also total fecundity, data are presented as somatic indices to facilitate comparisons between sampling periods and between studies. Fulton's condition factor was calculated as body weight/length^3 × 100, gonadosomatic index as gonad weight/body weight × 100, liver somatic index as liver weight/body weight × 100, and fecundity index as total number of eggs/body weight.

All statistical analyses of physiological indices were restricted to comparing Mildred Lake yellow perch with the yellow perch from the stocked ponds. Only yellow perch with actively maturing gonads were included in the analyses of the indices. Statistical analyses were performed this way due to multiple interactions (heterogeneity of slope) when off-site references were included, to keep statistical power similar at all sampling time points, and to simplify statistics in order to concentrate on the a priori hypotheses of the stocking experiment. Qualitative comparisons were deemed sufficient to assess the relevance of measured indices with regard to reference populations. All statistical testing was completed using the SYSTAT software package (Wilkinson 1990). The critical level of statistical differences for all analyses in this paper was assessed at $\alpha = 0.05$.

Results

Water chemistry

Water chemistry characteristics indicated a gradient of both organic compounds and major ions as shown by the measured water quality parameters (Table 2). The higher salinity in oil sands associated ponds was characterized by sulfate as the major anion followed by chloride. Sodium was the major cation, but elevations in potassium, calcium, and magnesium were also evident. The only indicator of elevated oil sands related organic compounds shown was total naphthenates. Total naphthenates demonstrated the same overall gradient as major ions. South Bison Pond water chemistry was influenced most, despite the lack of any oil sands tailings in the area, followed by Demonstration Pond and Deep Wetland. Oil sands also showed a gradient of influence in the reference lakes in this study. Mildred Lake had low levels of naphthenates as well as slightly elevated levels of chloride and sulfate. Sucker Lake had no apparent major ion effects but showed traces of naphthenates. Kimowin Lake, the only site entirely removed from the Athabasca oil sands deposit for which we had extensive water chemistry data, did not have detectable concentrations of naphthenates.

Oil sands exposed sites were also characterized by some elevations in levels of trace metals in water (Table 3). Increases in boron, lithium, and strontium followed the same gradient as salinity and naphthenate levels, indicating a probable association with oil sands and related clays. Zinc also showed a slight increase, particularly in Demonstration Pond. Levels of lead and selenium (not shown in Table 3) were also measured and found to be nondetectable in all samples analysed (<20 and <0.2 $\mu g \cdot L^{-1}$, respectively).

Temperature profiles of the experimental ponds and reference sites (data not shown) showed a nearly identical regime among the lakes and ponds. Dissolved oxygen profiles were more variable, with some sites demonstrating late winter oxygen deficits. Deep Wetland in particular had a significant fish kill during winter 1995–1996. All yellow perch and greater than 99% of fathead minnow perished. Sucker Lake had oxygen levels of 2.0 $mg \cdot L^{-1}$ in March 1997; however, a substantial number of yellow perch survived this event. All other ponds showed levels of late winter dissolved oxygen in excess of 60% saturation. Mildred Lake, which receives aeration through a continuous input of water pumped up from the Athabasca River, had greater than 85% saturation.

Perch survival

Yellow perch capture effort in the experimental ponds in fall 1995 indicated that Deep Wetland yellow perch had the best overall summer survival. Capture attempts in Demonstration Pond and South Bison Pond provided barely enough yellow perch for the sampling needs (nominally 20 males and 20 females), whereas Deep Wetland yielded greater than 150 yellow perch in one night of netting (representing 50% of the total number stocked). In 1996, CPUE (Fig. 2) was utilized to quantify survival. Demonstration Pond showed a significant reduction in CPUE between 1 week poststocking and August, after which the CPUE data were relatively stable. South Bison Pond also showed an initial decrease, but statistically significant differences did not occur until May 1997 (after about 80 yellow perch had been sacrificed for sampling purposes during fall 1996 and winter 1997). The yellow perch stocked into Demonstration Pond and South Bison Pond demonstrated superior survival in 1996 as opposed to the 1995 stocking effort.

Perch condition indices

Yellow perch condition factor responses to being stocked in the experimental ponds were sex dependent. Male condition factor remained unaffected by stocking, showing no statistically significant differences from the condition factor

© 1999 NRC Canada

Table 2. Mean water chemistry parameters ($mg \cdot L^{-1}$) (*n*, SEM) for experimental ponds and lakes during the open-water season of 1995 and 1996.

Site	pH	Cond. ($\mu S \cdot cm^{-1}$)	TDS	Na^+	K^+	Mg^{2+}	Ca^{2+}	Cl^-
1995								
Deep Wetland	8.7	489	348	45.3				6.9
	(3, 0.1)	(2, 19)	(2, 17)	(5, 1.5)				(3, 0.1)
Demonstration Pond	8.4	826	557	126	4.8	16.0	48.1	31.2
	(5, 0.2)	(5, 10)	(4, 4)	(6, 3.7)	(4, 0.4)	(4, 0.2)	(4, 0.7)	(6, 0.6)
South Bison Pond	7.9	3131	2392	430	12.5	87.9	200	116
	(1)	(1)	(1)	(1)	(1)	(1)	(1)	(1)
1996								
Deep Wetland	8.4	421	297	44.6	3.1	18.9	34.8	6.2
	(5, 0.1)	(5,9)	(5, 8)	(5, 1.2)	(5, 0.22)	(5, 0.6)	(5, 3.1)	(5, 0.2)
Demonstration Pond	8.5	788	565	139	4.3	16.0	45.9	36.1
	(9, 0.1)	(9, 7)	(9, 5)	(9, 2.8)	(9, 0.38)	(9, 0.3)	(9, 2.3)	(9, 0.9)
Mildred Lake	7.7	288	194	18.1	1.7	9.1	39.3	7.2
	(3, 0.3)	(3, 14)	(3, 7)	(3, 2.0)	(3, 0.1)	(3, 0.4)	(3, 2.2)	(3, 1.0)
South Bison Pond	8.0	1825	1594	246	8.4	57.1	132	78.6
	(5, 0.1)	(5, 94)	(3, 12)	(5, 15.6)	(5, 0.62)	(5, 4.1)	(5, 9.2)	(5, 3.6)
Sucker Lake	7.3	176	134	8.5	1.4	6.6	23.6	0.6
	(3, 0.1)	(3,)	(2, 16)	(2, 0.1)	(1)	(1)	(1)	(3, 0.3)
Kimowin Lake	7.7	242	171	11.7	2.8	11.7	31.2	0.4
	(3, 0.2)	(2, 1)	(2, 5)	(3, 0.1)	(3, 0.3)	(3, 0.4)	(3, 2.3)	(3, 0.1)

Note: Empty cells indicate that the parameter was not measured during the indicated period. TDS, total dissolved solids; TN, total nitrogen; TP, total phosphorus; DOC, dissolved organic carbon.

Table 3. Mean water trace metal concentrations ($\mu g \cdot L^{-1}$) (*n*, SEM) for experimental ponds and lakes during the open-water season of 1995 and 1996.

Site	Al	Sb	As	Ba	Be	B	Cd	Cr	Co	Cu	Fe
1995											
Demonstration Pond			1.0			415				1.5	
			(1)			(3, 72)				(3, 0.5)	
South Bison Pond			0.8	50			<2	<2			30
			(1)	(1)							(1)
1996											
Deep Wetland	20	<0.2	1.0	23	<1	80	<3	5	4.0	2.0	20
	(4, 5)		(2, 0.2)	(4, 3)		(4, 20)		(4, 3)	(4, 1)	(4, 1)	(4, 10)
Demonstration Pond	72	<0.2	1.0	40	2	484	<3	3	3.6	2.2	62
	(5, 22)		(2, 0.2)	(5, 4)	(5,1)	(5, 12)		(5, 1)	(5, 0.5)	(5, 0.4)	(5, 40)
Mildred Lake	<10	<0.2	0.4	67	3	37	<3	<2	<3	<1	143
			(1)	(3, 2)	(3, 1)	(3, 3)					(3, 50)
South Bison Pond	55	0.3	<0.3	40	3	637	<3	<2	3.8	2.5	18
	(4, 33)	(2, 0.1)		(4, 4)	(4, 1)	(4, 22)			(4, 0.6)	(4, 0.6)	(4, 7)
Sucker Lake	20			20	<1	40	5	6	<3	3	400
	(1)			(1)		(1)	(1)	(1)		(1)	(1)
Kimowin Lake	15			27	3	43	<3	3	<3	<1	20
	(3, 10)			(3, 3)	(3, 1)	(3, 5)		(3, 1)			(3, 5)

Note: Empty cells indicate that the parameter was not measured during the indicated period.

measured in Mildred Lake in each of the sample periods (Table 4). Female condition factor was higher, and statistically different, in yellow perch from the experimental ponds when compared with Mildred Lake in the falls of 1995 and 1996. Winter 1997 samples indicated no statistically significant differences among the three sites. Condition factors for both sexes in Mildred Lake and the experimental ponds fell within the range of variability shown in yellow perch captured in the off-site reference lakes. The range is characterized by the values computed for the stunted population of Sucker Lake (<1.2) and the population of Kimowin Lake (>1.5).

Liver size of stocked fish was consistently larger than that of Mildred Lake fish, the exception being that liver size in Deep Wetland males was unaffected in fall 1995 (Table 4). Yellow perch liver sizes in South Bison Pond and Demon-

© 1999 NRC Canada

SO_4^{2-}	CO_3^{2-}	NH_3^+	TN	TP	Total naphthenates	DOC
43.6	286	0.10	1.64	0.07	3.0	34.6
(3, 3.1)	(3, 10)	(3, 0)	(3, 0.02)	(3, 0.02)	(1)	(3, 1.6)
98.8	422	0.09	2.49	0.06	8.5	38.2
(6, 2.9)	(6, 12)	(6, 0.01)	(5, 0.61)	(5, 0.01)	(2, 1.1)	(6, 1.0)
1160	386					
(1)	(1)					
39.6	208	0.04	1.26	0.05	1.4	28.9
(5, 0.7)	(5, 11)	(5, 0.01)	(5, 0.06)	(5, 0.01)	(3, 0.2)	(5, 2.0)
97.9	335	0.07	2.48	0.07	5.6	35.8
(9, 0.9)	(6, 9)	(9, 0.01)	(7, 0.91)	(7, 0.02)	(5, 0.6)	(9, 1.3)
21.8	134	0.03	0.80	0.06	1.1	15.2
(3, 2.2)	(3, 4)	(3, 0.01)	(3, 0.1)	(3, 0.01)	(2, 0.1)	(3, 1.2)
747	184	0.06	0.91	0.05	9.1	30.7
(5, 38.4)	(5, 6)	(5, 0.02)	(5, 0.08)	(5, 0.01)	(3, 2.4)	(5, 1.9)
4.6	118	0.11	3.25	0.02	0.4	24.5
(3, 0.4)	(1)	(2, 0.07)	(1)	(1)	(1)	(3, 1.6)
3.6	175	0.06	3.68	0.06	<0.3	17.2
(3, 0.8)	(3, 4)	(3, 0.02)	(2, 1.64)	(2, 0.03)	(1)	(3, 1.2)

Li	Mn	Mo	Ni	Sr	Ti	V	Zn
43				340			9
(1)				(1)			(1)
			17				
11	20	<3	6	210	5	<2	10
(4, 1)	(4, 3)		(4, 1)	(4, 10)	(4, 2)		(4, 5)
36	4	6	7	332	4	<2	24
(5, 1)	(5, 1)	(5, 2)	(5, 1)	(5, 7)	(5, 1)		(4, 9)
6	56	<3	11	230	5	<2	4
(3, 1)	(3, 15)		(3, 3)	(3, 9)	(3, 1)		(3, 1)
79	19	<3	<5	1323	4	3	12
(4, 4)	(4, 7)			(3, 52)	(4, 1)	(4, 1)	(4, 5)
8	168	<3	<5	96	5	5	1
(1)	(1)			(1)	(1)	(1)	(1)
11	38	<3	<5	138	<3	<2	5
(3, 1)	(3, 14)			(3, 5)			(3, 2)

stration Pond were significantly larger in both sexes in winter 1997 when compared with either Mildred Lake fish or the upper extreme of the off-site reference lakes.

Reproductive indices and observations

Gonad size changes were also apparent in yellow perch stocked in the experimental ponds as compared with Mildred Lake yellow perch (Fig. 3). In fall 1995, male and female yellow perch from Deep Wetland had significantly larger gonad size than Mildred Lake yellow perch. Male and female yellow perch from the other experimental ponds showed no significant differences. In fall 1996, male and female yellow perch from Demonstration Pond and South Bison Pond both had significantly larger gonad size than Mildred Lake yellow perch. In female yellow perch, condition factor differences were reduced and gonad size differ-

© 1999 NRC Canada

Table 4. Mean (SEM) age, length, weight, condition factor, liver somatic index (LSI), percent spawning periodicity, and sample size for yellow perch used in this study.

	Females						
Capture location	Age (years)	Length (cm)	Weight (g)	Condition factor	LSI	Spawning periodicity (%)	*n*
Fall 1995							
Demonstration Pond	7.2	22.7	164	1.30	2.08	0	19
	(0.6)	(0.4)	(9)	(0.02) *a*	(0.05) *a*		
Deep Wetland	7.7	22.7	171	1.29	1.63	0	20
	(0.5)	(0.6)	(14)	(0.02) *a*	(0.07) *b*		
South Bison Pond	8.0	22.2	14(7)	1.27	1.88	0	21
	(0.6)	(0.3)		(0.02) *a*	(0.08) *ab*		
Mildred Lake	8.2	28.7	14(6)	1.19	1.30	19.0	47
	(0.3)	(0.3)		(0.01) *b*	(0.05) *c*		
Fall 1996							
Demonstration Pond	8.5	22.9	15	1.21	1.76	0	19
	(0.6)	(0.3)	(6)	(0.02) *ab*	(0.09) *a*		
South Bison Pond	8.7	23.8	185	1.27	1.68	0	20
	(0.6)	(0.4)	(10)	(0.02) *a*	(0.06) *a*		
Mildred Lake	7.9	22.9	148	1.16	1.31	24.1	23
	(0.5)	(0.4)	(7)	(0.02) *b*	(0.05) *b*		
Sucker Lake	4.5	18.4	79	1.18	1.39	0	27
	(0.2)	(0.4)	(6)	(0.01)	(0.07)		
Kimowin Lake	8.3	28.7	422	1.64	1.56	0	39
	(0.5)	(0.4)	(16)	(0.02)	(0.03)		
Winter 1997							
Demonstration Pond	6.7	22.0	165	1.25	3.04	0	20
	(0.4)	(0.4)	(9)	(0.02) *a*	(0.12) *a*		
South Bison Pond	8.1	24.5	230	1.23	2.96	0	21
	(2.0)	(0.4)	(11)	(0.01) *a*	(0.06) *a*		
Mildred Lake	7.7	21.8	147	1.21	1.67	12.1	29
	(0.3)	(0.3)	(6)	(0.02) *a*	(0.04) *b*		
Sucker Lake	4.0	18.8	93	1.15	2.20	9.1	20
	(0.1)	(0.4)	(5)	(0.01)	(0.08)		
Kimowin Lake	9.4	28.3	440	1.51	2.64	0	20
	(0.8)	(0.6)	(28)	(0.03)	(0.10)		
Cowper Lake	6.7	28.0	363	1.38	2.11	25.0	18
	(0.3)	(0.3)	(13)	(0.02)	(0.09)		

Note: Ages reflect the exact ages of the fish at the beginning of the previous growing season. Means within a column for a particular sampling date followed by the same letter are not significantly different ($p > 0.05$).

ences were accentuated over the period of time between the fall 1996 and the winter 1997 sample collections. Gonad sizes in Mildred Lake and the experimental ponds fell within, or exceeded, the range found in the off-site reference locations, with Sucker Lake once again being on the low end of the distribution and Kimowin Lake on the high end.

Fecundity estimates (Fig. 4) generally parallelled the gonad size data, indicating that during these sampling periods, increases in gonad size were due to an increase in the number of ovarian follicles and not a change in the follicle size. Only one example of the opposite possibility was observed in fall 1995 for South Bison Pond. Gonad size in South Bison Pond yellow perch was significantly lower than that measured in Deep Wetland and Demonstration Pond, but fecundity remained unaffected as a result of a decrease in follicle size. Fecundity data of yellow perch from the experimental ponds generally fell within, or exceeded, the fecundity estimates observed at the off-site reference sites.

During the spring of 1997, yellow perch stocked in the experimental ponds in 1996 were observed to undergo spawning in a normal fashion as indicated by the deposition of egg strings on small spruce trees introduced as spawning substrate. CPUE netting revealed that a large majority of the female yellow perch had spawned by the completion of these netting efforts in late May. The timing of spawning corresponded well to what was observed in Mildred Lake during spring 1997.

Of particular note was the appearance of spawning periodicity at some of the sites (Table 4). Spawning periodicity, or "resting", can be defined as the absence of any gonadal development in an individual capable of such development. In this case, female yellow perch that would not be spawning at age 4 or greater were evaluated as having a resting year. Since female gonads remain arrested in their previtellogenic state, spawning periodicity is easily observed by early September. Mildred Lake showed this phenomenon over the pe-

© 1999 NRC Canada

Males					
Age (years)	Length (cm)	Weight (g)	Condition factor	LSI	*n*
7.1	19.9	108	1.24	1.44	7
(1.0)	(0.5)	(10)	(0.03) *a*	(0.10) *ab*	
7.4	19.2	99	1.29	1.26	13
(0.7)	(0.1)	(3)	(0.02) *a*	(0.06) *bc*	
7.3	19.3	102	1.29	1.63	6
(1.1)	(0.6)	(11)	(0.03) *a*	(0.11) *a*	
7.1	19.2	96	1.26	1.10	14
(0.5)	(0.3)	(5)	(0.02) *a*	(0.05) *c*	
7.1	18.5	86	1.25	1.71	19
(0.3)	(0.2)	(3)	(0.01) *a*	(0.05) *a*	
7.6	19.6	104	1.27	1.25	21
(0.3)	(0.2)	(4)	(0.01) *a*	(0.10) *b*	
7.0	18.7	87	1.23	1.14	20
(0.6)	(0.2)	(4)	(0.01) *a*	(0.03) *c*	
4.0	15.9	53	1.17	1.41	20
(0.2)	(0.4)	(0.4)	(0.01)	(0.03)	
10.8	26.4	324	1.58	1.14	17
(0.7)	(0.8)	(22)	(0.04)	(0.07)	
5.9	18.1	81	1.24	3.18	21
(0.4)	(0.3)	(4)	(0.02) *a*	(0.21) *a*	
7.8	19.8	109	1.25	2.79	13
(0.6)	(0.3)	(7)	(0.02) *a*	(0.10) *a*	
8.2	17.7	78	1.27	1.81	12
(1.0)	(0.6)	(7)	(0.02) *a*	(0.13) *b*	
4.0	17.0	61	1.14	1.65	20
(0.1)	(0.4)	(4)	(0.01)	(0.09)	
8.2	23.4	248	1.50	2.13	22
(1.0)	(1.2)	(29)	(0.04)	(0.11)	
4.9	20.8	163	1.33	1.87	18
(0.6)	(1.3)	(31)	(0.03)	(0.11)	

riod of years framed by this study with frequencies ranging from 12 to 24% of the female population. Female yellow perch transferred from Mildred Lake to the experimental ponds that were age 4 and above did not show a single case of missing a reproductive season (n = 140 females examined), nor did any of the Kimowin Lake females examined (n = 59). However, periodicity was observed in female yellow perch at Sucker Lake and Cowper Lake.

Summary of physiological indices

Physiological indicator data have been aggregated and summarized in Table 5 as energy storage parameters (condition factor, liver size) and energy utilization parameters (gonad size, fecundity, spawning periodicity). Changes in the parameters relative to the lake of origin for the stocked yellow perch (Mildred Lake) over the study period provided a potentially useful means of assessing the impacts of experimental pond water exposure on stocked yellow perch. Changes are indicated only if all component measures of the parameter showed a significant change in the same direction. Response patterns between sites, for different stressor regimes, varied and were not consistent in maintaining unique response patterns. In no cases did the energy storage or utilization parameters show a significant negative impact (i.e., parameter decrease).

Discussion

Experiments on yellow perch stocked in ponds containing oil sands related reclamation water revealed no negative changes in somatic indices as a result of exposure. Yellow perch showed equal or superior ability to store and utilize energy for reproductive tissue growth relative to the lake from which they originated. Somatic indices in yellow perch from exposed areas generally fell within the range of indices measured at off-site reference lakes. Typically, the magni-

© 1999 NRC Canada

Fig. 2. Mean CPUE estimates performed using hoop nets in Demonstration Pond and South Bison Pond following the 1996 stocking effort. Error bars represent standard error of the mean. Asterisks indicate statistically significant differences between means ($p < 0.05$). The number at the base of each bar indicates the quantity of replicate net sets.

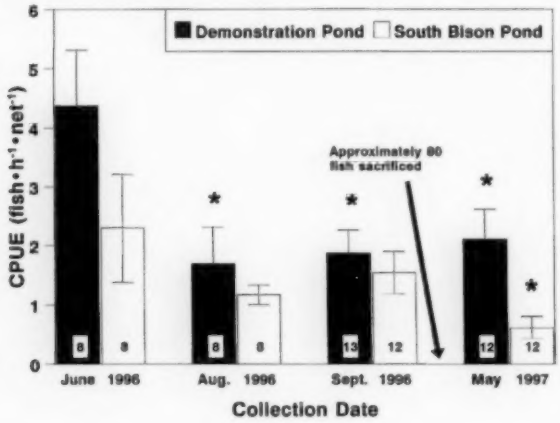

Fig. 3. Mean gonadosomatic index in (*a*) male and (*b*) female yellow perch captured at the experimental locations during fall 1995, fall 1996, and winter 1997. Error bars represent standard error of the mean. Means within sampling periods with the same letter are not significantly different ($p > 0.05$). Lake abbreviations as per Table 1.

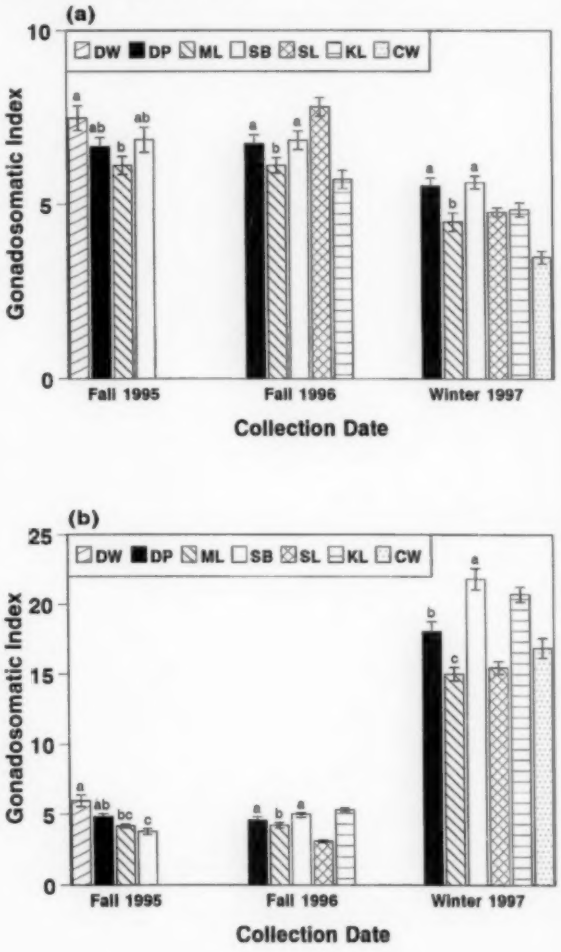

tude of differences between reference lake measurements exceeded changes that occurred in yellow perch stocked in experimental ponds.

Several chemical indicators of oil sands impacts on water quality were observed in this study. Increased salinity, with sulfate being the major anion, appears to be common in oil sands from this particular source. Sulfate salinity was closely parallelled by levels of naphthenic acids and by the trace metals boron, lithium, and strontium. In the sites tested, none of these marker compounds appeared to be present at sufficiently high levels to cause overt levels of acute lethality in adult yellow perch. However, levels of salinity in South Bison Pond were within a factor of 2 of the estimated 2000–4000 mg total dissolved solids·L^{-1} (sulfate saline) that yellow perch embryos can tolerate (Koel and Peterka 1995).

Initial declines in the numbers of yellow perch present in the experimental ponds were likely attributable to a delayed response precipitated by the trauma of capturing and transporting the fish. To what level this stress was influenced by the water chemistry of the experimental ponds remains unknown. Observed increases in 1996 poststocking survival probably resulted from efforts made to minimize handling and captivity time of yellow perch during stocking. The duration of the stocking experiments to date does not allow comment on possible long-term effects; further studies are required before conclusions about long-term risks can be drawn.

In this study, yellow perch, which are abundant in many boreal lakes and have a large geographic distribution and a home range limited to less than 1 km^2 (Fish and Savitz 1983), proved suitable for use within the context of the environmental framework developed by Munkittrick and Dixon (1989) and Gibbons and Munkittrick (1994). Given the short duration of the experiments reported here (2 years) relative to the life span of yellow perch (10+ years), it was not possible to assess changes in age distribution resulting from exposure to the experimental systems. The requirement for such data represents a practical limitation on the utility of monitoring frameworks for assessing the possible impacts of pulse events (e.g., tailings pond spills or flood events) and limits their use to situations where known stresses have been acting in a consistent manner for a period at least as long as a single, complete life cycle for the studied species.

A further, and quite serious, limitation of monitoring frameworks based on fisheries parameters is the choice of reference locations. For example, the recommendations of Canada's environmental effects monitoring protocol for fish require that one reference site be chosen as a basis for comparison with a possibly impacted site. The data from the off-site reference lakes presented in this study show that the use of a single reference location is at best misguided. In this study, the fortuitous choice of two off-site reference loca-

© 1999 NRC Canada

Fig. 4. Mean fecundity index in female yellow perch captured at the experimental locations during fall 1995, fall 1996, and winter 1997. Fecundity is expressed as number of eggs per gram of organ-corrected fish weight. Error bars represent standard error of the mean. Means within sampling periods with the same letter are not significantly different ($p > 0.05$). Lake abbreviations as per Table 1.

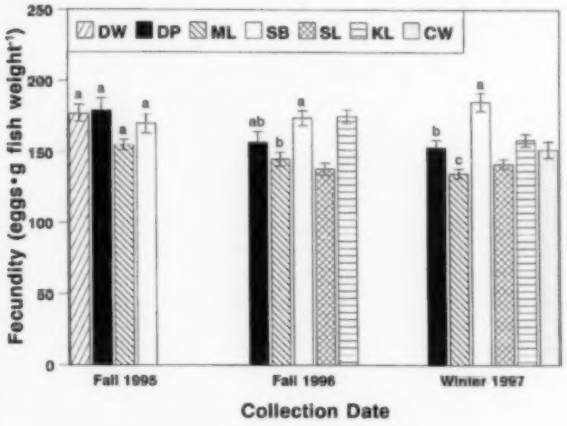

tions that reflect large differences in the measured fisheries parameters clearly demonstrates this problem. If the yellow perch monitoring parameters from either Sucker Lake or Kimowin Lake were compared directly with Demonstration Pond yellow perch parameters, two opposite conclusions would result. These results strongly indicate the need to know and understand the natural range of variability in fisheries parameters. Unfortunately, in order to accomplish this, a large number of sites need to be surveyed; this is both expensive and time consuming.

Despite the limitations of the monitoring strategy examined here, energy storage and utilization parameters were successfully used to characterize the response of stocked yellow perch to the experimental systems. Energy storage indices (condition factor, liver weight) showed no change or increased in yellow perch stocked in the experimental systems. The results suggest improved resource availability and a lack of any observable problems with adult yellow perch gonadal growth in the stocked ponds as compared with Mildred Lake. Examination of available diet, density, and competition data provides direct support for this conclusion. Yellow perch from the experimental ponds had the highest proportion of fish in their diet (Gould 1999) and were exceeded in condition only by fish from Kimowin Lake, whose diet consisted almost exclusively of abundant and calorie-rich prey (*Gammarus pulex* and *Hyalella azteca*). Sucker Lake yellow perch had the highest densities of all studied populations (authors' unpublished data). The population was dominated by large numbers of small fish, a pattern suggestive of food limitation and high intraspecific competition. The presence of white sucker (*Catostomus commersoni*), a known interspecific competitor, further suggests that Sucker Lake yellow perch were resource limited (Johnson 1977; Post and Cucin 1984).

The magnitude of condition factor differences in female yellow perch was reduced between fall 1996 and winter

Table 5. Relative changes in energy storage and utilization parameters (in that order) for yellow perch from the three experimental ponds as compared with Mildred Lake, the lake of origin for the stocked yellow perch.

	Deep Wetland	Demonstration Pond	South Bison Pond
Females			
Fall 1995	+ +	+ 0	+ 0
Fall 1996		0 +	+ +
Winter 1997		0 +	0 +
Males			
Fall 1995	0 +	+ 0	0 0
Fall 1996		0 +	0 +
Winter 1997		0 +	0 +

Note: +, significant increase; 0, no change; –, significant decrease. Changes are indicated only if all indices show a significant change in the same direction.

1997 and any statistical differences disappeared as a result. This suggested a seasonal change in condition factor. Such a change would be expected to occur if stored somatic energy reserves were utilized for gonad growth, since 75% of gonad growth occurs between fall and late winter. Kimowin Lake also showed a substantial drop in condition factor over this period. In contrast with changes observed in condition factor, liver size in yellow perch from the experimental ponds increased substantially between fall 1996 and winter 1997. Experimental pond yellow perch liver size was also larger than that of yellow perch in the off-site reference locations, particularly during winter 1997. The liver serves as the primary site of chemical metabolism and excretion and also as an energy storage organ. There is evidence to suggest that liver size may increase due to a petroleum-related chemical challenge under conditions where energy intake is controlled (Steadman et al. 1991; Truscott et al. 1992). Increased mixed-function oxygenase enzyme activity and bile polycyclic aromatic hydrocarbon metabolites in experimental pond yellow perch would suggest that this may be the case (van den Heuvel et al. 1999).

Energy utilization indices, gonad size, and fecundity for experimental pond yellow perch either showed significant increases or, when no significant change occurred, were higher than similar values derived for Mildred Lake yellow perch. The exception to this was South Bison Pond yellow perch in fall 1996. South Bison Pond yellow perch fecundity was similar to Mildred Lake yellow perch fecundity during this same period, indicating that smaller ovarian follicles relative to the other sites were responsible for the reduced gonad size. In 1996, yellow perch in South Bison Pond reversed this trend and had the highest fecundity and gonad size of any site examined. The reasons for this anomaly are unknown; however, fathead minnow were stocked during the same period of 1995 as the yellow perch. A rapid increase in the size of the fathead minnow population occurred between 1995 and 1996, possibly resulting in a better food base for yellow perch. It is also possible that the improved food source masked toxicological effects on gonad growth in 1996 but not in 1995.

Differences in gonad size in females were accentuated in winter 1997, as opposed to fall 1996, just as condition factor

© 1999 NRC Canada

differences disappeared over this period. This suggests that yellow perch in the experimental pond were successful at converting energy stored in the body into reproductive tissue. Thus, exposure to oil sands related reclamation waters does not appear to cause any deficiency in the metabolic redistribution of energy, as has been observed in white sucker exposed to pulp mill effluent (Munkittrick et al. 1994).

An unexpected phenomenon was the presence of resting years in reproduction or spawning periodicity in yellow perch from several of the locations examined. Periodicity could be considered a major energy utilization problem or merely the failure to accumulate sufficient energy to cue the initiation of gonadal recrudescence in the fall. Yellow perch stocked in the experimental ponds did not show spawning periodicity and appeared to have better energy stores than yellow perch from Mildred Lake. This would seem to suggest that the lack of gonad development in the resting fish was indeed related to food supply. However, two observations argue against this hypothesis: Sucker Lake yellow perch probably had the highest density and poorest food availability, yet periodicity was only infrequently observed. In addition, Cowper Lake yellow perch grew to sizes similar to Kimowin Lake yellow perch and showed the second highest condition factors in winter 1997 female yellow perch, yet showed a similar rate of spawning periodicity to that of Mildred Lake yellow perch. The observation of resting years is observed in other fish species, particularly at higher latitudes, and also shows contradictory data as to possible causes (Pulliainen and Korhonen 1993).

The results of this study indicate that the exposure of yellow perch to waters associated with oil sands reclamation does not compromise the short-term physiological status of exposed individuals. Irrespective of improved food supply in the experimental ponds, there was no direct evidence to suggest that oil sands related compounds were responsible for reduced survival, condition, or gonadal growth in yellow perch. It should be noted that physiological indices in adult fish may not be the most sensitive indicators of toxicant stress. Impacts may be masked by compensatory responses at both the individual and population level. This would imply that monitoring frameworks based on adult fish may not be the best tool for predicting potential risks to a population. Early life stages are generally thought to be a more sensitive stage of development and are therefore more likely to impact upon population status than are small changes in somatic indices at the adult stage of development.

Acknowledgements

Funding for this project was provided by Syncrude Canada Ltd. and by a Natural Sciences and Engineering Research Council of Canada collaborative research and development grant. The authors wish to thank Hans Boerger, Megan Harris, Betty Fung, Janice Cursons, Shauna Melnichuk, Niel and Rob Jevnings, Rachel Gould, Richard Fossen, and Lady for their enthusiastic technical support and guidance. The assistance of Larry Rhude, Alberta Fish and Wildlife, was also appreciated.

References

American Public Health Association, American Water Works Association, and Water Pollution Control Federation. 1985. Standard methods for examination of water and wastewater. 16th ed. American Public Health Association, Washington, D.C.

Boerger, H., MacKinnon, M., Van Meer, T., and Verbeek, A. 1992. Wet landscape option for reclamation of oil sand fine tails. *In* Proceedings of the 2nd International Conference on Environmental Issues and Management of Waste in Energy and Mineral Production. *Edited by* R.J. Singhal, A.K. Mehrota, K. Fytas, and J.L. Collins. A.A. Balkema, Rotterdam. pp. 1248–1261.

Colby, P.J., and Nepszy, S.J. 1981. Variation among stocks of walleye (*Stizostedion vitreum*): management implications. Can. J. Fish. Aquat. Sci. **38**: 1814–1831.

Fine Tailings Fundamentals Consortium. 1995. Volume II. Fine tailings and process water reclamation. *In* Advances in oil sands tailings research. Alberta Department of Energy, Oil Sands and Research Division, Edmonton, Alta. pp. 1–50.

Fish, P.A., and Savitz, J. 1983. Variations in home ranges of largemouth bass, yellow perch, bluegills, and pumpkinseeds in an Illinois lake. Trans. Am. Fish. Soc. **112**: 147–153.

Gibbons, W.N., and Munkittrick, K.R. 1994. A sentinel monitoring framework for identifying fish population responses to industrial discharges. J. Aquat. Ecosyst. Health, **3**: 227–237.

Gould, R. 1999.The effects of oil sands mine tailings on the benthic invertebrate community and diet of yellow perch (*Perca flavescens*). M.Sc. thesis, University of Waterloo, Waterloo, Ont.

Johnson, F.H. 1977. Responses of walleye (*Stizostedion vitreum*) and yellow perch (*Perca flavescens*) populations to removal of white sucker (*Catostomus commersoni*) from a Minnesota lake, 1966. J. Fish. Res. Board Can. **34**: 1633–1642.

Koel, T.M., and Peterka, J.J. 1995. Survival to hatching of fishes in sulfate-saline waters, Devils Lake, North Dakota. Can. J. Fish. Aquat. Sci. **52**: 464–469.

MacKinnon, M.D., and Boerger, H. 1986. Description of two treatment methods for detoxifying oil sands tailings pond water. Water Pollut. Res. J. Can. **21**: 496–512.

Munkittrick, K.R., and Dixon, D.G. 1989. A holistic approach to ecosystem health assessment using fish population characteristics. Hydrobiologia, **188/189**: 123–135.

Munkittrick, K.R., van der Kraak, G.J., McMaster, M.E., Portt, C.B., van den Heuvel, M.R., and Servos, M.R. 1994. Survey of receiving-water environmental impacts associated with discharges from pulp mills. 2. Gonad size, liver size, hepatic EROD activity and plasma sex steroid levels in white sucker. Environ. Toxicol. Chem. **13**: 1089–1101.

Post, J.R., and Cucin, D. 1984. Changes in the benthic community of a small Precambrian lake following the introduction of yellow perch. Can. J. Fish. Aquat. Sci. **41**: 1496–1501.

Pulliainen, E., and Korhonen, K. 1993. Does the burbot, *Lota lota*, have rest years between normal spawning seasons? J. Fish Biol. **43**: 355–362.

Steadman, B.L., Farag, A.M., and Bergman, H.L. 1991. Exposure-related patterns of biochemical indicators in rainbow trout exposed to No. 2 fuel oil. Environ. Toxicol. Chem. **10**: 365–374.

Truscott, B., Idler, D.R., and Fletcher, G.L. 1992. Alteration of reproductive steroids of male winter flounder (*Pleuronectes americanus*) chronically exposed to low levels of crude oil in sediments. Can. J. Fish. Aquat. Sci. **49**: 2190–2195.

U.S. Environmental Protection Agency. 1979. Methods for chemical analysis of water and wastes. EPA-600/4-79-020. EMSL, Cincinnati, Ohio.

© 1999 NRC Canada

van den Heuvel, M.R., Power, M., MacKinnon, M.D., and Dixon, D.G. 1999. Effects of oil sands related aquatic reclamation on yellow perch (*Perca flavescens*). II. Chemical and biochemical indicators of exposure to oil sands related waters. Can. J. Fish. Aquat. Sci. **56**. This issue.

Verbeek, A.G. 1994. A toxicity assessment of oil sands wastewater. M.Sc. thesis, University of Alberta, Edmonton, Alta.

Wilkinson, L. 1990. SYSTAT: the system for statistics. SYSTAT Inc., Evanston, Ill.

© 1999 NRC Canada

Effects of oil sands related aquatic reclamation on yellow perch (*Perca flavescens*). II. Chemical and biochemical indicators of exposure to oil sands related waters

M.R. van den Heuvel, M. Power, M.D. MacKinnon, and D.G. Dixon

Abstract: Adult yellow perch (*Perca flavescens*) were stocked into experimental ponds designed to emulate possible aquatic reclamation alternatives of the oil sands mining industry. After 5 and 11 months, mixed-function oxygenase (MFO) activity, liver conjugation enzymes, bile polycyclic aromatic hydrocarbon (PAH) equivalents, and plasma sex steroids were measured. Liver MFO activity and bile PAH equivalent concentration were closely correlated and showed the highest levels in the experimental ponds but also demonstrated a gradient of exposure among reference locations. Levels of steroid hormones in fall-captured fish did not show major differences among sites. However, during winter, yellow perch from three sites, including the experimental ponds, showed low levels of sex steroids in both males and females. Multivariate regressions showed no relationship between steroid hormone concentrations and gonad size or fecundity. Similarly, steroid hormones did not parallel the gradient of exposure as measured by MFO and bile PAH metabolites. Gonad size and fecundity also were not directly correlated with the gradient of exposure observed in this study. Although MFO activity and bile PAH equivalents were good indicators of exposure to oil sands related waters, they were not predictive of physiological endpoints, suggesting that the latter were influenced primarily by ecological and not by chemical factors.

Résumé : On a introduit des perchaudes (*Perca flavescens*) dans des étangs expérimentaux pour simuler les opérations possibles de récupération de sables bitumineux dans les milieux aquatiques par l'industrie minière. Après 5 et 11 mois, on a mesuré l'activité des oxygénases à fonction mixte (OFM), les enzymes hépatiques de conjugaison, les équivalents d'hydrocarbures aromatiques polycycliques (HAP) dans la bile et les stéroïdes sexuels plasmatiques. L'activité des OFM hépatiques et la concentration des équivalents HAP dans la bile étaient étroitement corrélées, et ces deux paramètres ont présenté les valeurs les plus élevées dans les étangs expérimentaux, mais ont aussi révélé l'existence d'un gradient d'exposition dans les sites de référence. Les niveaux d'hormones stéroïdes chez les poissons capturés à l'automne n'étaient pas très différents d'un site à l'autre. Cependant, durant l'hiver, les perchaudes mâles et femelles de trois sites, notamment des étangs expérimentaux, renfermaient de faibles concentrations de stéroïdes sexuels. Les régressions multivariées ont montré qu'il n'y avait pas de relation entre les concentrations d'hormones stéroïdes et la taille des gonades ou la fécondité. De même, les concentrations de stéroïdes ne suivaient pas le gradient d'exposition tel que mesuré par les OFM et les métabolites des HAP dans la bile. La taille des gonades et la fécondité n'étaient pas non plus directement corrélées avec le gradient d'exposition observé dans cette étude. Si l'activité des OFM et les équivalents HAP biliaires étaient de bons indicateurs de l'exposition aux eaux des sables bitumineux, ils ne permettaient pas de faire des prévisions concernant les paramètres physiologiques, ce qui laisse penser que ces derniers étaient déterminés principalement par des facteurs écologiques plutôt que par des facteurs chimiques.

[Traduit par la Rédaction]

Introduction

The oil sands industries of northern Alberta, Canada, are the largest producers of synthetic crude oil in the world, with over a billion barrels produced to date. This large and economically important industry will mine hundreds of square kilometres of muskeg-dominated northern boreal forest in order to remove the hydrocarbon-saturated sands located beneath the surface. The oil sands industries have a commitment to reclaim the landscape disturbed by the min-

Received August 25, 1998. Accepted February 17, 1999.
J14758

M.R. van den Heuvel[1] **and D.G. Dixon.** Department of Biology, University of Waterloo, Waterloo, ON N2L 3G1, Canada.
M. Power. Department of Agricultural Economics, University of Manitoba, Winnipeg, MB R3T 2N2, Canada.
M.D. MacKinnon. Syncrude Canada Ltd., Edmonton Research Center, 9421 17th Ave., Edmonton, AB T6N 1H4, Canada.

[1]Author to whom all correspondence should be addressed. Present address: New Zealand Forest Research Institute, Private Bag 3020, Rotorua, New Zealand. e-mail: mike.vandenheuvel@forestresearch.co.nz

© 1999 NRC Canada

ing operations. Out of necessity, this will involve reincorporating the tailings back into the landscape in an environmentally benevolent fashion.

Regardless of the method of reclamation used, surface waters will be produced or influenced by process activities and the resulting waters must be capable of supporting biological systems in viable ecosystems. The water quality properties associated with the process affected waters include elevated salinity and organic acids (naphthenic acids) as well as the increased concentrations of polycyclic aromatic hydrocarbons (PAH's). The relative concentrations of the chemical constituents will differ, depending on the reclamation methods used. It is expected that fish will eventually come into contact with oil sands reclamation waters or inhabit reclaimed aquatic systems. As such, it would be useful to have a suite of biochemical and chemical indicators of exposure to families of compounds associated with oil sands related waters.

Two indicators, mixed-function oxygenase (MFO) activity and bile PAH equivalent concentration, have been widely used to quantify exposure of fishes to petroleum hydrocarbons (Krahn et al. 1984; Hellou and Payne 1987; Payne et al. 1987; Collier and Varanasi 1991). In fishes, MFO generally refers to a measurement of a single cytochrome P450 isozyme, namely P4501A1 (Payne et al. 1987; Stegeman and Hahn 1995). Synthesis of MFO enzymes can be induced by exposure to many of the compounds that are metabolized by them, including PAH's. In the liver, P4501A1 is responsible for the initial oxidation (phase I) of hydrophobic organic compounds in order to facilitate biliary excretion. Oxidized hydrophobic organic compounds are rendered more water soluble via conjugation with glucuronic acid, glutathione, or sulfate. The conjugative metabolic reactions are referred to as phase II and are catalyzed by enzymes such as uridine 5′-diphosphate-glucuronosyl transferase (UDPGT), glutathione *S*-transferase (GST), and sulfatase. Because biliary excretion is the major route of excretion for PAH's, measurement of PAH metabolites in the bile can provide a sensitive indicator of exposure to PAH's.

Levels of plasma steroid hormones in fishes have been observed to decrease in response to PAH exposure (Thomas 1988; Stein et al. 1991) or petroleum hydrocarbon exposure (Truscott et al. 1983; Johnson et al. 1988; Truscott et al. 1992). Recently, plasma steroid hormones have been extensively used to examine the potential of pulp and paper mill effluents to affect fish reproduction (Munkittrick et al. 1991; Van Der Kraak et al. 1992; McMaster et al. 1996). The main estrogen and androgen in fishes, 17β-estradiol and 11-ketotestosterone, are the primary hormones responsible for gonadal development in females and males, respectively. Decreased levels of these steroid hormones and their common immediate precursor, testosterone, would therefore be expected to indicate the potential for contaminant-induced reduction in gonad size.

Toxicological literature has been flooded with research studying biochemical and chemical indicators of exposure to groups of anthropogenic compounds. For the most part, these parameters have been measured under the contention that they can be used as early-warning signs or predictors of damage at higher levels of ecological organization (National Research Council of Canada 1985). The term "indicator" has been coined to imply that measured parameters predict, or are correlated with, effects at a higher level of biological organization (McCarty and Munkittrick 1996). Attempts to causally link, or validate, indicators for effects at higher levels of biological organization are few (Holdway 1996, 1997; McCarty and Munkittrick 1996).

The purpose of this study was to examine the usefulness of MFO enzymes, conjugation enzymes, bile PAH metabolite concentrations, and plasma steroid hormones in yellow perch (*Perca flavescens*) as markers of exposure to oil sands mining related waters. The secondary aim of this work was to examine the potential of these biochemical and chemical endpoints as predictive indicators of physiological and population-level impacts in subsamples of individuals from yellow perch populations exposed to oil sands derived sources of water.

Materials and methods

Study site description and yellow perch stocking experimental design

Study site descriptions and chemical characteristics of the ponds and lakes used in this study are described in detail in van den Heuvel et al. (1999). Briefly, the main experimental pond, called the Demonstration Pond, was constructed in 1993 as an example of the water-capping reclamation strategy. Demonstration Pond is about 4 ha and contains oil sands mature fine tailings capped with a layer of surface drainage water. Two other experimental ponds located at the mine site, South Bison Pond and Deep Wetland, were constructed ponds without a bottom of fine tailings. Deep Wetland was constructed adjacent to and at the same time as Demonstration Pond. South Bison Pond receives drainage from a reclaimed pasture area and is 8 years older than the other two experimental ponds. Mildred Lake is an altered natural lake on the oil sands lease from which yellow perch were stocked into the experimental ponds. Three additional off-site reference locations were chosen in order to examine yellow perch populations that were completely isolated from any oil sands influence. Sucker Lake is located on the western edge of the Athabasca deposit, while Kimowin Lake and Cowper Lake are located in areas that do not receive any surface water drainage from above the oil sands geological deposit.

Yellow perch were removed from Mildred Lake in the springs of 1995 and 1996 and transferred into the experimental ponds as described in van den Heuvel et al. (1999). Subsamples of yellow perch were captured and sacrificed during September 1995 (hereafter referred to as fall 1995), May 1996 (spring 1996), September 1996 (fall 1996), and March 1997 (winter 1997).

Fish sampling

Yellow perch were captured as described in van den Heuvel et al. (1999). Blood was removed by caudal puncture using a 3-mL syringe (21 gauge or 23 gauge), placed into a 3-mL heparinized vacutainer, and placed on ice. After blood collection, yellow perch were dispatched with a sharp blow to the head. Within 8 h of collection, blood was spun at 500 × *g* for 10 min in a clinical centrifuge and plasma was frozen in liquid nitrogen.

Livers were removed and weighed, and a 1-g subsample for 7-ethoxyresorufin-*O*-deethylase (EROD) analysis was frozen in liquid nitrogen in a 2.0-mL cryovial. Gallbladders that contained bile were placed intact into 2.0-mL cryovials and frozen in liquid nitrogen. In fall 1995 and spring 1996, bile-containing gallbladders were pooled from each site, while in fall 1996 and winter 1997, gallbladders were collected on an individual fish basis. Liver samples for EROD measurement were stored at –80°C pending analy-

© 1999 NRC Canada

sis (maximum storage time of 3 months). All other samples were stored at –20°C until analysis.

EROD analysis

Hepatic MFO enzyme activity was estimated in postmitochondrial supernatant (PMS) as EROD activity using a modification of the fluorescence plate-reader technique developed by Kennedy and Jones (1994). Liver extracts were homogenized in a cryopreservative buffer (0.1 M phosphate, 1 mM EDTA, 1 mM dithiothreitol, and 20% glycerol, pH 7.4) and spun at 9000 × *g* to obtain the PMS. The EROD reaction mixture contained 0.1 M HEPES buffer, pH 7.8 (Sigma Chemical Co., St. Louis, Mo.), 5.3 mM Mg^{2+}, 0.5 mM NADPH (Boehringer Mannheim, Mannheim, Germany), 1.5 μM 7-ER (Sigma), and about 0.5 mg PMS protein·mL^{-1}. The reaction was stopped after 5 min by adding 0.5 mL of ice-cold acetonitrile containing the protein-binding reagent fluorescamine (Lorenzen and Kennedy 1993). Resorufin was determined on a Millipore Cytofluor model 2350 plate-reading fluorometer (530 nm excitation, 590 nm emission). Protein content was estimated from fluorescamine fluorescence (380 nm excitation, 420 nm emission) against bovine serum albumin (fraction V, Sigma).

Conjugation enzyme analysis

Microsomal and cytosolic fractions were prepared from PMS of female yellow perch captured during winter 1997. PMS was centrifuged for 1 h at 90 000 × *g*. The cytosol (supernatant) was removed and the microsomal pellet was suspended in cryopreservative buffer (previously described). Both cytosolic and microsomal fractions were frozen at –80°C until analysis. Measurement of UDPGT activity was measured in microsomal suspensions according to Castren and Oikari (1983). Protein content was determined by a modified fluorescamine fluorescence method (Lorenzen and Kennedy 1993). GST was measured according to Habig et al. (1974) as modified by Anderson et al. (1985).

Bile fluorescence analysis

Yellow perch gallbladders were thawed and the bile expressed from them. Bile was diluted by a factor of 10 with Milli-Q quality water. High-performance liquid chromatography (HPLC) – fluorescence analysis was used to estimate phenanthrene and benzo[a]pyrene equivalents adapted after the methods of Krahn et al. (1984). The HPLC was a Spectra-Physics model SP8100 pump, a Shimatzu RF-10A fluorescence detector, and a Spectra-Physics model SP4270 peak integrator. Bile samples (50 μL) were injected onto a 250 × 4.6 mm C-18 column with 5-μm particle size (Supelco, Mississauga, Ont.) and eluted with a linear gradient of 100% water (0.005% acetic acid) to 100% methanol over 15 min and then held at 100% methanol for an additional 45 min. Areas for all peaks eluting after 7 min of run time were added and compared with peak areas for standards of either phenanthrene (256 nm excitation, 380 nm emission) or benzo[*a*]pyrene (380 nm excitation, 430 nm emission).

Steroid hormone analysis

Steroid hormones were measured according to McMaster et al. (1992). Plasma samples were thawed and steroid hormones were extracted with diethyl ether. The plasma extract from females was analysed for estradiol and testosterone, while that from males was analysed for 11-ketotestosterone and testosterone using standard radioimmunoassay procedures.

Statistics

All statistical analyses were performed using SYSTAT software (Wilkinson 1990). EROD, bile PAH equivalent concentrations, and steroid hormone data were analysed by ANOVA followed by Tukey's test for all possible pairwise comparisons. Yellow perch EROD injection experiment data were analyzed by ANOVA followed by Dunnett's test. Prior to statistical testing, homoscedasticity was tested using Bartlett's test and normality was examined using probability plots. Heteroscedastic or nonnormal data were log transformed and retested prior to performing statistical tests requiring that these assumptions be met. Statistical significance was assessed at the $\alpha = 0.05$ level.

Results

Hepatic enzyme induction

Over the duration of the study, a consistent pattern of hepatic MFO (EROD) induction was observed in yellow perch exposed to oil sands related waters (Fig. 1). These data demonstrated a gradient of EROD activity with yellow perch from Kimowin Lake and Cowper Lake, the off-site reference locations remote from the Athabasca oil sands deposit, having the lowest levels of activity. Intermediate in EROD activity were Mildred Lake and Sucker Lake yellow perch. These reference sites were located on the oil sands deposit area and, in the case of Mildred Lake, at the mine site. Highest in EROD activity were yellow perch from the experimental ponds South Bison Pond, Demonstration Pond, and Deep Wetland. Male and female yellow perch both demonstrated similar trends in EROD activity. The absolute activity was consistently higher in male than in female yellow perch. The maximum magnitude of EROD induction (highest mean divided by the lowest) for males and females, respectively, was 9.6-fold in winter 1997 and 16.2-fold in fall 1996.

Phase II hepatic metabolism, as represented by GST and UDPGT activity measured in winter 1997, was not affected by exposure to oil sands reclamation related water (Table 1). GST activity in Sucker Lake during this period was shown to be significantly depressed. Due to the lack of changes in these enzyme activities during the winter 1997 period, further analysis on other capture periods was not conducted.

Bile PAH equivalent concentrations

Bile PAH equivalent concentrations measured at both phenanthrene and benzo[*a*]pyrene wavelengths showed similar trends as EROD activity. Due to the low number of individuals with bile present in the gallbladder, male and female yellow perch bile results were pooled for statistical analysis. Differences in both phenanthrene and benzo[*a*]pyrene bile PAH equivalent concentrations were observed for the fall 1996 and winter 1997 sampling periods (Fig. 2). During spring 1996 and fall 1995, bile samples were pooled, precluding statistical analysis, but similar trends were observed. Phenanthrene and benzo[*a*]pyrene endpoints were found to be highly correlated ($r^2 = 0.81$, $p < 0.001$, $n = 93$), indicating a similar source for both groups of compounds.

Multivariate regressions were used in order to determine if bile PAH equivalent concentrations were predictive of EROD activity. Data from individual fish were utilized from fall 1996 and winter 1997. Bile benzo[*a*]pyrene and phenanthrene equivalent concentrations were assessed individually using capture season and yellow perch gender as additional independent variables. There was no significant seasonal component of variation, and capture season was

© 1999 NRC Canada

Fig. 1. Mean ± SEM levels of EROD measured in liver PMS for (*a*) male and (*b*) female yellow perch. Sample sizes in males are $n = 12$ with the following exceptions. Fall 1995: Demonstration Pond, $n = 8$; South Bison Pond, $n = 6$; spring 1996: Demonstration Pond, $n = 4$; South Bison Pond, $n = 2$; fall 1996: Demonstration Pond, $n = 13$. Sample sizes in females are $n = 12$ with the following exceptions. Spring 1996: Demonstration Pond, $n = 4$; Mildred Lake, $n = 10$; South Bison Pond, $n = 8$; fall 1996: Sucker Lake, $n = 13$. Means within a sampling period with the same letter are not significantly different ($p > 0.05$). DW, Deep Wetland; DP, Demonstration Pond; ML, Mildred Lake; SB, South Bison Pond; SL, Sucker Lake; KL, Kimowin Lake; CW, Cowper Lake.

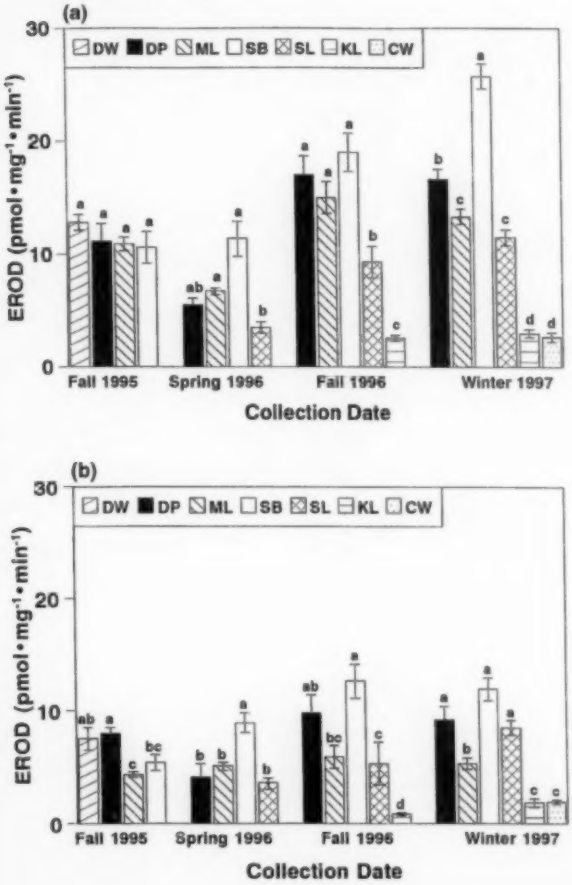

dropped from further analysis. Bile PAH equivalents were highly predictive ($p < 0.001$) of EROD activity when either phenanthrene or benzo[*a*]pyrene endpoints were used. A significant component of variation ($p < 0.05$) could be attributed to gender when phenanthrene equivalents were examined but not when benzo[*a*]pyrene equivalents were used as an independent variable.

Plasma sex steroid hormones

Significant differences in steroid hormones were observed during all capture periods. In females captured during fall sampling periods, only South Bison Pond (in 1995) and Sucker Lake (in 1996) had levels of estradiol that were significantly lower than values measured for the bulk of the other sites (Fig. 3). Testosterone in fall 1995 South Bison Pond female yellow perch was also significantly lower than for two of the other three sites examined. The winter steroid results demonstrated much more dramatic differences. During this sampling period, two discrete groups were observed. South Bison Pond, Demonstration Pond, and Sucker Lake female yellow perch had low plasma levels of both estradiol and testosterone as compared with Kimowin Lake, Cowper Lake, and Mildred Lake yellow perch. This trend was particularly apparent for testosterone where yellow perch from the latter three sites appeared to have increased testosterone levels from the previous fall, while those from the former three sites did not.

Males demonstrated few significant differences in steroid hormone levels in the fall capture periods (Fig. 4). Deep Wetland yellow perch had elevated testosterone concentrations compared with yellow perch from the other three sites examined during fall 1995. There were also significant differences between Kimowin Lake and Mildred Lake yellow perch 11-ketotestosterone in fall 1996. As in females, steroid differences in the late winter were much more dramatic. Identical groupings appeared as in females, with 11-ketotestosterone and testosterone in yellow perch from South Bison Pond, Demonstration Pond, and Sucker Lake being significantly lower than in male yellow perch from the remaining sites.

Comparisons of biochemical and physiological parameters

In order to determine if steroid hormone levels were predictive of physiological reproductive indicators, the reproductive indices gonadosomatic index (GSI) and fecundity somatic index (FSI, data from van den Heuvel et al. 1999) were compared with steroid levels on an individual fish basis using regression analysis. Either GSI or FSI was used as the dependent variable and steroid concentration, capture location, and capture season were used as the independent variables. Regressions showed a strong seasonal component of variability in gonad size in both males and females ($p < 0.001$), but there was no significant seasonal variation in female fecundity. For both estradiol and testosterone in female yellow perch, there were interactions between steroids and location of capture in the GSI–steroid regression and in the FSI–steroid regression ($p < 0.001$). This indicates that there was no consistent relationship between steroids and GSI or FSI within the individual capture locations; the relationship between steroids and GSI or FSI varied from location to location. A similar lack of relationship between gonad size and steroids was observed when mean data were compared. For example, in winter 1997, South Bison Pond female yellow perch had relatively low steroid levels, the largest ovaries, and highest fecundity (van den Heuvel et al. 1999). Conversely, Sucker Lake yellow perch captured during the same period had similarly low estradiol, relatively smaller ovaries, and low fecundity.

In males, there were no interactions between location and steroid levels for either steroid measured. There were also no relationships between steroids and GSI. As can be ob-

© 1999 NRC Canada

Table 1. Mean (SEM, *n*) hepatic activity levels of GST and UDPGT in female yellow perch captured during winter 1997.

Capture location	GST ($\mu mol \cdot mg^{-1} \cdot min^{-1}$)	UDPGT ($pmol \cdot mg^{-1} \cdot min^{-1}$)
Demonstration Pond	1.27 (0.08, 11) *a*	24.1 (4.0, 11) *a*
Mildred Lake	1.40 (0.09, 11) *a*	25.0 (7.6, 11) *a*
South Bison Pond	1.23 (0.09, 12) *a*	27.6 (4.4, 13) *a*
Sucker Lake	0.78 (0.12, 9) *b*	17.4 (3.8, 9) *a*
Kimowin Lake	1.20 (0.12, 10) *a*	18.4 (5.8, 10) *a*
Cowper Lake	1.55 (0.08, 10) *a*	16.0 (7.2, 10) *a*

Note: Means followed by the same letter are not significantly different ($p > 0.05$).

Fig. 2. Mean ± SEM levels of (*a*) benzo[*a*]pyrene and (*b*) phenanthrene equivalent concentrations in the bile of yellow perch as measured by HPLC–fluorescence. Sample sizes for fall 1996 and winter 1997 were $n = 10$. Fall 1995 and spring 1996 bars represent concentrations measured in pooled samples of bile (>10 individuals). Means within a sampling period with the same letter are not significantly different ($p > 0.05$). See Fig. 1 for site abbreviations.

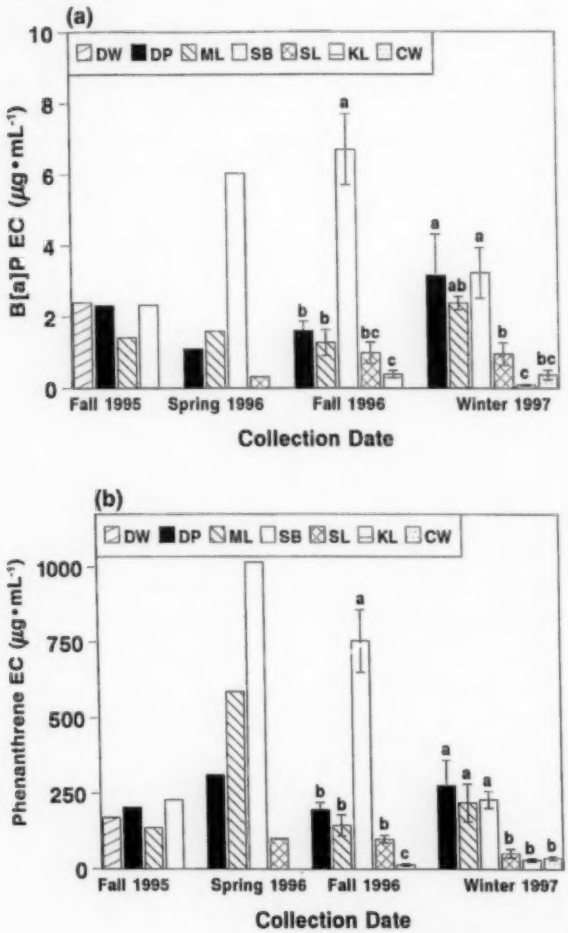

Fig. 3. Mean ± SEM levels of (*a*) estradiol and (*b*) testosterone in plasma of female yellow perch. Sample sizes are $n = 12$ with the following exceptions. Fall 1995: Demonstration Pond, $n = 13$; Mildred Lake, $n = 23$; winter 1997: Mildred Lake, $n = 11$; Sucker Lake, $n = 10$; Kimowin Lake, $n = 11$; Cowper Lake, $n = 9$. Means within a sampling period with the same letter are not significantly different ($p > 0.05$). See Fig. 1 for site abbreviations.

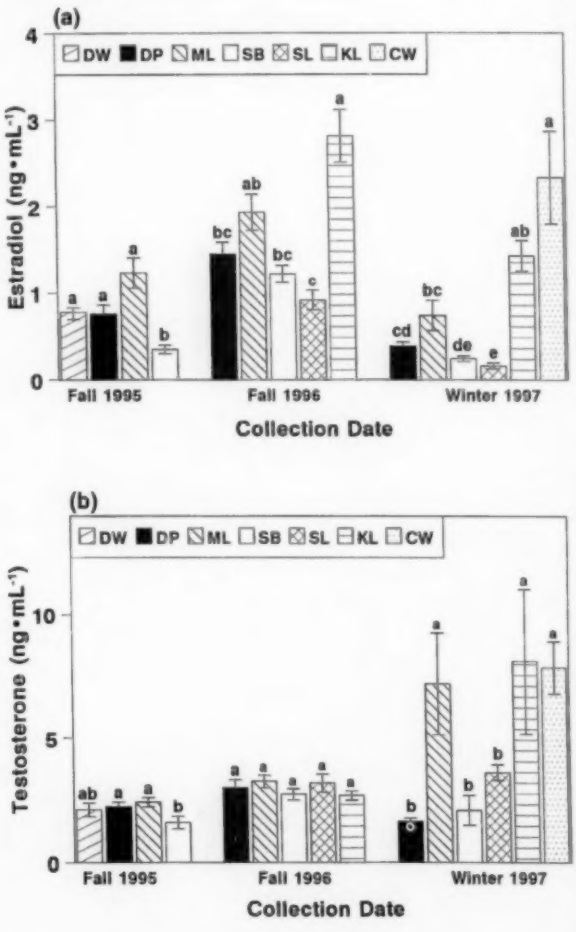

served from the mean steroid levels, there was a significant component of variability due to capture location.

Yellow perch plasma steroid hormones in females did not show the same gradient as the exposure-related indicators EROD and bile PAH equivalent concentrations. Regressions were performed by sex and capture season to determine if

© 1999 NRC Canada

Fig. 4. Mean ± SEM levels of (*a*) 11-ketotestosterone and (*b*) testosterone measured in male yellow perch. Sample sizes are $n = 12$ with the following exceptions. Fall 1995: Demonstration Pond, $n = 8$; Mildred Lake, $n = 13$; South Bison Pond, $n = 6$; winter 1997: Mildred Lake, $n = 10$; Kimowin Lake, $n = 9$; Cowper Lake, $n = 10$. Means within a sampling period with the same letter are not significantly different ($p > 0.05$). See Fig. 1 for site abbreviations.

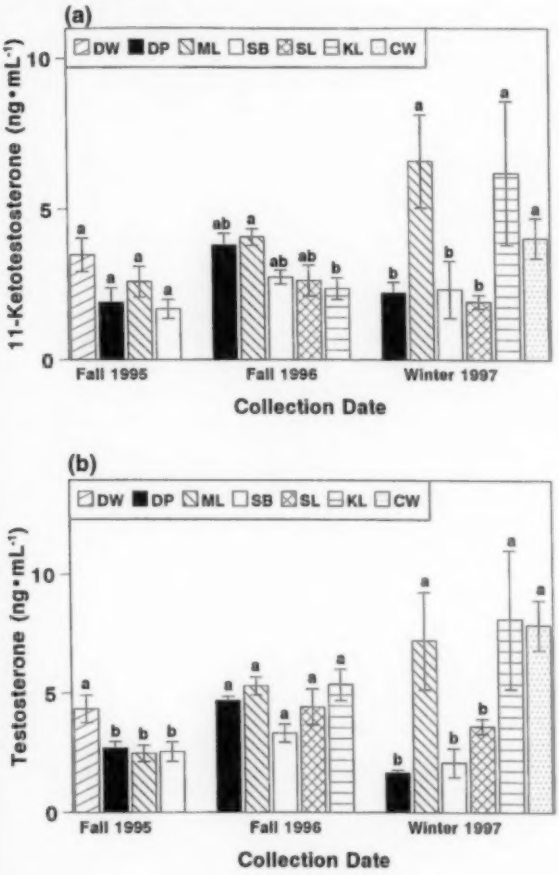

EROD was predictive of steroid levels. Capture location was also added as an independent variable in the regression. During fall 1995 capture dates, there were significant positive relationships between both 11-ketotestosterone and testosterone and EROD in male yellow perch and also between testosterone and EROD in females. However, during fall 1996, there was a negative relationship between estradiol and EROD in females and between testosterone and EROD in males. During winter 1997, when the most dramatic steroid differences occurred, capture location was a highly significant ($p < 0.001$) determinant of steroid levels, while EROD did not contribute significantly to the overall variability. This trend was apparent for both steroids in both sexes during the winter capture date. Similar regressions using bile PAH equivalent concentrations also showed a lack of any consistent trend between exposure indicators and steroid hormones.

EROD activity and bile PAH equivalent concentrations also could not be related to physiological indices of reproduction. In regressions using GSI as the dependent variable, in both males and females, there was a significant interaction between EROD activity and capture location ($p < 0.001$). This implies that the EROD–GSI relationship varied between capture location. In a regression using fecundity (FSI) as the dependent variable, there was also a significant location effect ($p < 0.001$). No significant interactions and no relationship between EROD and FSI were observed.

Discussion

This study demonstrated a gradient of exposure in yellow perch to oil sands related compounds as indicated by MFO and bile PAH metabolite endpoints; this was not reflected in the conjugation enzyme parameters measured. The highest exposure to the compounds to which these indicators are sensitive appeared to occur in the experimental reclamation related ponds, followed by yellow perch captured in lakes on, or receiving water from, the Athabasca oil sands deposit, and then by yellow perch in lakes located off the Athabasca deposit. Steroid hormones in yellow perch did not follow the same gradient and could not be consistently related to either measure of yellow perch exposure. Steroid hormones, hepatic MFO, and bile PAH equivalent concentrations were not correlated with physiological indices of adult yellow perch reproductive development, gonad size, and fecundity.

Levels of the conjugation enzymes GST and UDPGT did not appear to be related to exposure to water associated with oil sands. The only statistically significant depression occurred with GST in Sucker Lake yellow perch. This may have been a stress-related response due to the hypoxia that the yellow perch were undergoing at the time. Previous studies have identified the GST and UDPGT enzymatic endpoints as potential indicators of exposure to organic compounds (Celander et al. 1994). However, with the species of fish and sources of exposure examined in this study, these endpoints appeared to have no value as exposure indicators.

Hepatic EROD activity measured in experimental yellow perch was likely proportional to the exposure to PAH's originating from oil sands material. P4501A1 induction is indicative of exposure to several groups of planar compounds including dioxins and furans, polychlorinated biphenyls, and PAH's. In this case, the two former classes of compounds are known not to be associated with oil sands mining. The elevated bile PAH equivalent concentrations suggest the presence of PAH metabolites in the bile and thus exposure of these yellow perch to PAH's. Attempts were made to identify particular PAH metabolites in yellow perch bile extract derived from this study. No detectable levels of known PAH metabolites could be identified in the bile (authors' unpublished data). This result may be because the individual metabolites were present at concentrations too low for detection by a mass selective detector. Metabolites of biogenic compounds were also found in the bile in high concentrations, impairing the detection of molecules that may only be present at trace levels.

Exposure to PAH's appears to be diagnostic of exposure to waters associated with oil sands material. In the case of

© 1999 NRC Canada

South Bison Pond, the high responses observed in both MFO and bile PAH equivalent concentrations are almost certainly attributable to unextracted oil sands material, most likely the lean oil sands material that composes the pond basin and underlies the surrounding pasture. Demonstration Pond, which contains large amounts of previously extracted material (tailings), tends to show lower bile equivalent concentrations and hepatic MFO activity than South Bison Pond. In this case, we cannot rule out the possibility that this material is derived from the clays that compose the pond basin rather than from the tailings themselves. Observations from fall 1995 in the adjacent Deep Wetland would lend credence to the theory that the source of at least some PAH-like material is the pond construction material.

The gradient of oil sands related exposure also extends to some of the reference locations. Mildred Lake has obvious sources of this material, since the water pumped into Mildred Lake originates in the Athabasca River, which cuts directly through the Athabasca oil sands deposit. Also, the intake for Mildred Lake water is downstream of a point-source discharge from an adjacent oil sands upgrading plant. Sucker Lake, which is remote from any industry or human activity, also appears to have low-level exposure to what are likely oil sands derived compounds. This was unexpected, since the Athabasca oil sands would be expected to be far below the surface at this location and Sucker Lake is only on the eastern periphery of the deposit. Detectable levels of naphthenic acids in Sucker Lake water suggest that there may be a source of oil sands related compounds present in drainage waters entering the lake (van den Heuvel et al. 1999). Only Kimowin Lake and Cowper Lake appeared to have very low levels of exposure to PAH material. These two sites are completely removed from the Athabasca deposit and do not receive drainage water from any part of the oil sands area.

The exposure gradient observed in this study has important implications for the oil sands reclamation options. These results would indicate that it is essentially impossible to create or reclaim aquatic habitat on the oil sands area without having some exposure to organic (and inorganic) compounds present in the bitumen deposits. Although the indicators of exposure used in this study are specific for particular groups of compounds, PAH's in this case, it is likely that other bitumen-related organic compounds such as naphthenic acids will occur proportionally (they are also proportional to the inorganic compounds associated with oil sands, van den Heuvel et al. 1999). The severity of the exposure to these compounds will depend on the nature of the reclamation material present. It appears, ignoring other characteristics of the material, as if the previously extracted material (tailings) is no worse, and possibly better, than unextracted oil sands as a reclamation material with regard to exposure to compounds to which our exposure indicators were sensitive. This raises the question of what levels of exposure to compounds associated with these materials become detrimental to the integrity of populations of aquatic organisms.

At levels of exposure encountered in this study, no consistent relationships between the level of exposure to oil sands related compounds and steroid hormone concentrations could be found. Observations in rainbow trout (*Oncorhynchus mykiss*) would suggest that levels of estradiol in females during late vitellogenesis should begin to drop gradually, while testosterone levels remain high until ovulation (Scott and Sumpter 1983). It appeared that yellow perch in South Bison Pond, Demonstration Pond, and Sucker Lake had abnormal late winter steroid profiles, in that testosterone production had not increased or had decreased as compared with fall values. Yellow perch from the other three sites showed the increase in testosterone that would be expected based on the rainbow trout model. It is unlikely that the responsible mechanism is consistent among the three affected sites, since Sucker Lake yellow perch did not have similar levels of exposure to oil sands compounds as compared with yellow perch from the two experimental ponds. This suggests that these observations may not have been directly mediated by any chemicals present. The mechanism of response in Sucker Lake may be one of general stress in light of the low levels of dissolved oxygen during the winter ($2.0\ mg \cdot L^{-1}$, van den Heuvel et al. 1999). Elevated stress levels have been observed to have a potent effect on steroid synthesis (Jardine et al. 1996). The possibility that the alterations in late winter steroid profiles seen in Demonstration Pond and South Bison Pond yellow perch were directly or indirectly caused by contaminants remains. However, dietary and abiotic factors leading to stress, or indirect contaminant stress, in these organisms cannot be ruled out.

Another key finding was that the alterations in yellow perch steroid hormone profiles could not be related to gonad size indices in individuals. Differences in steroid levels among sites observed here varied by as much as 10-fold, yet were not correlated with gonad size. This raises questions relating to the use of steroids as monitoring tools. The magnitude of steroid change required to cause an alteration in gonadal growth remains essentially unknown. As with any toxicological response, the levels of steroid change required to cause a particular gonadal effect are probably highly dependent on modifying factors, particularly nutrition. Evidence from this study (van den Heuvel et al. 1999) indicates that South Bison Pond yellow perch in all probability had relatively high energy intake and storage as compared with yellow perch from many of the other sites. This improved nutritional regime may have been sufficient to mask physiological effects mediated by depressed steroid levels. Steroids were also measured at particular points in time during vitellogenesis. It must be recognized that gonad growth occurs over many months and steroids in the winter period (when the most significant differences occurred) may not be relevant to gonad growth that has occurred previously during the year.

This study has identified biochemical and chemical indicators of exposure to oil sands related compounds. However, due to the lack of relationship between these parameters and observations at the individual or physiological level, the measured indicators remain indicators of exposure, not indicators of toxicological effect. Our study could not factor out the effect of many biotic and abiotic modifying factors that invariably influence field-based measures. This raises obvious questions about the utility of the "biomarker" or "bioindicator" approach for making inferences about effects likely to be observed at higher levels of biological organiza-

© 1999 NRC Canada

tion. However, these observations do not detract from the value of biochemical tools when used to gain insight into the mechanisms of impaired physiological performance.

Acknowledgements

Funding was provided by a Natural Sciences and Engineering Research Council of Canada collaborative research and development grant and by Syncrude Canada Ltd. The authors wish to thank Hans Boerger, Evan Dobson, Terry Van Meer, Deib Birkholz, Rachel Gould, Megan Harris, Janice Cursons, Shauna Melnichuk, Larry Rhude, Niel and Rob Jevnings, Richard Fossen, and Lady for their assistance. Dr. Glen Van Der Kraak provided helpful insight on these data.

References

Anderson, T., Pesonen, M., and Johansson, C. 1985. Differential induction of cytochrome P-450 dependent monooxygenase, epoxide hydrolase, glutathione transferase and UDP glucuronosyl transferase activities in the liver of the rainbow trout by β-naphthoflavone or clophen A50. Biochem. Pharmacol. **34**: 3309–3314.

Castren, M., and Oikari, A. 1983. Optimal assay conditions for liver UDP-glucuronosyltransferase from the rainbow trout, *Salmo gairdneri*. Comp. Biochem. Physiol. C, Comp. Pharmacol. **76**: 365–369.

Celander, M., Naf, C., Broman, D., and Forlin, L. 1994. Temporal aspects of induction of hepatic cytochrome P450 1A and conjugating enzymes in the viviparous blenny (*Zoarces viviparus*) treated with petroleum hydrocarbons. Aquat. Toxicol. **29**: 183–196.

Collier, T.K., and Varanasi, U. 1991. Hepatic activities of xenobiotic metabolizing enzymes and biliary levels of xenobiotics in English sole (*Parophrys vetulus*) exposed to environmental contaminants. Arch. Environ. Contam. Toxicol. **20**: 462–473.

Habig, W.J., Pabst, M.J., and Jakoby, W.B. 1974. Glutathione *S*-transferases. The first enzymatic step in mercapturic acid formation. J. Biol. Chem. **249**: 7130–7139.

Hellou, J., and Payne, J.F. 1987. Assessment of contamination of fish by water-soluble fractions of petroleum: a role for bile metabolites. Environ. Toxicol. Chem. **6**: 857–862.

Holdway, D.A. 1996. The role of biomarkers in risk assessment. Hum. Ecol. Risk Assess. **2**: 263–267.

Holdway, D.A. 1997. Truth and validation in ecological risk assessment. Environ. Manage. **21**: 816–819.

Jardine, J.J., Van Der Kraak, G.J., and Munkittrick, K.R. 1996. Capture and confinement stress in white sucker exposed to bleached kraft pulp mill effluent. Ecotoxicol. Environ. Saf. **33**: 287–298.

Johnson, L.L., Casillas, E., Collier, T.K., McCain, B.B., and Varanasi, U. 1988. Contaminant effects on ovarian development in English sole (*Parophrys vetulus*) from Puget Sound, Washington. Can. J. Fish. Aquat. Sci. **45**: 2133–2146.

Kennedy, S.W., and Jones, S.P. 1994. Simultaneous measurement of cytochrome P4501A catalytic activity and total protein concentration with a fluorescence plate reader. Anal. Biochem. **222**: 217–233.

Krahn, M.M., Myers, M.S., Burrows, D.G., and Malins, D.C. 1984. Determination of metabolites of xenobiotics in the bile of fish from polluted waterways. Xenobiotica, **14**: 633–646.

Lorenzen, A., and Kennedy, S.W. 1993. A fluorescence-based protein assay for use with a microplate reader. Anal. Biochem. **214**: 346–348.

McCarty, L.S., and Munkittrick, K.R. 1996. Environmental biomarkers in aquatic toxicology: fiction, fantasy, or functional. Hum. Ecol. Risk Assess. **2**: 268–274.

McMaster, M.E., Munkittrick, K.R., and Van Der Kraak, G.J. 1992. Protocol for measuring circulating levels of gonadal sex steroids in fish. Can. Tech. Rep. Fish. Aquat. Sci. No. 1836.

McMaster, M.E., Van Der Kraak, G.J., and Munkittrick, K.R. 1996. An epidemiological evaluation of the biochemical basis for steroid hormonal depressions in fish exposed to industrial wastes. J. Gt. Lakes Res. **22**: 153–171.

Munkittrick, K.R., Portt, C.B., Van Der Kraak, G.J., Smith, I.R., and Rokosh, D.A. 1991. Impact of bleached kraft mill effluent on population characteristics, liver MFO activity, and serum steroid levels of a Lake Superior white sucker (*Catostomus commersoni*) population. Can. J. Fish. Aquat. Sci. **48**: 1371–1380.

National Research Council of Canada. 1985. The role of biochemical indicators in the assessment of ecosystem health — their development and validation. NRCC 24371. National Research Council of Canada, Ottawa, Ont.

Payne, J.F., Fancey, L.L., Rahimtula, A.D., and Porter, E.L. 1987. Review and perspective on the use of mixed-function oxygenase enzymes in biological monitoring. Comp. Biochem. Physiol. C, Comp. Pharmacol. **86**: 233–245.

Scott, A.P., and Sumpter, J.P. 1983. A comparison of the female reproductive cycles of autumn-spawning and winter-spawning strains of rainbow trout (*Salmo gairdneri* Richardson). Gen. Comp. Endocrinol. **52**: 79–85.

Stegeman, J.J., and Hahn, M.E. 1995. Biochemistry and molecular biology of monooxygenases: current perspectives on forms, functions, and regulation of cytochrome P450 in aquatic species. *In* Aquatic toxicology: molecular, biochemical, and cellular perspectives. *Edited by* D.C. Malins and G.K. Ostrander. CRC Press, New York. pp. 87–206.

Stein, J.E., Hom, T., Sanborn, H.R., and Varanasi, U. 1991. Effects of exposure to a contaminated-sediment extract on the metabolism and disposition of 17β-estradiol in English sole (*Parophrys vetulus*). Comp. Biochem. Physiol. C, Comp. Pharmacol. **99**: 231–240.

Thomas, P., 1988. Reproductive endocrine function of female Atlantic croaker exposed to pollutants. Mar. Environ. Res. **24**: 179–183.

Truscott, B., Walsh, J.M., Burton, M.P., Payne, J.F., and Idler, D.R. 1983. Effect of acute exposure to crude petroleum on some reproductive hormones in salmon and flounder. Comp. Biochem. Physiol. C, Comp. Pharmacol. **75**: 121–130.

Truscott, B., Idler, D.R., and Fletcher, G.L. 1992. Alteration of reproductive steroids of male winter flounder (*Pleuronectes americanus*) chronically exposed to low levels of crude oil in sediments. Can. J. Fish. Aquat. Sci. **49**: 2190–2195.

van den Heuvel, M.R., Power, M., MacKinnon, M.D., Van Meer, T., Dobson, E.P., and Dixon, D.G. 1999. Effects of oil sands related aquatic reclamation on yellow perch (*Perca flavescens*). I. Water quality characteristics and yellow perch physiological and population responses. Can. J. Fish. Aquat. Sci. **56**. This issue.

Van Der Kraak, G.J., Munkittrick, K.R., McMaster, M.E., Portt, C.B., and Chang, J.P. 1992. Exposure to bleached kraft pulp mill effluent disrupts the pituitary–gonadal axis of white sucker at multiple sites. Toxicol. Appl. Pharmacol. **115**: 224–233.

Wilkinson, L. 1990. SYSTAT: the system for statistics. SYSTAT Inc., Evanston, Ill.

© 1999 NRC Canada

Use of simulation–extrapolation estimation in catch–effort analyses

W.R. Gould, L.A. Stefanski, and K.H. Pollock

Abstract: All catch–effort estimation methods implicitly assume catch and effort are known quantities, whereas in many cases, they have been estimated and are subject to error. We evaluate the application of a simulation-based estimation procedure for measurement error models (J.R. Cook and L.A. Stefanski. 1994. J. Am. Stat. Assoc. 89: 1314–1328) in catch–effort studies. The technique involves a simulation component and an extrapolation step, hence the name SIMEX estimation. We describe SIMEX estimation in general terms and illustrate its use with applications to real and simulated catch and effort data. Correcting for measurement error with SIMEX estimation resulted in population size and catchability coefficient estimates that were substantially less than naive estimates, which ignored measurement errors in some cases. In a simulation of the procedure, we compared estimators from SIMEX with "naive" estimators that ignore measurement errors in catch and effort to determine the ability of SIMEX to produce bias-corrected estimates. The SIMEX estimators were less biased than the naive estimators but in some cases were also more variable. Despite the bias reduction, the SIMEX estimator had a larger mean squared error than the naive estimator for one of two artificial populations studied. However, our results suggest the SIMEX estimator may outperform the naive estimator in terms of bias and precision for larger populations.

Résumé : Dans toutes les méthodes d'estimation utilisant les captures et l'effort de pêche, on considère implicitement que les captures et l'effort sont des quantités connues, alors que dans bien des cas, ces valeurs ont été estimées et comportent une part d'erreur. Nous évaluons l'application, dans les études utilisant les captures et l'effort de pêche, d'une procédure d'estimation fondée sur une simulation pour les modèles d'erreur de mesure (J.R. Cook and L.A. Stefanski. 1994. J. Am. Stat. Assoc. 89: 1314–1328). Cette procédure implique une simulation et une étape d'extrapolation, d'où l'appellation d'estimation SIMEX. Nous décrivons l'estimation SIMEX en termes généraux et illustrons son utilisation par des applications à des données réelles et simulées de captures et d'effort. Avec la correction de l'erreur de mesure par l'estimation SIMEX, on a obtenu des estimations de la taille des populations et du coefficient de capturabilité qui étaient substantiellement inférieures aux estimations « naives » dans lesquelles on a ignoré les erreurs de mesure dans certains cas. Dans une simulation de la procédure, nous avons comparé les estimateurs SIMEX aux estimateurs naïfs qui ignorent les erreurs de mesure des captures et de l'effort pour déterminer la capacité de la procédure SIMEX de produire des estimations à biais corrigé. Les estimateurs SIMEX étaient moins biaisés que les estimateurs naïfs, mais ils étaient aussi dans certains cas plus variables. Malgré la réduction du biais, l'estimateur SIMEX comportait une erreur quadratique moyenne supérieure à celle de l'estimateur naïf pour l'une des deux populations artificielles étudiées. Cependant, nos résultats laissent penser que l'estimateur SIMEX peut donner de meilleurs résultats que l'estimateur naïf en ce qui concerne le biais et la précision pour les grandes populations.

[Traduit par la Rédaction]

Introduction

Catch–effort methods for estimating important demographic parameters naturally lend themselves to populations that are exploited by persons for economic or recreational purposes. The more traditional catch–effort regression models (Leslie and Davis 1939; DeLury 1947) have seen substantial use in commercial fisheries because of their ease of use and intuitive approach to estimation (Fischler 1965; Ralston and Tagami 1992). More recently, catch–effort maximum likelihood (ML) estimation (Seber 1982; Dupont 1983; Gould and Pollock 1997) has become a more feasible means of estimation with the advent of powerful computers.

All catch–effort estimation methods implicitly assume catch and effort are known quantities, a reasonable assumption in some situations, but not likely to be true for many large-scale commercial fisheries or animal populations that are annually hunted. Even in smaller freshwater fisheries, it is often unreasonable to census the entire population of fishermen because of limited resources (time, personnel, etc.). As a result, catch and effort are often estimated by on-site surveys (port or creel surveys) in which samples are taken from the population to estimate total catch and effort (Guthrie et al. 1991; Pollock et al. 1994; Hoenig et al. 1997). Off-site surveys (telephone, mail, etc.) are sometimes made in an attempt to completely census a population, but

Received July 15, 1998. Accepted February 26, 1999.
J14692

W.R. Gould.[1] University Statistics Center, Department of Economics and International Business, New Mexico State University, Las Cruces, NM 88003, U.S.A.
L.A. Stefanski and K.H. Pollock. Department of Statistics, North Carolina State University, Raleigh, NC 27695, U.S.A.

[1]Author to whom all correspondence should be addressed.
e-mail: wgould@nmsu.edu

© 1999 NRC Canada

these surveys can take place some time after removals have been made and usually provide less reliable data than on-site surveys.

Gould et al. (1997) studied effects of measurement error on catch–effort estimation by examining the magnitude and direction of bias in population size and catchability coefficient estimates as a function of measurement error variance. On average, measurement error in catch and effort caused population size estimates to be biased upwardly by as much as 20% or more in some cases. Except for DeLury's method, measurement error also positively biased the catchability coefficient estimates, although to a lesser extent than population size estimates. Because a conservative approach to management is necessary to ensure continued existence of a population for economic and aesthetic reasons, a positive bias in population size estimates is perhaps a more "serious" error than a negative bias. In either case, the need for bias correction is evident so that management decisions can be based on accurate information rather than misinformation.

Quenouille (1956) introduced the jackknife as a nonparametric estimate of bias which resulted in bias-corrected parameter estimates. The technique involves removal of one observation from the data, a recomputation of the parameter estimate in absence of the observation, repeated for all possible sets of data missing one observation. The average of parameter estimates is then used to estimate bias, which is subtracted from the original parameter estimate based on all observations to obtain a less-biased estimate. More recently, a simulation-based estimation procedure known as SIMEX, for simulation–extrapolation, has been developed for measurement error models (Cook and Stefanski 1994; Carroll et al. 1995) in which the measurement error variance is known or at least well estimated. Random sampling designs used in creel surveys or port samples of commercial fisheries will provide an estimate of measurement error variance, making the SIMEX procedure an attractive estimation method for catch–effort analyses with measurement error. The SIMEX method has been shown to produce less-biased parameter estimates in a variety of problems (Cook and Stefanski 1994) and has a strong connection to jackknife estimation (Stefanski and Cook 1995).

This article describes the SIMEX estimation method in general terms and presents an application of the method to catch–effort analysis where both catch and effort are estimated quantities (contain measurement error). We hope that the relative ease with which SIMEX is executed will encourage biologists to consider its use in correcting for biases in catch–effort estimates resulting from measurement error. For simplicity, we have chosen to examine a closed population, i.e., one in which there are no births or deaths or movement of any kind; however, the general technique is applicable to open populations as well. We present examples with real data to illustrate the SIMEX procedure, in the process describing the effects of measurement error on estimation, resulting in production of less-biased estimates of population size and catchability. Finally, we evaluate the performance of SIMEX estimation by examining simulation results from 500 generated data sets in which we compared the SIMEX estimate to the naive estimate obtained when errors in catch and effort are ignored.

Simulation–extrapolation estimation

Basically, the simulation–extrapolation procedure (SIMEX) consists of four main steps: (1) additional measurement error is added in known increments to the observed data; (2) for each increment of added measurement error, parameter estimates are computed from the further-contaminated data; (3) a trend is established between the parameter estimate and the added measurement error; and (4) the trend is extrapolated back to the case without measurement error. In the same sense as the bootstrap is a 'resampling' method, SIMEX can be considered a 'remeasurement' method. To describe the SIMEX method in a more detailed fashion, we define the following terms: Y_i = the response variable; V_i = a covariate measured without error; U_i = the true predictor; and X_i = the measured predictor, such that $X_i = U_i + \sigma Z_i$ ($i = 1,...,s$), where $Z_i \sim N(0,1)$, independent of U_i, V_i, and Y_i, and σ^2 is the known measurement error variance.

Estimators $\hat{\theta}_{\text{true}}$ and $\hat{\theta}_{\text{naive}}$ depend on $T\{Y_i, V_i, U_i\}_{i=1}^{s}$ and $T\{Y_i, V_i, X_i\}_{i=1}^{s}$, respectively. The simulation part of the SIMEX method occurs with steps 1 and 2. For $\lambda \geq 0$, measurement error is added to the observed (contaminated) data as

$$X_{b,i}(\lambda) = X_i + \lambda^{1/2}\sigma Z_{b,i},$$

$$Z_{b,i} \sim N(0,1),\ b = 1,...,B,\ i = 1,...,s$$

where λ is an adjusting constant for the magnitude of measurement error variance. The parameter estimate with the additionally contaminated data $\hat{\theta}_b(\lambda)$ then depends on $T\{Y_i, V_i, X_{b,i}(\lambda)\}_{i=1}^{s}$. To avoid dependence of the estimate on the specific random number generated, $Z_{b,i}$, the process is repeated over a sufficiently large number of repetitions, B, and parameter estimates are averaged to obtain

$$(1) \qquad \hat{\theta}(\lambda) = \frac{1}{B}\sum_{b=1}^{B} \hat{\theta}_b(\lambda)$$

When $\lambda = 0$, $\hat{\theta}_b(\lambda) = \hat{\theta}_{\text{naive}}$.

Plotting the trend between parameter estimates, $\hat{\theta}(\lambda)$, and the magnitude of added measurement error variance (λ) is informative in its own right in that it presents a graphical description of effects of measurement error on parameter estimation. It is well known that for simple linear regression models, measurement error has the effect of attenuating or flattening the slope of the regression line (Fuller 1987). However, for more complicated models, effects of measurement error are not easily understood. We present Leslie's method (Leslie and Davis 1939) of catch–effort estimation in the next section where it will become obvious why the effect of measurement error on this regression method is not self-evident. An analysis of measurement error effects with the simulation component of the SIMEX method will have implications as to whether bias correction is worthwhile and also will give an indication of the direction of bias.

The extrapolation component of the process is necessary for producing bias-corrected parameter estimates. Using a model that best describes the relationship between $\hat{\theta}(\lambda)$ and λ ($\lambda \geq 0$) and extrapolating back to $\lambda = -1.0$ yields the SIMEX estimator, $\hat{\theta}_{\text{SIMEX}}$. Stefanski and Cook (1995) show for suffi-

© 1999 NRC Canada

ciently smooth functions (Stefanski 1989), if the true extrapolant is used, the SIMEX estimator is unbiased. A rather simplistic justification for $\lambda = -1$ as the point at which measurement error is absent can be seen by examining the contaminated data:

$$X_{b,i}(\lambda) = X_i + (\lambda)^{1/2}\sigma Z_{b,i} = U_i + \sigma Z_i + (\lambda)^{1/2}\sigma Z_{b,i}.$$

The total error has variance $\sigma^2(1.0 + \lambda)$; thus at $\lambda = -1.0$, the measurement error variance is zero. The extrapolation component of the method basically assumes the relationship between the observed data and observed data contaminated with additional measurement error is the same as the relationship between the true data and observed data regarding parameter estimation. The graphical nature of the simulation component is instrumental in determining the type of extrapolant to be used. Cook and Stefanski (1994) present a discussion on the order-of-magnitude of asymptotic bias in the SIMEX estimator for different extrapolants and give examples where $\hat{\theta}_{SIMEX}$ is shown to be an unbiased and consistent estimator of θ.

Leslie's regression method

The catch–effort regression method proposed by Leslie and Davis (1939) regresses catch per unit effort (CPUE; u_i/v_i) against prior cumulative catch to estimate the catchability coefficient, k, and original population size, N. Leslie's method approximates the conditional binomial relationship between catch and prior cumulative catch with a linear model

$$u_i/v_i = \alpha + \beta \sum_{j=1}^{i-1} u_j + \varepsilon_i,$$

where $\alpha = kN$, $\beta = -k$, and the error terms, ε_i, are typically assumed to be normally distributed with mean zero and constant variance. The error terms represent random variation of catch per unit effort (CPUE) around its mean as well as approximation error (resulting from approximating the mean response by a linear function). When catch and effort are estimated, measurement errors further complicate the regression model. Two reasonable models for describing the nature of measurement errors in the estimated catch (n_i) and effort (f_i) are (*i*) an additive unbiased measurement error model $n_i = u_i + \delta_i$ and $f_i = v_i + \gamma_i$ and (*ii*) an additive unbiased measurement error model on the log scale.

These models contain two sources of measurement error in the response variable (CPUE). In addition, measurement error is cumulative in the explanatory variable. Clearly, errors in the regression variables are more complex than in simple regression examples presented in the statistical literature and thus, effects of measurement error on Leslie's method are not intuitively apparent. Similarly, effects of measurement error on catch–effort maximum likelihood estimation (Seber 1982; Dupont 1983) are not readily apparent either, but the smooth functions of bias demonstrated in Gould et al. (1997) suggested that SIMEX estimation may be a reasonable means of producing bias-corrected estimates given knowledge or good estimates of the measurement error variance.

Application of SIMEX estimation

We used real and simulated data sets to illustrate the SIMEX method and to evaluate its ability to produce bias-corrected estimates. Because no estimate of measurement error variance was available for the real data, we assumed estimates of the measurement error variance for demonstration purposes. For the simulated data, we first generated true unknown catches based on initial values of population size and effort. True catch and effort were then contaminated with known levels of measurement error and assumed the role of "observed" estimates of catch and effort collected in on-site surveys. Measurement error was then added to the observed catch and effort in a systematic manner. Parameter estimates of population size and catchability were computed with the further-contaminated data via maximum likelihood using program SURVIV (White 1983, 1986) and least squares estimation of Leslie's method using SAS (SAS Institute 1988). A relationship between the measurement error variance and parameter estimates was made and an appropriate extrapolant was used to compute the SIMEX estimator.

Catch–effort methods provide reasonable parameter estimates only when the population has been reduced enough to observe a significant decline in CPUE. In our simulations, the catchability coefficient, $k = 0.05$, and the sequence of efforts expended in removing individuals (v_i = 7.133, 8.133, 7.133, 6.133, 7.133; i = 1,...,5) were chosen to ensure a substantial depletion of the population (83% cumulative removal), thereby better isolating effects of measurement error on estimation. The sequence of efforts was originally intended to mimic hours spent electrofishing, but the units are arbitrary and could also represent hundreds of angler-hours or thousands of traps hauled in a commercial fishery. The capture probability at a given sample ($p_i = 1 - e^{-kf_i}$) ranged from 0.26 to 0.33. True catches (u_i) were generated as a sequence of conditional binomials:

$$g(u_i | \sum_{j=1}^{i-1} u_j) = \begin{pmatrix} N - \sum_{j=1}^{i-1} u_j \\ u_i \end{pmatrix} p_i^{u_i} (1 - p_i)^{N - \sum_{j=1}^{i-1} u_j}.$$

Uniform random numbers were generated for each individual remaining in the population and compared with the capture probability for that sampling period to determine capture or noncapture of an individual. Captures were then summed over each sampling period and resulted in the true unobserved catches, u_i. Given the unobserved catches, observed catches (n_i) were generated in a lognormal fashion,

$$n_i | u_i \sim \text{lognormal}(u_i, C\sigma^2_{u_i}),$$

where

$$n_i = e^{a + bZ_i}; \quad b = \left[\ln\left(\frac{C}{u_i} + 1 \right) \right]^{1/2},$$

$$a = \ln(u_i) - \frac{b^2}{2}, \quad Z_i \sim N(0,1),$$

© 1999 NRC Canada

Fig. 1. The SIMEX estimate ($\lambda = -1$) and naive estimate ($\lambda = 0$) for the population size (N) and catchability (k) of commercial-sized male blue crabs (Fischler 1965) using maximum likelihood (ML; ◆) and Leslie's regression method (■) for Poisson-like measurement error variance ($C = 1.0$).

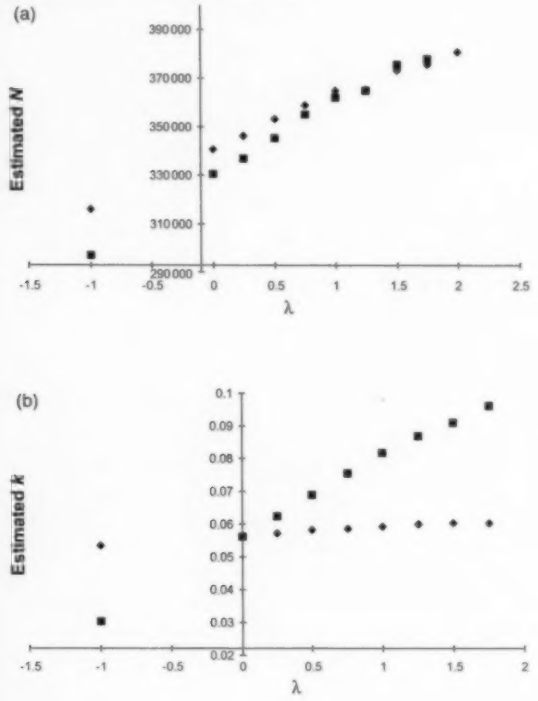

and C is a constant. In this way, the measurement error is unbiased with mean zero and variance that is dependent on variance of the true unknown catch. Ideally, choice of the measurement error model would be made with the aid of validation data or replicates to estimate the error distribution. In the absence of such information, the lognormal distribution provides a reasonable error model, especially for a theoretical description of the method. The lognormal distribution is commonly used to model variables with positively skewed distributions, e.g., counts (see Casella and Berger 1990, p. 110, for further description). In a similar manner, given the unobserved effort, v_i, observed effort, f_i, is

$$f_i | v_i \sim \text{lognormal}(v_i, C\sigma_{v_i}^2).$$

Setting $C = 1.0$ will result in Poisson-like variances, i.e., variance proportional to the respective mean, a reasonable condition for our investigation.

Having generated a sequence of catches and efforts that represent estimates of total catch and effort from on-site surveys, SIMEX estimation calls for adding additional measurement error in known amounts to the contaminated data and computing estimates of population size and catchability based on the further-contaminated data. Measurement error was added to the observed catch and effort in a manner similar to that in which observed values were generated from the true data. Catch and effort were generated conditional on the observed catch and effort respectively as

$$n_{b,i}(\lambda) | n_i \sim \text{lognormal}(n_i, C\lambda n_i)$$

and

$$f_{b,i}(\lambda) | f_i \sim \text{lognormal}(f_i, C\lambda f_i).$$

With $C = 1.0$,

$$(2) \qquad n_{b,i}(\lambda) = e^{a_\lambda + b_\lambda Z_{b,i}}, \quad b_\lambda = \left[\ln\left(\frac{\lambda}{n_i} + 1\right)\right]^{1/2},$$

$$a_\lambda = \ln(n_i) - (b_\lambda^2 / 2)$$

and

$$f_{b,i}(\lambda) = e^{a_\lambda + b_\lambda Z_{b,i}}, \quad b_\lambda = \left[\ln\left(\frac{\lambda}{f_i} + 1\right)\right]^{1/2},$$

$$a_\lambda = \ln(f_i) - (b_\lambda^2 / 2).$$

Effects of the magnitude of measurement error variance were demonstrated by systematically changing the value of the multiplying constant λ over a discrete, uniformly spaced range of values ($\lambda = 0.0$–2.0). For each value of λ, 2000 replications ($b = 1,\ldots,2000$) were performed to prevent the results from being dependent on any particular random number, $Z_{b,i}$. Each repetition of the simulation produced an estimate of the catchability coefficient and population size via maximum likelihood and Leslie's method. Parameter estimates were averaged over the repetitions after omitting extreme outliers (estimates below zero and greater than 500% of the true parameter value) and plotted against λ. Based on the work in Gould et al. (1997), we proposed to fit a linear extrapolant to the points for computation of the SIMEX estimators at $\lambda = -1.0$. Simulated data allowed us to compare the SIMEX estimator ($\lambda = -1.0$) to the naive estimator ($\lambda = 0$) to determine which estimates were closer to the true parameter values. All computer programs used are available from the senior author on request.

Example

Catch and effort data were taken from Fischler (1965) on a commercial-sized male blue crab (*Callinectes sapidus*) fishery. We estimated population size and the catchability coefficient via maximum likelihood estimation and Leslie's method ignoring measurement error and for various levels of additional measurement error, as determined by λ and the constant C. We present two scenarios for Fischler's data. Setting $C = 1.0$, we assumed a Poisson-like measurement error variance. Setting $C = 2.0$, we assumed measurement error variance larger than the mean. Although λ ranged from 0 to 2, we fit a simple linear model to population size estimates for values of λ between 0 and 1 and extrapolated back to $\lambda = -1.0$ to produce the SIMEX estimate of population size (Figs. 1 and 2). The SIMEX estimates of population size based on maximum likelihood estimation and Leslie's method were 7–10% lower than the naive estimates from the respective estimation methods (Fig. 1). The SIMEX estimates of the catchability coefficient were 5–46% lower than the naive estimate using maximum likelihood and Leslie's method, respectively. When the assumed measurement error

© 1999 NRC Canada

Fig. 2. The SIMEX estimate ($\lambda = -1$) and naive estimate ($\lambda = 0$) for the population size (N) and catchability (k) of commercial-sized male blue crabs (Fischler 1965) using maximum likelihood (ML; ◆) and Leslie's regression method (■) with measurement error variance greater than the mean ($C = 2.0$).

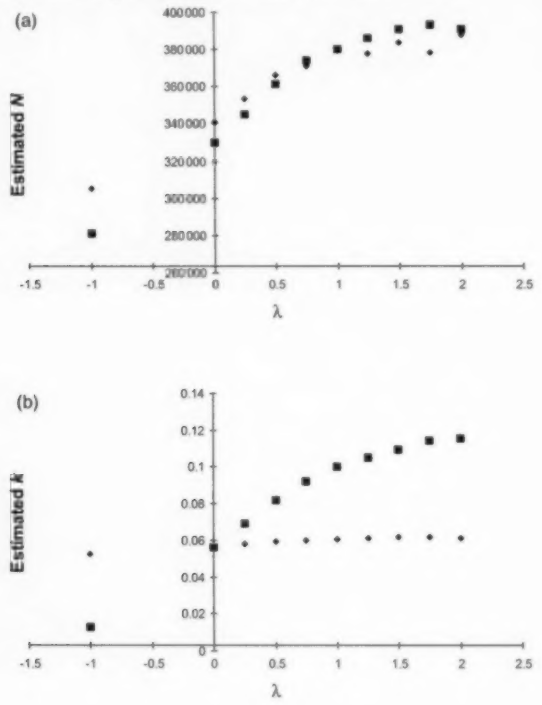

variance was greater ($C = 2.0$), the differences in the SIMEX estimates and naive estimates were greater (10–16% less for N, 7–78% for k) using maximum likelihood and Leslie's method, respectively (Fig. 2).

Simulation of SIMEX

We devised a simulation study to evaluate the performance of the SIMEX estimator for 500 independent data sets. We made time concessions by dropping the maximum likelihood approach from our analysis and computed parameter estimates only for Leslie's regression approach. We present results for observed data generated with Poisson-like variances ($C = 1.0$). For each of three levels of λ ($\lambda = 0.0$, 0.5, 1.0), we contaminated the observed catch and effort data as described in eq. 2, using $B = 500$ replications. The SIMEX estimator was determined by fitting a linear model to the estimates over the values of λ ($\lambda = 0.0$, 0.5, 1.0) with PROC REG in SAS (1988) and extrapolating back to $\lambda = -1.0$. Population size was computed for two artificial population sizes, $N = 10\,000$ and $N = 100\,000$, which might represent fisheries in sections of rivers or reservoirs.

Simulation results

Extreme outliers, values below 0 or over 500% larger than the true parameter, were excluded from our results to allow a better evaluation of general estimator performance because many measures used to evaluate estimator performance are not robust to outliers. We suspect that a biologist familiar with the population would likely throw out such estimates as reasonable values as well. However, we did record the failure rate (percentage of outliers) as another measure of estimator performance. The SIMEX population size estimator was less biased than the Leslie-based naive estimator for the smaller population ($N = 10\,000$); however, associated with the decrease in bias was an increase in estimated variance (Table 1*a*). This result is reflected in the larger mean square error of the SIMEX estimator and in another criterion we used for comparing estimators, known as Pitman's measure of closeness (Mood et al. 1974). Pitman's closeness measures the frequency with which one estimator is closer in absolute value to the true parameter than another estimator. The SIMEX estimator was closer in absolute value to the true population size than the naive estimator in 35% of the cases, indicating the naive estimator was more often closer (in absolute value) to the true parameter value than the SIMEX estimator, despite the SIMEX estimator being less biased.

Table 1. Distributional summary of population size (N) estimates, including measures of bias and precision, from the naive approach and SIMEX estimation excluding outliers (B_* repetitions).

(a) $N = 10\,000$	Naive ($B_* = 473$)	SIMEX ($B_* = 465$)
Mean	11147.3	9986.7
% relative bias	+11.5	−0.1
Standard deviation	4780.3	5165.0
Mean squared error	2.417×10^7	2.668×10^7
Pitman's measure of closeness (Mood et al. 1974)	64.5%	35.5%
(b) $N = 100\,000$	**Naive ($B_* = 475$)**	**SIMEX ($B_* = 464$)**
Mean	112210.1	98622.4
% relative bias	+11.2	−1.4
Standard deviation	52959.9	47450.3
Mean squared error	2.954×10^9	2.253×10^9
Pitman's measure of closeness (Mood et al. 1974)	65.6%	34.4%

For the larger population ($N = 100\,000$), the SIMEX estimator reduced bias and also was more precise than the naive estimator (Table 1*b*). However, it should be noted that the SIMEX estimator had more extreme values (36) than the naive approach (25). In 34% of the cases, the SIMEX estimator was closer (in absolute value) than the naive estimator to the true population size using Leslie's method, meaning that the naive estimator was closer to the true parameter in 66% of the cases.

Kernel density estimates (Silverman 1986) of population sizes from the SIMEX estimator and naive estimator (Figs. 3 and 4) were computed using S-PLUS (Statistical Sciences 1988). A normal kernel was used with a common bandwidth of $h = 1.06\,\sigma B_*^{-1/5}$ for all estimators in the study, where B_* is the number of repetitions excluding extreme observations. Although we have not attempted to make detailed contrasts between the two estimators, it is important to note the con-

© 1999 NRC Canada

Fig. 3. Kernel density estimates of population size (N = 10 000; B = 500 replications) from the SIMEX estimator and naive estimator represented by the solid and dotted lines, respectively.

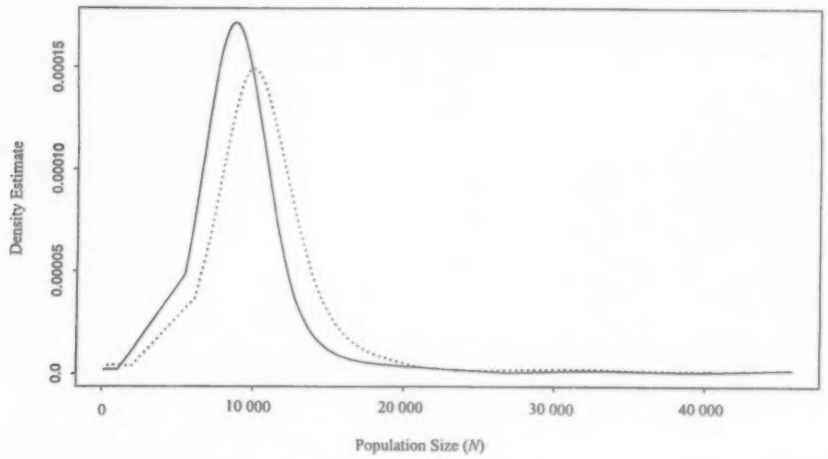

Fig. 4. Kernel density estimates of population size (N = 100 000; B = 500 replications) from the SIMEX estimator and naive estimator represented by the solid and dotted lines, respectively.

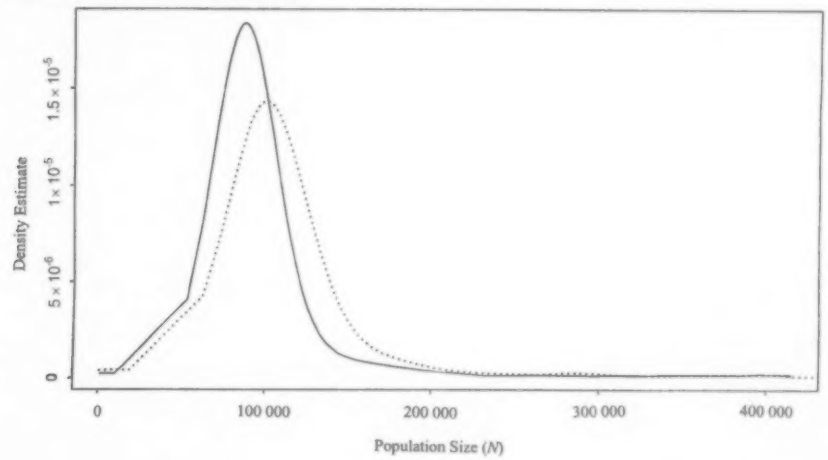

servativeness of the SIMEX estimator, which may be better from a management perspective.

Discussion

By sampling from a commercial or recreational fishery, it may be possible to provide managers with enough information to evaluate the status of some aspects of the fishery. Sampling reduces the expenses that would be involved in executing a census; however, costs of sampling can still be large in these systems. In justifying expenditures of such resources (time, personnel, etc.), it is important to consider the quality of collected data and its usefulness in demographic parameter estimation. Catch–effort estimation of population parameters using estimated quantities of catch and effort can be severely biased, depending on the magnitude of measurement error in catch and effort. SIMEX estimation readily lends itself as a possible bias correction technique in which an estimate of measurement error variance from an on-site survey is available. Even without measurement error, catch–effort methods may fail to produce reasonable estimates unless a perceptible decline in CPUE is observed. However, such a declination will usually result if the population is substantially depleted.

Our example illustrated the potential differences of SIMEX estimation over naive estimation. Differences between the SIMEX and naive estimates of population size were not large but became greater as measurement error variance increased. SIMEX estimation may be particularly useful in situations with large measurement error variances. Maximum likelihood estimation appeared more robust to measurement error than Leslie's method in the sense that differences between SIMEX and naive estimates were smallest using maximum likelihood estimation. Estimates of catchability from Leslie's method were particularly sensitive to measurement error. Using simulated data, Gould et al.

© 1999 NRC Canada

(1997) also demonstrated the greater sensitivity of Leslie's estimates to measurement error.

Simulations allowed us the luxury of knowing the true values of the parameters, which are not known when considering real data contaminated with measurement error. Having produced 500 estimates from the SIMEX estimator and the naive estimator, we were able to assess in some sense which estimator is better than the other. Our simulations showed that the SIMEX estimator reduced the bias from the naive estimator, but sometimes at the cost of lesser precision. When the gains in bias reduction are outweighed by losses in precision, as identified for the smaller population, the SIMEX estimator is not worth computing from a mean squared error perspective. Bias–variance tradeoffs are characteristic of measurement error problems, but there is value in identifying the "equilibrium point" so that informed decisions can be made about when measurement error correction is worthwhile. Our results for the larger population indicate that in some circumstances, the SIMEX estimator may be superior to the naive estimator with regard to mean squared error, etc. In particular, we believe the advantages to bias adjustment will be greater for larger populations and (or) larger sample sizes because precision increases under these conditions (e.g., see Gould and Pollock 1997). Further investigation using SIMEX with larger samples and a maximum likelihood approach may determine whether SIMEX estimation is of limited benefit or if estimation with measurement error is inherently difficult in catch–effort studies.

References

Carroll, R.J., Ruppert, D., and Stefanski, L.A. 1995. Measurement error in nonlinear models. Chapman and Hall, London, U.K.

Casella, G., and Berger, R.L. 1990. Statistical inference. Wadsworth & Brooks Cole, Pacific Grove, Calif.

Cook, J.R., and Stefanski, L.A. 1994. Simulation–extrapolation estimation in parametric measurement error models. J. Am. Stat. Assoc. **89**: 1314–1328.

DeLury, D.B. 1947. On the estimation of biological populations. Biometrics, **3**: 145–167.

Dupont, W.D. 1983. A stochastic catch–effort method for estimating animal abundance. Biometrics, **39**: 1021–1033.

Fischler, K.J. 1965. The use of catch–effort, catch sampling, and tagging data to estimate a population of blue crabs. Trans. Am. Fish. Soc. **94**: 287–310.

Fuller, W.A. 1987. Measurement error models. Wiley, New York.

Gould, W.R., and Pollock, K.H. 1997. Catch–effort maximum likelihood estimation of population parameters. Can. J. Fish. Aquat. Sci. **54**: 890–897.

Gould, W.R., Stefanski, L.A., and Pollock, K.H. 1997. The effects of measurement error on catch–effort estimation. Can. J. Fish. Aquat. Sci. **54**: 898–906.

Guthrie, D., Hoenig, J.M., Holliday, M., Jones, C.M., Mills, M.J., Moberley, S.A., Pollock, K.H., and Talhelm, D.R. (*Editors*). 1991. Creel and angler surveys in fisheries management. Am. Fish. Soc. Symp. No. 12, Bethesda, Md.

Hoenig, J.M., Jones, C.M., Pollock, K.H., Robson, D.S., and Wade, D.L. 1997. Calculation of catch rate and total catch in roving surveys of anglers. Biometrics, **53**: 306–317.

Leslie, P.H., and Davis, D.H.S. 1939. An attempt to determine the absolute number of rats on a given area. J. Anim. Ecol. **8**: 94–113.

Mood, A.M., Graybill, F.A., and Boes, D.C. 1974. Introduction to the theory of statistics. 3rd ed. MacGraw-Hill, Tokyo.

Pollock, K.H., Jones, C.M., and Brown, T.L. 1994. Angler surveys and their application to fisheries management. American Fisheries Society, Bethesda, Md.

Quenouille, M. 1956. Notes on bias and estimation. Biometrika, **43**: 353–360.

Ralston, S., and Tagami, D.T. 1992. An assessment of the exploitable biomass of *Heterocarpus laevigatus* in the main Hawaiian Islands. Part 1: trapping surveys, depletion experiment and length structure. Fish. Bull. (U.S.), **90**: 494–504.

SAS Institute Inc. 1988. SAS/STAT users guide, version 6.03, SAS Institute Inc., Cary, N.C.

Seber, G.A.F. 1982. The estimation of animal abundance and related parameters. Macmillan, New York.

Silverman, B.W. 1986. Density estimation for statistics and data analysis. Chapman and Hall, New York.

Statistical Sciences. 1988. S-PLUS guide to statistical and mathematical analysis. MathSoft, Inc., Seattle, Wash.

Stefanski, L.A. 1989. Unbiased estimation of a nonlinear function of a normal mean with application to measurement error models. Comm. Stat. Theory Meth. **18**: 4335–4358.

Stefanski, L.A., and Cook, J.R. 1995. Simulation extrapolation: the measurement error jackknife. J. Am. Stat. Assoc. **90**: 1247–1256.

White, G.C. 1983. Numerical estimation of survival rates from band-recovery and biotelemetry data. J. Wildl. Manage. **47**: 716–728.

White, G.C. 1986. Program SURVIV user's manual. Version 1.2. Environmental Science Group, Los Alamos, N.Mex.

© 1999 NRC Canada

Resource partitioning along three niche dimensions in a size-structured tropical fish assemblage

G.J. Piet, J.S. Pet, W.A.H.P. Guruge, J. Vijverberg, and W.L.T. Van Densen

Abstract: In Tissawewa, a tropical reservoir, the size-specific resource use of the 10 most important fish species was determined along three dimensions: trophic, spatial, and temporal. During this study, a drought occurred distinguishing two periods before and after the drought that differed markedly in availability of resources and fish biomass. In this study, differences in resource use between the two periods are presented together with their consequence on the partitioning of resources. A different approach is introduced into the calculation of niche breadth and niche overlap incorporating size-specific differences in resource use and interactions between resource dimensions. Comparison with conventional measures of niche breadth and niche overlap shows that conventional measures often misrepresent interactions between species. Condition and biomass were used as indicators of a species' fitness, and it is shown that fitness of most species is governed by the availability of resources and partitioning of these resources is an important mechanism allowing potential competitors to coexist. Resource partitioning along the trophic dimension was more important than along the spatial or temporal dimension.

Résumé : Dans le réservoir tropical Tissawena, on a déterminé l'utilisation des ressources selon la taille par les dix plus importantes espèces de poisson suivant trois dimensions, soit les dimensions trophique, spatiale et temporelle. Une sécheresse a sévi durant cette étude, de sorte que les périodes d'avant et d'après la sécheresse ont montré des différences marquées quant à la disponibilité des ressources et à la biomasse des poissons. Dans cette étude, on présente les différences dans l'utilisation des ressources entre les deux périodes ainsi que leur conséquence sur la répartition des ressources. On présente aussi une approche différente en ce qui concerne le calcul de l'étendue et du chevauchement des niches qui prend en considération des différences liées à la taille dans l'utilisation des ressources et les interactions entre les dimensions des ressources. La comparaison avec les mesures classiques de l'étendue et du chevauchement des niches montre que ces mesures ne reflètent souvent pas correctement les interactions entre espèces. On a utilisé l'indice de condition et la biomasse comme indicateurs de la valeur adaptative des espèces, et on a montré que la valeur adaptative de la plupart des espèces est fonction de la disponibilité des ressources; en outre, la répartition de ces ressources est un mécanisme important qui permet aux compétiteurs potentiels de coexister. La répartition des ressources suivant la dimension trophique était plus importante que celle suivant les dimensions spatiale et temporelle.

[Traduit par la Rédaction]

Introduction

Indices that represent a species' flexibility in resource use (e.g., niche breadth) or the levels of resource overlap between species (niche overlap) are often used to study population- or community-level effects of interspecific interactions. The indices most frequently used assume that (*i*) individuals within a population are ecologically identical and therefore overlap to the same degree with individuals of another species (Colwell and Fuentes 1975; Wissinger 1992) and (*ii*) resource overlap between two species along one resource dimension is independent of resource overlap along other resource dimensions.

While this first assumption may hold for birds and mammals, this is certainly not the case for fish, amphibians, and many invertebrate species. For fish the body weights of conspecific individuals commonly span up to four orders of magnitude (Werner 1986), and the ontogenetic changes in

Received January 10, 1997. Accepted January 18, 1999.
J13827

G.J. Piet.[1] Netherlands Institute of Ecology, Centre for Limnology, Nieuwersluis, The Netherlands, and Department of Zoology, Ruhuna University, Matara, Sri Lanka.
J.S. Pet. Department of Fish Culture and Fisheries, Wageningen Agricultural University, Wageningen, The Netherlands, and Department of Zoology, Ruhuna University, Matara, Sri Lanka.
W.A.H.P. Guruge. Department of Zoology, Ruhuna University, Matara, Sri Lanka.
J. Vijverberg. Netherlands Institute of Ecology, Centre for Limnology, Nieuwersluis, The Netherlands.
W.L.T. Van Densen. Department of Fish Culture and Fisheries, Wageningen Agricultural University, Wageningen, The Netherlands.

[1]Author to whom all correspondence should be addressed. Present address: Netherlands Institute for Fisheries Research, P.O. Box 68, 1970 AB IJmuiden, The Netherlands. e-mail: gerjan@rivo.dlo.nl

© 1999 NRC Canada

size are often accompanied by shifts in diet and (or) habitat (Werner and Gilliam 1984) to the extent that individuals of different ontogentic stages within the same population often differ more in resource use than individuals of different species (Polis 1984; Muotka 1990).

For a population consisting of ontogenetic stages differing in resource use, two components of niche breadth can be distinguished: the within-ontogenetic stage component and the between-ontogenetic stage component. Thus, since at a specific point in time (when resource availability changes) the number of ontogenetic stages per species is fixed, a species' flexibility in resource use will depend almost entirely on the within-ontogenetic stage component. Nevertheless, niche breadth has traditionally been estimated for a subset of the entire population, comprising one or more ontogenetic stages, thereby introducing an unknown between-ontogenetic stage component to the calculated niche breadth. Also, for indices of interspecific niche overlap, examples are known (e.g., Persson and Greenberg 1990; Osenberg et. al. 1992) where the interaction between populations would not be represented correctly by an index based on the resource use of the sampled subsets of the populations involved.

When studying coexistence of competing species, it is not sufficient to measure only interspecific competition. Often, intraspecific or intraguild competition (Werner and Gilliam 1984; Polis et. al. 1989; Wissinger 1992) can be the major factor in realizing coexistence of possible competitors by keeping the stronger competitor below the density necessary to eliminate the weaker competitor. For each species the relative roles of intraspecific and interspecific competition in determining the density of this species should be studied. This is also important when studying resource partitioning because the two types of competition act in opposing directions. In theory, increasing intraspecific competition forces a species to expand its niche whereas increased interspecific competition forces it to reduce it (Connell 1983).

In the same manner, ontogenetic shifts in resource use can bias the calculated niche overlap and niche breadth along each resource dimension, so niche overlap and niche breadth along one resource dimension depend on interactions with the other resource dimensions. Hence, niche occupation studies of a species along one dimension, ignoring niche shifts along any other dimension (including ontogenetic shifts), will be biased. Ross (1986) reviewed the work on resource partitioning in fish communities and distinguished three resource dimensions along which segregation was observed: trophic, spatial, and temporal. Interrelation between two resource dimensions is a common phenomenon when determining resource use but has never been taken into account when calculating the indices of resource use in a community. Interrelation between the trophic and spatial dimension is described by optimal foraging theory (MacArthur and Pianka 1966; Townsend and Winfield 1985), while interrelation between the temporal dimension and the trophic or spatial dimension was observed in studies of diel changes in feeding behavior and vertical distribution (e.g., Rudstam and Magnuson 1985; Levy 1990; Dervo et al. 1991; Hu and Tessier 1995; Gonzales and Tessier 1997; Piet and Guruge 1997). When studying the importance of these interactions the distinction between direct and nondirect interactions should be considered (Wootton 1993; Billick and Case 1994). Along the trophic dimension, no direct interactions are required because species respond to the level of resource depletion (exploitative competition, Schoener 1983), and although differences in resource depletion between habitats can be important, the time of day that resources are depleted will not make any difference. Contrary to the trophic dimension, interactions between the spatial and temporal dimensions can be of relevance because, here, species interact directly along the spatial dimension by capturing space (interference competition, see Park 1962).

In our study, three resource dimensions were distinguished: trophic, spatial, and temporal. A drought, markedly reducing fish density and changing resource availability, provided the opportunity to study the occurrence of niche shifts assuming that competition for resources was altered. For each species the size-specific resource use along each of the dimensions was determined before and after the drought, taking the effect of possible interrelation with the other two dimensions into account. We addressed the following questions. (*i*) Are the measures of niche overlap and niche breadth along one resource dimension influenced by ontogenetic shifts in the use of that resource or interaction in resource use between different resource dimensions? (*ii*) Does resource partitioning occur, and if so, what is the relative importance of the different dimensions in segregating species?

Methods

Study area

Tissawewa is a shallow (mean depth = 1.2 m), lowland reservoir of about 200 ha in Sri Lanka. The most abundant fish species were five cyprinids (*Amblypharyngodon melettinus*, *Barbus chola*, *Barbus dorsalis*, *Barbus sarana*, and *Rasbora daniconius*), a goby (*Glossogobius giuris*), a halfbeak (*Hyporamphus gaimardi*), two catfishes (*Mystus gulio* and *Mystus vittatus*), which were treated as *Mystus* spp., and two introduced exotic tilapias (*Oreochromis mossambicus* and *Oreochromis niloticus*). These species together made up more than 98% of the biomass as determined from experimental gillnet catches and bottom trawl surveys.

Sampling program

The sampling program started in September 1991 and continued until January 1994. During this sampling program the reservoir dried up during September and October 1992 due to extreme drought. Before desiccation of the reservoir (period 1), vegetation occurred only in the inshore zone and turbidity was high (mean Secchi depth transparency ±SD = 30 ± 8 cm) due to continuous suspension of a thick layer of detritus on the bottom. After refilling (period 2), vegetation was found throughout the reservoir and covered the entire water column. The water became significantly clearer (mean Secchi depth transparency ±SD = 127 ± 65 cm) due to a marked decrease of suspended detritus and phytoplankton.

A stratified sampling program was designed to determine the size-specific niche occupation per species along the three major resource dimensions, trophic, spatial, and temporal. Four different types of habitat were available in the reservoir, and one sampling station was chosen within each of these four habitats (Fig. 1). Station A represents the surface layer of the offshore zone, station B the bottom layer of the offshore zone, station C the intermediate zone, and station D the inshore zone. Each month, the four habitats were sampled simultaneously with monofilament multimesh gill nets (1.5 m depth; length varied between panels with following mesh sizes: 12.5-, 16-, 20-, 25-, 33-, 37-, and 50-mm stretched

© 1999 NRC Canada

Fig. 1. Morphometric map of Tissawewa during period 1 when vegetation was confined to the inshore zone (hatched). Positions of the sampling stations are indicated. Station A, surface layer offshore zone; station B, bottom layer offshore zone; station C, intermediate zone; station D, inshore zone.

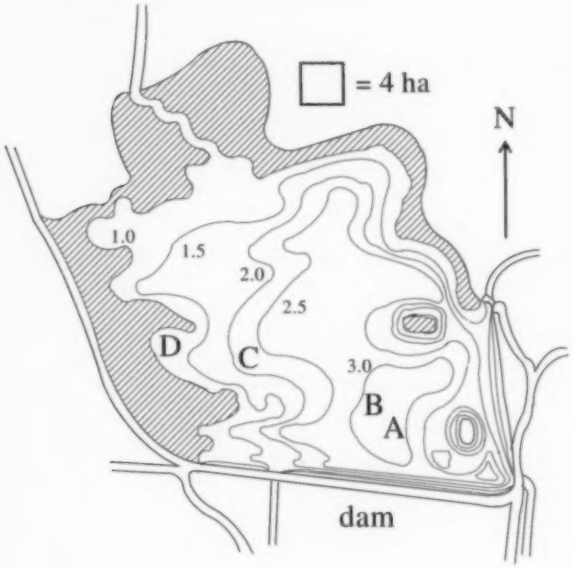

mesh) on four occasions: twice during the day and twice during the night. Because the relative positions of the stations were water level dependent, we used only data from 12 sampling occasions (five during period 1 and seven during period 2) when the water level was above 2.5 m at the deepest point to determine the habitat occupation. In addition to the gill nets, a bottom trawl (10-min hauls) and a cast net were used to ensure that the entire size range (>3 cm total length) of the available species was sampled. The fish caught with active gears were used only for length–weight measurements and gut content analyses. The entire size range was divided into six size-classes to study size-specific differences (Table 1). On each sampling occasion the size-specific diet and gut fullness of the different species were determined from pooled samples of a maximum of 10 specimens per species, size-class, gear type, station, and time of day. For each fish the percentage of fullness of the stomach or anterior one third of the gut was estimated according to five gut fullness categories (slightly modified according to Haram and Jones 1971): completely filled and swollen (100%), just filled over the full length and not swollen (75%), contents divided into different patches (50%), very few food particles (25%), and empty (0%). The contents of the stomach or anterior one third of the gut were analyzed for each pooled sample. The relative biovolumes of food items in the gut/stomach were estimated according to the points method (Hynes 1950) using a microscope. The following categories of contents were distinguished: fish, insects (both aquatic and terrestrial but not benthic), microcrustacean zooplankton (cladocerans and cyclopoid and calanoid copepods), gastropods, shrimp, fish eggs, chironomid larvae (benthic), microbenthos (mainly ostracods and some benthic cladocerans), poriferans, macrophytes, epiphytic filamentous algae, phytoplankton, and unrecognizable matter (both digested matter and detritus). To distinguish between ingested detritus and digested matter, the proportion of digested matter per size-class was calculated per period (Piet 1996). The proportion of detritus was calculated by subtracting the calculated proportion of digested matter from the observed proportion of unrecognizable matter.

Measures of niche breadth and niche overlap

Measures of niche overlap or niche breadth should be independent of the number of resource states considered, and availability as well as the degree of distinctness of the resource states from the organisms viewpoint should be taken into account (Colwell and Futuyma 1971; Colwell and Fuentes 1975; Petraitis 1979). For determining niche occupation along three dimensions, it is almost impossible to control the number of resource states, but the way that sampling was conducted ensured that resource states along the spatial and temporal dimensions were equally available. Only the availability of resource states along the trophic dimension could not be controlled, and because none of the known niche overlap indices (Colwell and Futuyma 1971; Petraitis 1979; Smith and Zaret 1982) could prevent bias arising from the number, availability, and degree of distinctness of resource states (Loreau 1990), the most straightforward measures of niche overlap (Schoener 1970) and niche breadth (Levins 1968) were chosen which at least have the advantage of compatibility with other published works (e.g., Moyle and Senanayake 1984).

Resource use along one dimension, expressed by niche breadth and niche overlap, can only be compared for populations within one ecosystem when sampling bias, which occurs if the size structure of the population(s) involved differs from that in the sample, is eliminated and if ontogenetic shifts are taken into account. This can be realized by calculating the niche breadth and niche overlap according to the method introduced in this study: size-specific resource use per species is determined for a number of size-classes per species, after which standardized measures of niche overlap and niche breadth for a population can be calculated from, respectively, the weighted niche overlaps and niche breadths of the size-classes. Weighting per size-class is according to their relative biomass. Theoretically the accuracy will improve with increasing number of classes.

Niche breadth per size-class, B, was calculated using the formula of Levins (1968):

$$B = -\sum_j P_j \log P_j$$

where P_j is the proportion associated with resource state j. To take into account possible size-specific differences in resource use, the niche breadth of a species, Bs, was calculated from the weighted niche breadth of different size-classes, B_c, according to the following formula:

$$Bs = \sum_{c=1}^{c=6} (B_c W_c)$$

where W_c is a weighting factor depending on the biomass proportion of the cth size-class. For classifying a species as a specialist or generalist, based on the measurement of niche breadth, the problem of the definition of categories was first recognized by Ricklefs (1966). He classified a species based on its niche breadth relative to a scale constructed by using as upper and lower bounds the extreme values found for all species combined (Colwell and Futuyma 1971). In this study, niche breadths of species and size-classes were shown relative to a scale between extreme values of all species/size-classes combined.

Gut fullness was assumed to be the best indicator of resource use along the temporal dimension for all species except for *H. gaimardi* and *Mystus* spp. (Piet and Guruge 1997). Because this variable does not allow determination of resource states and only two resource states (i.e., day and night) were distinguished for diel activity, niche breadth was not determined for this dimension. Species were simply designated as diurnal, nocturnal, or continuously active. A species was only characterized as either diurnal or nocturnal in case a distinct difference between daytime or nighttime was observed in gut fullness or in case a less distinct difference

© 1999 NRC Canada

Table 1. Total length ranges (in parentheses) of each size-class (1–6) and the size distribution of the 10 most common species, with their abbreviations.

	Relative biomass of size-class in gillnet catches (%)					
	1 (3.0–4.4 cm)	2 (4.5–6.9 cm)	3 (7.0–9.9 cm)	4 (10.0–13.9 cm)	5 (14.0–18.9 cm)	6 (≥19.0 cm)
A. melettinus (AM)	1	72	27	0	0	0
B. chola (BC)	T	11	59	30	T	0
B. dorsalis (BD)	T	1	11	51	37	T
B. sarana (BS)	0	3	8	27	48	14
G. giuris (GG)	0	1	4	27	26	41
H. gaimardi (HG)	0	0	14	53	33	0
Mystus spp. (MY)	0	T	13	65	21	2
O. mossambicus (OM)	T	9	18	45	26	2
O. niloticus (ON)	0	2	5	20	26	48
R. daniconius (RD)	0	26	73	2	0	0

Note: "T" indicates a proportion less than 0.5%.

was corroborated by a distinct difference in diel activity. Because most sampling was conducted at the onset of daytime and nighttime periods, it was assumed that a high gut fullness at nighttime corresponds to diurnal activity and vice versa.

Niche overlap among members of the size-structured assemblage was calculated using Schoener's (1970) formula:

$$S = 1 - 0.5D$$

where S is an index of similarity ranging from 0 to 1 and D is a measure of distance in multidimensional space between the proportions P of the resource state j along one resource dimension for assemblage members x and y:

$$D = \sum_{j=1}^{n} |P_{x_j} - P_{y_j}|$$

As niche breadth of a species was calculated from the niche breadths of its different size-classes, niche overlap $Ss_{x,y}$ of species x with species y was calculated from the weighted niche overlaps $S_{cx,cy}$ between all combinations of size-classes of the two species using the following formula:

$$Ss_{x,y} = 0.5 \sum_{cy=1}^{cy=6} \sum_{cx=1}^{cx=6} S_{cx,cy} W_{cx} W_{cy}$$

where W_{cx} and W_{cy} are the weighting factors depending on the biomass proportions of the size-classes cx and cy of species x and y, respectively.

In determining niche breadth and niche overlap along a particular dimension, the interaction between the trophic and spatial resource dimensions as well as between the spatial and temporal resource dimensions can bias results. Spatial differences in feeding behavior and diet were hardly observed for the Tissawewa fish assemblage (Piet 1996). In contrast, marked temporal (diel) differences were observed (Piet and Guruge 1997). Therefore, only the interaction between the spatial and temporal dimensions was incorporated into the measures calculated for the spatial dimension. Niche occupation along the trophic dimension was established using the relative biovolumes of the different food categories. Niche occupation along the spatial dimension was determined from the relative biomass distribution among the four habitats during daytime and nighttime separately. The relative catch per unit of effort (CPUE) in the gill nets and gut fullness during daytime or nighttime were chosen as indicators of the diel patterns along the temporal dimension. The relative CPUE is the ratio between the CPUE at one time of the day and the summed CPUE over both times of the day. If possible, resource use along each of the dimensions was determined for all size-classes of the main species.

The number of resource categories differed among the resource dimensions. For the trophic dimension the calculated overlap values appeared to depend on the number of food categories selected; lowering the number of food categories from the original 13 to eight (as applies for the spatial dimension) and subsequently to four (as applies for the temporal dimension) by combining similar food categories resulted in an increased average overlap for the species matrix. The increase of niche overlap with decreasing number of resource states observed for the trophic dimension indicates that niche overlap in field studies generally depends on the number of resource states that can be distinguished along a specific dimension. Determination of the importance of different resource dimensions in segregating potential competitors is therefore difficult because (*i*) the number of resource states varies between dimensions and (*ii*) subdivision of resources into different categories is subjective and differs between dimensions. Thus, unless along each resource dimension the same number of meaningful resource states are distinguished, studies of the importance of different dimensions in segregating competing species will always be biased and will underestimate the importance of the dimension with least resource states. This can be partly overcome by introducing a measure of overlap between two species relative to the entire assemblage (Colwell and Futuyma 1971). Instead of an overlap value between the theoretical extremes of the overlap range (0–100), the overlap value is adjusted relative to the minimum and maximum overlap value of all species pairs of the entire assemblage per dimension and per period. Comparison of adjusted niche overlaps along three dimensions of one species pair during one period displays the main dimension along which this species pair was segregated.

Condition

In fish ecology, condition is believed to be a good indicator of the general "well-being" or "fitness" of the population under consideration (Adams and McLean 1985), and several condition indices are used in fishery science as indicators of the length–weight relationship of a population. However, the conversion of the two-dimensional length–weight relationship into a single statistic results in a loss of information and, in many cases, an inaccurate representation of that relationship. After a review of the most common condition indices by Bolger and Connolly (1989), Cone (1989) propagated the calculation of estimates of ordinary least squares regression parameters as the most accurate method of examining length–weight relationships for fish populations. However, since regression parameters are commonly heterogeneous and slope and intercept are often inversely related, valid interpretation of the results is difficult (Bolger and Connolly 1989). A disadvantage of an alternative, the estimated weights of fish of fixed lengths from re-

© 1999 NRC Canada

gression equations specific to the groups of fish under consideration (De Silva 1985), is the dependency on the arbitrary choice of the length (Bolger and Connolly 1989). Therefore, we chose the calculated average weight per individual from regression equations for a population of a fixed size structure as an indicator of the species' condition. This average weight was calculated from the calculated weight of each size-class of this species multiplied by the proportion of that size-class in the species' biomass. To avoid bias caused by changes in the size structure of a species, a standard (average) size structure was used. The weight of a size-class in a particular period was calculated for the midrange length of this size-class using the length–weight relationship determined for that period.

Data analysis

Principal components analysis (PCA) biplots were used to describe size-specific resource use of each of the species. For each resource dimension and both periods separately, species and size-classes were positioned in the two-dimensional plane as was, in a separate graph, the contribution of each of the resource states. For comparison of overlap values between periods, a paired t test was used on the pairwise interactions of all species and size-classes involved. Spearman's R_s is a nonparametric correlations statistic that can be used as an indicator of how two sets in which species are ranked according to a specific measure (e.g., niche breadth or overlap with a particular species) correlate; R_s varies between 1 and –1.

Results

Niche overlap

Size-specific resource use of species along the trophic dimension is represented for periods 1 and 2 separately using a PCA biplot (Fig. 2). This technique clearly distinguishes groups of species/size-classes that share the same food resources. In general, three groups can be distinguished: the herbivorous species (*O. mossambicus*, *O. niloticus*, and *A. melettinus*), the benthivorous species (*B. chola*, *B. dorsalis*, and *B. sarana*), and the planktivorous/piscivorous species (*R. daniconius*, *H. gaimardi*, *G. giuris*, and *Mystus* spp.). Resource use of the herbivorous species hardly differs between periods; only juveniles of *A. melettinus* switch from detritus to zooplankton as their main food. In contrast, considerable diet shifts were observed for species of the other trophic groups: the juveniles of *B. chola*, *B. dorsalis*, and *Mystus* spp. shifted from zooplankton to chironomids and those of *G. giuris* from zooplankton to insects. For the adults of *B. dorsalis* and *B. sarana*, gastropods were partially replaced by insects and for the latter, partly by chironomids as well. The adults of *Mystus* spp. partially replaced their main prey, fish, with chironomids whereas the adults of *G. giuris* fed almost exclusively on fish and shrimps. Lastly, *H. gaimardi* shifted from zooplankton to insects and macrophytes. These diet shifts resulted in a significantly (pairwise t test, $p < 0.01$) higher overlap (Table 2) during period 2 as compared with period 1.

Size-specific resource use of species along the spatial dimension was represented for periods 1 and 2 separately (Fig. 3). Spatial segregation between groups of species often depended on the time of the day; during nighttime, species and size-classes were markedly more segregated than during daytime. *Hyporamphus gaimardi* and *R. daniconius* were segregated from all other species because only they occupied the surface layer during both daytime and nighttime. During daytime, few other species were found in the water column (e.g., *A. melettinus* and large size-classes of *Oreochromis* spp. and *B. sarana*), but most species occupied the bottom layer.

Considerable shifts in spatial distribution were observed between periods: as compared to period 1, there was a general tendency of species to avoid the surface layer and to shift from the shallow inshore zone towards the deeper offshore zone, during period 2. Only *H. gaimardi* and *R. daniconius* were distinctly segregated from all the other species that occupied the bottom layer: they occupied the surface layer at night, but in the daytime, they either remained in the surface layer (*H. gaimardi*) or descended into the water column (*R. daniconius*). As with the trophic dimension, segregation along the spatial dimension was significantly ($p < 0.01$) less during period 2 than during period 1 (Table 2).

Resource use along the temporal axis was determined from two variables, gut fullness and relative CPUE, both at daytime and at night. The groups that could be distinguished differed in that (*i*) gut fullness was distinctly higher during either daytime (e.g., *B. dorsalis*, large *G. giuris*, and large *Mystus* spp.) or nighttime (e.g., *O. mossambicus*, small *G. giuris*, and *B. sarana*) and (*ii*) relative CPUE was distinctly higher during either daytime (*R. daniconius*, *H. gaimardi*, and small *Mystus* spp.) or nighttime (*G. giuris* and *B. dorsalis*) (Fig. 4). As with the other niche dimensions, the average niche overlap along the temporal dimension was significantly ($p < 0.01$) higher during period 2 than during period 1 (Table 2).

Niche breadth

Among the 10 most common species, niche breadth along both the trophic and spatial dimensions differed considerably, between both size-classes and species (Fig. 5). The most specialized species along the trophic axis were the piscivore *G. giuris* and the detritivorous/herbivorous *A. melettinus*. In contrast, the benthivorous cyprinid *B. chola* and the tilapia *O. mossambicus* showed the most diverse diets. Although most species showed distinct changes in their niche breadth throughout ontogeny, some species became more specialized (e.g., *G. giuris* and *A. melettinus*) whereas others showed the opposite (e.g., *B. dorsalis*).

Along the spatial dimension, *H. gaimardi* and *Mystus* spp. showed a distinct preference for one specific habitat as opposed to species like *O. mossambicus* and *O. niloticus*, which showed no preference. In general, the smallest size-class appeared to be the least flexible in the choice of its habitat.

Based on their gut fullness and CPUE during daytime and nighttime, most species were characterized as diurnal. Exceptions were the barbs *B. chola* and *B. dorsalis*, which did not show any preference, *Mystus* spp. and *G. giuris*, which were considered nocturnal, and *R. daniconius*, which changed from a diurnal species during period 1 to a nocturnal species during period 2.

Bias in conventional measures of niche breadth and niche overlap

The bias in conventional measures of niche breadth and niche overlap caused by ignoring ontogenetic changes in

© 1999 NRC Canada

Fig. 2. PCA biplots showing resource use along the trophic dimension of species and size-classes during (*a*) period 1 and (*b*) period 2 and (*c*) the contribution of each of the resource states (arrows). Size-classes of one species are connected with a line. The smallest size-class is indicated with a cross and the largest with a dot. See Table 1 for species abbreviations. Resource states: FISH, fish; ADIN, adult insects; ZOOP, zooplankton; GAST, gastropods; SHRI, shrimps; CHIR, chironomids; EGGS, fish eggs; MIBE, microbenthos; MACR, macrophytes; BEEP, benthic and epiphytic algae; PHYT, phytoplankton; PORI, poriferans; DETR, detritus.

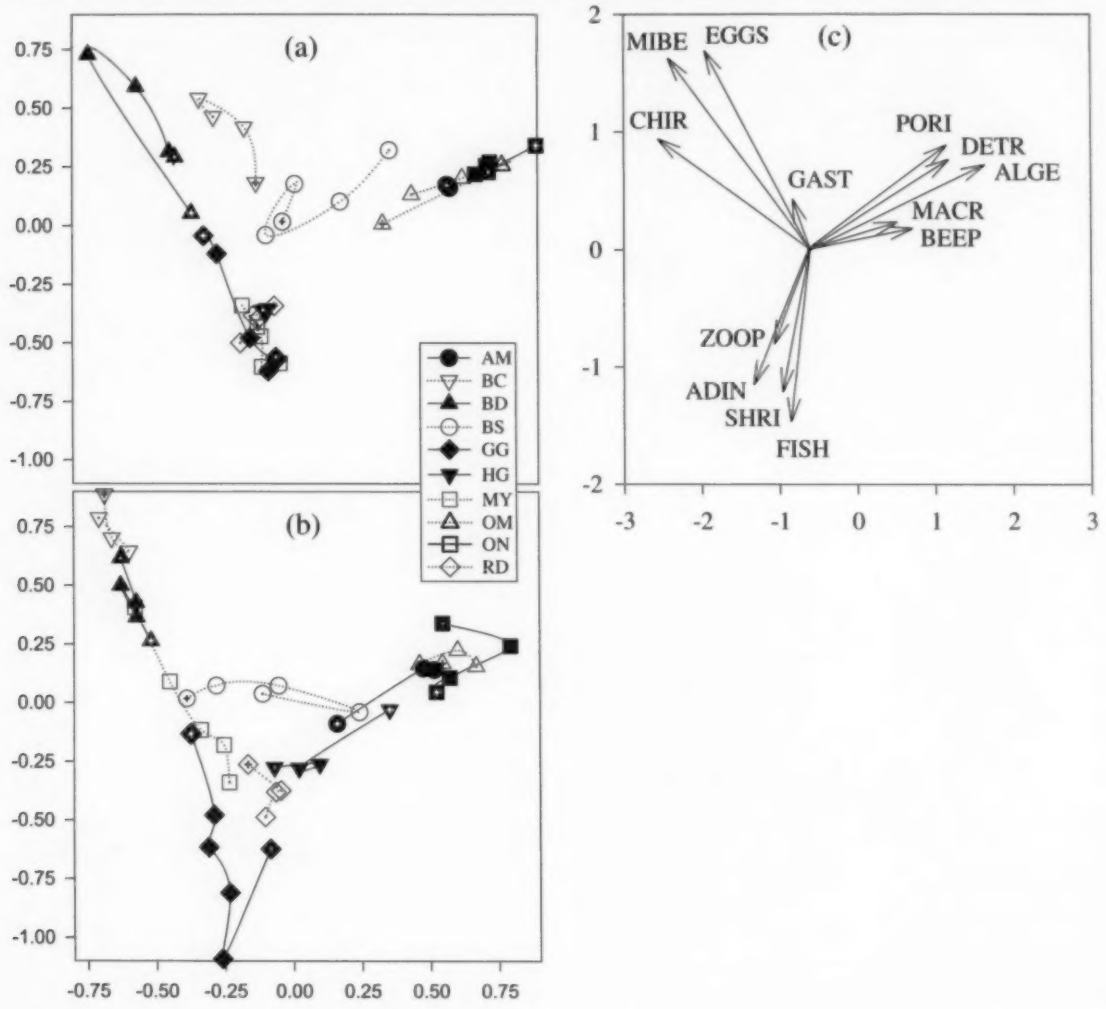

resource use can be determined by comparing the conventional measures based on the average resource use of a species with the size-specific measures of niche overlap and niche breadth. The bias was expressed by the correlation of the species' assemblage ranked according to the conventional and size-specific measures of the niche overlap or the niche breadth, respectively. Spearman's R_s was used as a measure of how well the size-specific measures correlated with the conventional measures. Of the 60 correlations (three dimensions, two periods, and 10 species; see Tables 2 and 3) for niche overlap, only one showed a perfect correlation ($R_s = 1$). On average (with 95% confidence limits), $R_s = 0.92 \pm 0.05$ for the trophic dimension, $R_s = 0.72 \pm 0.08$ for the spatial dimension, and $R_s = 0.76 \pm 0.06$ for the temporal dimension. For niche breadth, similar differences were observed, with $R_s = 0.90$ for the trophic dimension and $R_s = 0.79$ for the spatial dimension (Table 4). Also, compared with the size-specific measures, the conventional measures were systematically, and often significantly, higher.

The bias in conventional measures of niche breadth and niche overlap caused by ignoring the interaction of resource dimensions was studied for the spatial resource dimension by comparing the conventional measure based on the average spatial distribution of the species with the measure determined by the spatial distribution during daytime and nighttime separately. This shows that ignoring the interaction with the temporal dimension causes niche breadth to be overestimated (*t* test, $p = 0.08$), the ranked order of species based on their niche breadth to change ($R_s = 0.09$), and the average overlap of the entire assemblage to be overestimated

© 1999 NRC Canada

Table 2. Niche overlap values (×100) along the trophic (top table), spatial (middle table), and temporal (bottom table) dimensions.

27\53	AM	BC	BD	BS	GG	HG	MY	OM	ON	RD
AM	99 (88)\99 (48)	15 (7–27)	6 (4–14)	7 (0–15)	3 (1–11)	11 (2–22)	12 (7–32)	40 (32–46)	22 (16–47)	12 (5–51)
BC	24 (20–38)	95 (55)\95 (81)	74 (43–84)	35 (9–69)	15 (2–46)	25 (9–34)	52 (41–63)	29 (17–42)	19 (9–31)	26 (13–34)
BD	2 (2–7)	63 (21–76)	94 (55)\93 (53)	41 (4–78)	19 (1–45)	27 (7–35)	58 (39–82)	23 (8–30)	23 (4–28)	28 (10–30)
BS	2 (1–7)	20 (9–39)	41 (4–52)	86 (60)\81 (27)	24 (8–61)	46 (16–56)	42 (12–78)	42 (16–53)	35 (13–44)	48 (9–57)
GG	2 (1–7)	7 (2–51)	7 (2–74)	10 (2–39)	93 (9)\82 (37)	22 (7–57)	33 (8–76)	12 (6–26)	15 (6–23)	24 (6–53)
HG	2 (2–7)	19 (16–42)	17 (12–48)	15 (6–32)	6 (2–44)	99 (97)\89 (46)	47 (13–59)	42 (30–54)	57 (40–68)	64 (6–77)
MY	2 (2–7)	21 (7–43)	20 (2–56)	20 (8–35)	56 (8–88)	42 (10–84)	89 (14)\93 (66)	26 (14–38)	23 (10–27)	58 (19–64)
OM	80 (57–88)	32 (19–67)	7 (1–32)	15 (1–32)	4 (1–39)	8 (1–39)	7 (1–39)	90 (42)\88 (67)	53 (44–74)	37 (9–51)
ON	69 (62–75)	28 (23–49)	2 (0–13)	18 (6–31)	8 (0–17)	4 (2–14)	9 (0–23)	77 (49–90)	92 (71)\94 (67)	31 (7–40)
RD	2 (2–7)	22 (13–44)	19 (6–50)	19 (5–40)	7 (2–49)	84 (49–94)	47 (5–91)	8 (1–40)	3 (1–16)	97 (39)\95 (10)
29\62	AM	BC	BD	BS	GG	HG	MY	OM	ON	RD
AM	99 (88)\99 (48)	15 (7–27)	6 (4–14)	7 (0–15)	3 (1–11)	11 (2–22)	12 (7–32)	40 (32–46)	22 (16–47)	12 (5–51)
BC	24 (20–38)	95 (55)\95 (81)	74 (43–84)	35 (9–69)	15 (2–46)	25 (9–34)	52 (41–63)	29 (17–42)	19 (9–31)	26 (13–34)
BD	2 (2–7)	63 (21–76)	94 (55)\93 (53)	41 (4–78)	19 (1–45)	27 (7–35)	58 (39–82)	23 (8–30)	23 (4–28)	28 (10–30)
BS	2 (1–7)	20 (9–39)	41 (4–52)	86 (60)\81 (27)	24 (8–61)	46 (16–56)	42 (12–78)	42 (16–53)	35 (13–44)	48 (9–57)
GG	2 (1–7)	7 (2–51)	7 (2–74)	10 (2–39)	93 (9)\82 (37)	22 (7–57)	33 (8–76)	12 (6–26)	15 (6–23)	24 (6–53)
HG	2 (2–7)	19 (16–42)	17 (12–48)	15 (6–32)	6 (2–44)	99 (97)\89 (46)	47 (13–59)	42 (30–54)	57 (40–68)	64 (6–77)
MY	2 (2–7)	21 (7–43)	20 (2–56)	20 (8–35)	56 (8–88)	42 (10–84)	89 (14)\93 (66)	26 (14–38)	23 (10–27)	58 (19–64)
OM	80 (57–88)	32 (19–67)	7 (1–32)	15 (1–32)	4 (1–39)	8 (1–39)	7 (1–39)	90 (42)\88 (67)	53 (44–74)	37 (9–51)
ON	69 (62–75)	28 (23–49)	2 (0–13)	18 (6–31)	8 (0–17)	4 (2–14)	9 (0–23)	77 (49–90)	92 (71)\94 (67)	31 (7–40)
RD	2 (2–7)	22 (13–44)	19 (6–50)	19 (5–40)	7 (2–49)	84 (49–94)	47 (5–91)	8 (1–40)	3 (1–16)	97 (39)\95 (10)
39\44	AM	BC	BD	BS	GG	HG	MY	OM	ON	RD
AM	99 (88)\99 (48)	15 (7–27)	6 (4–14)	7 (0–15)	3 (1–11)	11 (2–22)	12 (7–32)	40 (32–46)	22 (16–47)	12 (5–51)
BC	24 (20–38)	95 (55)\95 (81)	74 (43–84)	35 (9–69)	15 (2–46)	25 (9–34)	52 (41–63)	29 (17–42)	19 (9–31)	26 (13–34)
BD	2 (2–7)	63 (21–76)	94 (55)\93 (53)	41 (4–78)	19 (1–45)	27 (7–35)	58 (39–82)	23 (8–30)	23 (4–28)	28 (10–30)
BS	2 (1–7)	20 (9–39)	41 (4–52)	86 (60)\81 (27)	24 (8–61)	46 (16–56)	42 (12–78)	42 (16–53)	35 (13–44)	48 (9–57)
GG	2 (1–7)	7 (2–51)	7 (2–74)	10 (2–39)	93 (9)\82 (37)	22 (7–57)	33 (8–76)	12 (6–26)	15 (6–23)	24 (6–53)
HG	2 (2–7)	19 (16–42)	17 (12–48)	15 (6–32)	6 (2–44)	99 (97)\89 (46)	47 (13–59)	42 (30–54)	57 (40–68)	64 (6–77)
MY	2 (2–7)	21 (7–43)	20 (2–56)	20 (8–35)	56 (8–88)	42 (10–84)	89 (14)\93 (66)	26 (14–38)	23 (10–27)	58 (19–64)
OM	80 (57–88)	32 (19–67)	7 (1–32)	15 (1–32)	4 (1–39)	8 (1–39)	7 (1–39)	90 (42)\88 (67)	53 (44–74)	37 (9–51)
ON	69 (62–75)	28 (23–49)	2 (0–13)	18 (6–31)	8 (0–17)	4 (2–14)	9 (0–23)	77 (49–90)	92 (71)\94 (67)	31 (7–40)
RD	2 (2–7)	22 (13–44)	19 (6–50)	19 (5–40)	7 (2–49)	84 (49–94)	47 (5–91)	8 (1–40)	3 (1–16)	97 (39)\95 (10)

Note: Indicated are the average niche overlap per period (period 1\period 2) in the upper left cell, the calculated interspecific niche overlap per species pair during period 1 (lower left half) and period 2 (upper right half), and for each species pair the minimum and maximum niche overlaps (in parentheses) of all size-class interactions. Across each table (upper left to lower right) are intraspecific niche overlap per species and the minimum overlap (in parentheses) between size-classes for period 1 (left) and period 2 (right). See Table 1 for species abbreviations.

© 1999 NRC Canada

Fig. 3. PCA biplots showing resource use along the spatial dimension of species and size-classes during (*a*) period 1 and (*b*) period 2 and (*c*) the contribution of each of the resource states (arrows). Size-classes of one species are connected with a line. The smallest size-class is indicated with a cross and the largest with a dot. See Table 1 for species abbreviations. Resource states: the first letter represents station (A, B, C, or D; see Fig. 1) and the second day (D) or night (N).

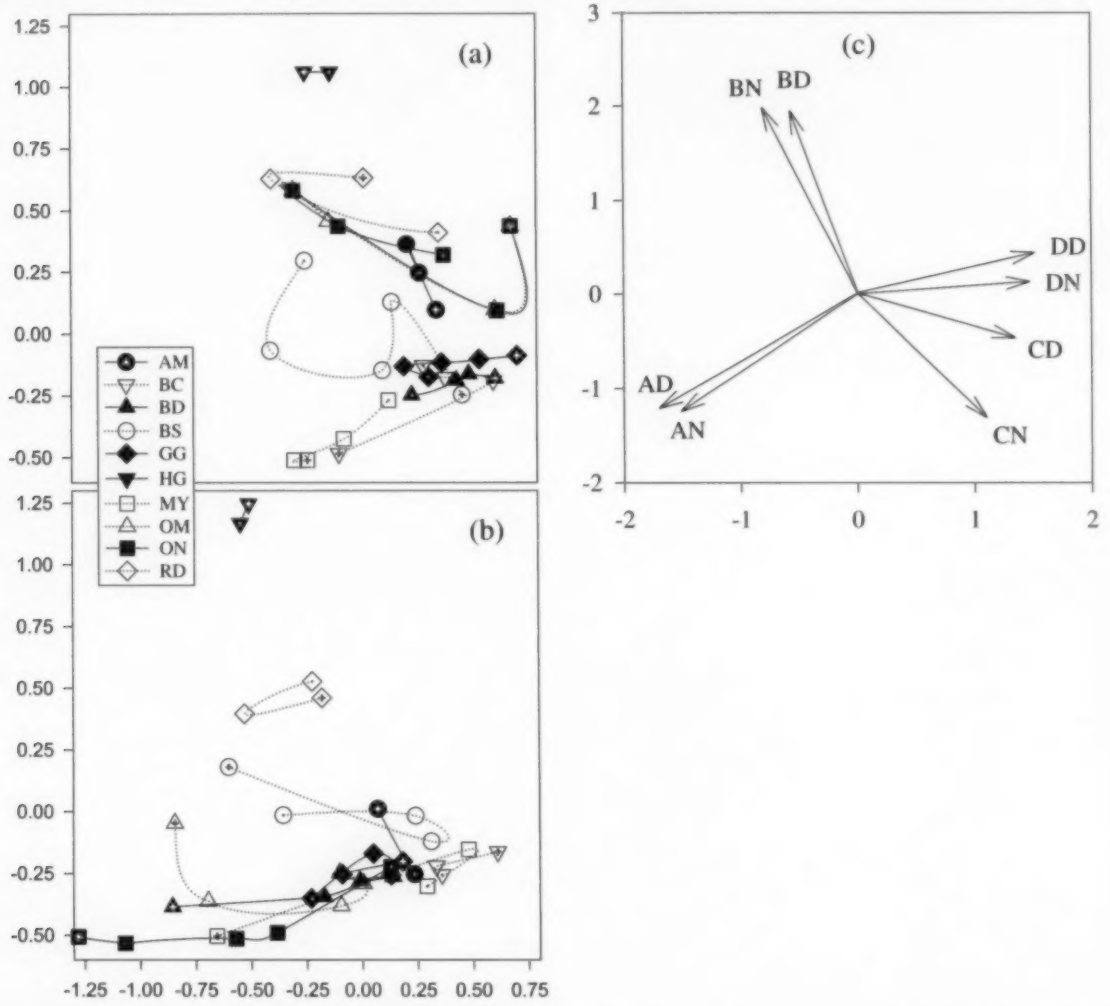

(*t* test, $p = 0.02$). In general, ignoring the interaction with the temporal dimension will systematically overestimate niche overlap along the spatial dimension if species exhibit an inverse diel spatial pattern (e.g., for *B. sarana* and *Mystus* spp. during period 1, niche overlap was 31% higher) and will underestimate overlap for species that exhibit a similar diel spatial pattern (e.g., for *A. melettinus* and *O. mossambicus* during period 1, niche overlap was 15% lower).

Resource partitioning

The importance of resource dimensions for a particular period can be determined by comparison of adjusted niche overlaps along three dimensions of one species pair during that period. During period 1, 80% of the species pairs were segregated along the trophic dimension, 9% along the spatial dimension, and 11% along the temporal dimension. During period 2, these values were 62, 20, and 18%, respectively.

Based on the data on resource use along the trophic, spatial, and temporal dimensions, an ecological "key" to the Tissawewa fish species was developed (Fig. 6). This key shows how the available resources were subdivided between species along three dimensions and how this was influenced by environmental changes.

Fish biomass and condition

Both fish biomass and condition differed markedly between periods (Table 5). Absolute biomass before the drought (period 1) was more than twice that after the drought (period 2). The species mainly affected by the changes was *A. melettinus* of which both biomass and condition were significantly lower during period 2 (*t* test, $p < 0.05$). Most species (*B. dorsalis*, *B. sarana*, *O. mossambicus*, and *R. daniconius*) showed a moderate decrease in biomass and a marked increase in condition whereas for *O. niloticus*,

© 1999 NRC Canada

Fig. 4. PCA biplots showing resource use along the temporal dimension of species and size-classes during (*a*) period 1 and (*b*) period 2 and (*c*) the contribution of each of the resource states (arrows). Size-classes of one species are connected with a line. The smallest size-class is indicated with a cross and the largest with a dot. See Table 1 for species abbreviations. Resource states: the first three letters represent relative CPUE (CAT) or gut fullness (FUL) and the last day (D) or night (N).

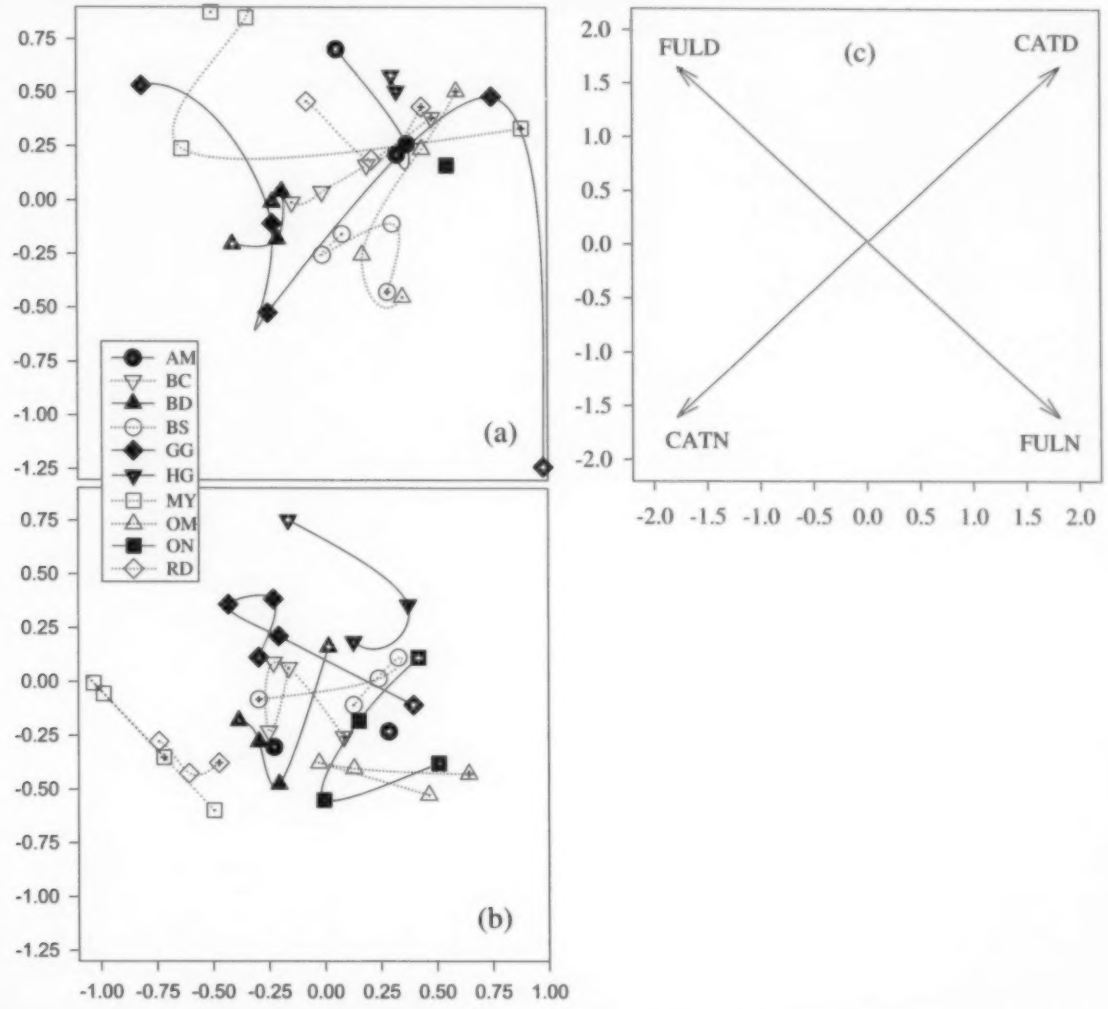

both biomass and condition increased. Notable were the strong increases in biomass of the piscivores *G. giuris* and *Mystus* spp. The changes between periods in biomass and condition appeared to be positively correlated, but because of the extreme increase in condition of *B. sarana*, this was not significant (R^2 = 0.47, p = 0.09). Without *B. sarana*, changes in biomass and condition were significantly correlated (R^2 = 0.91, p < 0.01).

Discussion

Conventional measures of niche breadth and niche overlap

Comparison of conventional measures of niche breadth and niche overlap with measures determined in this study shows that considerable bias can occur when ignoring ontogenetic changes in resource use and interactions with other resource dimensions in the calculation of these measures.

Ignoring the ontogenetic changes in resource use will bias niche breadth and consequently the distinction between generalists and specialists. Furthermore, it will result in a different characterization of species relationships based on resource use and will overestimate potential competition. For the species of the Tissawewa assemblage, ontogenetic differences in resource use were observed along each resource dimension. These size-specific shifts often minimized intraspecific competition and increased interspecific competition (with ontogenetic stages of other species). Juvenile stages, which exhibit a feeding behavior different from that of adult stages, often take up only a minor part of the biomass of a fish population and therefore have a relatively small impact on the calculated niche overlap between species. However, interspecific competition during the juvenile

© 1999 NRC Canada

Fig. 5. Niche breadth per species (bars) and per size-class (circles) along two dimensions. Niche breadth was calculated based on the resource use averaged between periods 1 and 2; the value is scaled relative to the extremes of all species/size-classes of that resource dimension combined. For each species the indicated size-classes increase from left to right. See Table 1 for size-classes and species abbreviations.

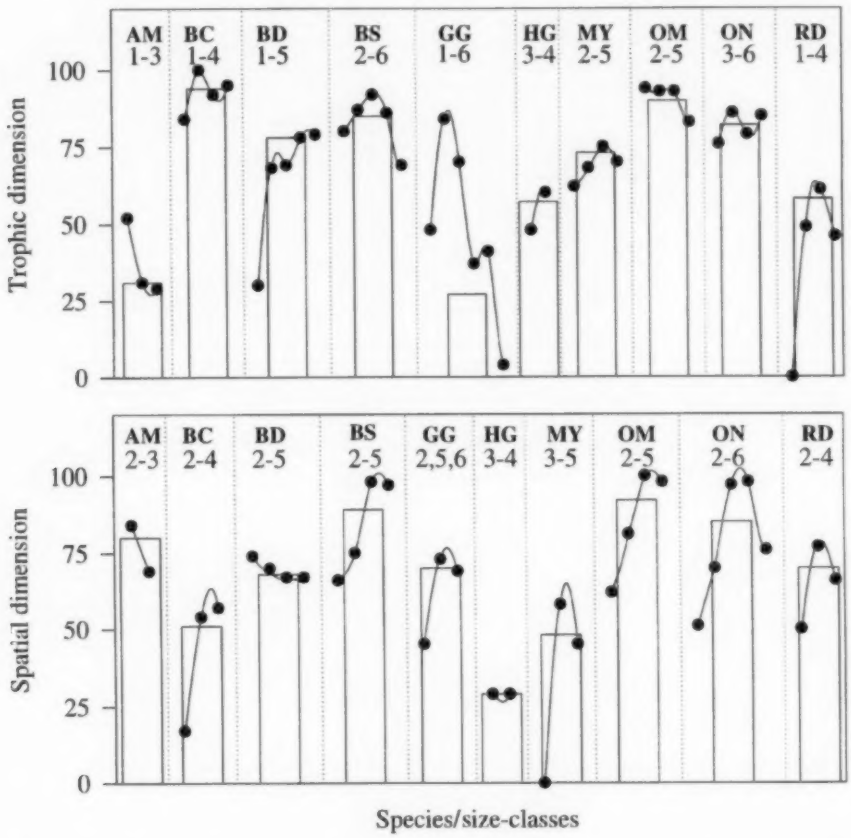

stage of a large species may reduce recruitment to larger size-classes, even though resources for these larger size-classes may not be limited, resulting in the so-called juvenile competitive bottleneck (Werner 1986; Persson and Greenberg 1990). Several species pairs that had only a minor overall overlap exhibited markedly higher overlaps between the juvenile stages (e.g., *B. dorsalis* and *G. giuris* during both periods) or between the juvenile stage of one species and the entire size range of an other species (e.g., the juvenile stages of *B. chola*, *O. mossambicus*, and *Mystus* spp. with *H. gaimardi* or *R. daniconius* during period 1). Besides these striking examples, almost all species display at a certain stage a higher overlap with other species, or ontogenetic stages of other species, than follows from the calculated overall niche overlap between species. Therefore, the impact that other species might have on the development of a certain species is often underestimated.

In this study, only the interaction between the spatial and the temporal dimensions was considered because in Tissawewa the spatial differences in diet (interaction trophic and spatial dimensions) are negligible (Piet 1996). In other environments where habitats differ more in food availability, this need not be the case. In general, ignoring the interaction with another resource dimension will underestimate niche overlap for species that exhibit a similar pattern along that dimension and overestimate overlap for species with a different pattern.

Importance of resource dimensions

During both periods the trophic dimension was markedly more important than the about equally important spatial and temporal dimensions. These findings correspond to those of Ross (1986), who reviewed resource partitioning and found that the trophic dimension is the most important dimension for segregating species. However, Ross (1986) found the trophic dimension to be only slightly more important than the spatial dimension, and these two dimensions were considerably more important than the diel temporal dimension.

The relatively higher importance during period 2 of the spatial and temporal dimensions in segregating species was caused solely by the fact that resource partitioning along the trophic dimension was lower during this period.

Competition

Comparison of resource use between periods showed several species exhibiting shifts in resource use, resulting in dif-

© 1999 NRC Canada

Table 3. Conventional niche overlap values (×100) along the trophic (top table), spatial (middle table), and temporal (bottom table) dimensions.

62\70	AM	BC	BD	BS	GG	HG	MY	OM	ON	RD
AM	100	66	61	69	57	61	66	78	66	67
BC	59	100	89	82	62	73	85	71	69	71
BD	59	85	100	78	60	66	86	66	63	66
BS	56	67	73	100	66	77	82	77	73	79
GG	49	57	57	54	100	59	67	59	57	63
HG	45	67	55	48	43	100	69	74	85	74
MY	56	69	65	61	83	60	100	68	63	77
OM	93	63	62	59	52	48	59	100	83	69
ON	79	67	66	64	58	49	65	85	100	67
RD	52	74	63	56	50	86	67	55	56	100
88\91	AM	BC	BD	BS	GG	HG	MY	OM	ON	RD
AM	100	92	92	91	91	90	91	93	90	82
BC	91	100	95	94	97	87	95	95	92	83
BD	90	98	100	95	96	87	96	97	95	84
BS	93	93	92	100	94	90	96	93	92	86
GG	87	92	92	89	100	87	95	95	94	84
HG	87	81	80	83	79	100	87	87	87	88
MY	85	86	87	86	83	77	100	95	94	83
OM	96	90	88	92	87	86	85	100	96	84
ON	93	87	86	89	82	84	80	92	100	85
RD	94	86	85	90	82	90	82	94	92	100
93\92	AM	BC	BD	BS	GG	HG	MY	OM	ON	RD
AM	100	97	92	99	97	90	86	98	98	90
BC	93	100	90	98	99	93	85	95	96	88
BD	90	97	100	92	91	83	93	92	90	98
BS	94	97	95	100	98	91	86	97	98	89
GG	89	96	97	93	100	91	86	95	95	89
HG	92	85	83	86	82	100	78	89	91	81
MY	93	94	92	92	92	88	100	85	84	96
OM	97	95	93	97	91	89	93	100	98	90
ON	97	96	94	96	92	89	95	98	100	88
RD	100	93	90	94	89	92	93	97	97	100

Note: Indicated are the average niche overlap per period (period 1\period 2) in the upper left cell and the calculated interspecific niche overlap per species pair during period 1 (lower left half) and period 2 (upper right half). See Table 1 for species abbreviations.

Table 4. Conventional and size-specific values of niche breadth (×100) for two resource dimensions.

	Trophic		Spatial	
	Conventional	Size-specific	Conventional	Size-specific
AM	37.2	44.9	82.4	88.4
BC	80.3	78.3	74.3	81.5
BD	69.2	61.1	79.0	82.2
BS	74.4	82.8	84.8	86.9
GG	34.4	59.0	79.7	80.0
HG	55.4	59.1	68.1	82.0
MY	66.0	61.7	73.5	82.2
OM	77.8	86.1	85.9	88.5
ON	72.4	71.8	83.8	88.0
RD	55.7	61.9	79.7	85.9

Note: The values were not scaled relative to the extremes. See Table 1 for species abbreviations.

ferent overlap values along several dimensions, both between species pairs and for the entire assemblage. The major shifts, where one food item was almost entirely replaced by another, were observed for all consumers of this food item, suggesting that these shifts were caused by a change in availability of this food item rather than a change in food preference. However, during period 1, when fish biomass was higher, average niche overlap along all dimensions was significantly lower, indicating that minor shifts occurred toward utilization of resources for which competition was less severe. Increased partitioning of resources when these are presumed limiting has also been observed in other studies (Zaret and Rand 1971; Werner and Hall 1977) and is strong circumstantial evidence for the importance of exploitative competition.

More circumstantial evidence for the importance of exploitative competition in structuring the Tissawewa fish community is based on (*i*) the condition of most fish species, which was highest during period 2 when fish biomass was lowest, and (*ii*) the correlation between changes in condition and changes in abundance. The only species with a significantly lower condition during period 2 was the detritivorous specialist *A. melettinus*. This is because during these peri-

© 1999 NRC Canada

Fig. 6. Ecological "key" to the Tissawewa fish assemblage indicating how species are segregated along the different dimensions during (*a*) period 1 and (*b*) period 2. For each species, habitat occupation is determined at the time the species is mainly active. See Table 1 for species abbreviations.

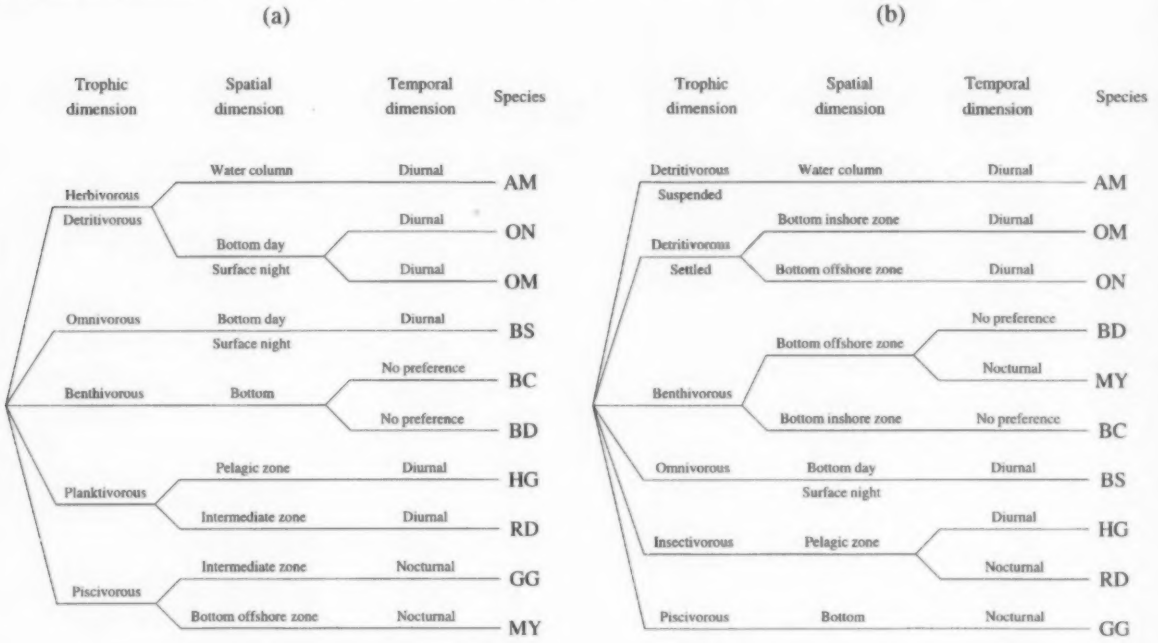

Table 5. Biomass expressed as CPUE and condition expressed as the calculated average weight per individual based on length–weight measurements and a standard population size structure as presented in Table 1.

	CPUE with gill nets ($g \cdot m^{-2} \cdot h^{-1}$)				Weight per individual (g)			
		Average per period				Average per period		
	N	1	2	Change (%)	*N*	1	2	Change (%)
AM	99 429	36.3	2.4	–174.7	1667	3.1	2.9	–7.1
BC	13 701	8.7	2.6	–108.7	1917	13.6	13.6	–0.5
BD	14 096	10.9	6.9	–44.5	2922	34.4	35.6	3.5
BS	4 971	2.8	2.3	–19.8	1618	49.2	60.3	20.2
GG	1 849	1.5	3.7	84.7	243		41.8	
HG	2 858	2.2	3.1	35.7	152		7.9	
MY	4 942	2.8	5.4	65.1	365		26.6	
OM	12 782	6	3.0	–66.1	3134	40.6	41.6	2.5
ON	2 048	1.1	1.7	37	823	105.9	112.6	6.1
RD	12 660	7.9	5.3	–39.8	1541	4.9	5	1.9
Total		80.2	36.4	–75.1				

Note: The average values of these variables are presented for the time before the drought (period 1) and after the drought (period 2). The calculated change per variable is relative to the average value of the two periods. *N* is the number of fish used to determine the variables. See Table 1 for species abbreviations.

ods, not only fish biomass changed but food availability as well. In fact the main food source of *A. melettinus*, suspended detritus, decreased from 7 to 2 mg $C \cdot L^{-1}$ (personal observations), a relatively larger decrease than that of the total fish biomass. Furthermore, changes in biomass of other species will hardly affect *A. melettinus*; because of its specialized feeding and high biomass during period 1, its abundance is expected to be mainly regulated through intraspecific competition. This is confirmed by the expansion of its niche, as indicated by a decrease in minimum overlap between size-classes from period 1 to period 2, when its main resource became scarce. The other species in which condition was not higher during period 2 was the benthivorous generalist *B. chola* feeding mainly on detritus and chironomids. Benthic detritus was almost negligible after the drought (Piet 1996) and competition for chironomids had increased considerably, since more species were utilizing this food source. The importance of increased interspecific competition to this generalist during period 2 is demonstrated by the reduction of its niche. All species for

© 1999 NRC Canada

which interspecific competition decreased while food availability was assumed to remain constant showed an increase in condition and abundance was relatively high. In contrast, species for which intra- or inter-specific competition was assumed to increase displayed a decrease in condition and abundance.

The inverse correlation between the average intraspecific niche overlap of a species and the change in condition between periods suggests that species that are more capable of reducing intraspecific competition through niche expansion have an advantage in a situation with little interspecific competition such as in period 2. The importance of a high potential for niche expansion is emphasized by the relatively high increases in abundance of species having large ontogenetic shifts such as the piscivores *G. giuris* and *Mystus* spp., even though availability of their preferred food source, fish, was lower. The relatively high biomass and condition during period 2 of species with large ontogenetic changes, and therefore a large between-ontogenetic stage component of niche breadth, supports the claim of Roughgarden (1972) that species with a greater potency for ecological release in the between-ontogenetic stage component of niche breadth have a higher colonizing ability.

Conclusions

Ontogenetic niche shifts can have a considerable impact on intra- and inter-specific competition and therefore should be considered when calculating niche overlap or niche breadth. Although the calculated values remain dependent on the number of resource states or their availability, including ontogenetic stages will at least remove or decrease sampling bias and provide insight into the actual potential of a species to adjust to perturbations or avoid competition. For the fish assemblage in Tissawewa, ontogenetic niche shifts are common phenomena and juvenile bottlenecks can occur because juveniles of several larger species share zooplankton as an important resource with each other and with two adult zooplanktivores. However, spatial segregation can play an important role because the juveniles occupy the inshore zone, while the adult zooplanktivores are mainly found in the pelagic or intermediate zone (Pet and Piet 1993).

With increasing niche breadth, interspecific competition becomes more important whereas the importance of intraspecific competition decreases. Therefore, if an assemblage is introduced into an environment where interspecific competition is relatively low, those species that are most capable of expanding their niche, thereby reducing intraspecific competition, will have an advantage, which will be expressed in a higher increase in abundance than other species. As the total fish biomass increases, interspecific competition will increase and niches will be reduced, thereby increasing intraspecific competition until a steady state is reached where abundance of each species depends on a balanced outcome of intra- and inter-specific competition.

Under the conditions prevailing before the drought, Tissawewa could be considered a typical shallow lowland reservoir. The change in fish biomass after the drought and subsequent niche shifts, together with changes in fitness of most fish species, suggests that in these shallow lowland reservoirs, resources are limiting and resource partitioning is an important mechanism for potential competitors to coexist. Resource partitioning will occur mainly along the trophic dimension in order to avoid exploitative competition.

Acknowledgments

The present study is part of the combined RU/WOTRO/NIOO-CL/WAU-DFCF Research Project on Inland Fisheries. The Department of Zoology of the Ruhuna University (RU) in Matara, Sri Lanka, is acknowledged for its hospitality and cooperation. The project was financially supported by grant W84-313 of the Netherlands Foundation for the Advancement of Tropical Research (WOTRO), the Center for Limnology (CL) of the Netherlands Institute of Ecology (NIOO), and the Department of Fish Culture and Fisheries (DFCF) of Wageningen Agricultural University (WAU). The authors wish to thank R.D. Gulati, W.M. Mooij, and E.A. Huisman for critically reviewing the manuscript. We also thank D.A.K. Gunasekara, N.W. Shanta, W. Sanath, W. Rohana, N.Y. Samaraweera, J.W. Jayasuriya, M.N.T. Munideewa, J.W.M. Wijsman, C. Soede, G.J.M. Gevers, and M.M. Fuchs for their assistance in the field. This is Publication No. 2482 of the Netherlands Institute of Ecology.

References

Adams, S.M., and McLean, R.B. 1985. Estimation of largemouth bass, *Micropterus salmoides* Lacepede, growth using the liver somatic index and physiological variables. J. Fish Biol. **26**: 111–126.

Billick, I., and Case, T.J. 1994. Higher order interactions in ecological communities: what are they and how can they be detected? Ecology, **75**: 1529–1543.

Bolger, T., and Connolly, P.L. 1989. The selection of suitable indices for the measurement and analysis of fish condition. J. Fish Biol. **34**: 171–182.

Colwell, R.K., and Fuentes, E.R. 1975. Experimental studies of the niche. Annu. Rev. Ecol. Syst. **6**: 281–310.

Colwell, R.K., and Futuyma, D.J. 1971. On the measurement of niche breadth and overlap. Ecology, **52**: 567–576.

Cone, R.S. 1989. The need to reconsider the use of condition indices in fishery science. Trans. Am. Fish. Soc. **118**: 510–514.

Connell, J. H. 1983. On the prevalence and relative importance of interspecific competition: evidence from field experiments. Am. Nat. **122**: 661–696.

Dervo, B.K., Hegge, O., Hessen, D.O., and Skurdal, J. 1991. Diel food selection of pelagic Arctic charr, *Salvelinus alpinus* (L.), in brown trout, *Salmo trutta* L., in Lake Atnsjo, SE Norway. J. Fish Biol. **38**: 199–210.

De Silva, S.S. 1985. Body condition and nutritional ecology of *Oreochromis mossambicus* (Pisces, Cichlidae) populations of man-made lakes in Sri Lanka. J. Fish Biol. **27**: 621–633.

Gonzales, M.J., and Tessier, A.J. 1997. Habitat segregation and interactive effects of multiple predators on a prey assemblage. Freshwater Biol. **38**: 179–191.

Haram, O.J., and Jones, J.W. 1971. Some observations on the food of the gwyniad *Coregonus clupeoides pennantii* Valenciennes of Llyn Tegid (Lake Bala), North Wales. J. Fish Biol. **3**: 287–295.

Hu, S.S., and Tessier, A.J. 1995. Seasonal succession and the strength of intra- and interspecific competition in a *Daphnia* assemblage. Ecology, **76**: 2278–2294.

© 1999 NRC Canada

Hynes, H.B.N. 1950. The food of fresh-water sticklebacks (*Gasterosteus aculeatus* and *Pygosteus pungitius*) with a review of methods used in studies of the food of fishes. J. Anim. Ecol. **19**: 36–58.

Levins, R. 1968. Evolution in changing environments: some theoretical explorations. Princeton University Press, Princeton, N.J.

Levy, D.A. 1990. Reciprocal diel vertical migration behavior in planktivores and zooplankton in British Columbia lakes. Can. J. Fish. Aquat. Sci. **47**: 1755–1764.

Loreau, M. 1990. The Colwell–Futuyma method for measuring niche breadth and overlap: a critique. Oikos, **58**: 251–253.

MacArthur, R.H., and Pianka, E.R. 1966. On optimal use of a patchy environment. Am. Nat. **100**: 603–609.

Moyle, P.B., and Senanayake, F.R. 1984. Resource partitioning among fishes of rainforest streams in Sri Lanka. J. Zool. (Lond.), **202**: 195–223.

Muotka, T. 1990. Coexistence in a guild of filter-feeding caddis larvae: do different instars act as different species? Oecologia, **85**: 281–292.

Osenberg, C.W., Mittelbach, G.G., and Wainwright, P.C. 1992. Two-stage life histories in fish: the interaction between juvenile competition and adult performance. Ecology, **73**: 255–267.

Park, T. 1962. Beetles, competition, and populations. Science (Washington, D.C.), **138**: 1369–1375.

Persson, L., and Greenberg, L.A. 1990. Juvenile competitive bottlenecks: the perch (*Perca fluviatilis*) – roach (*Rutilus rutilus*) interaction. Ecology, **71**: 44–56.

Pet, J.S., and Piet, G.J. 1993. The consequences of habitat occupation and habitat overlap of the introduced tilapia *Oreochromis mossambicus* (Peters) and indigenous fish species for fishery management in a Sri Lankan reservoir. J. Fish Biol. **43**: 193–208.

Petraitis, P.S. 1979. Likelihood measures of niche breadth and overlap. Ecology, **60**: 703–710.

Piet, G.J. 1996. On the ecology of a tropical fish community. Thesis, Wageningen Agricultural University, Wageningen, The Netherlands.

Piet, G.J., and Guruge, W.A.H.P. 1997. Diel variation in feeding and vertical distribution of ten co-occurring fish species: consequences for resource partitioning. Environ. Biol. Fishes, **50**: 293–307.

Polis, G.A. 1984. Age structure component of niche width and intraspecific resource partitioning: can age groups function as ecological species? Am. Nat. **123**: 541–564.

Polis, G.A., Myers, C., and Holt, R.D. 1989. The ecology and evolution of intraguild predation: potential competitors that eat each other. Annu. Rev. Ecol. Syst. **20**: 297–330.

Ricklefs, R.E. 1966. The temporal component of diversity among species of birds. Evolution, **20**: 235–242.

Ross, S.T. 1986. Resource partitioning in fish assemblages: a review of field studies. Copeia, **2**: 352–388.

Roughgarden, J. 1972. Evolution of niche width. Am. Nat. **106**: 683–718.

Rudstam, L.G., and Magnuson, J.J. 1985. Predicting the vertical distribution of fish populations: analysis of cisco, *Coregonus artedii*, and yellow perch, *Perca flavescens*. Can. J. Fish. Aquat. Sci. **42**: 1178–1188.

Schoener, T.W. 1970. Nonsynchronous spatial overlap of lizards in patchy habitats. Ecology, **51**: 408–418.

Schoener, T.W. 1983. Field experiments on interspecific competition. Am. Nat. **122**: 240–285.

Smith, E.P., and Zaret, T.M. 1982. Bias in estimating niche overlap. Ecology, **63**: 1248–1253.

Townsend, R.E., and Winfield, I.J. 1985. The application of optimal foraging theory to feeding behaviour in fish. *In* Fish energetics — new perspectives. *Edited by* P. Tytler and P. Calow. Croom Helm, London, U.K. pp. 67–97.

Werner, E.E. 1986. The mechanisms of species interactions and community organization in fish. *In* Community ecology. *Edited by* J. Diamond and T.J. Case. Harper and Row, New York.

Werner, E.E., and Gilliam, J.F. 1984. The ontogenetic niche and species interactions in size-structured populations. Annu. Rev. Ecol. Syst. **15**: 393–425.

Werner, E.E., and Hall, D.J. 1977. Competition and habitat shift in two sunfishes (Centrarchidae). Ecology, **58**: 869–876.

Wissinger, S.A. 1992. Niche overlap and the potential for competition and intraguild predation between siz-structured populations. Ecology, **73**:1431–1444.

Wootton, J.T. 1993. Indirect effects and habitat use in an intertidal community: interaction chains and interaction modifications. Am. Nat. **141**: 71–89.

Zaret, T.M., and Rand, A.M. 1971. Competition in tropical stream fishes: support for the competitive exclusion principle. Ecology, **52**: 336–342.

© 1999 NRC Canada

Estimation of tag reporting rates in age-structured multicomponent fisheries where one component has observers

William S. Hearn, Thomas Polacheck, Kenneth H. Pollock, and Wade Whitelaw

Abstract: For many tagging experiments, it is vital that fishers find and report all tags to scientists. If not, the tag reporting rate needs to be estimated so that fishing and natural mortality rates can be estimated. One way to estimate this rate is to have one fishery component (e.g., with observers) report every tag found from all fish that it catches. If the numbers of fish caught by all fishery components are also known and the tagged fish are mixed with the population (or subpopulation) being harvested, then one can estimate the reporting rate of underreporting fishery components. This procedure can fail if data are pooled over ages. We obtain maximum likelihood estimators for the reporting rate for each age and (or) each fishery component. We show how to estimate reporting rates if mixing of tagged and untagged fish occurs with some delay. We also obtain overall age-dependent reporting rates, which combine reporting rates from all components of the fishery. Our likelihood is part of an integrated likelihood that allows estimation of age-dependent fishing and natural mortalities in addition to the reporting rates. Our procedures are illustrated with some southern bluefin tuna (*Thunnus maccoyii*) tagging data.

Résumé : Dans de nombreuses expériences de marquage, il est essentiel que les pêcheurs trouvent et signalent toutes les marques aux scientifiques. Sinon, le taux de signalement des marques doit être estimé de façon à ce que les taux de capture et de mortalité naturelle puissent être estimés. Une façon d'estimer ce taux de signalement consiste à faire en sorte qu'une composante de la pêche (p. ex. avec les observateurs) signale chaque marque trouvée dans l'ensemble de ses prises. Si on connaît aussi les nombres de poissons capturés par toutes les composantes de la pêche, et si les poissons marqués sont intégrés à la population (ou la sous-population) exploitée, alors on peut estimer le taux de signalement par les composantes de la pêche qui ne signalent pas toutes les marques. Cette procédure peut échouer si les données sont groupées par âge. Nous obtenons des estimateurs du maximum de vraisemblance pour le taux de signalement pour chaque âge et/ou chaque composante de la pêche. Nous montrons comment estimer les taux de signalement quand le mélange des poissons marqués et non marqués se fait avec un certain retard. Nous obtenons aussi des taux globaux de signalement dépendants de l'âge, qui combinent les taux de signalement de toutes les composantes de la pêche. Notre coefficient de vraisemblance s'inscrit dans une vraisemblance intégrée qui permet l'estimation des mortalités par pêche et naturelle dépendantes de l'âge, ainsi que celle des taux de signalement. Nos procédures sont illustrées au moyen de données de marquage concernant le thon rouge du sud (*Thunnus maccoyii*).

[Traduit par la Rédaction]

Introduction

Tagging experiments are often used to estimate the mortality rates, population size, and commercial production of fish (and wildlife) populations. For harvested species, it is vital that catchers find and return all tags or that the fraction reported to scientists can be estimated (Brownie et al. 1985; Pollock et al. 1991). There are five main ways of estimating the tag reporting rate: (*i*) "plant", or "seed", uniquely numbered tags in catches before processing (Green et al. 1983), (*ii*) incorporate reporting rate estimates into models that estimate mortality rates from tag return data (Youngs 1974; Siddeek 1989, 1991; Hearn et al. 1998; Hoenig et al. 1998*a*), (*iii*) release some specially coloured or marked tags with very high rewards and publicise them to hopefully ensure that finders return 100% of these tags (Henny and Burnham 1976), (*iv*) use an angler sample survey or port sample to estimate the total number of tags available to be reported and hence the reporting rate (the sampling fraction is based on the sampling design used (Pollock et al. 1991)), and (*v*) have scientific observers inspect a part of the catch for tags. In addition the numbers of fish in both the inspected and uninspected catches are counted (or estimated in some way). The reporting rate of the tag returns from the uninspected catch can then be estimated (Paulik 1961;

Received October 13, 1998. Accepted February 26, 1999. J14830

W.S. Hearn,[1] T. Polacheck, and W. Whitelaw.[2] Commonwealth Scientific and Industrial Research Organisation (CSIRO) Marine Research, G.P.O. Box 1538, Hobart, Tasmania 7001, Australia.
K.H. Pollock.[3] Bureau of Resource Sciences, Fisheries Branch, P.O. Box E11, Kingston, ACT 2604, Australia.

[1]Author to whom all correspondence should be addressed. e-mail: bill.hearn@marine.csiro.au
[2]Present address: Oceanic Fisheries Programme, South Pacific Commission, BPD5 98848, Noumea Cedex, New Caledonia.
[3]Present address: Department of Statistics, Box 8203, North Carolina State University, Raleigh, NC 27695-8203, U.S.A.

© 1999 NRC Canada

Table 1. Hypothetical numbers of fish caught and numbers of fish with tags reported from five age-classes for two fishery components.

Age	c_1	r_1	α (%)	c_2	r_2	$\hat{\lambda}_2$
1	50	1	2.00	6000	60	0.500
2	1500	30	2.00	100	1	0.500
3	250	25	10.00	200	10	0.500
4	200	10	5.00	1200	30	0.500
5	120	3	3.00	720	9	0.500
Pooled	2120	69	3.25	8220	110	0.411

Note: Component 1 reports all tags from fish that it catches but component 2 does not. Percentage of tagged fish in catch is α (%). The reporting rate, λ_2, of component 2 is estimated from eq. 1 for each age and the pooled data.

Kimura 1976). The theory developed here concerns the last method and how it may be generalised (*a*) to more than two fishery components with age-structured catches, (*b*) to allow for delayed mixing of tagged fish from various sources, and (*c*) to obtain age-specific reporting rates that are required for estimating age-specific mortality rates.

The basis of method (*v*) is given in Kimura (1976). Suppose a substantial number of fish have been tagged and released and that sufficient time has elapsed for these to completely mix in, at least, the subpopulation that two fishery components harvest. In fishery component 1, c_1 fish are caught from which r_1 tags are returned. We assume that in this component, all the tags are returned, and so an estimate of the proportion of tagged fish in the population is r_1/c_1. In component 2, c_2 fish are caught from which r_2 tags are returned. For this component, we assume that an unknown proportion, the reporting rate λ_2, of the tags are returned, and so an estimate of the proportion of tagged fish in the population is $r_2/(\hat{\lambda}_2 c_2)$. Assuming that the tagged fish are perfectly mixed through both fisheries, i.e., the proportions of tagged fish are the same in both fishery components, so that

$$\frac{r_1}{c_1} \approx \frac{r_2}{\hat{\lambda}_2 c_2},$$

then, λ_2 can be estimated as

$$(1) \qquad \hat{\lambda}_2 = \frac{r_2 c_1}{c_2 r_1}.$$

Most fish populations are age structured. We show below that the age structure needs to be taken into account when estimating reporting rates, even if the reporting rates themselves are not age dependent (possibly a reasonable assumption if fish of all ages are processed in the same way). The proportion, by age, of the catch from the different fisheries will usually vary due to gear and to temporal and spatial effects. (Kimura (1976) considered time strata but did not develop in detail a methodology for age-structured fisheries.) Additionally, it is likely that tagging programs will result in differing proportions of fish being tagged among fish of various ages. (To tag the same proportion of fish of each age, for each year, would require an exacting experimental design and execution, which is unlikely to be achieved in practice and would likely conflict with the general experimental design for the purpose of the experiment. See Brownie et al. (1985) for experiments to estimate mortality rates.) Under both of these conditions, eq. 1 can lead to model bias in the estimate of λ_2. We illustrate how the estimate of λ_2 from eq. 1 can be seriously biased if age structure is not taken into account, with the hypothetical example in Table 1.

In this example, the estimate of λ_2 from the pooled data is biased by about 20% ($\hat{\lambda}_2 = 0.41$ versus 0.5 for every individual age). Alternatively, if only the data from ages 3 and 4 are considered, the pooled reporting rate (i.e., $\hat{\lambda}_2 = 0.37$) has even greater bias. On the other hand, if data from ages 1 and 2 are pooled, $\hat{\lambda}_2 = 0.5$. This is because the proportion of tags in their catches is the same (i.e., α = 2.00%), even though the age distributions of their fishery components' catches are different. Again, if data from ages 4 and 5 are pooled, then $\hat{\lambda}_2 = 0.5$. This is because the age distributions of their fishery components' catches are the same, even though the proportions of tagged fish in catches differ by age.

In the example in Table 1, $\hat{\lambda}_2$ is age independent. We also consider models in which reporting rates are intrinsically age dependent. This can occur even where the proportions, by age, of tagged fish in catches are the same, say because fish of different ages (sizes) may be processed differently after capture.

Initial nonmixing (or delayed mixing) of tagged fish with the general population is a well-known problem in tagging experiments and needs to be dealt with in many analyses of tag return data in order to be credible. Fishers often catch substantial numbers of fish soon after tagging because the tagging occurred in the vicinity of the fishery. This can result in an overestimate of the exploitation rate due to initial nonmixing (see Hoenig et al. (1998*b*) for mortality estimation models that take account of delayed mixing). If initial nonmixing is the same for all fishery components, then it will not affect estimates of reporting rates. This is unlikely to be the case if different fishery components are spatially or temporally segregated. In these situations, the analysis models need to account for the initial period of nonmixing.

In this paper, we develop maximum likelihood estimators for estimating potentially age-dependent reporting rates for two or more fisheries components, given that one of them reports 100% of the tagged fish and the total catch, by age, for each fishery component is known (e.g., if an observer program exists). Additionally, we show how delayed mixing of tagged fish can be accounted for in the reporting rate estimation procedure. These reporting rates can be used to produce an overall age-specific reporting rate across all fishery components weighted by the age structure of the catch. We illustrate our models with an example based on southern bluefin tuna (*Thunnus maccoyii*) tagging data. We conclude with a general discussion section.

Model development

Assumptions

The reporting rate assumptions are as follows.

(1) One fishery component reports 100% of the tagged fish that it catches.

(2) The catch-at-age distribution of this component has some ages in common with those of other components.

© 1999 NRC Canada

(3) The tagged fish are mixed in the subpopulation of fish that the fishers harvest. In some cases, mixing does not need to be immediate.

(4) The total numbers, by age, of fish harvested (including tagged fish) need to be known, or reliably estimated for each fishery component. Tagging programs are normally carried out for estimating general population parameters such as mortality rates and population size. However, estimates of or assumptions about reporting rates are essential components for estimating these general population parameters. In specific analyses, other assumptions besides the four listed above may apply. It should be noted that in estimating reporting rates, it is not necessary to know how many fish were tagged initially, which is perhaps surprising and may be important in some cases.

Likelihood function

We present a conditional likelihood for estimation of potentially age-dependent reporting rates. In a separate paper (K.H. Pollock, W.S. Hearn, and T. Polacheck, unpublished data), we show that this conditional likelihood is part of an integrated likelihood, which also provides estimates of age-dependent fishing and natural mortalities.

There are s fishery components, 1, 2,..., j,..., s, that catch fish in k age-classes, 1, 2,..., i,..., k, in which some of the fish have been tagged. The number of fish of age i in the total catch of component j is designated as c_{ji}, from which r_{ji} fish are reported as having tags.

For our general model A, the likelihood consists of two parts:

$$(2) \qquad L = L_1 \times L_2$$

where L_1 is the likelihood component of the tag recoveries in all the fishery components conditional on their total and L_2 is the likelihood component of the catches conditional on their total. The L_1 is the product multinomial

$$(3) \qquad L_1 = \prod_{i=1}^{k} P(r_{1i}, r_{2i}, \ldots, r_{si} | r_{\bullet i}) = \prod_{i=1}^{k} \binom{r_{\bullet i}}{r_{1i}, r_{2i}, \ldots, r_{si}} \prod_{j=1}^{s} \left[\frac{\lambda_{ji}\,\delta_{ji}}{\sum_{j=1}^{s} \lambda_{ji}\,\delta_{ji}} \right]^{r_{ji}}$$

where $r_{\bullet i} = \sum_{j=1}^{s} r_{ji}$ is the number of tag recoveries of age i in a particular year summed over all s fishery components, δ_{ji} is the fraction of the exploitation that occurs in component j for age i ($\Sigma_{j=1}^{s} \delta_{ji} = 1$), and λ_{ji} is the reporting rate for component j for age i fish ($\lambda_{1i} = 1.0$, i.e., there is 100% reporting of tags in component 1 for all ages i = 1, 2,..., k). The L_2 is also product multinomial:

$$(4) \qquad L_2 = \prod_{i=1}^{k} P(c_{1i}, c_{2i}, \ldots, c_{si} | c_{\bullet i}) = \prod_{i=1}^{k} \binom{c_{\bullet i}}{c_{1i}, c_{2i}, \ldots, c_{si}} \prod_{j=1}^{s} \delta_{ji}^{c_{ji}}$$

where $c_{\bullet i} = \sum_{j=1}^{s} c_{ji}$ is the catch of age i in a particular year summed over all s components. Note that eq. 4 could be generalised to allow for sampling errors in catch and catch-at-age estimation. It would also be possible to develop a similar likelihood to eq. 4 based on fishing effort if those data were available and believed to be more reliable than the catch component data. In fact, any other estimators of the fractions of fishing in each component of the fishery (j = 1, 2,..., s) could be incorporated.

We propose to fit three increasingly restrictive models: model A1, δ_{ji} and λ_{ji} distinct parameters; model A2, δ_{ji} and λ_j distinct parameters; model A3, δ_j and λ_j distinct parameters. For each model, a computer program can be used to provide maximum likelihood estimates. The most parsimonious model can be selected based on results of likelihood ratio tests (involving negative log likelihood) and Akaike's information criterion (AIC) (Akaike 1971, 1974; Buckland et al. 1993, pp. 112–114).

Model A1

For this general saturated model, which we refer to as model A1, the maximum likelihood estimators are explicit and take the following forms:

$$(5) \qquad \hat{\delta}_{ji} = \frac{c_{ji}}{c_{\bullet i}} \qquad i = 1, 2, \ldots, k \text{ and } j = 2, 3, \ldots, s$$

$$(6) \qquad \hat{\lambda}_{ji} = \frac{r_{ji}\,c_{1i}}{c_{ji}\,r_{1i}} \qquad i = 1, 2, \ldots, k \text{ and } j = 2, 3, \ldots, s.$$

Note that eq. 6 is basically just eq. 1 but indexed explicitly for each age and fishery component. Model A1 would be appropriate where age-dependent processing procedures or other factors lead to age-dependent reporting rates.

Model A2

Model A2 is appropriate in situations where reporting rates are fishery component dependent but not age dependent (i.e., $\lambda_{ji} = \lambda_j$). In this case, explicit maximum likelihood estimators cannot be obtained, but a numerical maximisation routine (e.g., MINIMD (programmed by D.E. Shaw, CSIRO Division of Mathematical and Information Sciences, P.O. Box 218, Lindfield, NSW, Australia) or SURVIV (White 1983)) can be used to numerically obtain the estimators and their variance–covariance matrix.

Model A3

This model gives rise to estimators that, we believe, are likely to be inappropriate in most situations. In the case of δ_{ji} and λ_{ji} being constant over all ages i, the maximum likelihood estimators reduce to the closed form, which is the pooled version of model A1 (i.e., the catch and the tag re-

© 1999 NRC Canada

coveries are pooled over all ages for each fishery component):

$$(7) \qquad \hat{\delta}_j = \frac{\sum_{i=1}^{k} c_{ji}}{\sum_{i=1}^{k} c_{\bullet i}}$$

$$(8) \qquad \hat{\lambda}_j = \frac{\sum_{i=1}^{k} r_{ji} \sum_{i=1}^{k} c_{1i}}{\sum_{i=1}^{k} c_{ji} \sum_{i=1}^{k} r_{1i}}.$$

for $j \neq 1$.

Alternative model

Another model based on different conditioning, which we call model B, is developed in the Appendix. It is derived by considering the proportion (α_i) of tagged fish in the population, which many readers might believe is a natural approach to estimating the reporting rates. The model is conditional on the catch numbers c_{ji}. For a given data set, the estimates of the λ's are the same, or almost the same, whether model A or B is used (we further examine this matter in the Results section and Appendix).

Delayed mixing

Nonmixing, which is the same in all components of the fishery, does not cause any complications. However, if mixing in one component (say the last one s) is not equal to the others for a specific period (e.g., up to a year) the direct (D for first period recoveries) and indirect recoveries (I) need to be separated in eq. 3. This yields

$$(9) \qquad L_1 = \sum_{i=1}^{k} \binom{r_{\bullet i}^{\mathrm{D}}}{r_{1i}^{\mathrm{D}}, r_{2i}^{\mathrm{D}}, \ldots, r_{si}^{\mathrm{D}}} \prod_{j=1}^{s} \left[\frac{\lambda_{ji}\,\delta_{ji}}{\sum_{j=1}^{s} \lambda_{ji}\,\delta_{ji}} \right]^{r_{ji}^{\mathrm{D}}}$$

$$\times \prod_{i=1}^{k} \binom{r_{\bullet i}^{\mathrm{I}}}{r_{1i}^{\mathrm{I}}, r_{2i}^{\mathrm{I}}, \ldots, r_{si}^{\mathrm{I}}} \prod_{j=1}^{s} \left[\frac{\lambda_{ji}\,\delta_{ji}}{\sum_{j=1}^{s} \lambda_{ji}\,\delta_{ji}} \right]^{r_{ji}^{\mathrm{I}}}.$$

All the parameters are the same in the two parts of the likelihood except that δ_{si} is different for the direct (δ_{si}^{*}) and indirect (δ_{si}) recoveries. For the indirect recoveries, δ_{si} truly reflects the catch rates. For the direct recoveries, $\delta_{si}^{*} = \delta_{si}\,\gamma_i$, where the mixing parameter γ_i is the relative size of the exploitation rate of component s compared with the other $s - 1$ components. If the sth component behaves the same as the others, $\gamma_i = 1$, then both sets of recoveries can be combined. A likelihood ratio test could be conducted to test if $\gamma_i = 1$, in which case, $\delta_{si}^{*} = \delta_{si}$. Note that reporting rates for component s cannot be estimated in the first year of a multiyear tagging program if mixing is not the same as in the other components. In this case, an alternative assumption must be made, e.g., γ_i is common across 2 or more years.

In applying delayed mixing to model A1, the maximum likelihood solutions take a closed form, with estimates for δ_{ji} from eq. 5 and for λ_{ji} (except for $j = s$) from eq. 6. When $j = s$:

$$(10) \qquad \hat{\lambda}_{si} = \frac{r_{si}^{\mathrm{I}} c_{1i} \sum_{j=1}^{s-1} r_{ji}}{r_{1i} c_{si} \sum_{j=1}^{s-1} r_{ji}^{\mathrm{I}}}$$

and the estimate of the mixing parameter is

$$(11) \qquad \hat{\gamma}_i = \frac{r_{si}^{\mathrm{D}} \sum_{j=1}^{s-1} r_{ji}^{\mathrm{I}}}{r_{si}^{\mathrm{I}} \sum_{j=1}^{s-1} r_{ji}^{\mathrm{D}}}.$$

Age-specific reporting rates for data pooled over fishery components

In the application of the reporting rate estimators (obtained by methods described in previous sections) to estimate the rates of fishing and natural mortalities, it will be necessary to have reporting rates for different ages pooled over the fishery components with potentially different age selectivities. Such an estimate can be derived from the weighted averages of the reporting rates for each age where the weights are the catches in each component at each age (c_{ji}):

$$(12) \qquad \hat{\lambda}_{i\text{pooled}} = \sum_{j=1}^{s} \hat{\lambda}_j\,\hat{\delta}_{ji}$$

where

$$\hat{\delta}_{ji} = \frac{c_{ji}}{c_{\bullet i}}.$$

Note that $\lambda_1 = 1.0$; consequently the first term in eq. 12 is δ_{1i}. An important feature of eq. 12 is that reporting rates can be estimated for ages that are not harvested by component 1, as long as there is some overlap in the ages harvested by the different fishery components. This may be critical in the analyses of tag return data from fisheries in which there are major differences in the age selectivities among the various fisheries components.

Example

Southern bluefin tuna is a highly migratory and long-lived species that begins to spawn at about 10–12 years of age in oceanic waters south of Java, mainly during October–March. Currently, Australian fishers catch juveniles (primarily 2 to 5 years old) from surface schools off southern Australia. The longline fishery (mostly Japanese) catches older juveniles (aged 3 years or more) and adults in ocean waters from 20°W in the Atlantic Ocean, across the Indian Ocean to 170°W near New Zealand in the Pacific Ocean. More de-

© 1999 NRC Canada

tailed information about the life history, biology, and fisheries of southern bluefin tuna is given in Caton (1991).

Tagging experiments

Juvenile southern bluefin tuna have been tagged in Australian waters since 1959. The double-tagging procedure mainly used is described in Hearn et al. (1991). We analyse data from fish tagged between 1990 and 1995.

Double-tagging experiments allow estimates to be made of the proportions of tags that are shed from fish (e.g., Beverton and Holt 1957; Kirkwood 1981; Hearn et al. 1991). Preliminary analyses indicate that shedding rates are very low in the 1990's. Hence, for these analyses, we overlook the impact of shedding.

The age of each caught fish was determined from its length and the date of tagging, using the slicing method, and the two-stanza von Bertalanffy growth curve that was recommended by the Southern Bluefin Tuna Workshop (Anonymous 1994) for 1980's catches. Polacheck and Preece (1996) found that growth in the 1990's is close to the 1980's curve. We do not assess the effects that bias and uncertainty, in the growth curve and slicing, have on our estimates of southern bluefin tuna reporting rates. This is a difficult matter to address and is beyond the scope of the current paper.

Much effort has been expended recovering tags from both the domestic and international southern bluefin tuna fisheries. CSIRO initiated an industry liaison position whose major objectives were to provide information to relevant fishers and to encourage the return of tags and recapture information. In addition to many port and processor visits, there was much publicity and information produced and distributed to the fishers. This was distributed, in English and Japanese, to Australian, Japanese, and New Zealand vessels by on-ground liaison personnel in Australia, New Zealand, and South Africa as well as by the Federation of Japan Tuna and ZENGYOREN (the two main Japanese fishing cooperatives). It was also distributed to vessels visited by observers from the Australian Fishing Zone (AFZ) and the Real Time Monitoring Program, on the high seas.

Each tag recovery, whether returned directly to CSIRO scientists or via observers or liaison personnel, was responded to with a reward as well as a certificate providing information on the release and recovery details. This "real time" feedback to the vessels has encouraged further returns. While every effort was made to inform the fishers of the tagging program, there were still many longline vessels fishing for southern bluefin tuna whose crews appeared to be unaware of the program. There were also a number of longline vessels whose crews appeared to ignore the tagging information and seemed not to cooperate with this joint Australian–Japanese tagging program.

Data selected to illustrate our reporting rate methods are from Japanese longliners operating east of the mid-Indian Ocean in 1992–1995. Each midyear since 1988, Japanese longline vessels have been permitted to catch a limited tonnage of southern bluefin tuna in the AFZ, under certain conditions. One is that Australian observers be put aboard some of the vessels for varying periods from a few days to a few weeks. Among other duties, observers record the number of fish caught and their length and also inspect fish for tags. For our example, it is these observed fish that we call component 1 and assume that 100% of their tags are reported. (Observers also collect tags from previously caught fish and publicise the tagging program.)

The longliners operating in the AFZ (the in-zone fishery) also undergo postseason catch inspections when they are asked for tags. This fleet, for the period they are operating in the AFZ without observers, we call component 2. We assume that component 1 is a random sample of the in-zone fishery, so mixing of tagged fish between fisheries 1 and 2 is considered to be immediate. Component 3 constitutes all Japanese longline vessels operating outside the AFZ on fishing grounds from east of New Zealand to the mid-Indian Ocean, but not off South Africa.

It is not necessary that tagged fish immediately mix between component 3 and components 1 and 2, but we have assumed that they have mixed by 8 months after tagging. The catch numbers and numbers of reported fish with tags for these three fishery components in 1992–1995 are listed in Table 2 by age. The numbers of reported fish with tags are split into two categories (Table 2): (*i*) those recaptured within the first 8 months after tagging (direct recoveries) and (*ii*) the remainder (indirect recoveries).

For each year, we select data sets for analyses from those ages where (*i*) $r_{1i} \neq 0$ (model A1 solution does not exist if $r_{1i} = 0$) and (*ii*) $\varepsilon_i > 10$ (this eliminates sets where $\varepsilon_i \leq 6$). On this basis, the ages selected were 2–3 years for 1992, 2–4 years for 1993, 2–5 years for 1994, and 3–6 years for 1995.

Results

Data in Table 2 were analysed by models A1, A2, and A3 (using MINIMD for maximising the likelihood in A2), with no accounting for possible delayed mixing, for various ages; the results are given in Table 3. By AIC, model A2 is the most appropriate model for the years 1992, 1994, and 1995. For these years, it is noted that the reporting rate for fishery component 2 is about twice that of component 3.

For 1993, model A1 is better than model A2 (Table 3). However, the best model for 1993 is a combination of models A1 and A2 (Table 3, model A1/2), in that the reporting rate is age independent for fishery component 2 but is age dependent for component 3.

As shown in the Appendix, models A1 and B1 give identical results, and so do models A3 and B3. We also mention in the Appendix that models A2 and B2 give similar estimates for λ's, but generally, they are not identical. To illustrate the last point, we estimated λ_2 and λ_3 by model B2 from the same data analysed by model A2 in Table 3. In a comparison of results, the λ's obtained using model B2 differ by –2.0 to 3.9% from those using model A2.

We investigated the effect of delayed mixing on the reporting rate estimates. Ages 2 and 3 are the only ones with direct recoveries (Table 2) because fish were only tagged up to 3 years of age. The results from model A1, incorporating delayed mixing for ages 2 and 3, are given in Table 4. Using the likelihood ratio test to compare model A1 estimates between mixing (Table 3) and delayed mixing (Table 4) assumptions, we show one case where the mixing parameter γ_i is significantly different from 1.0 (age 3 in 1994, $p = 0.037$) (Table 4). However, the numbers involved are small (Ta-

© 1999 NRC Canada

Table 2. Catch numbers (c_{ji}) for fishery components j = 1, 2, 3 (1 = observers, 2 = in-zone, and 3 = out-of-zone) and ages i = 1–6 years by calendar years 1992–1995.

	Fishery component	Age (years) 1	2	3	4	5	6	Total
1992								
Catches (c_{1i})	1	12	1 625	1 777	959	310	178	4 861
Recoveries								
Direct (r^{D}_{1i})		0	7	5	0	0	0	12
Indirect (r^{I}_{1i})		0	2	8	0	0	0	10
Total (r_{1i})		0	9	13	0	0	0	22
Catches (c_{2i})	2	143	20 293	31 749	13 624	5 829	2 936	74 574
Recoveries								
Direct (r^{D}_{2i})		0	18	5	0	0	0	23
Indirect (r^{I}_{2i})		0	10	33	3	0	0	46
Total (r_{1i})		0	28	38	3	0	0	69
Catches (c_{2i})	3	1 164	28 261	8 093	12 507	5 499	4 316	59 840
Recoveries								
Direct (r^{D}_{3i})		0	10	1	0	0	0	11
Indirect (r^{I}_{3i})		0	7	6	0	0	0	13
Total (r_{3i})		0	17	7	0	0	0	24
Sum over j ($r_{\cdot i}$)		0	54	58	3	0	0	115
1993								
Catches (c_{1i})	1	28	3 688	3 899	1 787	1 067	569	11 038
Recoveries								
Direct (r^{D}_{1i})		0	10	4	0	0	0	14
Indirect (r^{I}_{1i})		0	1	11	6	1	0	19
Total (r_{1i})		0	11	15	6	1	0	33
Catches (c_{2i})	2	226	17 071	26 425	16 426	10 786	5 964	76 898
Recoveries								
Direct (r^{D}_{2i})		0	23	8	0	0	0	31
Indirect (r^{I}_{2i})		0	6	54	25	3	0	88
Total (r_{2i})		0	29	62	25	3	0	119
Catches (c_{3i})	3	682	22 756	19 771	10 343	9 890	5 843	69 285
Recoveries								
Direct (r^{D}_{3i})		0	2	4	0	0	0	6
Indirect (r^{I}_{3i})		0	1	14	14	2	0	31
Total (r_{3i})		0	3	18	14	2	0	37
Sum over j ($r_{\cdot i}$)		0	43	95	45	6	0	189
1994								
Catches (c_{1i})	1	8	442	1 832	1 532	727	482	5 023
Recoveries								
Direct (r^{D}_{1i})		0	1	1	0	0	0	2
Indirect (r^{I}_{1i})		0	0	7	5	6	0	18
Total (r_{1i})		0	1	8	5	6	0	20
Catches (c_{2i})	2	230	3 579	12 438	12 026	5 744	4 343	38 360
Recoveries								
Direct (r^{D}_{2i})		0	6	7	0	0	0	13
Indirect (r^{I}_{2i})		0	1	12	36	7	0	56
Total (r_{2i})		0	7	19	36	7	0	69
Catches (c_{3i})	3	372	9 550	18 880	10 763	7 796	7 140	54 501
Recoveries								
Direct (r^{D}_{3i})		0	3	6	0	0	0	9
Indirect (r^{I}_{3i})		0	5	10	11	5	2	33
Total (r_{3i})		0	8	16	11	5	2	42
Sum over j ($r_{\cdot i}$)		0	16	43	52	18	2	131

© 1999 NRC Canada

Table 2 (*concluded*).

	Fishery component	Age (years) 1	2	3	4	5	6	Total
1995								
Catches (c_{1i})	1	0	111	569	761	439	220	2 100
Recoveries								
Direct (r_{1i}^{D})		0	0	2	0	0	0	2
Indirect (r_{1i}^{I})		0	0	9	12	6	3	30
Total (r_{1i})		0	0	11	12	6	3	32
Catches (c_{2i})	2	34	1 776	5 156	4 619	2 673	1 564	15 822
Recoveries								
Direct (r_{2i}^{D})		0	3	5	0	0	0	8
Indirect (r_{2i}^{I})		0	4	14	19	9	3	49
Total (r_{2i})		0	7	19	19	9	3	57
Catches (c_{3i})	3	98	6 977	6 312	10 302	11 344	8 942	43 975
Recoveries								
Direct (r_{3i}^{D})		0	11	3	0	0	0	14
Indirect (r_{3i}^{I})		0	18	20	19	12	6	75
Total (r_{3i})		0	29	23	19	12	6	89
Sum over j ($r_{\cdot i}$)		0	36	53	50	27	12	178

Note: Reported numbers of recaptured tagged fish (r_{ji}) for components j and ages i are split into direct (D, at liberty less than 8 months) and indirect (I) recaptures.

ble 2) and the test is not significant when the Yate's correction for continuity is applied, which gives $p = 0.121$.

Estimates of reporting rates and mixing parameters from the model A2 analysis, incorporating delayed mixing of 2- and (or) 3-year-old fish, are presented in Table 5. Using the likelihood ratio test to compare model A2 estimates between mixing (Table 3) and delayed mixing (Table 5) assumptions, we find that 1993 is the only year where a mixing parameter, γ_2, is significantly different from 1.0 ($p = 0.001$).

In summary, the "best" model for 1992, 1994, and 1995 is mixing model A2 (Table 3). For 1993, the mixing model A1/2 is selected by AIC (Table 3, AIC = 219 554.99), and the next best is delayed mixing model A2 (Table 5, AIC = 219 557.74). Both are better than mixing model A2 (Table 3, AIC = 219 567.63).

Using eq. 12 and the fishery component dependent reporting estimates (Table 3, model A2) and catch numbers (Table 2) as inputs, we obtained the weighted estimates of reporting rates, by age (Table 6). Note that we obtained two sets of estimates for 1993 by (*i*) applying the model A1/2 estimates of fishery component reporting rates in Table 3, by replacing λ_3 in eq. 12 with λ_{3i}, and (*ii*) using the delayed mixing model A2 estimates of λ_j in Table 5. These applications of eq. 12 are only illustrations, as they do not take into account all fishery components catching southern bluefin tuna.

Discussion

We believe that this paper makes an important contribution to the literature on reporting rate estimation for the following reasons: (*i*) it allows for two or more components of the fishery with different reporting rates and different age selectivities, (*ii*) it brings catch data into the tagging models as an auxiliary variable in a natural way, (*iii*) it allows estimation of reporting rates for ages, which were not sampled in component 1 if there are more than two fishery components, and (*iv*) it can be used as part of an integrated likelihood for tag recovery and catch data. The likelihood component L_2 (eq. 4) represents the component where the fractions of fishing by each fishery component are estimated (δ_{ji}). We have begun with the simplest possible multinomial likelihood, which assumes perfect catch and catch-at-age information. Clearly, we could extend this component to allow for catch and catch-at-age to be estimated according to some sampling procedure. We could also replace eq. 4 by a likelihood component based on relative fishing efforts in the different components. In addition, it might be possible to combine different sources of information to get even better estimators of the fishing fractions (δ_{ji}).

An alternative model (model B) for estimating reporting rates, based on different conditioning than model A, is presented in the Appendix. We provided evidence that indicates that the estimates of reporting rates from model B are similar to those from model A. Unlike model A, however, the likelihood for model B cannot be obtained from an integrated likelihood, involving fishing and natural mortality rates and reporting rates.

Delayed mixing is an important issue that we investigated. It is possible to estimate reporting rate using all the recoveries pooled (i.e., eqs. 3 and 4), provided that all fishery components have the tags nonmixed in the same way. We accommodated delayed mixing by including additional parameters in our model. If one component is nonmixed for a specified period, while another is initially mixed, then we show how to estimate these parameters by analysing recoveries of all fishery components that have been split into (*i*) direct recoveries (i.e., tags recovered during the specified period) and (*ii*) indirect recoveries (i.e., the remainder).

In the application to southern bluefin tuna, the models that

© 1999 NRC Canada

Table 3. Reporting rates (λ_j) and negative log likelihood (–LL) for components 2 and 3 by ages and calendar years 1992–1995, as estimated by models A1–A3 from data in Table 2, assuming initial mixing.

				Likelihood ratio test between successive models				
Model	Age (years)	λ_2	λ_3	–LL	df	χ^2	p	AIC
1992								
A1	2	0.2491	0.1086	40 224.76	4			80 457.52
	3	0.1636	0.1182	27 501.38	4			55 010.75
	Total			67 726.14	8			135 468.29
					2	1.33	0.514	
A2	2–3	0.1955	0.1032	67 726.80	6			135 465.60[a]
		(0.0322)	(0.0279)					
					2	13 602.68	0.000	
A3	2–3	0.1961	0.1021	74 528.14	4			149 064.28
1993								
A1	2	0.5696	0.0442	39 862.41	4			79 732.83
	3	0.6099	0.2366	45 321.93	4			90 651.86
	4	0.4533	0.4031	24 583.01	4			49 174.01
	Total			109 767.35	12			219 558.70
					2	0.30	0.861	
A1/2	2	0.5653	0.0440					
	3	0.5653	0.2227					
	4	0.5653	0.4835	109 767.50	10			219 554.99[b]
					2	16.64	0.000	
A2	2–4	0.5456	0.1980	109 775.82	8			219 567.63
		(0.1073)	(0.0479)					
					4	2 847.21	0.000	
A3	2–4	0.5671	0.1939	111 199.42	4			222 406.84
1994								
A1	2	0.8645	0.3703	9 653.77	4			19 315.54
	3	0.3498	0.1941	28 170.69	4			56 349.39
	4	0.9172	0.3131	21 521.47	4			43 050.95
	5	0.1477	0.0777	12 121.00	4			24 250.00
	Total			71 466.94	16			142 965.87
					6	7.71	0.260	
A2	2–5	0.4692	0.2011	71 470.79	10			142 961.58[c]
		(0.0872)	(0.0456)					
					4	2 553.38	0.000	
A3	2–5	0.4629	0.1929	72 747.48	4			145 502.97
1995								
A1	3	0.1906	0.1885	10 238.48	4			20 484.96
	4	0.2609	0.1170	12 331.02	4			24 670.03
	5	0.2464	0.0774	8 824.47	4			17 656.93
	6	0.1407	0.0492	5 505.59	4			11 019.18
	Total			36 899.55	16			73 831.10
					6	7.51	0.276	
A2	3–6	0.2141	0.1177	36 903.31	10			73 826.61[d]
		(0.0489)	(0.0263)					
					6	3 412.15	0.000	
A3	3–6	0.2218	0.1600	38 609.38	4			77 226.76

Note: Selection of models is based on the likelihood ratio test and AIC. Standard errors are in parentheses.
[a]Best model for 1992.
[b]Best model for 1993.
[c]Best model for 1994.
[d]Best model for 1995.

took age structure into account were better, according to AIC, than pooling data (model A3). In comparing results from models A2 and A3, the largest bias occurred in 1995 when the reporting rate of fishery component 3 was estimated to be $\lambda_3 = 0.1177$ by model A2 but $\lambda_3 = 0.1600$ by model A3 (+36% bias).

We believe that the reason why the estimate of the reporting rate λ_2 is consistently larger than λ_3 is because the in-

© 1999 NRC Canada

Table 4. Reporting rates (λ_j), mixing parameter (γ_i), and negative log likelihood (–LL) for components 2 and 3, ages 2 and 3 years, and calendar years 1992–1995 estimated by delayed mixing model A1 from data in Table 2.

Model A1	Age (years)	λ_2	λ_3	γ_i	–LL	df	AIC	p
1992	2	0.2491	0.1379	0.6857	40 224.57	5	80 459.14	0.538
	3	0.1636	0.1261	0.6833	27 501.32	5	55 012.63	0.729
1993	2	0.5696	0.0842	0.4242	39 862.21	5	79 734.43	0.527
	3	0.6099	0.2180	1.5476	45 321.71	5	90 653.42	0.507
1994	2	0.6444	1.0000	0.1233	9 651.59	4	19 311.18	0.037[a]
	3	0.3498	0.1724	1.4250	28 170.55	5	56 351.11	0.597
1995	3	0.1906	0.2138	0.4929	10 238.02	5	20 486.03	0.337

Note: The likelihood ratio test (p) compares results from mixing model A1 estimates (Table 3) and delayed mixing model A1 (this table).
[a]Applying Yate's correction for continuity gives $p = 0.121$.

Table 5. Reporting rates (λ_j), mixing parameters (γ_i), and negative log likelihood (–LL) for components 2 and 3, ages 2 and 3 years, and calendar years 1992–1995 estimated by delayed mixing model A2 from data in Table 2.

Model A2	Age (years)	λ_2	λ_3	γ_2	γ_3	–LL	df	AIC	p
1992	2–3	0.1963	0.1303	0.6091	0.7596	67 726.30	8	135 468.60	0.607
1993	2–4	0.5579	0.2718	0.1295	1.0000	109 769.87	9	219 557.74	0.001
1994	2–5	0.4579	0.2036	0.4548	1.4566	71 469.86	12	142 963.71	0.395
1995	3–6	0.2142	0.1181	na	0.9598	36 903.30	11	73 828.61	0.888

Note: The likelihood ratio test (p) compares results from mixing model A2 (Table 3) and delayed mixing model A2 (this table).

Table 6. Weighted estimates (eq. 12) of reporting rate λ by ages i = 2–6 years and calendar years 1992–1995.

	Weighted λ for age (years)					λ for fishery component	
	2	3	4	5	6	2	3
1992	0.1696	0.2119	0.1814	0.1733	0.1612	0.1955	0.1032
1993	0.3295	0.4639	0.5629	0.5494	0.5467	0.5653	0.0440[a]
							0.2227[b]
							0.4835[c]
1993	0.4458	0.4794	0.4819	0.4495	0.4432	0.5579	0.2718[d]
1994	0.2978	0.3458	0.3840	0.3498	0.3306	0.4692	0.2011
1995	0.1481	0.2007	0.1889	0.1623	0.1499	0.2141	0.1177

Note: For 1992, 1994, and 1995 the input fishery component reporting rates are from model A2 (Table 3). The first 1993 estimates are derived from model A1/2 (Table 3) estimates of fishery component reporting rates. The second 1993 estimates are derived from delayed mixing model A2 Table 5 estimates of fishery component reporting rates.
[a]Estimated reporting rate of component 3 at age 2 years (model A1/2 for 1993, Table 3).
[b]Reporting rate of component 3 at age 3 years (model A1/2 for 1993, Table 3).
[c]Reporting rate of component 3 at age 4 years and older (model A1/2 for 1993, Table 3).
[d]Reporting rate from delayed mixing model A2 for 1993 (Table 5).

zone fishery (component 2) has more contact with scientists and observers than the out-of-zone fishery (component 3). Additionally, all in-zone vessels are required to come into port after the completion of fishing, during which time, a tag liaison officer is able to personally visit most vessels to ask for tags and provide rewards. However, incomplete mixing might be an additional contributing factor.

The estimates of the southern bluefin tuna longline reporting rates were low in 1992 and 1995. However, low reporting rates are common in other species, e.g., $\lambda = 0.18$ for lake trout (*Salvelinus namaycush*) (Youngs 1974). A low reporting rate might be expected in 1992, as it was only the second year of the tagging program, when publicity coverage of the longline fishery was incomplete.

As an illustration, we obtained pooled estimates of age-specific reporting rates for three southern bluefin tuna fishery components for the years 1992–1995. These were weighted averages of the individual fishery component reporting rates with the weights being the catches in each component at each age (c_{ji}). This enables one to estimate fishing and natural mortalities, by age, by using one reporting rate adjustment for each age–year cell. In a companion paper, we show that these weighted averages are derived from an integrated likelihood, which allows for estimates of fishing and natural mortalities as well as reporting rates.

Acknowledgments

We acknowledge the vital contributions made by those involved in the tagging program during the 1990's and the AFMA observer program. Specifically, we thank Kevin Williams and Deidre Waddington (WW Fisheries), Yuji Kawai (Federation of Japan Tuna), the vessel visitation staff in Australia, New Zealand, and South Africa, and the fishing masters, captains, and crew of participating vessels. It is only through industry cooperation that tagging programs can

© 1999 NRC Canada

succeed. We thank Dr. Ann Cowling, Mr. Dennis Reid, and two referees for valuable comments on a previous draft of the paper. We thank the Bureau of Resource Sciences, Department of Primary Industries and Energy, Canberra, Australia, for their fellowship supporting K.H. Pollock.

References

Akaike, H. 1971. Information theory and an extension of the maximum likelihood principle. *In* Second International Symposium on Information Theory. *Edited by* B.N. Petrov and F.C. Sahi. Akademiai Kiado, Budapest, Hungary. pp. 267–281.

Akaike, H. 1974. A new look at the statistical model identification. IEEE Trans. Automated Control AC-19. pp. 716–723.

Anonymous. 1994. Report of the southern bluefin tuna trilateral workshop. Southern Bluefin Tuna Trilateral Workshop, Hobart, Australia, 17 January – 4 February 1994. (Available from Commission for Conservation of Southern Bluefin Tuna, P.O. Box 37, Deakin West, ACT 2600, Australia.)

Beverton, R.J.H., and Holt, S.J. 1957. On the dynamics of exploited fish populations. Fish. Invest. Ser. II Mar. Fish. G.B. Minist. Agric. Fish. Food No. 19.

Brownie, C., Anderson, D.R., Burnham, K.P., and Robson, D.S. 1985. Statistical inference from band recovery data: a handbook. 2nd ed. U.S. Fish Wildl. Serv. Resour. Publ. 156.

Buckland, S.T., Anderson, D.R., Burnham, K.P., and Laake, J.L. 1993. Distance sampling: estimating abundance of biological populations. Chapman and Hall, London and New York.

Caton, A.E. 1991. Review of aspects of southern bluefin tuna: biology, population and fisheries. *In* World meeting on stock assessment of bluefin tunas: strengths and weaknesses. *Edited by* R.B. Deriso and W.H. Bayliff. Inter-Am. Trop. Tuna Comm. Spec. Rep. 7. pp. 181–357.

Green, A.W., Matlock, G.C., and Weaver, J.E. 1983. A method for directly estimating the tag-reporting rate of anglers. Trans. Am. Fish. Soc. **112**: 412–415.

Hearn, W.S., Leigh, G.M., and Beverton, R.J.H. 1991. An examination of a tag-shedding assumption, with application to southern bluefin tuna. ICES J. Mar. Sci. **48**: 41–51.

Hearn, W.S., Pollock, K.H., and Brooks, E.N. 1998. Pre- and post-season tagging models: estimation of reporting rate and fishing and natural mortality rates. Can. J. Fish. Aquat. Sci. **55**: 199–205.

Henny, C.J., and Burnham, K.P. 1976. A reward band study of mallards to estimate band reporting rates. J. Wildl. Manage. **40**: 1–14.

Hoenig, J.M., Barrowman, N.J., Hearn, W.S., and Pollock, K.H. 1998*a*. Multiyear tagging studies incorporating fishing effort data. Can. J. Fish. Aquat. Sci. **55**: 1466–1476.

Hoenig, J.M., Barrowman, N.J., Pollock, K.H., Brooks, E.N., Hearn, W.S., and Polacheck, T. 1998*b*. Models for tagging data that allow for incomplete mixing of newly tagged animals. Can. J. Fish. Aquat. Sci. **55**: 1477–1483.

Kimura, D.K. 1976. Estimating the total number of marked fish present in a catch. Trans. Am. Fish. Soc. **105**: 664–668.

Kirkwood, G.P. 1981. Generalized models for the estimation of rates of tag shedding by southern bluefin tuna (*Thunnus maccoyii*). J. Cons. Cons. Int. Explor. Mer, **39**: 256–260.

Paulik, G.J. 1961. Detection of incomplete reporting of tags. J. Fish. Res. Board Can. **18**: 817–832.

Polacheck, T., and Preece, A. 1996. Preliminary comparisons of the growth rates of southern bluefin tuna in the 1990s with those in the 1960s and 1980s. Eighth Workshop on SBT Monitoring Surveys and Tagging Programs, Hobart, Australia, 23–25 July 1996. RMWS/96/6. (Available from Commission for Conservation of Southern Bluefin Tuna, P.O. Box 37, Deakin West, ACT 2600, Australia.)

Pollock, K.H., Hoenig, J.M., and Jones, C.J. 1991. Estimation of fishing and natural mortality when a tagging study is combined with a creel survey or port sampling. Am. Fish. Soc. Symp. **12**: 423–434.

Siddeek, M.S.M. 1989. The estimation of natural mortality in Irish Sea plaice, *Pleuronectes platessa* L., using tagging methods. J. Fish Biol. **35**(Suppl. A): 145–154.

Siddeek, M.S.M. 1991. Estimation of natural mortality of Kuwait's grooved tiger prawn *Penaeus semisulcatus* (de Haan) using tag–recapture and commercial fisheries data. Fish. Res. **11**: 109–125.

White, G.C. 1983. Numerical estimation of survival rates from band-recovery and biotelemetry data. J. Wildl. Manage. **47**: 716–728.

Youngs, W.D. 1974. Estimation of the fraction of anglers returning tags. Trans. Am. Fish. Soc. **103**: 616–618.

Appendix. Model B for estimating reporting rates

We present another conditional model, model B, for which we focus on the proportion (α_i) of tagged fish in the population of age i fish. We use similar notation as for model A. There are s fisheries, 1, 2,..., j,..., s, and k age-classes, 1, 2,..., i,..., k, in which some of the fish have been tagged. There are c_{ji} fish caught by fishery component j at age i, from which r_{ji} fish are reported as having tags.

At age i, the probability that a caught fish is tagged is α_i. For fishery component j, the probability that a tagged fish is caught and returned is $\lambda_{ji}\alpha_i$, where λ_{ji} is the reporting rate of age i fish for fishery component j. It is assumed that fishery component 1 reliably reports 100% of tags that it catches. Thus, for component 1, $\lambda_{1i} = 1.0$ for all ages 1, 2,..., i,..., k.

Given these assumptions, the likelihood function for λ_{ji} and α_i is a product of binomial distributions conditional on the catches c_{ji}:

$$\text{(A1)}\quad L(\lambda_{ji},\alpha_i) = \prod_{i=1}^{k}\binom{c_{1i}}{r_{1i}}\alpha_i^{r_{1i}}(1-\alpha_i)^{c_{1i}-r_{1i}}\prod_{j=2}^{s}\binom{c_{ji}}{r_{ji}}(\lambda_{ji}\alpha_i)^{r_{ji}}(1-\lambda_{ji}\alpha_i)^{c_{ji}-r_{ji}}.$$

As for model A, we propose three increasingly restrictive models: model B1, α_i and λ_{ji} distinct parameters; model B2, α_i and λ_j distinct parameters; model B3, α and λ_j distinct parameters.

© 1999 NRC Canada

Model B1

For this most general model, which we refer to as model B1, the maximum likelihood estimators are explicit and take the following forms:

$$\text{(A2)} \quad \hat{\alpha}_i = \frac{r_{1i}}{c_{1i}} \qquad i = 1, \ldots, k$$

$$\text{(A3)} \quad \hat{\lambda}_{ji} = \frac{r_{ji} c_{1i}}{c_{ji} r_{1i}} \qquad i = 1, \ldots, k \text{ and } j = 2, \ldots, s.$$

Note that models A1 and B1 give identical estimates of the λ's, which is expected, as they are general saturated models (somewhat analogous to fitting a straight line to two points).

Model B2

We present another model with less parameters, which we refer to as model B2, where reporting rates are fishery dependent but not age dependent (i.e., $\lambda_{ji} = \lambda_j$). In this case, explicit maximum likelihood estimators are not obtained, but a numerical maximisation routine (e.g., MINIMD or SURVIV) can be used to obtain the estimators iteratively. Models A2 and B2 give similar estimates for λ's, but because they are not saturated general models, their estimates are not expected to be identical in all cases. We illustrate this property in the Results section of the main text from analyses of southern bluefin tuna data.

Model B3

Another model is the case of α_i and λ_{ji} being constant over all ages i, for which the maximum likelihood estimators take the closed form

$$\text{(A4)} \quad \hat{\alpha} = \frac{\sum_{i=1}^{k} r_{1i}}{\sum_{i=1}^{k} c_{1i}}$$

$$\text{(A5)} \quad \hat{\lambda}_j = \frac{\sum_{i=1}^{k} r_{ji} \sum_{i=1}^{k} c_{1i}}{\sum_{i=1}^{k} c_{ji} \sum_{i=1}^{k} r_{1i}}.$$

Note that models A3 and B3 give identical estimates of the λ's, which is expected, as they are general saturated models for the pooled data.

© 1999 NRC Canada

Modeling the spatial dynamics of the U.S. purse-seine fleet operating in the western Pacific tuna fishery

H.F. Campbell and A.J. Hand

Abstract: Two qualitative choice models of the location decisions of U.S. purse-seine vessels operating in a total of sixty-five 5° grids in the western Pacific tuna fishery are developed and compared. A nested logit model in which decisions are first made about where to fish in the east–west plane, followed by a choice of grid in the north–south plane, performs better than a nonnested model in which all grids are considered simultaneously. The nested model can be used for the allocation of purse-seine fishery effort in a spatially disaggregated bioeconomic model of the regional tuna fishery.

Résumé : On présente et compare deux modèles de choix qualitatifs pour la détermination des lieux de pêche du thon à la senne coulissante par les bateaux américains dans un total de 65 grilles de 5° dans l'ouest du Pacifique. Un modèle logit hiérarchique dans lequel on choisit d'abord les lieux de pêche dans le plan est–ouest pour ensuite choisir des grilles dans le plan nord–sud donne de meilleurs résultats qu'un modèle non hiérarchique dans lequel toutes les grilles sont considérées simultanément. Le modèle hiérarchique peut être utilisé pour l'allocation de l'effort de pêche à la senne coulissante selon un modèle bio-économique spatialement désagrégé de la pêche régionale du thon.

[Traduit par la Rédaction]

Introduction

Very few bioeconomic models have included models of fleet dynamics, simply because most population dynamics models developed have been spatially aggregated: an even distribution of stocks is assumed and catch is therefore independent of the spatial distribution of fishing effort (Gillis et al. 1993). The only fleet spatial dynamics models that, to our knowledge, have been included in bioeconomic models are found in Hilborn and Walters (1987) and Sampson (1992). In both cases, no attempt was made to parameterise the explanatory variables in the model (value of catch per unit effort (VCPUE) in Hilborn and Walters (1987) and distance from port and VCPUE in Sampson (1992)).

Tuna species are highly migratory, and recent tuna population dynamics models have been spatially disaggregated. Examples are a model of the skipjack tuna (*Katsuwonus pelamis*) fishery in the Solomon Islands fishing zone by Kleiber and Hampton (1994) and a model of the western Pacific region's skipjack tuna fishery by Bertignac et al. (1997). Under preparation is a four-species (albacore (*Thunnus alalunga*), bigeye tuna (*Thunnus obesus*), yellowfin tuna (*Thunnus albacares*), and skipjack tuna), three-gear-type (longline, pole-and-line, and purse seine) model of the western Pacific tuna fishery (WPTF). In this model, which is being developed by Bertignac et al. (1997), stock levels, and hence fishing conditions, will vary with respect to both month and location defined by 5° squares. Initial versions of this model use the historical average level and spatial distribution of effort to predict catches, given the predicted distribution of fish stocks. However, a more complete model would also attempt to explain the movement of fishing effort in response to changes in fishing conditions.

A number of fleet spatial dynamics models (Bockstael and Opaluch 1983; Eales and Wilen 1986; Campbell et al. 1993; Dupont 1993; Morey et al. 1993) are set in a utility-theoretic qualitative choice framework. Use of a qualitative choice framework allows the influence of variables, such as catch rate expectations and distance from port, on choice of fishing location to be estimated. This type of approach has been motivated by the desire to learn more about what governs skippers' movement patterns (Bockstael and Opaluch 1983) and to test for the sharing of catch rate information (Campbell et al. 1993).

Qualitative choice models designed for these purposes have tended to use data at a low degree of spatial resolution because of the need for continuity of fishing effort across periods and locations (Campbell et al. 1993). In the present study, however, the application of a multinomial logit model to 5° grid catch effort data demonstrates that a qualitative choice framework can be applied even when a relatively fine degree of spatial resolution is required for consistency with a population dynamics model. This parametric approach is considered preferable to the use of arbitrary movement rules (Hilborn and Walters 1987; Anganuzzi 1994) in bioeconomic models.

In a recent study of purse-seine fleet movement, Vignaux (1996) analysed the movement of the purse-seine fleet oper-

Received January 6, 1998. Accepted December 15, 1998. J14370.

H.F. Campbell[1] **and A.J. Hand.** Department of Economics, University of Queensland, Brisbane, Queensland, 4072, Australia.

[1]Author to whom all correspondence should be addressed. e-mail: h.campbell@economics.eq.edu.au

© 1999 NRC Canada

Fig. 1. Western Pacific purse-seine tuna fishery (source: South Pacific Commission).

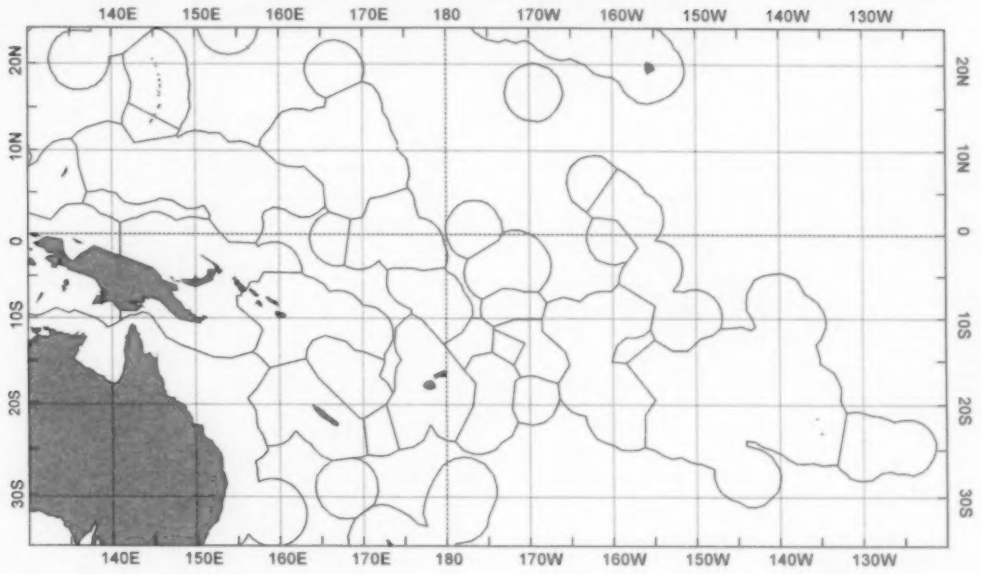

ating in the New Zealand hoki (*Macruronus novaezelandiae*) fishery and concluded that there is no evidence that there is sufficient information transfer for vessels to make decisions on the basis of other vessels' catch rates. The estimated parameters of the model developed in the present study suggest that this is not the case for the U.S. purse-seine fleet operating in the WPTF and that there is extensive information sharing.

Methods

Data

The U.S. fleet's current fishing agreement is the only comprehensive multilateral treaty with all of the Forum Fisheries Agency (FFA) member countries: Australia, Cook Islands, Federated States of Micronesia, Fiji, Kiribati, Marshall Islands, Nauru, New Zealand, Niue, Palau, Papua New Guinea, Solomon Islands, Tonga, Tuvalu, Vanuatu, and Western Samoa. Because the treaty is multilateral, the U.S. fleet is virtually unconstrained as to which parts of the fishery it can access. The U.S. fleet has been granted only very limited access to the Solomon Islands fishing zone, an aspect of the multilateral agreement that the U.S. Tuna Boat Association considers to be somewhat of an anomaly (T. Kingston, FFA, personal communication).

Further, the U.S. government pays for $US 14 million, i.e., 78%, of the $US 18 million annual access fee for the U.S. fleet. The $US 18 million annual fee was negotiated between the U.S. Tuna Boat Association and FFA member countries in June 1993 and was fixed for the contract period, i.e., until June 1998, with the number of boats used restricted to 55. The payment of fees by the U.S. government and the long-term nature of the agreement reduce the incentive for the fleet to underreport catch. This is in contrast with access arrangements for other distant water fishing nations that generally include a fee that is set at a notional 5% of expected revenue, with expected revenue based on logbook data, thereby providing an incentive to underreport catch (South Pacific Commission 1992). The absence of constraints on area fished and the high quality of catch and effort data make the U.S. purse-seine logbook data the most suitable data available for the modeling of fleet dynamics in the WPTF.

The data used in this study are for the March 1988 to December 1995 period. Data extending as far back as 1984 were also available, but the U.S. fleet started providing logbook entries for all waters fished in the region, high seas and exclusive economic zones (EEZ's), from March 1988 under the provisions of a new fishing agreement. Before this time, it was obliged to provide logbook entries only for catch taken within the EEZ's of FFA member countries.

The logbook data, aggregated across vessels, show for each month t and for each of the J grids, which are identified by their 5° latitude and longitude midpoints, how much catch of each species was taken by the fleet, how many days were fished, and how many sets were made. For each month, the number of observations in the data set is equal to the number of grids fished. While one hundred and thirty-six 5° longitude × 5° latitude grids (i.e., one hundred and thirty-six 5° square grids) were fished by the fleet in the March 1988 to December 1995 sample period, 97% of fishing effort occurred in 65 grids contained within the area extending from 135°E to 160°W in the longitudinal plane and from 10°N to 15°S in the latitudinal plane (see Fig. 1). Only fishing that occurred in this 65-grid sector is included in the model.

Since the model developed in the paper is estimated using data that are aggregated across vessels, the modeling of fleet dynamics is on the basis of grid-specific variables only. This is compatible with population dynamics models where within-fleet fishing effort is usually assumed to be homogenous.

Expectations about value per unit fishing effort

The fleet spatial dynamics model is a qualitative choice model that uses a number of "$t - 1$" variables to predict the redistribution of fishing effort in period t. One of the variables is catch rate expectations. Since grid-specific catch rates are characterised by large amounts of uncertainty and volatility, it was considered appropriate to follow the Eales and Wilen (1986) approach and utilise a submodel of catch rate expectations.

Relative grid profitability and therefore movement decisions are affected by prices if catch composition varies across grids. As catch composition does vary between grids, it was decided to use a

© 1999 NRC Canada

Fig. 2. Distribution of fishing effort for three different ENSO phases.

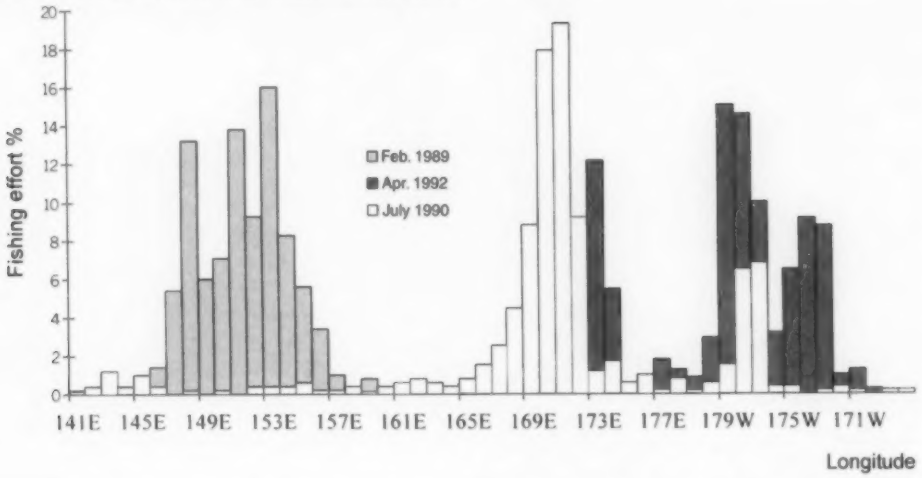

submodel of expectations for the value equivalent of catch rate expectations, expected value per unit effort (VPUE), instead of expected catch per unit effort (CPUE).

Further, because of concern that large changes in average productivity between months could affect the stability of the VPUE expectations parameter estimate in the qualitative choice model, the model was based on the relative value of catch expectations, as defined by the ratio of $VPUE_{jt}$ to the average VPUE in period t, $\Sigma_{j=1}^{J} VPUE_{jt}/J$ (this ratio is subsequently referred to as $VRatio_{jt}$), rather than on VPUE expectations directly.

Various types of expectations models have been used: Mangel and Clark (1983) and Campbell et al. (1993) used Bayesian updating of expectations, Bockstael and Opaluch (1983) used an adaptive expectations model, and Dupont (1993) used a rational expectations approach to modeling expected fish prices. Eales and Wilen (1986) used a naive expectations model in the sense that fishers are assumed to use yesterday's mean catch to predict today's expected catch. The assumption in the present study is that fishers' catch rate expectations are based on the previous period's catch (naive expectations) supplemented by seasonal and historical information about stock behaviour and information about the fishing locations of the fleet as a whole (rational expectations).

Expected catch rates, or more specifically, $VRatio_{jt}$ expectations for period t ($E(VRatio_{jt})$), are assumed to be a determinant of skippers' movement decisions (Hilborn and Ledbetter 1979; Bockstael and Opaluch 1983). These expectations may be updated many times during a single day as radio information is received from code group members and sightings of positive signs, such as bird life, are made. As monthly data are used in the present study, the objective is to develop a $VRatio_{jt}$ expectations model to proxy the outcome of the expectations formed within a month.

Spatial aggregation

Spatial aggregation up to the level at which there is at least some fishing in all grids in all periods has always been used in qualitative choice models of fleet spatial dynamics. Bockstael and Opaluch (1983), Eales and Wilen (1986), Campbell et al. (1993), and Dupont (1993) all aggregated sufficiently to ensure continuity of fishing effort before applying their data to qualitative choice models of fleet spatial dynamics. Because there are such substantial spatial shifts in the western Pacific tuna resource, aggregating to such an extent would leave the present model providing very little information about fleet dynamics.

Figure 2 shows the distribution of fishing effort within the main fishing area during three selected periods: April 1992, which had a Southern Oscillation index (SOI) lagged 3 months (SOI3) of –3.4, the lowest during the sample period; February 1989, which had an SOI3 of 1.9, the highest SOI for the period; and July 1990, which had an SOI3 equal to 0. Thus, Fig. 2 shows the distribution of fishing effort during two extreme SOI3 months and one midrange month. Other than some fishing around American Samoa, there was virtually no fishing in the eastern part of the fishery during February 1989 when SOI3 was very high. Conversely, when SOI3 was very low in April 1992, there was virtually no fishing in the western part of the fishery. When SOI3 was in the midrange, most fishing took place in the 163–173°E band, with a second smaller concentration of fishing effort at 177 and 179°W. Thus, vessels were fishing in a fairly concentrated area even when SOI3 was not at either of the extremes of its range.

In fact, the shifts in the resource induced by El Niño/Southern Oscillation (ENSO), as illustrated in Fig. 2, are so pronounced that no more than two grids could be used if continuity of fishing effort was required for the sample period. In order to allow a large number of grids to be included in the estimated model, values of zero were assigned to the CPUE in all grids in which there was no fishing in period $t - 1$. An expectations model that includes grids where no fishing occurred in $t - 1$ can be constructed, which in turn facilitates the use of utility functions for period $t - 1$, for all 65 grids. These utility functions are required in the qualitative choice model of fleet dynamics (see Qualitative choice models section). In this way, it is possible to develop a fleet spatial dynamics model set in a qualitative choice framework with a high degree of spatial resolution.

Catch rates in period t – 1

CPUE or its value equivalent, VPUE, has been used as the sole explanatory variable in all models of catch rate expectations developed to date (Bockstael and Opaluch 1983; Eales and Wilen 1986; Campbell et al. 1993). The use of $CPUE_{jt-1}$ or $VPUE_{jt-1}$ as a principal explanatory variable for $E(CPUE_{jt})$ or $E(VPUE_{jt})$ is due to the short-term nature of expectations about fishing conditions. Similarly, in the expectations model developed in this study, $VRatio_{jt-1}$ is used as the principal variable available for forecasting $VRatio_{jt}$. Reasons are now considered for the inclusion of a number of other variables in the expectations model.

Effect of stock and migratory effects on expectations

While $VRatio_{jt-1}$ is clearly an important explanatory variable in

© 1999 NRC Canada

a model of expectations about $VRatio_{jt}$, it has some limitations. The first problem is the weakening of the relationship between $VRatio_{jt-1}$ and $VRatio_{jt}$ caused by the migratory nature of tuna. The relationship may also be weakened by the "fish-down" effect. The fish-down effect is the reduction in CPUE that occurs in an area because of a reduction in stock as a result of fishing activity. Assume for the moment that tuna were not migratory; then, a large number of fishing days in grid j in period $t-1$ would tend to reduce the stock in that grid in period t. A lower initial stock in period t would be associated with a lower catch rate in that grid in period t for any given level of effort. This suggests that other things being equal, the stock effect will result in a lower expected value of $VRatio_{jt}$ the greater the number of days fished in grid j in period $t-1$.

VRatios in grids to the north, northeast, east, southeast, south, southwest, west, and northwest of grid j were also used as explanatory variables because the migratory nature of the stocks suggests that if there is high VRatio in a grid near grid j in period $t-1$, then expectations for grid j should be higher than otherwise. This is a reasonable assumption given that skippers do have a general understanding of migratory paths (Orbach 1977).

Proxies for the amount of search as an explanatory variable

Expectations will be higher the more searching occurring within an area. This is because skippers may share catch rate information and also because the probability of finding stocks depends on localised search for positive signs such as bird life or the schools themselves using binoculars and "spotter" helicopters. Days fished in grid j lagged once and twice, $Days_{jt-1}$ and $Days_{jt-2}$, are included in the model to account for the higher expectations for catch rates in grid j brought about by the greater amount of search. Due to the stock effect and migration, fishing in one grid may also imply that searching will be greater in surrounding grids, if sizeable aggregations are not found in that particular grid. Hence, it was considered reasonable to assume that search in a grid is also likely to be higher the greater the number of days fished in adjoining grids. Days fished in grids to the north, northeast, east, southeast, south, southwest, west, and northwest of grid j in period $t-1$ were therefore also used as explanatory variables for $E(VRatio_{jt})$. Due to the fish-down effect, however, more days fished in a previous period may lead to a reduction in catch rate expectations, and therefore, there is no a priori expectation for the sign of the coefficient on days fished.

Knowledge of areas with "favourable" conditions

Some grids are inherently more favourable to tuna than others due to currents, nutrient levels, water temperature, thermocline depth, and proximity to landmasses (Bertignac et al. 1997). Skippers, while perhaps not having a technical knowledge of these factors, do use their experience about where catch rates were higher in the past to form their expectations. Grid dummies, $Grid_{jt}$, are included in the expectations model to account for skippers' collective knowledge about such favourable conditions.

Effect of the SOI on water temperature and expectations

Figure 2 contrasts the distribution of fishing effort for three different levels of the SOI. Movements of the gravity centre of the 29° thermocline, the optimal level for tuna forage and therefore tuna, are strongly correlated with movements of the SOI (Lehodey et al. 1997). When there is an El Niño event, the index is large and negative and most fishing is in the east of the fishery because conditions (i.e., thermocline depth, water temperature, and currents) in the east become favourable. When there is a La Niña event, the index is large and positive and more stocks are found in the west and fishing effort follows.

Skippers may not have the detailed understanding of the relationship between the SOI and the distribution of tuna that biologists have. They do, however, use water temperature sensors, and discussions with operators have confirmed that they have a reasonably precise knowledge of the optimal water temperature for tuna. It is therefore appropriate to include the SOI in a model of catch rate expectations as a proxy for water temperature. As a given value of the SOI implies different water temperatures for different grids, it is necessary to include SOI3–grid interaction variables ($SOI3_t \times Grid_j$).

Distance of gravity centre of fishing effort from grid and change in distance of gravity centre from grid

Movements of the tuna fleet to a greater or lesser degree track the migratory patterns of tuna stocks. Assuming that information about the spatial distribution of the fleet is widely available, catch rate expectations for a particular grid will be higher the closer that grid is to the centre of gravity of the fleet. The rate of movement of the centre of gravity towards a particular grid may be an indicator of the rate at which the principal tuna aggregations are moving towards the grid. To pick up the effect of fleet movements on individual vessel catch rate expectations, the distance of the gravity centre of the fleet from grid j in period $t-1$, $Dist_{jt-1}$, and the changes in that distance between periods $t-1$ and $t-2$, $Distdif_{jt-1}$, and between periods $t-2$ and $t-3$, $Distdif_{jt-2}$, are included as explanatory variables.

Expectations model

With inclusion of all the abovementioned variables, the VRatio expectations model takes the following form:

$$
\begin{aligned}
(1)\qquad E(\mathrm{VRatio}_{jt}) = {} & \beta_0 + \beta_1 \mathrm{VRatio}_{jt-1} + \beta_2 \mathrm{Days}_{jt-1} \\
& + \beta_3\ \mathrm{Days}_{jt-2} + \beta_4\ \mathrm{SOI3}_t \\
& + \sum_{j=1}^{64} \gamma_j\ \mathrm{Grid}_{jt}\ \mathrm{SOI3}_t \\
& + \beta_6\ \mathrm{VRatio}^{\mathrm{N}}_{jt-1} + \beta_7\ \mathrm{VRatio}^{\mathrm{NE}}_{jt-1} \\
& + \beta_8\ \mathrm{VRatio}^{\mathrm{E}}_{jt-1} + \beta_9\ \mathrm{VRatio}^{\mathrm{SE}}_{jt-1} \\
& + \beta_{10}\ \mathrm{VRatio}^{\mathrm{S}}_{jt-1} + \beta_{11}\ \mathrm{VRatio}^{\mathrm{SW}}_{jt-1} \\
& + \beta_{12}\ \mathrm{VRatio}^{\mathrm{W}}_{jt-1} + \beta_{13}\ \mathrm{VRatio}^{\mathrm{NW}}_{jt-1} \\
& + \beta_{14}\ \mathrm{Days}^{\mathrm{N}}_{jt-1} + \beta_{15}\ \mathrm{Days}^{\mathrm{NE}}_{jt-1} \\
& + \beta_{16}\ \mathrm{Days}^{\mathrm{E}}_{jt-1} + \beta_{17}\ \mathrm{Days}^{\mathrm{SE}}_{jt-1} \\
& + \beta_{18}\ \mathrm{Days}^{\mathrm{S}}_{jt-1} + \beta_{19}\ \mathrm{Days}^{\mathrm{SW}}_{jt-1} \\
& + \beta_{20}\ \mathrm{Days}^{\mathrm{W}}_{jt-1} + \beta_{21}\ \mathrm{Days}^{\mathrm{NW}}_{jt-1} \\
& + \beta_{22}\ \mathrm{Dist}_{jt-1} + \beta_{23}\ \mathrm{Distdif}_{jt-1} \\
& + \beta_{24}\ \mathrm{Distdif}_{jt-2} + \sum_{y=1}^{64} \delta_y\ \mathrm{DGrid}_{yt} + \varepsilon_{jt}.
\end{aligned}
$$

Prices of $US 957/t for skipjack tuna, $US 1000/t for bigeye tuna, and $US 1063/t for yellowfin tuna (Hand and Forau 1997) are used to convert CPUE to VPUE before calculating the respective ratios.

Qualitative choice models

Qualitative choice models are appropriate where the underlying decision is between discrete alternatives. The discrete choice model is the type of qualitative choice model used in the present study. It is appropriate where there are more than two choices and if choice-specific variables are included within the utility function (Greene 1991*b*). In period t, each skipper chooses between J alter-

© 1999 NRC Canada

natives. The J alternatives are each characterised by a vector of attributes, x_{jt}:

$$(2)\quad U(\text{choice } j \text{ in period } t) = U_{jt} = \beta' x_{jt} + \varepsilon_{jt},\ j = 1, \ldots, J.$$

The random, period-specific terms (ε_{1t}, ε_{2t},..., ε_{Jt}) are assumed to be independently distributed, each with an extreme value (Gumbel) distribution, which can be shown to imply that the probability of choosing grid j in period t (Greene 1996) is

$$(3)\quad \Pr[y_t = J] = \frac{\exp(\beta' x_{jt})}{\sum_{j=1}^{J} \exp(\beta' x_{jt})}.$$

The model is parameterised using full information maximum likelihood (FIML) estimation.

Because the data are aggregated across vessels and within months, the dependent variable is expressed as a proportion of total fishing effort for the month in each grid, rather than taking on the 0, 1, 2,..., J form shown in eq. 3. This type of dependent variable can be used instead of the discrete dependent variable described in eq. 3 whenever the underlying choice is discrete (Greene 1991*b*, p. 418) such as the choice by each skipper between grids. The statistical package used to estimate the model, LIMDEP 7.0, automatically recognises the "proportions" type of dependent variable in qualitative choice models. Thus, in eq. 3, $\Pr[y_t = J]$ can be replaced by Proportion_{jt}, the proportion of total fishing effort in grid j at time t:

$$(4)\quad \text{Proportion}_{jt} = \frac{\exp(\beta' x_{jt})}{\sum_{j=1}^{J} \exp(\beta' x_{jt})}.$$

Since the proportions were calculated from groups containing different numbers of observations, they are weighted by the number of observations in each group in order to counteract the inherent heteroscedasticity resulting from observations with different variances. The hypothesised x_{jt} variables are as follows.

(*i*) Expected VRatio_{jt} ($E(\text{VRatio}_{jt})$). The importance of this variable, which measures the current performance of the fleet as a whole in grid j, will depend on the amount of information sharing among vessels.

(*ii*) Distance (kilometres) of the grid from the home port of American Samoa (DISTPT_{jt}) and distance (kilometres) from the previous period gravity centre of fishing effort (DISTGC_{jt}). These variables represent costs of travel. As most skippers and crew take time off around the end of the year, distance from the port is expected to be more important in the months of December, January, and February. Hence, interaction variables between DISTPT_{jt} and month dummy variables, DFeb_{jt}, DMar_{jt}, DApr_{jt}, DJune_{jt}, DJuly_{jt}, DAug_{jt}, DSept_{jt}, DOct_{jt}, DNov_{jt}, DDec_{jt}, are included. January is the default month.

(*iii*) Dummy variables for zero fishing effort in j in $t - 1$ (ZEROL_{jt-1}) and $t - 2$ (ZEROL_{jt-2}). These variables identify grids that have not been the object of recent search and for which no recent information is available.

The utility function used in the discrete choice model therefore takes the following form:

$$\begin{aligned}(5)\quad U_{jt} = {} & \beta_{1A}\ \text{EVSKJRatio}_{jt} + \beta_{1B}\ \text{EVYFTRatio}_{jt} \\ & + \beta_2\ \text{DISTGC}_{jt} + \beta_3\ \text{DISTPT}_{jt} \\ & + \beta_4\ \text{DFeb}_{jt} \times \text{DISTPT}_{jt} + \beta_5\ \text{DMar}_{jt} \times \text{DISTPT}_{jt} \\ & + \beta_6\ \text{DApr}_{jt} \times \text{DISTPT}_{jt} + \beta_7\ \text{DMay}_{jt} \times \text{DISTPT}_{jt} \\ & + \beta_8\ \text{DJune}_{jt} \times \text{DISTPT}_{jt} + \beta_9\ \text{DJuly}_{jt} \times \text{DISTPT}_{jt} \\ & + \beta_{10}\ \text{DAug}_{jt} \times \text{DISTPT}_{jt} + \beta_{11}\ \text{DSept}_{jt} \times \text{DISTPT}_{jt} \\ & + \beta_{12}\ \text{DOct}_{jt} \times \text{DISTPT}_{jt} + \beta_{13}\ \text{DNov}_{jt} \times \textit{DISTPT}_{jt} \\ & + \beta_{14}\ \text{DDec}_{jt} \times \text{DISTPT}_{jt} \\ & + \beta_{15}\ \text{ZEROL}_{jt-1} + \beta_{16}\ \text{ZEROL}_{jt-2} + \varepsilon_{jt}, \\ & j = 1, \ldots, 65,\ t = 1 = 1, \ldots, 94.\end{aligned}$$

To account for uncertainty, the variance in returns (Bockstael and Opaluch 1983) was also included in a preliminary version of the model but was found not to be statistically significant. This suggests that the size of intermonth fluctuations in grid-specific returns does not affect locational choice.

This result does not, however, necessarily mean that skippers are not risk averse. It could be indicative of a cooperative approach to search, which allows high-variance locations to be searched without penalty in the form of forgone catch, i.e., the other vessels will inform the searcher if they find a good aggregation. Also, because of the ENSO influence on resource distribution, nearly all grids experience large variability, making it difficult for skippers to include variance in the decision-making process.

Nested logit model

Discussions with operators in the WPTF revealed some knowledge of the ENSO-induced changes in the longitudinal distribution of the resource. An El Niño effect changes relative temperatures across grids in the east–west plane but not in the north–south plane. In fact, the large changes in the east–west distribution of the resource lead to the hypothesis that skippers make decisions in two stages: first, about where to fish in the east–west plane in response to changes in water temperature and (or) the ENSO phase (depending on whether they use the ENSO phase or water temperature in the formation of catch rate expectations) and, second, about where to fish in the north–south plane.

This hypothesis is tested using a nested logit model. Under the nested model, the choice of grid j is conditional upon the choice beforehand of the longitudinal band, m:

$$(6)\quad P_{jm} = P(j|m)P(m)$$

where $P(j|m)$ is the probability that the individual chooses grid j conditional on choosing m and $P(m)$ is the probability that the individual chooses longitudinal band m. The $P(j|m)$ is found using the following expression:

$$(7)\quad P(j|m) = \frac{\exp(\beta' x_{j|m})}{\Sigma_{q|m}\ \exp(\beta' x_{q|m})} = \frac{\exp(\beta' x_{j|m})}{e^{I_m}}$$

where q is the number of twigs on a branch ($q = 5$ for each m, i.e., five latitudinal bands for each longitudinal branch) and I_m is the inclusive value for branch m, $i_m = \log \Sigma_{q|m}\ \exp(\beta' x_{q|m})$. At the next level up, the probability of choosing branch m is defined as

$$(8)\quad P(m) = \frac{\exp(\gamma z_m + \tau_m I_m)}{\Sigma_w\ \exp(\gamma z_w + \tau_w I_w)}$$

where w is the number of branches in the model (13, one for each longitudinal band; see Fig. 3).

The general forms of the two utility functions required for the nested model are as follows:

$$(9)\quad U_m = \gamma Z_m + \varepsilon_m,\ m = 1, 2, \ldots, M$$

$$(10)\quad U_{j|m} = \beta' x_{j|m} + \varepsilon_{j|m},\ j = 1, 2, \ldots, J$$

© 1999 NRC Canada

Fig. 3. Decision trees for nested logit and nonnested logit models.

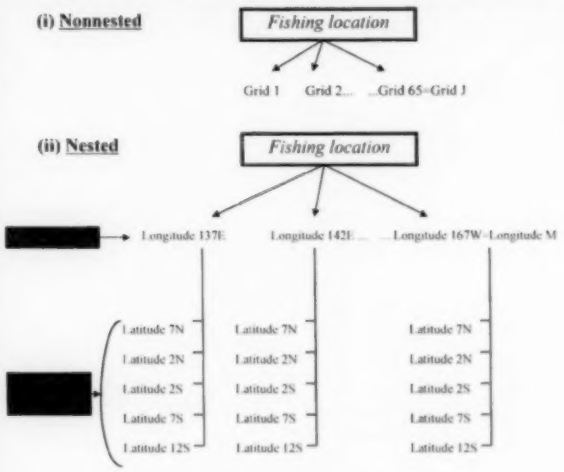

where Z_m is a vector of variables in the first-level (or branch) utility function, x_{jlm} is a vector of variables in the second-level (or twig) utility function, γ is a vector of coefficients for the Z_m variables, and β' is a vector of coefficients for the x_{jlm} variables.

Relative productivity in the longitudinal plane fluctuates mainly in response to changes in the ENSO phase, as reflected in the SOI level. This change in relative productivity enters the skippers' utility functions through their understanding of optimal water temperature and use of water temperature sensors. Water temperature is proxied using $SOI3_t$, and because $SOI3_t$ reflects different water temperatures in different longitudinal bands, interaction dummy variables between longitudinal bands and $SOI3_t$ were also included in the first-stage utility function. The specific form of eq. 9 is therefore

$$(11) \quad U_{mt} = \gamma_1 \, SOI3_t + \sum_{m=1}^{12} \gamma_{1+m} \, SOI3_t \times Long_{mt} + \varepsilon_{mt}$$

where $Long_{mt}$ is the longitudinal band dummy (see Fig. 3), with the easternmost longitudinal band being used as the default. The second-stage utility function is the same as eq. 5, except that it is now conditional upon m.

The nested model, compared with the nonnested model, is illustrated in Fig. 3. In the nonnested model, utility of each of the 65 grids is compared simultaneously. In the nested model, there is first a comparison of the expected utility across 13 longitudinal bands, which are identified using the 5° midpoint (less 30'). For example, 137E denotes the longitudinal band running from 135 to 140°E. The expected utilities (conditional upon choice of longitudinal band) from fishing in the five latitudinal bands (again identified using 5° midpoints) are evaluated in the second stage.

Equations 7 and 8 are estimated, for the nested model, using a proportions-dependent variable (as was the case for the nonnested model using eq. 4). Estimation is carried out using FIML.

Results

Catch rate expectations model results

The results of the ordinary least squares estimation of eq. 1 are shown in Table 1. $VRatio_{jt-1}$ was highly significant, showing that despite the stock and migratory effects, recent catch rates are important in determing expectations. $Days_{jt-1}$ was significant, suggesting that catch rates are positively related to the amount of search in an area. $Days_{jt-2}$ was not significant.

Of the "surrounding-grids" days fished variables, $Days^{E}_{jt-1}$, $Days^{SE}_{jt-1}$, $Days^{N}_{jt-1}$, and $Days^{W}_{jt-1}$ were significant in the $E(VRatio_{jt})$ model. The signs of the estimated surrounding-grid coefficients for the significant variables were all positive, which indicates that search in grid j in period t is greater if there is more fishing effort in the surrounding grids in the previous period.

The east, west, southwest, and south surrounding-grid $VRatio_{jt-1}$ variables were all significant at the 5% level of significance, and $VRatio^{NE}_{jt-1}$ was significant at the 7% level.

Log-likelihood ratio tests were used to test for the significance of four large groups of dummy variables used in the expectations model. The following restricted versions of the model were run and the statistic $\chi^2_{(k-1)} = -2(L_R - L_U)$ was calculated where L_R and L_U are the values of the log-likelihood ratio in the restricted and unrestricted models, k is the number of restrictions, and $k - 1$ is the degrees of freedom: restrict days fished in surrounding grids to a single average value ($\chi^2_{(6)} = 31.00$); restrict the surrounding grid $VRatio_{jt-1}$ variables to a single average value ($\chi^2_{(6)} = 28.96$); remove the 64 grid dummies ($\chi^2_{(63)} = 143.44$); and remove the proxies for closeness to optimal water temperature, the $SOI3_t$ and the 64 $SOI3_t \times Grid_j$ interaction variables ($\chi^2_{(64)} = 60.48$). On the basis of the log-likelihood ratio tests, these four groups of variables were retained in the model.

The model was then tested for the presence of multicollinearity amongst the continuous independent variables. The condition number of the characteristic roots of the 24 × 24 ($X'X$) matrix of the independent variables, excluding the dummies, was calculated to be 4.14, which is well below the critical value (Greene 1991*a*, p. 280). It was concluded that multicollinearity is not a problem. A Breusch–Pagan–Godfrey test of the null hypothesis of homoscedasticity was conducted (Greene 1991*a*, p. 421), and the value of the test statistic, $\chi^2_{(151)} = 109.479$, suggests that this hypothesis should not be rejected. It was concluded that heteroscedasticity is not a serious problem.

Qualitative choice model results

The results of the FIML estimation of eqs. 4 and 7 are shown in Table 2. The nonnested model was tested for the presence of multicollinearity by means of the condition number of the characteristic roots of the 16 × 16 ($X'X$) matrix of the independent variables. The condition number was 10.90, suggesting that multicollinearity is not a problem.

The positive and highly significant coefficient for $E(VRatio_{jt})$ in both models is in accordance with a priori expectations. The coefficient on $DISTGC_{jt}$ is also highly significant in both models, and it can therefore be concluded that vessels consider both expected revenues and the cost of moving when selecting fishing grids.

The coefficient on $DISTPT_{jt}$ is not significant in the nonnested model but is significant and positive in the nested model, suggesting that skippers are more likely to select grids farther from port. This counterintuitive result for the nested model is probably because this variable enters the utility function after the choice of longitudinal band has been made, and distance from port is not important in choosing between five grids within a particular longitudinal band.

© 1999 NRC Canada

Table 1. Estimated coefficients for catch rate expectations (VRatio) model.

Variable	Coefficient	*p* value	*t* ratio	Variable	Coefficient	*p* value	*t* ratio
$VRatio_{jt-1}$	0.130	0.0000	9.517	$VRatio^{E}_{jt-1}$	0.037	0.0073	2.686
$VRatio_{jt-2}$	–0.019	0.1598	–1.406	$VRatio^{SE}_{jt-1}$	0.010	0.4777	0.710
$Days_{t-1}$	0.001	0.0003	3.634	$VRatio^{N}_{jt-1}$	0.041	0.0033	2.938
$Days^{NE}_{t-1}$	–0.046	0.7520	–0.316	$VRatio^{NW}_{jt-1}$	–0.002	0.8682	–0.166
$Days^{E}_{t-1}$	0.745	0.0000	5.087	$VRatio^{W}_{jt-1}$	0.090	0.0000	6.455
$Days^{SE}_{t-1}$	0.435	0.0027	2.997	$VRatio^{SW}_{jt-1}$	0.029	0.0450	2.005
$Days^{N}_{t-1}$	0.243	0.1013	1.639	$VRatio^{S}_{jt-1}$	0.019	0.1758	1.354
$Days^{NW}_{t-1}$	0.037	0.8010	0.252	$Dist_{jt-1}$	–0.002	0.0828	–1.735
$Days^{W}_{t-1}$	0.377	0.0097	2.588	$Distdif_{jt-1}$	0.004	0.0019	3.110
$Days^{SW}_{t-1}$	0.044	0.7611	0.304	$Distdif_{jt-2}$	0.002	0.1809	1.338
$Days^{S}_{t-1}$	–0.148	0.3212	–0.992	$SOI3_{t}$	0.014	0.7672	0.296
$VRatio^{NE}_{jt-1}$	0.004	0.7780	0.282	Constant	0.058	0.3602	0.915
Adjusted R^2	0.20						
Log-likelihood	–3827.93						

Note: Degrees of freedom = 5957 for calculation of *p* values.

The significance of the group of variables measuring the interaction of the month dummies with the $DISTPT_{jt}$ variable was tested by means of a log-likelihood ratio test. In the restricted model the 11-month dummy variables were replaced by a single dummy representing the holiday season (November–February). A comparison of the log-likelihood ratios of the unrestricted and restricted model suggested that the restriction should be rejected ($\chi^2_{(10)} = 1927.4$).

Table 3 shows the cumulative proportional level of fishing effort for the entire 94-month sample period. A fleet fishing-month is equal to 1. Hence, in the grids with the most fishing effort for the sample period, 147°E, 2.30°S and 172°E, 2.30°S, there are 7 fleet fishing-months. The three columns for each longitudinal reference are for actual, nested model results, and nonnested model results, respectively. There are actually 94 units of fishing effort in the March 1988 to December 1995 period. However, LIMDEP rounds to the nearest discrete number, and as there is more rounding down than rounding up, the totals sum to less than 94.

Overall, the performance of the nested logit model, from observation of Table 3, appears better than that of the nonnested model. A formal test of the predictive power of the models is provided by the Hosmer–Lemeshow test (Hosmer and Lemeshow 1989, p. 141), which is similar to the Pearson test but applied to grouped data. The 6110 observations and predictions of the shares of fishing effort by grid and period were sorted according to the magnitude of the predicted values and divided into 10 equal groups. The null hypothesis that the predicted values match the observed values is tested by means of a χ^2 statistic: the value of the statistic was $\chi^2_{(8)} = 0.6335$ for the nonnested model and $\chi^2_{(8)} = 0.625$ for the nested model.

Elasticities

The elasticities (measuring the percent change in the value of the dependent variable in response to a 1% increase in the value of an independent variable) of proportion of fishing effort in grid *j* with respect to the variables included in eqs. 5 and 11 are calculated at the mean values of the explanatory variables and reported as part of the LIMDEP output. The elasticities with respect to $E(VRatio_{jt})$ (η_{VR}) and $Dist_{jt}$ (η_{Distj}) are shown in Table 4 for the four grids with the most fishing effort for the sample period. The η_{VR} is slightly above unity for nearly all of the choices and is quite consistent across models. The own elasticity with respect to distance is between –0.90 and –0.1.48 for the nested logit model but between –0.49 and –0.77 for the nonnested model.

Model selection and test for consistency with utility maximisation

While the nested model appears to be a better predictor, two formal model selection tests were conducted. Greene (1996) showed that at least one of the inclusive value parameters, τ_m, must differ from unity for the nested model not to reduce to the nonnested model. For each inclusive value parameter, the null hypothesis that its value is equal to unity was tested using a *t* ratio. In all cases, the null is easily rejected (the lowest *t* ratio in the 13 tests was 7.8). The null hypothesis that all of the inclusive value parameters are equal to unity was then tested by means of a log-likelihood ratio test. The value of the test statistic ($\chi^2_{(12)} = 5814$) suggests that the null hypothesis can be rejected. On the basis of these results, it was concluded that the nested model is preferred.

According to McFadden (1981), a globally sufficient condition for the nested logit model to be consistent with utility maximisation is that $0 < \tau_{m,m=1,\ldots,w} < 1$, where τ_m is the coefficient on the inclusive value, I_m. This condition is met in all cases except for τ_{11} and τ_{12}. Borsch-Supan (1985, 1990) demonstrated local sufficiency conditions that permitted values of $\tau > 1$ that are rarely met when $\tau > 2$. The null hypothesis $\tau > 2$ was tested for τ_{11} and τ_{12} by means of *t* tests. The test statistics (–48.27 and –31.18, respectively) suggested that local sufficiency conditions for utility maximisation are likely to be met.

© 1999 NRC Canada

Table 2. Fleet spatial dynamics (qualitative choice) model results.

Nested				Nonnested			
Variable	Coefficient	*p* value	*t* ratio	Variable	Coefficient	*p* value	*t* ratio
$E(\text{VRatio}_{jt})$	3.38	0.0000	132.40	$E(\text{VRatio}_{jt})$	3.018	0.0000	162.48
DISTGC_{it}	–0.09	0.0000	–40.69	DISTGC_{it}	–0.043	0.0000	–50.15
DISTPT_{jt}	0.05	0.0000	14.80	DISTPT_{jt}	–0.003	0.1499	–1.44
$\text{DFeb}_{jt} \times \text{DISTPT}_{jt}$	–0.14	0.0000	–25.11	$\text{DFeb}_{jt} \times \text{DISTPT}_{jt}$	–0.067	0.0000	–16.87
$\text{DMar}_{jt} \times \text{DISTPT}_{jt}$	–0.04	0.0000	–7.71	$\text{DMar}_{jt} \times \text{DISTPT}_{jt}$	0.06	0.0000	17.87
$\text{DApr}_{jt} \times \text{DISTPT}_{jt}$	–0.03	0.0000	–6.35	$\text{DApr}_{jt} \times \text{DISTPT}_{jt}$	–0.04	0.0000	–11.54
$\text{DMay}_{jt} \times \text{DISTPT}_{jt}$	0.02	0.0000	4.63	$\text{DMay}_{jt} \times \text{DISTPT}_{jt}$	0.02	0.0000	6.06
$\text{DJune}_{jt} \times \text{DISTPT}_{jt}$	0.05	0.0000	11.44	$\text{DJune}_{jt} \times \text{DISTPT}_{jt}$	0.05	0.0000	15.57
$\text{DJuly}_{jt} \times \text{DISTPT}_{jt}$	–0.06	0.0000	–14.06	$\text{DJuly}_{jt} \times \text{DISTPT}_{jt}$	0.001	0.8026	0.25
$\text{DAug}_{jt} \times \text{DISTPT}_{jt}$	0.03	0.0000	7.23	$\text{DAug}_{jt} \times \text{DISTPT}_{jt}$	0.02	0.0000	6.73
$\text{DSept}_{jt} \times \text{DISTPT}_{jt}$	–0.09	0.0000	–22.57	$\text{DSept}_{jt} \times \text{DISTPT}_{jt}$	–0.002	0.4593	–0.74
$\text{DOct}_{jt} \times \text{DISTPT}_{jt}$	–0.04	0.0000	–9.18	$\text{DOct}_{jt} \times \text{DISTPT}_{jt}$	0.02	0.0000	6.53
$\text{DNov}_{jt} \times \text{DISTPT}_{jt}$	–0.11	0.0000	–25.45	$\text{DNov}_{jt} \times \text{DISTPT}_{jt}$	–0.003	0.3271	–0.98
$\text{DDec}_{jt} \times \text{DISTPT}_{jt}$	–0.10	0.0000	–22.96	$\text{DDec}_{jt} \times \text{DISTPT}_{jt}$	–0.04	0.0000	–10.18
ZEROL_{jt-1}	–0.74	0.0000	–34.77	ZEROL_{jt-1}	–0.88	0.0000	–44.37
ZEROL_{jt-2}	–0.44	0.0000	–25.70	ZEROL_{jt-2}	–0.53	0.0000	–33.71
Branch utility function							
SOI3_t	–7.443	0.0719	–1.80				
$\text{SOI3}_t \times \text{Long}_{1t}$	0.999	0.0000	21.82				
$\text{SOI3}_t \times \text{Long}_{2t}$	0.913	0.0000	25.18				
$\text{SOI3}_t \times \text{Long}_{3t}$	1.023	0.0000	30.69				
$\text{SOI3}_t \times \text{Long}_{4t}$	0.978	0.0000	28.11				
$\text{SOI3}_t \times \text{Long}_{5t}$	0.813	0.0000	23.89				
$\text{SOI3}_t \times \text{Long}_{6t}$	0.890	0.0000	25.30				
$\text{SOI3}_t \times \text{Long}_{7t}$	0.693	0.0000	20.59				
$\text{SOI3}_t \times \text{Long}_{8t}$	0.414	0.0000	12.88				
$\text{SOI3}_t \times \text{Long}_{9t}$	0.365	0.0000	10.76				
$\text{SOI3}_t \times \text{Long}_{10t}$	0.854	0.0000	25.31				
$\text{SOI3}_t \times \text{Long}_{11t}$	0.717	0.0000	22.82				
$\text{SOI3}_t \times \text{Long}_{12t}$	1.040	0.0000	27.14				
R^2	0.306			R^2	0.293		
Log-likelihood	–157 500			Log-likelihood	–160 407		

Note: Degrees of freedom = 6081 for nested model *p* values and 6094 for nonnested model *p* values.

Independence of irrelevant alternatives

An important property of multinomial and discrete choice models is the independence of irrelevant alternatives (IIA). Under IIA, introduction of a new alternative leaves the relative odds of choosing among the existing alternatives unaltered. This property requires that all alternatives be perceived as distinct and independent, i.e., that errors in estimating the utility associated with each alternative be uncorrelated. A partial solution to this problem is to use a nested logit model because this allows the choice of alternatives to be correlated within, although not between, groups (Kling and Thomson 1996). Hence, this provides an additional econometric rationale for proceeding with the nested logit model instead of the discrete choice model, as it reduces the likelihood that the IIA does not hold.

Discussion

The main purpose of the analysis is to predict fleet movements, but the models also provide information about the process of generating and sharing information about migra-

© 1999 NRC Canada

Table 3. Actual (A), nested (N), and nonnested (NN) cumulative proportional fishing effort distribution, March 1988 to December 1995.

	Longitude																					
	137.3°E			142.30°E			147.30°E			152.30°E			157.30°E			162.30°E			167.30°E		
Latitude	A	N	NN	A	N	NN	A	N	NN	A	N	NN	A	N	NN	A	N	NN	A	N	NN
7.30°N	0	1	0	0	0	1	1	1	1	1	1	1	0	0	1	0	1	1	1	0	0
2.30°N	1	1	1	3	3	3	3	3	2	3	3	3	4	4	4	3	3	3	3	5	5
2.30°S	0	0	0	3	2	3	7	6	5	5	4	5	4	3	4	3	3	3	5	3	4
7.30°S	0	0	0	0	0	0	0	1	1	1	1	1	0	1	1	0	1	1	1	1	1
12.30°S	0	0	0	0	0	0	0	0	0	0	0	0	0	0	0	0	0	0	0	0	0
Total	1	2	1	6	5	7	11	11	9	10	9	10	8	8	10	6	8	8	10	9	10
	172.3°E			177.30°E			177.30°W			172.30°W			167.30°W			162.30°W			Total		
Latitude	A	N	NN	A	N	NN	A	N	NN	A	N	NN	A	N	NN	A	N	NN	A	N	NN
7.30°N	0	0	0	0	0	0	0	0	0	0	0	0	0	0	0	0	0	0	3	4	5
2.30°N	4	3	3	2	2	2	1	1	2	1	1	1	0	0	0	0	0	0	28	29	29
2.30°S	7	7	6	5	5	5	5	6	5	4	3	2	1	1	1	1	1	0	50	44	43
7.30°S	1	2	2	2	2	2	2	2	1	1	1	1	0	0	0	0	1	0	8	13	11
12.30°S	0	0	0	0	0	0	0	0	0	1	0	0	0	0	0	0	0	0	1	0	0
Total	12	12	11	9	9	9	8	9	8	7	5	4	1	1	1	1	2	0	90	90	90

tory fish stocks and about the costs of vessel movement in a spatially diverse fishery.

Fleet movements are predicted in two stages: first, relative catch rate expectations amongst grids are modeled, and then the spatial distribution of effort in response to these expectations, taking distance factors into account, is predicted using a qualititative choice model. Overall, the performance of the catch rate expectations model was good in comparison with that of other models such as those of Eales and Wilen (1986) and Vignaux (1996), with 20% of the variation in $VRatio_{jt}$ explained by the model.

As can be seen from the results of the qualitative choice models reported in Table 3, the nested logit model of the spatial allocation of effort performed better than the nonnested model: in the longitudinal plane, the nested model's cumulative predictions appear closer to the actual levels than the cumulative predictions from the nonnested model, with no longitudinal band having more than 2 full months separating the predicted from the actual cumulative proportion; in the latitudinal plane, the model overpredicted by more than 5 months full fishing the amount of fishing in the 7.30°S band. This was almost equal to the amount of underprediction in the 2.30°S band.

The catch rate expectations model suggests that information about the distribution of tuna stocks is based partly on historical patterns (as evidenced by the importance of the grid dummies), partly on information about water temperatures (as evidenced by the significant of the lagged SOI variable and its interaction with grids), and partly on the amount of search undertaken in a grid and its neighbours in the immediate past (as evidenced by the significance of the days fished variables). The model also suggests that because of the migratory nature of tuna stocks, the value of information is short-lived: $VRatio_{jt-2}$ was found to be insignificant in the VRatio expectations model, which suggests that migration effects over a 2-month period are so great as to remove any relationship between $VRatio_{jt-2}$ and $VRatio_{jt}$.

There is some conjecture about the extent of catch rate information sharing because information is expected to be undersupplied by the fleet vis-à-vis optimal levels because it is a public good, i.e., a good that benefits all simultaneously but that each individual has a limited incentive to supply. Further, Doulman's (1987, p. 144) comments would suggest that, apart from some small code groups set up for the purpose, there is very little sharing of catch rate information by the U.S. fleet:

> Japanese vessels tend to fish as a fleet and exchange information on the fishing grounds; U.S. vessels usually operate individually and competitively.

Orbach's (1977, pp. 104–105) comments suggest that code groups play a somewhat more central role:

> Of all the factors which go into the fishermen's decisions about when and where to look for fish, the most important is radio communications between the boats themselves.. They [the skippers] have approximately five million square miles of ocean to cover in search of a highly mobile quarry.

Orbach (1977, p. 112) also described the extent of skippers' involvement in information sharing code groups:

© 1999 NRC Canada

Table 4. Elasticities of proportion of effort in grids with respect to catch rate expectations and distance from the gravity centre of the fleet in period $t - 1$.

Choice		Nested		Nonnested	
		η_{VR}	η_{Dist_j}	η_{VR}	η_{Dist_j}
147°E, 2.30°S	Own Grid	1.160	–1.477	1.294	–0.778
	Grid in same branch	–0.435	0.278	–0.129	0.013
	Grid in other branch	–0.116	0.020		
172°E, 2.30°S	Own Grid	1.290	–0.897	1.464	–0.491
	Grid in same branch	–0.515	0.229	–0.147	0.017
	Grid in other branch	–0.109	0.025		
177°E, 2.30°S	Own Grid	1.185	–1.064	1.382	–0.594
	Grid in same branch	–0.516	0.292	–0.137	0.017
	Grid in other branch	–0.069	0.020		
177°W, 2.30°S	Own Grid	1.166	–1.439	1.249	–0.741
	Grid in same branch	–0.398	0.238	–0.147	0.015
	Grid in other branch	–0.115	0.027		

> Almost all of the boats in the fleet, even those which usually act as loners, belong to a code group. These are groups of anywhere from three or four to fourteen or fifteen boats who agree in principle to cooperate in the search for tuna.

This would appear to make Doulman's (1987) assertion that U.S. vessels sometimes form code groups of three or four vessels somewhat conservative. The extent to which information is shared, however, is an empirical question. Campbell et al. (1993) found that the U.S. purse-seine fleet shares catch rate information to a lesser extent than the Japanese purse-seine fleet. Their study was, however, limited to the Papua New Guinea fishing zone and also for one year only, 1985, a year in which there were just 927 days fished by the U.S. fleet in the WPTF. The U.S. purse-seine fleet's presence in the WPTF greatly expanded in the late 1980's (in response to the ENSO-induced decline in fishing condition in the eastern Pacific tuna fishery) to the stage where typically 6000–8500 fishing days are recorded per year, and hence, structural change in the way fishing operations are conducted is quite possible.

The highly significant and positive coefficients on the "fleetwide" $E(\text{VRatio}_{jt})$ variables in the qualitative choice models reported in Table 2 seem to confirm that the sharing of catch rate information by the U.S. fleet is commonplace, supporting Orbach's (1977) view. Some further support is obtained from the results of the catch rate expectations model reported in Table 1: search in a grid and surrounding grids in the previous month tends to raise the effort share in the following month, and movement of the centre of gravity of the fleet towards a grid in previous months also tends to increase effort share. The responsiveness of the fleet movements to fleetwide expectations about catch rates is measured by the elasticities η_{VR}, which show the percent change in the proportion of fishing effort in a grid in response to a 1% increase in relative catch rate expectations. The values for η_{VR}, reported in Table 4, suggest that the rate of information sharing is quite high.

While catch rate expectations are important in determining the spatial distribution of the fleet, it can be predicted that profit-maximizing skippers will also take into account the opportunity cost of travel time in choosing where to fish. The qualitative choice model supports this prediction, indicating that the further a grid is from the centre of gravity of fishing effort in the previous month the lower will be its effort share in the current month. The nonnested version of the model also confirmed that, in the holiday season, the larger the distance of a grid from from the home port (American Samoa) the lower will be its share in relative effort. This result was not obtained from the nested model because distance from home port is an important issue when choosing the longitude of the grid to be fished, but less so when choosing latitude.

Two refinements to the empirical model that could be considered if more disaggregated data became available are using marginal, instead of average, CPUE as an explanatory variable in the catch rate expectations model and using weekly rather than monthly updating of information about catch rates.

Expectations based on marginal CPUE might serve as a better explanatory variable in the qualitative choice model because marginal CPUE bears a closer relationship than average CPUE to the expected overall productivity of a grid for the coming month. This is because a small localised stock lightly fished could have the same average CPUE as a grid with a higher stock level and greater number of days fished, but would yield a much lower return to additional fishing effort. In contrast, the higher the marginal CPUE in grid j at time $t - 1$ the greater the expected productivity in grid j at time t, and therefore the higher the number of fishing days expected in the subsequent period. Marginal CPUE could be calculated using a final subset of CPUE observations in grid j in period $t - 1$. However, this would require data on CPUE by location at a more temporally disaggregated level, including perhaps data on individual purse-seine "shots" (a shot is the term given to each individual set-

© 1999 NRC Canada

Fig. 4. Distribution of fishing days and average CPUE.

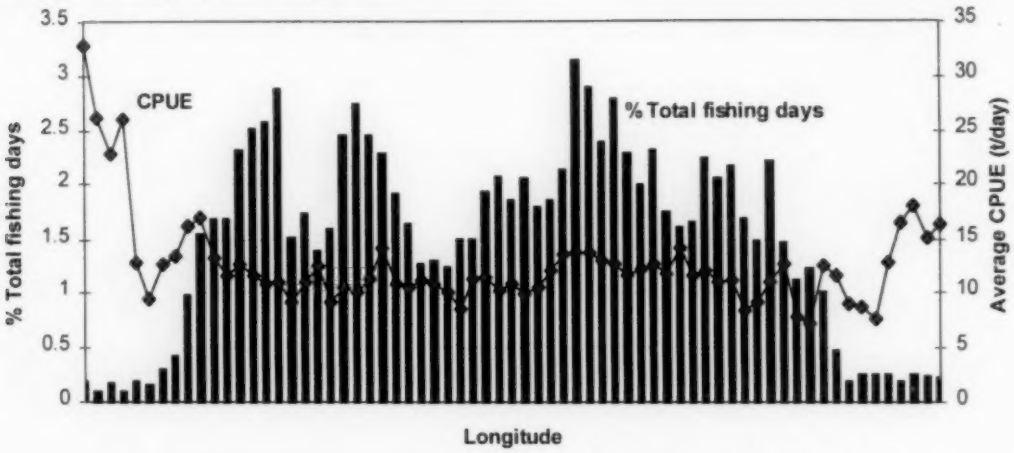

ting of the purse-seine net), which are not generally available at present for reasons of commercial confidentiality.

A further advantage of using marginal CPUE as an explanatory variable is that, in the long run, there is a tendency for average CPUE to be equalised across grids (see Fig. 4) because of the individual profit-maximization behaviour of fishers (Gordon 1954), and it is only because this equalisation generally takes longer than a month that variations in relative CPUE exist and can be used to predict the choice of grid. Marginal CPUE, on the other hand, measures inherent initial productivity and is independent of the subsequent level of effort applied to the grid.

The spatial resolution of 5° grids, while being consistent with the spatial resolution currently used in tuna population dynamics models, is much broader than the 1° grids that would ideally be used. However, commercial confidentiality limits the availablity and use of catch and effort data at this degree of spatial resolution. A solution to this problem could be to use the model presented in this study to redistribute fishing effort between 5° grids and then to use a simple movement rule to redistribute fishing effort within 5° grids. For example, Anganuzzi (1994) redistributed effort from one grid to the surrounding grids in direct proportion to the relative catch rates predicted by the population dynamics model. However, this approach does not fully model the predicted behaviour of profit-maximising individual vessels: in the absence of travel costs, they are all expected to move to the most productive grid first and then, when the fish-down effect reduces its ranking, move to the new first-ranked grid.

Conclusions

Bioeconomic models attempt to predict fish stock levels and catches corresponding to various levels of fishing effort. The predictions can be used to develop policies that meet objectives such as sustainability or economic efficiency. In the WPTF, highly mobile fishing fleets pursue highly migratory tuna stocks, and the locations of fish stocks and fleets may be as important to the final outcome as their levels. Current models of the fishery (Klieber and Hampton 1994; Bertignac et al. 1997) incorporate the migratory behaviour of tuna stocks but predict catches on the basis of the historical spatial distribution of the tuna fleets. A more complete approach would integrate the spatial dynamics of the fleets into the bioeconomic model.

Using the estimated parameters of the catch rate expectations and discrete choice models described in this paper, fishing effort can be redistributed on a monthly basis among 5° grids within the principal region of the WPTF; as noted above, the discrete choice model performs well in predicting effort distribution. The monthly updates of the spatial distribution of effort can be combined with monthly updates of the spatial distribution of stocks to give more accurate predictions of catches than a model that redistributes effort on the basis of historical averages. This refinement will be particularly important when the bioeconomic model is used to predict the effects of significant departures from the current level and composition of effort.

A further possibility offered by this type of model is that of simultaneously estimating the parameters of stock and fleet movement models. Current population dynamics models specify the catching power and historical spatial distribution of the fleets and estimate the stock parameters that will produce the observed catch distribution. However, there are two sides to the system, the fish stocks and the fleets, and it would be preferable not to have to make artificial assumptions about either when estimating the parameters of a bioeconomic model.

Acknowledgements

The authors would like to thank Tony Kingston and Len Rodwell from the Forum Fisheries Agency; Michel Bertignac and John Hampton from the South Pacific Commission; Dale Squires from the National Marine Fisheries Service, and Masao Nakada and Katsunori Yajima from Solomon Taiyo Ltd. for invaluable assistance. Sincere thanks also to the U.S. Tuna Boat Association for releasing U.S. purse-seine logbook data. Thanks also to the editors of the *Journal* and two referees for comments on an earlier draft of the manuscript. Funding was provided by the Australian Centre for International Agricultural Research, project 9405. Any remaining errors are attributable to the authors.

© 1999 NRC Canada

References

Anganuzzi, A.A. 1994. An aggregate model of effort distribution. Second FAO Expert Consultation on Interaction of Tuna Fisheries. Food and Agriculture Organization of the United Nations, Rome

Bertignac, M., Lehodey, P., and Hampton, J. 1997. Towards the incorporation of environmental parameters in tuna-fisheries simulation modelling: the case of the Pacific skipjack fisheries. Working Pap., South Pacific Commission South Pacific Commission, Noumea, New Caledonia.

Bockstael, N.E., and Opaluch, J.J. 1983. Discrete modelling of supply response under uncertainty: the case of the fishery. J. Environ. Econ. Manage. **10**: 125–137.

Borsch-Supan, A. 1985. Tenure choice and housing demand. *In* U.S. and German housing markets: comparative economic analysis. *Edited by* K.Stahl and R. Struyk. Urban Institute Press, Washington D.C. pp. 55–105.

Borsch-Supan, A. 1990. On the compatibility of nested logit models with utility maximization. J. Econometrics, **43**: 373–388.

Campbell, H.F., Meyer, G., and Nicholl, R.B. 1993. Search behaviour in the purse seine tuna fishery. Nat. Resour. Model. **7**: 15–35.

Doulman, D.J. (*Editor*). 1987. Tuna issues and perspectives in the Pacific Island region. Pacific Islands Development Programme, East-West Centre, Honolulu, Hawaii.

Dupont, D.P. 1993. Price uncertainty, expectations formation and fishers' location choices. Mar. Res. Econ. **8**: 219–247.

Eales, J., and Wilen, J.E. 1986. An examination of fishing location choice in the pink shrimp fishery. Mar. Res. Econ. **2**: 331–351.

Gillis, D.M., Peterman, R.M., and Tyler, A.V. 1993. Movement dynamics in a fishery: application of the ideal free distribution to spatial allocation of effort. Can. J. Fish. Aquat. Sci. **50**: 323–333.

Gordon, H.S. 1954. The economic theory of a common property resource: the fishery. J. Pol. Econ. **62**: 124–142.

Greene, W.H. 1991*a*. Econometric analysis. Maxwell MacMillan International Editions, New York.

Greene, W.H. 1991*b*. LIMDEP version 6.0 manual. Econometric Software, Plainview, N.Y.

Greene, W.H. 1996. LIMDEP version 7.0 manual. Econometric Software, Plainview, N.Y.

Hand, A.J., and Forau, P.S. 1997. Tuna prices for bioeconomic modelling of the western Pacific and Solomon Islands tuna fisheries. Tech. Pap. No. 3. ACIAR Project No. 9405: A Bioeconomic Analysis of Tuna Purse Seining in the Pacific Islands Region, January. ACIAR, Canberra, Australia.

Hilborn, R., and Ledbetter, M. 1979. Analysis of British Columbia salmon purse-seine fleet: dynamics of movement. J. Fish. Res. Board Can. **36**: 384–391.

Hilborn, R., and Walters, C.J. 1987. A general model for simulation of stock and fleet dynamics in spatially heterogeneous fisheries. Can. J. Fish. Aquat. Sci. **44**: 1366–1369.

Hosmer, D.W., and Lemeshow, S. 1989. Applied logistic regression. John Wiley & Sons, New York.

Kleiber, P., and Hampton, J. 1994. Modeling effects of FADs and islands on movement of skipjack tuna (*Katsuwonus pelamis*): estimating parameters from tagging data. Can. J. Fish. Aquat. Sci. **51**: 2642–2652.

Kling, C.L., and Thomson, C.J. 1996. The implications for model specification for welfare estimation in nested logit models. Am. J. Agric. Econ. **78**: 103–114.

Lehodey, P., Bertignac, M., Hampton, J., and Lewis, A. 1997. El Niño Southern Oscillation and tuna in the western Pacific. Nature (Lond.), **389**: 715–718.

Mangel, M., and Clark, C.W. 1983. Uncertainty, search and information in fisheries. J. Cons. Cons. Int. Explor. Mer, **41**: 93–103.

McFadden, D.L. 1981. Econometric models of probabilistic choice. *In* Structural analysis of discrete data. *Edited by* C.F. Manski and D.L. McFadden. Cambridge University Press, New York.

Morey, E.R., Rowe, R.D., and Watson, M. 1993. A repeated nested logit model of Atlantic salmon fishing, Am. J. Agric. Econ. **75**: 578–592.

Orbach, M.K. 1977. Hunters, seamen, and entrepreneurs — the tuna seinermen of San Diego. University of California Press, Berkeley, Calif.

Sampson, D.B. 1992. Fishing technology and fleet dynamics: predictions from a bioeconomic model. Mar. Res. Econ. **7**: 37–58.

South Pacific Commission. 1992. Non-reporting of catches by western Pacific seiners in data collected by coastal states. Working Pap. 6, Tuna and Billfish Assessment Programme, South Pacific Commission, Noumea, New Caledonia.

Vignaux, M. 1996. Analysis of vessel movements and strategies using commercial catch and effort data from the New Zealand hoki fishery. Can. J. Fish. Aquat. Sci. **53**: 2126–2136.

© 1999 NRC Canada

Modeling the size of snapper (*Pagrus auratus*) using temperature-modified growth curves

Russell B. Millar, Brian H. McArdle, and Shelton J. Harley

Abstract: Age–length keys from RV *Kaharoa* trawl surveys in the years 1984–1990 and 1992–1994 were used to estimate mean lengths-at-age of snapper (*Pagrus auratus*) in the Hauraki Gulf of New Zealand. A von Bertalanffy growth curve fitted to these lengths-at-age exhibited poor fit, and when the fit was restricted to only cohorts since 1968 (those for which sea surface temperature data were available) the estimated maximum length parameter dropped 5 cm. A power curve provided a better fit without an increase in the number of parameters and was not sensitive to the restriction to younger cohorts. When water temperature was added to the power curve model the residual plots indicated unexplained year effects and temporal correlation. These features were included using a mixed-effects model for repeated-measures data, and temperature was found to be statistically significant ($p < 0.0001$). This conclusion was corroborated via a simple randomization test. The model predicts growth over a year to change by the equivalent of 8 weeks if the average annual water temperature changes by 1°C. This is sufficient to predict a 4-year-old snapper from the 1986 cohort as having the equivalent of 6 months more growth (at the growth rate corresponding to average water temperature) than a 4-year-old fish from the 1990 cohort.

Résumé : Les clés associant âge et longueur établies à partir des campagnes de chalutage du RV *Kaharoa* de 1984–1990 et de 1992–1994 ont été utilisées pour évaluer la longueur moyenne selon l'âge des pagres (*Pagrus auratus*) dans le golfe Hauraki, en Nouvelle-Zélande. Une courbe de croissance de von Bertalanffy ajustée à ces longueurs selon l'âge était mal ajustée, et lorsque l'ajustement était limité uniquement aux cohortes depuis 1968 (celles pour lesquelles on possédait des données sur la température superficielle de la mer), l'estimation du paramètre de longueur maximale a chuté de 5 cm. Une courbe de puissance a fourni un meilleur ajustement sans augmenter le nombre de paramètres, et elle n'était pas sensible à la limitation aux jeunes cohortes. Lorsque la température de l'eau a été ajoutée au modèle de la courbe de puissance, les courbes résiduelles montraient des effets annuels et une corrélation temporelle inexpliqués. Ces éléments ont été inclus à l'aide d'un modèle à effets mixtes pour les données de mesures répétées, et on a constaté que la température était statistiquement significative ($p < 0{,}0001$). Cette conclusion a été corroborée par un simple test de randomisation. Le modèle prévoit que la modification de la croissance au cours d'une année équivaudra à 8 semaines si la température annuelle moyenne de l'eau varie de 1°C, ce qui est suffisant pour prédire qu'un pagre âgé de 4 ans, de la cohorte de 1986, présente un équivalent de croissance de 6 mois de plus (pour un taux de croissance correspondant à la température moyenne de l'eau) qu'un poisson âgé de 4 ans issu de la cohorte de 1990.

[Traduit par la Rédaction]

Introduction

Snapper (*Pagrus auratus*) (Sparidae) are a demersal fish found off the coasts of Japan, Taiwan, China, Philippines, Indonesia, southern Australia, Lord Howe, and the Norfolk Islands and around the North Island and upper South Island of New Zealand (Paul 1992; Annala and Sullivan 1997). In New Zealand, snapper support one of the most valuable coastal fisheries (Annala and Sullivan 1997) and is the most popular saltwater species sought by recreational anglers (Teirney et al. 1997).

Received April 21, 1998. Accepted March 4, 1999.
J14552

R.B. Millar.[1] Department of Statistics, University of Auckland, Private Bag 92019, Auckland, New Zealand.
B.H. McArdle and S.J. Harley. Department of Biological Sciences, University of Auckland, Private Bag 92019, Auckland, New Zealand.

[1]Author to whom all correspondence should be addressed.
e-mail: r.millar@auckland.ac.nz

In the Hauraki Gulf (Fig. 1), spawning of snapper typically peaks in late spring (November and December), and at 1 month, they are about 2.5 cm in length and near-perfect miniatures of the adult fish (Paul 1992). The minimum legal commercial size of 25 cm is typically reached at age 4 or 5. However, prerecruits from the 1981, 1989, and 1990 cohorts experienced growth slower than expected (Gilbert et al. 1996). The consequences for failing to account for this slow growth included negative biases in model estimates of mean recruitment and biomass projections (Gilbert et al. 1996) and the absence of the expected fish from the exploited population. The periods over which the slow growth was observed by Gilbert et al. (1996) coincided with the El Niño weather patterns of 1983 and 1991 that caused New Zealand's coastal waters to remain cool due to an increased flow of westerly and southwesterly winds (Paul 1992).

Interstock association between growth rate and temperature has been documented for many fish species (e.g., Taylor 1958; Brander 1995). Study of intrastock association has frequently used seasonal growth models (Cloern and Nichols 1978; Francis 1994) whereby temperature is implicitly modeled by including a sinusoidal term within a parametric

© 1999 NRC Canada

Fig. 1. Hauraki Gulf showing the location of the Leigh Marine Laboratory. The area surveyed by RV *Kaharoa* is contained between the dashed lines.

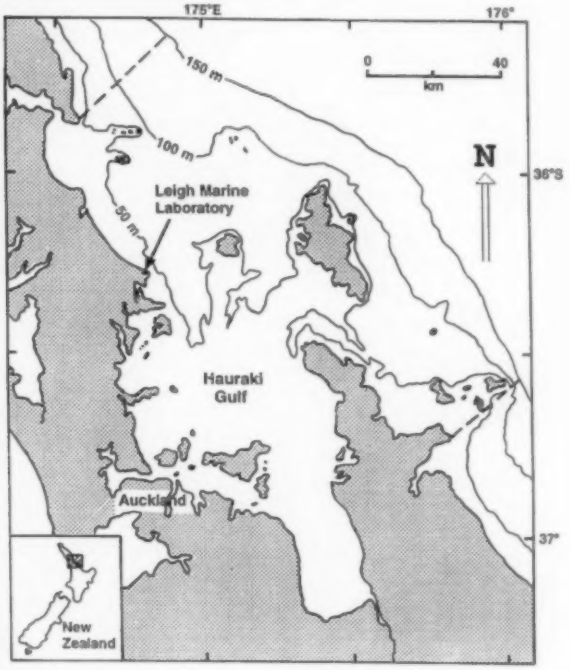

growth model (e.g., von Bertalanffy). Fountoura and Agostinho (1996) took this approach further by matching sinusoidal terms of differing frequencies with observed temperature data. A model that allows growth rate to depend explicitly on temperature was given by Campana and Hurley (1989) and used to fit to data on the size of larval Atlantic cod (*Gadus morhua*) and haddock (*Melanogrammus aeglefinus*). Francis (1994) found a positive correlation between sea surface temperature and growth of juvenile snapper by regressing the average juvenile growth rate (postmetamorphosis) against average sea surface temperature since metamorphosis.

The length data available for this present study were mean lengths-at-age of Hauraki Gulf snapper obtained from annual trawl surveys. The usual approach to investigating for a temperature association using such data is to calculate the average (or cumulative) temperature (or temperature anomaly) at each age for each cohort. This is then regressed against size-at-age (e.g., Nakken and Raknes 1987; Brander 1995). A different approach, that of Millar and Myers (1990), is used here. This is essentially a discretized version of the explicit modeling approach used by Campana and Hurley (1989), made appropriate for fitting to annual length-at-age data by modeling the annual growth increment as a function of annual temperature anomaly. As with the method of Campana and Hurley (1989), although it is the growth rate (or increment) that is explicitly modeled, it is length-at-age data to which the model is fitted. This approach has the advantage that the resulting temperature-modified growth curve can be used directly in future stock assessments. It has the disadvantage that the fit corresponds to a repeated-measures analysis due to the repeated sampling of cohorts over time, but this is no longer a great problem because of the increasing capability of existing software packages to fit such models.

This study examines the fitting of different temperature-modified growth curves to observed mean lengths-at-age (as estimated from age–length keys) and employs randomization, random effects, and repeated-measures methodology to ensure valid inference.

Methods

Data

The 28-m RV *Kaharoa* performed spring (October–November) surveys of snapper in the Hauraki Gulf (Fig. 1) in the years 1984–1990 and 1992–1994 inclusive (Langley 1995). All snapper caught were measured to the nearest centimetre below actual fork length, except when large catches necessitated measuring only a representative subsample. Lengths of snapper ranged from 5 to 75 cm. Otoliths were removed from subsamples of measured fish in order to construct an age–length key. Here, an age 1 fish is defined to be a fish from the spawning of the previous spring.

The subsampling of otoliths was stratified by length in some years and hence not a true random sample from all fish caught. Calculation of mean length-at-age therefore required an adjustment to remove bias in calculation of the proportion of length-at-age, p_{la}. This adjustment is a simple application of Bayes Theorem:

$$(1)\quad p_{la} = \text{Prob}(\text{length} = l \text{ given age} = a) = \frac{\text{Prob}(\text{length} = l \text{ and age} = a)}{\text{Prob}(\text{age} = a)} = \frac{\text{Prob}(\text{age} = a \text{ given length} = l)\ \text{Prob}(\text{length} = l)}{\Sigma_l\ \text{Prob}(\text{age} = a \text{ given length} = l)\ \text{Prob}(\text{length} = l)}.$$

The estimate of p_{la}, denoted $\hat{p}_{la}$, is given by replacing the probabilities in eq. 1 by the proportions obtained from the survey and the age–length key. Mean length-at-age a is then estimated as

$$(2)\quad \bar{l}_a = \sum_l \hat{p}_{la} l.$$

Ageing of snapper is believed to be very accurate (Francis et al. 1992), and hence the estimated $\bar{l}_a$, $a = 1, 2, \ldots$, will be (approximately) unbiased and mutually independent.

The RV *Kaharoa* deployed a trawl with codend mesh size not exceeding 40 mm (Francis et al. 1995, 1997). This mesh size is believed to release a high proportion of age 1 snapper (Francis et al. 1995), and hence, only age 2 and older fish were used here. In addition, the age–length key for 1988 did not contain data on any snapper above 30 cm, and to avoid bias in the mean length-at-age estimates, only ages 2, 3, and 4 were used in that year. This left 196 valid data points. Of these, 151 were from cohorts born no earlier than 1968, the first year for which sea-surface temperature data were available (Fig. 2).

The temperature data are the annual averages of daily sea surface temperatures measured at 9 a.m. by the Leigh Marine Laboratory (Fig. 1) in the northern end of the Hauraki Gulf. These water temperature data are the most extensive and reliable that were available and have previously been used in studies of snapper recruitment (Francis et al. 1995, 1997) and juvenile growth (Francis 1994). The mean annual temperature over the period 1968–1994 was 17.1°C, and the temperature anomaly, δ_t, in year t was therefore calculated as the annual temperature in year t minus 17.1.

© 1999 NRC Canada

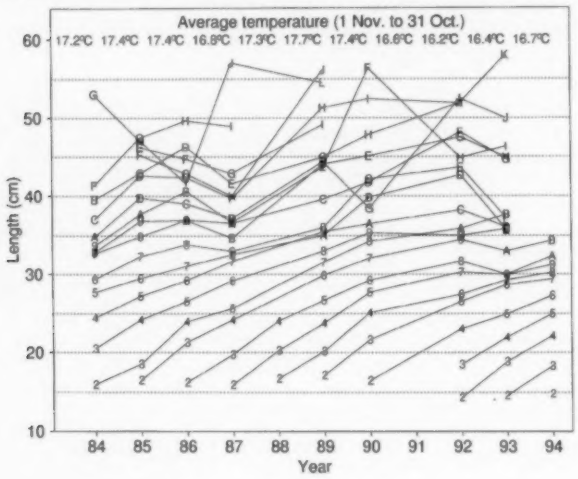

Fig. 2. Length-at-age data from cohorts born no earlier than 1968. Solid lines join cohorts. The letters A–L denote ages 10–21.

Models

Two growth models were considered, the von Bertalanffy and power models.

von Bertalanffy model

The three-parameter von Bertalanffy growth curve gives an animal of age a an expected length of

$$(3) \qquad l_a = E[L_a] = l_\infty(1 - c\ \exp(-ka)).$$

The parameter c will here be termed the "timing" parameter because it positions the growth curve on the horizontal (age) axis so that an age 0 fish is not required to have an expected length of zero. The growth rate of the von Bertalanffy model is

$$\frac{\partial l_a}{\partial a} = k(l_\infty - l_a).$$

Here, abiotic factors at time t are included by allowing k to be a function of t:

$$\frac{\partial l_{at}}{\partial a} = k_t(l_\infty - l_{at})$$

where a double subscript is required to reflect that expected length now depends on both age and time. Solving the above differential equation gives the expected length of an age a fish at time t as

$$(4) \qquad l_{at} = l_\infty(1 - c\ \exp(-\int_{t-a}^{t} k_y dy)).$$

Here, all surveys were conducted in spring and it was more convenient to use the discrete form of eq. 4:

$$(5) \qquad l_{at} = l_\infty(1 - c\ \exp(-\sum_{y=t-a+1}^{t} k_y))$$

where k_y quantifies the growth rate appropriate to the year spanning times $y - 1$ and y.

Power model

The power model essentially prescribes a growth curve that specifies expected length to be proportional to some power of age, and therefore, it does not have an upper theoretical limit on size. The formulation below includes a parameter β that acts in the same way as the timing parameter c in the von Bertalanffy model. The power model of growth used here is

$$(6) \qquad l_a = E[L_a] = \lambda(\beta + a)^\rho, \quad a \geq -\beta.$$

To include abiotic factors, it is more convenient to reexpress eq. 6 in the form $l_a = (\beta^* + ka)^\rho$, which has growth rate

$$\frac{\partial l_a}{\partial a} = \frac{k\rho}{l_a^{(1-\rho)/\rho}}.$$

Allowing k to depend on abiotic factors at time t gives

$$\frac{\partial l_{at}}{\partial_a} = \frac{k_t \rho}{l_{at}^{(1-\rho)/\rho}}$$

and solving the differential equation gives the expected length of an age a fish at time t as

$$l_{at} = (\beta^* + \int_{t-a}^{t} k_y dy)^\rho$$

which in the discrete time case becomes

$$(7) \qquad l_{at} = (\beta^* + \sum_{y=t-a+1}^{t} k_y)^\rho.$$

Modeling growth rate

Growth rate in year t was modeled as a linear function of the annual temperature anomaly δ_t using the following equation:

$$k_t = k(1 + b\delta_t).$$

For the discrete time von Bertalanffy (eq. 5), this results in expected length-at-age of

$$(8) \qquad l_{at} = l_\infty(1 - c\ \exp(-k(a + b \sum_{y=t-a+1}^{t} \delta_y)))$$
$$= l_\infty(1 - c\ \exp(-k(a + b\ \Delta_{at})))$$

where $\Delta_{at} = \Sigma_{y=t-a+1}^{t}\ \delta_y$ can be considered the cumulative temperature anomaly experienced by a fish that is of age a in year t. Similarly, for the discrete time power model (eq. 7), this gives

$$l_{at} = (\beta^* + k(a + b\Delta_{at}))^\rho$$

which can be reexpressed in the form

$$(9) \qquad l_{at} = \lambda(\beta + a + b\Delta_{at})^\rho.$$

Analysis

As a preliminary analysis, the expected lengths-at-age (and time) given by eqs. 3, 6, 8, and 9 were fitted to the estimated length-at-age data by nonlinear (weighted) least squares in both SAS (using PROC NLIN) and Splus (using function "nlmin"). (The results from the two implementations were identical.) It was evident from the age–length keys that variability in length increases with age. Over the range of data fitted, this relationship was well described by $\text{var}(L_{at}) \propto a$, i.e., the standard deviation of length is proportional to the square root of age. Hence, the weight associated with an estimated mean length at age a (eq. 2) was n_{at}/a, where n_{at} is the number of age a fish aged at time t.

It must be borne in mind that while the least-squares analysis used here is the usual way of fitting such models, it

© 1999 NRC Canada

amounts to a gross simplification of the error structure of the data. For example, it will be the case that abiotic factors cause the timing parameters c and β to vary somewhat from year to year. In addition, it is likely that unaccounted year effects on growth will be present because of limitations of the temperature-modified model (e.g., inadequacy of modeling growth rate as linear in temperature anomaly; other abiotic factors). Each cohort is measured repeatedly over time, and hence, these unaccounted for year effects will result in correlation between years within each cohort. Also, because of operational and random variation between the annual cruises of RV *Kaharoa* and the ageing of snapper, measurement errors may be correlated within year. There is strong evidence of this in the length-at-age data, e.g., nine cohorts of snapper have smaller measured lengths in 1993 than in 1992 (Fig. 2) despite being a year older.

Two approaches for obtaining more reliable inferences from the nonlinear least-squares model were deployed. First, a randomization test was performed whereby the temperature data were randomly permuted among years. This was done 1000 times, and on each occasion the model was fitted using these randomized temperatures and the log likelihood of the fit was recorded. The log likelihood from the actual fit (using the true temperature time series) was then compared with the 1000 log-likelihood values from the randomized temperature fits to determine whether the actual fit was better than could reasonably occur by chance if there were no relationship between temperature and growth.

The second approach was to explicitly incorporate the more complex error structure into the model by fitting year as a random effect and to model the within-cohort correlation:

$$(10) \quad L_{at} = l_{at} + \epsilon_{at} + \varepsilon_t.$$

where ε_t are independent Normal$(0,\tau^2)$ random effects to model year-specific measurement errors and ϵ_{at} are Normal $(0, \frac{a}{n_{at}}\sigma^2)$.

The repeated measurement of cohorts is modeled by assuming dependence structure on the ϵ_{at}. To investigate whether the timing of spawning could explain any within-cohort correlation, eq. 10 was also fitted with the timing parameter specified as a linear function of the temperature anomaly over spring (October–December) in the year of spawning:

$$(11) \quad \beta_t = \beta(1 + h\,\gamma_t)$$

where γ_t is the anomaly in spring water temperature for year t.

The Lindstrom and Bates (1990) fit of this model was obtained using both the Splus function "nlme" and the SAS macro "nlinmix" under the assumption that all ϵ_{at} are independent, i.e., without modeling the repeated measurement of cohorts over time. The SAS macro "nlinmix" also permitted the repeated-measures structure to be modeled, and this was done under the assumption of a first-order autoregressive error structure on ϵ_{at} over time within cohorts, i.e., for any positive integer d, the cohort that is age a at time t will be of age $a' = a + d$ at time $t' = t + d$ and the correlation between ϵ_{at} and $\epsilon_{a't'}$ is

$$(12) \quad \text{Corr}\,(\epsilon_{at}, \epsilon_{a't'}) = r^d, \; -1 \le r \le 1,$$

where r is a parameter to be estimated.

Results

The temperature-modified models (eqs. 8 and 9) require the cumulative temperature anomaly for each mean length-at-age value and hence can only be fitted to data from cohorts born no earlier than 1968, the first year in which temperature data were available. This reduces the sample size from 196 to 151. To enable comparison between the temperature-independent models (eqs. 3 and 6) and temperature-modified models (eqs. 8 and 9), the four models were fitted to these same 151 observations.

When fitted to the subset of 151 observations, the resulting log likelihoods (Table 1) show that the temperature-independent power model (eq. 6) provides a better fit than the von Bertalanffy model (eq. 3). These two models were also fitted to the complete set of 196 observations, and the power model remains the preferred (Table 1). The fit of the von Bertalanffy curve changed substantially when the additional observations were included (Fig. 3), whereas the power curve fit did not. In particular, the l_∞ parameter of the von Bertalanffy curve increased by 4.8 cm, or the equivalent of 2.6 SD, when the additional 45 observations were added. This suggests that these 45 observations are not compatible with the von Bertalanffy curve fitted to the 151 from the more recent cohorts. For this reason, and because the power curve fits have higher likelihood, it is only the results from temperature modified fits of the power curve that are given below.

Fixed-effects analysis

The temperature effect produced a highly significant improvement ($p < 0.0001$) in the log likelihood of the fitted model (Table 2). The estimated temperature effect is $\hat{b} = 0.252$, which implies that a year with a 1° temperature anomaly corresponds to a predicted 3-month delay (or advancement) in growth compared with an average temperature year. The residuals, when plotted against age (Fig. 4*a*), exhibit some minor structure, particularly a group of large negative residuals between ages 9 and 15. The strength of the year effect is evident in the plot of residuals against year (Fig. 4*b*) where it is seen that the large negative residuals correspond to the years 1993 and 1994. On the other hand, the years 1984 and 1985 are dominated by positive residuals.

The randomization procedure resulted in 21 of the 1000 fits with randomized temperature having a higher log likelihood than the fit using the actual temperatures. This gives a p value of 0.02. (While statistically significant, this p value is no where near as small as the p value (<0.0001) given by the model fit (Table 2).This is explained at the end of the Discussion.)

Mixed-effects and repeated-measures analyses

The inclusion of year as a random effect (eq. 10) in the fit of the temperature-modified power model (eq. 9) resulted in a statistically significant (Table 2) improvement (with the log likelihood increasing from –399.7 to –365.2, $p < 0.0001$; the result of Self and Liang (1987) shows that a conservative test is provided by assuming twice the difference in log likelihood between the fixed- and mixed-effects models to be χ^2 with 1 df). The temperature effect was estimated to be $\hat{b} = 0.149$ and remains statistically significant ($p < 0.0001$).

© 1999 NRC Canada

Table 1. Summary of fixed-effects fits of the von Bertalanffy curve (eq. 3) and power curve (eq. 6).

Model	l_∞ (cm)	c	k	λ	β	ρ	Log likelihood
151 observations							
von Bertalanffy	48.4	0.849	0.123				–442.4
Power				15.1	–0.856	0.395	–433.5
196 observations							
von Bertalanffy	53.2	0.843	0.100				–559.2
Power				14.9	–0.828	0.399	–541.8

Note: When restricted to cohorts for which temperature data were available (those cohorts born no earlier than 1968) the number of observations is reduced from 196 to 151.

Fig. 3. Power fit (eq. 6) (solid line) and von Bertalanffy fit (eq. 3) (short-dashed line) to length-at-age data on cohorts born no earlier than 1968 (dots). The long- and medium-dashed line are the corresponding fits to all length-at-age data (dots and crosses).

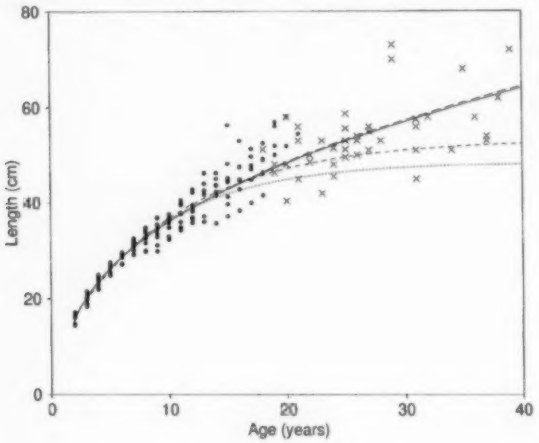

The residuals from the above mixed-effects fit show no pattern against year (Fig. 4*e*), although two large negative residuals arise from smaller than expected lengths of age 3 snapper in 1985 and 1992. All five residuals from the 1987 cohort are positive and all eight from the 1984 cohort are negative, and this indicates possible correlation within cohorts. Thus, there is some evidence for correlation within cohorts. (The multiple "comparisons" problem arises here because we are visually inspecting the residuals from 25 cohorts; hence, it is difficult to assess the strength of this evidence.)

The amount of within-cohort correlation explained by modeling the timing parameter using the spring water temperature anomaly was not statistically significant ($p > 0.05$). Alternatively, the repeated-measures analysis with autocorrelated errors was marginally significant ($p = 0.05$) and estimated the correlation between successive years to be $r = 0.19$. The estimates and diagnostics were little changed (e.g., $\hat{b} = 0.150$) and the residuals are not detectably different from those in Figs. 4*d*–4*f*.

Discussion

The estimated temperature effect of $\hat{b} = 0.252$ (Table 2) given by the fixed-effects model is an overestimate of the true effect, the overestimation arising from to the significant random year effect. For example, it was previously noted that nine cohorts shrunk in observed size between 1992 and 1993. This year was a cold one, and hence, this random year effect is inflating the temperature effect. The preferred model is the mixed-effects fit with autocorrelated errors within cohorts, specified by eqs. 9, 10, and 12. The estimated value of the temperature effect is $\hat{b} = 0.150$ (Table 2), which implies that a year with a 1° temperature anomaly corresponds to a predicted 8-week delay (or advancement) in growth compared with an average temperature year.

The power curve was used here rather than the von Bertalanffy curve because the temperature-independent fit was better and was not sensitive to restriction of the analysis to cohorts born no earlier than 1968. The temperature-modified fixed- and mixed-effects von Bertalanffy models were also fitted and gave similar results ($\hat{b} = 0.283$ and $\hat{b} = 0.164$, respectively) but always provided a worse fit than the power curve.

Figure 3 suggests that the von Bertalanffy fit is sensitive to the age range of the length-at-age data used. In particular, the l_∞ increased from 48.4 to 53.2 cm when the data from older cohorts were included. This phenomenon has arisen in previous investigations of snapper growth. The data of Paul (1976) suggest that snapper in the Hauraki Gulf have a von Bertalanffy growth curve with l_∞ of less than 50 cm. However, the recent stock assessment by Gilbert and Sullivan (1994) utilized length-at-age data containing older snapper and estimated an l_∞ of 58.8 cm.

The power curve does have indeterminate growth; however, the expected lengths-at-age do not get unreasonably extreme even at the upper limit of the snapper life span of 60 years (Paul 1992), at which age, a length of 78.1 cm is predicted from the preferred model under the assumption of constant temperature. Snapper as large as 100 cm have recently been tagged in the Leigh Marine Reserve (T. Willis, Leigh Marine Laboratory, University of Auckland, Auckland, New Zealand, personal communication). The oldest snapper in the database of age–length keys was 39 years old, corresponding to a predicted length of 65.3 cm. It was, in fact, 72 cm long. In the other extreme of age, the power curve would not adequately model length-at-age of very young fish. Indeed, because the timing parameter β is estimated to be –0.722, a length of zero is predicted at age 0.722 and the curve is not defined at ages less than this.

Both the von Bertalanffy and power curves must be considered, at best, approximations to snapper growth, and the accuracy of this approximation depends on the age range

© 1999 NRC Canada

Table 2. Summary of power curve (eq. 6) and temperature-modified power curve (eq. 9) fits to the cohorts born no earlier than 1968 (151 observations).

Model	λ	β	ρ	*b*	Log likelihood
Fixed effects					
Eq. 6	15.1 (0.7)	–0.856 (0.149)	0.395 (0.018)		–433.5
Eq. 9	15.0 (0.5)	–0.721 (0.119)	0.399 (0.014)	0.252 (0.028)	–399.7
Mixed effects					
Eqs. 6 and 10	14.2 (0.5)	–0.703 (0.115)	0.420 (0.016)		–382.5
Eqs. 9 and 10	14.6 (0.4)	–0.719 (0.097)	0.411 (0.014)	0.149 (0.024)	–365.2
Eqs. 9, 10, and 11	14.7 (0.4)	–0.749 (0.095)	0.408 (0.013)	0.153 (0.023)	–363.6
Eqs. 9, 10, and 12	14.6 (0.4)	–0.722 (0.099)	0.410 (0.014)	0.150 (0.026)	–363.3

Note: The mixed-effects fits all use the error structure of eq. 10 with year as a random effect. The model using eq. 11 uses the anomaly in spring water temperatue to model an effect on the timing parameter. The repeated-measures model fits the within-cohort autoregressive errors given by eq. 12 and is the preferred model. Standard errors are given in parentheses.

Fig. 4. Weighted residuals from the power curve (eq. 9) (*a–c*) fixed-effects fits and (*d–f*) mixed-effects fits plotted against age, year, and cohort.

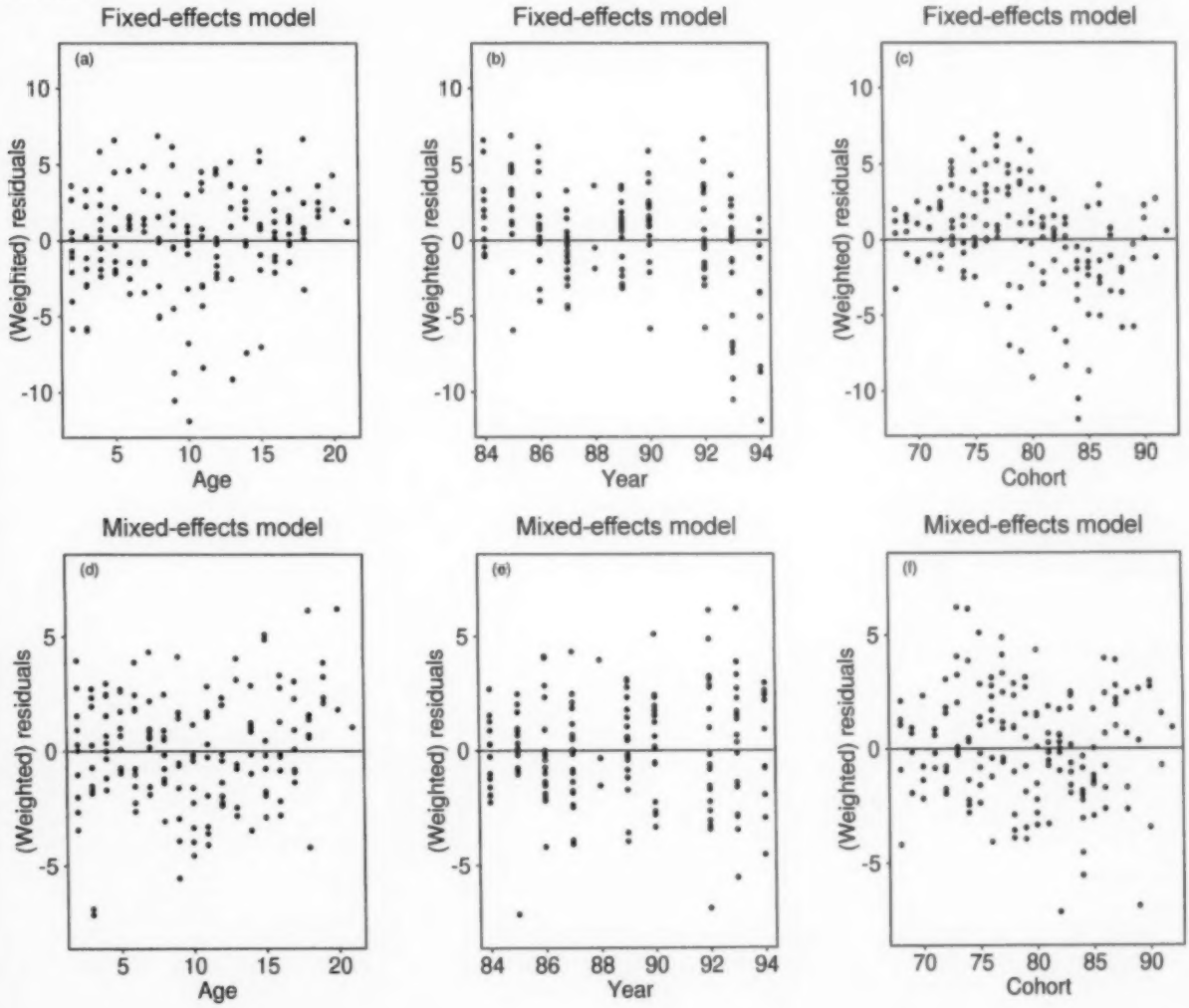

© 1999 NRC Canada

considered. In this application, with attention restricted to ages of 2 and older, the power curve was preferable.

The error term on each length-at-age measurement, ϵ_{at}, in eq. 10 implicitly incorporates the effect of individual variability in snapper length-at-age. However, it is well known that size-dependent fishing mortality will result in the observed lengths-at-age being biased. Most fishing gears select for recruited fish, and hence, faster growing fish are more likely to be removed than slower growing fish, thereby resulting in negative bias in the observed length-at-age data. The extent of this bias could be modeled (e.g., Deriso and Parma 1988), but this requires adequate knowledge about fishing mortalities, vulnerabilities at length, and the magnitude of individual variability in length-at-age. In the Hauraki Gulf snapper fishery, there is the complication that vulnerabilities have to be specified for multiple gear types, including the recreational fishery. The results of Deriso and Parma (1988) suggest that the bias here should not be severe because the fishing mortality in Hauraki Gulf snapper seldom exceeds 0.2. Moreover, it should be noted that the issue of bias is a somewhat moot point because for the purposes of estimating maximum surplus production or performing stock reduction analysis, the growth curves fitted here are arguably more appropriate to use than growth curves that are valid only under no fishing.

The mixed-effects model gave a highly significant p value (<0.0001) for the test of a temperature effect. This can be viewed as a model-based inference in that the p value is conditional on eq. 9 being a reasonable model of snapper length-at-age. Testing for a temperature effect is then simply a test of H_0: $b = 0$. This test was rejected and the estimate of b was about 0.15. On the other hand, the p value of 0.02 from the randomization is (very loosely speaking) indicating how effectively the water temperature time series serves as an explanatory variable in eq. 9 in comparison with any other arbitrarily chosen and unrelated time series (e.g., the time series of batting averages for your favourite baseball team from 1968 through 1994). It is perhaps a truer indicator of the evidence for a causal relationship between temperature and length-at-age but is less powerful than the model-based test and is restricted by the limited number of years of data. Funding permitting, we intend to reevaluate the strength of this relationship when the most recent years of data are added.

Acknowledgements

We are extremely grateful to the New Zealand Ministry of Fisheries for permission to use their snapper age–length data from RV *Kaharoa* cruises and to Dr. Malcolm Francis (National Institute for Water and Atmospheric Research) for providing the data and Fig. 1. Comments from the referees facilitated considerable improvement to the first draft.

References

Annala, J.H., and Sullivan, K.J. 1997. Report from the Fishery Assessment Plenary, May 1997: stock assessment and yield estimates. Ministry of Fisheries, Wellington, New Zealand.

Brander, K.M. 1995. The effect of temperature on growth of Atlantic cod (*Gadus morhua* L.). ICES J. Mar. Sci. **52**: 1–10.

Campana, S.E., and Hurley, P.C.F. 1989. An age- and temperature-mediated growth model for cod (*Gadus morhua*) and haddock (*Melanogrammus aeglefinus*) larvae in the Gulf of Maine. Can. J. Fish. Aquat. Sci. **46**: 603–613.

Cloern, J.E., and Nichols, F.H. 1978. A von Bertalanffy growth model with a seasonally varying coefficient. J. Fish. Res. Board Can. **35**: 1479–1482.

Deriso, R.B., and Parma, A.M. 1988. Dynamics of age and size for a stochastic population model. Can. J. Fish. Aquat. Sci. **45**: 1054–1068.

Fountoura, N.F., and Agostinho, A.A. 1996. Growth with seasonally varying temperatures: an expansion of the von Bertalanffy growth model. J. Fish Biol. **48**: 569–584.

Francis, M.P. 1994. Growth of juvenile snapper, *Pagrus auratus*. N.Z. J. Mar. Freshwater Res. **28**: 201–218.

Francis, M.P., Langley, A.D., and Gilbert, D.J. 1995. Snapper recruitment in the Hauraki Gulf. N.Z. Fish. Assess. Res. Doc. 95/17. NIWA, Wellington, New Zealand.

Francis, M.P., Langley, A.D., and Gilbert, D.J. 1997. Prediction of snapper (*Pagrus auratus*) recruitment from sea surface temperature. *In* Developing and sustaining world fisheries resources: the state of science and management. *Edited by* D.A. Hancock et al. Second World Fisheries Congress Proceedings. CSIRO Publishing, Collingwood, Australia. pp. 67–71.

Francis, R.I.C.C., Paul, L.J., and Mulligan, K.P. 1992. Ageing of adult snapper (*Pagrus auratus*) from otolith annual ring counts: validation by tagging and oxytetracycline injection. Aust. J. Mar. Freshwater Res. **43**: 1069–1089.

Gilbert, D.J., and Sullivan, K.J. 1994. Stock assessment of snapper for the 1992–1993 fishing year. N.Z. Fish. Assess. Res. Doc. 94/3. Ministry of Fisheries, Wellington, New Zealand.

Gilbert, D.J., Sullivan, K.J., Davies, N.M., McKenzie, J.R., Francis, M.P., and Starr, P.J. 1996. Population modelling of the SNA 1 stock for the 1995–96 fishing year. N.Z. Fish. Assess. Res. Doc. 96/15. Ministry of Fisheries, Wellington, New Zealand.

Langley, A. 1995. Trawl survey of snapper and associated species in the Hauraki Gulf, October–November 1994 (KAH9411). New Zealand Fisheries Data Report No. 61. NIWA, Wellington, New Zealand.

Lindstrom, M.J., and Bates, D.M. 1990. Nonlinear mixed effects models for repeated measures data. Biometrics, **46**: 673–687.

Millar, R.B., and Myers, R.A. 1990. Modelling environmentally induced change in growth for Atlantic Canada cod stocks. ICES CM 1990/G:24.

Nakken, O., and Raknes, A. 1987. The distribution and growth of northeast Artic cod in relation to bottom temperatures in the Barents Sea, 1978–1984. Fish. Res. **5**: 243–252.

Paul, L. 1976. A study on age, growth, and population structure of the snapper *Chrysophrys auratus* (Forster) in the Hauraki Gulf, New Zealand. Fish. Res. Bull. 13. MAF, Wellington, New Zealand.

Paul, L. 1992. The biology of snapper. *In* All you want to know about snapper. *Edited by* S. Mossman. New Zealand Fishing News, Auckland. pp. 3–15.

Self, S.G, and Liang, K.Y. 1987. Asymptotic properties of maximum likelihood estimators and likelihood ratio tests under nonstandard conditions. J. Am. Stat. Assoc. **82**: 605–610.

Taylor, C.C. 1958. Cod growth and temperature. J. Cons. int. Explor. Mer, **23**: 366–370.

Teirney, L.D., Kilner, A.D., Millar, R.B., Bradford, E., and Bell, J.D. 1997. Estimation of recreational harvests from 1991–92 to 1993–94. N.Z. Fish. Assess. Res. Doc. 97/15. Ministry of Fisheries, Wellington, New Zealand.

© 1999 NRC Canada

Size-dependent predation in piscivores: interactions between predator foraging and prey avoidance abilities

David Lundvall, Richard Svanbäck, Lennart Persson, and Pär Byström

Abstract: Body size is known to play a crucial role in predator–prey interactions. For a given predator size, it has been suggested that prey mortality should be a dome-shaped function dependent on prey body size. In this study, we experimentally tested (*i*) the suggested mechanisms responsible for the dome-shaped prey vulnerability function and (*ii*) whether a prey refuge affected the form of this function. As prey, we used young-of-the-year Eurasian perch (*Perca fluviatilis*), and as predator, larger Eurasian perch. The prey mortality as a function of prey size was dome shaped for large and medium predators but decreased monotonically with prey size for small predators. Capture success of predators decreased monotonically with increasing prey size and was lower for small predators. In refuge trials, the mortality of prey declined monotonically with prey size for all predator sizes. Refuge use of prey increased with the sizes of both prey and predator. Our results suggest that the hypothesized dome-shaped relationship on prey vulnerability can be altered by the presence of an absolute prey refuge. Our results further suggest that the ability to perform more flexible foraging behaviors is of increasing importance when prey size increases.

Résumé : On sait que la taille corporelle joue un rôle crucial dans les interactions prédateur–proie. Pour une taille donnée de prédateur, on a formulé l'hypothèse que la mortalité des proies devrait suivre une courbe en cloche qui serait fonction de la taille corporelle des proies. Dans la présente étude, nous avons testé expérimentalement (*i*) les mécanismes suggérés responsables de la courbe de vulnérabilité des proies en forme de cloche et (*ii*) si la présence d'un abri pour les proies influe sur la forme de cette courbe. Nous avons utilisé de jeunes perches communes (*Perca fluviatilis*) de l'année comme proies et des perches communes de plus grande taille comme prédateurs. La mortalité des proies en fonction de la taille de celles-ci suivait une courbe en cloche dans le cas des prédateurs de grande taille et de taille moyenne, mais décroissait de façon monotone suivant la taille des proies dans le cas des prédateurs de petite taille. Le succès de capture des prédateurs décroissait de façon monotone tandis que la taille des proies augmentait, et était plus faible chez les prédateurs de petite taille. En présence d'un abri, la mortalité des proies diminuait de façon monotone tandis que la taille de celles-ci augmentait pour toutes les tailles de prédateur. Les proies utilisaient davantage l'abri plus ces dernières et leurs prédateurs étaient gros. Nos résultats laissent penser que la courbe de vulnérabilité des proies qui, à titre d'hypothèse, devrait être en cloche peut être altérée par la présence d'un abri protégeant parfaitement les proies. Ils indiquent aussi que la capacité de manifester des comportements de recherche de nourriture plus souples augmente quand la taille des proies s'accroît.

[Traduit par la Rédaction]

Introduction

Predation in size-structured communities can have substantial impact on the structure and dynamics of prey populations, either directly by reducing prey numbers (e.g., Paine 1976; Tonn et al. 1992) or indirectly by inducing behavioral changes (Mittelbach 1981; Tonn et al. 1992; Persson and Eklöv 1995). When and to what extent a certain prey will be eaten depends on both predator and prey characteristics as well as environmental factors (e.g., Savino and Stein 1982; Tonn et al. 1991).

Received May 19, 1998. Accepted February 26, 1999.
J14594

D. Lundvall, R. Svanbäck,[1] L. Persson, and P. Byström. Department of Ecology and Environmental Science, Umeå University, S-901 87 Umeå, Sweden.

[1]Author to whom all correspondence should be addressed.
e-mail: Richard.Svanback@eg.umu.sc

The size range of prey that a predator potentially can feed on is constrained by the predator's ability to capture and handle the prey (Christensen 1996). The lower prey size limit can be set, both by difficulties in retaining the prey (Persson 1987) and by the predator's ability to detect the prey (Breck and Gitter 1983). The upper limit is set by physical constraints of the predator, such as the size of the feeding apparatus (e.g., mouth gape) (Hart and Hamrin 1988; Hambright 1991) and swimming capacity (Christensen 1996). The size relationship between predator and prey is perhaps the single most important component that affects capture success of piscivorous fish. Capture success has been shown to strongly depend on the relative sizes of predator and prey (Miller et al. 1988; Fuiman 1994) and has generally been suggested to decrease monotonically with prey size (Fuiman and Magurran 1994).

Considering the prey, both body size and developmental state significantly influence an animal's ability to avoid predators (e.g., Werner and Gilliam 1984; Fuiman and Magurran 1994). In fishes, early ontogeny is the most dy-

© 1999 NRC Canada

namic phase in the life cycle with rapid change in size and dramatic changes in morphology that have major implications for predator-avoidance capacity (Miller et al. 1988; Fuiman and Magurran 1994). Fish larvae possess several sensory systems presumed to be important for predator detection. During early ontogeny, these sensory systems undergo rapid development, which is thought to be crucial in determining escape performance of prey (Blaxter 1986; Fuiman 1989; Margulies 1989). An increase in absolute body size also acts on predator–prey interactions, as larger locomotor muscles provide more power to escape predators, and size also limits the numbers of potential gape-limited predators. In conjunction with the morphological and developmental consequences of growth, the behavioral repertoire of a fry also increases through learning. However, there are also penalties with development, as the transparency of the body decreases, which makes larvae more conspicuous to visual predators (Brownell 1985). Encounters with predators may also increase due to increased prey activity (Fuiman and Magurran 1994).

Bailey and Houde (1989) have suggested that the vulnerability of fish larvae should decrease monotonically with prey size for cruising invertebrate predators or filter-feeding fish. For raptorial predators (invertebrates and piscine), vulnerability was predicted to first increase with prey size to a maximum and decrease thereafter with increased size. The mechanisms for the dome-shaped form of prey vulnerability have been suggested to be a combined effect of increased encounter rate at small prey sizes and decreased capture success of larger prey (Fuiman and Magurran 1994; see also Fuiman 1989; Litvak and Legget 1992; Pepin et al. 1992).

To analyze the size-related changes in predator–prey interactions, we conducted a number of experiments with different predator and prey sizes where we focused on how different size-dependent abilities of predator and prey interact to shape the predator capture (prey escape) function. We first tested the hypothesis of Bailey and Houde (1989) as a general function for size-related predator–prey interactions related to encounter rate and capture success. Although previous studies have considered parts of the mechanisms generating the functional form of the size-related predator capture (prey escape) relationship, we consider the whole set of possible mechanisms producing the suggested dome-shaped function. These mechanisms include prey startling response, prey swimming capacities, predator swimming capacities, flexible predator behavior, predator capture success, and prey size. Second, we tested how the presence of a prey refuge affected the shape of the function. We predicted that the presence of a refuge should change the form of the prey vulnerability function. This change in form was hypothesized to result from the fact that the increase in encounter rate between prey and predator with increasing prey size should be counteracted by a simultaneous increase in prey ability to perceive risk and go into the refuge with increasing prey size.

Methods

Adult Eurasian perch (*Perca fluviatilis*) were used as predators and young-of-the-year (YOY) perch as prey in the experiments. The predators were caught with barb-free hooks in the vicinity of Umeå, Sweden. Some YOY perch (9.1–19.8 mm) were collected as embryos and hatched either indoors or in outdoor pools. YOY perch (19.8–47.6 mm) were also electrofished from lakes in the vicinity of Umeå. Predators were acclimatized to the indoor environment in holding tanks (500 L) for more than 2 weeks prior to experiments and prey for more than 24 h.

Three size-classes (total length, means ± SE) of predators were used: small (65.9 ± 5.8 mm), medium (127.9 ± 1.8 mm), and large (156.9 ± 1.7 mm) and eight prey size-classes (total length, means ± SE, $n > 75$ for all size-classes) were used: 9.1 ± 0.11, 14.6 ± 0.14, 19.8 ± 0.22, 24.9 ± 0.11, 29.7 ± 0.13, 35.0 ± 0.10, 39.9 ± 0.11, and 47.6 ± 0.16 mm The predator sizes where chosen to include perch that are normally not piscivorous (66 mm), perch that have started to include fish in their diet (120 mm), and perch that are mainly piscivorous (160 mm) (Persson et al. 1991). The small predators were the only predators that increased significantly in length during the experimental period. They increased in length (means ± SE) from 57.6 ± 1.1 mm on June 10 to 74.4 ± 1.3 mm on August 13. To minimize stress due to manipulation, measured prey were not used in trials the same day and the predator fishes were measured after each trial.

The fish were held in 500-L holding tanks between experiments with similar temperatures (18–20°C) as in the experimental aquaria. The water was changed regularly (>30% volume replacement per week). Prey fish were fed daily with live zooplankton. Predators were mainly fed with live roach (*Rutilus rutilus*) fry but also with earthworms and live zooplankton. Predators were starved for 24 h before experiments to standardize initial hunger level.

The trials were conducted in four 600-L glass aquaria (200 × 60 × 50 cm) with a water depth of 47 cm. The water was changed on a regular basis (>30% volume per week). Fluorescent tubes (4 × 30 W) were placed 55 cm above the water surface. The background was pale green and the exteriors of the bottom and side windows were covered with black plastic sheets. The front windows of the aquaria were divided with vertical (5 cm apart) and horizontal lines (10 cm apart) to estimate swimming speed. The aquaria were divided into one larger and one smaller compartment with a gray polyvinyl chloride sheet that could slide vertically. The smaller compartment (one third of the aquarium length) was used as an acclimatization chamber for the predators and the larger compartment was the experimental chamber. Trials were carried out with and without an absolute refuge. In trials with a refuge, a net (mesh size 10 mm for all prey sizes except for the largest prey size where a mesh size of 12.5 mm was used) divided the experimental arena into two equal parts, each consisting of one third of the length of the aquarium. In trials with refuge, the prey fish were placed in equal numbers on both sides of the net, and in trials without a refuge, prey fish were placed in the middle of the experimental arena. The experimental units were individual trials and each combination of predator, prey, and presence or absence of refuge was replicated four times. Swedish guidelines were followed concerning the care and welfare of the experimental fish.

Because piscivorous perch are mainly social foragers (Eklöv 1992; Eklöv and Diehl 1994), two predators were used in each trial. The predators were held in the acclimatization chamber for 4–12 h prior to a trial. We have found that larger fish need more time to acclimatize. Thirty prey fish were used in each trial (except the 47.6-mm prey size-class where only 20 were used due to difficulties in obtaining a sufficient number of prey), and prey fish were allowed to acclimatize in the arena for 30–60 min before predators were released by raising the polyvinyl chloride sheet for a few seconds. No predator was used more than once for each prey size, and surviving prey were not used in subsequent experiments to avoid the effect of learning in the prey.

The spatial distribution of the fry was measured in the aquaria after acclimatization but prior to the predation experiments for all size-classes of prey. Distributions were assessed both with and

© 1999 NRC Canada

Fig. 1. Mortality (M) of YOY perch (proportion of prey eaten, means ± SE) for small (squares, short-dashed line), medium (circles, long-dashed line), and large (triangles, solid line) predators (perch) in (a) trials without refuge and (b) trials with refuge. The regression lines in trials without refuge are $M = 0.95e^{-0.11(\text{prey size})}$, $M = 0.00063(\text{prey size})^{3.67}e^{-0.20(\text{prey size})}$, and $M = 0.00091(\text{prey size})^{3.19}e^{-0.14(\text{prey size})}$ for the small, medium, and large predators, respectively. The regression lines in trials with refuge are $M = 0.46e^{-0.076(\text{prey size})}$, $M = 0.37e^{-0.030(\text{prey size})}$, and $M = 0.29e^{-0.025(\text{prey size})}$ for the small, medium, and large predators, respectively.

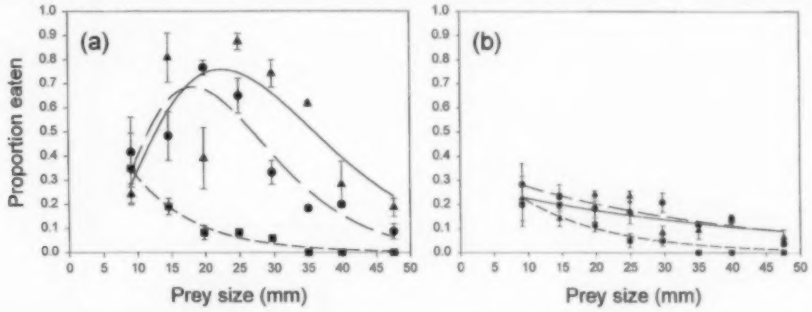

without the refuge net. The position of the prey (using the definition refuge side and arena side) was noted every minute for 5 min. There was no difference in spatial distribution of prey with respect to prey size and refuge treatment (two-way ANOVA for the proportion of prey on the refuge side of the aquaria; prey size: $F_{7,168} = 1.06$, $P = 0.39$; refuge: $F_{1,168} = 0.36$, $P = 0.55$). Mean (±SE) values were 51.8 ± 1.7% without refuge and 49.7 ± 0.3% with refuge.

In most trials, the predators started to attack prey within a few seconds after the entry into the arena. Trials were run for 10 min commencing with the first attack made by a predator. Presence or absence of three unambiguous events was recorded: attack, response from the prey, and capture. A predator attack was defined as a movement towards a prey that resulted in the predator "opening its mouth". We only recorded evasive behavior of prey, and a response was defined as a rapid acceleration when a predator attacked. Capture was defined as a predator swallowing a prey. Three different types of attack were observed: single, multiple, and two-predator. A single attack was defined as one predator attacking one prey once. During a multiple attack, a single predator pursued and repeatedly attacked a single prey. The attack sequence was said to end when the predator either succeeded in its attack, stopped following the prey and slowed down, or attacked another prey without reducing its attack speed. The failed first attack in a multiple-attack sequence was counted as a failed single attack. A two-predator attack occurred when two predators simultaneously attacked the same prey fish. In the analyses involving multiple and two-predator attacks, the refuge trials were not included to avoid an effect of low prey numbers on predator behavior, due to use of the refuge by prey.

Trials were recorded with an S-VHS video camera (focused on the middle third of the aquaria) and by two persons observing the behavior of one predator each. Observations were also voice recorded on the videotape. During a trial, the aquarium was shielded with two opaque, black plastic screens (1.5 × 1.5 m) to avoid any disturbances.

In trials with refuges, numbers of prey left in the refuge at the end of each trial were counted and expressed as a proportion of initial numbers (arena plus refuge), except for the 9.1-mm size-class where it was difficult to locate surviving prey. Mortality was measured as the number of successful attacks by the predators during the 10-min trial and was expressed as proportion of prey eaten.

Capture success was expressed as the proportion of attacks that ended in a prey ingestion. The capture success ratios of single, multiple, and two-predator attacks were based on the five first attacks of each attack type performed by each predator to reduce prey depletion effects. The maximum attack speed of predators and maximum escape speed of prey were measured two dimensionally with frame-by-frame analysis of the video recordings (50 frames/s). No consideration was given as to whether an attack was successful or not when swimming speed was measured. Swimming speeds of predators and prey in the 9.1-mm prey trials were not measured, as attack distances of predators were too short to allow accurate measurements. Also, prey escape responses were almost absent in 9.1-mm perch, making escape speed irrelevant. In the small predator trials with 35.0- to 47.6-mm prey size classes, attack and escape distances were judged to be too short for accurate measurements.

Statistics

ANOVA was generally used in the statistical analysis with the exception of the analysis of swimming speeds, where multiple regression was used. In the regression analyses including predator lengths, the overall mean length of medium and large predators was used. For the small predators, the mean length at each trial was used in the regression analyses due to the significant growth over the experimental period. Data were $\log(x)$ or $\log(x + 1)$ transformed prior to analysis, or, when proportions were tested, data were $\arcsin\sqrt{x}$ transformed. The significance level used was $P < 0.05$.

Results

Prey mortality and prey response

The mortality curves for the prey as a function of size in the absence of a refuge were dome shaped for the large and medium predators but monotonically decreased with prey size for the small predators (Fig. 1a). In trials with a refuge, mortality declined monotonically with prey size for all predator sizes (Fig. 1b). The mortality rate was affected by predator size, prey size, and refuge availability (three-way ANOVA; predator size: $F_{2,144} = 123.27$; prey size: $F_{7,144} = 28.89$; refuge: $F_{1,144} = 135.64$; predator size × prey size: $F_{14,144} = 5.03$; predator size × refuge: $F_{2,144} = 31.69$; prey size × refuge; $F_{7,144} = 5.24$; predator size × prey size × refuge: $F_{14,144} = 4.88$; $P < 0.001$ for all F values).

Both predator size and prey size affected proportions of prey in the refuge after a 10-min trial (Fig. 2) (two-way ANOVA; predator size: $F_{12,63} = 49.48$; prey size: $F_{12,63} = 8.04$; predator size × prey size: $F_{12,63} = 4.91$; $P < 0.001$ for all F values). The effect of predator size reflected the fact that the proportion of prey fish in the refuge was lower with small predator size (Tukey HSD test; $P < 0.001$), whereas no

© 1999 NRC Canada

Fig. 2. Proportion (P) of initial prey (YOY perch) number in the refuge at the end of the experiments (means ± SE) for small (squares, short-dashed line), medium (circles, long-dashed line), and large (triangles, solid line) predators (perch). The regression lines are $P = 0.68e^{-0.5((\text{prey size})-28/18)^2}$, $P = 0.13 + 0.20\ln(\text{prey size})$, and $P = 0.083 + 0.27\ln(\text{prey size})$ for the small, medium, and large predators, respectively. Arrows indicate the largest prey size captured for the small (S), medium (M), and large (L) predators in the trials.

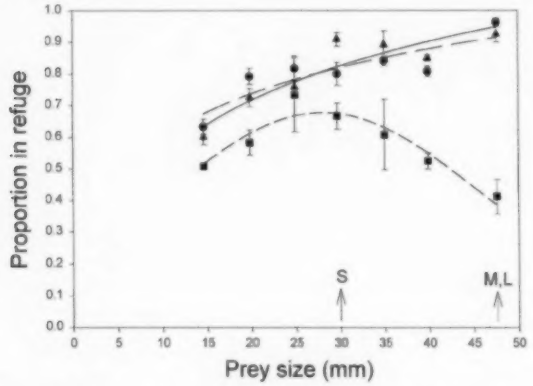

Table 1. Results of two- and three-way ANOVA's of the effects of predator (perch) and prey sizes (YOY perch) on (*a*) single-attack capture success, (*b*) multiple-attack capture success, (*c*) two-predator-attack capture success, and (*d*) occurrence of multiple attacks.

Test and source of variation	F	df	P
(*a*) Single-attack capture success			
Predator size	22.44	2, 144	<0.001
Prey size	54.57	7, 144	<0.001
Refuge	0.599	1, 144	0.439
Predator size × prey size	1.84	14, 144	0.037
Predator size × refuge	0.35	2, 144	0.705
Prey size × refuge	1.08	7, 144	0.377
Predator size × prey size × refuge	1.11	14, 144	0.354
(*b*) Multiple-attack capture success			
Predator size	1.67	1, 41	0.204
Prey size	1.99	7, 41	0.080
Predator size × prey size	1.38	7, 41	0.240
(*c*) Two-predator-attack capture success			
Predator size	4.97	1, 22	0.036
Prey size	1.97	6, 22	0.114
Predator size × prey size	0.46	6, 22	0.829
(*d*) Occurrence of multiple attacks			
Predator size	18.93	2, 134	<0.001
Prey size	2.92	7, 134	0.007
Refuge	0.04	1, 134	0.845
Predator size × prey size	1.84	14, 134	0.039
Predator size × refuge	0.90	2, 134	0.411
Prey size × refuge	1.12	7, 134	0.353
Predator size × prey size × refuge	1.50	14, 134	0.119

difference existed between medium and large predators (Tukey HSD test; $P = 0.996$). For the smallest predator, the proportion of prey in the refuge also decreased for the largest prey size-classes (Fig. 2).

Fig. 3. Single-attack capture success (means ± SE) of the small, medium, and large predators (perch) for different prey (YOY perch) sizes.

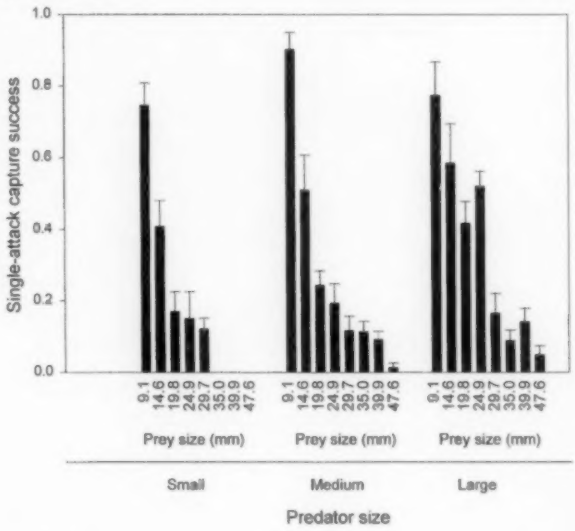

Prey responded frequently to attacks by the predators, and all attacked prey 19.8 mm and larger responded to attacks. For smaller prey, the response to predators decreased with decreasing prey size (86.8 ± 4.3% for 14.6-mm prey and 47.6 ± 2.1% for 9.1-mm prey; means ± SE from 24 trials (n = 3–25 in each trial) with the same prey size), but there was no effect of predator size on the response (one-way ANOVA; $F_{2,9} = 0.17$, $P = 0.84$). There was a significant difference in escape success between responding and nonresponding 9.1-mm prey for small (47.9 ± 11.4 versus 3.1 ± 3.1%; means ± SE; t test; $t_7 = 3.27$, $P = 0.014$) and medium predators (26.8 ± 5.8 versus 6.0 ± 5.0%; $t_7 = 3.90$, $P = 0.006$) but not for large predators (33.8 ± 12.6 versus 14.2 ± 8.6%; $t_7 = 1.68$, $P = 0.14$).

Capture success

Predator foraging behavior varied with prey size. The two smallest prey size-classes (9.1 and 14.6 mm) were dispersed solitarily and moved very slowly and irregularly. Predatory attacks on these prey were characterized by a slow stalking approach towards the prey ending with a short (~2–5 cm) burst attack. Predators and prey in the trials with larger prey were more active. The prey moved around in schools followed by one or both predators. The predators initiated attacks from longer distances at higher speeds, and attacks often involved pursuit of the prey. Repeated strikes at the same prey within an attack sequence (multiple attacks) occurred frequently in the medium and large predator trials. Situations where a prey that had just escaped an attack from one predator suffered one or more attacks from the second predator (two-predator attacks) were also observed but not as frequently as multiple attacks. Multiple and two-predator attacks were performed to a very low extent by the small predators. The small predators were therefore excluded from

© 1999 NRC Canada

Fig. 4. Capture success (means ± SE) of the medium and large predators (perch) for different prey (YOY perch) sizes for (*a*) multiple attacks and (*b*) two-predator attacks.

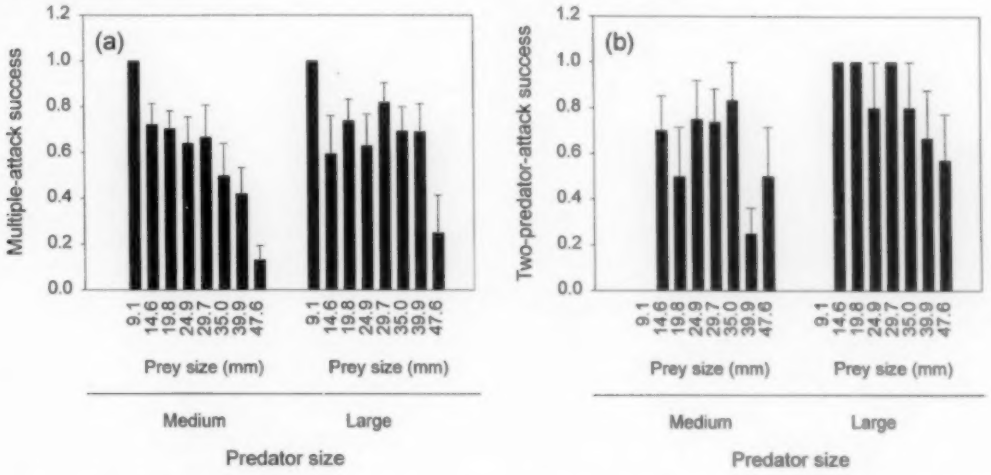

Fig. 5. Proportion of failed first strike in a single attack that resulted in a multiple attack (means ± SE) for the small, medium, and large predators (perch) for different prey (YOY perch) sizes.

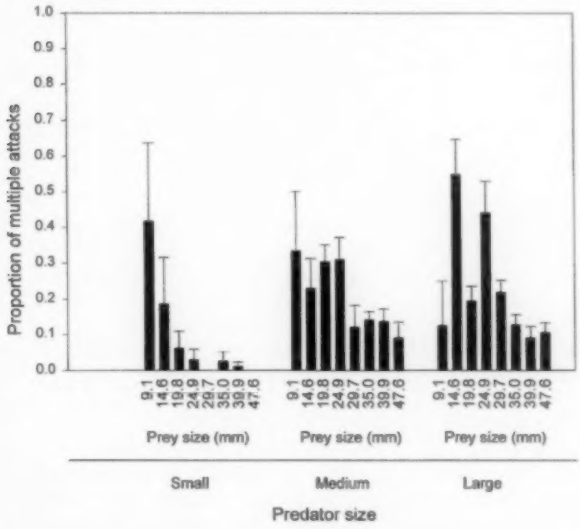

the analyses of capture success for these attack types. The presence of a refuge had no effect on capture success (Table 1). Data on capture success for refuge and nonrefuge experiments were therefore pooled in analyzing capture success (Figs. 3 and 4). The medium and large predators were capable of capturing and ingesting all sizes of prey presented, whereas the largest prey that the small predators were capable of capturing were the 29.7-mm prey.

Single attacks were the dominant attack type for all predator and prey sizes (93.4 ± 1.5, 83.9 ± 1.4, and 84.8 ± 1.7% of all attacks performed for small, medium, and large predators, respectively; means ± SE, $n = 64$ for all predator sizes). The capture success in single attacks increased with predator size and decreased with prey size (Table 1*a*; Fig. 3). The significant interaction between predator and prey size for single-attack capture success was a result of the faster decline in capture success with prey size for the small predators (Table 1*a*).

Capture success for multiple attacks by the medium and large predators was higher than the single-attack capture success (paired t test; medium predators: $t_{27} = 7.79$, $P < 0.001$; large predators: $t_{28} = 5.78$, $P < 0.001$) and was not affected by predator size but tended to decline with prey size (Table 1*b*; Fig. 4*a*). The proportion of failed single attacks that resulted in multiple attacks generally declined with prey size in a pattern dependent on predator size (Table 1*d*; Fig. 5). The frequency of multiple attacks performed by the small predators declined rapidly from about 30% for 9.1-mm prey size to nearly zero for 24.7-mm and larger prey. For the medium and large predators, multiple attacks accounted for 30–40% of the total number of attacks for the smallest prey sizes, which declined to about 10% for the largest prey sizes.

The small predators performed a total of only three two-predator attacks, which all failed, during the 32 trials conducted. The success rate of two-predator attacks of the medium and large predators was higher than the single-attack capture success (paired t test; medium predators: $t_{17} = 4.93$, $P < 0.001$; large predators: $t_{17} = -6.13$, $P < 0.001$). The two-predator-attack capture success was only affected by predator size, which had a positive effect on the capture success (Table 1*c*; Fig. 4*b*). Of all successful two-predator attacks performed by the medium and large predators, 90 and 91% of the prey, respectively, were captured by the "interfering" predator, i.e., not the predator that performed the first attack.

Although infrequent, the proportion of prey captured in multiple and two-predator attacks combined increased with increasing prey size (Fig 6) (regressions: medium predators, $r^2 = 0.77$, $P = 0.0027$; large predators, $r^2 = 0.75$, $P = 0.0035$).

Predator and prey swimming performances

Both predator attack speed and prey escape speed were positively related to predator and prey sizes (Fig. 7) (regressions: prey escape speed, $r^2 = 0.86$, $P < 0.0001$; predator at-

© 1999 NRC Canada

Fig. 6. Proportion of prey (YOY perch) captured (C) in multiple and two-predator attacks by the medium (circles, $C = 10^{0.0154L-0.9289}$, adjusted $r^2 = 0.767$; L = size) and large predators (perch) (triangles, $C = 10^{0.0167L-1.1770}$, adjusted $r^2 = 0.747$) as a function of prey size.

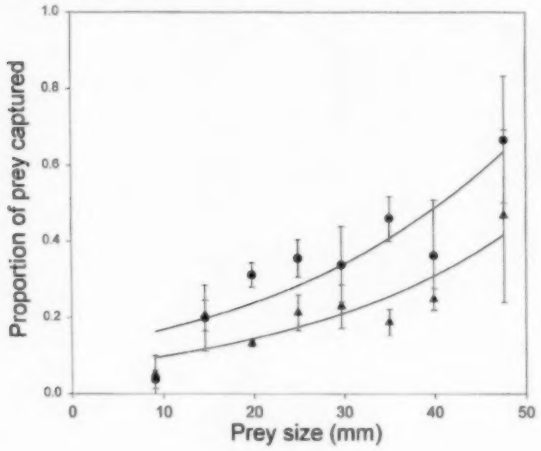

tack speed, $r^2 = 0.55$, $P < 0.0001$). Predator and prey speeds were, however, mostly influenced by prey size. The swimming speed of the small predators was markedly lower than that of the medium and large predators. Prey swam slower when exposed to the small predators than when exposed to the larger predators. The swimming speed difference between predators and prey seemed, however, to be rather constant and independent of predator size throughout the whole size range for prey that were successfully captured.

Discussion

Size-dependent vulnerability and predator and prey performance

Mortality in size-structured populations is highly size dependent (Werner and Gilliam 1984). For a predator of a given size, the capture success has been shown to decline with increasing prey size (Webb 1981; Brownell 1985; Luecke et al. 1990; Fuiman 1994; Christensen 1996), which we also found in our study. Furthermore, we showed that the capture success of predators depended on predator size.

Our results for the medium and large predators supported the hypothesis of Bailey and Houde (1989) regarding the dome-shaped curve for the vulnerability of the prey for a given predator size. The smallest size-class of predators used in our experiments is normally not piscivorous (Persson et al. 1991), and the highest mortality caused by a predator of this size was in the smallest size of prey and prey mortality declined rapidly with increasing prey size (Fig. 1*a*). If smaller sizes of prey had been examined, the mortality function of the smallest predators may also have been dome shaped. The position of the peak of the function also increased with predator size. Satiation, where it occurred, apparently affected prey mortality at the declining end of the prey mortality function. However, the demonstrated decline in capture success of the predators will inevitably lead to a decrease in mortality at larger prey sizes, and predator satiation only contributes to the effect of capture success.

Predator and prey activities in the 9.1- and 14.6-mm prey trials were low, which led to a low mortality of these prey despite the fact that predators had the highest capture success on the 9.1- and 14.6-mm prey size-classes. The short reactive distance that predators display for small prey (Howick and O'Brien 1983) is likely to make it relatively easy for a small prey to move out of the of the predator's visual field and escape. This suggests that the low attack rates on the smallest prey size-classes, resulting in the dome-shaped mortality function, were a result of a low encounter rate. As the densities of YOY perch presented to the predators in the trials were higher than those observed in natural populations (e.g., Wang and Eckmann 1994; Byström et al. 1998), low encounter rates between piscivorous perch and larval perch partly explain the low larval perch mortality observed in some natural systems (Byström et al. 1998).

Development of sensory and motor systems during the larval period decreases the vulnerability of larvae as they become better equipped to detect and avoid predators (Hunter 1981; Blaxter 1986). Correspondingly, we found that the capture success decreased with prey size for all predators. Enhanced burst swimming speed of prey fish with increasing size has been recognized as one of the mechanisms altering the outcomes of attacks (Taylor and McPhail 1985). Other mechanisms important in escaping an attack are the startle response of the prey and timing of the response, which will be enhanced with increasing prey size (Fuiman 1994; Webb 1981).

Since the startle response seems to be important in predator avoidance (Webb 1981), its development is probably crucial in the early life history of fishes. In our experiment, only the smallest prey size (9.1 mm) was inefficient in responding to an attack. The absence of responses is probably attributable to an undeveloped sensory system; thus, prey fail to initiate a motor response in time to elude a strike. In accordance with the results of Fuiman (1989), we found that responding prey had a better chance of surviving an attack, although this may not be true when attacked by the largest predators used in our experiment, as no difference could be shown between responding and nonresponding prey fish. This could be because the evasive maneuver achieved by the startle response was not sufficient to evade the suctorial pressure wave generated by the large predators. We found no difference in response rate to different predator sizes, which may suggest that predator size is not as important as predator species with different attack modes in explaining the response rate of the prey (Webb 1982). One possible explanation for this lack of predator size dependence is that prey fish used the lateral line to a considerable degree to gain information on predation risk.

Prey refuges and the mortality function

Structured habitats that may function as a refuge for prey have been shown to reduce overall predation risk (e.g., Savino and Stein 1982; Turner and Mittelbach 1990; Persson and Eklöv 1995), and small species or small size-classes of larger species are often confined to habitats with complex physical structure (e.g., Mittelbach 1981; Werner and Hall 1988). Theories of vulnerability for prey in vegetation sug-

© 1999 NRC Canada

Fig. 7. Maximum escape speed (S_{prey}) of the prey (YOY perch) (solid circles, $S_{prey} = 2.854(L_{pred.})^{0.178}(L_{prey})^{0.801}$, adjusted $r^2 = 0.858$; L = size) and pursuit speed ($S_{pred.}$) of the predators (perch) (open circles, $S_{pred.} = 5.466(L_{pred.})^{0.278}(L_{prey})^{0.555}$, adjusted $r^2 = 0.550$) of the small, medium, and large predator trials as a function of prey size.

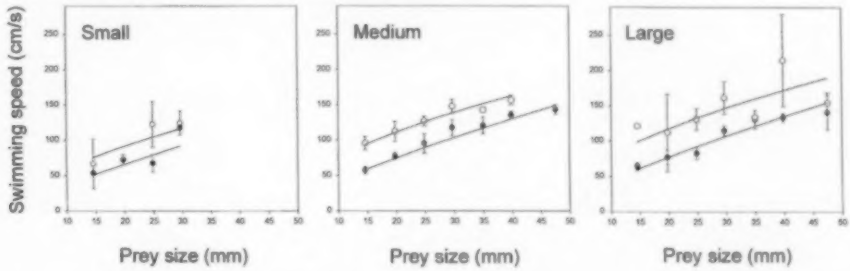

gest that the shape of the vulnerability curve as a function of prey size is hump shaped, as in the case without refuge, but has a lower peak (Persson and Crowder 1997). The shape of the mortality curve in our refuge trials was not hump shaped, but rather monotonically declining with prey size for all predator sizes. The reason behind this relationship might be that prey ability to make use of the refuge effectively increased with size, causing a monotonic decrease in prey fish mortality with size. Our results thus show that the presence of refuge per se may change the form of the mortality function from a hump-shaped curve to a monotonically decreasing curve. It could be argued that this result is an artifact of the absolute refuge used in our experiments. However, pond experimental data using perch as predator have shown that the mortality rate in prey fish is the same for absolute refuges and vegetation refuges, where the predators may enter the refuge, suggesting that results from experiments with absolute refuges have relevance for field conditions (Persson and Eklöv 1995).

Swimming speed and maneuverability

The swimming speed capacity of fish increases asymptotically with increasing body length (e.g., Beamish 1978), which implies that if predator and prey are of the same species, the prey would theoretically never be able to outswim the predator. However, prey pursuit can be assumed to require some degree of controlled maneuvering by the predator, as the pursuit is performed in response to prey movements, and therefore, predator attack speed is lower than maximum swimming speed. Christensen (1996) hypothesized that swimming speed capacity limits the maximum prey size captured by predators, which suggests that the capture success of piscivorous perch is closely linked to predator swimming capacity within the whole size range of available prey. However, besides speed alone, agile and accurate maneuvering is likely to be required in order to capture an escaping prey. Our finding that the predators seemed to adjust their attack speed to the escape speed of the prey, despite a capacity to swim faster, suggests that this behavior increases capture success and that maneuverability may be more important than a large speed advantage. The fact that the capture success declined with increasing prey size despite the predators' abilities to maintain adjusted pursuit speeds further indicates that the maneuverability of the predators decreases with increasing swimming speed.

To conclude, our results support the presence of a dome-shaped form of the size-dependent prey vulnerability function as suggested by Bailey and Houde (1989). We have also provided a number of mechanisms explaining this functional form based on encounter rate and capture success relationships. Encounter rate increased with prey size, which explains the ascending part of the vulnerability function. Prey escape speed and prey escape abilities increased with prey size, causing a decrease in the vulnerability of the prey. Capture success was lower for small predators, which resulted in a monotonical decrease in mortality of prey with increasing prey size. Importantly, we have also shown that the presence of a prey refuge can alter the form of the prey vulnerability function from a dome-shaped form to a monotonically decreasing form as a function of prey size. We suggest that this was due to the fact that the increase in encounter rate with increasing prey size was counteracted by a simultaneous increase in the prey's ability to use the refuge with increasing prey size. The impact of prey refuges on the qualitative form of the size-dependent prey vulnerability function that we have demonstrated is of major importance to consider, as prey fish in natural situations generally use prey refuges to avoid piscivorous predators.

Acknowledgements

We would like to thank Rohlf Dahlström for supplying us with the experimental fish. We also wish to thank Peter Eklöv and two anonymous reviewers who provided helpful comments on earlier versions of the manuscript. Support from the Swedish Natural Science Research Council to Lennart Persson and from the Swedish Council for Forestry and Agricultural Research to Lennart Persson and Pär Byström is greatfully acknowledged.

References

Bailey, K.M., and Houde, E.D. 1989. Predation on eggs and larvae of marine fishes and the recruitment problem. Adv. Mar. Biol. **25**: 1–83.

Beamish, F.W.H. 1978. Swimming capacity. *In* Fish physiology. Vol. VII. Locomotion. *Edited by* W.S. Hoar and D.J. Randall. Academic Press, New York. pp. 101–187.

Blaxter, J.H.S. 1986. Development of sense organs and behaviour of teleost larvae with special reference to feeding and predatory avoidance. Trans. Am. Fish. Soc. **115**: 98–114.

Breck, J.E., and Gitter, M.J. 1983. Effect of fish size on reactive distance of bluegill (*Lepomis macrochirus*) sunfish. Can. J. Fish. Aquat. Sci. **40**: 162–167.

© 1999 NRC Canada

Brownell, C.I. 1985. Laboratory analysis of cannibalism by larvae of the cape anchovy *Engrualis capensis*. Trans. Am. Fish. Soc. **114**: 512–518.

Byström, P., Persson, L., and Wahlström, E. 1998. Competing predators and prey — juvenile bottlenecks in whole lake experiments. Ecology, **79**: 2153–2167.

Christensen, B. 1996. Predator foraging capabilities and prey antipredator behaviours: pre- versus postcapture constrains on size-dependent predator–prey interactions. Oikos, **76**: 368–380.

Eklöv, P. 1992. Group foraging versus solitary foraging efficiency in piscivorous predators: the perch, *Perca fluviatilis*, and pike, *Esox lucius*, patterns. Anim. Behav. **44**: 313–326.

Eklöv, P., and Diehl, S. 1994. Piscivore efficiency and refuging prey: the importance of predator search mode. Oecologia, **98**: 344–353.

Fuiman, L.A. 1989. Vulnerability of Atlantic herring larvae to predation by yearling herring. Mar. Ecol. Prog. Ser. **51**: 291–299.

Fuiman, L.A. 1994. The interplay of ontogeny and scaling in the interactions of fish larvae and their predators. J. Fish Biol. **45**: 55–79.

Fuiman, L.A., and Magurran, A.E. 1994. Development of predator defences in fishes. Rev. Fish Biol. Fish. **4**: 145–183.

Hambright, K.D. 1991. Experimental analysis of prey selection by largemouth bass: role of predator mouth width and prey body depth. Trans. Am. Fish. Soc. **120**: 500–508.

Hart, P., and Hamrin, S.F. 1988. Pike as a selective predator. Effects of prey size, availability, cover and pike jaw dimensions. Oikos, **51**: 220–226.

Howick, G.L., and O'Brien, W.J. 1983. Piscivorous behaviour of largemouth bass. Trans. Am. Fish. Soc. **112**: 508–516.

Hunter, J.R. 1981. Feeding ecology and predation of marine fish larvae. *In* Marine fish larvae. *Edited by* R. Lasker. Washington Sea Grant, University of Washington Press, Seattle, Wash. pp. 33–79.

Litvak, M.K., and Legget, W.C. 1992. Age and size-selective predation on larval fishes: the bigger-is-better hypothesis revisited. Mar. Ecol. Prog. Ser. **81**: 13–24.

Luecke, C., Rice, J.A., Crowder, L.B., Yeo, S.E., and Binkowski, F.P. 1990. Recruitment mechanism of bloater in Lake Michigan: an analysis of the predator gauntlet. Can. J. Fish. Aquat. Sci. **47**: 524–532.

Miller, T.J., Crowder, L.B., Rice, J.A., and Marschall, E.A. 1988. Larval size and recruitment mechanism in fisheries: toward a conceptual framework. Can. J. Fish. Aquat. Sci. **45**: 1657–1670.

Mittelbach, G.G. 1981. Foraging efficiency and body size: a study of optimal diet and habitat use by bluegills. Ecology, **62**: 1370–1386.

Paine, R.T. 1976. Size-limited predation: an observational and experimental approach with the *Mytilus–Piaster* interaction. Ecology, **57**: 858–873.

Pepin, P., Shears, T.H., and de Lafontaine, Y. 1992. Significance of body size to the interaction between a larval fish (*Mallotus villosus*) and a vertebrate predator (*Gasterosteus aculeatus*). Mar. Ecol. Prog. Ser. **81**: 1–12.

Persson, L. 1987. The effects of resource availability and distribution on size class interactions in perch, *Perca fluviatilis*. Oikos, **48**: 148–160.

Persson, L., and Crowder, L.B. 1997. Fish–habitat interactions mediated via ontogenetic niche shifts. *In* The role of submerged macrophytes in structuring the biological community and bio-geochemical dynamics in lakes. *Edited by* E. Jeppesen, Ma. Søndergaard, Mo. Søndergaard, and K. Christoffersen. Springer-Verlag, Berlin. pp. 3–23.

Persson, L., and Eklöv, P. 1995. Prey refuges affecting interactions between piscivorous perch and juvenile perch and roach. Ecology, **76**: 70–81.

Persson, L., Diehl, S., Johansson, L., Andersson, G., and Hamrin, S.F. 1991. Shifts in fish communities along the productivity gradient of temperate lakes — patterns and the importance of size-structured interactions. J. Fish Biol. **38**: 281–293.

Savino, J.F., and Stein, R.A. 1982. Predator–prey interaction between largemouth bass and bluegills as influenced by simulated, submersed vegetation. Trans. Am. Fish. Soc. **111**: 255–266.

Taylor, E.B., and McPhail, J.D. 1985. Burst swimming and size-related predation of newly emerged coho salmon *Oncorhynchus kisutch*. Trans. Am. Fish. Soc. **114**: 546–551.

Tonn, W.M., Paszkowski, C.A., and Holopainen, I.J. 1991. Selective piscivory perch: effects of predator size, prey size and prey species. Verh. Int. Ver. Limnol. **24**: 2406–2411.

Tonn, W.M., Paszkowski, C.A., and Holopainen, I.J. 1992. Piscivory and recruitment: mechanisms structuring prey populations in small lakes. Ecology, **73**: 951–958.

Turner, A.M., and Mittelbach, G.G. 1990. Predator avoidance and community structure: interactions among piscivores, planktivores and plankton. Ecology, **71**: 2241–2254.

Wang, N., and Eckmann, R. 1994. Distribution of perch (*Perca fluviatilis*) during their first year of life in Lake Constance. Hydrobiologia, **277**: 135–143.

Webb, P.W. 1981. Responses of northern anchovy, *Engrualis mordax*, larvae to predation by a biting planktivore, *Amphiprion percula*. U.S. Natl. Mar. Fish. Serv. Fish. Bull. **79**: 727–735.

Webb, P.W. 1982. Avoidance responses of fathead minnow to strikes by four teleost predators. J. Comp. Physiol. **147**: 371–378.

Werner, E.E., and Gilliam, J.F. 1984. The ontogenetic niche and species interactions in size-structured populations. Annu. Rev. Ecol. Syst. **15**: 393–425.

Werner, E.E., and Hall, D.J. 1988. Ontogenetic habitat shifts in bluegill: the foraging rate – predation risk trade-off. Ecology, **69**: 1352–1366.

© 1999 NRC Canada

Effects of light, prey size, and turbidity on reaction distances of lake trout (*Salvelinus namaycush*) to salmonid prey

Jason L. Vogel and David A. Beauchamp

Abstract: Most studies on visual foraging by fish have focused on reaction distances to invertebrate prey; however, these acuity-based results considerably overestimate reaction distances of piscivores to prey fish. In laboratory experiments, we quantified reaction distance of adult lake trout (*Salvelinus namaycush*) to rainbow trout (*Oncorhynchus mykiss*) and cutthroat trout (*Oncorhynchus clarki*) as a function of light (0.17–261 lx), prey size (55, 75, and 139 mm), and turbidity (0.09, 3.18, and 7.40 NTU). Reaction distances increased rapidly with increasing light from <25 cm at 0.17 lx to about 100 cm at a light threshold of 17.8 lx. Reaction distance declined as a decaying power function of turbidity. By constructing equations that describe the combined effects of light and turbidity on reaction distances, we can begin to model prey detection capabilities of piscivores at any depth at any time of day in natural environments.

Résumé : La plupart des études sur le rôle de la vision dans la recherche de nourriture par les poissons se sont concentrées sur les distances de réaction à l'égard des proies invertébrées; cependant, ces études fondées sur l'acuité visuelle surestiment considérablement les distances de réaction des piscivores à l'égard des poissons proies. Dans des expériences en laboratoire, nous avons quantifié la distance de réaction de touladis (*Salvelinus namaycush*) adultes à l'égard de truites arc-en-ciel (*Oncorhynchus mykiss*) et de truites fardées (*O. clarki*) en fonction de l'éclairage (0,17–261 lux), de la taille des proies (55, 75, 139 mm) et de la turbidité (0,09, 3,18 et 7,40 NTU). Les distances de réaction ont augmenté rapidement avec l'accroissement de l'éclairage, passant de <25 cm, à 0,17 lux, à environ 100 cm, à partir de 17,8 lux. La distance de réaction a diminué avec l'accroissement de la turbidité suivant une fonction exponentielle décroissante. En établissant des équations qui décrivent les effets combinés de la lumière et de la turbidité sur les distances de réaction, nous pouvons commencer à modéliser les capacités de détection des proies des piscivores à n'importe quelle profondeur et n'importe quel moment de la journée dans les milieux naturels.

[Traduit par la Rédaction]

Introduction

Although the influence of predation on the structure and dynamics of aquatic communities has been well documented (Carpenter et al. 1985; Kerfoot and Sih 1987; Northcote 1988; Carpenter and Kitchell 1993), little is known about how pelagic piscivores detect prey. Except in turbid systems, visual foraging is effective in limnetic systems because vision provides greater search volume and offers more precise orientation to prey than other sensory systems (Guthrie and Muntz 1993). Numerous studies have examined visual feeding by zooplanktivores (e.g., Vinyard and O'Brien 1976; Confer et al. 1978; Wright and O'Brien 1984; Henderson and Northcote 1985), but only three studies have measured visual responses of piscivores to prey fish (Cerri 1983; Howick and O'Brien 1983; Miner and Stein 1996), and none of these examined the combined effects of light, turbidity, and prey size. By studying the combined effects of these three factors simultaneously, we can determine the relative importance of each and include interactions that would not be apparent from one- or two-factor experiments.

Visual foraging models depend on improved parameterization of the prey encounter and selection process to predict feeding rates (Eggers 1977; Wright and O'Brien 1984; Aksnes and Giske 1993; Beauchamp et al. 1999). Such models generally estimate a search volume approximated by a cylinder with radius equal to the reaction distance and length equal to the distance traveled during the foraging period (Eggers 1977). Since estimates of search volume will vary in proportion to the square of reaction distance, visual foraging models will be quite sensitive to errors in reaction distance estimates. Thus, estimates of reaction distance as a function of light, turbidity, and prey size can be incorporated into a general pelagic piscivore foraging model. Such a model would improve our understanding of how physical and biotic processes constrain prey detection in time and space. This approach would simulate how predators perceive availability of different prey types and thus should lend insight into why the magnitude of piscivory varies among systems (Beauchamp et al. 1999).

Fish use different visual systems to detect large prey like

Received March 9, 1998. Accepted March 26, 1999.
J14495

J.L. Vogel and D.A. Beauchamp.[1] Utah Cooperative Fisheries and Wildlife Research Unit[2] and Berryman Institute, Department of Fisheries and Wildlife/Ecology Center, Utah State University, Logan, UT 84322-5255, U.S.A.

[1]Author to whom all correspondence should be addressed. e-mail: daveb@cc.usu.edu

[2]The Unit is jointly sponsored by the Biological Resources Division of the U.S. Geological Survey, Utah State University, Utah Division of Wildlife Resources, and the Wildlife Management Institute.

© 1999 NRC Canada

fish versus smaller invertebrate prey. Breck (1993) demonstrated that an acuity-based model for zooplanktivores grossly overestimated reaction distances by piscivores to prey fish. In pelagic systems where piscivory involves relatively large prey under generally low light conditions, visual acuity should be less important than detecting the contrast between prey and its background (Eggers 1977; Cerri 1983; Breck 1993). Contrast will be affected by available light, turbidity, and the backscattering of light between predator and prey (Loew and McFarland 1990; Aksnes and Giske 1993; Breck 1993). In contrast-limited systems, reaction distances to prey are expected to be independent of or minimally dependent on prey size at large distances (Eggers 1977; Breck 1993). Thus, a visual foraging model for piscivores should be constructed from measurements of piscivores reacting to prey fishes rather than extrapolating from zooplanktivore foraging models.

Salmonids are top predators in many northern cold-water lakes and reservoirs; however, little is known about the relationship between their feeding behavior and the temporal and spatial distribution of prey. Lake trout (*Salvelinus namaycush*) have been introduced both legally and illegally into many lakes in western North America and potentially threaten the ecological integrity of existing salmoniform-dominated communities in the region like Yellowstone Lake (Varley and Schullery 1995), Bear Lake (Ruzycki and Wurtsbaugh 1995), and Flathead Lake (McIntyre 1998). In this study, reaction distances of lake trout to prey-sized rainbow trout (*Oncorhynchus mykiss*) and cutthroat trout (*Oncorhynchus clarki*) were measured experimentally as a function of light intensity, turbidity, and prey size in a laboratory tank. By examining the prey detection capabilities of lake trout, we hope to gain insight into how the role of this potential predator and competitor might differ among waters of different optical characteristics, morphometry, and species assemblage.

Methods

Fish exhibit characteristic or stereotypic behaviors when reacting to prey. Upon detection, fish orient head-on to prey (Confer and Blades 1975). This suggests that fish are better able to monitor the prey's position using binocular vision in the frontal field, as has been observed in cichlids (Ingle 1968) and sunfish (Confer and Blades 1975). Reaction distance was determined by measuring the distance from where the fish first orients toward the prey (Vinyard and O'Brien 1976; Howick and O'Brien 1983). This definition can be used for the predator's reaction to prey or, conversely, for the reaction of prey to the predator (Howick and O'Brien 1983; Savitz and Bardygula 1989; Miner and Stein 1996).

Reaction distances were measured for lake trout (330–456 mm total length, $N = 19$) taken from first-generation offspring of wild brood stock. For 1–4 months prior to the experiments, these predators were conditioned to feed on live prey similar to those used in experiments. Prey fish (acquired from several hatcheries in the area) were either rainbow or cutthroat trout depending on the availability of each size-class (mean ± SE total length: 55 ± 1 mm, 75 ± 2 mm, and 139 ± 2 mm). The prey fish at these sizes (55–139 mm) had the same basic morphometric characters and coloration (dark with parr marks). Since the two prey species were not visually different in appearance, both prey species were utilized. Small prey fish (55 mm) were used for the clear-water treatment but were not available for other treatments. Subsequently, only 75- and 139-mm prey fish were available for measuring reaction distances across all combinations of light and turbidity. The fish-holding facility was indoors, and fish experienced 11 h of daylight and 13 h of darkness (building hours 07:00–1800). Fish were held in rectangular and circular tanks supplied with river water maintained at 9–11°C.

To determine how light level, turbidity, and prey size influenced the reaction distances of lake trout to juvenile rainbow and cutthroat trout, reaction distances were measured in a rectangular tank (4.5 m long × 1 m wide × 1 m high). The experimental arena was lined inside with semirigid opaque gray plastic sheets; bottom sheets were etched and painted with a white grid (10 × 25 cm rectangles) on the bottom to aid in measuring reaction distances. The experimental tank, overhead lights, and camera frame were shrouded in two layers of black plastic to exclude any external sources of light. Light levels were generated from four fluorescent lights with two light tubes per fixture (50-W fluorescent tubes) hung end-to-end about 1 m above the water. Light intensities were controlled by adding multiple layers of fiberglass window screen over the lights until the desirable light condition was achieved (Neverman and Wurtsbaugh 1992). Light intensity declined exponentially ($r^2 = 0.998$, df = 11, $P < 0.001$) as layers of window screen were added:

$$(1) \qquad \text{lx} = 273.1e^{-0.504s}$$

where s is the number of layers of screen. Light intensities ranged from 0.17 to 261 lx measured to the nearest 0.1 lx at the water surface with a Spur Scientific (model 840006C) light meter.

Turbidities were controlled by adding various amounts of bentonite clay to achieve three turbidity levels of 0.09, 3.18, and 7.40 nephalometric turbidity units (NTU) measured with a LaMotte (model 2008) turbidity meter. The bentonite clay remained in suspension without circulators during each 4-h experiment.

We used one lake trout and one to three rainbow or cutthroat trout prey in each trial. Before the experiments, lake trout were deprived of food for at least 48 h and were held in the experimental arena for at least 1 h at experimental light intensities and turbidities (Vinyard and O'Brien 1976) with water temperatures between 9 and 11°C. Four to 11 predators were tested individually at each combination of light, turbidity, and prey size.

Predators were placed at one end of the tank behind an opaque sliding door with prey at the opposite end in a 38-L glass aquarium (50.8 cm long × 25.4 cm wide × 30.5 cm deep) inside the large experimental tank to eliminate all but visual stimuli. Inside the prey's aquarium, a piece of rigid gray plastic sheeting was used to confine the prey fish to a smaller region (50.8 cm long × 5 cm wide × 30.5 cm deep) to keep them oriented generally perpendicular to the predator, yet allowed the prey fish to swim freely in this space. Some preliminary experiments (55-mm prey size and 0.09 NTU level at 17.8 and 184 lx) showed no significant differences between mean reaction distances to tethered prey outside the aquarium and those to prey in the aquarium ($F_{3,37} = 0.9$, $P = 0.445$). Consequently, we used the fish inside the aquarium for all subsequent experiments, since this eliminated all but visual stimuli and simplified the measurements of reaction distance. The predator was released and allowed to swim freely in the tank for 1–4 h. Periodically, prey fish and predators were allowed to swim freely in the arena to prevent predators from becoming conditioned to a specific prey location.

Reaction distances of lake trout to prey were recorded using two Polaris CCD black and white surveillance cameras (model VT-90D) with two, four-head Magnavox videocassette recorders (model VRT 242) (with 8-h videotapes), and tapes were replayed later for analysis. When light levels were outside the range of the video cameras (i.e., <0.6 lx), reaction distances were measured directly. Two observers were stationed at the end of the tank and recorded measurements for a specified period of time, with both observers coming to a consensus after a reaction distance behavior was observed. Cameras could record at light levels down to 0.6 lx

© 1999 NRC Canada

Fig. 1. Reaction distances of lake trout (330–456 mm total length) to 55-, 75-, and 139-mm prey as a function of light (0.17–240 lx) in clear water (0.09 NTU). Data points represent the means ± 2 SE of individual average reaction distances for 4–11 lake trout at each combination of light and prey size.

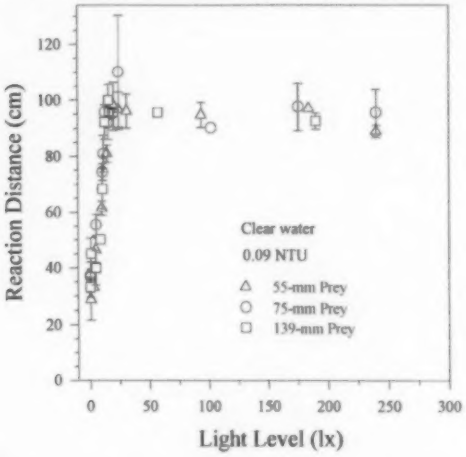

in the low-turbidity treatment but were only effective in light levels to ≥4 lx in higher turbidity treatments.

Reaction distances were measured from video recordings using two methods, depending on the angle at which a predator approached the prey fish. When the predator reacted in a direct line perpendicular to the prey and continued this line up to a specific prey in the aquarium, this point was marked by pausing the videocassette recorder at the beginning of the behavior. The distance was then determined by counting the rectangles between the fish and prey item. However, if the predator swam at some angle to the prey, again following this line up to a specific prey in the aquarium, the lateral and longitudinal distances were recorded and a reaction distance was calculated using the Pythagorean theorem.

Reaction distances of lake trout were measured for three prey sizes (55, 75, and 139 mm) in clear water (0.09 NTU) and for two prey sizes (75 and 139 mm) at 3.18 and 7.40 NTU. Reaction distance was analyzed as a linear function of prey size, a piecewise linear function of light level, and a linear function of $\log_e$-transformed turbidity. Turbidities were $\log_e$ transformed to capture the exponential decline in reaction distance reported in other studies (Vinyard and O'Brien 1976; Wright and O'Brien 1984; Miner and Stein 1996). Interaction among light, prey size, and turbidity was included. Regressions were performed on the mean reaction distances calculated individually for each predator (N = 4–11) within each combination of light, turbidity, and prey size. All piecewise linear regression models were fit using PROC NLIN in SAS release 6.12 (SAS Institute Inc. 1996); this procedure iteratively estimated the intercept, breakpoint, and slope parameters. Significance levels for regression parameter estimates (i.e., nonzero slopes, difference between slopes) were obtained from t tests. The R^2 values were computed as (regression SS/uncorrected total SS). An F-test for significance of the entire regression was computed (Zar 1984).

Results

Reaction distances were not affected by prey size (Fig. 1). Over all light levels (0.17–240 lx), the slopes of reaction distances to different prey fish sizes were not significantly different in clear water (0.09 NTU; t = 0.570, df = 27, P = 0.574), at 3.18 NTU (t = 1.36, df = 14, P = 0.195), or at 7.40 NTU (t = 1.92, df = 15, P = 0.074).

Fig. 2. Unified model of lake trout reaction distances as a function of light (0.17–261 lx) and turbidity (0.09, 3.18, and 7.4 NTU) pooled over the three prey sizes. Data points represent the means ± 2 SE of individual average reaction distances for 4–11 lake trout at each combination of light and turbidity.

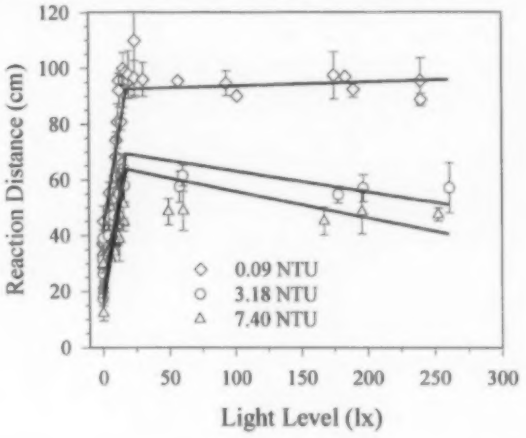

Reaction distances (RD) were highly correlated with light and turbidity (R^2 = 0.984, breakpoint = 17.83 lx, P < 0.001) (Fig. 2):

(2) Increasing limb: RD = 26.84 + 2.81(lx) – 6.09 ln(turbidity) – 0.025 ln(turbidity)(lx)

(3) Level limb: RD = 77.79 – 0.046(lx) – 6.09 ln(turbidity) – 0.025 ln(turbidity)(lx).

Reaction distances increased rapidly from the lowest light level (0.17 lx) to a threshold or breakpoint at 17.83 lx (termed the saturation intensity threshold (SIT) by Henderson and Northcote 1985). Above SIT, reaction distance declined gradually with a small, but significantly negative slope (–0.046) for the effect of light (t = 2.24, df = 68, P = 0.028). Reaction distances declined with increasing turbidity, and there was a significant interaction between light and turbidity (t = 3.75, df = 68, P < 0.001). As light or turbidity increased, the interaction term –0.025 ln(turbidity)(lx) gradually reduced the reaction distance, suggesting that both factors increased backscattering between piscivore and prey fish.

Discussion

By examining the combined effects of light, turbidity, and prey size on reaction distances of piscivorous fish, we gained new insights into the prey detection capabilities of piscivores under different optical conditions expected over a diel cycle and throughout the water column in many salmonid lakes. In this study, reaction distances increased rapidly to a plateau at light ≥17.8 lx, declined with increasing turbidity, but showed no effect of prey size. This threshold effect is significant because it sets an upper limit on reaction distances to prey. Thus, as predators or prey ascend above the SIT depth, increasing light contributes no further advantage for prey detection and no further risk to prey. In fact, prey fish appear to have the advantage over predators at

© 1999 NRC Canada

higher light levels in terms of greater reaction distances (Howick and O'Brien 1983) and more effective predator evasion (Savitz and Bardygula 1989; Petersen and Gadomski 1994). Previous studies have also reported different light thresholds for maximum reaction distances of different fishes to both zooplankton and fish prey; however, these thresholds have rarely been measured precisely: 50–180 lx for lake trout reacting to zooplankton (Confer et al. 1978), 3 lx for Dolly Varden (*Salvelinus malma*) and 5–56 lx for cutthroat trout reacting to zooplankton (Henderson and Northcote 1985), ≥10 lx for bluegill (*Lepomis macrochirus*) reacting to zooplankton (Vinyard and O'Brien 1976), and 5.59 lx for largemouth bass (*Micropterus salmoides*) reacting to bluegill (Howick and O'Brien 1983). This variability in reaction distances among species and the differences in reaction distances to zooplankton versus prey fish represent a fertile area for continued research to define differences in foraging potential among species and under different environmental conditions. Species-specific differences in prey detection capabilities under different optical conditions could have important implications for predatory or competitive advantages of some species over others. Valuable insights can be gained by examining the role of temporal–spatial changes in the visual environment in habitat partitioning, competitive advantage, foraging–predation risk trade-offs, and other interactions.

Maximum reaction distances were achieved at relatively low light intensities that corresponded to ambient midday light intensities at 10–40 m depths in mesotrophic to mesooligotrophic lakes. Thus, piscivores enjoy nearly maximum turbdity-specific reaction distances to prey fish through a range of depths where light is at or above SIT. During crepuscular periods, reaction distances decline rapidly with depth and change rapidly over short time scales. At night, reaction distances will be extremely low, even at the surface. The interaction term between light and turbidity suggests that, above SIT, reaction distances should decline gradually as light increases because increased backscattering reduces the contrast between prey and its background (Cerri 1983; Loew and McFarland 1990; Guthrie and Muntz 1993). This decline becomes more pronounced with higher turbidity. Thus, prey detection could be inhibited near the surface in bright sunlight and improve with depth until ambient light drops below SIT.

Our reaction distances for lake trout differed somewhat from those of Howick and O'Brien (1983) for largemouth bass. Prey size was not a significant factor affecting the reaction distance of lake trout to salmonid prey (55–139 mm) in our experiments, and maximum reaction distances were about 1 m. In contrast, Howick and O'Brien (1983) determined that reaction distances of largemouth bass increased with increasing prey size in clear water over a wide range of light levels (0.195–3340 lx), and maximum reaction distances were about 2 m. Prey size may presumably become important for reaction distances by lake trout at some smaller (<55 mm) prey size, but the shift from a contrast- to an acuity-based prey detection system may only become relevant when feeding on small translucent larval prey fishes. Prey detection might also depend more on the cross-sectional area rather than on the length of prey (Eggers 1977; Aksnes and Giske 1993). If so, then reaction distances should be greater for deep-bodied prey (e.g., bluegill) than for fusiform prey (e.g., cyprinids and salmonids). Interestingly, Howick and O'Brien (1983) found that reaction distances of largemouth bass were actually greater with fusiform redfin shiner (*Lythrurus umbratilis*, previously *Notropis umbratilis*) than with bluegill. These differences could also result from interspecific differences in foraging mode, different neurophysiological prey detection capabilities, or differences in experimental methods. Largemouth bass are predominantly sit-and-wait predators, whereas salmonids tend to be cruising predators. Prey movement increased reaction distances in clear-water situations for planktivores (Wright and O'Brien 1984) and for largemouth bass responding to smaller prey fish (Howick and O'Brien 1983). In our experiments, prey fish were allowed to swim in a confined area, so movement might have influenced reaction distance. For cruising salmonids, even motionless prey would appear to move through the visual field. Although the implications of these different feeding modes on prey detection are currently unknown, it is important to identify these as potentially important factors for determining reaction distance.

We used a neutral gray background, whereas Howick and O'Brien (1983) used a "clear" back to their experimental arena without describing the background color that resulted from this arrangement. Consequently, we cannot determine whether a difference in background coloration might explain the difference in reaction distances measured in this study compared with Howick and O'Brien (1983). Given the natural variability in background colors in lakes, we decided that gray offered the best reproducible compromise in background coloration.

Turbidity was a significant factor in reducing the reaction distances of lake trout. Miner and Stein (1996) examined turbidity effects on reaction distances between prey fish and piscivores over a much larger range (0.3–91.0 NTU) than in this study, but >80% of the observed decline in reaction distance occurred over 0–5 NTU. Moreover, the turbidities used in our experiments reflected the natural range expected in cold-water salmonid systems (except for some glacial lakes: 5–120 NTU; Koenings et al. 1990). Other experiments have focused largely on planktivorous centrarchids, which often experience turbidity levels around 20 NTU in midwestern and southern lakes and reservoirs (Vinyard and O'Brien 1976).

The experimental conditions under which reaction distances were estimated in this study should be considered before applying the reaction distance functions to natural systems. Light levels in this study were indicative of light levels in natural systems from midday (20–200 lx) at depths of 25–40 m through midcrepuscular periods (0.17 lx) at depths of 0–10 m (Henderson and Northcote 1985). We conducted these experiments in a shallow rectangular arena that was essentially a two-dimensional system and cannot duplicate the scale or complexities of lakes. Depth should be considered in future refinements of this approach. Coho salmon (*Oncorhynchus kisutch*) showed longer reaction distances to zooplankton above the horizontal visual plane (Dunbrack and Dill 1984), and Confer et al. (1978) obtained similar results with lake trout. Results from our study suggest that similar reaction distance measurements should be feasible in

© 1999 NRC Canada

larger three-dimensional arenas because the predators react to prey at much shorter distances than the visual detection range of humans or video equipment. Maximum reaction distances by predators were only 1 m in clear water under relatively high light intensity in our experiments. In natural conditions, we have observed lake trout attacking tui chub (*Gila bicolor*) at reaction distances of about 1 m at a depth of 20 m during early dusk in Lake Tahoe (NTU = 0.01, 360 lx).

Visual foraging models for top predators show considerable potential for enhancing our understanding of how piscivores influence the structure and function of limnetic communities (Beauchamp et al. 1999). The results of this study provide key parameters for estimating visual detection capabilities of a piscivore over a range of optical conditions. The resulting reaction distance functions simplify the modeling process, since only light and turbidity are required for a common size range of fusiform prey fishes (for prey 55–139 mm) encountered by salmonids in limnetic systems. To apply this model to specific lakes, basin-specific data (turbidity, light extinction coefficient, temporal changes in incident light levels, and diel prey distribution) can be collected quickly, and relatively inexpensively, thus making it a potentially powerful management tool.

Acknowledgments

Funding was provided by the Vice President for Research at Utah State University and the Berryman Institute. The Utah Water Research Laboratory and Utah Cooperative Fisheries and Wildlife Research Unit provided facilities, and Utah Division of Wildlife Resources provided fish. We thank Rick Orme, Jeff Godfrey, Michael Ward, Carl East, and Mike Mazur for their help with design, construction, and videotape analysis, Susan Durham for statistical assistance, Dana K. Vaughan, and Chris Luecke for review of this manuscript. This paper was derived from a thesis by Jason L. Vogel in partial fulfilllment of a Master of Science degree at Utah State University.

References

Aksnes, D.L., and Giske, J. 1993. A theoretical model of aquatic visual feeding. Ecol. Model. **67**: 233–250.

Beauchamp, D.A, Baldwin, C.M., Vogel, J.L., and Gubala, C.P. 1999. Estimating diel, depth-specific foraging with a visual encounter rate model for pelagic piscivores. Can. J. Fish. Aquat. Sci. **56**(Suppl. 1). In press.

Breck, J.E. 1993. Foraging theory and piscivorous fish: are forage fish just big zooplankton? Trans. Am. Fish. Soc. **122**: 902–911.

Carpenter, S.R., and Kitchell, J.F. 1993. The trophic cascade in lakes. Cambridge University Press, New York.

Carpenter, S.R., Kitchell, J.F., and Hodgson, J.R. 1985. Cascading trophic interactions and lake productivity. BioScience, **35**: 634–639.

Cerri, R.D. 1983. The effect of light intensity on predator and prey behaviour in cyprinid fish: factors that influence prey risk. Anim. Behav. **31**: 736–742.

Confer, J.L., and Blades, P.I. 1975. Omnivorous zooplankton and planktivorous fish. Limnol. Oceanogr. **20**: 571–579.

Confer, J.L., Howick, G.L., Corzette, M.H., Kramer, S.L., Fitzgibbon, S., and Landesberg, R. 1978. Visual predation by planktivores. Oikos, **31**: 27–37.

Dunbrack, R.L., and Dill, L.M. 1984. Three-dimensional prey reaction field of the juvenile coho salmon (*Oncorhynchus kisutch*). Can. J. Fish. Aquat. Sci. **41**: 1176–1182.

Eggers, D.M. 1977. The nature of prey selection by planktivorous fish. Ecology, **58**: 46–59.

Guthrie, D.M., and Muntz, W.R.A. 1993. Role of vision in fish behavior. *In* Behaviour of teleost fishes. 2nd ed. *Edited by* T.P. Pitcher. Chapman and Hall, London, U.K. pp. 89–121.

Henderson, M.A., and Northcote, T.G. 1985. Visual prey detection and foraging in sympatric cutthroat trout (*Salmo clarki clarki*) and Dolly Varden (*Salvelinus malma*). Can. J. Fish. Aquat. Sci. **42**: 785–790.

Howick, G.L., and O'Brien, W.J. 1983. Piscivorous feeding behavior of largemouth bass: experimental analysis. Trans. Am. Fish. Soc. **112**: 508–516.

Ingle, D. 1968. Spatial dimension of vision in fish. *In* The central nervous system and fish behavior. *Edited by* D. Ingle. University of Chicago Press, Chicago, Ill. pp. 51–60.

Kerfoot, W.C., and Sih, A. 1987. Predation: direct and indirect impacts on aquatic communities. University Press of New England, Hanover, N.H.

Koenings, J.P., Burkett, R.D., and Edmundson, J.M. 1990. The exclusion of limnetic Cladocera from turbid glacier-meltwater lakes. Ecology, **71**: 57–67.

Loew, E.W., and McFarland, W.N. 1990. The underwater visual environment. *In* The visual system of fish. *Edited by* R.H. Douglas and M.B.A. Djamgoz. Chapman and Hall, London, U.K. pp. 1–44.

McIntyre, J.D. 1998. An assessment of bull trout and lake trout interactions in Flathead Lake, Montana. A report to the Montana Bull Trout Restoration Team; Montana Fish, Wildlife and Parks; and Confederated Salish and Kootenai Tribes. Available from Montana Fish, Wildlife and Parks, 490 Meridian, Kalispell, MT 59901, U.S.A.

Miner, J.G., and Stein, R.A. 1996. Detection of predators and habitat choice by small bluegills: effects of turbidity and alternative prey. Trans. Am. Fish. Soc. **125**: 97–103.

Neverman, D., and Wurtsbaugh, W.A. 1992. Visual feeding by Bear Lake sculpin. Trans. Am. Fish. Soc. **121**: 395-398.

Northcote, T.G. 1988. Fish in the structure and function of freshwater ecosystems: a "top down" view. Can. J. Fish. Aquat. Sci. **45**: 361–379.

Petersen, J.M., and Gadomski, D.M. 1994. Light-mediated predation by northern squawfish on juvenile chinook salmon. J. Fish Biol. **45**(Suppl. A): 227–242.

Ruzycki, J.R., and Wurtsbaugh, W.A. 1995. Examination of the factors controlling the abundance of Bear Lake forage fishes: piscivore population and consumption estimates. Final Report. Department of Fisheries and Wildlife/Ecology Center, Utah State University, Logan, Utah.

SAS Institute Inc. 1996. SAS/STAT software: changes and enhancements for release 6.12. SAS Institute Inc., Cary, N.C.

Savitz, J., and Bardygula, L. 1989. Analysis of the behavioral basis for changes in salmon diets. Illinois–Indiana Sea Grant Rep. IL-IN-SG-R-89-3.

Varley, J.D., and Schullery, P. 1995. The Yellowstone Lake crisis: confronting a lake trout invasion. Report to the Director of the National Park Service. Yellowstone Center for Resources, Yellowstone National Park, Wyo.

Vinyard, G.L., and O'Brien, W.J. 1976. Effects of light and turbidity on the reactive distance of bluegill (*Lepomis macrochirus*). J. Fish. Res. Board Can. **33**: 2845–2849.

Wright, D.I., and O'Brien, W.J. 1984. The development and field test of a tactical model of the planktivorous feeding of white crappie (*Pomoxis annularus*). Ecol. Monogr. **54**: 65–98.

Zar, J.E. 1984. Biostatistical analysis. 2nd ed. Prentice-Hall, Englewood Cliffs, N.J.

© 1999 NRC Canada

Density-dependent habitat selection by juvenile Atlantic salmon (*Salmo salar*) in experimental riverine habitats

Tammo P. Bult, Stephen C. Riley, Richard L. Haedrich, R. John Gibson, and Jan Heggenes

Abstract: We investigated habitat use of Atlantic salmon (*Salmo salar*) parr in experimental riverine enclosures made up of pool, riffle, and run habitats over a range of densities (0.1–1.25 fish·m^{-2}) to test the implicit assumption in habitat modelling that habitat selection does not change with population density. Results indicated that habitat use changed with population density, with relatively more parr in pools and fewer in runs at higher population densities. Temperature influenced parr distribution, with relatively more parr in runs and fewer in riffles and pools at higher temperatures. Parr distribution was primarily affected by hydromorphological differences among pool, riffle, and run habitats. Effects of population density and temperature on use of pool, riffle, and run habitats were often as large as effects of hydromorphological differences among pool, riffle, and run habitats on fish distributions over the range of temperatures and densities observed. Results varied considerably, despite controlled experimental conditions. We concluded that habitat selection by juvenile Atlantic salmon parr may be density dependent and potentially quite variable.

Résumé : Nous avons étudié l'utilisation de l'habitat par les tacons de saumon atlantique (*Salmo salar*) dans des enceintes lotiques expérimentales constituées d'habitats de fosses, de radiers et de plats selon un intervalle de densité (0,1 à 1,25 poisson/m^2) afin de vérifier le postulat implicite en modélisation de l'habitat selon lequel le choix de l'habitat n'est pas relié à la densité de la population. Les résultats ont montré que l'utilisation de l'habitat varie en fonction de la densité de la population, avec plus de tacons dans les fosses et moins dans les plats lorsque la densité de population est forte. La température a influencé la distribution des tacons, avec un nombre plus élevé dans les plats et un nombre moindre dans les radiers et les fosses à température élevée. La distribution des tacons a été influencée principalement par les différences hydromorphologiques entre les habitats de fosses, de radiers et de plats. Les effets de la densité de la population et de la température sur l'utilisation des habitats de fosses, de radiers et de plats étaient souvent aussi importants que les effets des différences hydromorphologiques entre les divers habitats sur la distribution des poissons dans les intervalles de température et de densité examinés. Les résultats varient considérablement malgré les conditions expérimentales contrôlées. Nous avons conclu que le choix de l'habitat par les jeunes tacons de saumon peut être fonction de la densité et se révéler variable.

[Traduit par la Rédaction]

Introduction

Organism density is often used to identify important habitats and as an indicator of habitat quality (for a discussion, see Van Horne 1983). In fisheries management, relationships between fish density and habitat are often mathematically described in habitat models. Microhabitat models describe the distribution of individual fish over small-scale (<1 m^2) habitat features; macrohabitat models describe fish densities as a function of intermediate- to large-scale habitat features (>10 m^2).

In spite of the widespread use of habitat modelling techniques to predict fish distributions, some underlying assumptions are seldom explicitly stated, tested, or discussed, with most research effort seemingly focused on the development of local models for different river systems or regions (e.g., DeGraaf and Bain 1986) or on the spatiotemporal generality of models (e.g., Bozek and Rahel 1992). Two implicit assumptions in habitat modelling are that (*i*) organism density and habitat quality are positively correlated and (*ii*) habitat selection does not change with density. The objective of this

Received September 23, 1997. Accepted March 30, 1999.
J14218

T. Bult.[1] National Institute for Coastal and Marine Management, P.O. Box 8039, 4330 EA Middelburg, The Netherlands.
S.C. Riley. 310 5th Avenue East, Prince Rupert, BC V8J 1R9, Canada.
R.L. Haedrich. Department of Biology, Memorial University of Newfoundland, St. John's, NF A1C 5S7, Canada.
R.J. Gibson. 29 North Avenue, Mount Merrion, Co. Dublin, Ireland.
J. Heggenes. Department of Biology and Nature Conservation, Agricultural University of Norway, P.O. Box 14, N-1432, Åas-NLH, Norway.

[1]Author to whom all correspondence should be addressed. e-mail: T.P.BULT@RIKZ.RWS.MINVENW.NL

© 1999 NRC Canada

study was to investigate if use of pool, riffle, and run habitats by juvenile Atlantic salmon (*Salmo salar*) is affected by population density.

Previous work has shown that salmonids select positions in streams based on their competitive abilities and the profitability of positions in terms of potential net energy intake rate and predation risk, with profitability of positions being much determined by the physical habitat in terms of cover, bottom topography, and current flow patterns (Fausch 1984; Hughes and Dill 1990; Hughes 1992*a*, 1992*b*; Grand 1997; Grand and Dill 1997). As such, the area within a stream may be regarded as a hierarchy of potential positions, ranging from inaccessible to ideal, with each fish choosing the most profitable position that its rank in the social hierarchy will allow (Fausch 1984; Hughes 1992*a*). Territoriality, small-scale spacing behavior, or preemptive exclusion will thus regulate use of preferred positions and space that, if in short supply, are assumed to regulate population density (Bohlin 1977; Grant and Kramer 1990). From this, the physical habitat may be regarded as a template determining distribution patterns of fish (Hughes 1992*b*).

These processes suggest that salmonid distributions may be best described using the ideal-despotic distribution theory of Fretwell (1972). This theory describes how animals select their habitats assuming that they are "ideal" in knowing where profitability is highest but where access to resources is governed by territorial behaviors. When organisms distribute ideal despotic, the most desirable positions will be occupied first, followed by positions in progressively less desirable habitats. Because of this, the average gain per individual may differ and habitat use may change with density. From this, habitat models may vary with population density.

The ideal-free distribution theory (Fretwell and Lucas 1970) contrasts with this ideal-despotic theory in that access to resources is not restricted by territorial behaviors but all individuals are equal and "free" to move among patches without constraints or restrictions. When organisms distribute ideal-free, fitness of individuals declines with density as individuals occupy the best habitats, the average gain per individual will stabilise to be equal in all habitats, and the fraction of a population in each habitat should equal the fraction of resources occurring there (cf. input matching; Parker 1974). When organisms distribute ideal-free among habitats and the rate of resource renewal in these habitats is not affected by the organisms' density or distribution and all habitats are occupied at low population densities, then relative densities in habitats do not vary with population density.

We hypothesised that riffles and runs would offer the best feeding positions for parr, as drift is concentrated in these habitats, even though there are areas in these habitats that are relatively inhospitable due to high water velocities. By contrast, parr can occupy most of the total area of pool habitat with low energy expenditure, but the "quality" of individual positions in these areas may not be as high due to the lack of large water velocity gradients (Fausch 1984; Hughes and Dill 1990). Because of this, we expected parr to be most dense in riffle or run habitat at low overall densities, but pools would support more parr at higher densities. This process may be best described using the ideal-despotic rather than ideal-free theory.

Material and methods

Study site

The study was conducted in an abandoned spawning channel in the North Harbour River on the Avalon Peninsula of Newfoundland, Canada (47°12′N, 53°37′W), in late August to early October of 1993 and 1994. This channel was used as part of an experimental transplant of pink salmon (*Oncorhynchus gorbuscha*) in the late 1950's and 1960's (Lear 1975). The channel parallels the main stem of North Harbour River for a distance of about 550 m. The width of the channel ranges between 1.5 and 5 m and a sluice at the intake allowed for control of water flow. The most probable natural predators present at the channel included osprey (*Pandion haliaetus*), mink (*Mustela vison*), and American eel (*Anguilla rostrata*). North Harbour River is further described in DeGraaf and Bain (1986).

Three sections of the channel were blocked off by metal posts and wire mesh (0.6 × 0.6 cm, zinc coated). Sections were about 25 m long and had a surface area of about 100 m^2. Within each section, a riffle–run–pool sequence was created. The sequence of the habitats within the main sections was varied: travelling along the channel in an upstream direction, the first section (section 1) consisted of a run–riffle–pool sequence, the second section (section 2) of a riffle–pool–run sequence, and the third section (section 3) of a pool–riffle–run sequence.

To determine the surface area of subsections (= habitat within section), the length of each subsection was measured at three equally spaced transects parallel to the flow and the width was measured at every metre perpendicular to the flow, all to the nearest 0.05 m. Substrate (according to the American Geophysical Union as in Platts et al. (1983)), water depths (metres) and water velocities (metres per second at 60% of depth) were measured in all subsections at seven equidistant points in four equally spaced transects, established perpendicular to the flow.

The average surface area of pool, riffle, and run sections was 46.7 m^2 (range 41.5–51.3 m^2), 37.4 m^2 (range 33.1–41.9 m^2), and 19.2 m^2 (range 15.3–24.6 m^2), respectively. The average depth of pool, riffle, and run sections was 0.284, 0.106, and 0.228 m, respectively. The average water velocity of pool, riffle, and run sections was 0.071, 0.255, and 0.265 $m \cdot s^{-1}$, respectively. The substrate in the channel consisted primarily of coarse to very coarse gravel (16–64 mm). We randomly placed 10 particles of large cobble (128–256 mm) into each subsection to increase small-scale habitat variation.

Experimental procedures

Atlantic salmon parr were introduced into the three experimental sections at densities of 0.1, 0.25, 0.5, 0.75, and 1.0 fish$\cdot m^{-2}$ in 1993 and at densities of 0.1, 0.25, 0.5, 0.6, 0.75, 1.0, and 1.25 fish$\cdot m^{-2}$ in 1994. This range of densities is similar to the range of densities of 1+ and older parr observed in various stations in two nearby rivers (Northeast Trepassey Brook and Freshwater River; Gibson et al. 1993). Prior to introducing fish, all fish present in the experimental sections were removed. In 1993, each density was repeated within each section. In 1994, each density was established once within each section. The sequence of input densities was varied randomly within each section.

The lengths of the parr used in the experiment varied from 7.0 to 11.5 cm fork length (mostly 1+ fish). Fish were caught by electrofishing a variety of pool, riffle, and run habitats. These were located downstream of the entrance to the spawning channel to minimise possible homing behavior after introduction (cf. Saunders and Gee 1964). In 1993, all fish were anaesthetised (tricaine methanesulfonate), measured, weighed, and marked with an adipose fin clip before introduction into the sections. In 1994, the fish were introduced into the sections immediately after cap-

© 1999 NRC Canada

ture, without further handling. The difference in procedures was necessary because of the higher afternoon water temperatures in 1994, which made the fish more sensitive to handling, and because of logistics. The marking in 1993 allowed us to check for holes in the fencing material and to determine if fish caught for introduction had been used previously. No fish were introduced that were known to have been used previously. At introduction, fish were evenly distributed over the surface of the experimental sections.

After a 3-day period, the habitats within each experimental section were blocked with barrier nets. These nets had heavy chains attached to the footropes, which allowed us to block the habitats completely within 2 s and minimised parr redistribution. All fish were then removed by electroshocking until no more fish were captured even after repeated passes. The downstream section 1 was always emptied first, followed by sections 2 and 3. We did not vary this sequence because our activities in the channel caused suspension of silt and debris. Fish were removed from the sections in the morning. In the afternoon, new fish were caught for introduction and were released into the sections.

At the time of removal, water temperature and water level were recorded at a fixed location in the pool subsections. The discharge (cubic metres per second) in the spawning channel was measured at different water levels to establish a relationship between discharge and water level.

On several occasions, the enclosures did not work properly, with fish escaping or entering the experimental sections. We tried to repeat observations where the enclosures had obviously malfunctioned. Forty-six observations, out of a total of 60, were eventually used in the analyses after removal of observations where the enclosure was not considered to have worked.

Acclimation period

We conducted two experiments to assess if a 3-day acclimation period was sufficient to establish a stable fish distribution and to determine if the location where fish were introduced influenced the final distribution. In the first experiment, fish were introduced by even distribution over the surface of the sections and the acclimation period was varied from 3 to 13 days. In the second experiment, fish were introduced in different locations within the experimental sections (upstream, downstream, even) and removed after 3 days.

A general effect of acclimation period or introduction method on the distribution of the fish was not detectable (T.P. Bult, unpublished data). However, the acclimation period might have affected the fish distributions in section 2, with fish moving from the run to the pool habitat at longer acclimation periods. The introduction method might have affected the distributions in section 3, with more fish in the upstream subsection at upstream introductions, but upstream introductions coincided with higher temperatures and temperature effects could not be clearly separated from introduction effects.

Calculation procedures

We did not analyse our data by explaining the density in one habitat as a function of the density in a contrasting habitat, an approach often used when studying density-dependent habitat selection (cf. Rodríguez 1995). We did this because habitat densities of individual removals were not independent in our experiment. We quantified selection of parr for pool, riffle, and run habitat by using selection indices (SI):

$$(1) \qquad \mathrm{SI}_{\mathrm{h1-h2}} = \log_{10}(D_{\mathrm{h1}} + 0.01) - \log_{10}(D_{\mathrm{h2}} + 0.01)$$

where $\mathrm{SI}_{\mathrm{h1-h2}}$ is a selection index (–), quantifying selection for habitat 1 over habitat 2, and D_{h1} is the fish density in habitat 1 (fish per square metre).

If the distribution over habitats is proportional, i.e., an x-fold increase in density in the run habitat due to an increase in population density shows an x-fold increase in the pool habitat as well, selection indices do not change with population density. If habitat selection is density dependent, selection indices vary with population density.

The explanatory variables discharge and section density were rescaled using a logarithmic transformation. Transformations were done assuming a multiplicative effect on selection indices. To avoid spurious correlations, selection indices were analysed as a function of the section density at introduction rather than at removal. This was valid because the overall density at introduction did not vary considerably from the density at removal, as we removed observations where the enclosure did not work properly and fish were able to enter or escape the experimental sections.

To facilitate a comparison of changes in the distribution of the fish among sections and years due to temperature, discharge, or fish densities, selection indices were rescaled relative to the average selection index observed per section per year:

$$(2) \qquad \mathrm{RSI}_{\mathrm{h1-h2}\,s,y,i} = SI_{\mathrm{h1-h2}\,s,y,i} - \frac{\sum_{j=1}^{n_{s,y}} \mathrm{SI}_{\mathrm{h1-h2}\,s,y,j}}{n_{s,y}}$$

where $\mathrm{RSI}_{\mathrm{h1-h2}\,s,y,i}$ is the relative selection index (–), quantifying $\mathrm{SI}_{\mathrm{h1-h2}}$ of observation i in section s in year y, relative to the average observed $\mathrm{SI}_{\mathrm{h1-h2}}$ of section s in year y ($\mathrm{SI}_{\mathrm{h1-h2}\,s,y,i}$), and $n_{s,y}$ is the number of observations on section s in year y.

For analyses based on relative selection indices, the explanatory variables temperature (T), discharge (DIS), and section density (DE) were adjusted relative to the average temperature, discharge, and density per section per year:

$$(3) \qquad T_{\mathrm{ad},i} = T_i - \frac{\sum_{j=1}^{n_{s,y}} T_j}{n_{s,y}}$$

$$(4) \qquad \mathrm{DIS}_{\mathrm{ad},i} = \log_{10}(\mathrm{DSI}_i) - \frac{\sum_{j=1}^{n_{s,y}} \log_{10}(\mathrm{DSI}_j)}{n_{s,y}}$$

$$(5) \qquad \mathrm{DE}_{\mathrm{ad},i} = \log_{10}(\mathrm{DE}_i) - \frac{\sum_{j=1}^{n_{s,y}} \log_{10}(\mathrm{DE}_j)}{n_{s,y}}.$$

The use of relative selection indices and the rescaling of eqs. 3–5 focused the analyses on changes in habitat use relative to deviances from the average conditions within each section and year and was done because we were primarily interested in changes in selection indices due to changes in water temperature, discharge, and density rather than differences in selection indices among sections and years and because a clear separation of section and year effects from temperature, discharge, and density effects was not possible. This is because temperatures in section 3 were always higher than in sections 1 and 2, and temperatures in section 2 were always higher than in section 1, due to the sequence in which sections were sampled in the course of the day. The average discharge, temperature, and section density varied among years. In addition, the unbalanced design of the experiment, especially after removal of several of the observations because of malfunctioning of the enclosures, precluded a clear separation of effects. The use of relative selection indices, rather than selection indices, and the

© 1999 NRC Canada

Fig. 1. Selection of pool habitat versus run habitat ($SI_{pool-run}$ (–)) at varying densities within the experimental sections in 1993 (solid circles) and 1994 (open circles) (n = 46).

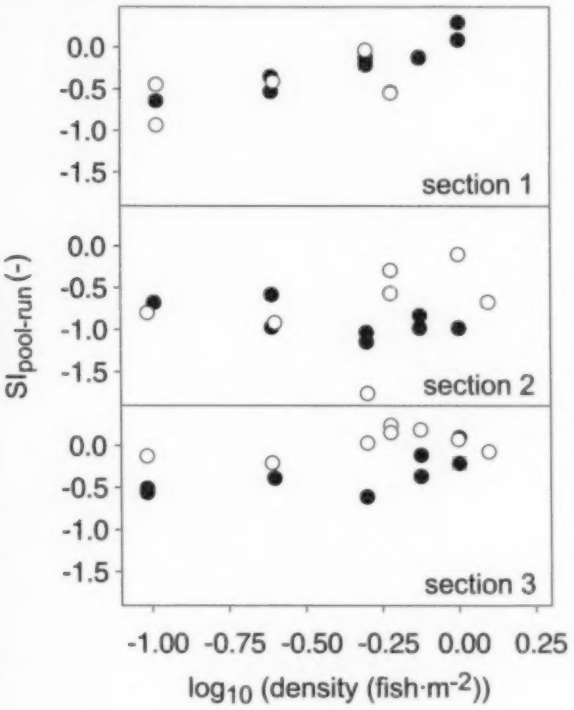

rescaled temperature, section, density, and discharge data facilitated analysis aimed at general changes in habitat selection behavior due to temperature, discharge, and density but was less suitable for analyses aimed at revealing differences among sections and years.

Condition factors (CF) of individual fish were calculated as the residuals of a $\log_{10}$(length (centimetres)) versus $\log_{10}$(weight (grams)) regression analysis using data from 1993. We tested for differences between the condition of fish at introduction and at removal by means of a t test on the differences in average CF of fish at introduction and removal. In addition, we tested if fish in the pool, riffle, and run habitats differed in length or CF and if these differences were subject to changes in overall densities. For these analyses, we used data from both 1993 and 1994 and subtracted the average CF and length of fish in the pool, riffle, and run habitats from the average observed CF and length of all fish within each removal event (RCF and RL, respectively).

Analyses were done using SAS statistical software (SAS Institute Inc. 1988). Residual analyses involved a visual check for patterns in plots of residual versus predicted values as well as tests for normality. Tests for normality involved both a visual check and the Shapiro–Wilks statistic (α = 0.05). If residuals deviated from normality, p values were obtained by randomisation to test the significance of effects of habitat variables on fish densities: Observations on response variables were randomised 5000 times, using sampling without replacement, with observations of explanatory variables held constant. A p value was obtained by calculating the proportion of randomisations with F ratios larger than the observed F ratio. A 5% level was used as a screening criterion to separate "significant" effects from "nonsignificant" effects.

Results

In 1993, the temperature at removal varied from 13.0 to 19.0°C (mean = 15.9, SD = 1.6) and the discharge varied from 0.069 to 0.165 $m^3 \cdot s^{-1}$ (mean = 0.121, SD = 0.029). In 1994, the temperature at removal varied from 11.0 to 19.5°C (mean = 13.9, SD = 2.3) and the discharge varied from 0.079 to 0.131 $m^3 \cdot s^{-1}$ (mean = 0.093, SD = 0.012).

The run habitat was preferred over the pool habitat and the pool habitat was preferred over the riffle habitat in all sections. Few fish were observed in riffle habitats and most fish were observed in the run and pool habitats. The average density in the run habitat was 2.6 times the density in the pool habitat (average $SI_{pool-run}$ = –0.42) and 24.5 times the density in the riffle habitat (average $SI_{riffle-run}$ = –1.39).

Density significantly affected $SI_{pool-run}$, with more fish moving from the run to the pool habitat at higher section densities (Fig. 1; Table 1: p = 0.011, n = 46). This effect was similar among all sections (interaction density × $SI_{pool-run}$ nonsignificant). Figure 1 shows that in sections 1 and 3, a selection for runs ($SI_{pool-run}$ negative) at low section densities shifted towards a selection for pools ($SI_{pool-run}$ positive) at higher section densities. Section densities did not significantly affect $SI_{riffle-run}$ and $SI_{riffle-pool}$. Discharge did not significantly affect $SI_{pool-run}$, $SI_{riffle-run}$, or $Si_{riffle-pool}$ (p > 0.082, n = 46). Water temperatures significantly affected $SI_{pool-run}$ and $SI_{riffle-run}$, with fish moving from the riffle to the run and from the pool to the run habitat at higher temperatures (Table 1). Effects of temperature on $SI_{pool-run}$ differed significantly among sections and years, while effects of temperature on $SI_{riffle-run}$ were similar among sections and years. A model including the variables section, year, temperature, density, and all possible interaction terms showed none of the variables to be significant for $SI_{riffle-pool}$ and $SI_{riffle-run}$ (p > 0.07, n = 46). $SI_{pool-run}$ was affected by temperature and density, but these effects were significant only as part of an interaction term with section and (or) year.

Section densities significantly affected $RSI_{pool-run}$ in sections 1 and 3 and $RSI_{riffle-pool}$ in section 3, with more fish moving from the run to the pool habitat (sections 1 and 3) and from the riffle to the pool habitat (section 3) at higher densities (Table 2). Density did not affect relative selection indices in section 2. Discharge affected $RSI_{pool-run}$ and $RSI_{riffle-pool}$ in section 3, with fish moving from the pool to the run and riffle habitats at higher discharges. Water temperature significantly affected $RSI_{pool-run}$ in section 2, with fish moving from the pool to the run habitat at higher temperatures.

When combining data from all sections, $RSI_{pool-run}$ was significantly affected by section density (Fig. 2; Table 2) and water temperature (Fig. 3; Table 2). A stepwise regression approach showed that $RSI_{pool-run}$ was significantly related to both temperature (n = 46, partial r^2 = 0.129, p = 0.008) and section density (n = 46, partial r^2 = 0.164, p = 0.005):

$$(6) \qquad RSI_{pool-run} = 0.3482DE - 0.0553T$$

$$(n = 46,\ r^2 = 0.293,\ p = 0.001).$$

$RSI_{riffle-run}$ was significantly affected by water temperature (Fig. 3; Table 2) (n = 46, r^2 = 0.188, p = 0.003):

© 1999 NRC Canada

Table 1. Selection of pool versus run habitat ($SI_{pool-run}$), riffle versus run habitat ($SI_{riffle-run}$), and riffle versus pool ($SI_{riffle-pool}$) habitat by parr as a function of parr density (DE, $\log_{10}$(density (fish·m^{-2})) and the temperature at removal (T,°C) in three experimental sections (SE) in 1993 and 1994 (Y).

Analysis	Variable	df	$SI_{pool-run}$	$SI_{riffle-run}$	$SI_{riffle-pool}$
Density	SE	2	**<0.001**	<0.001	<0.001
	Y	1	0.351	0.216	0.064
	DE	1	**0.011**	0.859	0.108
	SE × Y	2	0.054	0.295	**0.017**
	DE × SE	2	0.230	0.165	0.146
	DE × Y	1	0.803	0.343	0.270
	DE × SE × Y	2	0.131	0.572	0.540
Temperature	SE	2	**0.014**	0.865	0.475
	Y	1	**0.002**	0.636	**0.031**
	T	1	**0.010**	**0.009**	0.250
	SE × Y	2	**0.030**	0.665	0.212
	T × SE	2	**0.001**	0.802	0.128
	T × Y	1	**0.002**	0.895	0.057
	T × SE × Y	2	0.062	0.686	0.493

Note: Values of p were based on type III sums of squares and 46 observations. Significant effects are boldfaced ($\alpha = 0.05$).

Table 2. Selection of pool versus run habitat ($RSI_{pool-run}$), riffle versus run habitat ($RSI_{riffle-run}$), and riffle versus pool habitat ($RSI_{riffle-pool}$) by parr as a function of temperature, discharge, and section density (correlation coefficients r and p values (r/p)).

Variable	Section	n	Temperature	Discharge	Density
$RSI_{pool-run}$	1	15	–0.504/0.055	+0.319/0.246	**+0.743/0.002**
$RSI_{pool-run}$	2	15	**–0.723/0.002**	+0.075/0.789	+0.060/0.832
$RSI_{pool-run}$	3	16	+0.216/0.421	**–0.710/0.002**	**+0.632/0.009**
$RSI_{pool-run}$	Total	46	**–0.339/0.021**	–0.018/0.907	**+0.405/0.005**
$RSI_{riffle-run}$	1	15	–0.358/0.191	+0.209/0.455	+0.420/0.119
$RSI_{riffle-run}$	2	15	–0.476/0.073	+0.109/0.699	+0.097/0.731
$RSI_{riffle-run}$	3	16	–0.495/0.051	+0.397/0.128	–0.402/0.124
$RSI_{riffle-run}$	Total	46	**–0.434/0.003**	+0.211/0.159	+0.014/0.928
$RSI_{riffle-pool}$	1	15	+0.115/0.683	–0.092/0.744	–0.287/0.299
$RSI_{riffle-pool}$	2	15	+0.095/0.737	+0.054/0.849	+0.054/0.849
$RSI_{riffle-pool}$	3	16	–0.461/0.073	**+0.614/0.011**	**–0.581/0.018**
$RSI_{riffle-pool}$	Total	46	–0.162/0.283	+0.213/0.155	–0.285/0.055

Note: Temperature, discharge, and density observations were rescaled prior to analyses. Significant correlations are boldfaced ($\alpha = 0.05$); n, number of observations).

(7) $$RSI_{riffle-run} = -0.0862T.$$

$RSI_{riffle-pool}$ was not significantly affected by water temperature, section density, or discharge.

To obtain an impression of the relative importance of habitat, temperature, and section density for the selection behavior of the fish, $SI_{pool-run}$ and $SI_{riffle-run}$ were compared with $\Delta RSI_{pool-run}$ and $\Delta RSI_{riffle-run}$, with $\Delta RSI_{pool-run}$ and $\Delta RSI_{riffle-run}$ calculated based on eqs. 6 and 7 and by varying the temperatures from 12 to 19°C ($\Delta RSIt_{pool-run}$, $\Delta RSIt_{riffle-run}$) and section densities from 0.1 to 1.0 fish·m^{-2} ($\Delta RSId_{pool-run}$). Similarities in the absolute values of selection index and ΔRSI would indicate that effects were comparable. $SI_{pool-run}$, $\Delta RSId_{pool-run}$, and $\Delta RSIt_{pool-run}$ were –0.42, 0.35, and –0.39, respectively. $SI_{riffle-run}$ and $\Delta RSIt_{riffle-run}$ were –1.39 and –0.60, respectively.

The CF of parr at removal was 0.013 less than at introduction ($n = 25$, $t = 0.8286$, $p < 0.001$). This parallels a 1.6% reduction in weight (significant). This change in fish condition was not related to section density ($\log_{10}$(section density)) ($n = 25$, $r^2 = 0.0009$, $p = 0.889$). Fish from the pool, riffle, and run habitats did not differ in RCF ($n = 119$, $F_{2,116} = 1.88$, $p = 0.157$) but did differ in RL ($n = 121$, $F_{2,118} = 23.38$, $p < 0.001$). Parr in pool habitats were 0.35 cm larger than parr in run habitats (significant, GT2, $\alpha = 0.05$). Parr in riffle habitats were 0.2 cm smaller than parr in run habitats (not significant, GT2, $\alpha = 0.05$) and 0.55 cm smaller than parr in pool habitats (significant, GT2,

© 1999 NRC Canada

Fig. 2. Selection of pool habitat versus run habitat ($RSI_{pool-run}$ (–)) at varying densities within the experimental sections in 1993 and 1994 (n = 46; open circles, section 1; solid triangles, section 2; solid squares, section 3). Densities ($\log_{10}$(fish·m^{-2})) were rescaled relative to the average density per section per year.

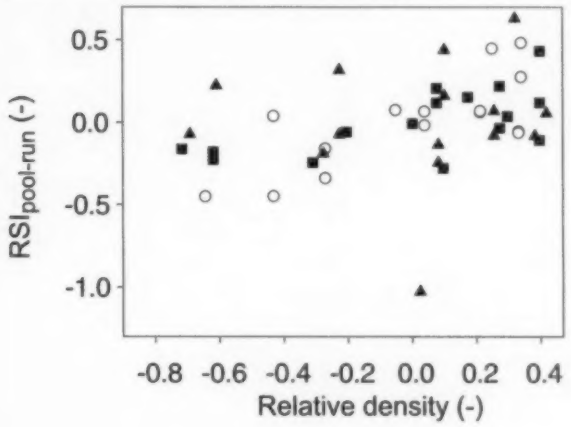

α = 0.05). RL and RCF were not significantly correlated with section density ($\log_{10}$(section density)) for the pool (RL: n = 46, r = –0.129, p = 0.398; RCF: n = 45, r = –0.127, p = 0.418), riffle (RL: n = 29, r = –0.044, p = 0.819; RCF: n = 29, r = –0.232, p = 0.226), and run habitats (RL: n = 46, r = –0.093, p = 0.537; RCF: n = 45, r = 0.152, p = 0.319).

Discussion

Our results indicated that section density and temperature affected habitat use, with parr distributions shifting towards pools from runs at higher densities and towards runs from pools and riffles at higher temperatures. Riffles were strongly avoided, possibly due to a lack of overhanging cover in combination with shallow depths (cf. Gibson 1978). The effects of population density and temperature on fish distributions were often comparable with the effect of hydrological and morphological differences between pool–riffle–run habitats over the range of densities observed. As neither temperature nor population density information is included in current habitat modelling approaches, a reconsideration of these models is warranted, as temperatures at one place often vary over more than 7°C within a few hours in summertime (when most habitat models are developed) and juvenile salmonid populations can vary in excess of one order of magnitude among years (cf. Kennedy and Crozier 1993).

Effects of density and temperature on habitat use were found regardless of the upstream–downstream sequence of the habitats within the enclosures. This indicates that habitat selection was primarily aimed at differences between pool–riffle–run habitats rather than the upstream or downstream location of habitats within sections. Habitat use may have been affected by preconditioning and availability of habitats in the main river. However, it is unlikely that observed density-dependent effects are the result of this, as all fish were pooled before introduction and randomly allocated to the experimental sections.

Fig. 3. Selection of pool habitat versus run habitat ($RSI_{pool-run}$ (–)) and selection of riffle habitat versus run habitat ($RSI_{riffle-run}$ (–)) at varying temperatures within the experimental sections in 1993 and 1994 (n = 46; open circles, section 1; solid triangles, section 2; solid squares, section 3). Temperatures were rescaled relative to the average temperature per section per year.

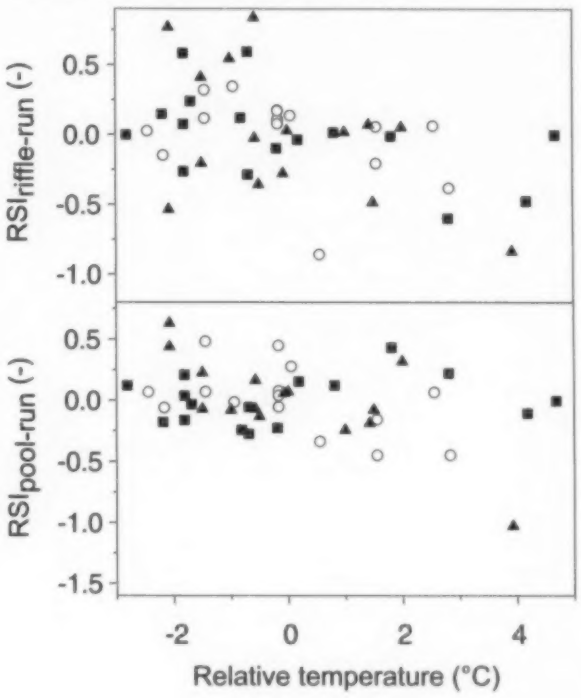

Lengths of parr in pools were largest and lengths of parr in riffles smallest. Parr lost 1.6% of their weight during the experiment, suggesting that most fish had not been feeding during a large part of their stay in the experimental sections. We suspect that this loss of weight is most likely due to handling rather than food scarcity because the condition of the fish did not vary with section density, implying that amount of food was not the cause. Fish had been moved into a new area and probable changes in levels of exploratory and agonistic behavior as a result of this introduction probably reduced feeding behavior (cf. Symons 1971). In addition, the experiment was conducted under seminatural conditions, with flow entering from the river and (presumably) a natural benthic invertebrate community in the channel. We therefore had no reason to expect that food would be more scarce than in the main channel of the North Harbour River.

These results suggest that the ideal-despotic theory may be more appropriate for describing parr distributions than the ideal-free theory, as both runs and pools were used at low section densities and relative densities in pools and runs changed with section density. However, lacking information on the resource distribution as experienced by the fish and also small-scale habitat selection observations, we could not infer with certainty which one of these theoretical models, or combination of models, was most appropriate. If fish select ideal-free for habitats at a spatial scale much smaller than

© 1999 NRC Canada

that of pools, riffles, and runs, a disproportionate distribution at increasing population densities at the larger scales of pool, riffle, and run habitats could result when small-scale secondary habitats within the larger scale pool–riffle–run habitats are occupied only after primary small-scale habitats are filled. If fish select ideal-despotic, a disproportionate distribution could result regardless of the spatial scale at which selection occurs. This also underlines the need for quantitative information on the scales at which fish are associated with their environment.

We suspect that the observed shift in habitat use is best described by a combination of ideal-free and ideal-despotic behavior occurring at small spatial scales. Runs offered relatively more primary positions than pools, and pools offered more intermediate-quality positions than runs. Primary positions were defended first, and because of this, habitat use shifted from runs to pools with increasing density. Parr have been observed to be territorial in riffles and less aggressive in pools (Kalleberg 1958; Gibson 1978; Gibson and Cunjak 1986). If parr densities are limited by territoriality, as suggested by Grant and Kramer (1990), or by small-scale spacing behavior, parr in our run habitats may have occupied primary spots by ideal-despotic behavior, whereas parr in the pool habitats may have displayed more of an ideal-free behavior (cf. Gotceitas and Godin 1992). From this, one may expect the larger and more competitive individuals in the run habitat, which is contrary to our findings that showed that individuals in the pool habitat were larger than those in the run habitat. Possibly, the larger individuals occupied the deeper habitats because of competitive segregation or differences in habitat selection between smaller and larger individuals (Bohlin 1977, 1978; Kennedy and Strange 1986), which may be an adaptation to avoid predation.

The observed shift in selection from pool and riffle habitats to run habitat at higher temperatures may be explained in terms of energy maximisation. At higher temperatures, routine metabolic rates increase and therefore oxygen demands do as well (Brett 1962). Fish that hold positions on the bottom of run and riffle habitats, using their pectoral fins and water currents, may be more efficient in taking up oxygen than fish that are positioned in pool areas, as oxygen uptake for fish in pool habitats will be more of an active process of opercular ventilation and swimming. Riffle habitats were avoided, particularly at higher temperatures, possibly because of an increased risk of predation at low water levels in combination with high temperatures in these habitats.

Results differed with respect to the generality of the observed effects. Analyses based on selection indices suggest that density affected fish distributions only under certain conditions (temperatures, sections, years), as no general temperature or density effect was found based on a model including section, year, density, temperature, and all possible interaction terms. However, when temperature and density were treated within separate models, a general effect of temperature and density was observed (Table 1). Analyses based on relative selection indices also suggest a general effect of temperature and density on habitat use (Table 2). These differences may be partly due to the effects of section, year, density, and temperature being confounded in combination with the unbalanced design of the experiment. However, they may also suggest a limited generality of results. In addition, selection indices varied widely, even within sections and years (Fig. 1), and in spite of our efforts to make habitats in the different sections as similar as possible, large differences were found in habitat use among sections (Fig. 1; Table 1).

The observed variation in habitat use among sections and years may be due to variable habitat selection behaviors or a mismatch between the scale of observations at pools, riffles, and runs and the much smaller spatial scale at which fish select habitats (<1 m^2). The habitats as experienced by fish may therefore be seen as far more diverse than suggested by variables that are based on environmental conditions averaged over larger scales. From this, a macrohabitat approach will only give an indirect impression on habitat use. This suggests that a macrohabitat modelling approach is likely to explain only a limited portion of the observed variation of fish density observations, that models are not likely to perform well when extrapolated over space or time, and that managerial decisions from habitat models may be improved when habitat models take into account variability or flexibility in habitat use.

Bohlin (1977, 1978) previously studied density-dependent habitat use by brown trout (*Salmo trutta*). From small-scale experiments (riverine enclosure 217 m in length, stream aquarium 3.6 m in length), he showed that habitat use of age 1+ trout varied with population density. Elliott (1986) also concluded that habitat use of brown trout was density dependent. However, these studies did not provide information on how the effect of population level on fish distributions compared with the effect of the physical habitat. Bohlin (1977) further showed that distributions of age 1+ trout may be explained by intracohort competition for territories of different quality and that distributions of age 0+ trout may be affected by older fish by intercohort competition or predation, resulting in deeper areas being occupied by larger fish. Bohlin (1977, 1978) also showed that these processes of intercohort competition or predation may affect age 0+ trout abundance at the population level as well, i.e., small space–time scale behavioral processes had large space–time scale effects. Effects of density on distribution by social interactions were also studied by Hughes (1992*a*, 1992*b*) who showed that when numbers of Artic grayling (*Thymallus arcticus*) increase, positions are occupied in an order that reflects the desirability of positions and the dominance rank of individuals. Social interactions thus regulate fish distribution, and habitat use may vary with population size. These findings were in line with results from our study that showed that habitat use varied with section density and that larger parr were found in pools and smaller ones in riffles.

Our results contrast with the findings of Rodríguez (1995), who studied density-dependent interactions between sympatric salmon and brook trout (*Salvelinus fontinalis*) based on 12 pool–riffle pairs and concluded that interspecific interactions changed habitat selection among pools and riffles with density as brook trout were displaced from riffles to pools at increasing salmon densities but intraspecific interactions did not. This contrast with our study may be due to a limited generality of the observed patterns, which in turn may be partly due to a mismatch between the scale of observations at pools, riffles, and runs and the much smaller spatial scale at which fish select habitats. The occur-

© 1999 NRC Canada

rence of brook trout may be more indicative of the quality of small-scale habitat features within pools and riffles as experienced by salmon than the definition of pools and riffles itself, i.e., relationships between salmon and brook trout densities may not necessarily be due to interspecific interactions alone. In addition, intraspecific effects may be more easily detectable in the absence of interspecific effects, i.e., in sympatry, intraspecific effects are simply hidden by stronger interspecific interactions. Our experimental setup with repeated use of standardised habitats should be more able to pick up the effect of intraspecific interactions on habitat use and contrast this effect with the effect of the physical habitat itself, which may account for the fact that we did observe density-dependent habitat selection due to intraspecific interactions and Rodríguez (1995) did not.

Conclusions

We concluded that habitat selection by juvenile Atlantic salmon parr is temperature and density dependent. Parr densities in pool–riffle–run habitats became more similar at increasing population densities. From this, fluctuations in population abundance mainly induce fluctuations in abundance in habitats that harbour low densities at low overall population density (secondary habitats): at higher population densities, the occupied habitat will expand to increasingly include secondary habitats; at lower population densities, the occupied habitat will contract into the primary habitats. The implications are that habitat models may be expected to vary with temperature and population density. Therefore, habitat quality assessments based on density information and conclusions with respect to preferred and avoided habitat probably also vary with temperature and population density and can therefore influence subsequent managerial actions such as the creation of preferred habitats and discharge regulations. In addition, the results illustrate that the quality of habitats can only be evaluated within the context of all available habitat, as habitat quality is a relative rather than an absolute measure (Heggenes 1991), and point to a fundamental problem of extrapolating habitat suitability criteria from one region or river to another or from one flow level to another because under different conditions, habitat availability will certainly differ. The results varied among years and experimental enclosures, despite controlled experimental conditions. This may be due to variable selection behaviors or a discrepancy in spatial scales of observations (pool–riffle–run) and habitat selection behaviors (<1 m^2). How fish select their habitats and how variable or flexible this behavior is may be best addressed using an experimental setup because conditions are much in control of the researcher. Additional field observations are needed to assess whether the results of such experiments can be extrapolated to scales relevant to fisheries management. In short, our results underline the need for information on habitat selection behavior for fish habitat management.

Acknowledgements

This study was supported via a Natural Sciences and Engineering Research Council of Canada grant to R.L.H. and a contract with the Canadian Centre for Fisheries Innovations. The manuscript was greatly improved by the comments of D. Methven, M. Rodríguez, D.C. Schneider, and three anonymous reviewers. We gratefully acknowledge the field assistance of J.K. Bult, G. Crutcher, L. Janes, and J. Robinson and would like to thank J. Armstrong, E. Beall, and E. Garcia-Vazquez for initial discussions about the experiment.

References

Bohlin, T. 1977. Habitat selection and intercohort competition of juvenile sea-trout *Salmo trutta*. Oikos, **29**: 112–117.

Bohlin, T. 1978. Temporal changes in the spatial distribution of juvenile sea-trout *Salmo trutta* in a small stream. Oikos, **30**: 114–120.

Bozek, M.E., and Rahel, F.J. 1992. Generality of microhabitat suitability models for young colorado river cutthroat trout (*Oncorhynchus clarki pleuriticus*) across sites and among years in Wyoming streams. Can. J. Fish. Aquat. Sci. **49**: 552–564.

Brett, J.R. 1962. Some considerations in the study of respiratory metabolism in fish, particulary salmon. J. Fish. Res. Board Can. **19**: 1025–1038.

DeGraaf, D.A., and Bain, L.H. 1986. Habitat use by and preferences of juvenile Atlantic salmon in two Newfoundland rivers. Trans. Am. Fish. Soc. **115**: 671–681.

Elliott, J.M. 1986. Spatial distribution and behavioural movements of migratory trout *Salmo trutta* in a lake district stream. J. Anim. Ecol. **55**: 907–922.

Fausch, K.D. 1984. Profitable stream positions for salmonids: relating specific growth rate to net energy gain. Can. J. Zool. **62**: 441–451.

Fretwell, S.D. 1972. Populations in a seasonal environment. Princeton University Press, Princeton, N.J.

Fretwell, S.D., and Lucas, H. 1970. On the territorial behaviour and other factors influencing habitat distribution in birds. Acta Biotheor. **19**: 1–36.

Gibson, R.J. 1978. The behavior of juvenile Atlantic salmon (*Salmo salar*) and brook trout (*Salvelinus fontinalis*) with regard to temperature and to water velocity. Trans. Am. Fish. Soc. **107**: 703–712.

Gibson, R.J., and Cunjak, R.A. 1986. An investigation of competitive interactions between brown trout (*Salmo trutta* L.) and juvenile Atlantic salmon (*Salmo salar* L.) in rivers of the Avalon Peninsula, Newfoundland. Can. Tech. Rep. Fish. Aquat. Sci. No. 1462.

Gibson, R.J., Stansbury, D.E., Whalen, R.R., and Hillier, K.G. 1993. Relative habitat use, and inter-specific and intra-specific competition of brook trout (*Salvelinus fontinalis*) and juvenile Atlantic salmon (*Salmo salar*) in some Newfoundland rivers. *In* Production of juvenile Atlantic salmon, *Salmo salar*, in natural waters. *Edited by* R.J. Gibson and R.E. Cutting. Can. Spec. Publ. Fish. Aquat. Sci. No. 118. pp. 53–69.

Gotceitas, V., and Godin, J.J. 1992. Effects of location of food delivery and social status on foraging site selection by juvenile Atlantic salmon. Environ. Biol. Fishes, **35**: 291–300.

Grand, T.C. 1997. Foraging site selection in juvenile coho salmon (*Oncorhynchus kisutch*): ideal free distributions of unequal competitors. Anim. Behav. **53**: 185–196.

Grand, T.C., and Dill, L.M. 1997. The energetic equivalence of cover to juvenile coho salmon (*Oncorhynchus kisutch*): ideal free distribution theory applied. Behav. Ecol. **8**: 437–447.

Grant, J.W.A., and Kramer, D.L. 1990. Territory size as a predictor of the upper limit to population density of juvenile salmonids in streams. Can. J. Fish. Aquat. Sci. **47**: 1724–1737.

Heggenes, J. 1991. Comparisons of habitat availability and habitat use by an allopatric cohort of juvenile Atlantic salmon *Salmo*

© 1999 NRC Canada

salar under conditions of low competition in a Norwegian stream. Holarct. Ecol. **14**: 51–62.

Hughes, N.F. 1992*a*. Ranking of feeding positions by drift-feeding Arctic grayling (*Thymallus arcticus*) in dominance hierarchies. Can. J. Fish. Aquat. Sci. **49**: 1994–1998.

Hughes, N.F. 1992*b*. Selection of positions by drift feeding salmonids in dominance hierarchies: model and test for Arctic grayling (*Thymallus arcticus*) in subarctic mountain streams, interior Alaska. Can. J. Fish. Aquat. Sci. **49**: 1999–2008.

Hughes, N.F., and Dill, L.M. 1990. Position choice by drift feeding salmonids: model and test for Arctic grayling (*Thymallus arcticus*) in subarctic mountain streams, interior Alaska. Can. J. Fish. Aquat. Sci. **47**: 2039–2048.

Kalleberg, H. 1958. Observations in a stream tank of territoriality and competition in juvenile salmon and trout (*Salmo salar* L., and *S. trutta* L.). Inst. Freshwater Res. Drottningholm Rep. **39**: 55–98.

Kennedy, G.J.A., and Crozier, W.W. 1993. Juvenile Atlantic salmon (*Salmo salar*) — production and prediction. *In* Production of juvenile Atlantic salmon, *Salmo salar*, in natural waters. *Edited by* R.J. Gibson and R.E. Cutting. Can. Spec. Publ. Fish. Aquat. Sci. No. 118. pp. 179–188.

Kennedy, G.J.A., and Strange, C.D. 1986. The effects of intra- and inter-specific competition on the distribution of stocked juvenile Atlantic salmon (*Salmo salar* L.) in relation to depth and gradient in an upland trout (*Salmo trutta* L.) stream. J. Fish Biol. **39**: 199–214.

Lear, W.H. 1975. Evaluation of the transplant of Pacific pink salmon (*Oncorhynchus gorbuscha*) from British Columbia to Newfoundland. J. Fish. Res. Board Can. **32**: 2343–2356.

Parker, G.A. 1974. The reproductive behaviour and the nature of sexual selection in *Scatophaga stercoraria* L. (Diptera: Scatophagidae). IX. Spatial distribution of fertilisation rates and evolution of male search strategy within the reproductive area. Evolution, **28**: 93–108.

Platts, W.S., Megahan, W.F., and Minshall, G.W. 1983. Methods for evaluating stream, riparian, and biotic conditions. U.S. For. Serv. Gen. Tech. Rep. INT-138.

Rodríguez, M.A. 1995. Habitat-specific estimates of competition in stream salmonids: a field test of the isodar model of habitat selection. Evol. Ecol. **9**: 169–184.

SAS Institute Inc. 1988. SAS/STAT users guide, release 6.03 edition. SAS Institute Inc., Cary, N.C.

Saunders, R.L., and Gee, J.H. 1964. Movements of young Atlantic salmon in a small stream. J. Fish. Res. Board Can. **21**: 27–36.

Symons, P.E.K. 1971. Behavioral adjustment of population density to available food by juvenile Atlantic salmon. J. Anim. Ecol. **40**: 569–587.

Van Horne, B. 1983. Density as a misleading indicator of habitat quality. J. Wildl. Manage. **47**: 893–901.

© 1999 NRC Canada

Gillnet selectivity for North Sea Atlantic cod (*Gadus morhua*): model ambiguity and data quality are related

Holger Hovgård, Hans Lassen, Niels Madsen, Thomas Moth Poulsen, and David Wileman

Abstract: Gillnet selectivity curves for North Sea Atlantic cod (*Gadus morhua*) were fitted to catch data obtained with six different mesh sizes. The selectivity curves investigated included frequently used selectivity models following the normal, lognormal, and gamma distributions. Another group of selectivity models that take the method of capture (gilled, maxillae, or "randomly" enmeshed) into consideration was also included. The best description of the selection data was found for the latter models. Therefore, the capture processes and girth measurements should be recorded as a matter of routine and such data used when constructing and evaluating gillnet selectivity models. The shape of the selectivity curve for those size intervals where there were satisfactory catch information was well defined, while the selection curve was ambiguous outside the interval with adequate data. Ambiguities in the shape of the selectivity curve can be diminished by choosing an appropriate range in mesh sizes and ensuring that the mesh sizes match the size distribution of the population fished. It is furthermore suggested that the estimated length distribution of the fish encountering the nets be robust to misspecification of the selectivity model.

Résumé : Les courbes de sélectivité des filets maillants pour la capture de la morue franche (*Gadus morhua*) de la mer du Nord ont été ajustées aux données sur les captures obtenues avec six tailles de mailles différentes. Les courbes de sélectivité étudiées comprenaient des modèles de sélectivité fréquemment utilisés suivant des distributions normales, lognormales et gamma. On a également inclus un autre groupe de modèles de sélectivité qui tiennent compte de la méthode de capture (maillés par les ouïes, les maxillaires ou maillés « au hasard »), ces derniers offrant la meilleure description des données de sélection. Les procédés de capture et les mesures de la circonférence devraient donc être consignés systématiquement et ces données utilisées pour construire et évaluer les modèles de sélectivité des filets maillants. La forme de la courbe de sélectivité pour ces intervalles de tailles pour lesquels on disposait de données satisfaisantes sur les captures était bien définie, tandis que la courbe de sélection était floue à l'extérieur de l'intervalle présentant des données pertinentes. On peut réduire les ambiguïtés de la forme de la courbe de sélectivité par le choix d'une plage appropriée de tailles de mailles et en s'assurant que ces tailles correspondent à la répartition des tailles dans la population de poissons exploitée. En outre, il semble que l'estimation de la distribution des longueurs des poissons emmaillés soit robuste à l'égard de la mauvaise spécification du modèle de sélectivité.

[Traduit par la Rédaction]

Introduction

Information on the size distribution of the population being fished is not available in most gillnet selectivity experiments and the selectivity must therefore be estimated indirectly, i.e., the size–frequency distribution of the population and the selectivity parameters are estimated simultaneously. This is possible if (*i*) fishes of a given size are equally available to nets of different mesh size fishing concurrently and (*ii*) the selectivity depends on the fish size and mesh size only and this dependence is smooth. The second assumption will be met if, for instance, the selectivity relationship can be formulated as an analytical function but is often more restrictively formulated as the principle of geometric similarity (Baranov 1948) or the selectivity curve belongs to a family of bell-shaped selection curves (Holt 1963). Selectivity curves may be constructed by nonparametric methods (Gulland and Harding 1961; Jensen 1973). Parametric presentations of the selectivity curve are most often theoretical density distributions from statistics, e.g., the normal distribution (Holt 1963), a skewed normal distribution (Regier and Robson 1966), the lognormal distribution (McCombie and Fry 1960), or the gamma distribution (Henderson and Wong 1991). In some cases the sum of two distributions has been used (Hamley and Regier 1973; Hovgård 1996*a*).

Received March 9, 1998. Accepted March 23, 1999.
J14496

H. Hovgård[1] **and H. Lassen.**[2] Danish Institute for Fisheries Research, Charlottenlund Slot, DK 2920 Charlottenlund, Denmark.
N. Madsen, T. Moth Poulsen,[3] **and D. Wileman.** Danish Institute for Fisheries Technology and Aquaculture, North Sea Centre, DK 9850 Hirtshals, Denmark.

[1]Author to whom all correspondence should be addressed. e-mail: hoh@dfu.min.dk
[2]Present address: ICES, Palægade 2-4, DK 1261 Copenhagen, Denmark.
[3]Present address: MAEP Aquaqulture Extension Project, Mascanda Mymensingh, P.O. Box 33, Mymensing 2200, Bangladesh.

© 1999 NRC Canada

Millar (1995) found that two sets of longline data fitted fundamentally different selectivity curves equally well and he suggested that a similar ambiguity should be expected for gillnet selectivity. Millar and Holst (1997) further explored this problem using gillnet selectivity data and concluded that it can never be established that a particular selection curve is the right one.

"Ambiguity" can be used in different contexts: (*i*) different catch processes can lead to the same selectivity model and therefore, estimation of the selectivity curve cannot be distinguished between these processes or (*ii*) selection curves with fundamentally different form, e.g., S-shaped and bell-shaped, cannot be distinguished based on the available data. A third but trivial form of ambiguity is where different mathematical formulations within the data window represent the same curve. The first problem needs to be addressed by redesigning the experiment. Millar (1995) and Millar and Holst (1997) discussed the second type of ambiguity.

The purpose of the present paper is to evaluate the extent of the ambiguity found for gillnet selectivity curves and its consequences for the estimated size distribution of the population encountering the nets. Obviously, one can only hope to estimate the selectivity for the range of fish lengths and mesh sizes where data are available, and in practice the data quality limits the accuracy with which the selectivity curve can be estimated. Within the available data window the selection curve can be estimated apart from a constant reflecting that the estimated selectivity is relative and not absolute.

The analyses were carried out on experimental catch data obtained from six different mesh sizes including those typically used in the commercial North Sea coastal Atlantic cod (*Gadus morhua*) fisheries. The ambiguity is investigated by fitting selectivity models to the same data set and investigating if these models fit the data equally well. The models investigated include frequently used selectivity models (normal, lognormal, and gamma distributions) together with models formulated to take into account different catch processes. The models are evaluated by using auxiliary information such as recordings of the catch processes and girth measurements. The paper concludes with suggestions on how the level of ambiguity can be diminished at the experimental planning state by choosing the range and spacing of the mesh sizes.

Materials and methods

Fishing gear and operational procedures

The data were collected within an EU-AIR research project (Anonymous 1997). The project focused on commercially used gill nets but also included nets with smaller mesh sizes. Here the analysis is restricted to the Danish cod fishery experiments. The catches in this group of experiments were high and details of how the cod were caught were collected.

The nets consisted of six different mesh sizes of silver–grey multimonofilament twine (each monofilament Japanese No. 1.5, 330 denier, and about 0.2 mm in diameter) with the numbers of filaments increasing with mesh size. The measured mesh sizes and the number of filaments (given in parentheses) were 90.1 mm (3), 99.4 mm (4), 107.7 mm (4), 122.8 mm (4), 133.5 mm (4), and 150.7 mm (6). All nets were of equal height (3.8 m), while the mean net length differed slightly between mesh sizes (69.2–71.5 m). The float lines were fitted with power floats (buoyancy 38 g/m) and the sink lines were braided lead line (weight 70 g/m). The nets were mounted as typical commercial Danish nets, i.e., with slack in the lead line relative to the float line (hanging ratios of 0.38 and 0.5 for the float line and lead line, respectively). Each fleet of nets consisted of six nets, one of each of the six different mesh sizes. The nets were arranged in random order and open spaces were left between the individual nets to restrict herding effects between nets. Four to 10 fleets of nets were deployed simultaneously. The average soak time was 22 h. The measure of fishing effort used in the model presented below is the product of net length and soak time.

The experimental fisheries were carried out by a chartered commercial gillnet vessel fishing in the central North Sea off the Danish coast at depths between 7 and 28 m. Four experiments were carried out: November 1994 and February, April, and December 1995. The total numbers of cod caught during these experiments were 2608, 1101, 3230, and 1010 individuals, respectively.

Catches

The total catch of cod was sorted by mesh size and all cod were measured to the nearest centimetre. The length–frequency distributions of the catches (Fig. 1) show clear differences among mesh sizes. The catch in numbers decreased with increasing mesh size.

In the first and third experiments, girths were measured with a polyethylene string with a standardised tension of 300 g as measured by an angling spring balance. Girth measurements were carried out on 520 cod at three different body positions: (*i*) perpendicular to the proximal end of the maxillary, (*ii*) immediately behind the gill cover, and (*iii*) at the maximum girth (behind the gills where the soft body was fattest). The ratios between girth and length were analysed by ANOVA using the relationship

$$M_{\mathrm{m}} = \log\left(\frac{\text{girth}}{\text{fish length}}\right)$$

where the subscript "m" represents maxillary, gill, or maximum girth. The log transformation was chosen to stabilise the variance. Neither the experiment effect nor the interaction between experiment and the measuring site was significant at a 5% significance level. Cod girth to length ratios were estimated to be 0.31, 0.47, and 0.48 for maxillary, gill, and maximum girth, respectively. The latter two estimates were not statistically different at a 5% significance level, implying that girth at the position of the gills is a fairly accurate measure of the maximum girth of cod.

In the first experiment, it was observed that some cod, far too small to be gilled, were entangled by their teeth. This happened for all mesh sizes. Therefore, in the fourth experiment the way in which cod were caught was recorded by carefully unravelling the cod as the nets came onboard the vessel. This study was restricted to a period of calm weather and encompassed 180 cod. Of these, 87 were classified as gilled, 52 were enmeshed behind the maxillae, 36 were entangled by their teeth, and five were otherwise entangled (Fig. 2).

Selectivity curve models examined

The selectivity curves examined include three theoretical distributions frequently used to describe gillnet selectivity: the normal, lognormal, and gamma distributions (Table 1). These standard models were supplemented with models formulated to take into account the observed catch processes.

The first of these models was based on Hovgård (1996*a*) where the selectivity was described by the sum of two normal distributions accounting for gilling and maxillary enmeshing, respectively. In the present work, this model was expanded to account for cod caught by their teeth or otherwise entangled by adding a constant, c, to the summed normal distributions and adjusting the maximum selection to 100%. This model has six parameters (Table1).

© 1999 NRC Canada

Fig. 1. Length–frequency distributions of Atlantic cod catches aggregated over all experiments. Cod above 80 cm are included in the 80-cm group.

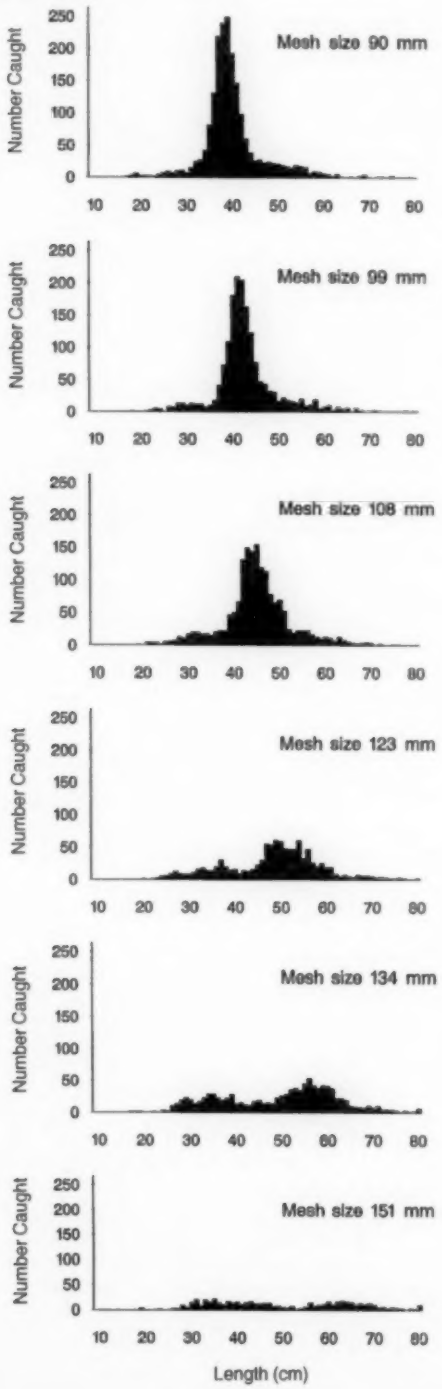

The catch process was clearly different for small and large cod (Fig. 2). Three further models were therefore constructed that include independent descriptions of the selection on the left- and

Fig. 2. Observations of the method of capture recorded for part of the catch during the fourth experiment. The catches from all mesh sizes are shown together on the transformed length scale (fish length/mesh size).

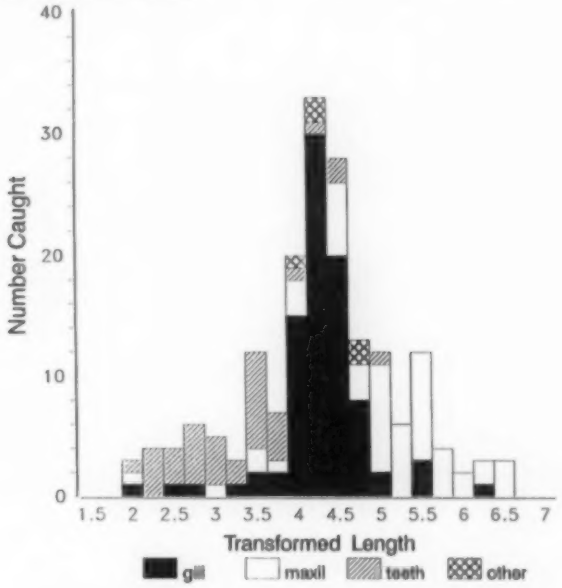

right-hand sides of the modal length (length of maximum selection). The most general of these three models is a five-parameter model: for sizes below the modal length the selectivity curve is described by a constant, c_1, plus the ascending part of a normal distribution with parameters (k, s_1) whereas for fish sizes above the modal length the curve is described by a second constant, c_2, plus the descending part of a normal distribution with parameters (k, s_2). The two constants c_1 and c_2 account for fish that were not gilled, i.e., enmeshed behind the maxillae, attached by their teeth, or otherwise entangled. These constants with $c_1 \neq c_2$ were introduced to allow these catch processes to differ for cod that are able to swim through the mesh lumen and are mainly caught by their teeth if not gilled (c_1) and those that are unable to swim through the mesh lumen and are mainly enmeshed behind the maxillae if not gilled (c_2). Table 1 presents the mathematical formulation of this model. This general model can be reduced: (*i*) $s_1 = s_2$ but $c_1 \neq c_2$ corresponding to a symmetrical selectivity curve for cod that are gilled but an overall selectivity curve that is skewed because of the two different levels of the other methods of capture and (*ii*) $c_1 = c_2$ but $s_1 \neq s_2$ corresponding to a common probability of capture by means other than gilling for small and large fish. Both the main model and the two reduced models were examined in the analysis.

Estimation algorithm

The catch in numbers, $C_{e,l,m}$, by experiment (e), length (l), and mesh size (m) can be expressed as

$$C_{e,l,m} = P_m E_{e,m} S_{l,m} N_{e,l} + \varepsilon$$

where P_m is the fishing power (the efficiency of the various nets), $E_{e,m}$ is the effort equal to the product of the net length and the soak time, $S_{l,m}$ denotes the selectivity, and $N_{e,l}$ is the relative number of fish available to any of the mesh sizes. Such relationships are subject to noise, ε. Catch and effort are measured quantities; the measured net length has been included as an exogenous parameter whereas soak time was ignored, as all mesh sizes were used concurrently in each fleet of nets. The parameters to be estimated are

© 1999 NRC Canada

Table 1. Gillnet selection models used in the analysis of the Atlantic cod catches.

Model	Selection curve on the transformed length scale	Selection curve formulation on the centimetre scale
Normal	$\text{sel}(t, k, s) = \exp\left[\frac{-(t-k)^2}{2s^2}\right]$	sel(l, ms k, ms s)
Lognormal	$\text{sel}(t, k, s) = \frac{1}{t}\exp\left[k - \frac{s^2}{2} - \frac{(\ln(t)-k)^2}{2s}\right]$	sel(l, ln(ms) + k, s)
Gamma	$\text{sel}(t, \alpha, \beta) = \left[\frac{1}{(\alpha-1)\beta}\right]^{(\alpha-1)} \exp\left[\alpha - 1 - \frac{t}{\beta}\right]$	sel(l, α, ms β)
Binormal	$\text{sel}(t, k_1, k_2, s_1, s_2, c, b) = \frac{1}{1 + b\exp((k_1-k_2)^2/2s_2^2) + c}\left[\exp\left[\frac{-(t-k_1)^2}{2s_1^2}\right] + b\exp\left[\frac{-(t-k_2)^2}{2s_2^2}\right] + c\right]$	sel(l, ms k_1, ms k_2, ms s_1, ms s_2, c, b)
Two-sided	For $t < k$: $\text{sel}(t, k, s_1, s_2, c_1, c_2) = (1-c_1)\exp\left[\frac{-(t-k)^2}{2s_1^2}\right] + c_1$	sel(l, ms k, ms s_1, ms s_2, c_1, c_2)
	For $t \geq k$: $\text{sel}(t, k, s_1, s_2, c_1, c_2) = (1-c_2)\exp\left[\frac{-(t-k)^2}{2s_2^2}\right] + c_2$	

Note: For the two-sided model, two reduced models were examined: (*i*) assuming $s_1 = s_2$ and (*ii*) assuming $c_1 = c_2$. All models are formulated in accordance with the principle of geometric similarities (Baranov 1948) and are expressed using the transformed length (t). Selection curves for individual mesh sizes (ms) for length cm (l, cm) may be derived by using the parameters given on the right.

(*i*) the selectivity parameters describing the selectivity curve $S_{l,m}$ (Table 1), (*ii*) the fishing power P_m, and (*iii*) the relative number of fish available in each centimetre group within each experiment $N_{e,l}$. Due to the multiplicative model structure, there are an infinite number solutions, but these only differ by a factor that is defined by setting the maximum selection to 100%. The fishing power was expressed as

$$P_m = \left(\frac{R}{R_{\text{mean}}}\right)^{\alpha}$$

where R is the ratio mesh size to number of filaments and R_{mean} is the average ratio over all nets, i.e., the power of the average net is set at 1.

The estimates were obtained by least squares estimation (Lehmann 1983). A square root transformation of the observed catches was introduced before applying these data in the least squares estimation procedure to make the variance of the residuals independent of the mean catch. This square root transformation is appropriate for Poisson-distributed measurement noise (Elliott 1993) The least squares estimators are found from

$$L = \sum_e \sum_l \sum_m \left[\sqrt{C_{e,l,m}} - \sqrt{P_m E_{e,m} S_{l,m} N_{e,l}}\right]^2 = \text{Min}.$$

This can be solved explicitly for $N_{e,l}$:

$$N_{e,l} = \left[\frac{\sum_m \sqrt{C_{e,l,m} P_m E_{e,m} S_{l,m}}}{\sum_m P_m E_{e,m} S_{l,m}}\right]^2.$$

The $N_{e,l}$'s are inserted into the least squares minimisation expression for the estimations. The SAS NLIN procedure (SAS Institute Inc. 1991) was used to find the minimum of the least squares expression, i.e., to obtain the parameter estimates, the variance, and the covariance.

The goodness of the model fit was evaluated by comparing the observed and predicted catches for the individual experiments (see Fig. 3 for an example) and by inspection of residual plots for all experiments combined (Fig. 4). As the analysis of the various selectivity models was made on the same catch data, the sum of the squared residuals may be used as a summary statistic when comparing the quality of the various fits.

The estimated selectivity curves were based on the principle of geometric similarity, i.e., the selection is only dependent on transformed length (fish length/mesh size) and the parameters are expressed relative to this size scale. The selectivity curves for each mesh size expressed as a function of fish size, e.g., measured in centimetres, may be derived as shown in Table 1.

Results

The residual plots in Fig. 4 show marked systematic trends for the normal, lognormal, and gamma models indicating poor fits by these models. In contrast, little pattern is seen in the residual plots (Fig. 4) derived from the binormal model and the three models where selection is described independently on the two sides of the mode. In these models, there is a prevalence of small negative residuals for transformed lengths above about 7, these being caused by a dominance of zero catches for sizes considerably above the mode. The normal, lognormal, and gamma models show large sum of squares values compared with the four others (Table 2). Using this sum of squares measure to rank the models gives (1) (best) binormal, (2) full two-sided, (3) two-sided with $s_1 = s_2$, and (4) two-sided with $c_1 = c_2$. The differences in sum of squares between these four models are, however, small.

The estimated selectivity curves for the normal, lognormal, and gamma models are very similar (Fig. 4) and show rather disperse bell-shaped curves with modal length of about 4.7 (transformed length). This common form differs

© 1999 NRC Canada

Fig. 3. Example of the model fit (two-sided model applied to the catch information from the first experiment). Circles indicate the observed catch; lines show the model predictions.

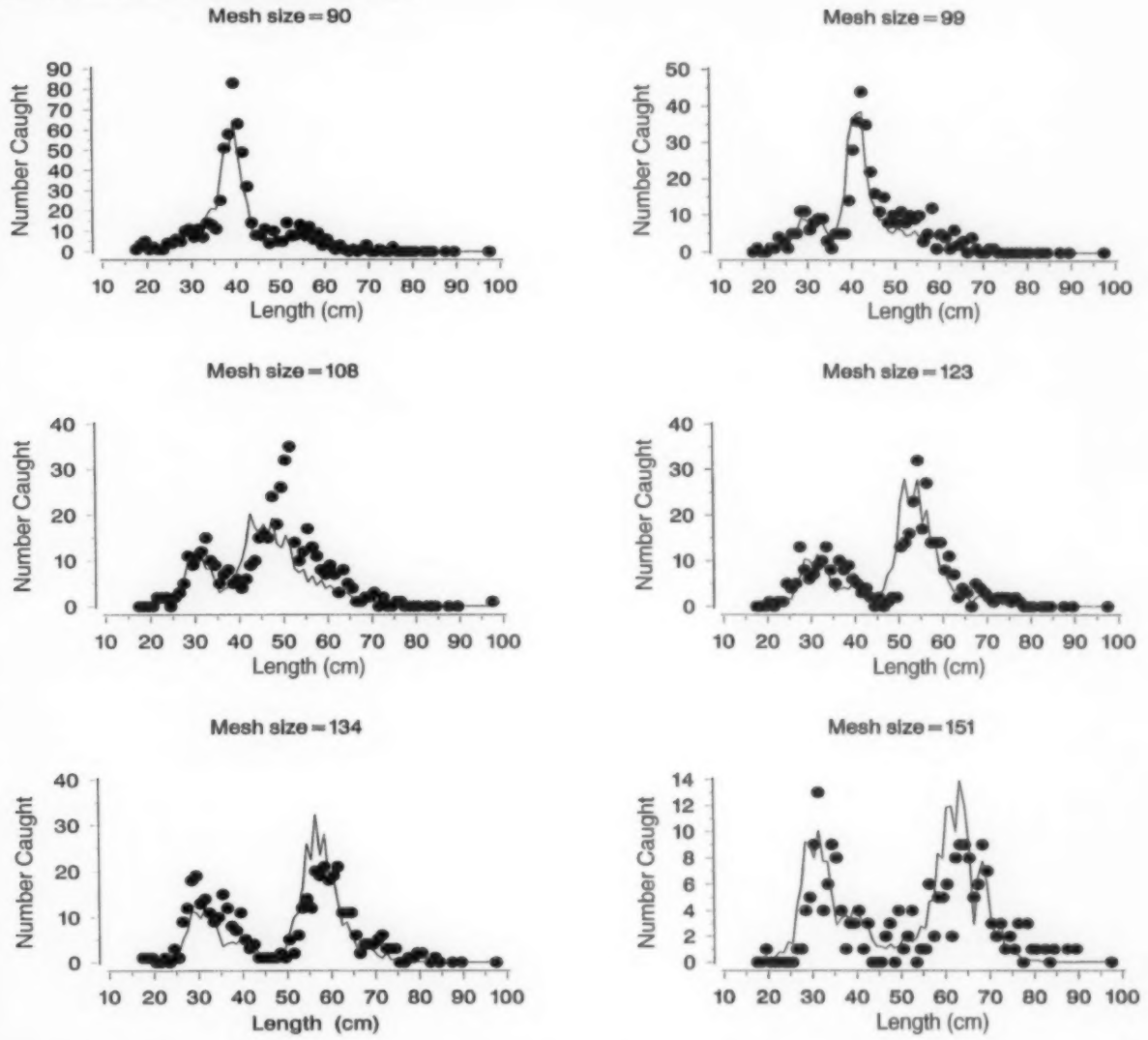

from those obtained using the four other models. The shapes of these four other selectivity curves, also shown in Fig. 4, are quite similar with respect to both the level of entangling of the smaller fish, c_1 or c approximately equal to 0.07, and the modal length of about 4.3. All these four curves show a narrow selection range around the mode. The estimated full two-sided model and the model using the reduction $s_1 = s_2$ are hardly distinguishable across all fish sizes. There is, however, considerable difference between these two and the two other selectivity curves for transformed lengths above 5. The residual plots do not help to distinguish how well the models fit the catch data in this size range.

The estimated values for α in the fishing power expression are in all cases found between 0 and 1. The contrast in the power ratio is small, however, and overall, this leads to only small differences in power between mesh sizes: the maximum differences are found for the binormal model where the power ranges from 0.90 to 1.13 (Table 2).

The selectivity of the total fleet of nets is calculated by summing the contributions from individual nets taking into account differences in fishing power and in net length. The seven models show pronounced similarities for cod in the range of 35–75 cm (Fig. 5). As a consequence the population estimates are similar between models within this range (Fig. 6). Outside this interval the total selectivity curves approach a constant value, either the values derived by summing the constant entangling effects (c_1, c_2) or zero for the models lacking such constant terms. The bell-shaped part of the aggregated selectivity curve is bounded by the cod that were gilled in the smallest and the largest mesh sizes, so choosing a range of mesh sizes results in a particular "selection window" within which the population will be well sampled.

© 1999 NRC Canada

Fig. 4. Estimated selectivity curves (left panels) and the associated residual plots (right panels) for the seven selectivity models examined.

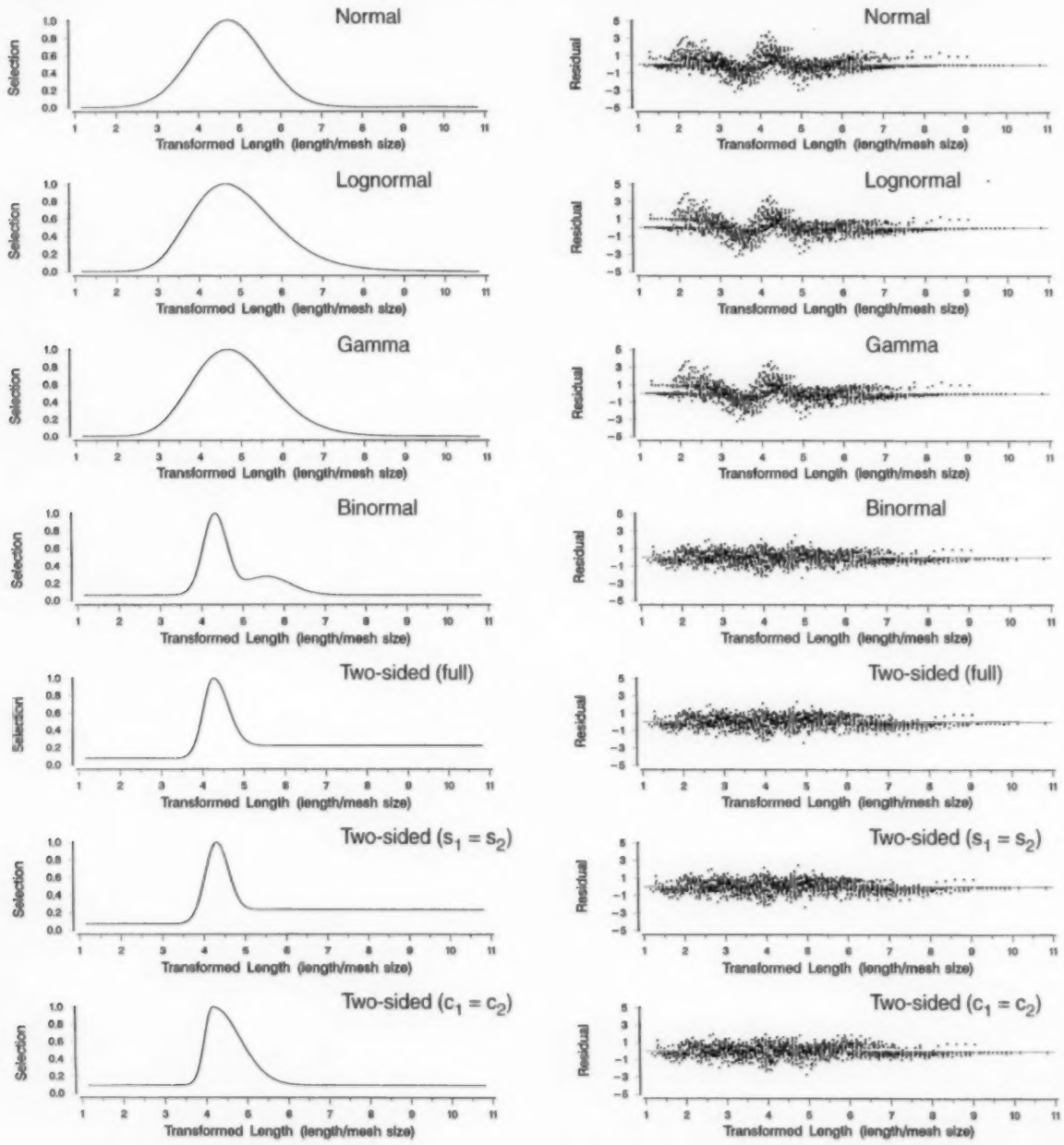

Discussion

The least squares estimation procedure used in the present work is similar to that of Hovgård (1996*a*) except for the use of the square root transformation that corresponds to assuming that the catches are randomly distributed, i.e., follow a Poisson distribution. Other authors have used maximum likelihood estimation (e.g., Kirkwood and Walker 1986; Millar 1995; Millar and Holst 1997). Wileman et al. (1996) provided a detailed description of the maximum likelihood estimation procedure applied to towed gear selection. A similar statistical technique may be preferable also for indirect estimation of selectivity of static gears. However, Erzini and Castro (1998) showed for gillnet selectivity analysis that least squares and maximum likelihood estimation procedures usually give similar results. We find that the critical point is

© 1999 NRC Canada

Table 2. Estimated selection and power parameters for the seven models examined.

Model	Selection parameters	Power parameter	Estimated powers by different nets (nets denoted by their mesh size in cm)						Residual sum of squares
			9.0	9.9	10.8	12.2	13.3	15.1	
Normal	$(k, s) = (4.75, 0.82)$	0.21	1.01	0.97	0.99	1.02	1.03	0.97	1437
Lognormal	$(k, s) = (1.57, 0.19)$	0.24	1.01	0.97	0.99	1.02	1.04	0.97	1369
Gamma	$(\alpha, \beta) = (29.18, 0.17)$	0.18	1.01	0.98	0.99	1.01	1.03	0.98	1321
Binormal	$(k_1, k_2, s_1, s_2, c, b) = (4.34, 5.62, 0.29, 0.52, 0.06, 0.25)$	0.74	1.04	0.90	0.96	1.06	1.13	0.91	677
Full two-sided	$(k, s_1, s_2, c_1, c_2) = (4.27, 0.25, 0.35, 0.07, 0.20)$	0.59	1.03	0.92	0.97	1.04	1.10	0.93	703
Two-sided ($s_1 = s_2$)	$(k, s_1, c_1, c_2) = (4.33, 0.28, 0.07, 0.21)$	0.64	1.03	0.92	0.96	1.05	1.11	0.92	707
Two-sided ($c_1 = c_2$)	$(k, s_1, s_2, c_1) = (4.18, 0.20, 0.64, 0.08)$	0.52	1.03	0.93	0.97	1.04	1.09	0.94	728

Note: The effect of the estimated power parameter is applied to the individual nets to directly express the estimated power difference.

Fig. 5. Aggregated selectivity of the fleets of experimental nets for the seven models examined. The aggregated selection is the sum of the products of the selectivity and fishing power for each of the six nets of different mesh size and is scaled to give maximum selection of 100%.

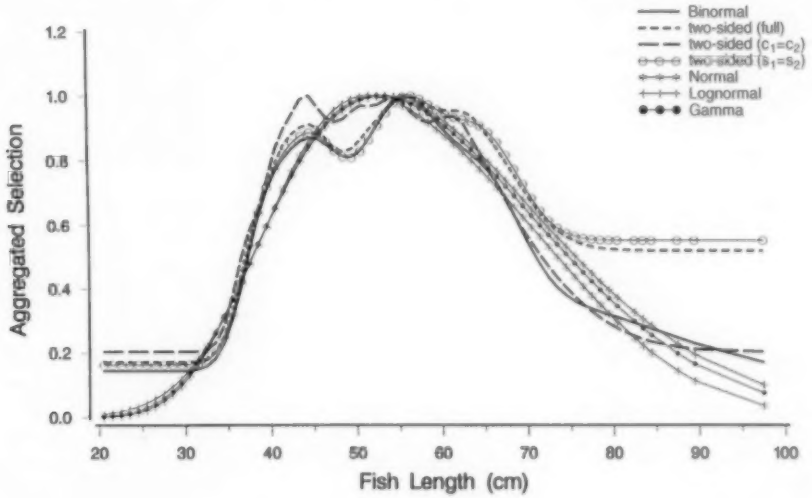

to pinpoint relevant models of the gillnet selectivity and not whether the model is fitted using maximum likelihood or least squares techniques.

The most commonly used selectivity models (normal, lognormal, and gamma models) gave curves with a wide selection range around the modal length caused by fish being caught that were of a size far different from the modal value. Expanding the models with specific terms to account for constant random entangling diminished the selection ranges considerably while at the same time leading to considerably better fits. The inclusion of random enmeshing or entangling terms, i.e., allowing catches to be taken without being mesh size dependent, does not appear to have been included in previous formulations of gillnet selectivity. Although this catch process may seem rather uninteresting in itself, the present analysis suggests that it may be important to account for it when estimating selection. The information on how fish were caught (Fig. 2) supports the use of this group of models, as (*i*) cod entangled by their teeth were mainly found at transformed lengths below 4, corresponding to the part of the selectivity curve with constant selection to the left of the mode, (*ii*) the medium-sized cod, which were gilled, dominated in the transformed length interval 4–5, matching the estimated mode of the selectivity curve, and (*iii*) cod enmeshed by their maxillae were found predominantly at transformed lengths above 5, corresponding to the part of the estimated selectivity curve to the right of the mode).

While the catch process information supports the use of models including forms of capture other than being gilled, the information does not particularly support selection or rejection of any of the four such model formulations examined. The two-parameter models (normal, lognormal, and gamma) fit the data much worse that the other model, even taking the fewer parameters into account. The other models with more parameters (four to six) fit about equally well,

© 1999 NRC Canada

Fig. 6. Estimated relative population length–frequency of Atlantic cod encountering the nets in the first experiment. The estimates from the different models are scaled to produce an equal abundance of 100 cod in the interval 35–75 cm. Extreme estimates, found for small cod sizes in the models lacking a specification of random entangling, are reduced to a value of 10 to enhance the presentation. See legend on Fig. 5 for model definition.

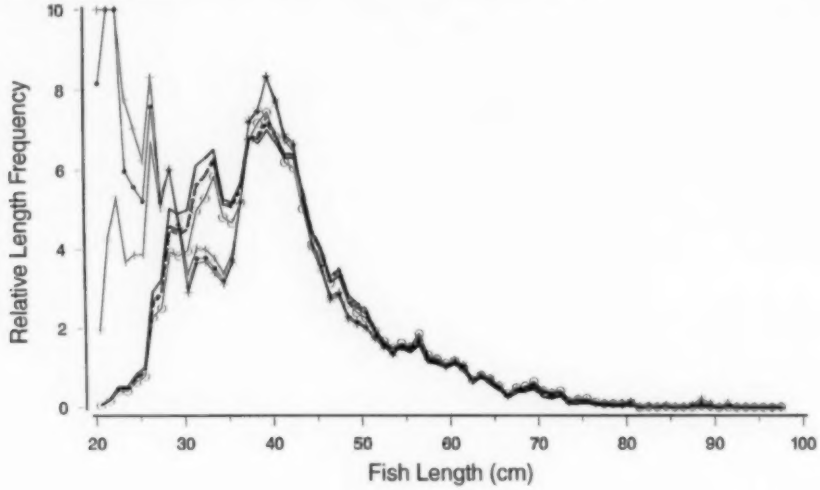

and based on statistical consideration alone the model with the fewer parameters (two-sided with $s_1 = s_2$ or with $c_1 = c_2$) should be preferred. These models, however, represent different catch processes, and information on these processes may therefore help towards an understanding of which model best describes the system.

The catches of enmeshed fish depend on a fit between the fish size and the mesh perimeter, and therefore, girth information may also be used when interpreting the catch processes. The mesh perimeter and gill girth match perfectly at a transformed length of 4.26, i.e., very similar to the estimated modal value (k) found in the four accepted models (Table 2). For the maxillary catch process, a similar geometric fit is found at a transformed length of 6.45. The geometric fit is clearly different from the estimated second modal value (k_2) of 5.57 found in the binormal model (Table 2). This estimate is difficult to relate to the cod being enmeshed directly behind the maxillae, as it correspond to fish being retained optimally at a girth of only 0.86 times the mesh perimeter. Hovgård (1996*a*) conducted experiments in Greenland with small mesh size monofilament nylon nets and presented selectivity curves for cod with two modes at transformed length values of 4.74 and 6.99. These modes are separated, as would be expected from the maxillary and gill girth measurements made in the present study (expected maxillae mode found at $k_2 = k_1(c_{gill}/c_{maxil})$, where the c's denote the girth to length ratios). Hovgård (1996*a*) inferred that the bimodality could easily be overlooked in experiments where the selectivity of the mesh sizes used does not match the size composition in the population fished. This can be seen to have been the case in the present study: compare the selection window (Fig. 5) and the estimated fish size distribution (Fig. 6). The abundant size-classes of fish in the population correspond to the part of the selectivity curve at or below the modal length. This is reflected in the catch compositions (Fig. 1) where only 11% of the catches are above a transformed length of 5 and only 2.5% are above 6. This implies that it will be difficult to discern a possible secondary mode expected geometrically at a transformed length of 6.45. This poor match between the selectivity of the fleets of nets and the population resulted in spite of efforts to enhance the selection window (i.e., the range of cod lengths sampled well by the fleets) by adding mesh sizes below those used commercially.

The binormal model and the families of two-sided models gave very similar selectivity curves for transformed lengths below 5 (Fig. 4). Few cod with a transformed length above 5 were caught and the observations were very scattered. This suggests that the selectivity curve be well estimated in the length interval where there are significant catches, in this study, for transformed lengths between 2.5 and 5. Outside this range, there is significant ambiguity in the determination of the selectivity curve such that the estimated selection depends on the model specification rather than on the observed data. The same conclusion may be drawn from the analysis made by Millar (1995) that fitted different selectivity curve models to cod and snapper longline data. Good snapper catch data were restricted to the interval 25–45 cm (see Ralston 1990), and within this size interval the selectivity curves are almost identical (Millar 1995, his fig. 4) For Millar's (1995) cod analysis, the hook selectivity curves that gave equally good fits also produced very similar expected selectivities over the size ranges where the catch information was acceptable.

When estimating gillnet selectivity curves from experiments with nets of several different mesh sizes, differences in fishing power between the nets should be considered. In some cases, (e.g., Hovgård 1996*b*), large differences in catch rates are observed between nets of adjacent mesh sizes, suggesting considerable power differences. The fishing power of gill nets appears to be related to the mesh size to twine diameter ratio (see Hovgård (1996*b*) for a short discussion).

© 1999 NRC Canada

For multimonofilament nets, catches have been reported to increase when the number of filaments was reduced (Steinberg 1985). Ongoing experiments on Baltic cod suggest similarly that an increase in the number of filaments in a multimonofilament twine from four to six decreases catch numbers by about a third (D. Wileman, personal communication). The exact relationship between the numbers of filaments and their dimensions and the resulting fishing power differences has not been evaluated in the literature. The power function used in this paper provides a simple and flexible formulation. For estimation purposes, fishing power is often confounded with other selectivity parameters (e.g., Millar and Holst 1997). Therefore, fishing power should be qualified by specially designed experiments. In the present experiment the selectivity parameter estimates were insensitive to the inclusion of a fishing power term.

Millar's (1995) longline analysis is inconclusive with respect to finding a general form for longline selectivity curves, although the lognormal model provided reasonable fits for both cases examined. For gill nets, the ambition of finding a universal form for the selectivity curve, applicable to all species, seems unrealistic, as enmeshing may take place at different locations (projections, spines, behind the gill cover, etc.) for different species (Trent and Pristas 1977; Marais 1985). The advantage of adapting the selectivity model to the observed catch processes seems evident from the present analysis where the realistic models perform better than "standard" selectivity models. Therefore, auxiliary information such as observations of catch processes and girth measurements should be recorded in gillnet selectivity experiments. This information is needed in the formulation and evaluation of selectivity models.

The uncertainty in the form of the selectivity curve found in the present study is due to data not being adequate. This suggests that attention should be paid to the experimental design. In order to obtain adequate data, large catches are required and the experimental design should focus on achieving this. Large catches can only be expected in the selection window, i.e., the length range [$k \times$ smallest mesh size, $k \times$ largest mesh size]. On the transformed length scale the selection window can be expressed as

$$\text{Selection window} = \left[\frac{k}{R}, Rk\right]$$

where R is the ratio between the largest and the smallest mesh size used. This formulation illustrates that the numbers caught are expected to be bigger around k. Similarly, fewer fish are expected for relative fish sizes R times above or below k. As the present study shows, the actual size interval with large catches may be considerable narrower than stipulated by the selection window when there is a poor match between the mesh sizes and the population size distribution. For experimental planning, this implies (*i*) an appropriate choice of the range of mesh sizes so that the widest possible interval on the transformed scale is potentially well covered by catches and (*ii*) an appropriate choice of individual mesh sizes so that these match the fish sizes in the population. Considering that most fish stocks are presently heavily exploited, and therefore dominated by young age groups, higher catch numbers should generally be expected when using relatively small mesh sizes. For roundfish, initial guesses of k can be obtained from gill girth measurements. Sechin (1969) provided a formalised approach for such estimations.

The present study found the total selectivity (i.e., the selection aggregated over all mesh sizes) to be rather insensitive to the choice of selectivity model within the selection window. As a result, the estimated population length–frequency distributions were found to be essentially similar for all selectivity models within the selection window. Holst and Moth Poulsen (1995), in their analysis of plaice catches from trammel nets using widely different parametric and nonparametric models, found that these all estimated similar size distributions. The estimated size distribution of the population therefore apeears to be largely independent of the choice of the selectivity model, but of course not of the selectivity data.

The estimated relative length distribution of the fish refers to those fish encountering the nets (Hamley 1975). If the encountering rate is a simple function of fish length ($A(l)$) (Rudstam et al. 1984), then the estimated length–frequency will be biased by this function, i.e., $N^{\text{encounter}} = N^{\text{population}}A(l)$. Ignoring the behavioural aspects of the encounter process has similar effects for the population size distribution estimate for other gears. For instance, correcting the observed length–frequency in a trawl codend according to the mesh selectivity only produces the true stock size distribution if the herding/escapement processes found in front of the trawl and inside the trawl before the fish enter the codend affect all fish sizes equally (Isaksen and Valdemarsen 1994).

Acknowledgment

The data were collected as part of the EU research project AIR2-93-1122 "Selectivity of gill nets in the North Sea, English Channel and Bay of Biscay" financed by the Commission of the European Communities. The project results are described in detail in Anonymous (1997). Financial support from the Commission and from the Danish Ministry for Food, Agriculture and Fisheries is gratefully acknowledged. The authors thank two anonymous referees whose comments helped in improving the quality of the paper.

References

Anonymous. 1997. Selectivity of gill-nets in the North Sea, English Channel and Bay of Biscay. EU Rep. No. AIR2-93-1122.

Baranov, F.I. 1948. Theory and assessment of fishing gear. Chap. 7. Theory of fishing with gillnets. Pishchepromizdat, Moscow. (Translated from Russian by the Ontario Department of Lands and Forests. Maple, Ont.)

Elliott, J.M. 1993. Some methods for the statistical analysis of samples of benthic invertebrates. Freshwater Biol. Assoc. Sci. Publ. No. 25.

Erzini, K., and Castro, M. 1998. An alternative methodology for fitting selectivity curves to pre-defined distributions. Fish. Res. **34**: 307–313.

Gulland, J.A., and Harding, D. 1961. The selection of *Clarias mosambicus* (Peters) by nylon gill nets. J. Cons. Cons. Int. Explor. Mer, **26**: 215–222.

Hamley, J.M. 1975. Review of gillnet selectivity. J. Fish. Res. Board Can. **32**: 1943–1969.

© 1999 NRC Canada

Hamley, J.M., and Regier, H.A. 1973. Direct estimates of gillnet selectivity to walleye (*Stizostedion vitreum vitreum*). J. Fish. Res. Board Can. **30**: 817–830.

Henderson, D.A., and Wong, J.I. 1991. A method for estimating gillnet selectivity of walleye (*Stizostedion vitreum vitreum*) in multimesh multifilament gill nets in Lake Erie, and its application. Can. J. Fish. Aquat. Sci. **48**: 2420–2428.

Holst, R., and Moth Poulsen, T. 1995. Numerical recipes and statistical methods for gillnet selectivity. ICES CM 1995/B:18 (mimeo.). International Council for the Exploration of the Sea, Charlottenlund, Denmark.

Holt, S.J. 1963. A method for determining gear selectivity and its application. Int. Comm. Northwest Atl. Fish. Spec. Publ. **5**: 106–115.

Hovgård, H. 1996*a*. A two-step approach to estimating selectivity and fishing power of research gill nets used in Greenland waters. Can. J. Fish. Aquat. Sci. **53**: 1007–1013.

Hovgård, H. 1996*b*. Effect of twine diameter on fishing power of experiment gill nets used in Greenland waters. Can. J. Fish. Aquat. Sci. **53**: 1014–1017.

Isaksen, B., and Valdemarsen, J.W. 1994. By-catch reduction in trawls by utilising behaviour differences. *In* Marine fish behaviour in capture and abundance estimation. *Edited by* A. Ferno and S. Olsen. Fishing News Books, Blackwell, Oxford, U.K. pp. 69–83.

Jensen, K.W. 1973. Selectivity of trout gill nets. Jagt-Fiske-Fritidsliv, **1**: 1–4. (Translated from Norwegian; Fish. Res. Board Can. Transl. Ser. No. 2629.)

Kirkwood, G.P., and Walker, T.I. 1986. Gill net mesh selectivities for gummy shark, *Mustelus antarticus* Gunther, taken in south-eastern Australian waters. Aust. J. Mar. Freshwater Res. **37**: 689–697.

Lehmann, E.L. 1983. Theory of point estimation. John Wiley & Sons, New York.

Marais, J.F.K. 1985. Some factors influencing the size of fishes caught in gillnets in Eastern Cape estuaries. Fish. Res. **3**: 251–261.

McCombie, A.M., and Fry, F.E.J. 1960. Selectivity of gill nets for lake whitefish, *Coregonus clupeaformis*. Trans. Am. Fish. Soc. **89**: 176–184.

Millar, R.B. 1995. The functional form of hook and gillnet selection curves cannot be determined from comparative catch data alone. Can J. Fish. Aquat. Sci. **52**: 883–891.

Millar, R.B., and Holst, R. 1997. Estimation of gillnet and hook selectivity using log-linear models. ICES J. Mar. Sci. **54**: 471–477.

Ralston, S. 1990. Size selection of snappers (Lutjanidae) by hook and line gear. Can. J. Fish. Aquat. Sci. **47**: 696–700.

Regier, H.A., and Robson, D.S. 1966. Selectivity of gill nets, especially to lake whitefish. J. Fish. Res. Board Can. **23**: 123–454.

Rudstam, L.G., Magnuson, J.J., and Tonn, W.M. 1984. Size selectivity of passive fishing gear: a correction for encounter probability applied to gill nets. Can. J. Fish. Aquat. Sci. **41**: 1252–1255.

SAS Institute Inc. 1991. SAS/STAT users guide. Vol 2. GLM-VARCOMP. SAS Institute Inc., Cary, N.C.

Sechin, Yu.T. 1969. A mathematical model for the selectivity curve of a gill net. Rybn. Khoz. **45**(9): 56–58. (Translated from Russian by the International Pacific Halibut Commission, Seattle, Wash.)

Steinberg, R. 1985. Einfluss der Netzfarbe und Garnstärke in dorsch-stellnetzen. Inf. Fisch. Wiss. **32**: 77–79. (In German.)

Trent, L., and Pristas, P.J. 1977. Selectivity of gill nets on estuarine and coastal fishes from St. Andrew Bay, Florida. Fish. Bull. U.S. **75**: 185–198.

Wileman, D.A., Ferro, R.S.T., Fonteyne, R., and Millar, R.B. 1996. Manual of methods of measuring the selectivity of towed fishing gears. ICES Coop. Res. Rep. No. 215.

© 1999 NRC Canada

An assessment of light-based geoposition estimates from archival tags

David W. Welch and J. Paige Eveson

Abstract: Archival tags record information about the environment of tagged animals over long periods of time (months to years). In theory, position can be estimated from a record of changes in light intensity with time. We describe two approaches to estimating geoposition based on estimating either the time of maximal rate of change in light intensity or the time that a reference light intensity is reached. Digital signal processing is investigated as a method of increasing the signal-to-noise ratio of the light record. Our test data suggest that the daily position of a tagged animal can potentially be estimated within an average error of about 140 km (SD's of 0.9° of longitude and 1.2° of latitude), approaching the resolution of the best eddy-resolving physical oceanographic models of ocean currents. The source of the remaining large-scale errors in geoposition appears to be extrinsic to the tags and may be related to large-scale weather systems. The accuracy of current archival tags is sufficient to permit an assessment of the open-ocean migration pathways of animals such as maturing salmon and may be sufficient for use in some parts of the continental shelf as well.

Résumé : Les marques d'archivage enregistrent des données sur l'environnement dans lequel évoluent les animaux marqués sur de longues périodes (mois ou années). En théorie, la position peut être estimée à partir d'un enregistrement des changements temporels dans l'intensité lumineuse. Nous décrivons deux méthodes d'estimation de la position géographique fondées sur l'estimation du moment où le taux de changement de l'intensité lumineuse est maximal ou du moment où une intensité lumineuse de référence est atteinte. Nous examinons l'utilisation du traitement du signal numérique comme méthode pour augmenter le ratio signal/bruit de l'enregistrement de l'intensité lumineuse. Nos données indiquent que la position quotidienne d'un animal marqué peut être estimée avec une erreur moyenne d'environ 140 km (É-T's de 0,9° de longitude et 1,2° de latitude), ce qui s'approche de la résolution des meilleurs modèles océanographiques physiques de description spatiale des tourbillons pour les courants océaniques. La source des erreurs importantes restantes dans la position géographique semble ne pas dépendre des marques et pourrait être liée à des systèmes météorologiques à grande échelle. La précision des marques d'archivage actuelles est suffisante pour permettre une évaluation des voies migratoires océaniques d'animaux comme le saumon en période de maturation, et pourrait être suffisante pour en permettre aussi l'utilisation dans certaines régions de la plate-forme continentale.

[Traduit par la Rédaction]

Introduction

Recently developed archival tags have memory capacities sufficient to store information about the physical environment of a tagged animal over long periods of time. In addition to recording depth and temperature, the tags also record light intensity. Because sunrise and sunset occur later for observers located farther west and day length varies with latitude, it is possible to estimate geoposition from the light data by establishing the times of dawn and dusk and then converting these values into estimates of longitude and latitude using existing navigational routines (e.g., Hill 1994).

Archival tags have been used in a number of marine studies in the 1990's (e.g., Gunn et al. 1994; Godo and Michalsen 1997; Sturlaugsson and Thorisson 1997), but most applications have focussed on defining the depth and temperature characteristics of tagged animals. Relatively few studies have attempted to track movement, with DeLong et al.'s (1992) reconstruction of the possible migration route of an elephant seal (*Mirounga angustirostris*) from the light record being a promising exception. Perhaps the best example to date of such a study made no use of light to estimate geoposition, but instead used specific hydrological characteristics of the North Sea to convincingly demonstrate surprisingly large-scale movements of plaice (Metcalfe and Arnold 1997). Unfortunately, the hydrographic properties of the North Sea that made this study a success are not frequently duplicated. Thus, a more generally applicable approach to estimating geoposition is needed.

Several studies suggest that geoposition estimates from phototags are perhaps on the order of ±0.5° of longitude and ±1° of latitude. However, only one experiment comparing the *known* position of the tag with the estimated position is available (Gunn et al. 1994), and it was limited by the short duration (14 days) and relatively short distances covered (450 km). In order to rigorously assess the true accuracy of archival tags for estimating geoposition, we conducted three

Received July 17, 1998. Accepted March 2, 1999.
J14693

D.W. Welch[1] and J.P. Eveson. Department of Fisheries and Oceans, Pacific Biological Station, Nanaimo, BC V9R 5K6, Canada.
[1]Author to whom all correspondence should be addressed.
e-mail: welchd@pac.dfo-mpo.gc.ca

© 1999 NRC Canada

experiments covering a span of several thousand kilometres (study 1) and many months at sea (study 2 and 3).

Geoposition accuracy depends not only on the performance of the tags, but also on the algorithm used to derive position estimates. We use the data from our studies to evaluate several algorithms. Any light-based geoposition algorithm involves determining the times of dawn and dusk. Dawn and dusk have usually been defined as the times corresponding to some reference illumination level. We introduce an alternative definition based on the times when the maximum rate of increase and decrease in light intensity occurs. This definition has a clear physical interpretation and also has several potentially desirable features that help minimize the effect of sensor drift (e.g., degradation in the sensors with time or fouling of the transparent surface of the detector by plant or animal growths). In this paper, we also evaluate the use of digital signal processing (filtering) techniques to enhance the geoposition signal relative to the noise.

Methods

Estimating geoposition

If the rotational axis of the earth were perpendicular to the plane of the earth's orbit around the sun, the sun would rise or set 4 min later for each degree of longitude west that an observer moved, irrespective of latitude (1° of latitude equals 111 km at all longitudes; at 50°N, 1° of longitude equals 111 km·cos(50°), or 71.4 km). The earth's rotational axis is actually tilted relative to the sun, resulting in day length varying with both latitude and day of the year. Thus, knowing the times of dawn and dusk is sufficient information in principle to determine the geographical coordinates (or geoposition) of the observer each day (Hill 1994).

Estimation of latitude is inherently more uncertain than that of longitude. Near the spring and fall equinoxes, day length is almost 12 h at all latitudes, so small errors in estimating day length can have large effects on the accuracy of the estimated latitude. For example, at 50°N and 5 days away from the equinox, a misspecification in day length of 1 min results in an error of about 1.5° (over 150 km) in estimated latitude. However, this sensitivity falls rapidly. We found in our experiments that acceptable geoposition estimates could be obtained outside a period of about ±7 days around the equinox.

Sources of error

Accurately estimating the times of dawn and dusk from a light record is not simple. When light enters the earth's atmosphere, it is refracted due to thermal and pressure gradients and the resulting path is curved. Thus, archival tags measure light as though the upper rim of the sun was on the horizon before it is actually there. Furthermore, when the tags are submerged in water, the light undergoes partial reflection and refraction at and beneath the air–sea interface. The amount of light scattering is maximal when the light enters the water almost parallel to the surface, which is precisely the case near sunrise and sunset, and will be further degraded by wave state. Such factors are impossible in practice to control for and necessarily limit our ability to estimate the times of dawn and dusk.

Thickness of cloud cover, presence of shadows, and spurious light from artificial sources may all affect the measured light intensity. If the horizon is obstructed by mountains, the times of dawn and dusk estimated from the light record will be too late and too early, respectively, since they will correspond to the rising and setting of the sun behind the mountains as opposed to the true horizon for the geoid. Noise in the electronics of the archival tags will also affect the measured light levels.

Other problems specific to the attachment of archival tags to free-swimming fish may also contribute to errors. Fouling from algae growing on the tags over time can be a problem, since this gradually reduces measured light levels. The fact that the fish are moving is a problem in itself, since determining geoposition requires estimates of dawn and dusk at the same location.

A particularly important issue for some species, which we do not consider here, is the effect of vertical movement within the water column. Such movements complicate the estimation of geoposition because light intensity is rapidly attenuated with depth. We will consider this issue elsewhere (D.W. Welch and J.P. Eveson, unpublished), but note that in principle, attenuation of the light record can be corrected for by using the depth measurements recorded by most archival tags to calculate the light level at a constant depth.

Estimating times of dawn and dusk

Reference light level

Dawn and dusk are commonly defined as the times corresponding to civil twilight. Civil twilight occurs when the upper edge of the sun's disk reaches an angle of $\zeta = 96°$ to the zenith (i.e., 6° below the horizon) and has been stated to correspond to an illumination level equal to the night light level plus 5% of the difference between day and night levels when light is measured on a logarithmic scale (Hill 1994).

This definition of dawn and dusk has been adopted in several previous studies (Gunn et al. 1994; Hill 1994), but we found that it does not work well for all tag designs. We considered a more general approach in which instead of a reference light level of 5%, we estimate the best value for the reference light level independently for each tag. We refer to this as the k% method. The light sensors in some tags measure night light levels that are inappropriate for this method because they detect the variation in nighttime light level caused by the phase of the moon. Consequently, we investigated a modified method that specifies the reference light level to be k% of the maximum daytime light level (equivalent to assuming that the nighttime level equals zero in the original definition). We refer to this as the k_{max} method. As the reference level of illumination, k, changes, the corresponding zenith angle, ζ, also varies and can be estimated from the data.

Daytime and nighttime levels of illumination were estimated by averaging the light readings within a 2.5-h span on either side of local noon and midnight and then used to calculate the k% or k_{max} reference light level. We applied a two-stage curve-fitting procedure to estimate the time at which the reference light level was reached. Specifically, we first identified a rough estimate of the true time of dawn or dusk and fit a fourth-order polynomial through the observations within a 2-h span of this approximation using least squares. The time at which the reference light level intersected the fitted curve was taken as our initial estimate of dawn or dusk. This estimate was refined by repeating the procedure, this time fitting a fourth-order polynomial through the data within a 0.5-h span of the initial estimate.

Maximum rate of change

An alternative definition of twilight with a clearer physical basis is the time at which light intensity changes most rapidly. This occurs as the center of the sun's disk reaches the horizon and the greatest surface area of the sun is occluded by the horizon per unit time (i.e., when $\zeta = 90°$, excluding complicating effects caused by the presence of an atmosphere and ocean).

To identify the times of most rapid change, we took the first-difference of the light data as follows. Let $L(t_i)$ denote the light

© 1999 NRC Canada

reading at time t_i, $i = 1, \ldots, n$. Then the first-difference is given by $\Delta L(t_i) = L(t_i) - L(t_{i-1})$. (This introduces a bias in our estimated times of dawn and dusk of $-1/2\Delta t$ that must be corrected for later.) The local maxima and minima of the differenced record occur when light intensity is increasing and decreasing most rapidly and give us our estimated times of dawn and dusk, respectively.

To estimate the maxima (minima) in the differenced data, we identified the largest (smallest) value in the differenced data for each day, took the nearest 50 observations, and fit a fourth-degree polynomial through the data by least squares. The estimated time of dawn (dusk) for each day was obtained by differentiating the fitted equation with respect to time and finding the appropriate zero in the derivative. Figure 8, discussed later, provides examples of how well this curve-fitting approach describes the observational data.

Signal processing algorithm

The desired signal for estimating geoposition is the 24-h cycle in sunlight, but it is distorted by noise from other sources including artificial light sources, changes in cloud thickness, sea state, fish orientation, and electronic errors. The goal of digital signal processing is to design a filter that increases the signal-to-noise ratio in the data by excluding some of the noise while retaining most of the signal. This is typically achieved by performing a frequency-dependent alteration of a data sequence.

We chose to use a Chebyshev type II low-pass filter to process the data because this has a maximally flat frequency response over the passband and therefore imposes minimal distortion at frequencies below the cutoff (Rabiner and Gold 1975). Chebyshev filters are one class of infinite impulse response filters. Although infinite impulse response filters are typically very efficient in achieving a given frequency response in the gain, they introduce complicated frequency-dependent phase shifts. These effects can be avoided by applying the filter twice with the data reversed in time sequence before the second filtering. The filter can be tuned to a specific light record by altering input parameters such as the frequency cutoff, the transition width, the passband ripple (i.e., the level of distortion at low frequencies), and the stopband attenuation (i.e., the suppression in variability at high frequencies).

Description of studies

To date, we have completed three test studies in the Gulf of Alaska using archival tags manufactured by several companies. The first involved placing tags on two moving vessels, the second had tags fixed to an underwater mooring at Ocean Station P (50°N, 145°W), and in the third experiment, tags were hung from an offshore weather buoy, Nomad North (54°N, 139°W).

Study 1

Two tags from Northwest Marine Technology (NMT) (Shaw Island, Wash., U.S.A.), serial Nos. 157 and 161, and two SBT200 tags from Zelcon Technic Pty (Glenorchy, Tasmania, Australia), serial Nos. 633 and 639, were fixed to the bow of the F/V *Columbia* in the Gulf of Alaska from October 10 to November 12, 1995. Two NMT tags (serial Nos. 154 and 165) were also placed aboard the CCGS *W.E. Ricker* from September 29 to October 23, 1995. Zelcon was unable to supply tags in time to be mounted on the CCGS *W.E. Ricker*. Because they were attached to a moving vessel, the tags underwent large positional changes in a day, and they were also exposed periodically to artificial light sources on the ship.

Both the NMT and the Zelcon archival tags used 8-bit analog-digital converters, which allowed the light level to be recorded as one of 256 discrete intervals. However, the architecture of the tags differed. The NMT tag estimated and returned the longitude based on a proprietary internal algorithm, and we used these numbers without further processing.[2] In contrast, the Zelcon tag stored the measured light data to which we applied our geoposition algorithms.

Study 2

To eliminate the problems caused by movement and artificial light sources, a second experiment was conducted in which tags were attached to a stationary subsurface mooring located at Station P in 4 km of water. Because Station P is located at 50°N, 145°W in the Gulf of Alaska and is 1500 km offshore, the horizon is unobstructed by mountains that could disrupt the actual time of sunrise or sunset. In addition, the top of the mooring is 38 m below the surface and has no flashing lights or other surface navigational aids that could influence the light readings. Thus, deploying tags at Station P provides an excellent situation in which to examine the potential accuracy of archival tags.

On February 29, 1996, two Zelcon SBT200 tags (the same model used in the first study) were mounted at the top of the subsurface mooring. The mooring was retrieved on May 20, 1996, the initial tags were removed, and two more SBT200 tags as well as two prototype Zelcon SBT2000 tags were attached. These tags were retrieved on August 27, 1996.

The SBT2000 tags incorporated several technological modifications including photodiode-based rather than photoresistor-based light sensors, which substantially reduced a memory effect intrinsic to photoresistor sensors. Also, the SBT200 tags used a switching procedure between high and low light sensitivity modes that was changed by the manufacturer in an attempt to correct a problem that we identified in the first study.

Study 3

The third study involved four archival tags manufactured by Wildlife Computers (16150 NE 85th St., No. 226, Redmond, WA 98052, U.S.A.) whose tags recorded light data. The original intent was to deploy the tags at the subsurface mooring Station P in February 1997, but severe weather conditions prevented recovery of the mooring. Instead, the tags were deployed on March 9, 1997, at an offshore weather buoy, Nomad North. The Nomad surface mooring, located at about 54°N, 139°W, is in 3.5 km of water off the continental shelf and beyond visible range of coastal mountains. The mooring was retrieved and the tags removed on June 12, 1997.

The experimental protocol involved hanging a heavy chain with chafing gear off the weather buoy with four tags attached at 10 m to the chain. The tags were mounted such that their light sensors faced perpendicularly out into the water column. Normal practice would be to face the sensors upward to face the surface, but concern for the physical integrity of the mounting during winter and spring storms prevented this.

Comparison of relative accuracy

For each study, we evaluated the accuracy of the geoposition estimates obtained from the different tags and algorithms. The k%, k_{max}, and differencing methods were applied directly to the raw light data and also to the filtered light data to get estimated times of dawn and dusk. Existing navigational routines were used to convert each set of dawns and dusks to daily geoposition estimates, which could then be compared with the true location.

The performance of each algorithm depends on the input parameters, such as the value of k in the reference light level methods and

[2] Recently developed archival tags produced by NMT apparently also store the light record and provide an estimate of latitude, but we have not examined the positional accuracy of these tags.

© 1999 NRC Canada

Fig. 1. Actual and estimated noontime positions of the F/V *Columbia*. The study region shown is the Gulf of Alaska. The estimated positions were derived for the Zelcon tags using the k_{max} light level algorithm.

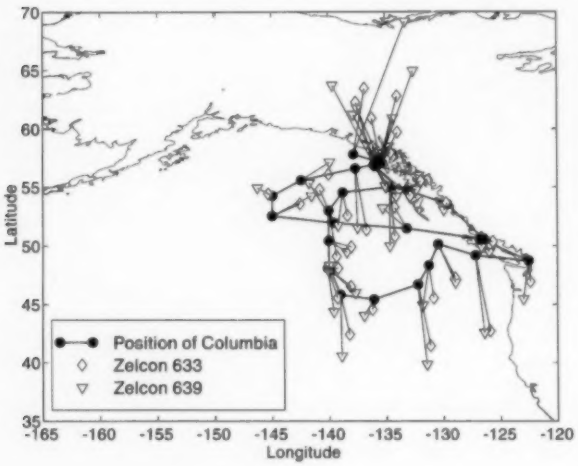

the filter characteristics when the Chebyshev filter is applied. Furthermore, a zenith angle ζ must be specified for use in the navigational routines, and the value chosen greatly influences the results.

To ensure a fair evaluation, we compared the "best" performance of each algorithm. The optimal parameter values and ζ for each method were found by minimizing the mean squared error in kilometres between the estimates and the true position. Mean squared error was chosen as the optimization criterion because it combines the variance and the absolute error of the estimates, both of which we would like to be small. Kilometres were used as the unit of comparison instead of degrees to account for the fact that the distance represented by 1° of longitude varies with latitude.

Results

For the first two studies, deficiencies in either the experimental design (study 1) or the design of the tags (study 2) limited our ability to unambiguously evaluate geoposition accuracy. Thus, we limit our presentation to the algorithm giving the best results, the k_{max} method. For the third experiment, we present a detailed comparison of geoposition algorithms.

Study 1

The actual midday positions of the ship track for the F/V *Columbia* are shown in Fig. 1 along with the estimated positions using the Zelcon tags. The NMT tags could not be included on the map because they provided only longitude estimates. The estimates for the Zelcon tags were derived using the k_{max} light level algorithm applied to the raw light data (filtering did not give a significant improvement). The optimal values of k and the ζ corresponding to this k were determined for each tag (Table 1).

The patterns of latitudinal and longitudinal errors were very similar between tags (Fig. 2), which suggests that the cause of the errors was external to the tags. Statistics on the uncertainty in latitude and longitude and the average position (Table 1) show that tag 633 performed significantly better than tag 639, with an average error of almost 100 km less. As expected, latitude was estimated with greater uncertainty than longitude. Our evaluation of the NMT tags was limited to longitude, for which all tags gave an SD of about ±2°.

Table 1. Summary of position estimates for the F/V *Columbia* and CCGS *W.E. Ricker* (study 1).

Tag ID	No. of estimable days	k_{max} (%)	ζ (°)	SD latitude (°)	SD longitude (°)	Average error (km)
F/V *Columbia* (Oct. 10 – Nov. 12, 1995)						
Zelcon 633	34	90	92.3	3.1	1.1	291.6
Zelcon 639	34	95	91.2	4.2	1.8	388.6
NMT 157	34	—	—	—	2.3	—
NMT 161	34	—	—	—	2.1	—
CCGS *W.E. Ricker* (Sept. 29 – Oct. 23, 1995)						
NMT 154	25	—	—	—	1.8	—
NMT 165	25	—	—	—	2.1	—

Note: All results were obtained using the k_{max} method with k optimized separately for each tag. The NMT tags calculated longitude internally using a proprietary algorithm; they did not calculate latitude.

Study 2

The Zelcon SBT200 tags from the first stage of the experiment (tags 634 and 635) were at sea during the time of the spring equinox, when accurate estimation of latitude using day length is impossible. We chose to be conservative and base our evaluation on the period starting 12 days after the equinox (Table 2). Again, geoposition estimates are reported for the k_{max} light level algorithm, where both k and ζ were optimized separately for each tag.

Both tags performed quite well, with an average error of about 130 km. A time series plot of estimated latitudes and longitudes (Fig. 3) indicates that the daily estimates were similar between tags and that there was no obvious pattern to the errors.

Of the two SBT200 tags used in the second deployment (tags 633 and 639), we were only successful in downloading data from tag 633. The reason for the failure of tag 639 was unknown. The light record from the successful tag extended the duration of the experiment and did not include days near the equinox; thus, geoposition estimates could be obtained for a total of 93 days. Unfortunately, both prototype SBT2000 tags stopped recording well before the end of the experiment, one on June 5, after only 15 days at sea, and the other on June 18. Furthermore, the tags recorded very different light histories, with the most striking difference being that one of the tags recorded a zero light level each night.

© 1999 NRC Canada

Fig. 2. Changes over time in positional error in (*a*) latitude and longitude for tags aboard the F/V *Columbia* and (*b*) longitude for NMT tags aboard the CCGS *W.E. Ricker.*

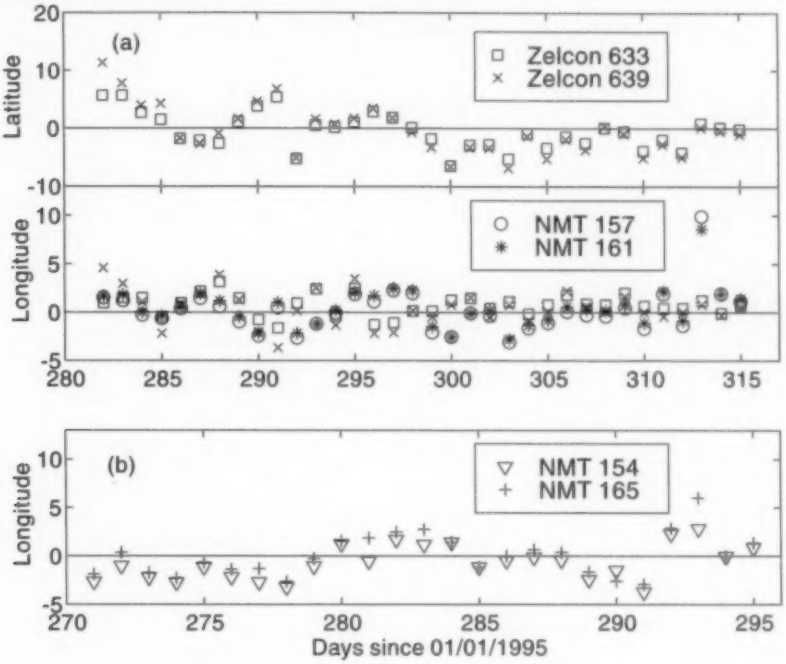

Table 2. Summary of position estimates for Station P (study 2).

Tag ID	No. of estimable days	k_{max} (%)	ζ (°)	SD latitude (°)	SD longitude (°)	Average error (km)
			Apr. 2 – May 19, 1996			
Zelcon 634	47	45	94.9	1.1	0.6	127.7
Zelcon 635	47	50	93.9	1.3	0.7	132.5
			May 21 – Aug. 20, 1996			
Zelcon 633	93	40	95.5	1.3	0.9	154.9
Zelcon 2001	28	35	86.2	4.4	3.0	513.2
Zelcon 2002	15	2	90.9	1.0	1.2	123.2

Note: Reported results are for the k_{max} method with k optimized separately for each tag. Results are calculated for the period starting 12 days after the spring equinox.

The accuracy of tag 633 was slightly worse than that for tags in the first stage of the experiment, perhaps because the number of days for which position was estimated was double. The latitude estimates drifted north and then south over time, and the longitude estimates drifted east (Fig. 4). Tag 2001 gave very inaccurate position estimates, with an average error of over 500 km (Table 2), the reason for which was not clear. Although tag 2002 performed much better, giving results comparable with those of tags 634 and 635 in the first stage of the experiment, it recorded data for such a short duration that evaluation is difficult.

Study 3

Upon recovery, we found that an algae film covered both the inner and outer surfaces of the protective Plexiglas boxes in which the Wildlife tags had been mounted plus the tag surfaces themselves, tripling the effective fouling through which the tags measured ambient light levels. The four tags recorded very similar light histories for the full duration of the experiment. Their light records show a decrease in peak daytime levels beginning in May, which likely corresponded to the development of fouling. Because all tags were at a depth of 10 m, a study of depth effects on the light records and geoposition estimates was impossible.

We estimated geoposition using the k_{max} method applied to both the raw and filtered light data and the differencing method applied to just the filtered data. (Taking the first difference of the raw light record magnified the variability in the data so much that maxima and minima could not be identified; therefore, filtering was essential before using the differencing method.) The k% method was not used because the Wildlife tags recorded light intensities on a logarithmic scale, which exaggerated the relative importance of lower light levels. As a result, the light readings at night varied greatly over time depending on the cycle of the moon and did not give useful nighttime reference levels.

The input parameters needing to be optimized varied ac-

© 1999 NRC Canada

Fig. 3. Changes over time in estimated (*a*) latitude and (*b*) longitude at Station P during the first deployment of study 2. Geoposition estimates for times within 12 days of the equinox were excluded. Horizontal lines indicate the true latitude and longitude.

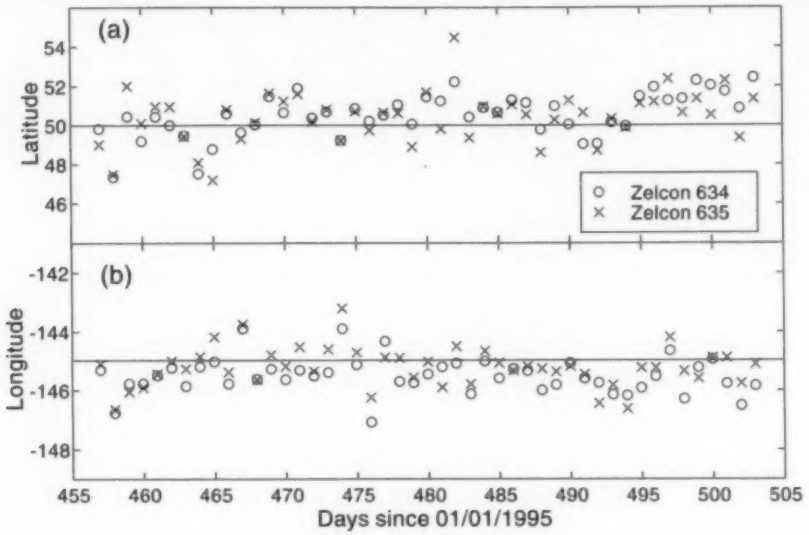

Fig. 4. Changes over time in estimated (*a*) latitude and (*b*) longitude for Zelcon model 200 and 2000 tags at Station P during the second deployment of study 2. Note the change in scale from the previous figures.

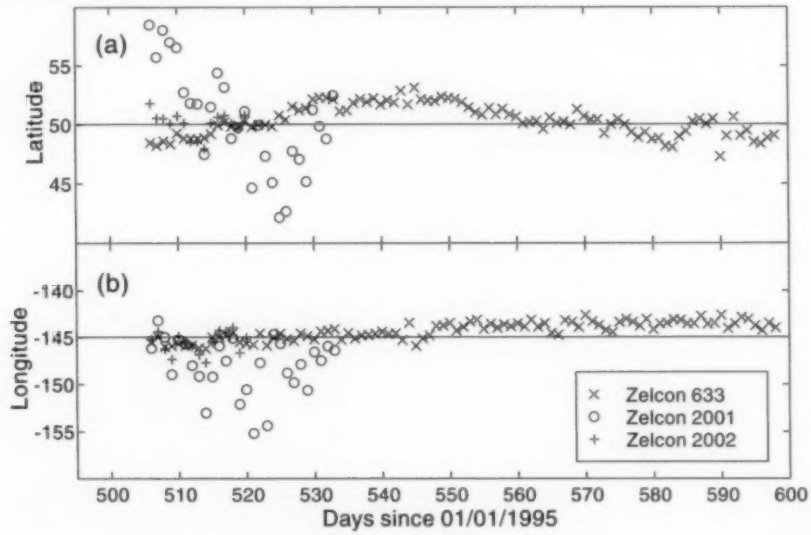

cording to the algorithm being used. The following is a summary of the methods applied and the values optimized:

Method	Values to be optimized
k_{max} applied to raw data	k and ζ
k_{max} applied to filtered data	Filter characteristics, k, and ζ
Differencing applied to filtered data	Filter characteristics and ζ

Initial assessment showed that the major determinant of filter performance was the cutoff frequency. The shape of the filter rolloff with frequency or the degree of attenuation at frequencies above the cutoff played only minor roles in determining tag accuracy but substantially increased the time required to estimate optimal parameters. For simplicity, we set the filter gain to change over a frequency span of ±20% of the cutoff and the minimum suppression at frequencies higher than this as 30 dB, or about 3% of the initial power.

Some interesting observations can be made regarding the estimated optimal parameter values (Table 3). The best value

© 1999 NRC Canada

Fig. 5. Identification of the optimal Chebyshev frequency cutoff for four Wildlife tags using the (*a*) k_{max} light level algorithm and (*b*) differencing algorithm. A cutoff of 30 min resulted in the smallest errors for the k_{max} = 70% light level algorithm, whereas a higher cutoff of 144 min was best for differencing. All tags give similar results (lines), but note the significant differences in mean squared error between tags for the k_{max} technique.

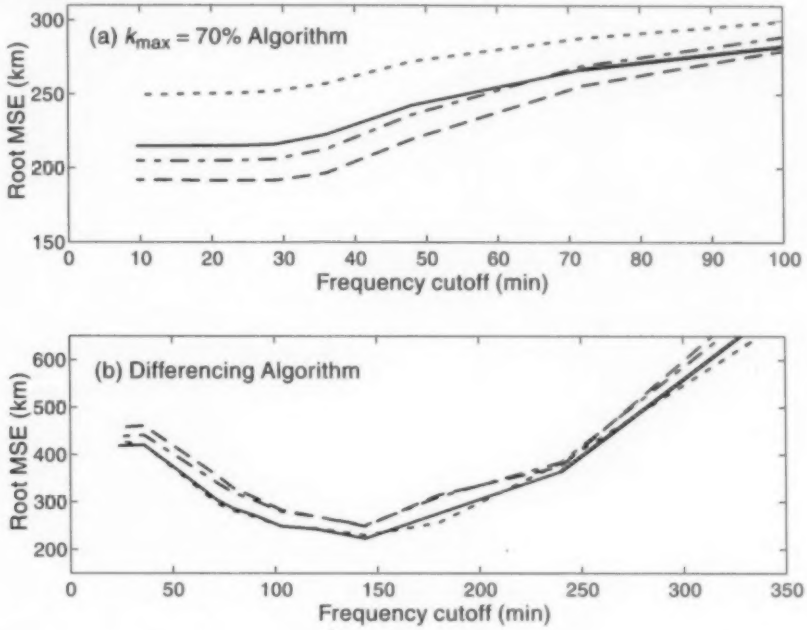

Table 3. Estimated optimal values of parameters necessary for each estimation method used in study 3.

Method	Wildlife tag ID	ζ (°)	Frequency cutoff (min)	k_{max} (%)
k_{max}, raw data	031	94.8	—	70
	032	94.6	—	70
	033	94.8	—	70
	034	94.8	—	70
k_{max}, filtered data	031	94.8	13.1	70
	032	94.6	11.1	70
	033	94.8	24.0	70
	034	94.8	14.4	70
Differencing, filtered data	031	97.2	144	—
	032	97.0	144	—
	033	97.4	144	—
	034	97.4	144	—

Note: When the method included the use of a low-pass Chebyshev filter, only the frequency cutoff was optimized. The other filter parameters were set to a transition width of ±20% of the cutoff, stopband attenuation of 30 dB, and passband ripple of 1 dB.

Table 4. Comparison of geoposition estimates for the Nomad North buoy (study 3).

	Method		
Wildlife tag ID	k_{max}, raw data	k_{max}, filtered data	Differencing, filtered data
Average error (km)			
031	142.0	141.9	144.9
032	164.5	164.5	153.1
033	125.1	124.6	155.9
034	139.1	138.8	161.9
Average	142.7	142.5	154
SD latitude (°)			
031	1.2	1.2	1.3
032	1.4	1.4	1.3
033	1.1	1.0	1.4
034	1.1	1.1	1.4
Average	1.2	1.2	1.4
SD longitude (°)			
031	0.9	0.9	1.0
032	0.9	0.9	0.9
033	0.9	0.9	1.1
034	0.9	0.9	1.0
Average	0.9	0.9	1

for k was 70% for all four tags, regardless of whether raw or filtered data were used. The optimal frequency cutoff for the Chebyshev filter when used in conjunction with the differencing algorithm was 144 min, or 2.4 h, for all tags, meaning that changes in light intensity on time scales of 144 min or less were suppressed. The optimal cutoff value when filtering was used in conjunction with the k_{max} method was more variable, ranging from 11 to 24 min depending on the tag. However, the error in the geoposition estimates was essentially identical for any frequency cutoff less than about 30 min (Fig. 5), meaning that only variations in light occur-

© 1999 NRC Canada

Fig. 6. Changes over time in estimated latitude (*a* and *b*) and longitude (*c* and *d*) using the k_{max} and differencing methods to estimate geoposition for the Nomad North experiment. Horizontal lines indicate the true latitude and longitude. The strong coherence between tags (different symbols) for a given method indicates that the geoposition errors are the result of extrinsic causes rather than problems with the tags themselves.

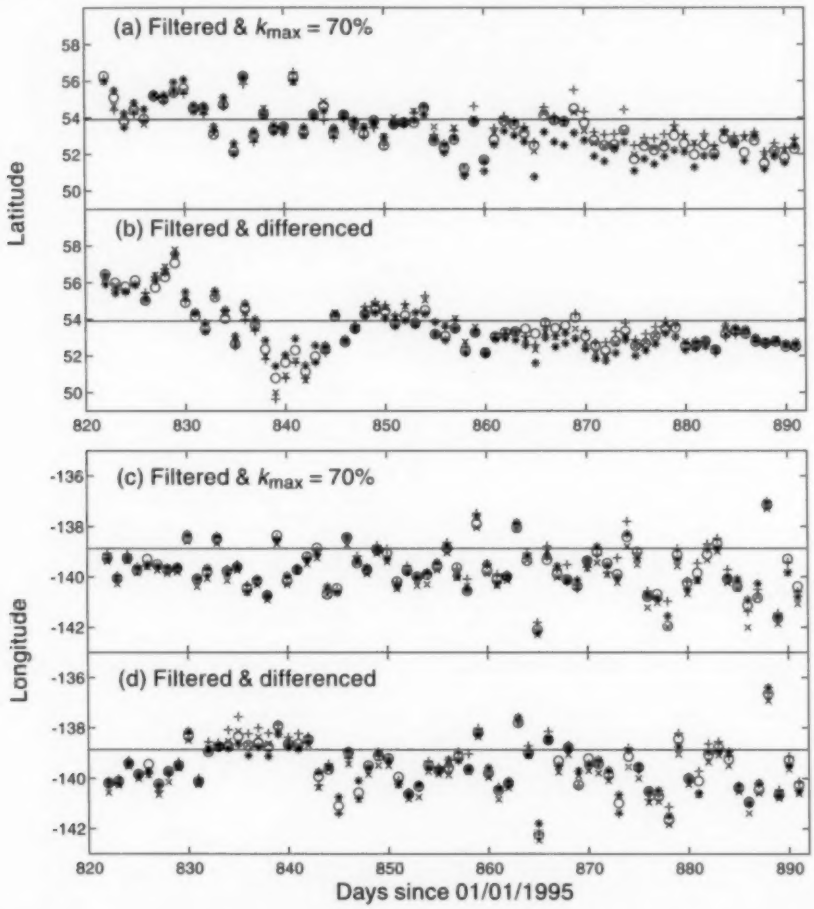

ring on time scales less than 30 min needed to be suppressed for the k_{max} method.

The uncertainty and average error of the daily geoposition estimates were very similar across tags and methods (Table 4). The k_{max} method performed marginally better than the differencing method whether or not filtered data were used; filtering made virtually no difference in the outcome. The average results across tags suggest that the Wildlife tags are capable of estimating geoposition within an uncertainty of about ±1.2° (≅130 km) in latitude and ± 0.9° (≅ 60 km) in longitude.

It is interesting to note that the relative ranking of the performance of the tags was the same whether raw or filtered data were used with the k_{max} method but varied between the k_{max} and differencing methods (Table 4, average error). For example, the tags that had the lowest geoposition error when using the k_{max} = 70% definition of twilight (033 and 034) and that were up to 40 km more accurate than tags 031 and 032 were significantly less accurate than tags 031 and 032 when using the differencing approach to estimate the times of dawn and dusk. The best method is therefore partly dependent on which tags are recovered (best-case return rates from field experiments are likely in the range of 10–30%).

For each method, there was good agreement among the four tags in their daily latitude and longitude estimates (Fig. 6). (Estimates for the k_{max} method applied to raw data are not shown, since they are almost identical to those using filtered data). Although the patterns of error in latitude and longitude differed for the $_{kmax}$ and differencing methods, some similar features existed such as a small drift southward in the latitude estimates in early May (around day 850, when fouling developed) and an increase in longitudinal variability over time. The estimates also showed a small amount of serial correlation, especially in latitude.

Discussion

In our first study, the errors in geoposition were larger than desired for all tags. This was at least partially caused by

© 1999 NRC Canada

Fig. 7. Estimated mean position ±1 SD in latitude and longitude for studies 2 (first deployment) and 3, calculated using the daily estimates from all tags within a study (two Zelcon tags in study 2 and four Wildlife tags in study 3). The results presented are for the k_{max} method applied to unfiltered data. The true locations of Station P (study 2) and the Nomad North buoy (study 3) are indicated.

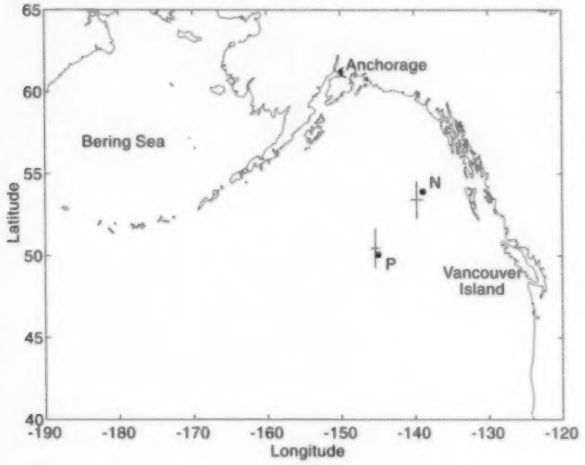

the ship's movement because over a day of sailing the times of dawn and dusk change from those that would be observed at a stationary position. For example, when the ship heads west, dusk occurs later than if the ship had remained at the same position where dawn was initially observed. This effectively increases the length of day and the time of midday and results in incorrect position calculations. Although a fish travels at a slower rate than a vessel, the effect of movement is still potentially substantial. For example, a 50-cm salmon migrating due east or west could change day length by about 1 min, assuming a 12-h day and a sustained migration rate of one body length per second. The resulting error in geoposition ranges from about 10 km to over 100 km depending on the time of year and the location of the fish. However, it should be possible to partially correct for this source of error by calculating an average east–west rate of movement and then correcting the estimates of day length to compensate for the movement.

The results from study 3 and from the first deployment in study 2 are promising. A map of the North Pacific Ocean (Fig. 7) shows the average position estimate ±1 SD achieved by tags in these two studies, along with the corresponding true locations; the results indicate that current archival tags are capable of resolving large-scale patterns of movement in fish migration. Although movement patterns in most coastal regions could not be resolved at the levels of accuracy achieved thus far using the light record alone, it may be possible to improve the estimates with the inclusion of depth and temperature information.

In our third experiment the optimal cutoff value for the Chebyshev filter was consistently higher, as expressed in minutes, when using the differencing method than when using the k_{max} method. A higher cutoff means that variations in light occurring on more times scales are being suppressed,

Fig. 8. Estimated times of dawn and dusk for day 865 (solid vertical lines) derived using two methods applied to tag 031. DF, differencing applied to filtered data; KR: k_{max} applied to raw data. Broken vertical lines indicate the actual times of dawn and dusk calculated from astronomical considerations (for each method, the estimate of ζ given in Table 3 was used). The solid horizontal line indicates the k_{max} light level. The large departure from the true times of dawn and dusk is not reflected in the variability in the data around the fitted curves. Note that the light measurements (dots) are spaced 1 min apart.

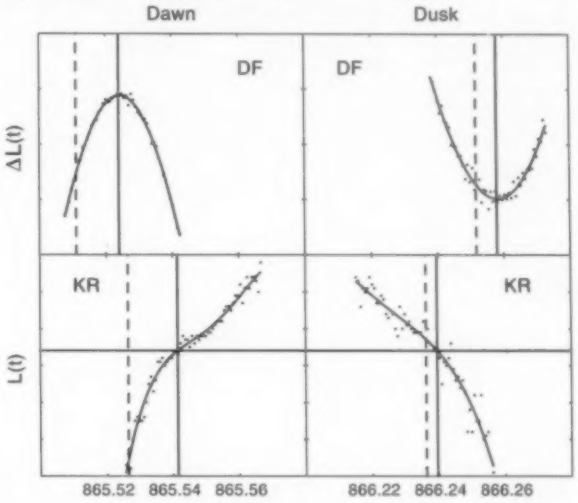

so that the filtered data are smoother than would be obtained with a lower cutoff. Thus, more highly smoothed data worked better for the differencing method than for the k_{max} method. This result may in part be related to the enhancement of high-frequency noise by differencing and the corresponding need for greater suppression of variation at these frequencies during filtering.

The optimal estimated angle of the sun at twilight (ζ) and the optimal parameter values required in the geoposition algorithms changed between methods and tag architectures. Because we knew the true position of the tags, we were able to determine the optimal values for each experiment. In an experiment on free-ranging animals, this would not be possible. As a result, it is important to conduct a pilot or parallel study at a known location, ideally in the same geoposition region and at the same time as the field study. Provided that all archival tags of the same model give consistent results, then the parameters determined for the tag(s) used in the pilot study would also be valid for the tags used in the field study. Our third experiment provides evidence that optimal parameter estimates are highly consistent across tags, so applying the parameters derived for one tag to the other three would have obtained equally good results.

Another practical difficulty in studying free-ranging fish is the changes in depth that will occur and the corresponding effect on recorded light intensities. Short-term tagging studies indicate that vertical movements of Pacific salmon are relatively limited, with almost all time spent within the surface mixed layer (e.g., Ogura and Ishida 1992, 1995; Ogura 1994). However, even in this case, light attenuation with

© 1999 NRC Canada

depth is significant and would need to be corrected to a constant depth. For other animals with more pronounced vertical movements, these difficulties will be more acute.

Previous studies of tag performance generally had a duration of only 1 week or less. We found that the length of the experiment has an important influence on the degree of error in estimates of geoposition. A large fraction of the total variation is the result of systematic and coherent changes in geoposition over long time scales that are shared between all tags (cf. Fig. 6). Because of this serial correlation, a subset of only a few days of the record will reveal much less variability. Furthermore, the zenith angle can be chosen to center the mean of a subset of estimates near the true location. However, the angle that is needed will differ with each subset of days so that one value cannot be chosen to give equally good results over the entire record. The level of error in geoposition estimates is therefore likely to be significantly underestimated in experiments of short duration (<1–2 months).

One source of error in our estimation procedures stems from our approach of having the computer algorithms estimate the times of dawn and dusk without human intervention. This decision was necessary because of the large number of estimations performed. Although data from a single recovery of a tagged animal would likely be subject to a closer visual inspection, the relative performance of the estimation algorithms that we report is unlikely to change. Indeed, we have been told of cases where investigators rejected more than one third of the available record because visual examination suggested that the data had too many outliers. A more objective approach seems called for, particularly when geoposition estimates for free-swimming animals must be rejected without an absolute basis for deciding upon what is "good" or "bad".

An important finding is that the major source of errors in geoposition appears to be external to the tags, as suggested by the high degree of consistency in the time series of latitude and longitude estimates among tags from the same experiment. Further indication that the major source of errors is external to the tags can be obtained by closer examination of those days when the greatest errors in geoposition are evident (Fig. 8). For both the k_{max} and differencing techniques, dawn and dusk occur at times much different from the expected times based on astronomical calculations. More importantly, the magnitude of the error is not indicated by the minute-to-minute variation in the recorded light levels. Some external source appears to have significantly changed the time that twilight occurred in a way that was clearly not reflected in the variability of the residual errors around the fitted light curve. We suspect that the movement of weather systems through the study area may have caused these changes by increasing cloud cover, wind strength, and sea state, all of which would result in decreased light levels. It is surprising, however, that these changes are observed even when the estimated times of dawn and dusk are based on the rate of change in light level. A proportionate reduction in light level that persists over periods of hours to days should not have a large effect on the time of maximal change, since we identify this time based on the difference in light level between adjacent samples. More work is needed to establish what atmospheric and oceanographic conditions contributed to the remaining errors and to determine the role of the sensitivity of the light sensors used in the tags.

Use of "smoothing" techniques such as running means or medians to average daily geoposition estimates is one approach to reduce the variability in estimates of latitude and longitude. This only works well if the errors in geoposition are random and independent. Our mooring experiments suggest that daily estimates are serially correlated, where the major source of positional uncertainty is due to estimates (latitude in particular) either drifting slowly or cycling irregularly up and down. As we have noted, a possible explanation for this is meteorological conditions giving consecutive days of good weather (little or no cloud cover) followed by consecutive days of poor weather. Although some smoothing of the migration track may be desirable, the degree of smoothing will need to be carefully evaluated, as will the actual improvement in the positional accuracy obtained.

Further improvements in the accuracy of geoposition estimates obtained from light records may be attainable by conducting fixed-location studies concurrently with a field program. Systematic deviations from the fixed study locations might be used to apply a "correction" to the estimated geoposition of a free-ranging animal. This approach would be particularly valuable if the patterns of deviation from the true location were not only coherent between multiple tags at a single location, as we have shown, but were also coherent between tags at different locations within the general study region. Such experiments have not yet been performed but would provide strong evidence that the major source of the remaining error observed is due to large-scale meteorological processes.

Conclusions

The tags and methods that we have studied are capable of estimating geoposition with an average error of about 140 km (SD's of ±1.2° of latitude and ±0.9° of longitude). The level of accuracy needed from archival tags depends on the specific application intended. Currently available archival tags are not suitable for use in regional-scale studies where the anticipated level of movement is comparable with the error in the position estimates; such studies will remain restricted to the short-term use of acoustic tags (days to weeks). However, basin-scale studies of ocean migration over long time periods are now clearly feasible using archival tags.

At present, the best eddy-resolving models of surface currents in the open North Pacific are capable of estimating currents to a maximum resolution of about 100 km (e.g., LeBlond and Endoh 1996; Semtner and Chervin 1988), a level of error comparable with that of the archival tags examined. It should therefore be possible to take the movement record derived for a free-swimming animal in the surface layer and remove the component of movement due to the currents to provide both a true heading and swimming speed for the tagged animal. This information would contribute a great deal to identifying actual migration paths of salmon on a geographical scale of 100–150 km as well as to resolving the question of whether or not salmon use bicoordinate navigation during their open-ocean migrations (Neave 1964; Quinn and Groot 1984; Quinn 1990). Both are exciting research areas.

© 1999 NRC Canada

Acknowledgements

Many individuals have contributed to the development of the archival tag technology reported here; we wish to acknowledge all of them. We particularly want to thank the companies who contributed tags for use in the experiments that we have reported and for their useful comments, particularly Phil Ekstrom of NMT for an especially valuable review. We also wish to express our thanks to Dr. John Gunn and his colleagues at CSIRO, who helped pioneer the development of archival tags. They not only provided us with copies of their astronomical routines to convert times of dawn and dusk to latitude and longitude, but also shared in a number of very useful discussions with us in the early stages of our study. This study was partially supported by GLOBEC-Canada.

References

DeLong, R.L., Stewart, B.S., and Hill, R.D. 1992. Documenting migrations of northern elephant seals using day length. Mar. Mammal Sci. **8**: 155–159.

Godo, A.R., and Michalsen, K. 1997. The use of data storage tags to study cod natural behaviour and availability to abundance surveys in the Barents Sea. ICES C.M. 1997/W:18.

Gunn, J., Polachek, T., Davis, T., Sherlock, M., and Betlehem, A. 1994. The development and use of archival tags for studying the migration, behaviour and physiology of southern bluefin tuna, with an assessment of the potential for transfer of the technology to groundfish research. ICES C.M. Mini:2.1.

Hill, R.D. 1994. Theory of geolocation by light levels. *In* Elephant seals: population ecology, behaviour, and physiology. *Edited by* B.J. LeBouef and R.M. Laws. University of California Press, Berkeley, Calif. pp. 227–236.

LeBlond, P.H., and Endoh, M. 1996. Modelling of the subarctic North Pacific circulation. PICES Sci. Rep. No. 5. Institute of Ocean Sciences, P.O. Box 6000, Sidney, BC V8L 4B2, Canada.

Metcalfe, J.D., and Arnold, G.P. 1997. Tracking fish with electronic tags. Nature (Lond.), **387**: 665–666.

Neave, F. 1964. Ocean migrations of Pacific salmon. J. Fish. Res. Board Can. **21**: 1227–1244.

Ogura, M. 1994. Migratory behaviour of Pacific salmon (*Oncorhynchus* spp.) in the open sea. Bull. Natl. Res. Inst. Far Seas Fish. No. 31.

Ogura, M., and Ishida, Y. 1992. Swimming behaviour of coho salmon, *Oncorhynchus kisutch*, in the open sea as determined by ultrasonic telemetry. Can. J. Fish. Aquat. Sci. **49**: 453–457.

Ogura, M., and Ishida, Y. 1995. Homing behaviour and vertical movements of four species of Pacific salmon (*Oncorhynchus* spp.) in the central Bering Sea. Can. J. Fish. Aquat. Sci. **52**: 532–540.

Quinn, T.P. 1990. Current controversies in the study of salmon homing. Ecol. Ethol. Evol. **2**: 49–63.

Quinn, T.P., and Groot, C. 1984. Pacific salmon (*Oncorhynchus*) migrations: orientation versus random movement. Can. J. Fish. Aquat. Sci. **41**: 1319–1324.

Rabiner, L.R., and Gold, B. 1975. Theory and application of digital signal processing. Prentice Hall, Inc., Englewood Cliffs, N.J.

Semtner, A.J., and Chervin, R.M. 1988. A simulation of the global ocean circulation with resolved eddies. J. Geophys. Res. **93**(C12): 15 502 – 15 522.

Sturlaugsson, J., and Thorisson, K. 1997. Migratory pattern of homing Atlantic salmon (*Salar salar* L.) in coastal waters W-Iceland, recorded by data storage tags. ICES C.M. 1997/CC:09.

© 1999 NRC Canada

CANADIAN CONFERENCE FOR FISHERIES RESEARCH•CFFR-2000

Fredericton, New Brunswick, 6-8 January, 2000

Programme Themes and Call for Papers:
(http://www.phys.ocean.dal.ca/ccffr)

- Fin and shellfish culture
- Recreational fisheries
- Research directed at conservation of wild salmonids
- Biotic and abiotic interactions in marine and freshwater systems
- Joint CCFFR/SCL session (to be announced)

Papers addressing the major themes are encouraged, although submission on other themes related to fisheries and aquatic habitat biology are also welcome. We hope that session 4 will attract papers from students and postdoctoral fellows working on GLOBEC projects. GLOBEC (GLOBal ocean ECosystem dynamics) is an international research program that examines how living marine resources are affected by variability in their environment.

The **DEADLINE** for abstracts is **10 September 1999.**

CCFFR has moved to an electronic process for developing the program. See:
http://www.phys.ocean.dal.ca/ccffr

CONFERENCE CANADIENNE DE LA RECHERCHE SUR LES PECHES: CCRP-2000

Fredericton, New Brunswick, les 6-8 janvier 2000

Les Principaux Thèmes Abordés et Appel Pour Contributions:
(http://www.phys.ocean.dal.ca/ccffr)

- Culture des poissons, des crustacés et des mollusques
- Pêcheries récréatives
- Recherches dirigées vers la conservation des salmonidés sauvages
- Interactions biotiques et abiotiques dans les systèmes marins et dulcicoles
- Session Conjointe CCRP/SCL: (sera annoncée ultérieurement)

Des contributions reliées aux thèmes principaux sont particulièrement sollicitées, mais des contributions sur d'autres thèmes reliés aux sciences halieutiques et à la biologie des habitats aquatiques sont également bienvenues. Nous espérons que la session 4 attirera des contributions provenant d'étudiants et de stagiaires post-doctoraux oeuvrant dans des projets a GLOBEC. GLOBEC (GLOBal ocean ECosystem dynamics) est un programme de recherche international qui examine la façon avec laquelle les ressources vivantes marines sont affecttées par la variabilité de leur environnement.

La **DATE LIMITE** pour la soumission des résumés est **le 10 septembre 1999.**

La CCRP est un processus entièrement électronique pour la préparation du programme. Voir:

http://www.phys.ocean.dal.ca/ccffr

ASSIGNMENT OF COPYRIGHT

Ms. No. _____

To: NATIONAL RESEARCH COUNCIL OF CANADA ("NRC") Research Press

From: _____

_____

_____

_____

(name and address of author signing this form)

This refers to the manuscript entitled: _____

_____

written by myself and the following additional author(s): _____

_____

for publication in: _____

1. I declare that the list of authors fairly conforms to academic conventions about who should be listed. I declare that the manuscript, or its equivalent, has not been submitted for publication elsewhere. If it is accepted for publication by the National Research Council of Canada, I will ensure that it, or its equivalent, is not submitted for publication elsewhere.

2. I declare that I am (check ONE):

☐ (a) the sole owner of the copyright relating to the manuscript,	and →	I **assign** to NRC the entire copyright.
☐ (b) a part owner of the copyright, in conjunction with interests held by co-authors or their employers,	and →	I **assign** to NRC my entire interest in the copyright, and I expect the co-authors to also sign a form like this one.
☐ (c) an agent of my employer with authority to assign the copyright owned by the employer, who is: _____,	and →	I **assign** to NRC, on behalf of my employer, my employer's entire interest in the copyright relating to the manuscript, and I expect the co-authors to also sign a form like this one.
☐ (d) a public servant in Canada (federal, provincial or territorial) or the United Kingdom, so that the copyright is owned by Her Majesty,	and →	I have obtained the approval of my employer, according to the terms of my employment, to grant NRC **non-exclusive permission** to publish the manuscript and administer the copyright.
☐ (e) a public servant of the United States of America, and subject to the law that creates no U.S. copyright for the manuscript,	and →	I **assign** to NRC, on behalf of my employer, my employer's entire interest in any copyright that may exist outside the U.S., and I expect the co-authors to sign a form like this one.

3. I understand that my submission of this document does not guarantee publication, and that publication will not occur until **all authors** have provided a copyright transfer. If the manuscript is not published within 2 years after I sign this, the assignment is revoked.

Signed at _____ on _____

(City and Province/State) (Date)

_____

(Signature)

[Standard NRC form; alterations not acceptable.]

Comments on Copyright Transfer
(with extracts from the *Copyright Act*, Revised Statutes of Canada 1985, chapter C-42, as amended)

The publisher is not permitted to publish the manuscript without permission or an assignment of ownership of copyright. For greatest flexibility, and to be prepared to deal with future uses of the published material, the publisher requires ownership.

The owner may assign the right, but that assignment must be in writing:

13.(4) The owner of the copyright in any work may assign the right, either wholly or partially, and either generally or subject to territorial limitations, and either for the whole term of the copyright or for any other part thereof, and may grant any interest in the right by licence, but no assignment or grant is valid unless it is in writing signed by the owner of the right in respect of which the assignment or grant is made, or by his duly authorized agent.

The owner may be the author, but in many cases, the owner is the author's employer:

13.(3) Where the author of a work was in the employment of some other person under a contract of service or apprenticeship and the work was made in the course of his employment by that person, the person by whom the author was employed shall, in the absence of any agreement to the contrary, be the first owner of the copyright, but where the work is an article or other contribution to a newspaper, magazine or similar periodical, there shall, in the absence of any agreement to the contrary, be deemed to be reserved to the author a right to restrain the publication of the work, otherwise than as part of a newspaper, magazine or similar periodical.

The only exception to taking ownership arises when the manuscript is covered by Crown copyright owned by a Canadian government.

12. Without prejudice to any rights or privileges of the Crown, where any work is, or has been, prepared or published by or under the direction or control of Her Majesty or any government department, the copyright in the work shall, subject to any agreement with the author, belong to Her Majesty and in that case shall continue for the remainder of the calendar year of the first publication of the work and for a period of fifty years following the end of that calendar year.

Governments, and in particular the federal government, do not have a simple mechanism for assigning ownership of this particular type of Crown asset. Therefore, when an author is a public servant so that there is Crown copyright in the manuscript, a simple permission to use is acceptable to the publisher, if it is granted by a person with appropriate authority.

CESSION DU DROIT D'AUTEUR

Document n° _____

Au : CONSEIL NATIONAL DE RECHERCHES DU CANADA («CNRC») - Presses scientifiques

De : _____

_____

_____

_____

(nom et adresse de l'auteur qui signe le présent formulaire)

La présente cession porte sur le document intitulé : _____

_____

rédigé par moi, en collaboration avec l'auteur/les auteurs suivant(s) : _____

_____

aux fins de publication dans : _____

1. Je déclare que la liste des auteurs ci-dessus respecte les pratiques usuelles de rédaction savante quant aux personnes dont le nom doit être cité. Je déclare que le document ou son équivalent n'a pas été soumis à quelque autre organisme aux fins de publication. Si le CNRC accepte de publier le document, je m'assurerai que celui-ci ou son équivalent n'est soumis à aucun autre organisme aux fins de publication sans en obtenir la permission préalable du CNRC.

2. Je déclare être (UN SEUL choix) :

☐	(a) le seul titulaire de droit d'auteur afférent au document,	et →	je **cède** le droit d'auteur intégral au CNRC.
☐	(b) un titulaire partite du droit d'auteur, de concert avec des coauteurs ou leurs employeurs,	et →	je **cède** ma part du droit d'auteur au CNRC et m'attends à ce que les coauteurs signent une entente comparable.
☐	(c) un agent de mon employeur ayant l'autorité de céder le droit d'auteur appartenant à l'employeur, nommément : _____,	et →	je **cède** au CNRC, au nom de mon employeur, la part entière du droit d'auteur afférent au document appartenant à mon employeur, et m'attends à ce que les coauteurs signent une entente comparable.
☐	(d) un fonctionnaire du Canada (fédéral, provincial ou territorial) ou du Royaume-Uni, donc le droit d'auteur appartient à Sa Majesté,	et →	j'ai obtenu de mon employeur, en vertu de mes conditions d'emploi, l'autorisation d'accorder au CNRC la **permission non exclusive** de publier le document et de gérer le droit d'auteur.
☐	(e) un fonctionnaire des États-Unis d'Amérique, donc sujet à la loi qui n'associe aucun droit d'auteur américain au document,	et →	je **cède** au CNRC, au nom de mon employeur, la part entière de quelque droit d'auteur en vigueur ailleurs qu'aux É.-U. appartenant à mon employeur, et m'attends à ce que les coauteurs signent une entente comparable.

3. Je comprends que la soumission du document ne garantit aucunement sa publication et que la publication ne pourra être réalisée tant que **tous les auteurs** n'auront pas signé une cession du droit d'auteur. Si le document n'est pas publié dans les deux années suivant ma signature des présentes, la cession sera automatiquement révoquée.

Signé à _____, le _____

(ville et province/état) (date)

_____

(signature)

[Formulaire normalisé du CNRC; aucune modification permise]

Commentaires sur la cession du droit d'auteur
(accompagnés d'extraits de la *Loi sur le droit d'auteur*, Lois révisées du Canada 1985, chapitre C-42 modifié)

L'éditeur ne peut publier un document sans la permission ou une cession du droit d'auteur. Pour des raisons de souplesse et en vue de l'utilisation future du document publié, l'éditeur doit devenir titulaire du droit d'auteur.

Le titulaire peut céder le droit, mais cette cession doit être faite par écrit :

13.(4) Le titulaire du droit d'auteur sur une oeuvre peut céder ce droit, en totalité ou en partie, d'une façon générale, ou avec des restrictions territoriales, pour la durée complète ou partielle de la protection; il peut également concéder, par une licence, un intérêt quelconque dans ce droit; mais la cession ou la concession n'est valable que si elle est rédigée par écrit et signée par le titulaire du droit qui en fait l'objet, ou par son agent dûment autorisé.

Le titulaire peut être l'auteur, mais dans plusieurs cas, le titulaire est l'employeur de l'auteur:

13.(3) Lorsque l'auteur est employé par une autre personne en vertu d'un contrat de louage de service ou d'apprentissage, et que l'oeuvre est exécutée dans l'exercice de cet emploi, l'employeur est, à moins de stipulation contraire, le premier titulaire du droit d'auteur; mais lorsque l'oeuvre est un article ou un autre contribution, à un journal, à une revue ou à un périodique du même genre, l'auteur, en l'absence de convention contraire, est réputé posséder le droit d'interdire la publication de cette oeuvre ailleurs que dans un journal, une revue ou un périodique semblable.

La seule exception dans la cession du droit d'auteur est lorsque le document est associé au droit d'auteur de la Couronne, qui appartient au gouvernement du Canada .

12. Sous réserve de tous les droits ou privilèges de la Couronne, le droit d'auteur sur les oeuvres préparées ou publiées par l'entremise, sous la direction ou la surveillance de Sa Majesté ou d'un ministère du gouvernement, appartient, sauf stipulation conclue avec l'auteur, à Sa Majesté et, dans ce cas, il subsiste jusqu'à la fin de la cinquantième année suivant celle de la première publication de l'oeuvre.

Les gouvernements, en particulier le gouvernement fédéral, ne disposent pas d'un mécanisme simple de cession de droit d'auteur pour ce genre de biens de la Couronne. C'est pourquoi lorsqu'un auteur est un fonctionnaire et que, par conséquent, le droit d'auteur appartient à la Couronne, une simple permission d'usage est suffisante pour l'éditeur, pour autant que celle-ci ait été octroyée par une personne jouissant de l'autorité nécessaire pour ce faire.

Russell B. Millar, Brian H. McArdle, and Shelton J. Harley	**1278–1284**	Modeling the size of snapper (*Pagrus auratus*) using temperature-modified growth curves
David Lundvall, Richard Svanbäck, Lennart Persson, and Pär Byström	**1285–1292**	Size-dependent predation in piscivores: interactions between predator foraging and prey avoidance abilities
Jason L. Vogel and David A. Beauchamp	**1293–1297**	Effects of light, prey size, and turbidity on reaction distances of lake trout (*Salvelinus namaycush*) to salmonid prey
Tammo P. Bult, Stephen C. Riley, Richard L. Haedrich, R. John Gibson, and Jan Heggenes	**1298–1306**	Density-dependent habitat selection by juvenile Atlantic salmon (*Salmo salar*) in experimental riverine habitats
Holger Hovgård, Hans Lassen, Niels Madsen, Thomas Moth Poulsen, and David Wileman	**1307–1316**	Gillnet selectivity for North Sea Atlantic cod (*Gadus morhua*): model ambiguity and data quality are related
David W. Welch and J. Paige Eveson	**1317–1327**	An assessment of light-based geoposition estimates from archival tags

National Research Council Canada
Ottawa, Canada K1A 0R6

Conseil national de recherches Canada
Ottawa, Canada K1A 0R6

Postage paid at Ottawa
Publications mail
Registration No. 1240579

Port payé à Ottawa
Poste-publication
Enregistrement n° 1240579

Canadian Journal of Fisheries and Aquatic Sciences

Volume 56, Number 7, July 1999

Journal canadien des sciences halieutiques et aquatiques

Volume 56, numéro 7, juillet 1999

Isabelle Roy and Landis Hare	**1143–1149**	Relative importance of water and food as cadmium sources to the predatory insect *Sialis velata* (Megaloptera)
Kenneth H. Reckhow	**1150–1158**	Water quality prediction and probability network models
Jill B.K. Leonard and Stephen D. McCormick	**1159–1171**	Effects of migration distance on whole-body and tissue-specific energy use in American shad (*Alosa sapidissima*)
M.J. Unwin, M.T. Kinnison, and T.P. Quinn	**1172–1181**	Exceptions to semelparity: postmaturation survival, morphology, and energetics of male chinook salmon (*Oncorhynchus tshawytscha*)
Yvan Simard and Diane Lavoie	**1182–1197**	The rich krill aggregation of the Saguenay – St. Lawrence Marine Park: hydroacoustic and geostatistical biomass estimates, structure, variability, and significance for whales
Bryan D. Neff, Peng Fu, and Mart R. Gross	**1198–1205**	Microsatellite evolution in sunfish (Centrarchidae)
Ulrich G. Reinhardt	**1206–1212**	Predation risk breaks size-dependent dominance in juvenile coho salmon (*Oncorhynchus kisutch*) and provides growth opportunities for risk-prone individuals
M.R. van den Heuvel, M. Power, M.D. MacKinnon, T. Van Meer, E.P. Dobson, and D.G. Dixon	**1213–1225**	Effects of oil sands related aquatic reclamation on yellow perch (*Perca flavescens*). I. Water quality characteristics and yellow perch physiological and population responses
M.R. van den Heuvel, M. Power, M.D. MacKinnon, and D.G. Dixon	**1226–1233**	Effects of oil sands related aquatic reclamation on yellow perch (*Perca flavescens*). II. Chemical and biochemical indicators of exposure to oil sands related waters
W.R. Gould, L.A. Stefanski, and K.H. Pollock	**1234–1240**	Use of simulation–extrapolation estimation in catch–effort analyses
G.J. Piet, J.S. Pet, W.A.H.P. Guruge, J. Vijverberg, and W.L.T. Van Densen	**1241–1254**	Resource partitioning along three niche dimensions in a size-structured tropical fish assemblage
William S. Hearn, Thomas Polacheck, Kenneth H. Pollock, and Wade Whitelaw	**1255–1265**	Estimation of tag reporting rates in age-structured multicomponent fisheries where one component has observers
H.F. Campbell and A.J. Hand	**1266–1277**	Modeling the spatial dynamics of the U.S. purse-seine fleet operating in the western Pacific tuna fishery

Continued on inside back cover / Suite au verso

Canada

Printed in Canada by / Imprimé au Canada par
University of Toronto Press Inc.
Typesetting by / Typographie par
NRC Research Press / Presses scientifiques du CNRC

0706-652X(199907)56:7;1-L